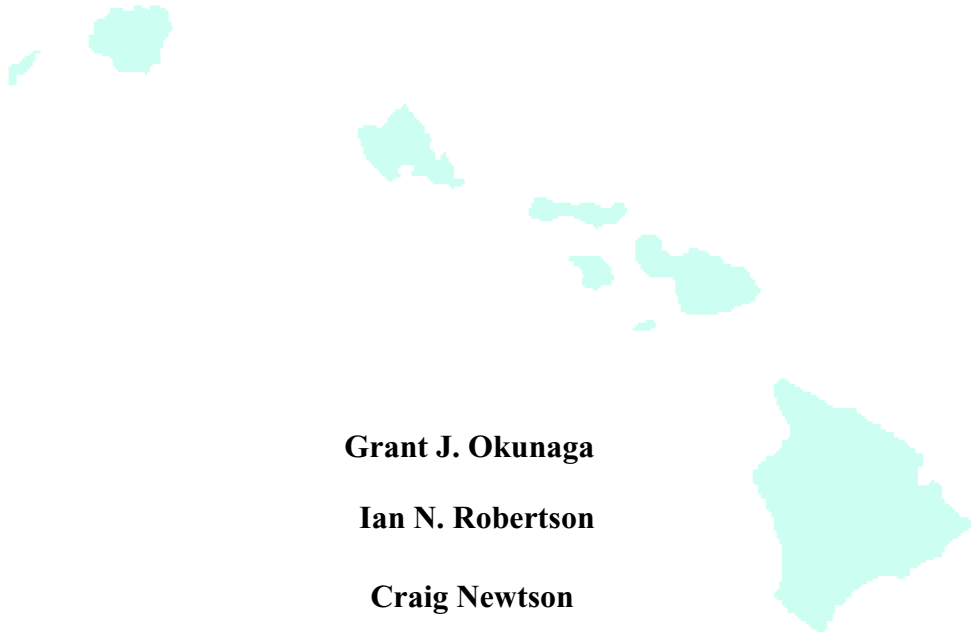


**LABORATORY STUDY OF CONCRETE PRODUCED WITH  
ADMIXTURES INTENDED TO INHIBIT CORROSION**



**Grant J. Okunaga**

**Ian N. Robertson**

**Craig Newtonson**



**Prepared in cooperation with the State of Hawaii Department of Transportation,  
Highways Division and U.S. Department of Transportation, Federal Highway  
Administration**

**UNIVERSITY OF HAWAII  
COLLEGE OF ENGINEERING**

**DEPARTMENT OF CIVIL AND ENVIRONMENTAL ENGINEERING**

**Research Report UHM/CEE/05-05**

**December 2005**



LABORATORY STUDY OF CONCRETE PRODUCED WITH ADMIXTURES  
INTENDED TO INHIBIT CORROSION

Grant J. Okunaga

Ian N. Robertson

Craig Newton

Prepared in cooperation with the:

State of Hawaii  
Department of Transportation  
Harbors Division  
and  
U.S. Department of Transportation  
Federal Highway Administration

Research Report UHM/CEE/05-05  
December 2005



## **Acknowledgements**

This report is based on a Master of Science thesis prepared by Grant Okunaga under the direction of Dr. Ian Robertson of the Department of Civil and Environmental Engineering at the University of Hawaii at Manoa, and Dr. Craig Newton of the Department of Civil and Environmental Engineering at New Mexico State University.

The authors wish to acknowledge the considerable contributions made by the State of Hawaii Department of Transportation (HDOT), Ameron Hawaii, and Hawaiian Cement during this project. Funding for this project was provided by the HDOT. Aggregates and other constituents for the concrete mixtures were donated by Ameron Hawaii and Hawaiian Cement.

The authors also acknowledge Drs. H. Ronald Riggs and Gregor Fischer for their contribution in reviewing this report and providing valuable suggestions. Special thanks are also extended to laboratory technicians Andrew Oshita and Miles Wagner for their technical assistance. Appreciation is also extended to Donn Kakuda, John Uno, and Gaur Johnson for their assistance in the Structures Laboratory.



## **ABSTRACT**

A study was conducted to evaluate the properties and effectiveness of concrete produced with Hawaiian aggregates and a variety of admixtures that are added to concrete to protect the embedded reinforcing steel from corrosion. The corrosion inhibiting admixtures investigated in this study include DCI, Rheocrete CNI, Rheocrete 222+, FerroGard 901, Xypex Admix C-2000, Pro-Crylic (a latex modifier), silica fume and fly ash. Concrete mixtures for each admixture were designed by varying proportions of the mixtures to provide the best comparison of each admixture's corrosion resistance. The corrosion resistance of the mixtures was tested by exposing test specimens to ponding cycles of a chloride solution designed to model marine environments. Physical properties of the concrete mixtures including compressive strength, elastic modulus, Poisson's ratio, and air permeability were measured. Electrical tests measuring the electrical current, half-cell potential, corrosion rate and concrete resistivity were used to monitor the corrosion in the test specimens during the ponding cycles. Finally, chemical tests were performed to measure the chloride concentration and pH at the level of the reinforcing steel. Results as of June 2004 show all of the corrosion inhibiting admixtures except for Xypex typically performed better than their control counterparts.



## TABLE OF CONTENTS

Abstract.....	v
List of Figures.....	xiii
List of Tables.....	xvii
Chapter 1 Introduction.....	1
1.1 Introduction.....	1
1.2 Objective.....	2
1.3 Scope.....	2
Chapter 2 Background and Literature Review.....	5
2.1 Introduction.....	5
2.2 Concrete Corrosion.....	5
2.3 Corrosion Inhibiting Admixtures.....	7
2.3.1 Calcium Nitrite-Based Corrosion Inhibitors.....	7
2.3.2 Rheocrete 222+.....	8
2.3.3 FerroGard 901.....	9
2.3.4 Xypex Admix C-2000.....	10
2.3.5 Pro-Crylic Latex Modifier.....	10
2.3.6 Silica Fume.....	11
2.3.7 Fly Ash.....	12
2.4 Testing.....	13
2.4.1 Physical and Mechanical Tests.....	13
2.4.2 Chemical Tests.....	15
2.4.3 Electrical Tests.....	16

2.5 Summary .....	20
Chapter 3 Experimental Procedures.....	21
3.1 Introduction.....	21
3.2 Materials .....	21
3.2.1 Coarse Aggregate.....	21
3.2.2 Fine Aggregate.....	22
3.2.3 Cement .....	23
3.3 Mixtures .....	23
3.3.1 Control Mixtures.....	24
3.3.2 DCI Mixtures .....	27
3.3.3 CNI Mixtures .....	28
3.3.4 Rheocrete Mixtures.....	29
3.3.5 FerroGard Mixtures .....	31
3.3.6 Xypex Mixtures .....	32
3.3.7 Latex Mixtures.....	33
3.3.8 Silica Fume Mixtures.....	34
3.3.9 Fly Ash Mixtures .....	39
3.3.10 Other Admixtures.....	43
3.4 Test Specimens .....	44
3.4.1 Mixing Preparation .....	46
3.4.2 Mixing Process.....	47
3.4.3 Casting and Curing Process .....	48
3.4.4 Testing Preparation .....	48

3.5 Testing Period .....	50
3.5.1 Electrical Tests .....	50
3.6 Testing Procedure for Physical and Mechanical Tests .....	50
3.6.1 Slump, Compressive Strength, Elastic Modulus, and Poisson Ratio Tests .....	50
3.6.2 Air Permeability .....	50
3.7 Testing Procedure for Chemical Tests .....	51
3.7.1 Chloride Concentration .....	51
3.7.2 pH .....	52
3.8 Testing Procedure for Electrical Tests .....	53
3.8.1 Current Test .....	53
3.8.2 Half-Cell Potential, Linear Polarization Resistance and Resistivity Measurements .....	53
3.9 Summary .....	53
Chapter 4 Results and Discussion of Mechanical Tests .....	55
4.1 Introduction .....	55
4.2 Slump, Compressive Strength, Elastic Modulus and Poisson's Ratio .....	55
4.2.1 Control Mixtures .....	55
4.2.2 Rheocrete Mixtures .....	57
4.3 Air Permeability .....	60
4.3.1 Control Mixtures .....	61
4.3.2 Calcium Nitrate Mixtures .....	62
4.3.3 FerroGard Mixtures .....	62
4.3.4 Rheocrete Mixtures .....	63

4.3.5 Latex Mixtures .....	63
4.3.6 Silica Fume Mixtures .....	64
4.3.7 Air Permeability Summary .....	64
4.4 Summary .....	64
Chapter 5 Results and Discussion of Chemical Tests .....	67
5.1 Introduction .....	67
5.2 Chloride Concentration Tests .....	67
5.2.1 Introduction .....	67
5.2.2 Control Mixtures .....	68
5.2.3 Calcium Nitrate Mixtures .....	70
5.2.4 FerroGard Mixtures .....	72
5.2.5 Rheocrete Mixtures .....	74
5.2.6 Latex Mixtures .....	76
5.2.7 Silica Fume Mixtures .....	78
5.2.8 Summary .....	80
5.3 pH Tests .....	80
5.3.1 Introduction .....	80
5.3.2 Control Mixtures .....	81
5.3.3 Calcium Nitrate Mixtures .....	82
5.3.4 Latex Mixtures .....	83
5.3.5 Silica Fume Mixtures .....	84
5.3.6 Other Mixtures .....	85
5.4 Summary .....	85

Chapter 6 Results and Discussion for Electrical Tests .....	87
6.1 Introduction.....	87
6.2 Accuracy of Electrical Current Tests .....	87
6.3 Accuracy of Gecor6 Electrical Tests .....	88
6.3.1 Introduction.....	88
6.3.2 Half-Cell Potential .....	90
6.3.3 Corrosion Rate from Linear Polarization.....	91
6.3.4 Concrete Resistivity .....	92
6.4 Presentation of Electrical Test Results .....	93
6.4.1 Electrical Current Tests.....	93
6.4.2 Half-Cell Potential Tests.....	96
6.4.3 Corrosion Rate Tests.....	99
6.4.4 Concrete Resistivity Tests.....	101
6.5 Ponding Cycles .....	104
6.5.1 Control Mixtures.....	104
6.5.2 Calcium Nitrite-Based Corrosion Inhibiting Admixtures.....	106
6.5.3 Rheocrete Mixtures .....	108
6.5.4 FerroGard Mixtures .....	110
6.5.5 Xypex Mixtures .....	111
6.5.6 Latex Mixtures .....	112
6.5.7 Silica Fume Mixtures.....	113
6.5.8 Fly Ash Mixtures .....	115
6.6 Summary.....	117

Chapter 7 Summary and Conclusions.....	119
7.1 Introduction.....	119
7.2 Summary.....	119
7.3 Conclusions.....	122
references .....	125
Appendix.....	127
A.1 List of Appendix Figures .....	129

## LIST OF FIGURES

<u>Figure</u>	<u>Page</u>
Figure 3-1: Geometry of a Typical Test Specimen.....	44
Figure 3-2: Laboratory Specimens in Holmes Hall Basement .....	45
Figure 3-3: Typical Longitudinal Specimen Cross Section.....	47
Figure 3-4: Typical Test Specimen Setup.....	49
Figure 3-5: Location of Chloride Sample .....	52
Figure 4-1: Average Compressive Strength of Kapaa and Halawa Control Mixtures .....	57
Figure 4-2: Average Compressive Strength of Kapaa and Halawa Rheocrete Mixtures .....	60
Figure 5-1: Progression of Chloride Concentrations for Kapaa Control Mixtures.....	69
Figure 5-2: Chloride Concentrations for Kapaa Control Mixtures.....	70
Figure 5-3: Progression of Chloride Concentrations for Kapaa DCI Mixtures .....	71
Figure 5-4: Chloride Concentrations for Kapaa DCI Mixtures .....	72
Figure 5-5: Progression of Chloride Concentrations for Kapaa FerroGard Mixtures .....	73
Figure 5-6: Chloride Concentrations for Kapaa FerroGard Mixtures .....	74
Figure 5-7: Progression of Chloride Concentrations for Kapaa Rheocrete Mixtures.....	75
Figure 5-8: Chloride Concentrations for Kapaa Rheocrete Mixtures.....	76
Figure 5-9: Progression of Chloride Concentrations for Kapaa Latex Mixtures.....	77
Figure 5-10: Chloride Concentrations for Kapaa Latex Mixtures .....	78
Figure 5-11: Progression of Chloride Concentrations for Kapaa Silica Fume Mixtures...79	
Figure 5-12: Chloride Concentrations for Kapaa Silica Fume Mixtures.....	80
Figure 5-13: pH for Kapaa Control Mixtures .....	82

Figure 5-14: pH for Kapaa DCI Mixtures.....	83
Figure 5-15: pH for Kapaa Latex Mixtures .....	84
Figure 5-16: pH for Kapaa Silica Fume Mixtures .....	85
Figure 6-1: Accuracy of Corrosion Potential in Predicting Corrosion .....	91
Figure 6-2: Accuracy of Corrosion Rate in Predicting Corrosion .....	92
Figure 6-3: Accuracy of Concrete Resistivity in Predicting Corrosion .....	93
Figure 6-4: Example of Electrical Current Measurements Not Indicating Corrosion .....	95
Figure 6-5: Example of Electrical Current Measurements Indicating Corrosion .....	96
Figure 6-6: Example of Half-Cell Potential Measurements Not Indicating Corrosion .....	97
Figure 6-7: Example of Half-Cell Potential Measurements Indicating Corrosion .....	99
Figure 6-8: Example of Corrosion Rate Measurements Not Indicating Corrosion .....	100
Figure 6-9: Example of Corrosion Rate Measurements Indicating Corrosion .....	101
Figure 6-10: Example of Concrete Resistivity Measurements Not Indicating Corrosion.....	103
Figure 6-11: Example of Concrete Resistivity Measurements Indicating Corrosion .....	104
Figure 6-12: Ponding Cycle Results for Kapaa and Halawa Control Mixtures.....	105
Figure 6-13: Ponding Cycle Results for Kapaa DCI Mixtures .....	106
Figure 6-14: Ponding Cycle Results for Kapaa CNI Mixtures .....	107
Figure 6-15: Ponding Cycle Results for Halawa CNI Mixtures.....	108
Figure 6-16: Ponding Cycle Results for Kapaa Rheocrete Mixtures.....	109
Figure 6-17: Ponding Cycle Results for Halawa Rheocrete Mixtures.....	110
Figure 6-18: Ponding Cycle Results for Kapaa FerroGard Mixtures .....	111
Figure 6-19: Ponding Cycle Results for Kapaa Xypex Mixtures .....	112

Figure 6-20: Ponding Cycle Results for Kapaa Latex Mixtures.....	113
Figure 6-21: Ponding Cycle Results for Kapaa Silica Fume Mixtures.....	114
Figure 6-22: Ponding Cycle Results for Halawa Silica Fume Mixtures.....	115
Figure 6-23: Ponding Cycle Results for Kapaa Fly Ash Mixtures.....	116
Figure 6-24: Ponding Cycle Results for Halawa Fly Ash Mixtures.....	117



## LIST OF TABLES

<u>Table</u>	<u>Page</u>
Table 2-1: Interpretation of Half-Cell Potential Results.....	17
Table 2-2: Interpretation of Corrosion Rate Results.....	18
Table 2-3: Interpretation of Concrete Resistivity Results.....	20
Table 3-1: Summary of Admixture Usage with Various Mixtures.....	24
Table 3-2: Mixture Proportions for Kapaa Control Mixtures.....	26
Table 3-3: Mixture Proportions for Halawa Control Mixtures.....	27
Table 3-4: Mixture Proportions for Kapaa DCI and CNI Mixtures.....	28
Table 3-5: Mixture Proportions for Halawa CNI Mixtures .....	29
Table 3-6: Mixture Proportions for Kapaa Rheocrete Mixtures.....	30
Table 3-7: Mixture Proportions for Halawa Rheocrete Mixtures.....	31
Table 3-8: Mixture Proportions for Kapaa FerroGard Mixtures .....	32
Table 3-9: Mixture Proportions for Kapaa Xypex Mixtures .....	33
Table 3-10: Mixture Proportions for Kapaa Latex Mixtures.....	34
Table 3-11: Mixture Proportions for Kapaa Force 10,000D Silica Fume Mixtures.....	37
Table 3-12: Mixture Proportions for Halawa Force 10,000D Silica Fume Mixtures.....	38
Table 3-13: Mixture Proportions for Halawa Rheomac SF100 Silica Fume Mixtures .....	39
Table 3-14: Mixture Proportions for Kapaa Fly Ash Mixtures .....	41
Table 3-15: Mixture Proportions for Halawa Fly Ash Mixtures .....	42
Table 4-1: Physical Properties of Kapaa Control Mixtures.....	55
Table 4-2: Physical Properties of Halawa Control Mixtures.....	56
Table 4-3: Physical Properties of Kapaa Rheocrete Mixtures .....	58

Table 4-4: Physical Properties of Halawa Rheocrete Mixtures .....	59
Table 4-5: Air Permeability Results for Kapaa Control Mixtures .....	62
Table 4-6: Air Permeability Results for Kapaa DCI Mixtures .....	62
Table 4-7: Air Permeability Results for Kapaa FerroGard Mixtures .....	63
Table 4-8: Air Permeability Results for Kapaa Rheocrete Mixtures .....	63
Table 4-9: Air Permeability Results for Kapaa Latex Mixtures .....	64
Table 4-10: Air Permeability Results for Kapaa Silica Fume Mixtures .....	64

## CHAPTER 1 INTRODUCTION

### 1.1 Introduction

Reinforced concrete is one of the most common building materials used today due to its strength and durability. Reinforced concrete structures are commonly used for marine structures such as piers and wharves. However when exposed to a marine environment, reinforced concrete structures can deteriorate rapidly due to the ingress of chlorides. As the chloride concentration levels at the reinforcing steel increase, the passive protective layer on the reinforcing steel formed from the high alkalinity of the concrete begins to break down. As the protective layer deteriorates, the reinforcing steel begins to corrode causing spalls or delaminations throughout the concrete structure.

Two of the main ingredients in concrete are the coarse and fine aggregates. In Hawaii, the aggregates used for concrete mixtures are unique. Consequently, concrete created with these aggregates will have unique properties. This study investigates the effect of common corrosion inhibiting admixtures used in concrete produced with materials available in Hawaii.

There are many different types of corrosion protection systems used to prevent the ingress of chlorides from reaching the reinforcing steel. One method is the use of corrosion inhibiting admixtures that can be added at the batch plant or during the mixing process. These admixtures are designed to prevent corrosion in various ways. Chemical admixtures inhibit corrosion by increasing the chloride concentration levels required to initiate the corrosion process and also slow the rate of corrosion on the reinforcing steel. Other types of admixtures are waterproofing admixtures or pozzolans intended to reduce the permeability of the concrete. By reducing the permeability, the ingress of chlorides is

also reduced. The use of admixtures during the mixing process is widely considered to be the least expensive method of corrosion prevention and is investigated in this study.

Another method of corrosion protection is providing a layer of protection on the reinforcing steel such as epoxy coated or stainless steel clad reinforcing bars. Other methods of corrosion protection that can be performed on existing reinforced concrete structures include cathodic protection, which uses a sacrificial anode and electrochemical removal of chlorides.

## **1.2 Objective**

The objective of this research project is to investigate the effects of corrosion inhibiting admixtures in concrete mixtures that have been engineered specifically for Hawaiian aggregates to protect the embedded steel in reinforced concrete from corrosion. The corrosion inhibiting admixtures used in this research study were DAREX Corrosion Inhibitor (DCI), Rheocrete CNI, Rheocrete 222+, FerroGard 901, Xypex Admix C-2000, Pro-Crylic latex-modifier, and pozzolans such as silica fume and fly ash. Various concrete mixtures designed using each of the admixtures were prepared and exposed to a simulated marine environment of saltwater ponding cycles. Mechanical and chemical tests were performed on each mixture including slump, compressive strength, chloride concentration, air permeability, and pH tests. Non-destructive electrical tests to evaluate the corrosion of the reinforcing steel included half-cell potential tests, corrosion rate from linear polarization resistance tests, concrete resistivity tests and electrical current tests.

## **1.3 Scope**

This report discusses the findings and status of the research project as of June 2004. Chapter 2 presents a literature review describing the corrosion process of

reinforced concrete, a background of the admixtures tested, and the mechanical, chemical and electrical tests performed in this study. Chapter 3 describes the experimental procedures for mixing of the concrete mixtures, and testing and monitoring procedures for all of the test specimens. The results from the mechanical tests are provided in Chapter 4. Chapter 5 presents the results of the chemical tests. The electrical test results are presented in Chapter 6. Finally, Chapter 7 provides a summary of the research and discusses the conclusions of the study.



## CHAPTER 2 BACKGROUND AND LITERATURE REVIEW

### 2.1 Introduction

This chapter begins with a discussion of the basic theory of the corrosion process in reinforced concrete. Also presented in this chapter is a discussion of each of the different concrete admixtures tested in this study. Finally this chapter presents a description of the physical, mechanical, chemical and electrical tests used in this study to assess the concrete test specimens.

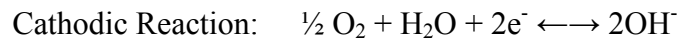
### 2.2 Concrete Corrosion

Corrosion is the process involving the deterioration or degradation of a metal. The corrosion process is typically caused by either a chemical or electrochemical reaction with the surrounding environment. For reinforced concrete structures, the concrete protects the steel from most chemical corrosive reactions; therefore the corrosion in reinforced concrete is typically caused by an electrochemical reaction.

The electrochemical corrosion process creates an electrochemical corrosion cell similar to a battery. The components required for the electrochemical process are an anode, a cathode, a conducting environment for ionic movement and an electrical connection between the anode and the cathode for the flow of electrical current. In reinforced concrete, the anode forms on an area of reinforcing steel where the passive protective layer is breached and oxidation begins to occur. At the anode the oxidation process causes electrons to be released by the following chemical reaction.



These free electrons travel along the reinforcing steel, which provides an electrical connection to a cathode located on another location on the reinforcing steel. At the cathode, the free electrons are used in the reduction process, which produces hydroxyl ions (OH<sup>-</sup>) with the following chemical reaction.



The moist concrete surrounding the reinforcing steel provides a conducting environment allowing the hydroxyl ions to travel back to the anode. The hydroxyl ions then react with the ferrous ions to form hydrous iron oxides. As the electrochemical process continues the corrosion products build up at the anode and begin to occupy more volume than the original reinforcing steel.

The natural high pH of concrete surrounding the reinforcing steel creates a natural layer of iron oxide or passive layer, which protects the steel from corrosion. However, as aggressive ions such as chloride ions from a saltwater environment flow through the concrete and reach the steel, this protective layer begins to break down. Once the chlorides reach the breach the protective layer, the electrochemical process begins. As the corrosion products occupy more volume than the original reinforcing steel at the anode, the concrete begins to expand. Eventually this expansive force will crack the concrete causing spall and delaminations. Chlorides are then allowed easier access to the reinforcing steel through these cracks and the corrosion process is accelerated. The expansive stress in the reinforced concrete decreases the bond between the reinforcing steel and the concrete. The decrease in bond between the reinforcing steel and the concrete and the deterioration of the reinforcing steel can eventually severely weaken the reinforced concrete structure.

## 2.3 Corrosion Inhibiting Admixtures

In this study DCI, Rheocrete CNI, Rheocrete 222+, FerroGard 901, Xypex Admix C-2000, fly ash, silica fume, and Pro-Crylic, a latex modifier, were added to concrete mixtures to test their corrosion inhibiting ability in a simulated chloride environment. This section provides a description of each of the admixtures and their effect on the properties of concrete.

Due to the similarities in names, Rheocrete CNI will be referred to as “CNI”, and Rheocrete 222+ will be referred to as “Rheocrete”. Also to reduce the length of the admixtures titles, FerroGard 901 will be referred to as “FerroGard”, and Xypex Admix C-2000 shall be referred to as “Xypex”. Also the latex modifier, Pro-Crylic, was used to represent all latex modifiers, and will be referred to herein as “Latex”.

### 2.3.1 Calcium Nitrite-Based Corrosion Inhibitors

Rheocrete CNI is a calcium nitrite based corrosion inhibiting admixture manufactured by Degussa containing a minimum of 30% calcium nitrite by mass. The recommended dosage for this admixture is 1 to 6 gallons per cubic yard, depending on the severity of the corrosion environment and anticipated chloride loading of the structure. According to the manufacturer the dosage for Rheocrete CNI can be computed using the following equation.

$$\text{Dosage}(\text{gal}/\text{yd}^3) = 0.411 \times \frac{\text{Anticipated Chloride Loading}(\text{lb}/\text{yd}^3)}{\text{Chloride – to – Nitrite Ratio}} \quad (2.1)$$

The water content of Rheocrete CNI is approximately 7.3 lb/gal and should be used in the calculation of the water-to-cement ratio of the concrete. However, to follow the Hawaii Harbors Division practice on all projects through 1998, Rheocrete CNI and

other calcium nitrite-based corrosion inhibitors such as DCI were used as an equal replacement for water. Consequently, the actual water-to-cement ratios decreased from the design water-to-cement ratios because only 70% of these admixtures are water. The remaining 30% of the admixture is calcium nitrite. For the mixtures in this study, water was replaced in equal portions with the calcium nitrite based corrosion inhibitors.

Due to the accelerated concrete setting times from this admixture, a retarding or hydration control admixture may be added to the concrete to offset the acceleration affects. According to the manufacturer, Rheocrete CNI may be used in combination with any other admixture manufactured by Degussa. When other admixtures are used, each admixture should be added individually during mixing. No information was provided as to whether Rheocrete CNI affects the hardened and plastic properties of the concrete. Also other than an adjustment for water, this admixture does not require any changes in mixture proportions.

DCI is also a calcium nitrate corrosion inhibiting admixtures identical to Rheocrete CNI and is manufactured by Grace Construction Products.

### *2.3.2 Rheocrete 222+*

Rheocrete 222+ is an organic corrosion-inhibiting admixture manufactured by Degussa. This admixture “restricts the ingress of chlorides and moisture and slows the rate of corrosion by forming a protective film on the reinforcing steel”. The recommended dosage for Rheocrete 222+ is 1 gallon per cubic yard. This admixture does not require a reduction of water in the mixture proportions and is not included in the water-to-cement ratio calculation. Rheocrete 222+ should not be mixed with any other admixtures prior to being introduced into the concrete and may be added with the

concrete batch water. The manufacturer claims Rheocrete 222+ does not significantly affect the hardened and plastic properties of the concrete. This admixture also should not significantly alter the compressive strength and permeability of the concrete.

### *2.3.3 FerroGard 901*

Ferrogard 901 is a liquid concrete admixture manufactured by Sika Corp. formulated to protect embedded reinforcing steel from corrosion. This admixture is an active, dual-purpose corrosion inhibitor, which contains a combination of aminoalcohols, and organic and inorganic inhibitors. FerroGard 901 works by protecting both the anodic and cathodic parts of the corrosion cell and forms a continuous protective film around the reinforcing steel presenting a physical barrier to chlorides and other deleterious substances. The manufacturer claims “FerroGard 901 is able to displace chloride ions from the metal surface to protect concrete from chloride-induced corrosion”. The recommended dosage of FerroGard 901 is 2 gallons per cubic yard of concrete. However, for extremely high chloride and severe marine exposure, the recommended dosage rate is increased to 3 gallons per cubic yard. When adding the dosage of FerroGard 901, the equivalent amount of water should be reduced. The weight of FerroGard 901 is included in the water-to-cement ratio calculation for mix designs. For best results, this admixture should be added directly to freshly mixed concrete, but can also be added to a ready-mix truck at the concrete plant or at the job site. The manufacturer claims FerroGard 901 does not affect the properties of hardened concrete, such as compressive strengths and permeability. Also this admixture does not require any changes in the mixture proportions or placement of fresh concrete.

#### *2.3.4 Xypex Admix C-2000*

Xypex Admix C-2000 is an admixture that provides chemical treatment for the waterproofing protection and improvement of concrete. This admixture consists of portland cement, very fine treated silica sand and various active, proprietary chemicals. When added during mixing, these chemicals react with the moisture in the fresh concrete as well as the by-products of cement hydration (calcium hydroxide, mineral salts, mineral oxides and unhydrated and partially hydrated cement particles) to cause a catalytic reaction, which generates a non-soluble crystalline formulation throughout the pores and capillary tracts of the concrete. This creates a permanent seal against the penetration of water or liquids from any direction into the concrete.

Xypex Admix C-2000 is added to the coarse and fine aggregates and mixed thoroughly for 2 to 3 minutes. Then, the cement and water are added following standard mixing practices. According to the manufacturer, Xypex may affect the setting time of the concrete causing a retardation of set. The amount of retardation depends upon the concrete mixture proportions and dosage of the admixture. However, under normal conditions, Xypex will provide a normal set concrete. The manufacturer also claims that concrete containing this admixture may develop higher ultimate strengths when compared to plain concrete.

#### *2.3.5 Pro-Crylic Latex Modifier*

Pro-Crylic is an acrylic polymer liquid admixture manufactured by Bonded Materials Company. This admixture is designed to improve the adhesion and other physical properties of portland cement mortar, plaster and concrete. The manufacturer

claims that mixtures with Pro-Crylic will exhibit improved adhesive qualities, moisture retention, flexibility, toughness and chemical resistance.

Pro-Crylic is added by substituting a portion of the water used in the concrete mixture with the admixture. During the mixing process this admixture is added before the sand and cement. After the addition of Pro-Crylic, the fresh concrete should not be mixed for more than 5 minutes. After hardening, concrete mixed with Pro-Crylic should not be immersed continuously in water until after at least 3 to 4 days air cure time.

Pro-Crylic and other types of latex admixtures added to concrete are designed to decrease the water absorptivity and increase the resistivity of the concrete. The latex admixture acts as a barrier in the concrete and restricts the saltwater from coming into contact with the reinforcing steel.

#### *2.3.6 Silica Fume*

In this study, two different types of silica fume were tested. The first type of silica fume used was Force 10,000D, which is a microsilica-based concrete admixture designed by W.R. Grace Construction Products. According to the manufacturer, this admixture improves the concrete by increasing the concrete strength, reducing the permeability and increasing the resistivity and durability. When using this admixture, the manufacturer recommends using the lowest practical w/c ratios and superplasticizers to provide adequate workability. The recommended dosage of Force 10,000D is between 7.5% and 15% microsilica by weight of cement.

The second type of silica fume used in this study is Rheomac SF 100 manufactured by Degussa. Rheomac SF 100 is a densified silica fume mineral admixture designed to increase concrete service life, strength, and modulus of elasticity. The

manufacturer also claims this admixture reduces the permeability of the concrete and increases the durability, resistance to sulfate attack and resistance to alkali-silica reactivity.

Silica fume works as a corrosion inhibiting admixture because the pozzolanic microsilica reacts with the calcium hydroxide and water during the mixing phase to produce more aggregate-binding calcium silicate gel. This additional glue improves the bonding in the concrete matrix and helps to reduce the permeability. Simultaneously during the chemical process, the calcium hydroxide content is reduced. High amounts of calcium hydroxide make the concrete more vulnerable to sulfate and chemical attacks as well as adverse alkali-aggregate reactions. By reducing the calcium hydroxide, the durability of the concrete improves. The extremely small size of the microsilica particles also helps to improve corrosion protection. The average microsilica particle size is about 0.15 micrometers, while the typical portland cement particle size is 26 micrometers. Due to the large difference in size, there are over 50,000 particles of microsilica for each grain of cement in concrete mixtures where 10% of cement by weight is replaced by silica fume. The microsilica particles fill the voids between the cement particles reducing the permeability of the concrete and improving the paste-to-aggregate bond of the microsilica concrete. The use of silica fume in concrete mixtures also reduces the pH in the concrete.

### *2.3.7 Fly Ash*

Fly ash is another pozzolan, like silica fume, used as an admixture in concrete mixtures. This admixture is a fine residue that results from the combustion of pulverized coal and is carried from the combustion chamber of the furnace by exhaust gases. Fly ash that is available commercially is usually a by-product of thermal power generating

stations. This admixture works similarly to silica fume and other pozzolanic materials by making concrete more economical, increasing compressive strength and reducing concrete permeability.

## **2.4 Testing**

This section provides a brief discussion of the theories and basic concepts for all of the physical, mechanical, chemical, and electrical tests.

### *2.4.1 Physical and Mechanical Tests*

The physical tests performed in this study include the slump test and air content test that were performed during immediately after the mixing process, and the air permeability test which was performed after the conclusion of the specimen corrosion cycling. The mechanical tests performed in this study measured the compressive strength, modulus of elasticity and Poisson's ratio.

#### *2.4.1.1 Slump Test*

The slump test, performed according to ASTM C 143, is the most widely accepted method used to measure the consistency of fresh concrete. A concrete mixture with a high slump value is desired as it indicates a wet and fluid concrete mixture and increases workability. Concrete mixtures with lower slump values are stiff and difficult to mold. A concrete mixture with a low slump value typically requires additional rodding or vibration to properly consolidate before hardening.

#### *2.4.1.2 Air Content*

In this study the air content was measured using the pressure method according to ASTM C 231. This test is based on Boyle's law, which relates pressure to volume. The

test is performed by adding a sample of freshly mixed concrete into the instrument chamber where a pressure is applied that compresses the air within the concrete sample, including the air in the pores of the concrete. A calibrated pressure-type meter accurately measures the air content in the fresh concrete.

#### *2.4.1.3 Compressive Strength*

Concrete compressive strength tests were performed according to ASTM C 39 using cylindrical specimens 6 inches in diameter by 12 inches in height.

#### *2.4.1.4 Modulus of Elasticity*

The modulus of elasticity, also known as the elastic modulus, and Poisson's ratio tests followed ASTM C 469. The modulus of elasticity measures the ratio of stress to strain in the elastic range of the stress versus strain curve for the concrete. The Poisson's ratio test measures the ratio of lateral to axial strain of the concrete

#### *2.4.1.5 Air Permeability Test*

The air permeability of the concrete test specimens was measured using the James Poroscope-Plus by NDT James Instruments Inc. The permeability of the concrete is a major factor in the durability of concrete as it measures the ease of movement of gases through the surface layer of the concrete. Concrete with a high permeability can lead to the ingress of air and moisture into the concrete and cause corrosion of the reinforcing steel. A low permeability in concrete can minimize the diffusion of water, chlorides, oxygen and carbon dioxide and significantly reduce the corrosion of the reinforcing steel.

The moisture content of the concrete has a major effect on the permeability. Fully saturated concrete is almost impermeable to air. For effective testing the concrete should be dry and near the surface moisture content measured.

For this study, the air permeability was measured using the Figg number. The Figg number was the time in seconds required for the pressure to increase from  $-7.98$  psi to  $-7.25$  psi ( $-55$  kPa to  $-50$  kPa) in a vacuum cavity in the test specimen.

#### *2.4.2 Chemical Tests*

In this study, the chemical tests measured the pH and chloride concentrations in the specimens after the conclusion of the cycling process.

##### *2.4.2.1 pH Test*

Concrete surrounding the embedded reinforcing steel provides a protective barrier preventing corrosion. The natural alkalinity of concrete provides a high pH environment, usually greater than 12.5, and inhibits the corrosion of reinforcing steel by allowing a passive and non-corroding protective oxide film to form around the steel. The pH level is typically measured from a sample of the concrete dust or powder collected from the area surrounding the reinforcing steel. This sample is mixed with 10 drops of distilled water per gram of concrete powder. A pH meter is then inserted into the solution to measure the pH, similar to the method for testing aqueous solutions.

##### *2.4.2.2 Chloride Content Test*

The chloride content or concentration in hardened concrete significantly affects the corrosion of the embedded reinforcing steel. Typical concrete has a high alkalinity, which provides a protective passive layer around the reinforcing layer. When chloride

ions are allowed to ingress through the concrete to the level of the reinforcing steel they can interact with sufficient moisture and oxygen to break down this protective barrier and corrode the reinforcing steel.

### *2.4.3 Electrical Tests*

This section provides a discussion of the basic concepts for each of the electrical tests used to measure the corrosion activity of the test specimens. The electrical tests performed in this study measured the half-cell potential, corrosion rate or polarization resistance and the concrete resistivity.

#### *2.4.3.1 Half-Cell Potential Test*

The half-cell potential test was first developed in the 1950's and has been widely used as a non destructive test to assess the corrosion in reinforced concrete structures. This electrical test measures the corrosion potential of the embedded reinforcing steel against a reference half-cell which is placed on the exterior surface of the concrete. The reference half-cells typically used are saturated calomel and copper/copper sulfate cells. The half-cell potential test requires an electrical connection to the embedded reinforcing steel below the reference cell. A small electrical current is then applied to the steel and the change in the half-cell potential is measured.

Results of the half-cell potential tests are then compared to the limiting values shown in Table 2-1. A half-cell potential reading less than -350 mV indicates a 90% probability of corrosion. Values between -350 mV and -200 mV indicate an "uncertain" result, and values greater than -200 mV indicate a 10% probability of corrosion the location of the half-cell.

Table 2-1: Interpretation of Half-Cell Potential Results

Measured Potential (mV)	Statistical Risk of Corrosion Occurring (%)
< -350	90
Between -350 and -200	Uncertain
> -200	10

A major drawback to the half-cell potential test is that this test only provides a qualitative measurement of corrosion. The potential values measured only provide a probable indication of corrosion. Also the large region of -200 mV to -350 mV values do not provide any conclusive information if corrosion exists or not in the reinforcing steel below.

#### 2.4.3.2 Corrosion Rate from Linear Polarization

The corrosion rate test, also known as the polarization resistance test, is an electrochemical technique, which is capable of detecting the onset of corrosion during the early stages. The principle behind this technique is that a linear relationship exists between the potential and applied currents. There are three methods to determine the corrosion rate or linear polarization resistance. They are the galvanostatic method, potentiostatic method and the potentiodynamic method.

For this study the corrosion rate was determined from the Gecor6 testing instrument by first measuring the polarization resistance  $R_p$ , which is the change in potential divided by the applied current as shown below.

$$R_p = \frac{\Delta E}{\Delta I}$$

The corrosion current is then determined using the “Stearn and Geary” relationship, which is shown below. In this equation B is the Stern-Geary constant, which was taken as 26 mV by the Gecor6 instrument.

$$I_{corr} = \frac{B}{R_p}$$

The corrosion current  $I_{corr}$  is then integrated over the surface area A of steel bar being polarized to determine the corrosion rate  $i_{corr}$ . For this study, the surface area A of steel in each test specimen was calculated to be 41.89 in<sup>2</sup>. This relationship to determine the corrosion rate, which was recorded in this study, is shown below.

$$i_{corr} = \frac{I_{corr}}{A}$$

Results of the corrosion rate tests are then compared to the limiting values shown in Table 2-2. A corrosion rate reading less than 1.0 uA/cm<sup>2</sup> indicates a high corrosion rate. Values between 0.5 uA/cm<sup>2</sup> and 1.0 uA/cm<sup>2</sup> indicate a moderate corrosion rate.. Values between 0.2 uA/cm<sup>2</sup> and 0.5 uA/cm<sup>2</sup> indicate a low corrosion rate. Finally values less than 0.2 uA/cm<sup>2</sup> indicate no corrosion.

Table 2-2: Interpretation of Corrosion Rate Results

Corrosion Rate (uA/cm <sup>2</sup> )	Level of Corrosion Rate
> 1.0	High
Between 0.5 and 1.0	Moderate
Between 0.2 and 0.5	Low
Less than 0.2	No Corrosion

The major limitation to the corrosion rate measurement or linear polarization method is accurately measuring the surface area of the reinforcing steel below. For the

test specimens in this study, the surface area can easily be calculated if the testing instrument is properly aligned on each test specimen. However in field testing of large concrete structures, the surface area of embedded steel directly below the testing instrument is difficult to accurately determine. An overestimation of the surface area of reinforcing steel can lead to an underestimated corrosion rate, while an underestimation will yield an overestimated corrosion rate.

#### *2.4.3.3 Resistivity Test*

The resistivity or concrete resistivity test measures the electrical resistance to current flow within the concrete. Concrete resistivity values are determined by measuring the potential difference or resistance from a pulse between the sensor counter-electrode of the Gecor6 and the reinforcing steel network. The concrete resistivity is then calculated by the following formula.

$$\text{Concrete resistivity} = 2 \cdot R \cdot D$$

Where: R = potential difference or resistance measured

D = diameter of the counter-electrode center

Results of the concrete resistant tests are then compared to the limiting values shown in Table 2-3. A concrete resistivity reading less than 5 kohm cm indicates a very high concrete rate. Values between 5 kohm cm and 10 kohm cm indicate a high corrosion rate. Values between 10 kohm cm and 20 kohm cm indicate a moderate to low corrosion rate. Finally values greater than 20 kohm cm indicate low corrosion.

Table 2-3: Interpretation of Concrete Resistivity Results

Resistivity (kohm cm)	Level of Corrosion Rate
< 5	Very High
Between 5 and 10	High
Between 10 and 20	Moderate/Low
> 20	Low

The major limitation to the concrete resistivity test is that the test is inaccurate after recent surface wetting as this can lead to a low resistivity at the surface of the concrete and significant errors in the results. For this reason, field testing of existing concrete structures after recent rainfall can cause low surface concrete resistivity and errors in the estimating of the concrete resistivity.

## 2.5 Summary

This chapter presented an overview of the corrosion process of embedded reinforcing steel in concrete. Also presented was a background of each of the corrosion inhibiting admixtures tested in this study. Finally this chapter discusses the various physical, mechanical, chemical and electrical tests performed in this study.

## CHAPTER 3 EXPERIMENTAL PROCEDURES

### 3.1 Introduction

This chapter describes the materials used in all of the concrete mixtures and the design of each mixture. The concrete mixing, casting and curing procedures are also described. The experimental procedures for measuring concrete properties such as compressive strength, chloride concentration, air permeability and pH are also described. The procedures for electrical tests used to measure the half-cell potential, linear polarization, resistivity, and electrical current, which assess the corrosion in the reinforcing steel are also presented.

### 3.2 Materials

#### 3.2.1 Coarse Aggregate

Coarse aggregates used in this study were obtained from two different quarries located on the island of Oahu. The first quarry is the Kapaa Quarry, operated by Ameron. The other quarry is the Halawa quarry, which is operated by Hawaiian Cement. These are two of the largest quarries on the island and manufacture a large portion of the concrete for the island of Oahu. For simplicity concrete mixes will be referred to herein as “Kapaa” and “Halawa” depending on the source of the coarse and fine aggregate used in the mixture.

This project used coarse aggregates from both quarries because the material properties vary from each quarry. Although the aggregates from the Halawa quarry contain particles that are extremely porous, both sources are routinely used for concrete production on Oahu. By testing the admixtures in concrete mixture proportions from

both batch plants, a comparison of the quality of aggregates from each quarry can be made.

Information on coarse aggregate particle size distribution, specific gravity and absorption for coarse aggregates used in the Kapaa mixtures were reported by Pham and Newtonson (2001).

### *3.2.2 Fine Aggregate*

To satisfy the gradation and fineness modulus requirements of ASTM C 33, three different fine aggregates were used in this study. The first is an aeolian deposit known as dune sand from the island of Maui. The second was crushed basalt or basalt sand obtained from the Kapaa quarry. The third was crushed basalt or basalt sand obtained from the Halawa quarry.

A previous study determined that Maui dune sand alone does not meet the fineness modulus requirements of ASTM C 33 (Pham 2001). However, a proper mixture of Maui dune sand and basalt sand can satisfy this ASTM requirement. For the Kapaa mixtures, a blended mixture of 34.3% Maui dune sand and 65.7% Kapaa basalt sand was used. For the Halawa mixtures, a blended mixture of 43.0% Maui dune sand and 57.0% Kapaa basalt sand was used.

Grain size distribution tests according to ASTM C 136 determined that the fineness modulus values of the blended fine aggregate were consistent with the standards set in ASTM C 33.

Detailed results of the particle size distribution, fineness modulus, bulk specific gravity and absorption for fine aggregates used in the Kapaa mixes are presented by Pham and Newtonson (2001).

### *3.2.3 Cement*

The cement used in this study was a Type I-II cement produced on the island of Oahu by Hawaiian Cement.

### **3.3 Mixtures**

The Kapaa aggregate mixtures consisted of a set of control mixtures and eight sets of mixtures that used different admixtures intended to reduce corrosion. For the Halawa aggregates, mixtures were designed using CNI, Rheocrete 222+, two types of silica fume, fly ash and a control mixture. For each admixture, specific mixture proportions were created to vary different parameters such as water-cement ratios, paste contents, admixture dosages or pozzolan contents. A summary of all the concrete mixes used in this study is presented in Table 3-1.

Table 3-1: Summary of Admixture Usage with Various Mixtures

Admixture	w/(c+p)	Paste Content	Pozzolan Content	Admixture Dosage	Latex Content
Kapaa Control	3 levels	2 levels	--	--	--
Halawa Control	3 levels	2 levels	--	--	--
Kapaa DCI	2 levels	2 levels	--	3 levels	--
Kapaa CNI	2 levels	2 levels	--	3 levels	--
Halawa CNI	2 levels	2 levels	--	3 levels	--
Kapaa Rheocrete 222+	3 levels	2 levels	--	1 level	--
Halawa Rheocrete 222+	3 levels	2 levels	--	1 level	--
Kapaa Xypex Admix C-2000	3 levels	2 levels	--	1 level	--
Kapaa Pro-Crylic Latex Modifier	2 levels	--	--	--	3 levels
Kapaa Force 10,000D Silica Fume	2 levels	2 levels	3 levels	--	--
Halawa Force 10,000D Silica Fume	2 levels	2 levels	3 levels	--	--
Kapaa Rheobuild SF100 Silica Fume	2 levels	2 levels	3 levels	--	--
Kapaa Fly Ash	2 levels	2 levels	3 levels	--	--
Halawa Fly Ash	2 levels	2 levels	3 levels	--	--

### 3.3.1 Control Mixtures

The control mixtures for the Kapaa aggregates were proportioned by modifying an actual concrete mixture design by Ameron (Kapaa) that was used for improvements on Pier 39 (Phase 2) in Honolulu, Hawaii. This specific mix was chosen as a model because it was considered effective for protecting the reinforcing steel. Control mixtures using

Halawa aggregates were modeled after the Kapaa mixtures but adjustments were made for the difference in aggregate properties.

Control mixes were designed using both Kapaa and Halawa aggregates. Three different w/c (water-to-cement) ratios were tested for the control mixes. The w/c ratios tested were 0.35, 0.40, and 0.45. The paste content was also varied for the control mixtures.

For the Kapaa control mixtures, a paste content of 31.2% was tested because it was identical to the mixture used on Pier 39 (Phase 2). Also a slightly higher paste content of 32.5% was tested based on the design recommendations of the PCA (Portland Concrete Association). These will be referred to herein as “low” and “high” paste contents. The Halawa control mixtures had a low paste content of 28.3% and a high paste content of 29.7%.

There are six Kapaa control mixes denoted as C1 to C6, which tested the three w/c ratios, and two paste contents. A summary of the Kapaa control mixtures can be found in Table 3-2. The Halawa control mixes were denoted as HC1 to HC6 and also varied the w/c ratios and paste contents. A summary of the admixture dosages of the Halawa control mixes can be found in Table 3-3.

Table 3-2: Mixture Proportions for Kapaa Control Mixtures

Material or Property	C1	C2	C3	C4	C5	C6
w/c	0.35	0.40	0.45	0.35	0.40	0.45
Paste Volume (%)	31.2	31.2	31.2	32.5	32.5	32.5
Design Slump (in) (mm)	4 (100)	4 (100)	4 (100)	4 (100)	4 (100)	4 (100)
Coarse Aggregate (lb/yd <sup>3</sup> ) (kg/m <sup>3</sup> )	1,576 (935)	1,576 (935)	1,576 (935)	1,576 (935)	1,576 (935)	1,576 (935)
Maui Dune Sand (lb/yd <sup>3</sup> ) (kg/m <sup>3</sup> )	431.0 (255.7)	431.0 (255.7)	431.0 (255.7)	411.5 (244.1)	411.5 (244.1)	411.5 (244.1)
Kapaa Basalt Sand (lb/yd <sup>3</sup> ) (kg/m <sup>3</sup> )	825.6 (489.8)	825.6 (489.8)	825.6 (489.8)	788.2 (467.6)	788.2 (467.6)	788.2 (467.6)
Cement (lb/yd <sup>3</sup> ) (kg/m <sup>3</sup> )	786.1 (466.4)	733.2 (435.0)	683.7 (405.6)	819.6 (486.3)	762.5 (452.4)	712.8 (422.9)
Water (lb/yd <sup>3</sup> ) (kg/m <sup>3</sup> )	275.1 (163.2)	292.1 (173.3)	307.7 (182.6)	286.9 (170.2)	305.0 (181.0)	320.8 (190.3)
Daratard (oz./sk) (ml/sk)	3 (88.7)	3 (88.7)	3 (88.7)	3 (88.7)	3 (88.7)	3 (88.7)
Darex (oz./sk) (ml/sk)	2 (59.1)	2 (59.1)	2 (59.1)	2 (59.1)	2 (59.1)	2 (59.1)
Design Air Content (%)	4	4	4	4	4	4

Table 3-3: Mixture Proportions for Halawa Control Mixtures

Material or Property	HC1	HC2	HC3	HC4	HC5	HC6
w/c	0.35	0.40	0.45	0.35	0.40	0.45
Paste Volume (%)	28.3	28.3	28.3	29.7	29.7	29.7
Design Slump (in) (mm)	4 (100)	4 (100)	4 (100)	4 (100)	4 (100)	4 (100)
Coarse Aggregate (lb/yd <sup>3</sup> ) (kg/m <sup>3</sup> )	1,642 (974.1)	1,642 (974.1)	1,642 (974.1)	1,642 (974.1)	1,642 (974.1)	1,642 (974.1)
Maui Dune Sand (lb/yd <sup>3</sup> ) (kg/m <sup>3</sup> )	572.7 (339.8)	572.7 (339.8)	572.7 (339.8)	547.0 (324.5)	547.0 (324.5)	547.0 (324.5)
Halawa Basalt Sand (lb/yd <sup>3</sup> ) (kg/m <sup>3</sup> )	759.2 (450.4)	759.2 (450.4)	759.2 (450.4)	725.2 (430.2)	725.2 (430.2)	725.2 (430.2)
Cement (lb/yd <sup>3</sup> ) (kg/m <sup>3</sup> )	786.1 (466.4)	733.2 (435.0)	683.7 (405.6)	819.6 (486.3)	762.5 (452.4)	712.8 (422.9)
Water (lb/yd <sup>3</sup> ) (kg/m <sup>3</sup> )	275.1 (163.2)	292.1 (173.3)	307.7 (182.6)	286.9 (170.2)	305.0 (181.0)	320.8 (190.3)
Daratard (oz./sk) (ml/sk)	3 (88.7)	3 (88.7)	3 (88.7)	3 (88.7)	3 (88.7)	3 (88.7)
Darex (oz./sk) (ml/sk)	2 (59.1)	2 (59.1)	2 (59.1)	2 (59.1)	2 (59.1)	2 (59.1)
Design Air Content (%)	4	4	4	4	4	4

### 3.3.2 DCI Mixtures

Kapaa DCI mixtures were based on control mixtures C2 and C4, but replacing water in increments of 2, 4, and 6 gallons with DCI admixture for 1 yd<sup>3</sup> of concrete. Water-to-cement ratios of 0.35 and 0.40 were tested. Six DCI mixtures using Kapaa aggregates were denoted as D1 to D6. Mixtures D1, D2, and D3 are based on the Kapaa control mixture C4 while mixtures D4, D5, and D6 are based on the Kapaa control mixture C2. The mixture proportions for the DCI mixtures are shown in Table 3-4. No mixtures were designed using DCI with aggregate from Halawa.

### 3.3.3 CNI Mixtures

DCI and Rheocrete CNI are similar calcium nitrite-based corrosion inhibiting admixtures both containing 30% calcium nitrite. Due to their similarity, the Rheocrete CNI mixtures were designed by simply replacing DCI with Rheocrete CNI. The Rheocrete CNI mixtures using Kapaa aggregate were denoted as CNI1 to CNI6 and their mixture proportions are shown in Table 3-4.

Table 3-4: Mixture Proportions for Kapaa DCI and CNI Mixtures

Material or Property	D1 CNI1	D2 CNI2	D3 CNI3	D4 CNI4	D5 CNI5	D6 CNI6
w/c	0.35	0.35	0.35	0.40	0.40	0.40
Paste Volume (%)	32.5	32.5	32.5	31.2	31.2	31.2
Design Slump (in) (mm)	4 (100)	4 (100)	4 (100)	4 (100)	4 (100)	4 (100)
Coarse Aggregate (lb/yd <sup>3</sup> ) (kg/m <sup>3</sup> )	1,576 (935)	1,576 (935)	1,576 (935)	1,576 (935)	1,576 (935)	1,576 (935)
Maui Dune Sand (lb/yd <sup>3</sup> ) (kg/m <sup>3</sup> )	411.5 (244.1)	411.5 (244.1)	411.5 (244.1)	431.4 (256.0)	431.4 (256.0)	431.4 (256.0)
Kapaa Basalt Sand (lb/yd <sup>3</sup> ) (kg/m <sup>3</sup> )	788.2 (467.6)	788.2 (467.6)	788.2 (467.6)	825.6 (489.8)	825.6 (489.8)	825.6 (489.8)
Cement (lb/yd <sup>3</sup> ) (kg/m <sup>3</sup> )	819.6 (486.3)	819.6 (486.3)	819.6 (486.3)	733.2 (435.0)	733.2 (435.0)	733.2 (435.0)
Water (lb/yd <sup>3</sup> ) (kg/m <sup>3</sup> )	270.2 (160.3)	253.5 (150.4)	236.8 (140.5)	275.4 (163.4)	258.7 (153.5)	242.0 (143.6)
Liquid DCI / CNI (gal/yd <sup>3</sup> ) (l/m <sup>3</sup> )	2 (9.9)	4 (19.8)	6 (29.7)	2 (9.9)	4 (19.8)	6 (29.7)
Daratard (oz./sk) (ml/sk)	3 (88.7)	3 (88.7)	3 (88.7)	3 (88.7)	3 (88.7)	3 (88.7)
Darex (oz./sk) (ml/sk)	2 (59.1)	2 (59.1)	2 (59.1)	2 (59.1)	2 (59.1)	2 (59.1)
Design Air Content (%)	4	4	4	4	4	4

Six CNI mixtures using Halawa aggregates were also designed similarly and are denoted as HCNI1 to HCNI6. Mixtures HCNI1 to HCNI3 are based on Halawa control

mixture HC4 while mixtures HCNI4 to HCNI6 are based on control mixture HC2. The mixture proportions for these mixtures can be found in Table 3-5.

Table 3-5: Mixture Proportions for Halawa CNI Mixtures

Material or Property	HCNI1	HCNI2	HCNI3	HCNI4	HCNI5	HCNI6
w/c	0.35	0.35	0.35	0.40	0.40	0.40
Paste Volume (%)	28.3	28.3	28.3	29.7	29.7	29.7
Design Slump (in) (mm)	4 (100)	4 (100)	4 (100)	4 (100)	4 (100)	4 (100)
Coarse Aggregate (lb/yd <sup>3</sup> ) (kg/m <sup>3</sup> )	1,642 (974.1)	1,642 (974.1)	1,642 (974.1)	1,642 (974.1)	1,642 (974.1)	1,642 (974.1)
Maui Dune Sand (lb/yd <sup>3</sup> ) (kg/m <sup>3</sup> )	572.7 (339.8)	572.7 (339.8)	572.7 (339.8)	547.0 (324.5)	547.0 (324.5)	547.0 (324.5)
Kapaa Basalt Sand (lb/yd <sup>3</sup> ) (kg/m <sup>3</sup> )	759.2 (450.4)	759.2 (450.4)	759.2 (450.4)	725.2 (430.2)	725.2 (430.2)	725.2 (430.2)
Cement (lb/yd <sup>3</sup> ) (kg/m <sup>3</sup> )	819.6 (486.3)	819.6 (486.3)	819.6 (486.3)	733.2 (435.0)	733.2 (435.0)	733.2 (435.0)
Water (lb/yd <sup>3</sup> ) (kg/m <sup>3</sup> )	270.2 (160.3)	253.5 (150.4)	236.8 (140.5)	275.4 (163.4)	258.7 (153.5)	242.0 (143.6)
Liquid DCI / CNI (gal/yd <sup>3</sup> ) (l/m <sup>3</sup> )	2 (9.9)	4 (19.80)	6 (29.70)	2 (9.90)	4 (19.80)	6 (29.70)
Daratard (oz./sk) (ml/sk)	3 (88.7)	3 (88.7)	3 (88.7)	3 (88.7)	3 (88.7)	3 (88.7)
Darex (oz./sk) (ml/sk)	2 (59.1)	2 (59.1)	2 (59.1)	2 (59.1)	2 (59.1)	2 (59.1)
Design Air Content (%)	4	4	4	4	4	4

### 3.3.4 Rheocrete Mixtures

Rheocrete mixtures were designed by adding 1 gal/ yd<sup>3</sup> of Rheocrete 222+ to each of the control mixtures. The Rheocrete mixtures using Kapaa aggregates were designed from the Kapaa control mixtures and are denoted as RHE1 to RHE6. Mixture proportions for these mixes can be found in Table 3-6.

Table 3-6: Mixture Proportions for Kapaa Rheocrete Mixtures

Material or Property	RHE1	RHE2	RHE3	RHE4	RHE5	RHE6
w/c	0.35	0.40	0.45	0.35	0.40	0.45
Paste Volume (%)	31.2	31.2	31.2	32.5	32.5	32.5
Design Slump (in) (mm)	4 (100)	4 (100)	4 (100)	4 (100)	4 (100)	4 (100)
Coarse Aggregate (lb/yd <sup>3</sup> ) (kg/m <sup>3</sup> )	1,576 (935)	1,576 (935)	1,576 (935)	1,576 (935)	1,576 (935)	1,576 (935)
Maui Dune Sand (lb/yd <sup>3</sup> ) (kg/m <sup>3</sup> )	431.0 (255.7)	431.0 (255.7)	431.0 (255.7)	411.5 (244.1)	411.5 (244.1)	411.5 (244.1)
Kapaa Basalt Sand (lb/yd <sup>3</sup> ) (kg/m <sup>3</sup> )	825.6 (489.8)	825.6 (489.8)	825.6 (489.8)	788.2 (467.6)	788.2 (467.6)	788.2 (467.6)
Cement (lb/yd <sup>3</sup> ) (kg/m <sup>3</sup> )	786.1 (466.4)	733.2 (435.0)	683.7 (405.6)	819.6 (486.3)	762.5 (452.4)	712.8 (422.9)
Water (lb/yd <sup>3</sup> ) (kg/m <sup>3</sup> )	275.1 (163.2)	292.1 (173.3)	307.7 (182.6)	286.9 (170.2)	305.0 (181.0)	320.8 (190.3)
Rheocrete 222+ (gal/yd <sup>3</sup> ) (l/m <sup>3</sup> )	1 (4.95)	1 (4.95)	1 (4.95)	1 (4.95)	1 (4.95)	1 (4.95)
Daratard (oz./sk) (ml/sk)	3 (88.7)	3 (88.7)	3 (88.7)	3 (88.7)	3 (88.7)	3 (88.7)
Darex (oz./sk) (ml/sk)	2 (59.1)	2 (59.1)	2 (59.1)	2 (59.1)	2 (59.1)	2 (59.1)
Design Air Content (%)	4	4	4	4	4	4

Six Rheocrete mixtures using Halawa aggregates were designed from the Halawa control mixtures and denoted as HRHE1 to HRHE6. Mixture proportions for the Halawa Rheocrete mixtures can be found in Table 3-7.

Table 3-7: Mixture Proportions for Halawa Rheocrete Mixtures

Material or Property	HRHE1	HRHE2	HRHE3	HRHE4	HRHE5	HRHE6
w/c	0.35	0.40	0.45	0.35	0.40	0.45
Paste Volume (%)	28.3	28.3	28.3	29.7	29.7	29.7
Design Slump (in) (mm)	4 (100)	4 (100)	4 (100)	4 (100)	4 (100)	4 (100)
Coarse Aggregate (lb/yd <sup>3</sup> ) (kg/m <sup>3</sup> )	1,642 (974.1)	1,642 (974.1)	1,642 (974.1)	1,642 (974.1)	1,642 (974.1)	1,642 (974.1)
Maui Dune Sand (lb/yd <sup>3</sup> ) (kg/m <sup>3</sup> )	572.7 (339.8)	572.7 (339.8)	572.7 (339.8)	547.0 (324.5)	547.0 (324.5)	547.0 (324.5)
Kapaa Basalt Sand (lb/yd <sup>3</sup> ) (kg/m <sup>3</sup> )	759.2 (450.4)	759.2 (450.4)	759.2 (450.4)	725.2 (430.2)	725.2 (430.2)	725.2 (430.2)
Cement (lb/yd <sup>3</sup> ) (kg/m <sup>3</sup> )	786.1 (466.4)	733.2 (435.0)	683.7 (405.6)	819.6 (486.3)	762.5 (452.4)	712.8 (422.9)
Water (lb/yd <sup>3</sup> ) (kg/m <sup>3</sup> )	275.1 (163.2)	292.1 (173.3)	307.7 (182.6)	286.9 (170.2)	305.0 (181.0)	320.8 (190.3)
Rheocrete 222+ (gal/yd <sup>3</sup> ) (l/m <sup>3</sup> )	1 (4.95)	1 (4.95)	1 (4.95)	1 (4.95)	1 (4.95)	1 (4.95)
Daratard (oz./sk) (ml/sk)	3 (88.7)	3 (88.7)	3 (88.7)	3 (88.7)	3 (88.7)	3 (88.7)
Darex (oz./sk) (ml/sk)	2 (59.1)	2 (59.1)	2 (59.1)	2 (59.1)	2 (59.1)	2 (59.1)
Design Air Content (%)	4	4	4	4	4	4

### 3.3.5 FerroGard Mixtures

FerroGard mixtures were designed by replacing 3 gallons of water per cubic yard (14.85 l/m<sup>3</sup>) of concrete with FerroGard 901 for each of the control mixtures. Six FerroGard mixtures for the Kapaa mixes were based on the Kapaa control mixtures and denoted as FER1 to FER6. The mixture proportions for these mixtures are shown in Table 3-8. No FerroGard mixtures were designed using Halawa aggregate.

Table 3-8: Mixture Proportions for Kapaa FerroGard Mixtures

Material or Property	FER1	FER2	FER3	FER4	FER5	FER6
w/c	0.35	0.40	0.45	0.35	0.40	0.45
Paste Volume (%)	31.2	31.2	31.2	32.5	32.5	32.5
Design Slump (in) (mm)	4 (100)	4 (100)	4 (100)	4 (100)	4 (100)	4 (100)
Coarse Aggregate (lb/yd <sup>3</sup> ) (kg/m <sup>3</sup> )	1,576 (935)	1,576 (935)	1,576 (935)	1,576 (935)	1,576 (935)	1,576 (935)
Maui Dune Sand (lb/yd <sup>3</sup> ) (kg/m <sup>3</sup> )	431.0 (255.7)	431.0 (255.7)	431.0 (255.7)	411.5 (244.1)	411.5 (244.1)	411.5 (244.1)
Kapaa Basalt Sand (lb/yd <sup>3</sup> ) (kg/m <sup>3</sup> )	825.6 (489.8)	825.6 (489.8)	825.6 (489.8)	788.2 (467.6)	788.2 (467.6)	788.2 (467.6)
Cement (lb/yd <sup>3</sup> ) (kg/m <sup>3</sup> )	786.1 (466.4)	733.2 (435.0)	683.7 (405.6)	819.6 (486.3)	762.5 (452.4)	712.8 (422.9)
Water (lb/yd <sup>3</sup> ) (kg/m <sup>3</sup> )	250.1 (148.4)	267.1 (158.5)	282.7 (167.7)	262.0 (155.4)	280.0 (166.1)	295.8 (175.5)
Ferrogard 901 (gal/yd <sup>3</sup> ) (l/m <sup>3</sup> )	3 (14.85)	3 (14.85)	3 (14.85)	3 (14.85)	3 (14.85)	3 (14.85)
Daratard (oz./sk) (ml/sk)	2 (59.1)	2 (59.1)	2 (59.1)	2 (59.1)	2 (59.1)	2 (59.1)
Darex (oz./sk) (ml/sk)	2 (59.1)	2 (59.1)	2 (59.1)	2 (59.1)	2 (59.1)	2 (59.1)
Design Air Content (%)	4	4	4	4	4	4

### 3.3.6 Xypex Mixtures

Xypex mixtures were designed by replacing 2% of the mass of cement in the control mixtures with Xypex Admix C-2000. Six Xypex mixtures using Kapaa aggregates were denoted as XYP1 to XYP6. The mixture proportions for Kapaa Xypex mixtures are shown in Table 3-9. No mixtures were designed using Xypex with aggregate from Halawa.

Table 3-9: Mixture Proportions for Kapaa Xypex Mixtures

Material or Property	XYP1	XYP2	XYP3	XYP4	XYP5	XYP6
w/(c+xyp)	0.35	0.40	0.45	0.35	0.40	0.45
Paste Volume (%)	31.2	31.2	31.2	32.5	32.5	32.5
Design Slump (in) (mm)	4 (100)	4 (100)	4 (100)	4 (100)	4 (100)	4 (100)
Coarse Aggregate (lb/yd <sup>3</sup> ) (kg/m <sup>3</sup> )	1,576 (935)	1,576 (935)	1,576 (935)	1,576 (935)	1,576 (935)	1,576 (935)
Maui Dune Sand (lb/yd <sup>3</sup> ) (kg/m <sup>3</sup> )	431.0 (255.7)	431.0 (255.7)	431.0 (255.7)	411.5 (244.1)	411.5 (244.1)	411.5 (244.1)
Kapaa Basalt Sand (lb/yd <sup>3</sup> ) (kg/m <sup>3</sup> )	825.6 (489.8)	825.6 (489.8)	825.6 (489.8)	788.2 (467.6)	788.2 (467.6)	788.2 (467.6)
Cement (lb/yd <sup>3</sup> ) (kg/m <sup>3</sup> )	770.4 (457.1)	718.5 (426.3)	670.0 (397.5)	803.2 (476.5)	747.3 (443.3)	698.6 (414.4)
Water (lb/yd <sup>3</sup> ) (kg/m <sup>3</sup> )	275.1 (163.2)	292.1 (173.3)	307.7 (182.5)	286.9 (170.2)	305.0 (180.9)	320.8 (190.3)
Xypex (lb/yd <sup>3</sup> ) (kg/m <sup>3</sup> )	15.72 (9.33)	14.70 (8.72)	13.70 (8.13)	16.40 (9.73)	15.80 (9.37)	14.30 (8.48)
Darex (oz./sk) (ml/sk)	2 (59.1)	2 (59.1)	2 (59.1)	2 (59.1)	2 (59.1)	2 (59.1)
Design Air Content (%)	4	4	4	4	4	4

### 3.3.7 Latex Mixtures

Latex-modified mixtures were designed by adding latex amounts of 2.5, 5, and 7.5% of the mass of cement to the control mixtures. Six latex-modified mixtures using Kapaa aggregates were denoted as L1 to L6. Mixtures L1, L2, and L3 were based on Kapaa control C1. Mixtures L4, L5, and L6 were based on Kapaa control C2. The mixture proportions for the Kapaa latex-modified mixtures can be shown in Table 3-10. No latex-modified mixtures were designed using aggregate from Halawa.

Table 3-10: Mixture Proportions for Kapaa Latex Mixtures

Material or Property	L1	L2	L3	L4	L5	L6
w/c	0.35	0.35	0.35	0.40	0.40	0.40
Paste Volume (%)	31.2	31.2	31.2	31.2	31.2	31.2
Design Slump (in) (mm)	4 (100)	4 (100)	4 (100)	4 (100)	4 (100)	4 (100)
Coarse Aggregate (lb/yd <sup>3</sup> ) (kg/m <sup>3</sup> )	1,576 (935)	1,576 (935)	1,576 (935)	1,576 (935)	1,576 (935)	1,576 (935)
Maui Dune Sand (lb/yd <sup>3</sup> ) (kg/m <sup>3</sup> )	414.2 (245.7)	397.3 (235.7)	380.5 (225.7)	412.2 (244.5)	399.5 (237.0)	383.8 (227.7)
Kapaa Basalt Sand (lb/yd <sup>3</sup> ) (kg/m <sup>3</sup> )	793.4 (470.7)	761.1 (451.5)	728.9 (432.4)	795.3 (471.8)	765.2 (454.0)	735.1 (436.1)
Cement (lb/yd <sup>3</sup> ) (kg/m <sup>3</sup> )	786.1 (466.4)	786.1 (466.4)	786.1 (466.4)	733.2 (435.0)	733.2 (435.0)	733.2 (435.0)
Water (lb/yd <sup>3</sup> ) (kg/m <sup>3</sup> )	216.2 (128.3)	157.2 (93.3)	98.3 (58.3)	237.1 (140.7)	182.1 (108.0)	127.1 (75.4)
Latex liquid (lb/yd <sup>3</sup> ) (kg/m <sup>3</sup> )	78.6 (46.6)	157.2 (93.3)	235.8 (140)	73.3 (43.5)	146.6 (87.0)	220.0 (130.5)
Design Air Content (%)	4	4	4	4	4	4

### 3.3.8 Silica Fume Mixtures

The silica fume mixtures were designed based on the concrete mixtures used in the Ford Island Bridge Project and according to PCA and used Force 10,000D silica fume. The Ford Island Bride mixture was similar to the Pier 39 improvements in that it was designed to be effective in protecting the reinforcing steel from corrosion.

Eleven silica fume mixtures using Kapaa aggregates were designed and denoted as SF1 to SF11. Ten of these mixtures contain silica fume, while SF1 is a control mixture for both silica fume and fly ash mixtures. Water cement ratios of 0.36 and 0.45 were tested. Mixtures SF1 thru SF6 were designed by modifying the Ford Island Bridge mixture. Mixtures SF7 thru SF11 were based on mixture design recommendations according to PCA.

Mixture SF1 was designed as a control mixture containing 0% silica fume since no control mixture using Kapaa aggregates had a water-to-cement ratio of 0.36. Mixes SF2 thru SF4 include silica fume contents of 5, 10 and 15% respectively, by replacing the equivalent weight of cement with silica fume, however allowing the paste content to vary. Mixtures SF5 and SF6 keep the paste contents constant with SF2, but use silica fume contents of 10% and 15% respectively. The intent of these three mixtures was to keep the paste content constant as the silica fume content varied.

Mixtures SF7 thru SF11 follow design recommendations according to PCA and have a w/c ratio of 0.45. Mixtures SF7 thru SF9 include silica fume contents of 5, 10 and 15% respectively, by replacing an equivalent weight of cement with silica fume, but allowing the paste content to vary. Mixtures SF10 and SF11 keep the paste contents constant with SF7 while varying the silica fume contents. The mixture proportions for all of the silica fume mixtures using Kapaa aggregate are presented in Table 3-11.

Two different types of silica fume, Force 10,000D and Rheomac SF100, were tested using Halawa aggregates. The Force 10,000D is the same silica fume used in the Kapaa silica fume mixtures and allows this study to compare the aggregate properties of both Kapaa and Halawa while keeping the specific type of silica fume constant. The Rheomac SF100 silica fume was tested only with the Halawa aggregates because this is the silica fume used in concrete mixtures designed at the Halawa batch plant. Using the Rheomac SF100, allows this study to compare the properties of typical silica fume mixtures from the Kapaa and Halawa plants.

A total of six mixtures were created using Force 10,000D and Halawa aggregate. They are denoted as HSF1 to HSF4, and HSF7 and HSF8. The numbering system is not

ordered sequentially because the corresponding mixture numbers in both the Kapaa and Halawa silica fume mixtures refers to the same mix design. For example, HSF1 is a control mixture with a w/c ratio of 0.36 and is modeled the same as SF1 except it uses the Halawa aggregates. HSF2 to HSF4 include silica fume contents of 5, 10 and 15% respectively, by replacing the equivalent weight of cement in HSF1 with silica fume and allowing the paste content to vary. This is the same design procedure as SF2 thru SF4 of the Kapaa aggregate mixtures. HSF7 and HSF8 include silica fume contents of 5% and 10% respectively by replacing the equivalent weight of cement with silica fume. However, these mixtures have a w/c ratio of 0.45, and follow design procedures detailed by the PCA. It should be noted that a mixture with w/c ratio of 0.45 and silica fume content of 15% was not prepared for this experiment. The mixture proportions for all of the silica fume mixtures using Force 10,000D silica fume and Halawa aggregate are presented in Table 3-12.

Six silica fume mixtures using Rheomac SF100 silica fume and Halawa aggregates were also prepared and denoted as HSF-R2 to HSF-R4, and HSF-R7 to HSF-R9. Mixtures HSF-R2 to HSF-R4 use HSF1 as a control mixture (0% silica fume, w/c ratio = 0.36) and replace equivalent weights of cement with Rheomac SF100 silica fume in increments of 5, 10, and 15% respectively. Mixtures HSF-R7 to HSF-R9 similarly replace equivalent weights of cement with silica fume. However, these mixtures follow the design procedures of the PCA and have a w/c ratio of 0.45. The mixture proportions for all of the silica fume mixtures using Rheomac SF100 silica fume and Halawa aggregate are presented in Table 3-13.

Table 3-11: Mixture Proportions for Kapaa Force 10,000D Silica Fume Mixtures

Material or Property	SF1	SF2	SF3	SF4	SF5	SF6	SF7	SF8	SF9	SF10	SF11
w/(c+sf)	0.36	0.36	0.36	0.36	0.36	0.36	0.45	0.45	0.45	0.45	0.45
Paste Volume (%)	32.6	32.9	33.3	33.6	32.9	32.9	34.7	35.0	35.3	34.7	34.7
Design Slump (in) (mm)	8-10 (200-250)										
Coarse Aggregate (lb/yd <sup>3</sup> ) (kg/m <sup>3</sup> )	1,668 (989)										
Maui Dune Sand (lb/yd <sup>3</sup> ) (kg/m <sup>3</sup> )	537.6 (319.0)	531.3 (315.2)	525.4 (311.7)	519.2 (308.0)	531.3 (315.2)	531.3 (315.2)	497.9 (295.4)	492.2 (292.0)	486.5 (288.6)	497.9 (295.4)	497.9 (295.4)
Kapaa Basalt Sand (lb/yd <sup>3</sup> ) (kg/m <sup>3</sup> )	712.6 (422.8)	704.3 (417.9)	696.4 (413.2)	688.2 (408.3)	704.3 (417.9)	704.3 (417.9)	660.1 (391.6)	652.5 (387.1)	644.8 (382.6)	660.1 (391.6)	660.1 (391.6)
Cement (lb/yd <sup>3</sup> ) (kg/m <sup>3</sup> )	811 (481.1)	771 (457.4)	729.9 (433.0)	689.35 (409.0)	722.62 (428.7)	675.77 (400.9)	717.8 (425.8)	680.0 (403.4)	642.2 (381.0)	674.0 (399.9)	631.1 (374.4)
Water (lb/yd <sup>3</sup> ) (kg/m <sup>3</sup> )	292 (173.2)	292 (173.2)	292 (173.2)	292 (173.2)	289.05 (171.5)	286.21 (169.8)	340.0 (201.7)	340.0 (201.7)	340.0 (201.7)	337.0 (200.0)	334.1 (198.2)
Silica Fume (lb/yd <sup>3</sup> ) (kg/m <sup>3</sup> )	0 (0)	40.00 (23.73)	81.10 (48.12)	121.65 (72.17)	80.29 (47.64)	119.25 (70.75)	37.78 (22.42)	75.56 (44.83)	113.33 (67.24)	74.89 (44.43)	111.36 (66.07)
Design Air Content (%)	1	1	1	1	1	1	1	1	1	1	1

Table 3-12: Mixture Proportions for Halawa Force 10,000D Silica Fume Mixtures

Material or Property	HSF1	HSF2	HSF3	HSF4	HSF7	HSF8
w/(c+sf)	0.36	0.36	0.36	0.36	0.45	0.45
Paste Volume (%)	29.7	30.1	30.4	30.8	32.6	32.9
Design Slump (in) (mm)	8-10 (200-250)	8-10 (200-250)	8-10 (200-250)	8-10 (200-250)	8-10 (200-250)	8-10 (200-250)
Coarse Aggregate (lb/yd <sup>3</sup> ) (kg/m <sup>3</sup> )	1,737 (1,031)	1,737 (1,031)	1,737 (1,031)	1,737 (1,031)	1,737 (1,031)	1,737 (1,031)
Maui Dune Sand (lb/yd <sup>3</sup> ) (kg/m <sup>3</sup> )	562.4 (333.7)	556.0 (329.9)	549.5 (326.0)	543.1 (322.2)	521.1 (309.2)	515.1 (305.6)
Kapaa Basalt Sand (lb/yd <sup>3</sup> ) (kg/m <sup>3</sup> )	745.5 (442.3)	737.1 (437.3)	728.4 (432.1)	719.9 (427.1)	690.8 (409.8)	682.8 (405.1)
Cement (lb/yd <sup>3</sup> ) (kg/m <sup>3</sup> )	811.0 (481.1)	771.0 (457.4)	729.9 (433.0)	689.4 (409.0)	717.8 (425.8)	680.0 (403.4)
Water (lb/yd <sup>3</sup> ) (kg/m <sup>3</sup> )	292 (173.2)	292 (173.2)	292 (173.2)	292 (173.2)	340.0 (201.7)	340.0 (201.7)
Silica Fume (lb/yd <sup>3</sup> ) (kg/m <sup>3</sup> )	0 (0)	40.00 (23.73)	81.10 (48.11)	121.65 (72.17)	37.78 (22.41)	75.56 (44.83)
Daratard (oz./sk) (ml/sk)	0 0.0	0 0.0	0 0.0	0 0.0	0 0.0	0 0.0
Darex (oz./sk) (ml/sk)	0 0.0	0 0.0	0 0.0	0 0.0	0 0.0	0 0.0
Design Air Content (%)	1	1	1	1	1	1

Table 3-13: Mixture Proportions for Halawa Rheomac SF100 Silica Fume Mixtures

Material or Property	HSF-R2	HSF-R3	HSF-R4	HSF-R7	HSF-R8	HSF-R9
w/(c+sf)	0.36	0.36	0.36	0.45	0.45	0.45
Paste Volume (%)	30.1	30.4	30.8	31.9	32.2	32.6
Design Slump (in) (mm)	8-10 (200-250)	8-10 (200-250)	8-10 (200-250)	8-10 (200-250)	8-10 (200-250)	8-10 (200-250)
Coarse Aggregate (lb/yd <sup>3</sup> ) (kg/m <sup>3</sup> )	1,737 (1,031)	1,737 (1,031)	1,737 (1,031)	1,737 (1,031)	1,737 (1,031)	1,737 (1,031)
Maui Dune Sand (lb/yd <sup>3</sup> ) (kg/m <sup>3</sup> )	556.0 (329.9)	549.5 (326.0)	543.1 (322.2)	521.1 (309.2)	515.1 (305.6)	509.1 (302.0)
Kapaa Basalt Sand (lb/yd <sup>3</sup> ) (kg/m <sup>3</sup> )	737.1 (437.3)	728.4 (432.1)	719.9 (427.1)	690.8 (409.8)	682.8 (405.1)	674.8 (400.3)
Cement (lb/yd <sup>3</sup> ) (kg/m <sup>3</sup> )	771.0 (457.4)	729.9 (433.0)	689.4 (409.0)	717.8 (425.8)	680.0 (403.4)	642.2 (381.0)
Water (lb/yd <sup>3</sup> ) (kg/m <sup>3</sup> )	292.0 (173.2)	292.0 (173.2)	292.0 (173.2)	340.0 (201.7)	340.0 (201.7)	340.0 (201.7)
Silica Fume (Rheo) (lb/yd <sup>3</sup> ) (kg/m <sup>3</sup> )	40.00 (23.73)	81.10 (48.11)	121.65 (72.17)	37.78 (22.41)	75.56 (44.83)	113.33 (67.24)
Daratard (oz./sk) (ml/sk)	0 0.0	0 0.0	0 0.0	0 0.0	0 0.0	0 0.0
Darex (oz./sk) (ml/sk)	0 0.0	0 0.0	0 0.0	0 0.0	0 0.0	0 0.0
Design Air Content (%)	1	1	1	1	1	1

### 3.3.9 Fly Ash Mixtures

Fly ash was used in ten Kapaa mixtures denoted as FA2 to FA11. The numbering system follows the same logic as the silica fume mixtures SF2 to SF11. The Kapaa fly ash mixtures follow the same design procedures as their numbered silica fume counterparts. Again SF1 is used as a control mixture because it does not contain fly ash or silica fume. The mixture proportions for all of the fly ash mixtures using Kapaa aggregate are presented in Table 3-14.

Six fly ash mixtures using Halawa aggregates were denoted as HFA2 to HFA4 and HFA7 to HFA9. The numbering system and design procedures follow the same logic as the Kapaa fly ash counterparts, mixtures FA2 to FA4, and FA7 to FA9. Mixture HSF1 is used as a control mixture because it uses Halawa aggregates, but does not contain fly ash or silica fume. The mixture proportions for all of the fly ash mixtures using Halawa aggregate are presented in Table 3-15.

Table 3-14: Mixture Proportions for Kapaa Fly Ash Mixtures

Material or Property	FA2	FA3	FA4	FA5	FA6	FA7	FA8	FA9	FA10	FA11
w/(c+fa)	0.36	0.36	0.36	0.36	0.36	0.45	0.45	0.45	0.45	0.45
Paste Volume (%)	32.8	33.0	33.2	32.8	32.8	34.6	34.8	35.0	34.6	34.6
Design Slump (in) (mm)	8-10 (200-250)									
Coarse Aggregate (lb/yd <sup>3</sup> ) (kg/m <sup>3</sup> )	1668 (989)									
Maui Dune Sand (lb/yd <sup>3</sup> ) (kg/m <sup>3</sup> )	533.9 (316.8)	530.2 (314.6)	526.4 (312.3)	533.9 (316.8)	533.9 (316.8)	500.4 (296.9)	496.9 (294.8)	493.5 (292.8)	500.4 (296.9)	500.4 (296.9)
Kapaa Basalt Sand (lb/yd <sup>3</sup> ) (kg/m <sup>3</sup> )	707.74 (419.9)	702.8 (416.9)	697.8 (414.0)	707.7 (419.9)	707.7 (419.9)	663.3 (393.5)	658.7 (390.8)	654.1 (388.1)	663.3 (393.5)	663.3 (393.5)
Cement (lb/yd <sup>3</sup> ) (kg/m <sup>3</sup> )	771.0 (457.4)	729.9 (433.0)	689.4 (409.0)	725.5 (430.4)	681.1 (404.1)	717.8 (425.8)	680.0 (403.4)	642.2 (381.0)	676.4 (401.3)	635.4 (377.0)
Water (lb/yd <sup>3</sup> ) (kg/m <sup>3</sup> )	292.0 (173.2)	292.0 (173.2)	292.0 (173.2)	290.2 (172.2)	288.5 (171.1)	340.0 (201.7)	340.0 (201.7)	340.0 (201.7)	338.2 (200.6)	336.4 (199.6)
Fly Ash (lb/yd <sup>3</sup> ) (kg/m <sup>3</sup> )	40.00 (23.73)	81.10 (48.12)	121.65 (72.17)	80.61 (47.82)	120.19 (71.31)	37.78 (22.42)	75.56 (44.83)	113.33 (67.24)	75.15 (44.59)	112.13 (66.53)
Design Air Content (%)	1	1	1	1	1	1	1	1	1	1

Table 3-15: Mixture Proportions for Halawa Fly Ash Mixtures

Material or Property	HSF1	HFA2	HFA3	HFA4	HFA7	HFA8	HFA9
w/(c+fa)	0.36	0.36	0.36	0.36	0.45	0.45	0.45
Paste Volume (%)	29.7	29.9	30.1	30.4	32.5	32.6	32.8
Design Slump (in) (mm)	8-10 (200-250)						
Coarse Aggregate (lb/yd <sup>3</sup> ) (kg/m <sup>3</sup> )	1737 (1,031)						
Maui Dune Sand (lb/yd <sup>3</sup> ) (kg/m <sup>3</sup> )	562.4 (333.7)	558.6 (331.4)	554.6 (329.0)	550.8 (326.8)	523.5 (310.6)	519.9 (308.4)	516.3 (306.3)
Kapaa Basalt Sand (lb/yd <sup>3</sup> ) (kg/m <sup>3</sup> )	745.5 (442.3)	740.4 (439.3)	735.2 (436.2)	730.1 (433.2)	693.3 (411.3)	689.1 (408.8)	684.3 (406.0)
Cement (lb/yd <sup>3</sup> ) (kg/m <sup>3</sup> )	811.0 (481.1)	771.0 (457.4)	729.9 (433.0)	689.4 (409.0)	717.8 (425.8)	680.0 (403.4)	642.2 (381.0)
Water (lb/yd <sup>3</sup> ) (kg/m <sup>3</sup> )	292.0 (173.2)	292.0 (173.2)	292.0 (173.2)	292.0 (173.2)	340.0 (201.7)	340.0 (201.7)	340.0 (201.7)
Fly Ash (lb/yd <sup>3</sup> ) (kg/m <sup>3</sup> )	0.0 (0)	40.0 (23.73)	81.1 (48.11)	121.7 (72.17)	37.8 (22.41)	75.6 (44.83)	113.3 (67.24)
Design Air Content (%)	1	1	1	1	1	1	1

### *3.3.10 Other Admixtures*

In addition to the corrosion inhibiting admixtures, mixtures also included other admixtures commonly used in practice. Daracem 19, Darex II AEA, and Daratard HC, all manufactured by W.R. Grace & Co., were added in various combinations to each of the mixtures to achieve the desired concrete properties.

Daracem 19 is a high range water reducer (HRWR) or superplasticizer that increases the workability of the concrete. As the water-cement ratio in a mixture decreases, so does the workability of the concrete. This admixture is useful in mixtures with low water-cement ratios because it increases the workability of the concrete without sacrificing concrete strength. The manufacturer specifies a dosage between 6 and 20 fl. oz. per 100 lbs (390 and 1300 mL per 100 kg) of cement. Daracem 19 was added to the concrete mixtures to achieve a preferred slump.

Darex II AEA is an air-entraining admixture which produces a stable air void system. This admixture is used to protect concrete from damage from freezing and thawing. The Darex dosage was 3 oz./sk (88.7 mL/sk), or 3 oz. per 94 lb sack of cement.

Daratard HC is a set-retarding admixture which, when added to fresh concrete, allows the set time to be delayed or controlled. This admixture allows additional time for the concrete to be placed and is useful when concrete needs to be tremied or pumped. The standard dosage for Daratard HC is 2 oz./sk (59.1 mL/sk), or 2 oz. per 94 lb sack of cement.

It should be noted that these three admixtures were not used for all of the mixes. Certain corrosion inhibiting admixtures could not be used in conjunction with these admixtures due to potential chemical reactions that could adversely affect the concrete

properties. These admixtures were also omitted to obtain the desired workability of the concrete.

### 3.4 Test Specimens

Test specimens were 4.5 inches in width, 6 inches in height and 11 inches in length (114 by 152 by 279 mm). Each specimen contained four No. 4 reinforcing steel bars instead of three according to ASTM G 109. A second No.4 reinforcing bar was added at the top of the test specimen because certain linear polarization resistance measurements require the second top bar to serve as a counterelectrode. The Gecor6 testing instrument used in this study however, did not require the additional reinforcing bar. The cross section and geometry of a typical test specimen is shown in Figure 3-1. All other corrosion testing procedures followed ASTM G 109.

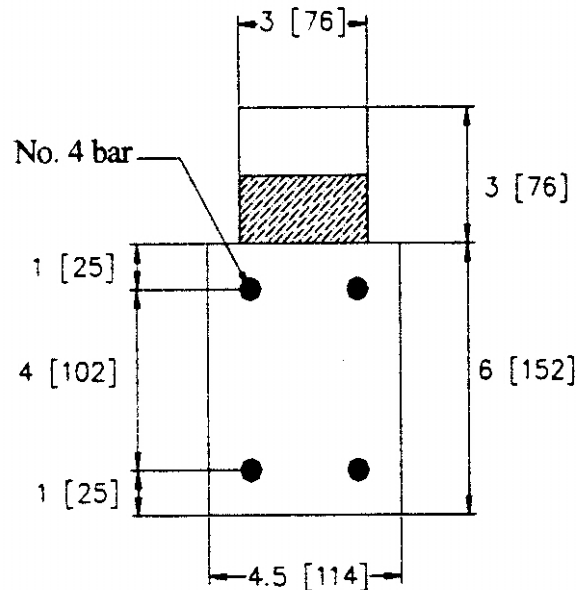


Figure 3-1: Geometry of a Typical Test Specimen

A total of twelve test specimens were produced for each of the Kapaa mixtures C1 to C6, DCI1 to DCI 6, FER1 to FER6, RHE1 to RHE6, SF1 to SF7 and L1 to L6. For all

the other mixes a total of four specimens were produced. The total number of specimens was reduced for later mixtures due to the limited space in the basement of the structures lab in Holmes Hall where the specimens were stored during the ponding cycle tests. Figure 3-2 shows the test specimens during testing in the Holmes Hall basement. The additional specimens produced for Kapaa control, DCI, Rheocrete, FerroGard, silica fume, and latex-modified mixes were used to monitor the progression of chloride concentration, permeability, and pH during the early ponding cycles.

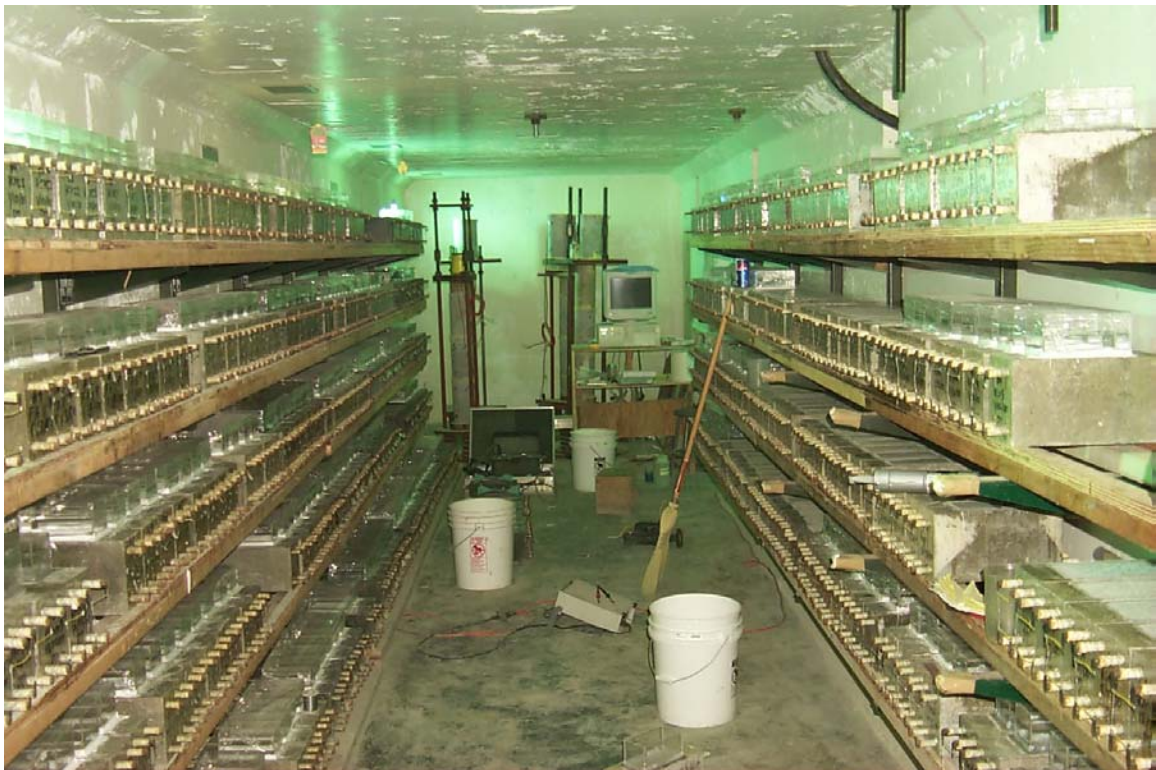


Figure 3-2: Laboratory Specimens in Holmes Hall Basement

In addition to the test specimens, three 6 by 12 inch (152 by 304 mm) cylindrical specimens were poured for each mixture to determine the compressive strength according to ASTM C 39. One of these cylinders was also used to measure the elastic modulus and Poisson's ratio according to ASTM C 469.

### *3.4.1 Mixing Preparation*

For each mixture, a butter batch, which was a smaller quantity of the main mix, was mixed before the main batch. The purpose of the butter batch was to coat the inside of the concrete mixer because some fine aggregates, paste, and water remain stuck to the inside of the mixer, thus distorting the mixture proportions. A butter batch is required in this study because of the relatively small amount of concrete mixed. The excess concrete stuck to the sides of a mixer is a substantial amount that can affect the concrete properties. In construction practices a butter batch is generally not required because the volume of concrete mixed in a concrete truck is large enough that the excess remaining on the sides of the mixer has little effect on the final product. The butter batch also provides an estimate of the amount of Daracem 19, or superplasticizer, which was required to reach the desired slump and workability in the main batch.

Coarse aggregate used in both the butter batch and main batch of each mixture was first weighed and then allowed to soak in water for 24 hours prior to mixing. This practice allowed the coarse aggregate to be fully saturated. The fine aggregates, crushed basalt sand and Maui dune sand, were placed in an oven at a temperature of 110°C for 48 hours before mixing. This practice produced fine aggregates with a moisture content of zero. These two procedures allowed an extremely precise measurement of aggregates and mixing water in each mix.

The steel reinforcing bars used in the test specimens were soaked in a 10% sulfuric acid solution for 10 minutes to remove any initial corrosion. The bars were then wire brushed to clean off any excess residue. A layer of electroplater's tape was placed on each bar covering three inches at both ends of each bar. The taped bars were carefully

placed into the specimen molds so that the tape provided protection for 1.5 inches (38 mm) from each end of the test specimen. The geometry of the taped reinforcing bars for a typical specimen is shown in Figure 3-3.

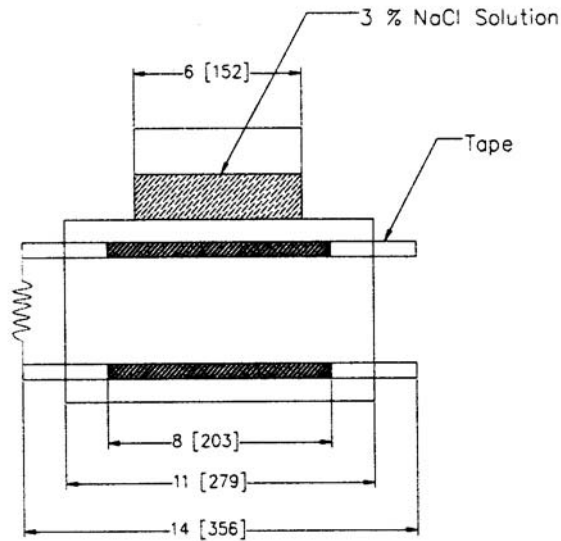


Figure 3-3: Typical Longitudinal Specimen Cross Section

#### 3.4.2 Mixing Process

Fine aggregates were removed from the oven and weighed in buckets for both the butter batch and main batch. A plastic sheet or cover was placed on the bucket to prevent any moisture absorption. The fine aggregates were then allowed to cool for three or four hours. Cement and pozzolans were also weighed out and covered in buckets.

Just prior to mixing, the soaking coarse aggregate was poured into a wire-mesh sieve to drain the excess water and then weighed. The water gained during the soaking process was deducted from the mixing water for each mixture. All mixing procedures were conducted according to ASTM C 192.

### *3.4.3 Casting and Curing Process*

Fresh concrete was placed in each test specimen in two layers. After each layer the concrete was consolidated using a vibrator. Care was taken to avoid over-consolidation in the test specimens. Fresh concrete was also placed in prepared cylinder molds in three equal layers. After each layer, the concrete was rodded 25 times using a 0.625 in. (16 mm) diameter steel rod.

The test specimens and cylinders were removed from the molds approximately 24 hours after casting. An additional layer of electroplater's tape was placed on the ends of each bar to provide additional protection from moisture during the curing process. The specimens were then placed in a curing tank to cure for 28 days. After the curing process, all specimens were removed from the curing tank and the cylinders were used to determine the compressive strength, elastic modulus and Poisson's ratio of the concrete, in accordance with ASTM C 31.

### *3.4.4 Testing Preparation*

After 28 days, the test specimens were removed from the curing process. The surfaces of the test specimens were then allowed to dry. Plastic dams 3 in. (76 mm) wide, 6 in. (150 mm) long, and 3 in. (76mm) tall were placed on the top of each specimen. The dams were secured to the concrete by applying silicone glue to the outside surfaces of the dams. All four of the vertical sides and the top surface area outside of the dams were sealed with epoxy. After the epoxy coating dried, the specimens were placed into the basement of the structures lab in Holmes Hall. This provided a laboratory environment with a relative constant temperature of 73°F (27.8°C) and humidity of 54%.

At one end of the test specimen the electroplater's tape was cut on all four of the reinforcing bars. The exposed reinforcing end was then cleaned to create an electrical connection. A 100-ohm resistor and two electrical wires were spot welded to the cleaned reinforcing at one end of the specimen as shown in .

A 0.106 gal (400 mL) volume of a 3% NaCl (Sodium Chloride) solution was poured into each plastic dam. To minimize evaporation a transparent plastic wrap was tightly secured around the tops of the plastic dams. This solution remained ponding in the dam for two weeks (14 days). After two weeks of the wet cycle, the transparent wrap and NaCl solution were removed. The specimens were then allowed to dry for two weeks (14 days). One complete cycle consisted of two weeks of the wet condition and two weeks of the drying condition, a total of 4 weeks (28 days). The cycle was repeated continuously to accelerate corrosion of the reinforcing steel.

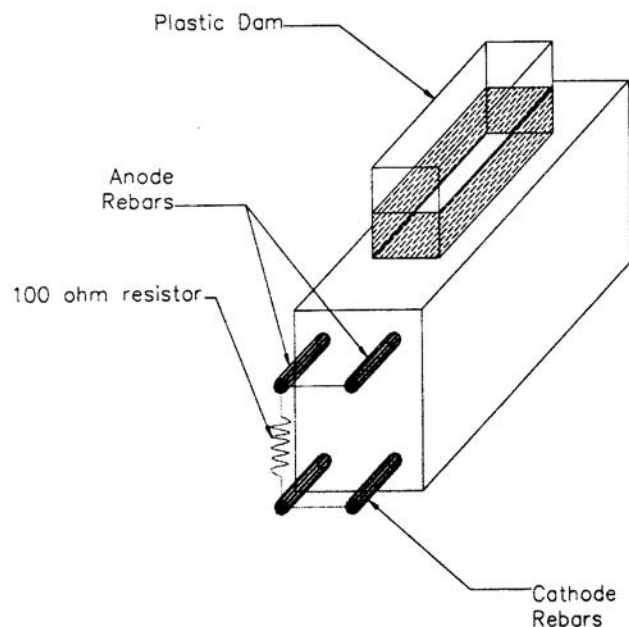


Figure 3-4: Typical Test Specimen Setup

### **3.5 Testing Period**

#### *3.5.1 Electrical Tests*

After each ponding or wet cycle, electrical tests measuring the corrosion potential of the top bars relative to a copper/copper sulfate electrode, the electrical resistance, and the corrosion rate were performed. The current measured between the top and bottom bars in each specimen was measured on the seventh day after draining or the middle of the dry period.

### **3.6 Testing Procedure for Physical and Mechanical Tests**

#### *3.6.1 Slump, Compressive Strength, Elastic Modulus, and Poisson Ratio Tests*

For each mixture an initial slump test, which was not recorded, was performed on the butter batch. Using this measurement, an accurate estimate of the amount of superplasticizer required in the main batch to obtain the desired workability could be made. When the desired workability appeared to be achieved by a visual inspection, a slump test was also performed on the main batch. This slump test was recorded and reported for each concrete mixture. Slump tests on the butter and main batches were performed in accordance with ASTM C 143. Compressive strength was measured according to ASTM C 39, and the modulus of elasticity and Poisson's ratio were measured according to the methods described in ASTM C 469.

#### *3.6.2 Air Permeability*

The air permeability of each test specimen was measured by drilling a 0.39 in. (10 mm) diameter hole on the top surface of each specimen to a depth of 1.58 in. (40 mm). All loose dust was blown out of the hole and a molded silicon plug was wedged into the

hole. A needle was then carefully inserted into the plug in the area between the bottom of the plug and the bottom of the hole. Air was pumped out through the needle, creating a vacuum in the small cavity below the plug. The time recorded for the pressure to drop from -7.98 psi to -7.25 psi (-55 kPa to -50 kPa) was measured. All air permeability measurements were performed using a Poroscope Plus (P-6050, James Instruments, Inc.). All test procedures followed the instrument's instruction manual.

### **3.7 Testing Procedure for Chemical Tests**

#### *3.7.1 Chloride Concentration*

The chloride concentration of each test specimen was measured at the depth of the reinforcing steel. Using a drill, a 0.75 in. (19mm) diameter hole was drilled in the center of the two top reinforcing bars. Dust samples were collected from a depth of 0.5 in. to 1.0 in. (13mm to 25mm), which is at the exact level of the reinforcing steel as shown in Figure 3-5. A 0.106 oz (3 gram) sample of dust was dissolved in 0.676 fl. oz. (20 mL) of extraction liquid provided by James Instruments, Inc. The dust sample was allowed to react with the chloride ions and the liquid acid for at least 15 minutes. Chloride concentration was then measured using the Chloride Test System (CL-200, James Instruments, Inc.). All test procedures followed the instrument's instruction manual.

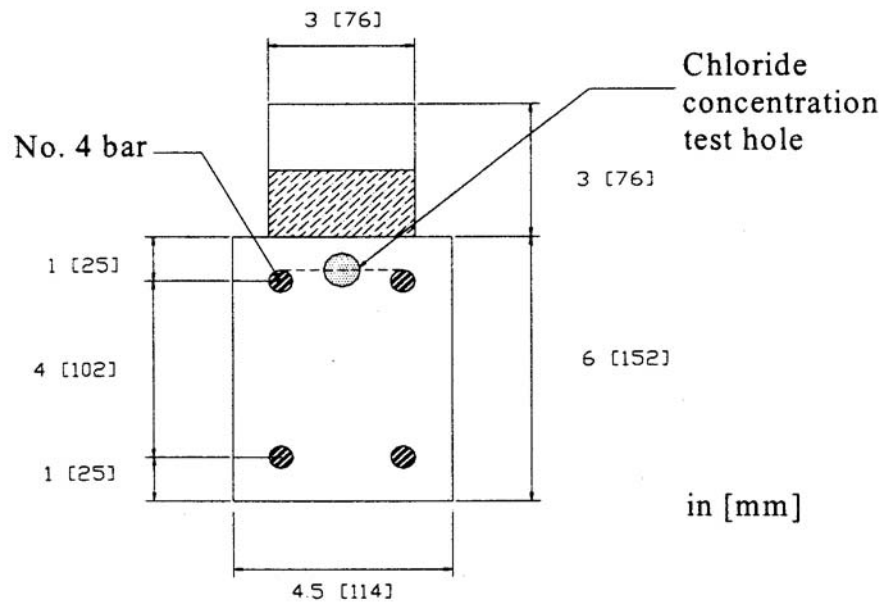


Figure 3-5: Location of Chloride Sample

### 3.7.2 pH

After chloride concentration and air permeability tests were performed, the top portion of the specimen was broken off at the top reinforcing bars. After removing the top reinforcing bars, a drill was used to collect dust samples of the concrete surrounding the reinforcing to be used in the pH measurement. Approximately 0.211 to 0.317 oz. (6 to 9 grams) of dust collected was mixed with 10 drops (10 grams) of distilled water. A pH probe was placed into the solution to measure the pH. All measurements were performed using a portable microprocessor pH meter (HI 8624, Hanna Instruments). All test procedures followed the instrument's instruction manual.

## **3.8 Testing Procedure for Electrical Tests**

### *3.8.1 Current Test*

Using a voltmeter the positive probe was attached to the top bars and the negative probe was attached to the bottom bars. The voltage difference between the top and bottom bars was measured. The voltage was then converted into the current using Ohm's Law taking into account the resistor connecting the top and bottom bars. The voltage measurement was recorded and then converted into the current because it provided a more accurate reading of the current.

### *3.8.2 Half-Cell Potential, Linear Polarization Resistance and Resistivity Measurements*

The half-cell potential, polarization resistance and resistivity measurements were measured using the Gecor6 Corrosion Rate Meter (James Instruments Inc.). The testing procedure was performed according to the instrument's manual.

## **3.9 Summary**

This chapter described all of the materials used in the concrete mixtures and their proportioned mix designs for this study. Also discussed were all procedures for preparing, pouring, and curing of the concrete specimens. Finally this chapter describes the testing procedures for all physical, mechanical, chemical and electrical tests.



## CHAPTER 4 RESULTS AND DISCUSSION OF MECHANICAL TESTS

### 4.1 Introduction

This chapter presents the results and discussion of the findings of the mechanical tests on the various concrete mixtures. The mechanical tests performed in this study measured the slump, compressive strength, elastic modulus, Poisson's ratio, air content and air permeability. Unfortunately test results for some of the Halawa mixtures are not available. Comparisons are presented here only when results are available for both Kapaa and Halawa mixtures.

### 4.2 Slump, Compressive Strength, Elastic Modulus and Poisson's Ratio

#### 4.2.1 Control Mixtures

The physical properties for the Kapaa control mixtures and are shown in Table 4-1 as presented in Pham and Newton (2001).

Table 4-1: Physical Properties of Kapaa Control Mixtures

Material or Property	C1	C2	C3	C4	C5	C6
w/c	0.35	0.40	0.45	0.35	0.40	0.45
Paste Volume (%)	31.2	31.2	31.2	32.5	32.5	32.5
Design Slump (in) (mm)	4 (100)	4 (100)	4 (100)	4 (100)	4 (100)	4 (100)
Actual Slump (in) (mm)	3.75 (94)	4.25 (106)	8.50 (213)	3.75 (94)	5.50 (138)	8.50 (213)
Compressive Strength (psi) (Mpa)	7620 (52.5)	7050 (48.6)	5780 (39.9)	8140 (56.1)	6530 (45.0)	6440 (44.4)
Elastic Modulus (psi) (Mpa)	3900 (26.9)	3200 (22.1)	3750 (25.9)	4100 (28.3)	3850 (26.5)	3750 (25.9)
Poisson's Ratio	-	0.17	-	-	0.17	0.22

The physical properties for the Halawa control mixtures and are shown in Table 4-2.

Table 4-2: Physical Properties of Halawa Control Mixtures

Material or Property	HC1	HC2	HC3	HC4	HC5	HC6
w/c	0.35	0.40	0.45	0.35	0.40	0.45
Paste Volume (%)	31.2	31.2	31.2	32.5	32.5	32.5
Design Slump (in) (mm)	4 (100)	4 (100)	4 (100)	4 (100)	4 (100)	4 (100)
Actual Slump (in) (mm)	3.75 (94)	3.00 (75)	6.00 (150)	5.50 (138)	5.00 (125)	6.50 (163)
Compressive Strength (psi) (Mpa)	7046 (48.6)	5270 (36.3)	4086 (28.2)	7249 (50.0)	5060 (34.9)	4327 (29.8)
Elastic Modulus (psi) (Mpa)	4107 (28.3)	3862 (26.6)	3135 (21.6)	4603 (31.7)	3070 (21.2)	3193 (22.0)
Poisson's Ratio	0.25	0.30	0.24	0.32	0.24	0.26

A comparison of the compressive strengths of the Kapaa and Halawa control mixtures is presented in Figure 4-1. For all control mixtures, concrete using Halawa aggregates had lower compressive strength than the same mixtures with Kapaa aggregates. The decrease in strength varied from 8% to 33% with the largest difference for mixtures with the highest water-to-cement ratio. The decrease in strength was similar for mixtures with low and high paste contents.

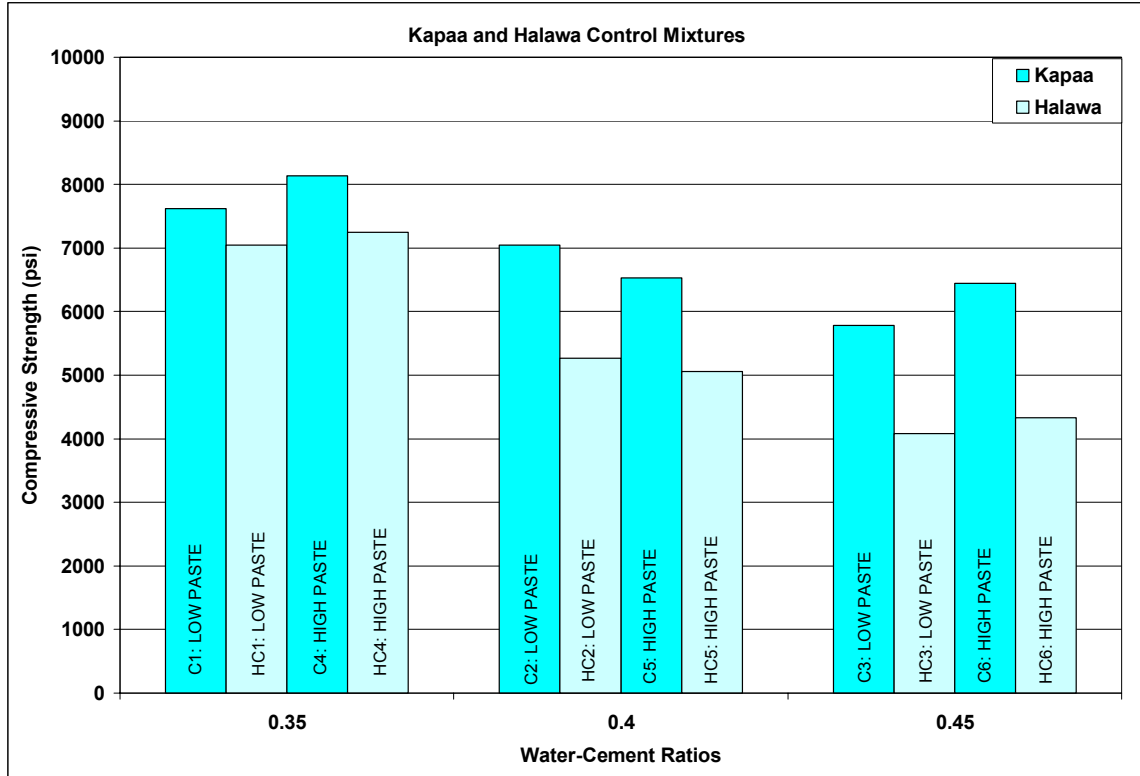


Figure 4-1: Average Compressive Strength of Kapaa and Halawa Control Mixtures

#### 4.2.2 Rheocrete Mixtures

The physical properties for Kapaa Rheocrete mixtures are shown in Table 4-3 as presented by Pham and Newton (2001).

Table 4-3: Physical Properties of Kapaa Rheocrete Mixtures

Material or Property	RHE1	RHE2	RHE3	RHE4	RHE5	RHE6
w/c	0.35	0.40	0.45	0.35	0.40	0.45
Paste Volume (%)	31.2	31.2	31.2	32.5	32.5	32.5
Design Slump (in) (mm)	4 (100)	4 (100)	4 (100)	4 (100)	4 (100)	4 (100)
Actual Slump (in) (mm)	4.25 (106)	5.25 (131)	9.50 (238)	5.50 (138)	8.50 (213)	10.00 (250)
Compressive Strength (psi) (Mpa)	8240 (56.8)	6530 (45.0)	5960 (41.1)	7270 (50.1)	6640 (45.8)	6460 (44.5)
Elastic Modulus (psi) (Mpa)	3650 (25.2)	3650 (25.2)	3650 (25.2)	4000 (27.6)	3500 (24.1)	3200 (22.1)
Poisson's Ratio	0.22	0.22	0.22	0.23	0.23	0.22
Design Air Content (%)	4.0	4.0	4.0	4.0	4.0	4.0
Air Content (%)	2.80	6.50	2.60	4.80	3.60	1.50

The physical properties for the Halawa Rheocrete mixtures are shown in Table

4-4.

Table 4-4: Physical Properties of Halawa Rheocrete Mixtures

Material or Property	HRHE1	HRHE2	HRHE3	HRHE4	HRHE5	HRHE6
w/c	0.35	0.40	0.45	0.35	0.40	0.45
Paste Volume (%)	31.2	31.2	31.2	32.5	32.5	32.5
Design Slump (in) (mm)	4 (100)	4 (100)	4 (100)	4 (100)	4 (100)	4 (100)
Actual Slump (in) (mm)	6.50 (163)	4.50 (113)	8.00 (200)	- (-)	6.50 (163)	- (-)
Compressive Strength (psi) (Mpa)	5910 (40.7)	5980 (41.2)	4527 (31.2)	7267 (50.1)	4772 (32.9)	4685 (32.3)
Elastic Modulus (psi) (Mpa)	3580 (24.7)	3591 (24.8)	4259 (29.4)	4517 (31.1)	3377 (23.3)	3286 (22.7)
Poisson's Ratio	0.19	0.19	0.24	0.26	0.22	0.21
Design Air Content (%)	4.0	4.0	4.0	4.0	4.0	4.0
Air Content (%)	3.00	4.25	3.50	-	5.90	-

A comparison of the compressive strengths of the Kapaa and Halawa Rheocrete mixtures is presented in Figure 4-2. As with the control mixtures the Halawa mixtures generally have lower compressive strength than the equivalent Kapaa mixtures.

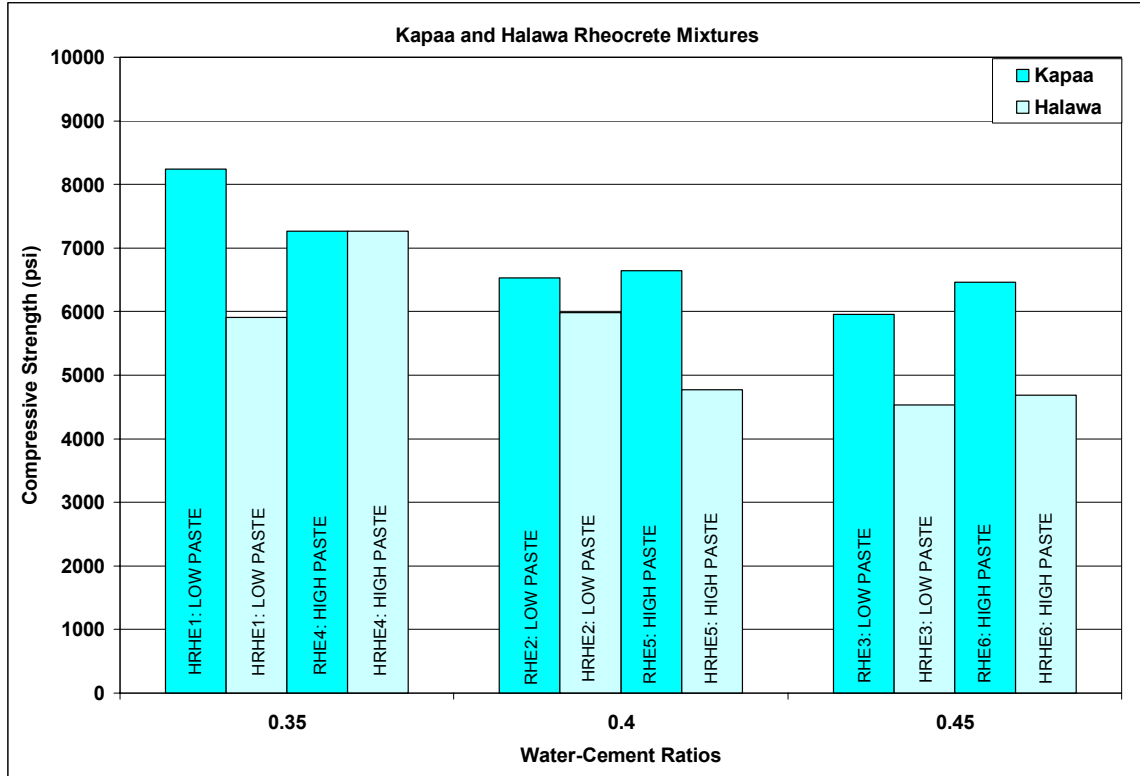


Figure 4-2: Average Compressive Strength of Kapaa and Halawa Rheocrete Mixtures

### 4.3 Air Permeability

The air permeability values obtained in this study were to be combined with the results presented in an earlier study (Pham 2001). However there was a significant difference between results from the earlier study and those collected in this study. It was believed that the previous study (Pham 2001) performed the air permeability tests soon after the test specimens were removed from the saltwater ponding cycles. The results obtained in this study are from test specimens that were allowed to dry. Depending on the test specimen, the time period from the last ponding cycle to air permeability testing ranged from a few months to over a year.

As discussed previously in Chapter 2, the moisture content of the concrete has a major effect on the permeability. Test specimens from the previous laboratory study

(Pham 2001) were probably close to fully saturated conditions causing the concrete to be almost impermeable to air. By allowing the specimens to remain outside of the laboratory environment for a significant amount of time after the ponding cycles, the concrete would have dried to near the surface moisture content. It should also be noted that the results presented in this study are consistent with the field tests presented in an earlier portion of this research study (Bola 2000) For these reasons, the results from this study were not combined with the previous results in the earlier laboratory study (Pham and Newtonson 2001).

In the previous laboratory study (Pham 2001) the water permeability of the concrete mixtures was measured in addition to the air permeability. However it was concluded that the water permeability test did not provide an accurate permeability measurement due to the large variations and standard deviations of the results on test specimens from the same concrete mixture. Therefore in this study no water permeability tests were performed.

#### *4.3.1 Control Mixtures*

Results of the air permeability tests for the control mixtures using Kapaa aggregates are presented in Table 4-5. All of the control mixes were rated as having a fair protective quality.

Table 4-5: Air Permeability Results for Kapaa Control Mixtures

Mix	Air Permeability (Figg Number)	Protective Quality
C1	182	Fair
C2	232	Fair
C3	213	Fair
C4	-	-
C5	134	Fair
C6	184	Fair
Avg	189	Fair

#### 4.3.2 Calcium Nitrate Mixtures

Results of the air permeability tests for the DCI mixtures using Kapaa aggregates are presented in Table 4-6.

Table 4-6: Air Permeability Results for Kapaa DCI Mixtures

Mix	Air Permeability (Figg Number)	Protective Quality
D1	190	Fair
D2	163	Fair
D3	90	Not Very Good
D4	124	Fair
D5	117	Fair
D6	340	Good
Avg	171	Fair

#### 4.3.3 FerroGard Mixtures

Results of the air permeability tests for the FerroGard mixtures using Kapaa aggregates are presented in Table 4-7.

Table 4-7: Air Permeability Results for Kapaa FerroGard Mixtures

Mix	Air Permeability (Figg Number)	Protective Quality
FER1	196	Fair
FER2	179	Fair
FER3	182	Fair
FER4	194	Fair
FER5	130	Fair
FER6	92	Not Very Good
Avg	162	Fair

#### 4.3.4 Rheocrete Mixtures

Results of the air permeability tests for the Rheocrete mixtures using Kapaa aggregates are presented in Table 4-8.

Table 4-8: Air Permeability Results for Kapaa Rheocrete Mixtures

Mix	Air Permeability (Figg Number)	Protective Quality
RHE1	301	Good
RHE2	155	Fair
RHE3	205	Fair
RHE4	185	Fair
RHE5	165	Fair
RHE6	182	Fair
Avg	199	Fair

#### 4.3.5 Latex Mixtures

Results of the air permeability tests for the latex mixtures using Kapaa aggregates are presented in Table 4-9.

Table 4-9: Air Permeability Results for Kapaa Latex Mixtures

Mix	Air Permeability (Figg Number)	Protective Quality
LA1	19	Poor
LA2	272	Fair
LA3	56	Not Very Good
LA4	164	Fair
LA5	93	Not Very Good
LA6	349	Good
Avg	159	Fair

#### 4.3.6 Silica Fume Mixtures

Results of the air permeability tests for the silica fume mixtures using Kapaa aggregates are presented in Table 4-10.

Table 4-10: Air Permeability Results for Kapaa Silica Fume Mixtures

Mix	Air Permeability (Figg Number)	Protective Quality
SF1	1236 *	Excellent
SF2	187	Fair
SF3	162	Fair
SF4	296	Fair
SF7	299	Fair
SF8	287	Fair
SF9	254	Fair
Avg	247	Fair

\* Excluded from Average

#### 4.3.7 Air Permeability Summary

Most mixtures with Halawa aggregates rated “Fair” based on the air permeability tests. Half of the specimens with the latex admixture rated below “Fair”.

### 4.4 Summary

This chapter presented the results of the mechanical tests performed in this study. Results from fresh concrete tests include the slump and air content tests. The compressive strength, elastic modulus and Poisson’s ratio was also measured using the 6

inch diameter by 12 inch height cylinders. Results of the air permeability tests, which were performed after the conclusion of the saltwater ponding cycles and after allowing the test specimens to dry for at least two months, are presented.



## **CHAPTER 5 RESULTS AND DISCUSSION OF CHEMICAL TESTS**

### **5.1 Introduction**

This chapter presents the results of the chemical tests performed to assess the chloride concentration, and pH. These tests can only be performed after a test specimen has been removed from the saltwater ponding cycling as these tests require sampling that destroys the test specimen. The results reported here do not include any specimens that did not reach failure. The mixtures that were not tested include all mixtures containing Halawa aggregates as well as fly ash and Xypex mixtures using Kapaa aggregates as the majority of the specimens in these mixtures had not yet reached failure.

### **5.2 Chloride Concentration Tests**

#### *5.2.1 Introduction*

This section presents the results of chloride concentration tests for the control, DCI, Rheocrete, FerroGard, latex-modified, and silica fume mixtures with Kapaa aggregates. These mixtures had documented results from previous chloride concentration tests performed in the early stages of cycling (Pham and Newton 2001). Each individual mixture contained 12 specimens. Five of the twelve test specimens were removed from cycling prior to failure to monitor the chloride concentration during the initial saltwater ponding cycles. These specimens were targeted for exposure to 0, 2, 4, 6 and 15 cycles. However, they were not always removed at the specified cycle. Nevertheless, these specimens still provide an accurate record of the ingress of chlorides. Also presented is a comparison of the average of the final chloride concentrations of the remaining specimens after failure of the entire mixture.

After the first five specimens were removed, the remaining data points are from test specimens that failed the electrical current test and were removed from the ponding cycling. If more than one test specimen was removed at a specific cycle, the average of their chloride concentrations was plotted. It should be noted that when chloride concentrations reaches 1% by mass of cement, corrosion initiates.

### *5.2.2 Control Mixtures*

The progression of chloride concentration over the ponding cycles for the control mixtures using Kapaa aggregates are presented in Figure 5-1. Mixture C6 results appear to be unreliable after cycle 15. The remaining mixtures show that mixtures with a w/c ratio of 0.35 had lower levels of chlorides as mixtures at the level of the steel. Mixtures C1 and C4 display significantly lower chloride concentrations than their 0.40 and 0.45 counterparts. The data also show that mixtures with higher paste contents performed better than their lower paste counterparts. High paste mixtures C4, C5, and C6 generally had lower chloride concentrations than their counterparts C1, C2 and C3. Chloride concentrations in the control specimens show that low w/c ratios and high paste contents reduce the ingress of chlorides.

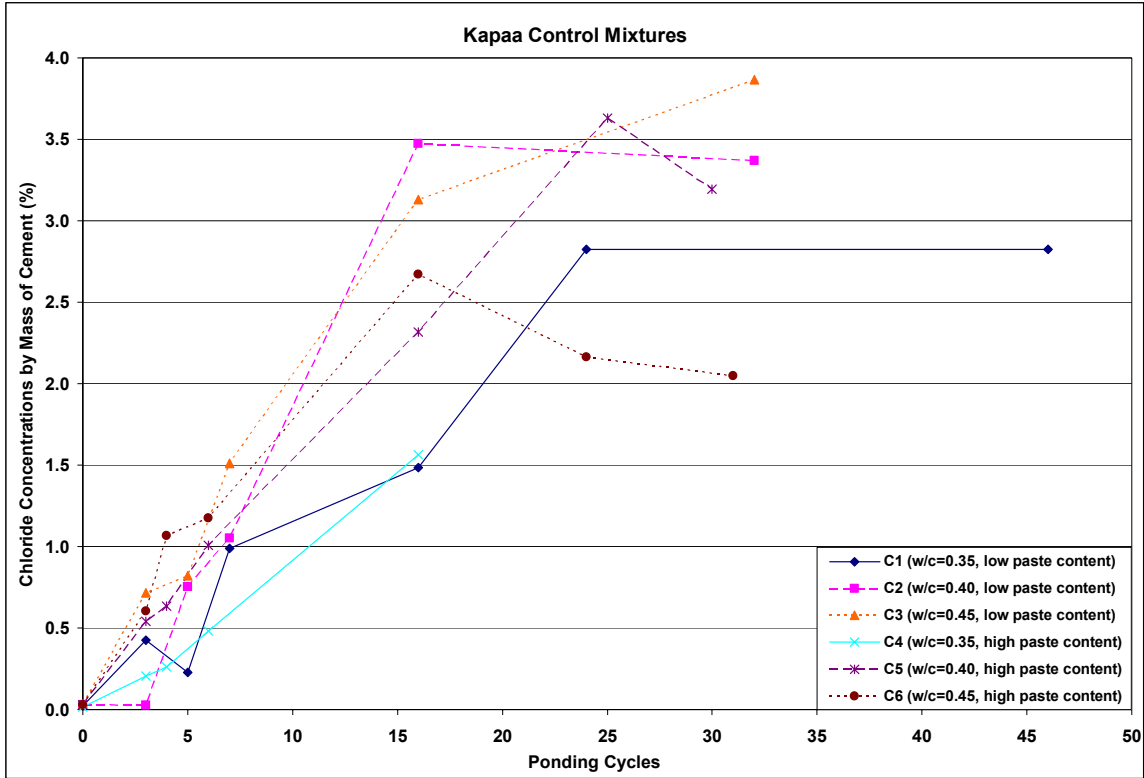


Figure 5-1: Progression of Chloride Concentrations for Kapaa Control Mixtures

The final chloride concentration results for the Kapaa control mixtures are presented in Figure 5-2. Also presented on the graph is the number of ponding cycles each mixture was exposed at the time chloride concentration tests were performed. Mixture C4 is still cycling and has yet to fail, therefore the chloride concentration at 16 cycles is presented. When this mixture fails, the final chloride concentrations will typically be higher as indicated by the dashed lines. Since mixture C4 is still cycling, no conclusions can be made for the 0.35 w/c ratio mixtures. However, the results for the 0.40 and 0.45 mixtures show that high paste mixtures had lower final chloride concentrations than their low paste counterparts. There was a significant difference in final chloride concentration values for the 0.45 w/c ratio mixtures.

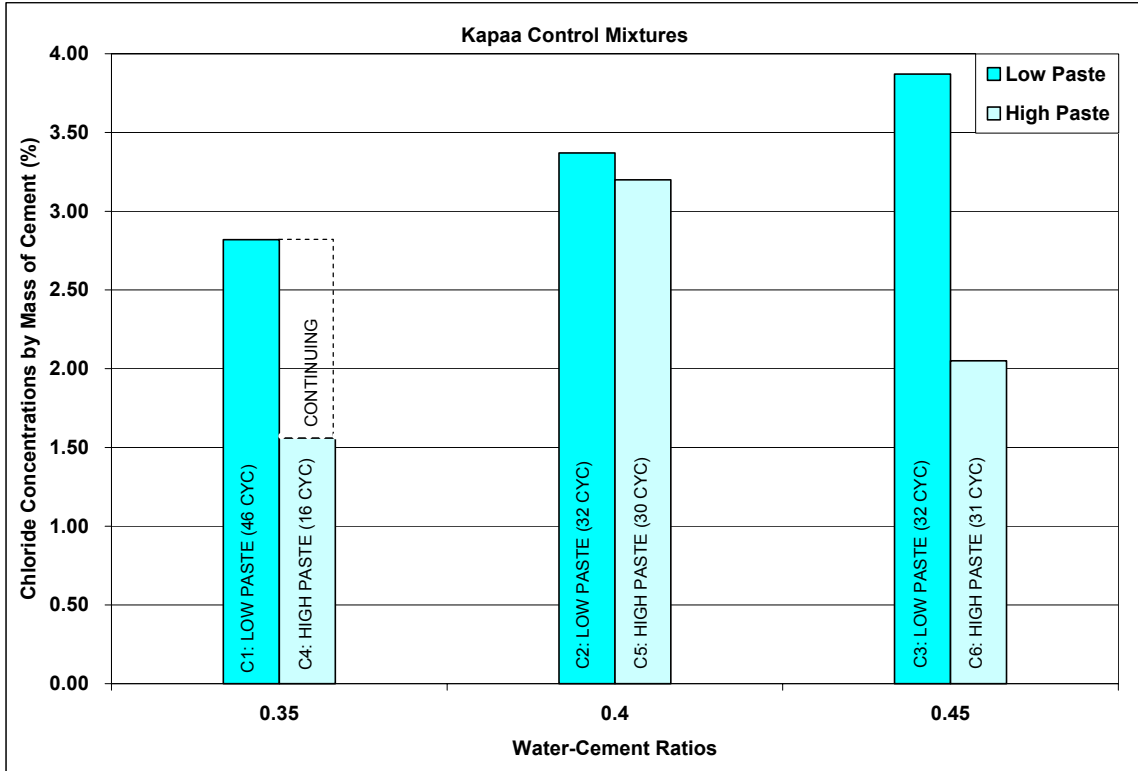


Figure 5-2: Chloride Concentrations for Kapaa Control Mixtures

### 5.2.3 Calcium Nitrate Mixtures

The chloride results for the DCI mixtures using Kapaa aggregates are presented in Figure 5-3. The graph shows that the lower w/c ratios protect better against the ingress of chlorides, as mixtures D1 thru D3 have the lowest chloride concentrations over time. The data also shows that the larger amounts of DCI tend to reduce the chloride concentration. Mixtures D2 and D3 (4 and 6 gal/cy) had lower concentrations than D1 (2 gal/cy). Also chloride concentrations decreased from D4 to D5 to D6, showing that as the amount of DCI increased, the chloride concentrations decreased. This trend probably occurred because as the DCI levels increased, the actual water-to-cement ratios decreased farther from their design values. This was because water was replaced with equal proportions of DCI to follow Harbor Division practice, however DCI consists of a mixture of calcium

nitrite and water. Therefore the actual water-to-cement ratios are lower than their design water-to-cement ratios.

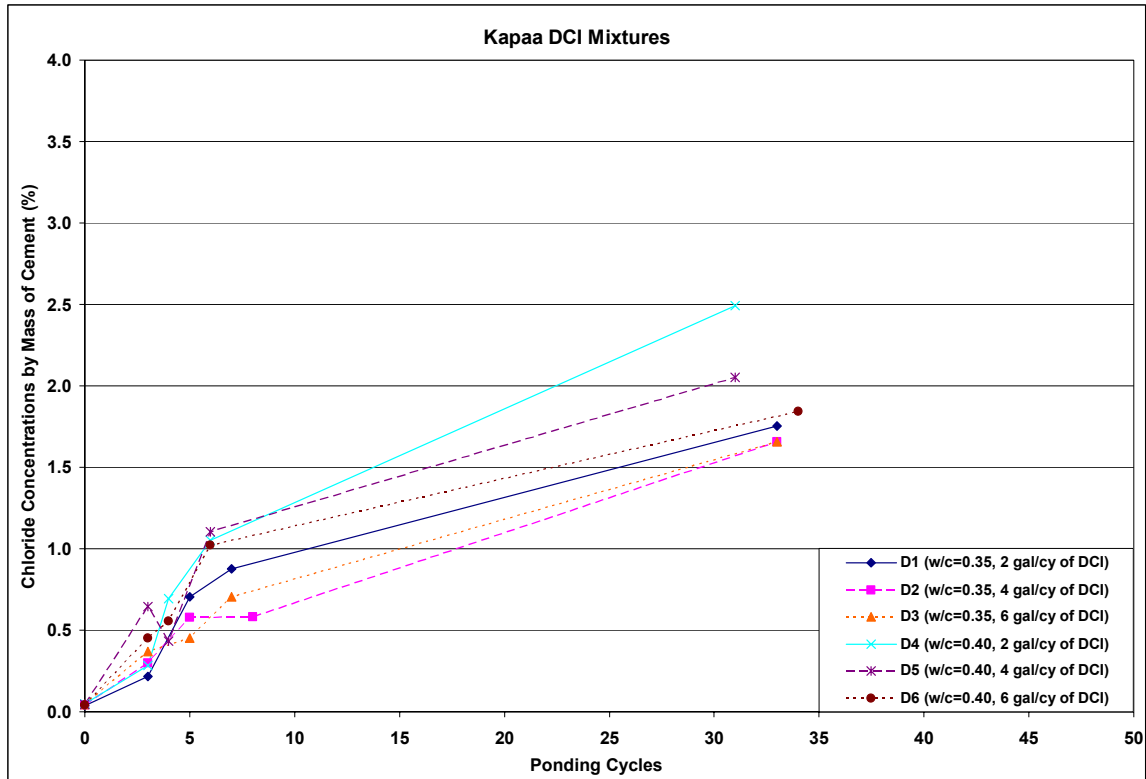


Figure 5-3: Progression of Chloride Concentrations for Kapaa DCI Mixtures

Figure 5-4 shows a comparison of the final chloride concentrations between the specimens with DCI and the corresponding control specimens. No conclusions can be made from the mixtures with w/c ratio of 0.35 all of these mixtures including the control mixture are still cycling. The mixtures with DCI dosages of 4 and 6 gal/cy with w/c ratios of 0.40 are still cycling as they have not failed. However, the final chloride concentration value of mixture D4 shows a lower chloride concentration than its control counterpart. Also the results show that the control and DCI mixtures with a 0.40 w/c ratio were all tested after 31 to 34 ponding cycles. The results also show that as the DCI dosage was increased, the chloride concentrations over the same number of ponding cycles decreased. However, the added chloride protection is not due to the calcium

nitrite, but because of the lower water-to-cement ratio of these mixtures as calcium nitrite mixtures are composed of only 70% water. Also the DCI concentrations were significantly lower than the control counterpart mixture C2.

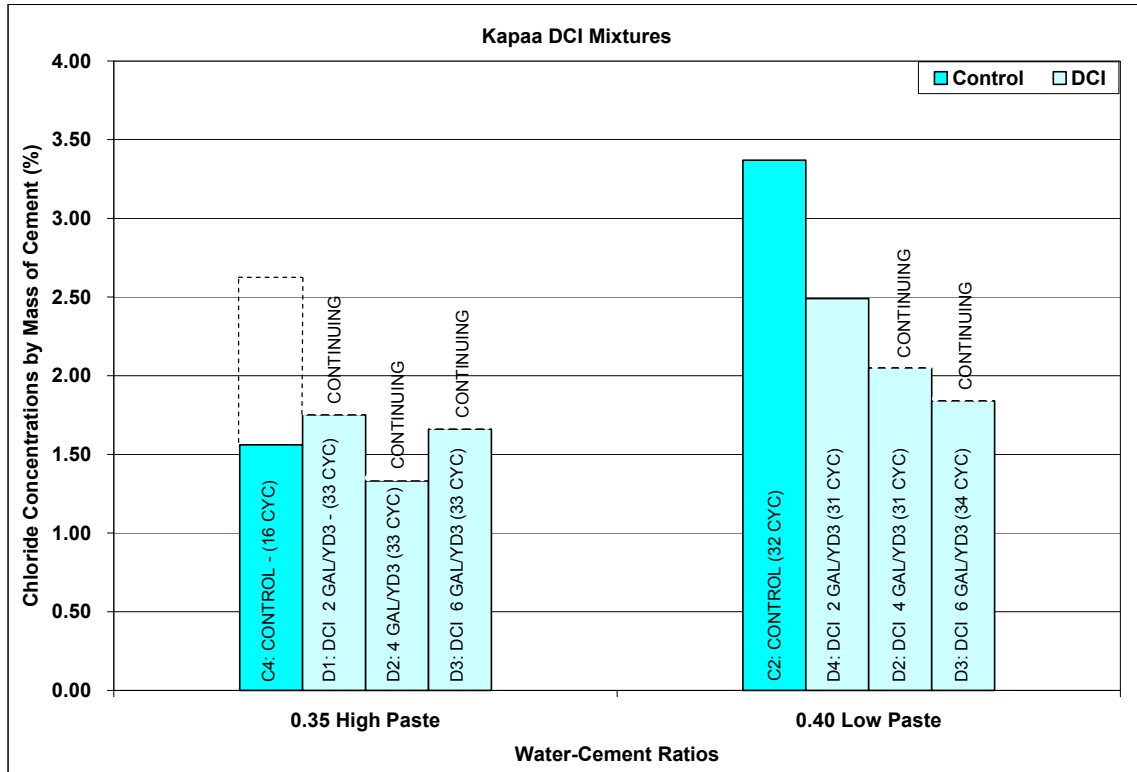


Figure 5-4: Chloride Concentrations for Kapaa DCI Mixtures

#### 5.2.4 FerroGard Mixtures

The chloride results for the FerroGard mixtures using Kapaa aggregates are presented in Figure 5-5. All FerroGard mixtures contained the same amount of the admixture, varying only the w/c ratios and paste contents. The two mixtures with the lowest chloride concentrations are FER1 and FER4. Again this shows that there is a significant difference in chloride concentrations with a low w/c ratio of 0.35. No other conclusions can be made from the remaining mixtures.

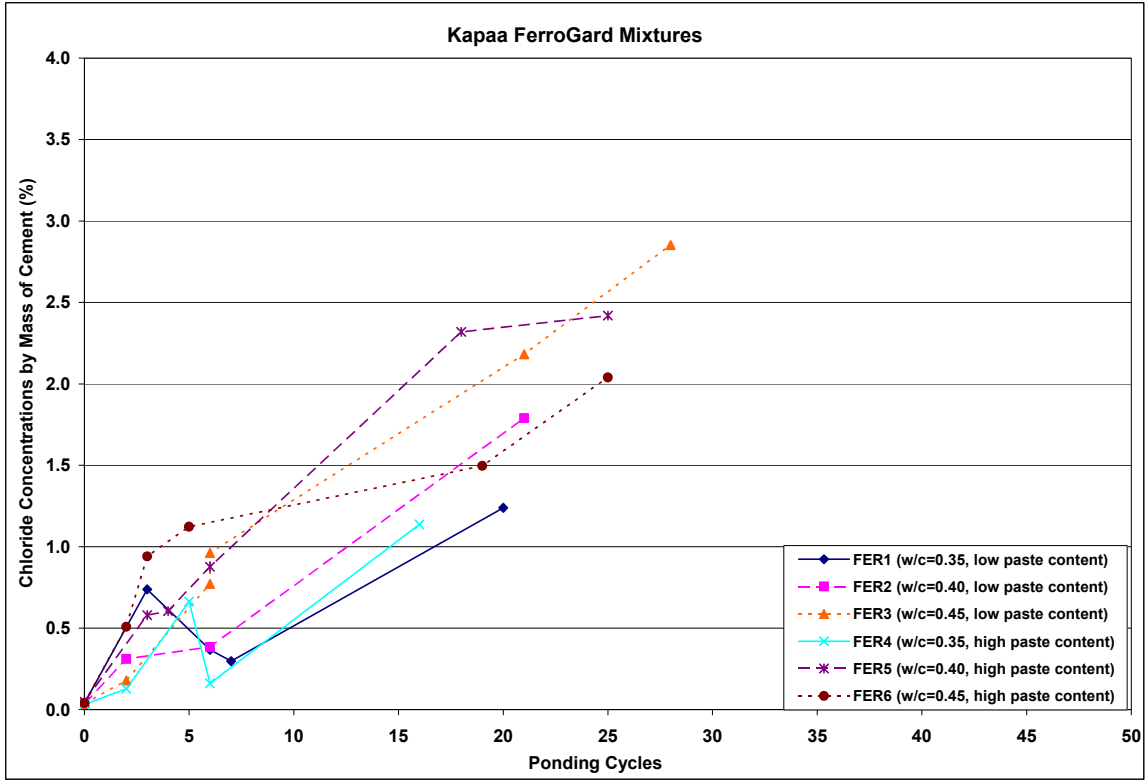


Figure 5-5: Progression of Chloride Concentrations for Kapaa FerroGard Mixtures

Figure 5-6 shows a comparison of the final chloride concentrations between the FerroGard mixtures and the corresponding control specimens. No conclusions can be made from the mixtures because the majority of these mixtures are still cycling

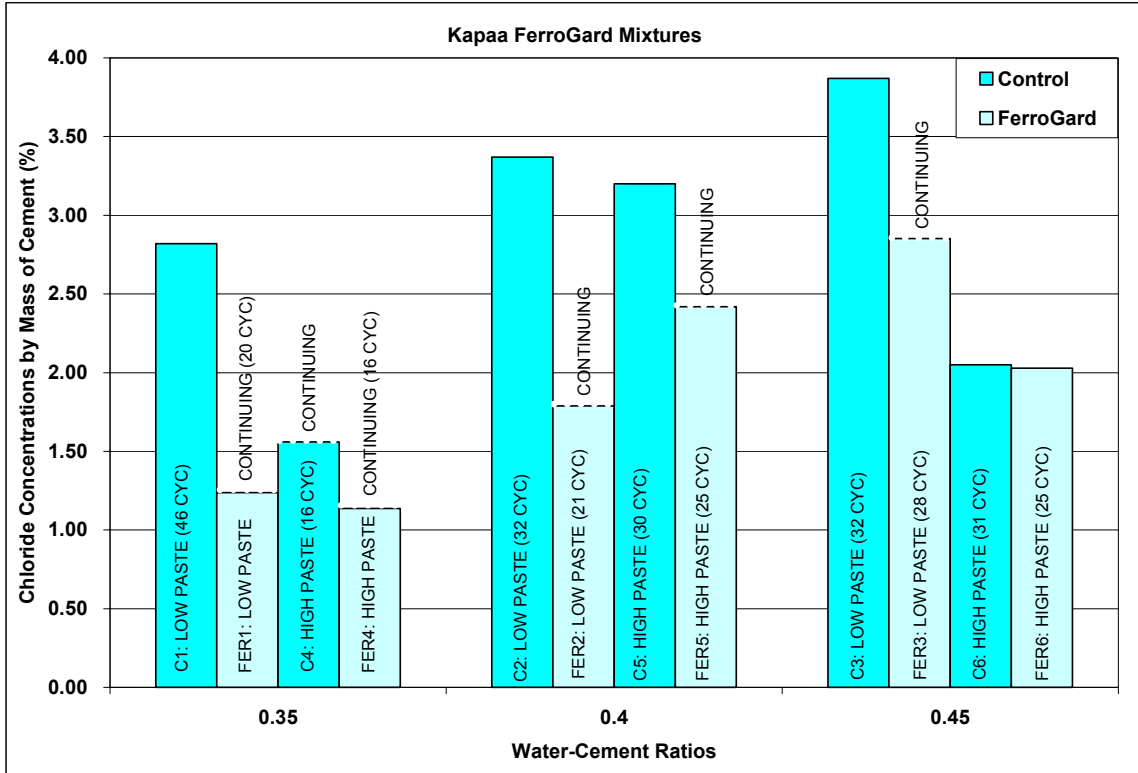


Figure 5-6: Chloride Concentrations for Kapaa FerroGard Mixtures

### 5.2.5 Rheocrete Mixtures

The chloride results for the Rheocrete mixtures using Kapaa aggregates are presented in Figure 5-7. Due to the lack of data points for RHE3 and the short ponding cycles, no significant conclusions can be made. It does show that RHE1 and RHE4 are two of the three mixtures with the lowest chloride concentrations and suggest that the low w/c ratio has an impact on the results.

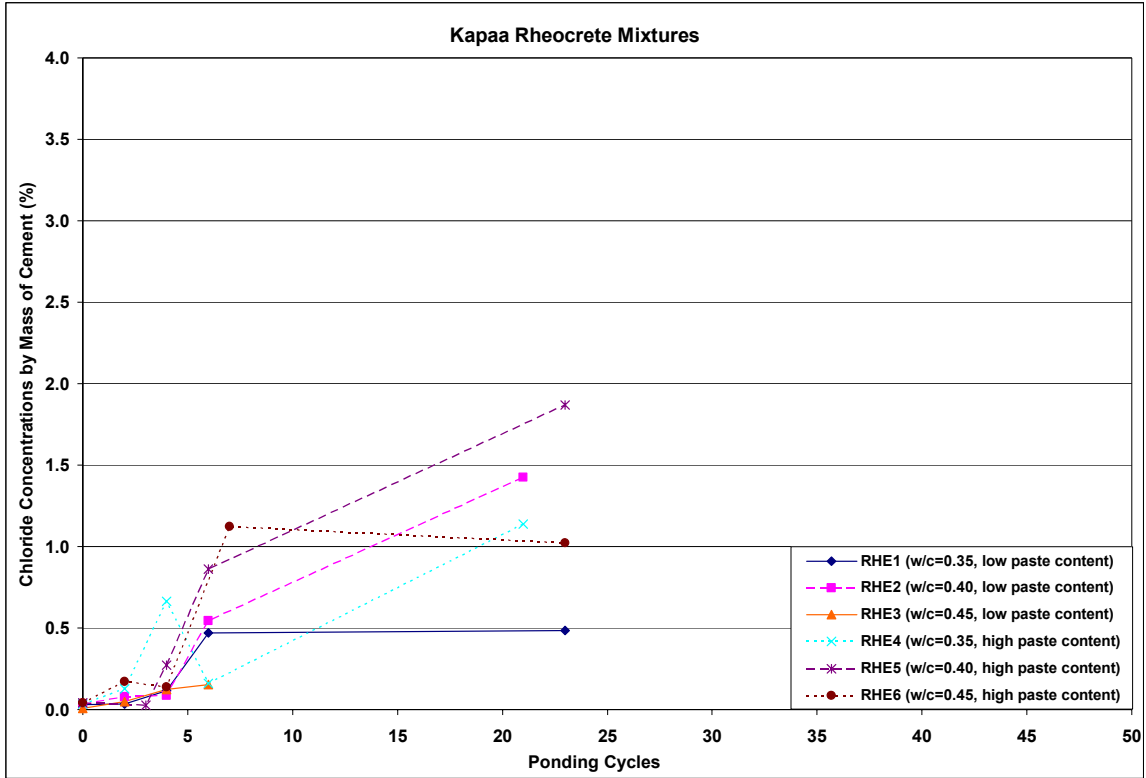


Figure 5-7: Progression of Chloride Concentrations for Kapaa Rheocrete Mixtures

Figure 5-8 shows a comparison of the final chloride concentrations between the Kapaa Rheocrete mixtures and the corresponding control specimens. No conclusions can be made from the mixtures because the majority of these mixtures are still cycling.

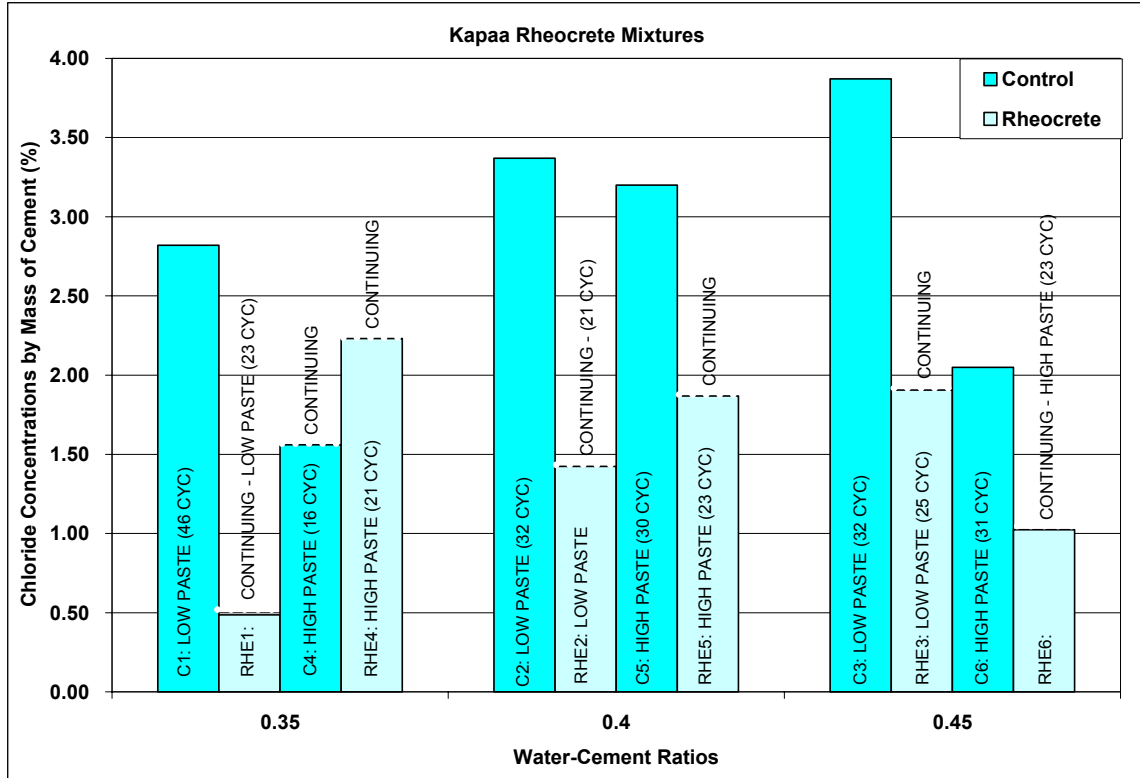


Figure 5-8: Chloride Concentrations for Kapaa Rheocrete Mixtures

### 5.2.6 Latex Mixtures

The chloride results for the latex-modified mixtures using Kapaa aggregates are presented in Figure 5-9. After 23 ponding cycles, mixtures L1 and L4 had the lowest chloride concentration values. These two mixtures contain the lowest levels of the latex admixture. Also the data shows L2 and L3, mixtures with w/c ratios of 0.35, significantly higher in chlorides than the other mixtures. This does not agree with the chloride concentrations for other mixtures which show that w/c ratios of 0.35 performed better than their 0.40 and 0.45 counterparts. This is most likely due to excessive overmixing of the latex mixtures and because the test specimens were not air cured. Problems with the latex mixtures including low compressive strength and high permeability were noted in an earlier study by Pham and Newton (2001).

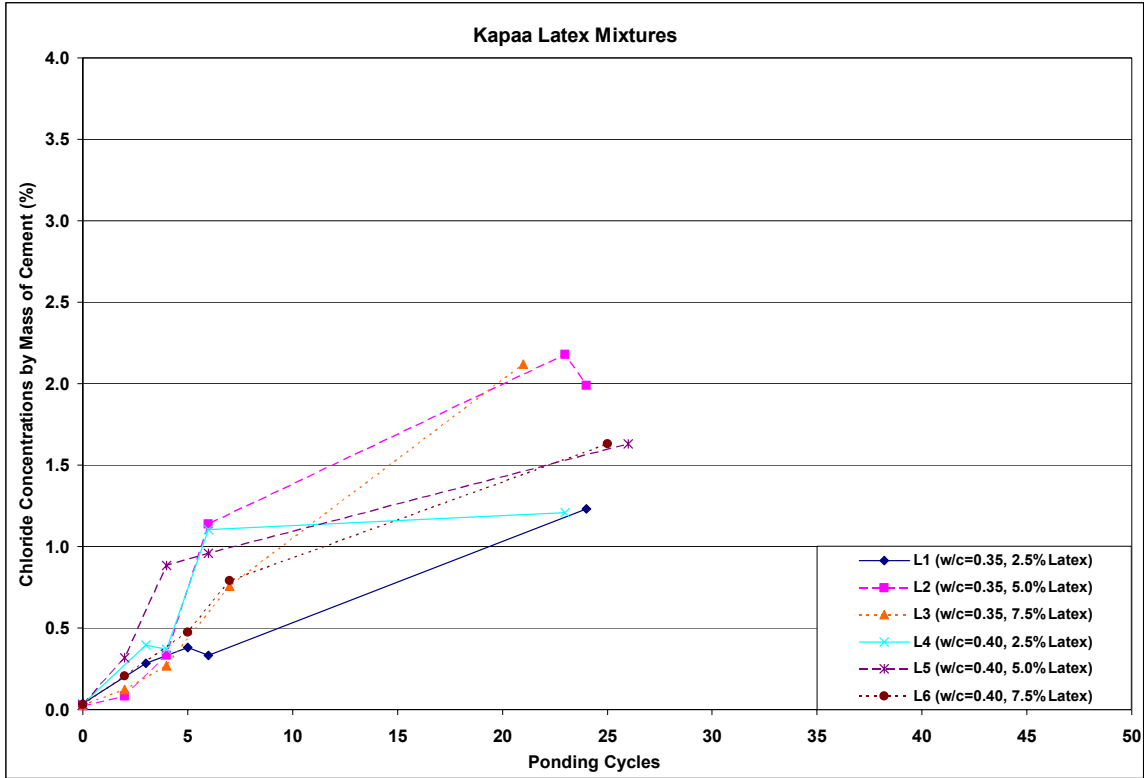


Figure 5-9: Progression of Chloride Concentrations for Kapaa Latex Mixtures

Figure 5-10 shows a comparison of the final chloride concentrations between the Kapaa Latex mixtures and the corresponding control specimens. No conclusions can be made from the mixtures because the majority of these mixtures are still cycling.

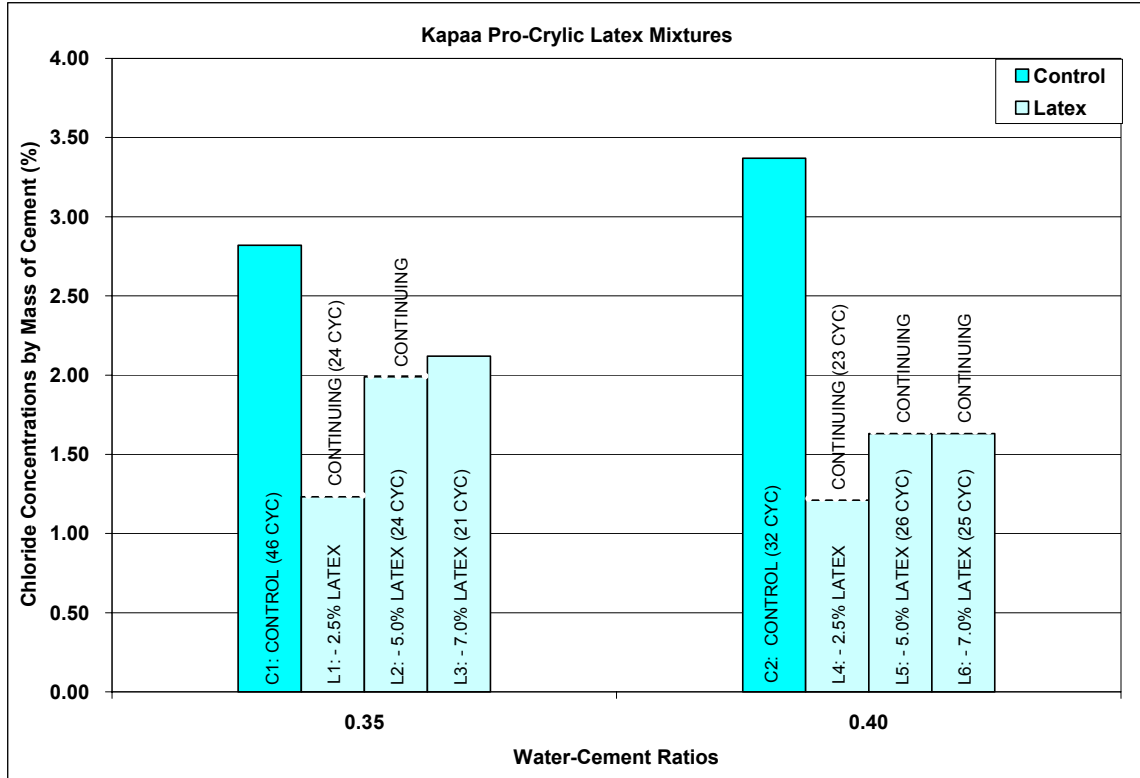


Figure 5-10: Chloride Concentrations for Kapaa Latex Mixtures

### 5.2.7 Silica Fume Mixtures

The chloride results for the silica fume mixtures using Kapaa aggregates are presented in Figure 5-11. The graph shows that increased silica fume contents resulted in reduced chloride concentrations. The three silica fume mixtures with the lowest chloride concentrations are SF2 thru SF4 which have w/c ratios of 0.36. Mixture SF1 also had a w/c ratio of 0.36, however this is a control mixture which contains no silica fume. The graph also shows that mixtures SF4 and SF9 which contained 15% silica fume performed significantly better than their equivalent w/c ratio counterparts with lower silica fume contents. SF9 (w/c ratio of 0.45) had a lower chloride concentration than SF1 (w/c ratio of 0.36), showing that the 15% silica fume compensated for the higher w/c ratio in SF9.

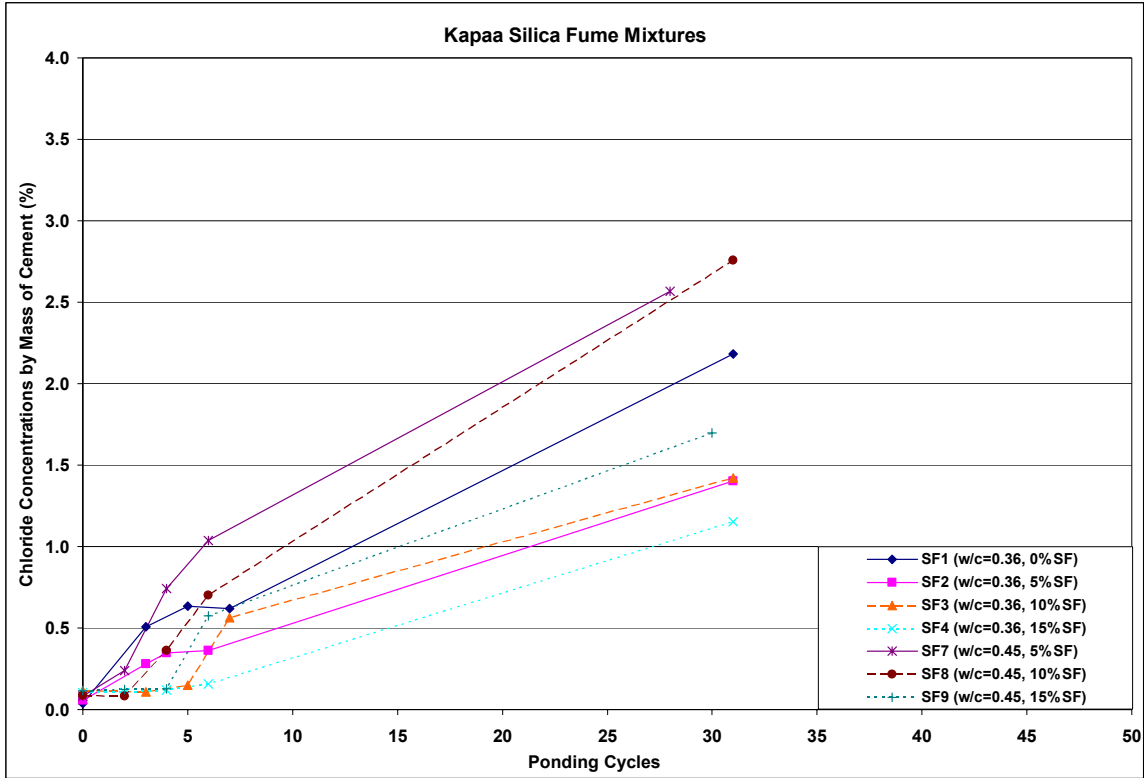


Figure 5-11: Progression of Chloride Concentrations for Kapaa Silica Fume Mixtures

Figure 5-12 shows a comparison of the final chloride concentrations between the Kapaa silica fume mixtures and the corresponding control specimens. The mixtures with a 0.36 w/c ratio similar to the Ford Island Bridge project are all still cycling. However, though these mixtures continue to be cycling, they were all tested after 31 ponding cycles. These results show that the silica fume mixtures had significantly lower chloride concentrations. The mixtures with a 0.45 w/c ratio designed according to PCA were all tested between 28 and 31 cycles. However, no conclusions could be made from the results.

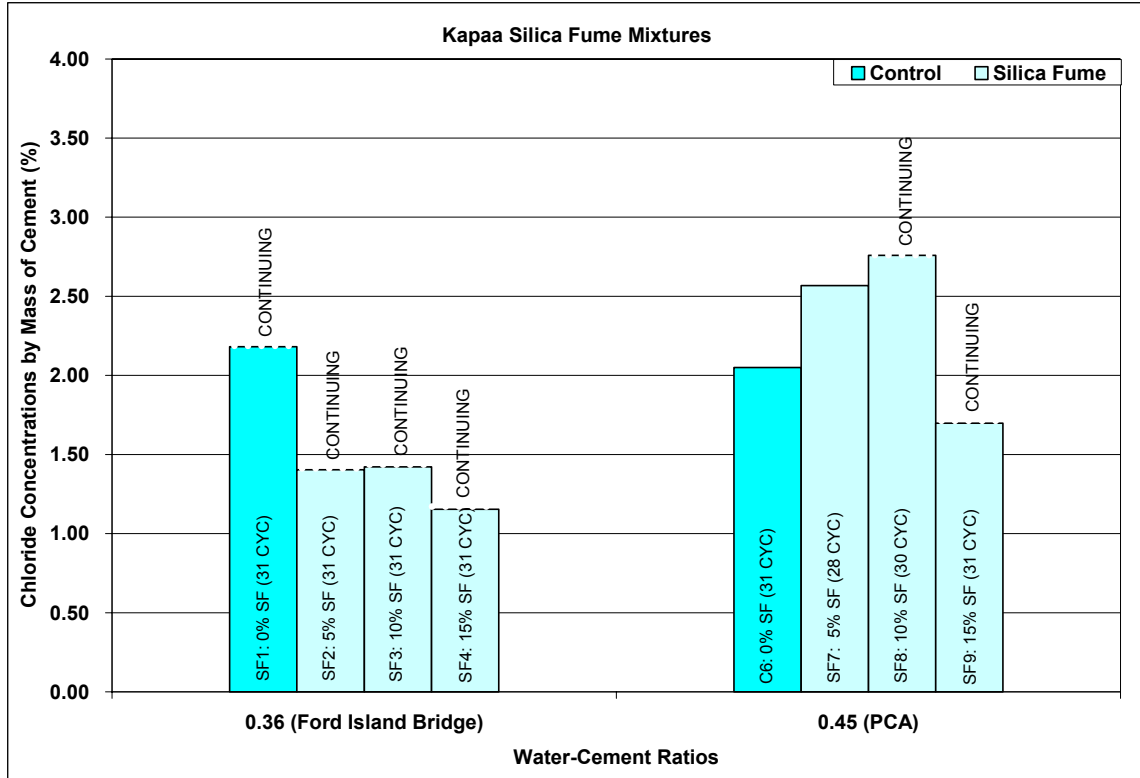


Figure 5-12: Chloride Concentrations for Kapaa Silica Fume Mixtures

### 5.2.8 Summary

The chloride concentration results generally show that a low w/c ratio of 0.35 or 0.36 provided better protection from the ingress of chlorides than equivalent mixtures with w/c ratios of 0.40 and 0.45. The majority of the mixtures that have finished cycling with corrosion inhibiting admixtures showed a reduction in chloride concentration compared with the control mixtures. The addition of 15% silica fume provides significantly more protection in decreasing chloride concentrations.

## 5.3 pH Tests

### 5.3.1 Introduction

This section presents the results of pH tests for the control, DCI, latex-modified, silica fume mixtures, with Kapaa aggregates. The Kapaa control, DCI, latex and silica

fume mixtures include documented results from previous pH tests performed in the early ponding stages (Pham 2001). Current data were added to these previous results. Results for the early ponding stages of the Rheocrete and FerroGard test specimens of the early ponding stages were inadvertently misplaced. The pH samples for testing were taken after the same number of ponding cycles as the chloride concentrations. All pH monitoring and testing intervals are the same as the chloride concentration tests.

### *5.3.2 Control Mixtures*

The pH results for the control mixtures using Kapaa aggregates are presented in Figure 5-13. All pH values fall between 12.0 and 13.0. The results show a trend of pH decreasing as the mixtures are subjected to increased ponding cycles. After 23 ponding cycles, all of the test specimens report pH values below 12.5, the typical pH level for normal concrete. There does not appear to be any correlation between pH and the w/c ratio of paste content of the Kapaa control mixtures.

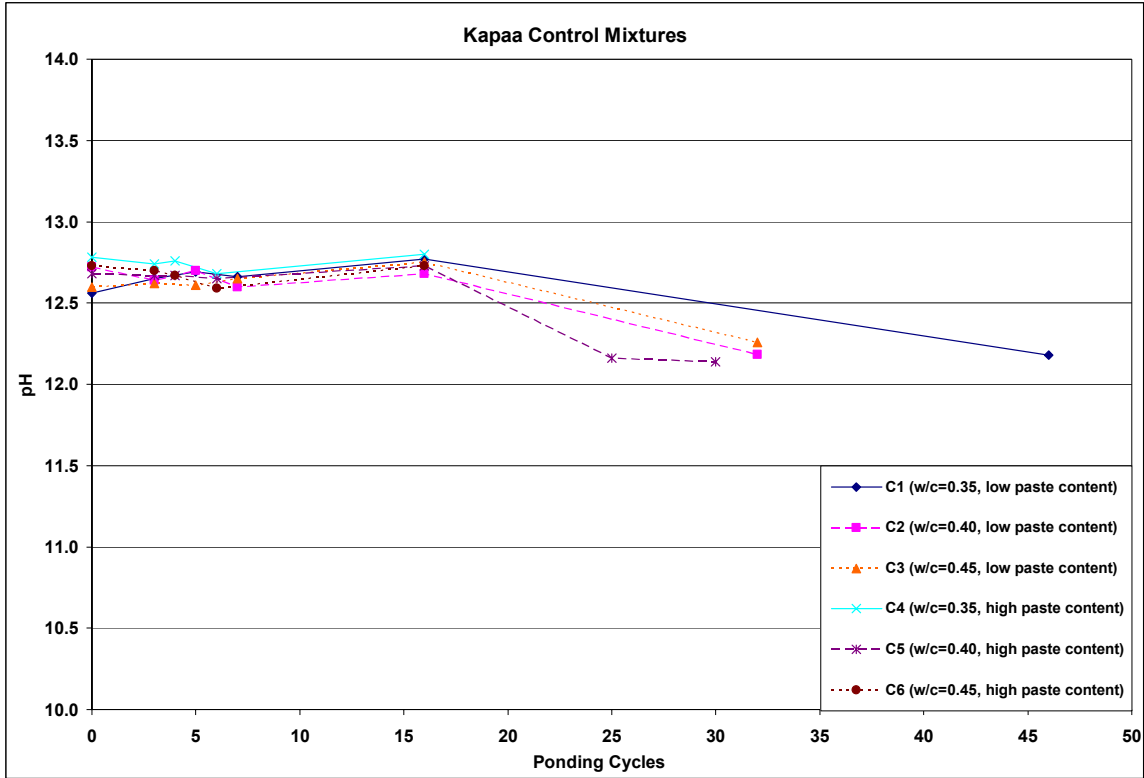


Figure 5-13: pH for Kapaa Control Mixtures

### 5.3.3 Calcium Nitrate Mixtures

The pH results for the DCI mixtures using Kapaa aggregates are presented in Figure 5-14. The results show a drop in pH from approximately 12.75 before being subject to saltwater ponding, to between 12.0 and 12.5 after 30 or more ponding cycles. No test specimens have reached a pH of below 12.00. All test specimens report pH values below 12.5, the typical pH level for normal concrete. There does not appear to be any correlation between pH and the amount of DCI in the mixture.

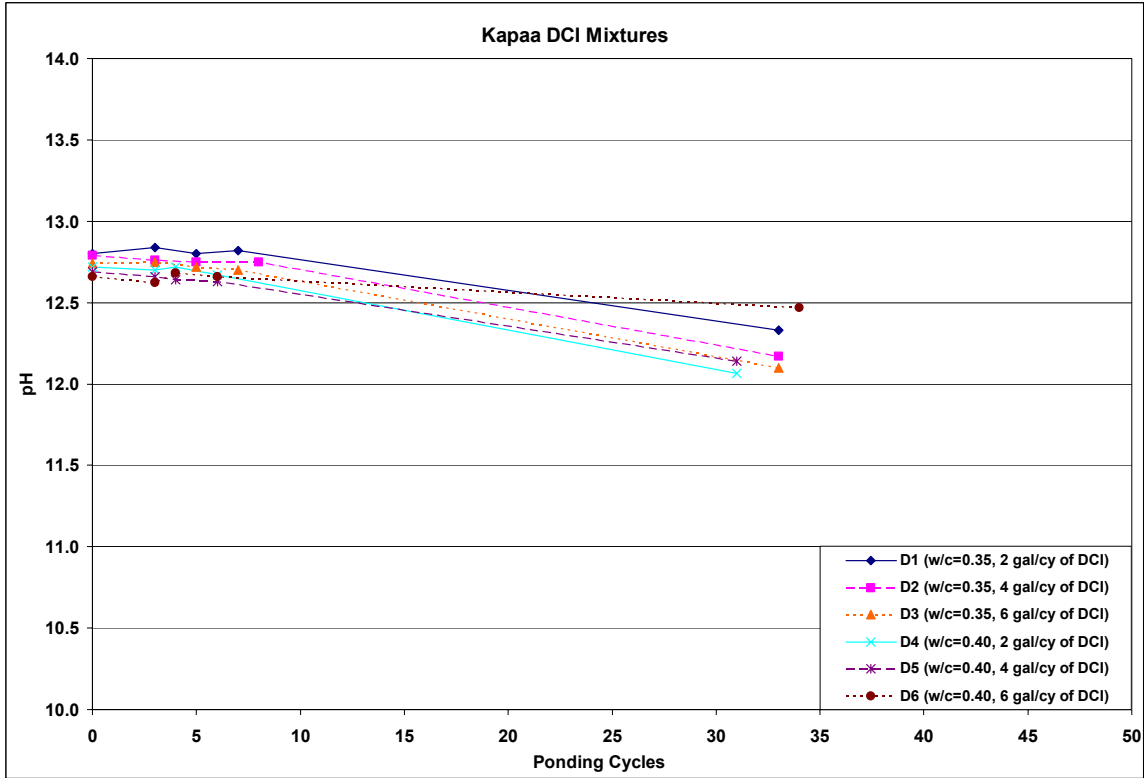


Figure 5-14: pH for Kapaa DCI Mixtures

#### 5.3.4 Latex Mixtures

The pH results for the latex mixtures using Kapaa aggregates are presented in Figure 5-15. The results show the latex mixtures initial pH values are around 13.0 and slowly dropped to the 12.0 to 12.5 range after 20 ponding cycles. None of the pH values for the test specimens reach a pH below 12.0. There is no correlation between pH level and the varying latex content.

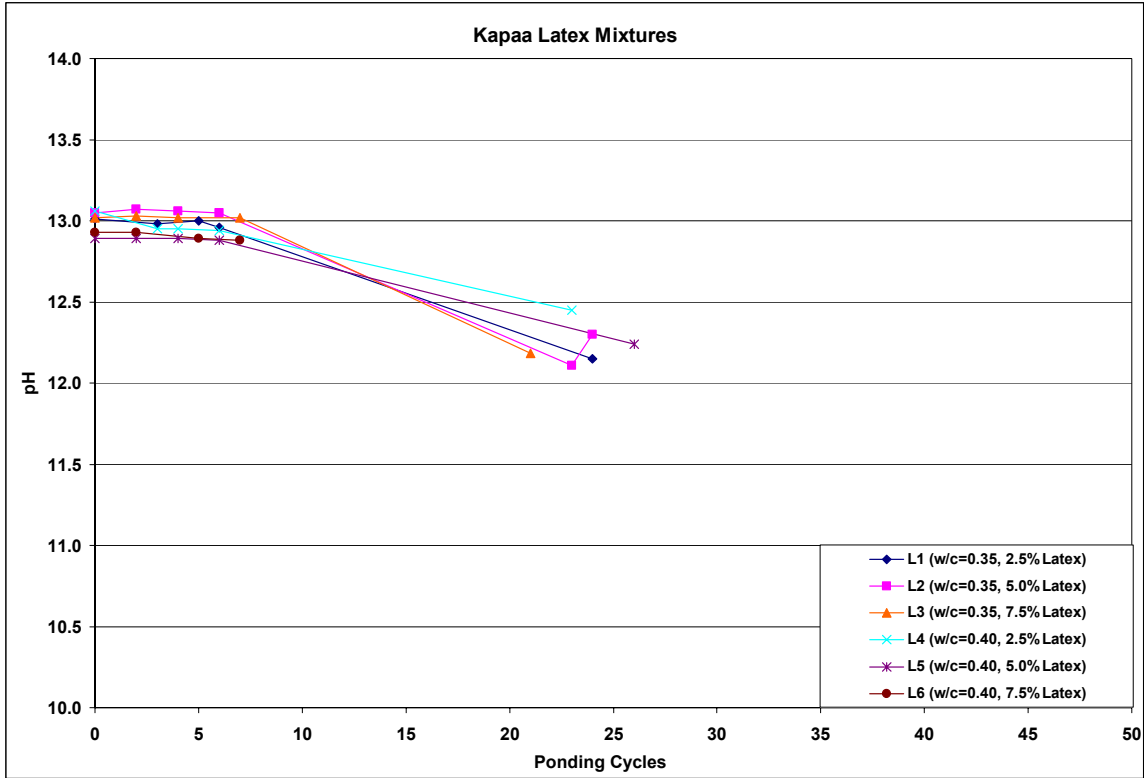


Figure 5-15: pH for Kapaa Latex Mixtures

### 5.3.5 Silica Fume Mixtures

The pH results for the silica fume mixtures using Kapaa aggregates are presented in Figure 5-16. All pH values fall between 12.0 and 13.0. The results show the silica fume mixtures initial pH values are around 12.8 and slowly dropped to the 12.0 to 12.6 range. After about 30 ponding cycles, all but one of the test specimens report pH values below the typical pH level of 12.5 for normal concrete. None of the pH values for the test specimens reach a pH below 12.0.

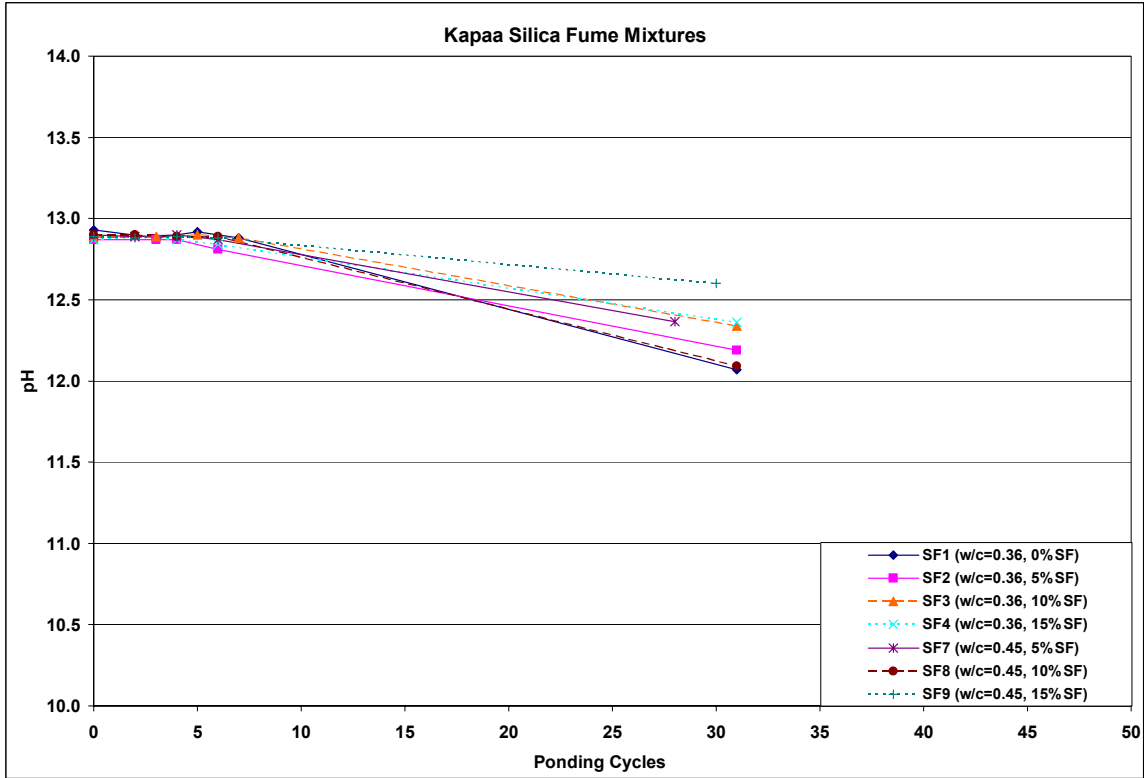


Figure 5-16: pH for Kapaa Silica Fume Mixtures

### 5.3.6 Other Mixtures

Due to the limited space in the laboratory and the increasing number of laboratory tests to perform, it was decided that the remaining mixtures would not monitor the change in pH in the concrete versus the number ponding cycles. As anticipated, the pH data recorded from the four concrete mixtures tested show a similar trend of declining pH values over time that eventually fell below 12.5.

## 5.4 Summary

This chapter presented the results of the chemical tests. The chloride tests for all of the mixtures tested showed a trend of increasing chloride levels as the test specimens were exposed to the saltwater ponding cycles. Also the pH results show a trend of the pH

levels dropping below the typical 12.5 value for normal concrete due to exposure to the saltwater ponding cycles

## **CHAPTER 6 RESULTS AND DISCUSSION FOR ELECTRICAL TESTS**

### **6.1 Introduction**

This chapter begins with a discussion of the accuracy of each of the four electrical tests. The electrical tests performed for this study measured the electrical current, half-cell potential, corrosion rate, and concrete resistivity. Also included is an explanation for each of the electrical tests to help understand and diagnose the graphs presenting these results. Due to the large number of graphs, all of the electrical test results are presented in the Appendix. Sample graphs are included in this chapter for illustration purposes. Finally the overall failure results of each mixture when compared to the electrical current tests, which were assumed to indicate corrosion initiation, are presented. Though many of the concrete mixtures have not yet failed, there is a significant amount of data to provide initial conclusions regarding each corrosion inhibiting admixture when compared to the corresponding control mixture.

### **6.2 Accuracy of Electrical Current Tests**

For this study, the electrical current test was assumed to provide the most accurate indication of the corrosion in the test specimens. This test could be performed numerous times on a single test specimen and yield exactly the same result. The first reading, which was taken immediately after the curing process, but before the initial saltwater ponding cycles were typically ignored as the concrete was still curing and was saturated with water. However after the initial readings, all test specimens typically had electrical current readings close to  $0.00\mu\text{A}$ . Once the electrical current values began to drop, indicating signs of corrosion activity, they typically reached the failure limit of  $-10.00\mu\text{A}$  in a few ponding cycles.

The only concern with the accuracy of the electrical current test was caused by insufficient electrical connections between the reinforcing bars on the test specimen. Though the saltwater ponding cycles were designed to provide an accelerated corrosion environment, most tests extended over a period of a few years. Over time, the wires, welds, and resistors completing the electrical connection had to be replaced due to accidental damage during testing and from exposure due to the saltwater environment. When an electrical connection was damaged, the electrical current test would show a drastic decrease from the previous cycle readings. To address this error, all test specimens that tested below the  $-10.00 \mu\text{A}$  were kept cycling for an additional three saltwater ponding cycles to verify the corrosion readings according to ASTM G 109. Also an inspection was performed on the electrical connections of all test specimens that showed a large decrease in electrical current values during a single ponding cycle. Often the electrical connection had failed and required repair for these specimens.

The electrical current test is only really suitable for a laboratory setting due to the use of specially designed test specimens. The remaining three electrical tests are non-destructive tests performed using the Gecor6 testing instrument manufactured by James Instruments. Using this instrument, these tests can be performed in the field. The first section in this chapter discusses the accuracy of the Gecor6 electrical measurements when compared to the electrical current readings.

### **6.3 Accuracy of Gecor6 Electrical Tests**

#### *6.3.1 Introduction*

The electrical current test was assumed to provide a reliable indication of corrosion activity on the reinforcing steel in the test specimens, however additional tests

measuring the half-cell potential, corrosion rate and concrete resistivity were performed using the Gecor6 instrument to verify the results. The Gecor6 instrument began experiencing testing problems and eventually malfunctioned in July 2004. However, a significant amount of data was recorded before this failure. Due to the significant amount of time taken to perform these tests, only the Kapaa mixtures were monitored using the Gecor6. The following section individually presents the accuracy of each of the Gecor6 electrical test results when compared to the electrical current test results.

The following errors should be taken into account in analysis of the Gecor6 test results. According to ASTM specifications, when the electrical current readings on the test specimens fall below  $-10.00 \mu\text{A}$ , the specimen has failed. However, significant corrosion exists before this limit is reached. To provide a better comparison of the Gecor6 electrical tests and electrical current test results, the Gecor6 results were compared to an electrical current failure limit of  $-2.50 \mu\text{A}$  instead of the required  $-10.00 \mu\text{A}$ . This  $-2.50 \mu\text{A}$  limit was chosen after analyzing the electrical test results and determining that test specimens typically experienced corrosion soon after reaching this limit.

As discussed earlier, when a test specimen reached the corrosion limit of  $-10.00 \mu\text{A}$ , the test specimen was determined to have failed, however it was allowed to remain cycling in the saltwater ponding for an additional 3 cycles to verify the results. This procedure meant that the majority of electrical readings occurred when no corrosion was indicated by the electrical current test. Approximately 94% of the electrical measurements were performed when the electrical current results read higher than  $-2.50$

$\mu\text{A}$  indicating no corrosion. Only 6% of the electrical readings were taken when current results read lower than  $-2.50 \mu\text{A}$  indicating corrosion had initiated.

### *6.3.2 Half-Cell Potential*

The results of the accuracy of the half-cell potential tests are shown below in Figure 6-1. This graph shows that approximately 81% of all half-cell potential test results that indicated a “high” potential for corrosion agreed with the electrical current tests of less than  $-2.50 \mu\text{A}$ , indicating corrosion was present. This percentage was slightly lower than the 90% accuracy indicated by the Gecor6 manufacturer. When the corrosion potential readings indicated an “uncertain” result, 12% of these results had electrical current test results less than  $-2.50$ . Finally, when the half cell potential tests indicated a “low” corrosion reading, approximate 0.4% of the results had an electrical current reading less than  $-2.50 \mu\text{A}$ . The increase in accuracy for test specimens with “low” half-cell potential readings was probably influenced by the fact that the majority of readings were taken when the electrical current indicated no corrosion was present.

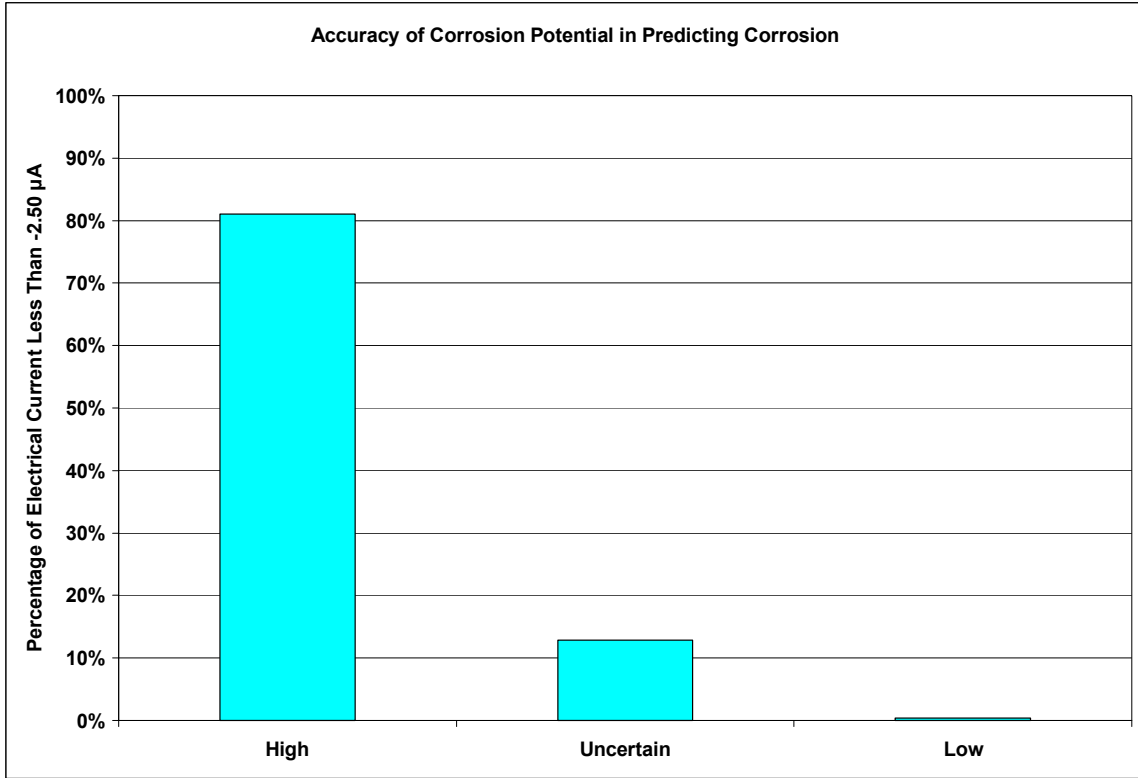


Figure 6-1: Accuracy of Corrosion Potential in Predicting Corrosion

### 6.3.3 Corrosion Rate from Linear Polarization

The results of the accuracy of the corrosion rate tests are shown below in Figure 6-2. This graph shows that 84% of all corrosion rate test results that indicated a “high” rate of corrosion agreed with the electrical current tests of less than -2.50 µA, indicating corrosion. When the corrosion rate values indicated a “moderate” rate of corrosion, 64% of these results had electrical current test results less than -2.50 µA. When the corrosion rate values indicated a “low” rate of corrosion, 32% of these results had electrical current test results less than -2.50 µA. Finally, when the corrosion rate tests indicated a “none”, or no corrosion rate, 4% of the results had an electrical current reading less than -2.50 µA.

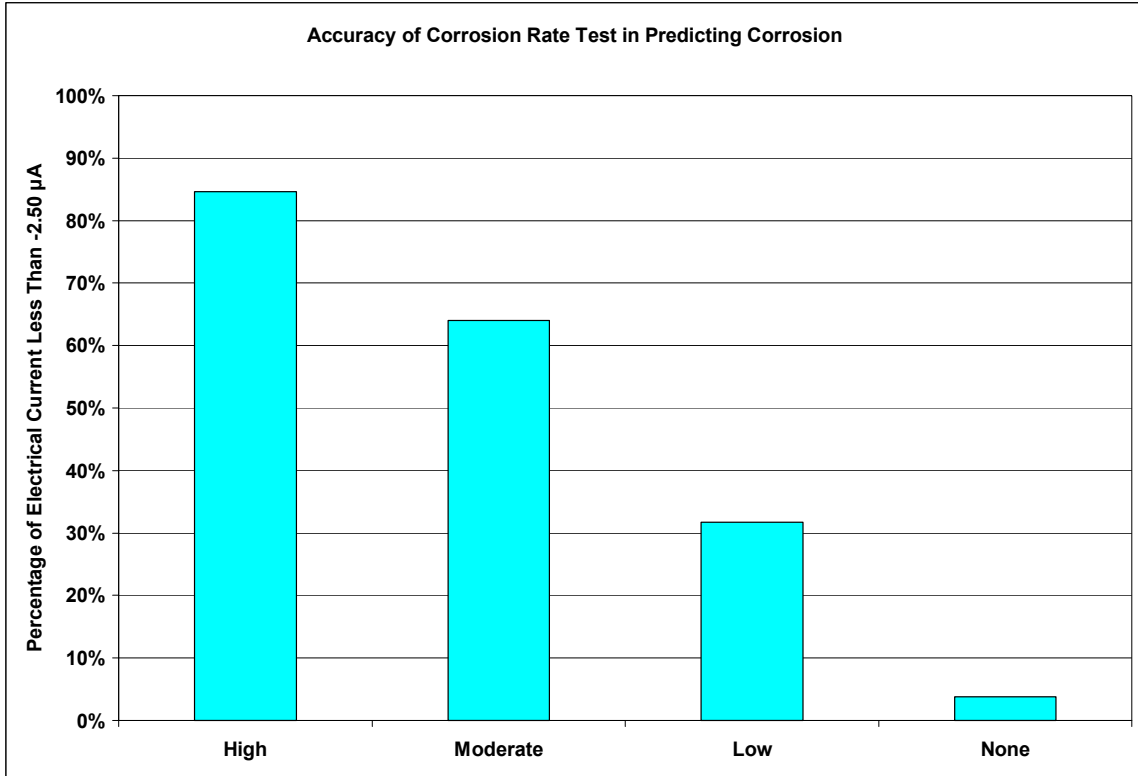


Figure 6-2: Accuracy of Corrosion Rate in Predicting Corrosion

#### 6.3.4 Concrete Resistivity

The results of the accuracy of the concrete resistivity tests are shown below in Figure 6-3. This graph does not show any correlation between the concrete resistivity and the electrical current tests. The graph shows that when the resistivity indicates “very high” corrosion, only 8% of the electrical current tests were less than -2.50 µA. When the resistivity indicated “high” corrosion, 6% of the electrical current tests indicate corrosion. When the resistivity values indicate “moderate/low” and “low” corrosion, only 5% and 2% of the electrical current tests indicate corrosion.

No correlation between the concrete resistivity values and the electrical current values could be determined similar to a previous study by Bola and Newton 2000.

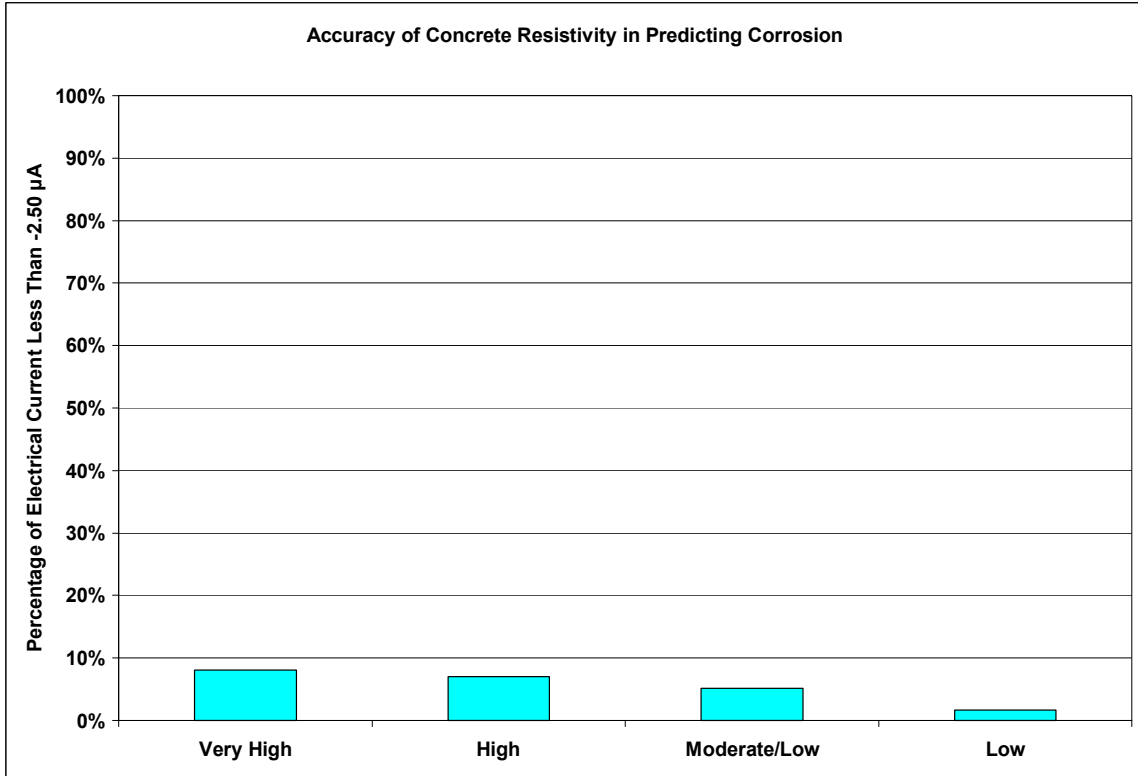


Figure 6-3: Accuracy of Concrete Resistivity in Predicting Corrosion

#### 6.4 Presentation of Electrical Test Results

Electrical tests were performed during each ponding cycle for each individual test specimen until July 2004. Results from all four of the electrical tests for all of the mixtures are presented individually in Appendix A. This section describes the presentation of each of the electrical test results as graphs describing the corrosion limits for each test. Sample graphs are shown for the Kapaa Control Mixture C4 with very little corrosion activity. Samples are also included for the Kapaa Control Mixture C5, which showed significant corrosion activity and eventual failure of the mixture.

##### 6.4.1 Electrical Current Tests

Electrical current test results were plotted versus the number of saltwater ponding cycles. A sample plot of a typical mixture not meeting the ASTM limit of  $-10.0 \mu\text{A}$  for

corrosion failure is shown in Figure 6-4. Each of the lines in the plot presents the electrical current results of a single test specimen. In this figure, test specimens #1 thru #7 are monitored for Kapaa control mixture C4. A horizontal line at  $-10.00 \mu\text{A}$  on the y-axis indicates the ASTM limiting electrical current value for corrosion failure. All readings above this limit indicate the test specimen has not failed. If the electrical current readings for a specimen fall below this limit, it is considered to have failed. In this plot, none of the specimen's readings drop below this limit and therefore none of the specimens has failed. This figure shows electrical current readings in the early ponding stages are very close to zero, indicating that no corrosion has taken place. Some corrosion activity is indicated in test specimen #2 at around 25 cycles. However, the readings fall above the  $-10.00 \mu\text{A}$  limit and so the ponding cycling is continued. As reported by Kakuda (2004) however, it is likely that corrosion is presented on the reinforcing bars since the electrical current reading has exceeded  $-2.50 \mu\text{A}$ . Similar signs of corrosion initiation are noted in specimens #6 and #7 at around 30 cycles, and specimens #3, #4 and #5 at around 40 cycles.

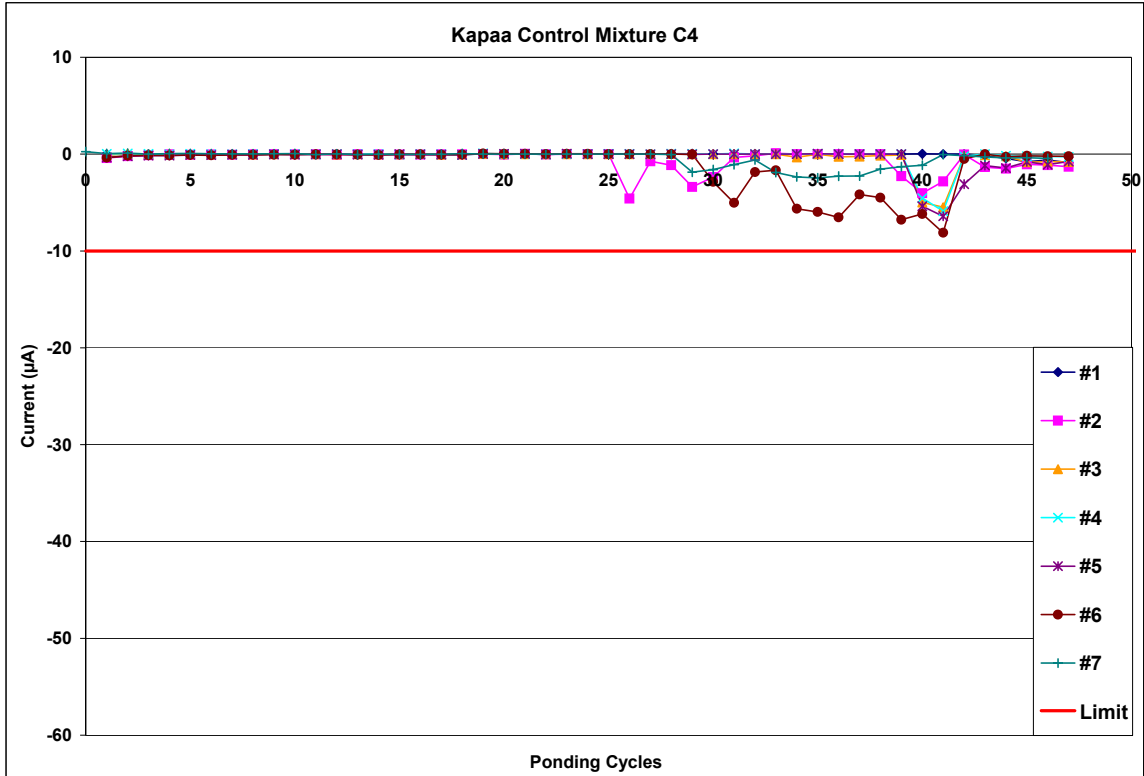


Figure 6-4: Example of Electrical Current Measurements Not Indicating Corrosion

Figure 6-5 shows a sample plot of a concrete mixture showing signs of corrosion failure as defined by ASTM G 109. Again each of the lines in the plot records the electrical current results of a single test specimen. This figure plots test specimens #1 thru #7 for Kapaa control mixture C5. All of the test specimens in this mixture eventually fall below the -10.00 µA limit. After a specimen has fallen below the corrosion limit, the specimen is monitored for another three ponding cycles. This is done to insure that the electrical current reading that indicated corrosion was accurate. Due to the large number of specimens being monitored, specimens were not always removed from cycling after three cycles of corrosion failure. After half of the specimens in a single mixture failed, the mixture was declared failed. For mixtures where 7 specimens were monitored, once 4 of the specimens exceeded the corrosion limit, the mixture had failed. For the mixtures where 4 total specimens were monitored, once two of the

specimens had reached the  $-10.00 \mu\text{A}$  limit, the mixture was declared failed. At this point, all remaining test specimens for that mixture were removed from cycling.

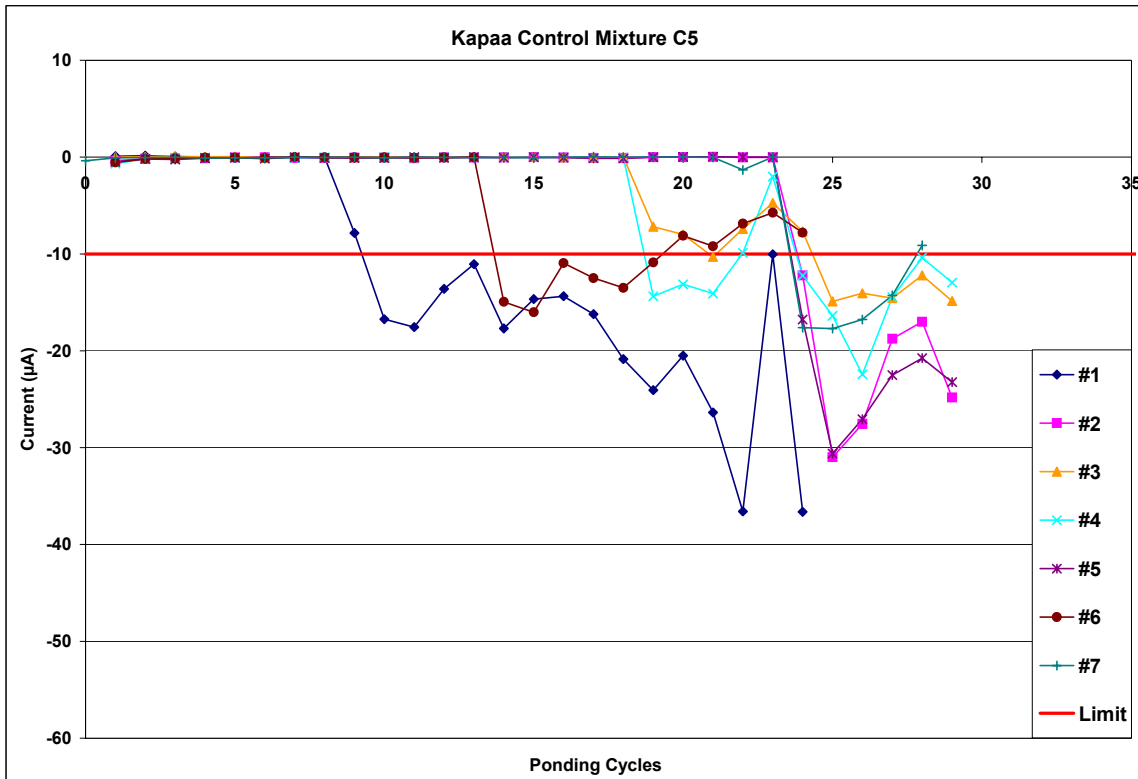


Figure 6-5: Example of Electrical Current Measurements Indicating Corrosion

#### 6.4.2 Half-Cell Potential Tests

The half-cell potential test results were plotted versus the number of saltwater ponding cycles, similar to the electrical current results. A sample plot of a typical mixture not showing signs of corrosion failure is shown in Figure 6-6. In this figure, test specimens #1 thru #7 are monitored for Kapaa control mixture C4 as a line on the graph. The green line at  $-200 \text{ mV}$  indicates the limiting half-cell potential value for a “low” probability of corrosion. All half-cell potential values above this  $-200 \text{ mV}$  limit indicate a 10% probability of corrosion. A horizontal line at  $-350 \text{ mV}$  indicates the limiting half-cell potential value for a “high” probability of corrosion. Half-cell potential values that

fall below the -350 mV limit indicate a “high” probability or 90% probability of corrosion. Readings between the -200mV and -350 mV limits indicate an “uncertain” probability of corrosion.

Figure 6-6 shows the majority of the half-cell potential readings before 15 ponding cycles fall above the -200 mV limit indicating a “low” probability of corrosion. However, there is significant scatter in the half-cell results indicating unreliable output. Sudden drops in half-cell readings occur at the same time as days in the electrical current readings. For example specimen #2 at 25 cycles and specimens #6 and #7 and 30 cycles. This agrees with the electrical current readings which indicated that no corrosion had begun during this period. As the ponding cycles increase and the specimens approach failure according to the electrical current results, the number of readings that fall in the “uncertain” region increase, indicating a greater potential for corrosion

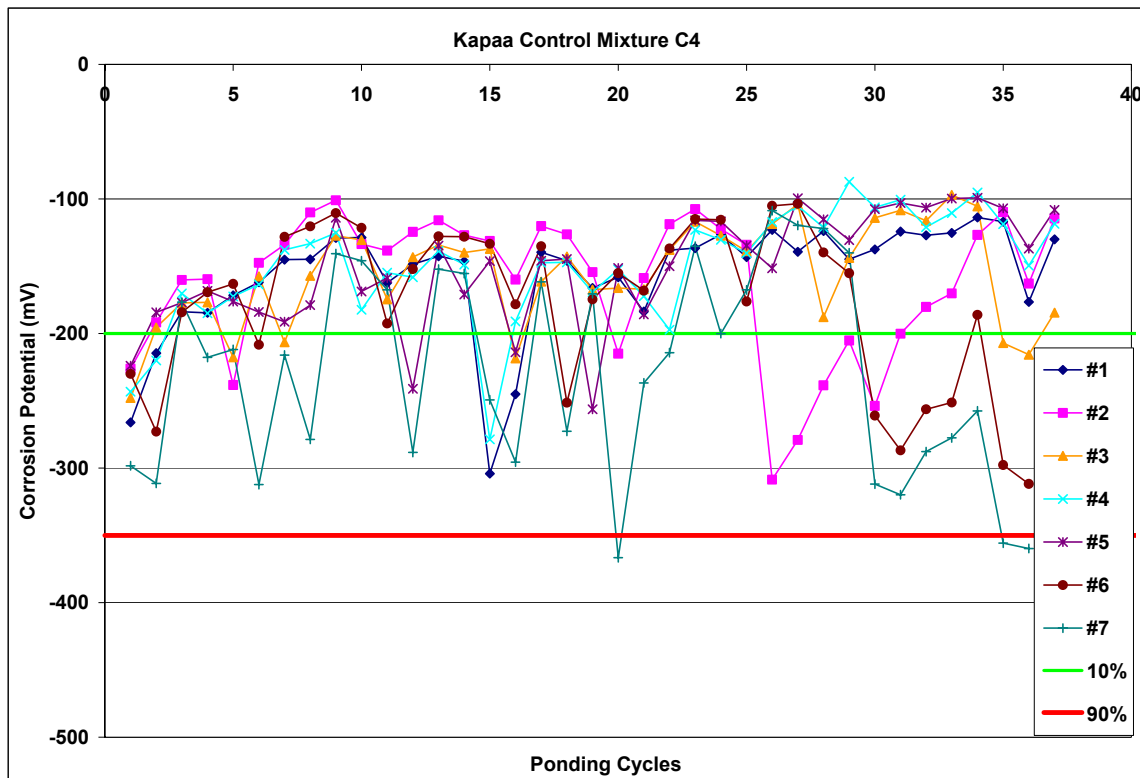


Figure 6-6: Example of Half-Cell Potential Measurements Not Indicating Corrosion

Figure 6-7 shows an example of a mixture with significant corrosion according to the half-cell potential results. The majority of the half-cell potential readings before 10 ponding cycles fall above the -200 mV limit indicating a “low” probability of corrosion. Again there is considerable scatter in these results in both the “10% probable corrosion” and the “uncertain” region. At approximately 12 ponding cycles specimen #1 shows a “high” probability of corrosion. By 25 cycles, more than half of the specimens have fallen below the -350 mV limit. A few cycles later this mixture was removed because more than half of the specimens had failed according to the electrical current results. The sudden drops in half-cell readings again correspond well with a drop in electrical current readings for the same specimen (Figure 6-5). Similar observations can be made of all of the half-cell potential plots included in Appendix A. It appears that the half-cell potential readings are consistent with the electrical current results.

A study by Kakuda (2004) involved breaking the test specimens open to visually inspect the reinforcing steel for corrosion. This study determined that the half-cell potential measurements were unconservative in detecting corrosion in the reinforcing steel. A high” probability of corrosion limit of -280 mV instead -350 mV limit set by the manufacturer was proposed. This limit appears to be more appropriate for as the majority of the half-cell potential measurements from specimens indicating corrosion in Figure 6-7 fall below the -280 mV limit.

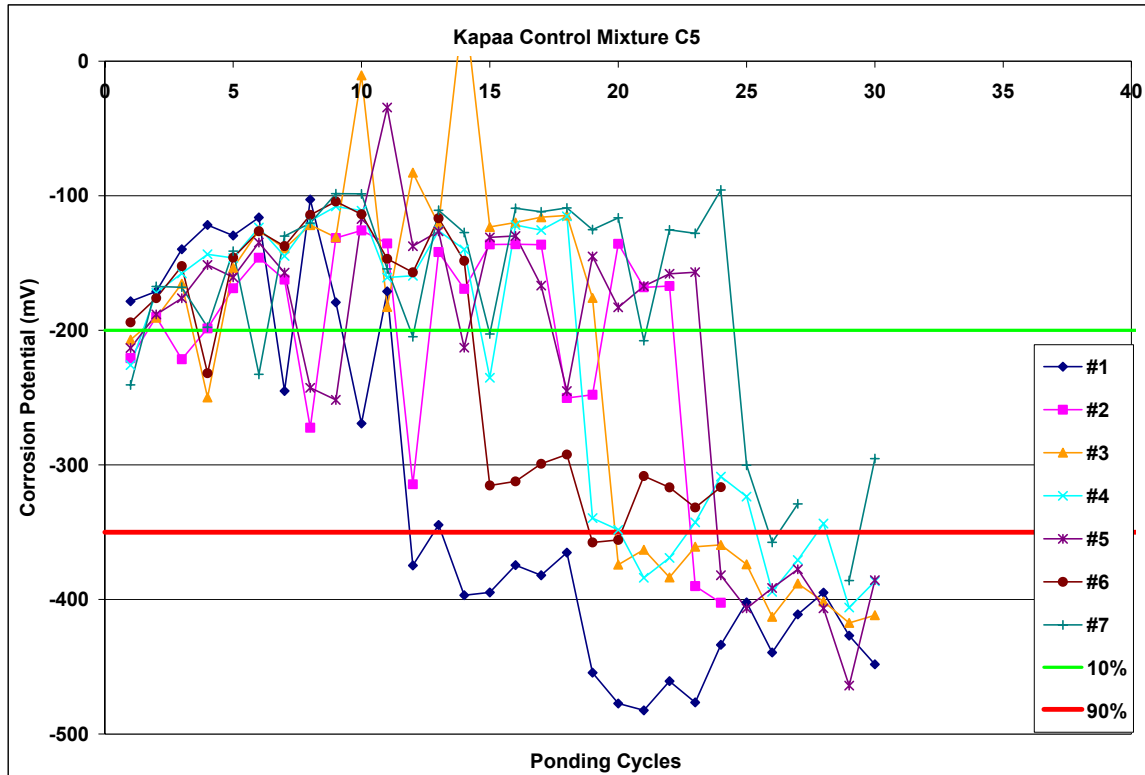


Figure 6-7: Example of Half-Cell Potential Measurements Indicating Corrosion

#### 6.4.3 Corrosion Rate Tests

The corrosion rate test results were plotted versus the number of saltwater ponding cycles, with individual test specimen results indicated by a line on each plot. A sample plot of Kapaa control mixture C4 in Figure 6-8 presents a typical mixture not showing signs of corrosion failure. In this figure, the horizontal line at  $0.2 \mu\text{A}/\text{cm}^2$  indicates the limiting corrosion rate value for “low” corrosion activity. The horizontal line at  $0.5 \mu\text{A}/\text{cm}^2$  indicates the limiting corrosion rate value for “moderate” corrosion activity, and the  $1.0 \mu\text{A}/\text{cm}^2$  line indicates the limiting corrosion rate value for “high” corrosion activity. All values below the  $0.2 \mu\text{A}/\text{cm}^2$  limit fall in the region indicating “no” corrosion activity. Values above  $0.2 \mu\text{A}/\text{cm}^2$ , but below  $0.5 \mu\text{A}/\text{cm}^2$  fall in the region of “low” corrosion activity. Values above  $0.5 \mu\text{A}/\text{cm}^2$ , but below  $1.0 \mu\text{A}/\text{cm}^2$  fall

in the region of “moderate” corrosion activity. Finally all values above the horizontal line at  $1.0 \mu\text{A}/\text{cm}^2$  fall in the region of “high” corrosion activity.

Figure 6-8 shows some of the initial readings fall in the “low” corrosion region however after the first few ponding cycles all but a few of the corrosion rate readings falling in the region indicating “no” corrosion activity. The values that do not fall in the “no” corrosion activity region fall only slightly above the  $0.2 \mu\text{A}/\text{cm}^2$  limit in the “low” corrosion region. The corrosion rate results in this plot agree the electrical current results which also show no corrosion activity has occurred in the specimens in this mixture.

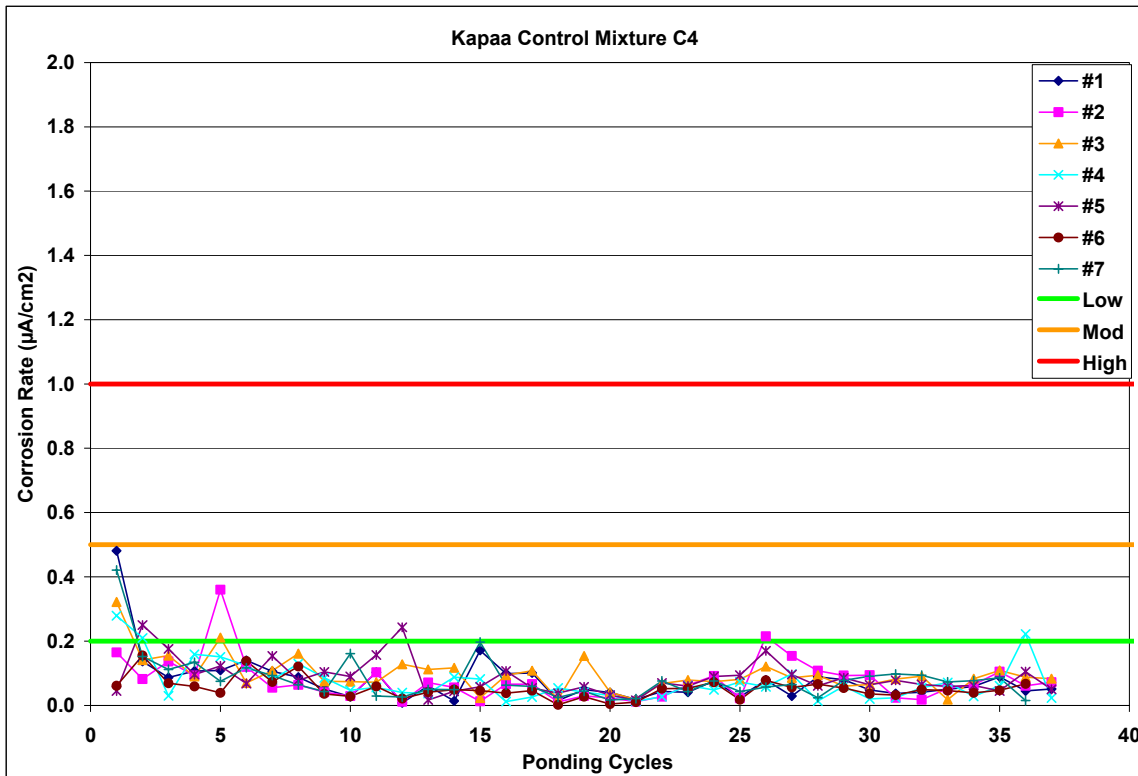


Figure 6-8: Example of Corrosion Rate Measurements Not Indicating Corrosion

Figure 6-9 presents an example of corrosion rate readings for a concrete mixture that shows significant corrosion activity. After a few of the initial readings, the majority of the values up to approximately 14 ponding cycles fall in the “no” corrosion region with a few values falling slightly above the  $0.2 \mu\text{A}/\text{cm}^2$  in the “low” corrosion region.

This would appear to be accurate as no corrosion should have occurred in the initial ponding cycles. After 20 ponding cycles, it appears that significant corrosion activity had occurred in two specimens (#6 and #7) since the corrosion rate readings rise to the “high” corrosion region. Also corrosion activity appears to occur in other specimens as the corrosion rate values increase significantly to the upper area of the “low” corrosion region.

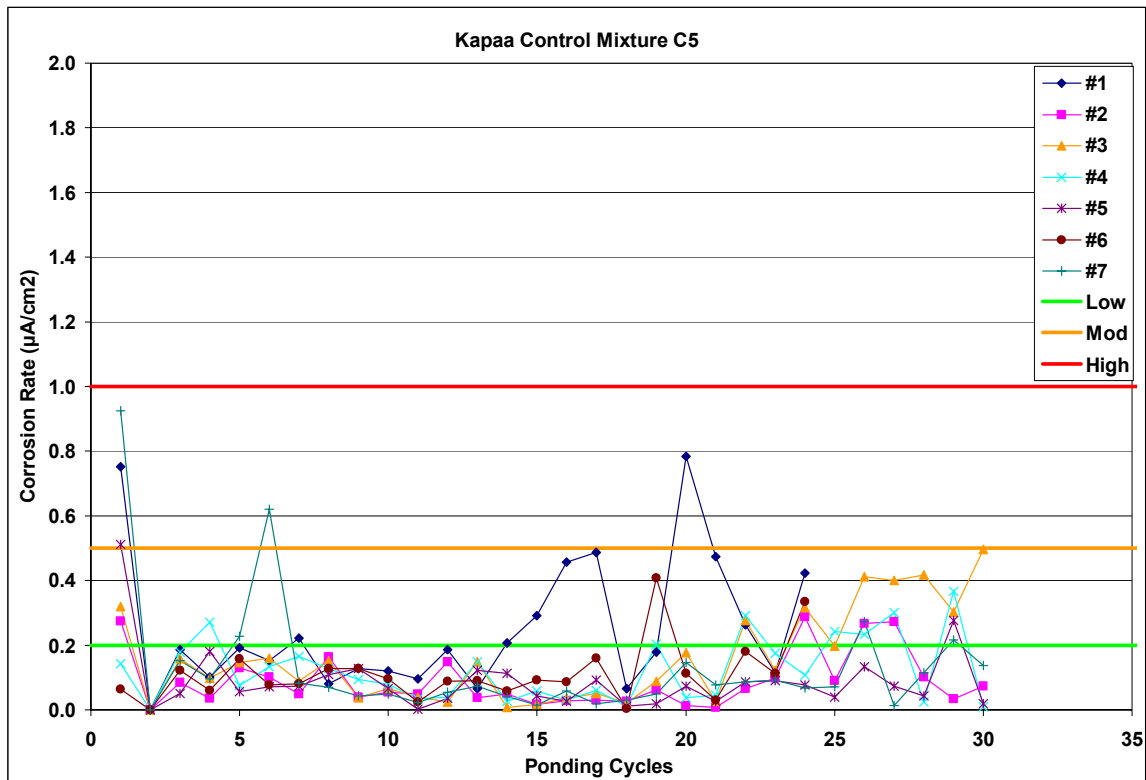


Figure 6-9: Example of Corrosion Rate Measurements Indicating Corrosion

#### 6.4.4 Concrete Resistivity Tests

The concrete resistivity test results were also plotted versus the number of saltwater ponding cycles, with individual test specimen results indicated by a line on each plot. It should be noted that a previous study (Bola and Newton 2000) as well as this study found that the concrete resistivity results did not show a direct correlation with the

electrical current results and the other electrical tests of the Gecor6 instrument. A sample plot of Kapaa control mixture C4 in Figure 6-10 presents a typical mixture not showing signs of corrosion failure according to the electrical current results. In this figure, the horizontal line at 20 kohm/cm indicates the limiting concrete resistivity value for a “low” corrosion activity. The horizontal line at 10 kohm/cm indicates the limiting concrete resistivity value for a “moderate” corrosion activity, and the 5 kohm/cm indicates the limiting corrosion rate value for a “high” corrosion activity. All values above the 20 kohm/cm limit fall in the region of “no” corrosion activity. Values below the 20 kohm/cm limit, but above the 10 kohm/cm fall in the region of “moderate/low” corrosion activity. Values below the 10 kohm/cm limit, but above the 5 kohm/cm fall in the region of “high” corrosion activity. Finally all values below the horizontal line limit of 5.0  $\mu\text{A}/\text{cm}^2$  fall in the region of “very high” corrosion activity.

Figure 6-10 shows the concrete resistivity readings for mixture C4 indicate high to very high corrosion during the early ponding cycles. However, the concrete resistivity results do not show any correlation to the electrical current results.

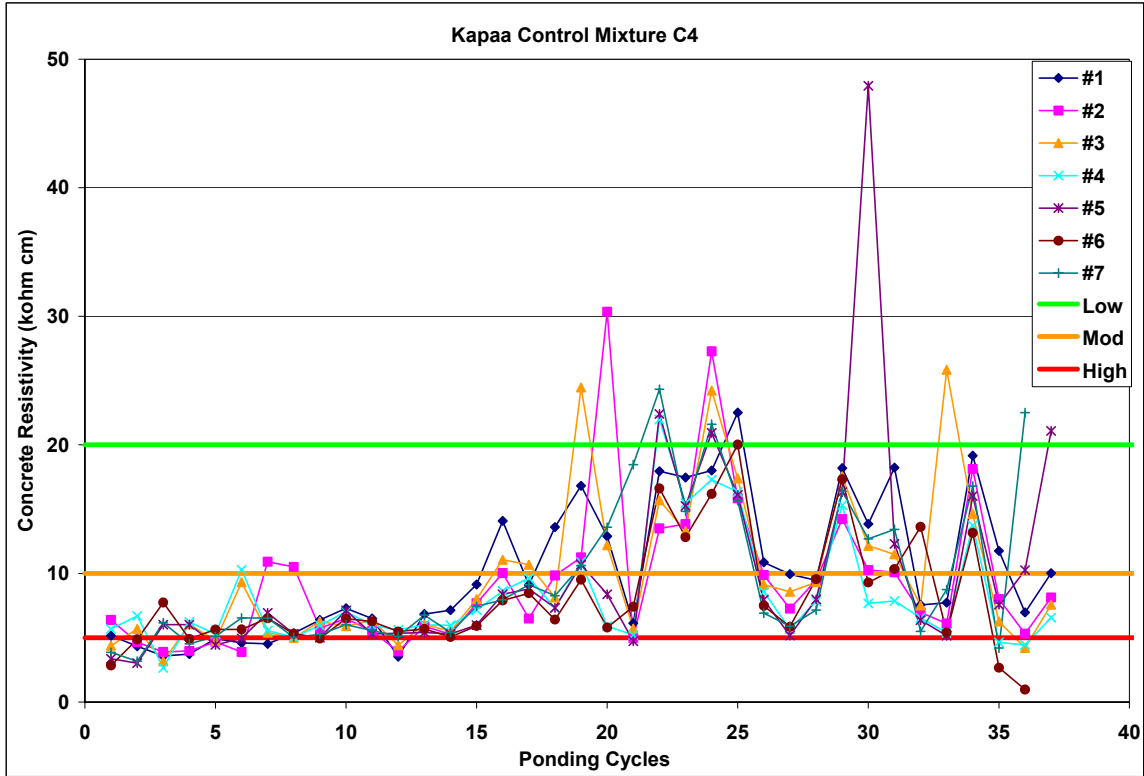


Figure 6-10: Example of Concrete Resistivity Measurements Not Indicating Corrosion

Figure 6-11 shows the concrete resistivity readings for mixture C5 that indicated significant corrosion and eventual failure of the mixture according to electrical current results. However, the concrete resistivity results do not show any correlation to the electrical current results. The majority of the concrete resistivity values fall in the “high” and “very high” corrosion region throughout all of the ponding cycles. Since the data does not show a change from “low” to “high” corrosion activity as the other Gecor6 test results, the concrete resistivity values do not appear to show any correlation with the other tests.

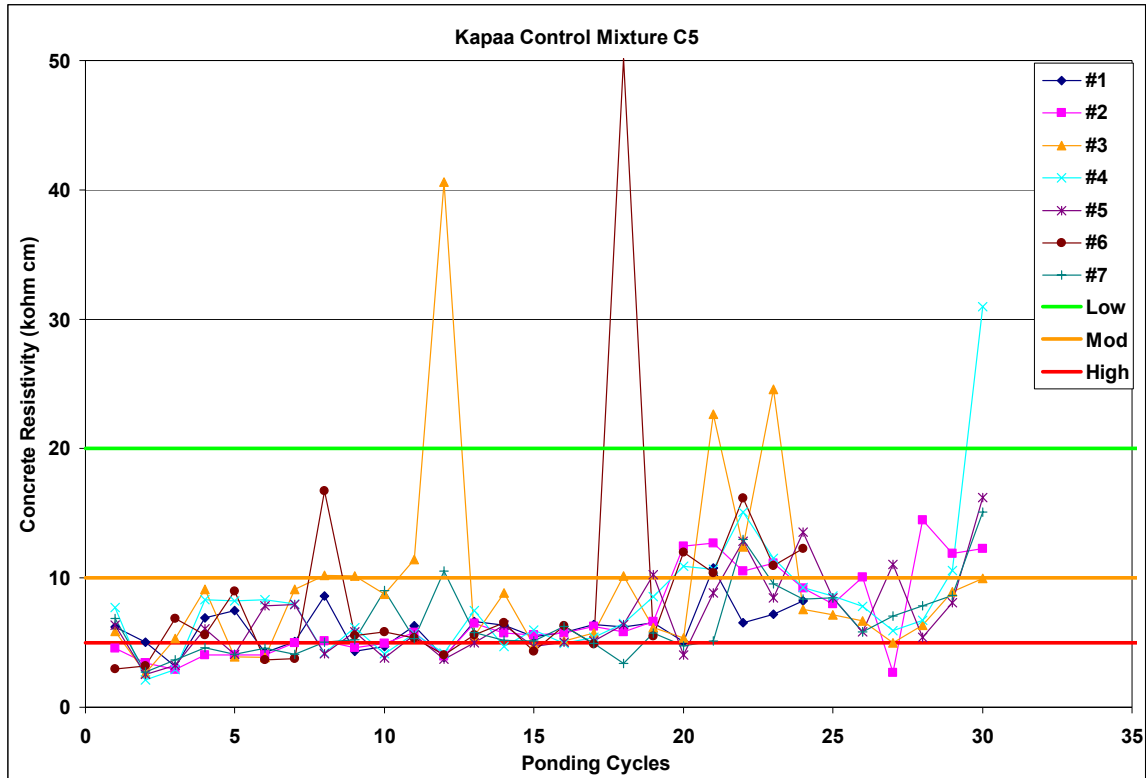


Figure 6-11: Example of Concrete Resistivity Measurements Indicating Corrosion

## 6.5 Ponding Cycles

This section discusses the final results of the electrical current tests, which determine when each mixture has reached its corrosion failure. Many of the mixtures are currently still cycling, however some initial observations can be made. All of the results presented are from measurements up to July 2004.

### 6.5.1 Control Mixtures

The ponding cycle results for both the Kapaa and Halawa control mixtures are shown in Figure 6-12. All of the control mixtures with w/c ratio of 0.45 have failed. The results show that all Kapaa mixtures outperformed their Halawa counterpart for the 0.35 w/c ratio control mixtures.

Control mixtures with w/c ratios equal to 0.4 however show completely different results. For these control mixtures, the Halawa mixtures outperformed their Kapaa equivalents. Halawa control mixture HC5, a 0.4 w/c ratio high paste mixture, is significantly outperforming its Kapaa equal. Except for mixture C2, 0.40 w/c ratio low paste mixture, all 0.4 w/c ratios with both Kapaa and Halawa aggregates have outperformed their 0.45 w/c counterpart.

No results between Kapaa and Halawa control mixtures with w/c ratios of 0.35 can be determined as only C1 has failed. All of these mixtures however have performed significantly better than their 0.4 and 0.45 w/c ratio equivalents. Of all of the Kapaa control mixtures, C4, w/c ratio 0.35 high paste, appears to be performing significantly better than the other Kapaa control mixtures.

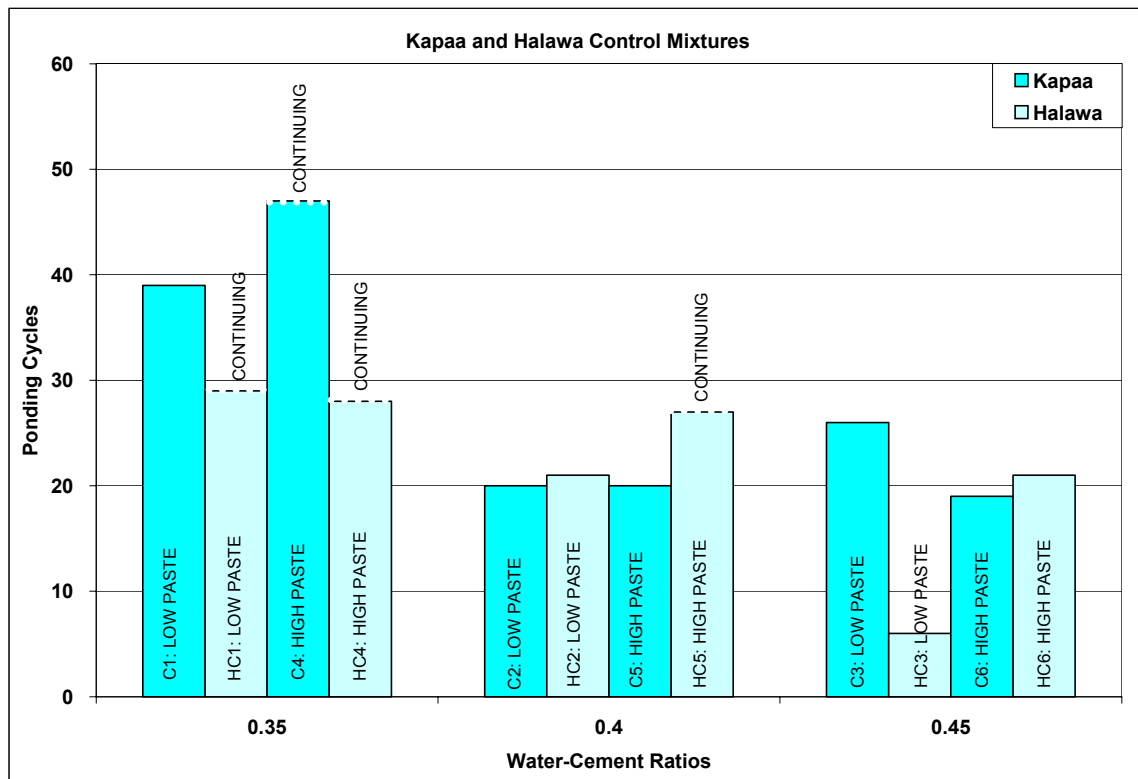


Figure 6-12: Ponding Cycle Results for Kapaa and Halawa Control Mixtures

### 6.5.2 Calcium Nitrite-Based Corrosion Inhibiting Admixtures

The ponding cycle results of the Kapaa DCI mixtures are shown in Figure 6-13.

The results show that DCI outperformed their control counterpart for the low paste mixtures with w/c ratios of 0.40 regardless of the DCI dosage. Mixture D4 that contained the smallest dosage of DCI (2 gal/yd<sup>3</sup>) failed first, while the remaining mixtures with higher DCI dosages have not yet failed.

DCI mixtures with high paste contents and w/c ratios of 0.35 however did not show similar results. D3 which contained the highest DCI dosage (6 gal/yd<sup>3</sup>) failed first, even before the control equivalent. The control mixture, C4, and lower DCI dosage mixtures, D1 and D2, are still cycling. It should be noted however that the DCI mixtures are performing the best among the Kapaa mixtures.

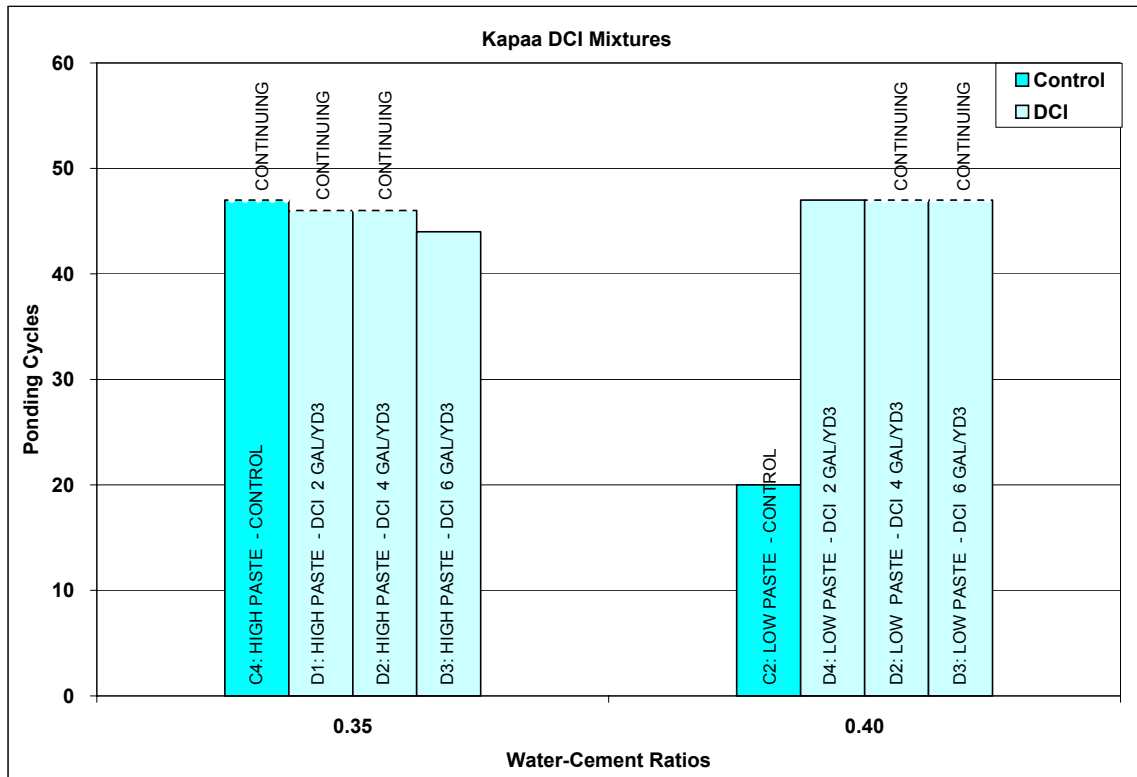


Figure 6-13: Ponding Cycle Results for Kapaa DCI Mixtures

The ponding cycle results of the Kapaa CNI mixtures are shown in Figure 6-14. Since the CNI admixture is practically identical to DCI, the same results were expected. The results show that CNI mixtures with low paste and w/c ratios of 0.40 performed significantly better than their control counterpart. No conclusion can be made as to how substantially better these mixtures performed because all three mixtures are still cycling. For mixtures with high paste contents and 0.35 w/c ratios no conclusions can be made because all Kapaa CNI mixtures and their control are still cycling in the laboratory conditions.

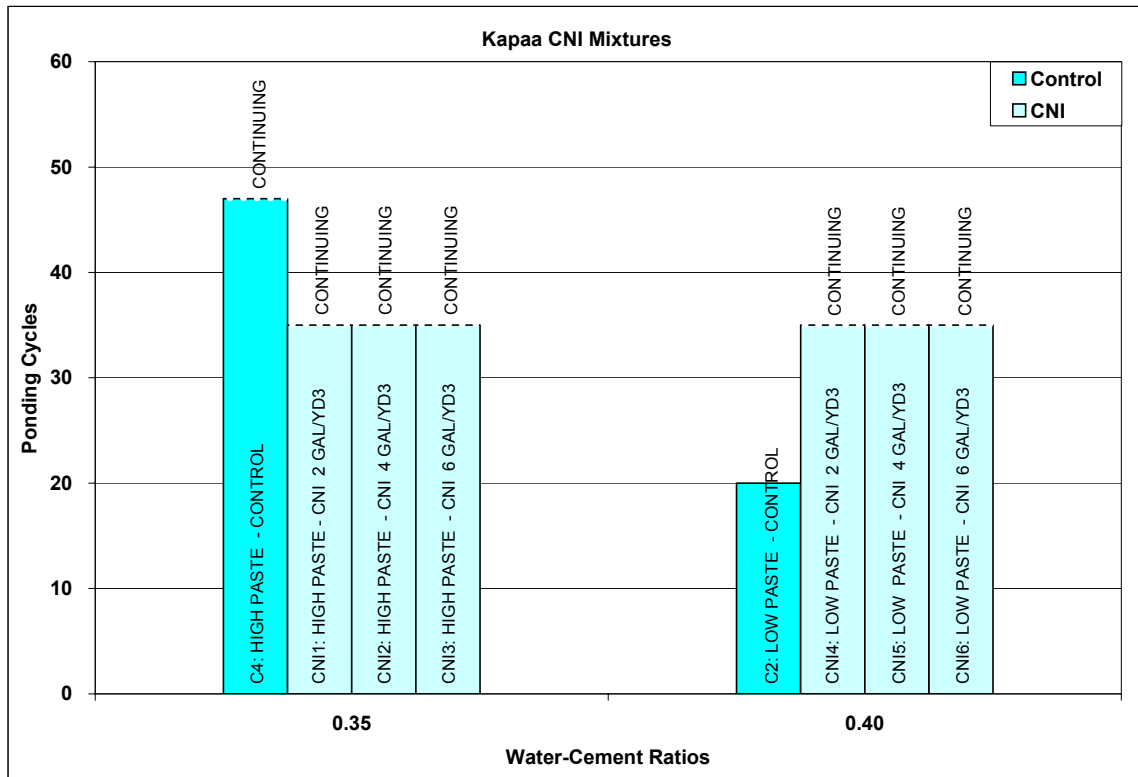


Figure 6-14: Ponding Cycle Results for Kapaa CNI Mixtures

Results showing the ponding cycles for the Halawa CNI mixtures are shown in Figure 6-15. Since the Halawa CNI mixtures are designed identical to the Kapaa CNI mixtures, similar results were expected. The Halawa CNI mixtures show the same results as their Kapaa CNI counterparts. The CNI mixtures with low paste and w/c ratios of 0.40

performed better than their control counterpart. No conclusion can be made as to how much better these mixtures performed because all three mixtures are still cycling. For mixtures with high paste content and 0.35 w/c ratio no conclusions can be made because all Kapaa CNI mixtures and their control are also still cycling in the laboratory testing conditions.

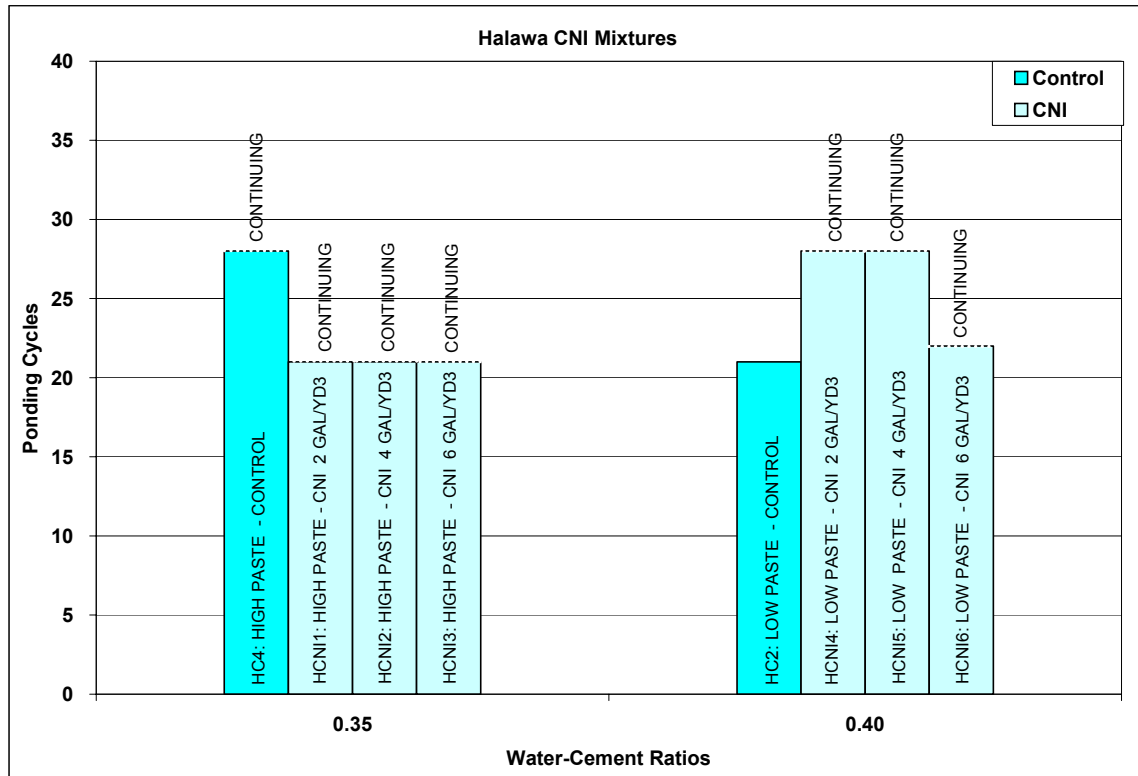


Figure 6-15: Ponding Cycle Results for Halawa CNI Mixtures

### 6.5.3 Rheocrete Mixtures

The dosage of Rheocrete 222+ in the Kapaa and Halawa Rheocrete mixtures was kept at a constant 1 gal/cy. The only variables between these mixtures are the three w/c ratios and the two paste volumes. The ponding cycle results for the Kapaa Rheocrete mixtures are shown in Figure 6-16. All of the Rheocrete mixtures are still cycling in the laboratory conditions, however the 0.40 and 0.45 w/c ratio control specimens have

already failed. For mixtures with 0.35 w/c ratios no conclusions can be made because the RHE1 has yet to surpass C1, and both C2 and RHE2 mixtures are also still cycling in the laboratory testing conditions.

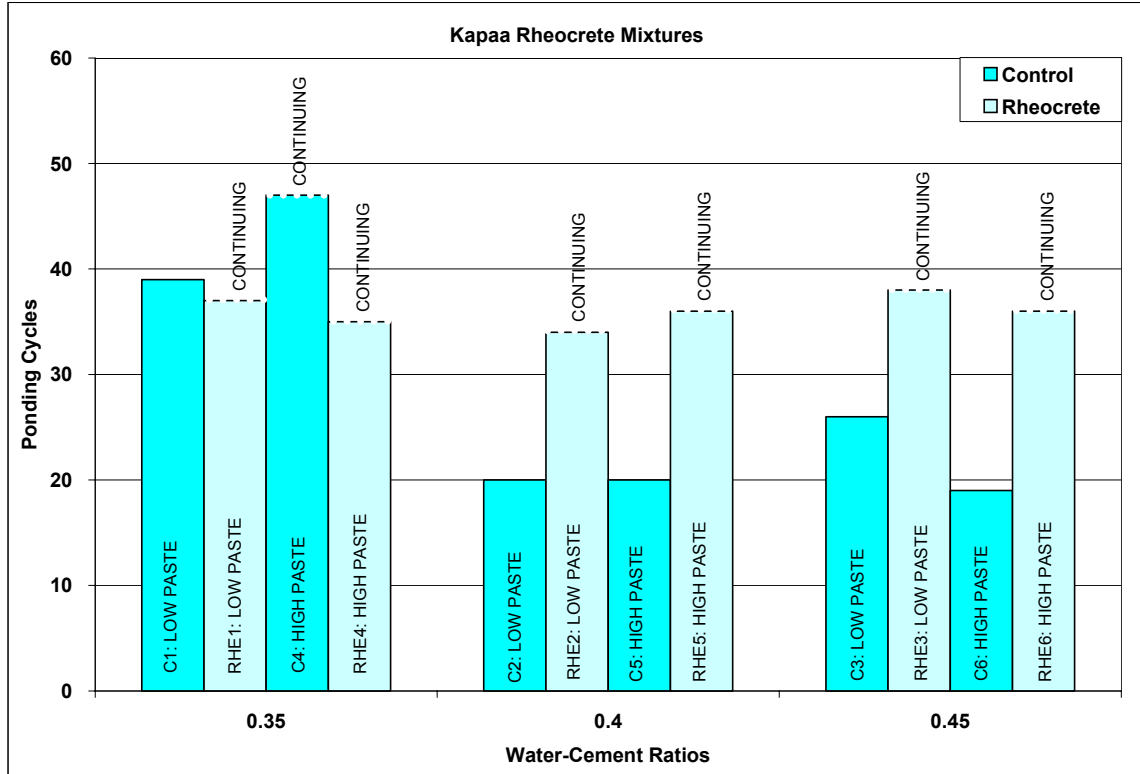


Figure 6-16: Pounding Cycle Results for Kapaa Rheocrete Mixtures

The pounding cycle results for the Rheocrete mixtures using Halawa aggregates are shown in Figure 6-17. No conclusions can be determined from the mixtures with 0.35 w/c ratio as HRHE1 and HRHE4 and their control equivalents HC1 and HC4 are still cycling under laboratory testing. The Rheocrete mixtures with w/c ratios of 0.40 and 0.45 both show the low paste mixtures performing better than the controls, however the high paste mixtures did not perform as well as their equivalent control mixtures. The data shows that HRHE5 performed significantly worse than HC5, while HRHE3 significantly surpassed HC3.

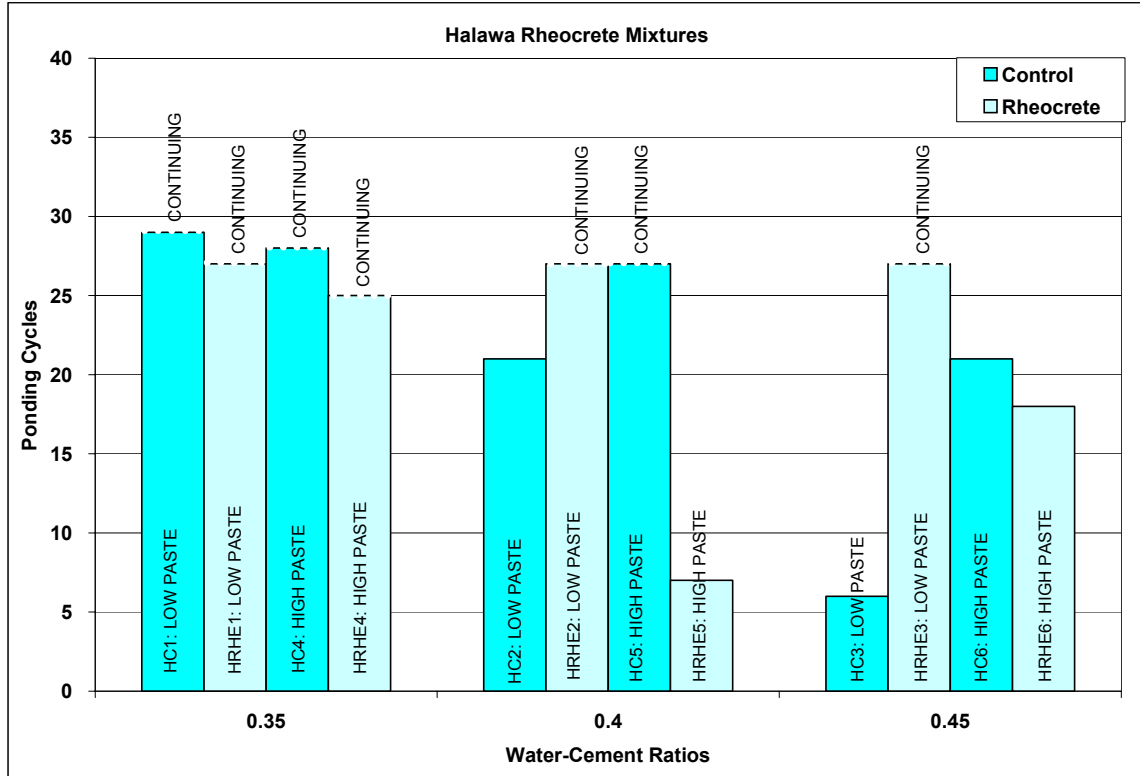


Figure 6-17: Ponding Cycle Results for Halawa Rheocrete Mixtures

#### 6.5.4 FerroGard Mixtures

Ponding cycle results for the FerroGard mixtures are shown in Figure 6-18. All but one of the Kapaa FerroGard mixtures is still cycling in the laboratory. The only mixture using this admixture to fail was FER6, a 0.45 w/c ratio high paste mixture. This mixture failed significantly faster than the other FerroGard mixtures, with a similar performance as the comparable control mixture C6. Results from this admixture show that four of the remaining five mixtures have already outperformed their control equals, which have failed. Only one FerroGard mixture has yet to outperform its control mixture. However, both C4 and FER4 are still cycling in the laboratory.

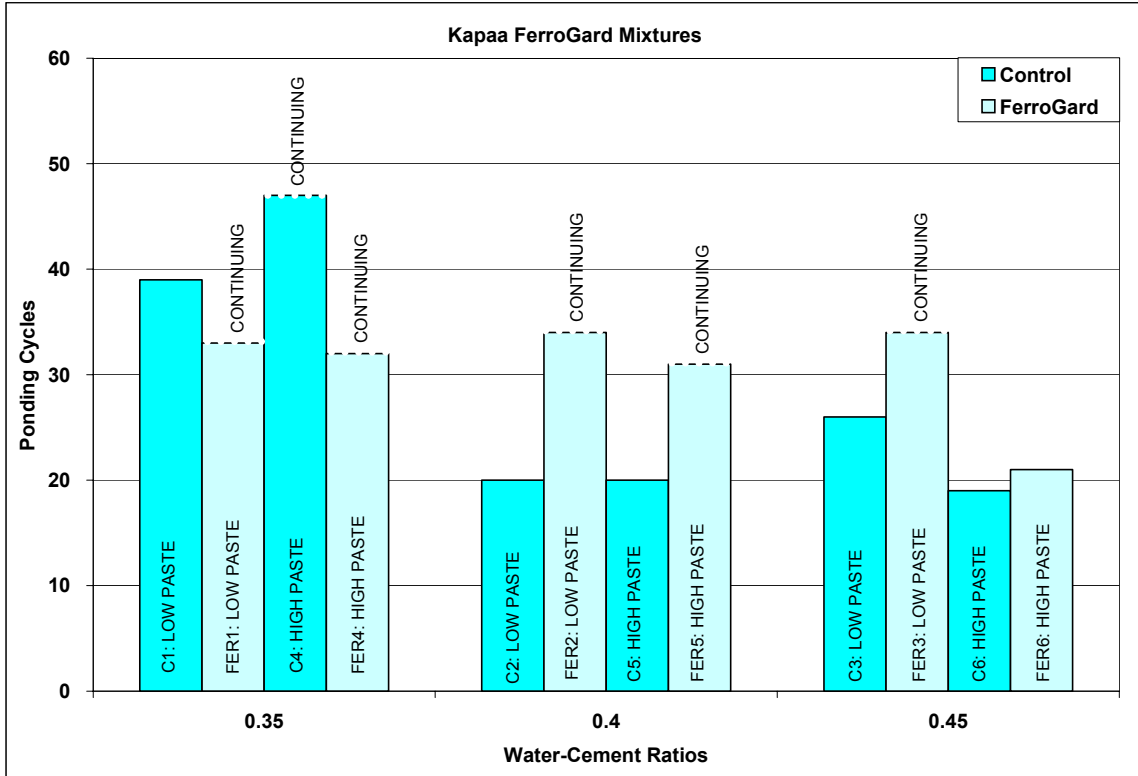


Figure 6-18: Ponding Cycle Results for Kapaa FerroGard Mixtures

### 6.5.5 Xypex Mixtures

Results showing the performance of Xypex mixtures with Kapaa aggregates are presented in Figure 6-19. The Xypex mixtures with w/c ratios of 0.35 severely underperformed their control counterparts. The Xypex mixtures with w/c ratios of 0.40 and 0.45 show mixed results with certain Xypex outperforming the control mixtures and others underperforming their control counterpart.

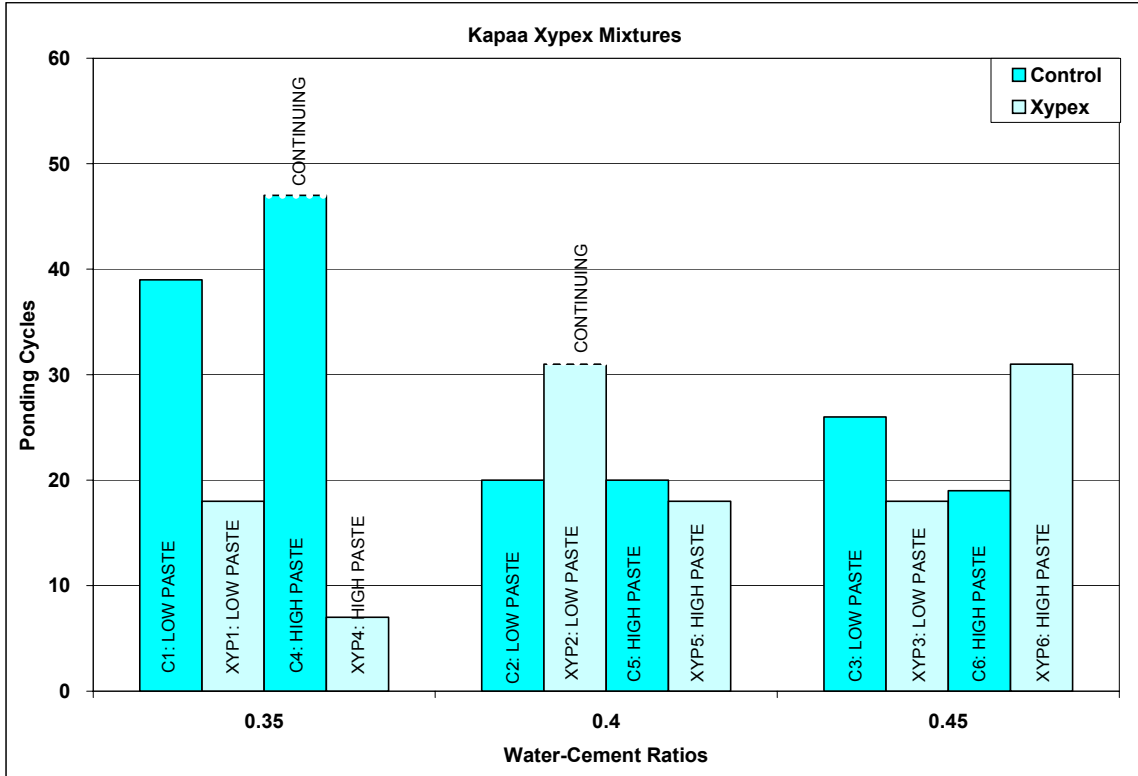


Figure 6-19: Ponding Cycle Results for Kapaa Xypex Mixtures

### 6.5.6 Latex Mixtures

The ponding cycle results for the latex mixtures using Kapaa aggregates are presented in Figure 6-20. No conclusions can be determined from the mixtures with 0.35 w/c ratios as L1 and L2 are still performing under laboratory testing, while L3 severely underperformed its control mixture equivalent. The latex mixtures with w/c ratios of 0.40 are significantly performing better than the control mixture and have yet to fail in the laboratory testing.

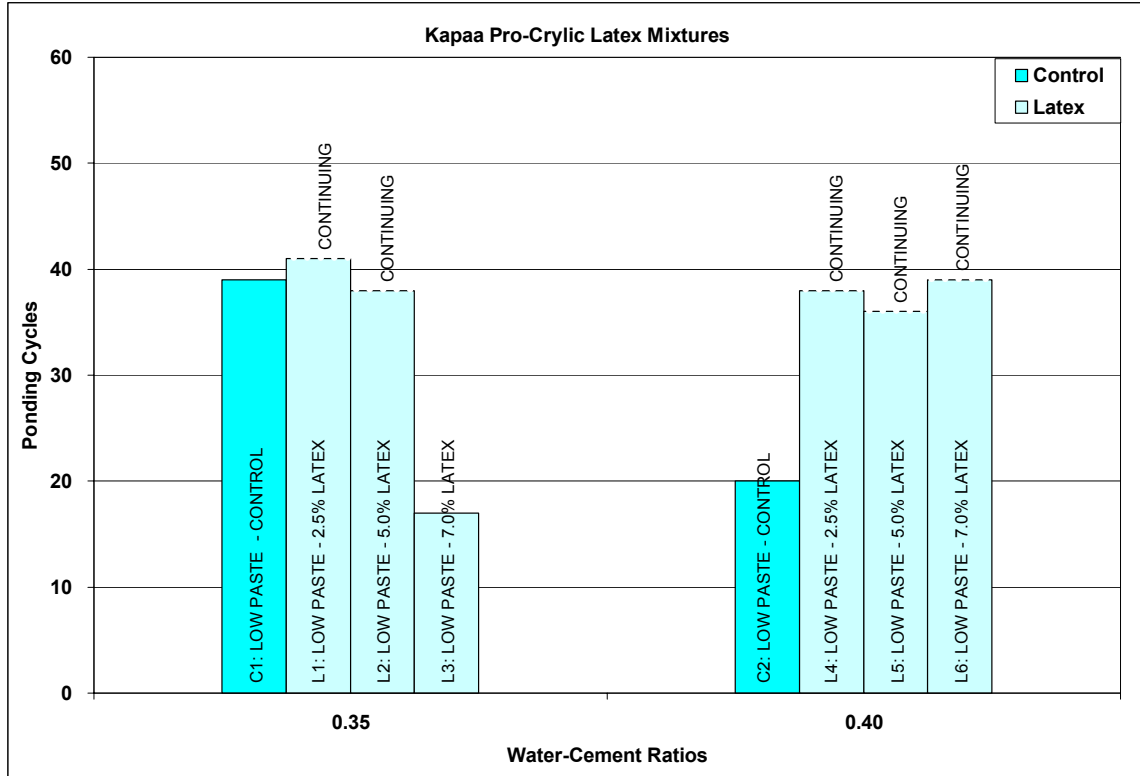


Figure 6-20: Ponding Cycle Results for Kapaa Latex Mixtures

### 6.5.7 Silica Fume Mixtures

Results of the silica fume mixtures using Kapaa aggregates are presented in Figure 6-21. No conclusions could be made from the silica fume mixtures with 0.36 w/c ratio that were modeled after the Ford Island Bridge mixtures because all of these mixtures are still cycling under laboratory conditions. The results show that silica fume mixtures designed according to the PCA guidelines with w/c ratios of 0.45 all outperformed their control counterparts. Four of the five mixtures are still cycling, so no conclusions can be made between mixtures with varying amounts of silica fume.

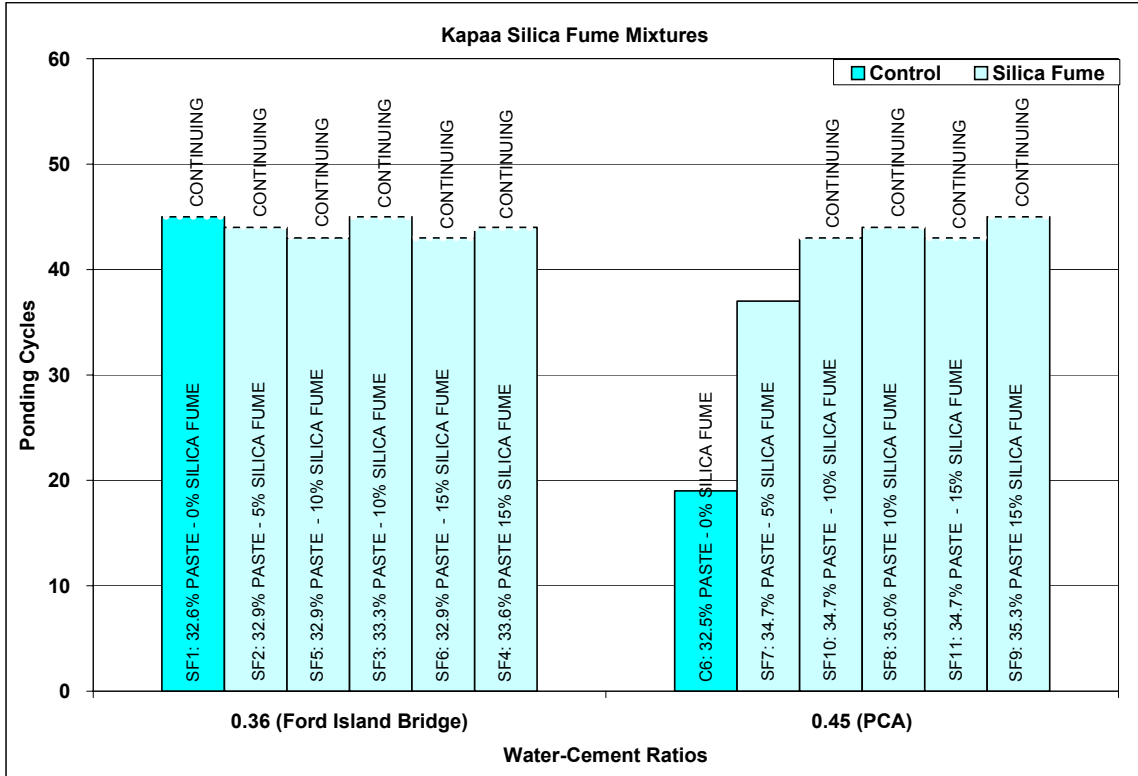


Figure 6-21: Ponding Cycle Results for Kapaa Silica Fume Mixtures

Results of the silica fume mixtures using Halawa aggregates are presented in Figure 6-22. The results show that silica fume mixtures designed according to PCA with w/c ratios of 0.45 outperformed their control counterpart regardless of the amount of silica fume. The three Halawa silica fume mixtures are still cycling, therefore no conclusions can be made regarding the amount of silica fume. All three of the silica fume mixtures with 0.36 w/c ratio that were modeled after the Ford Island Bridge mixture as well as the equivalent control mixture are still cycling. No conclusions could be made regarding these mixtures.

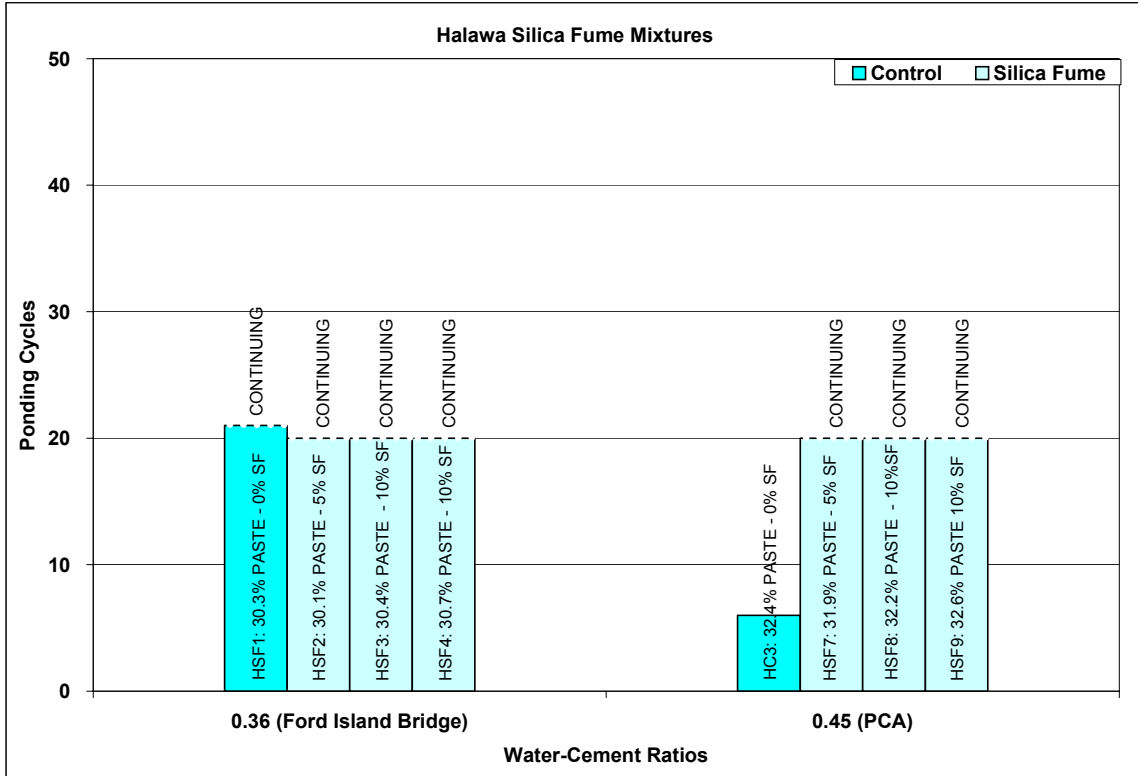


Figure 6-22: Ponding Cycle Results for Halawa Silica Fume Mixtures

### 6.5.8 Fly Ash Mixtures

Results of the fly ash mixtures using Kapaa aggregates are presented in Figure 6-23. No conclusions can be made regarding the fly ash mixtures with w/c ratios of 0.36 because most are still cycling in the laboratory testing. The results for the fly ash mixtures designed according to PCA with w/c ratios of 0.45 all outperformed their control counterpart regardless of the amount of fly ash.

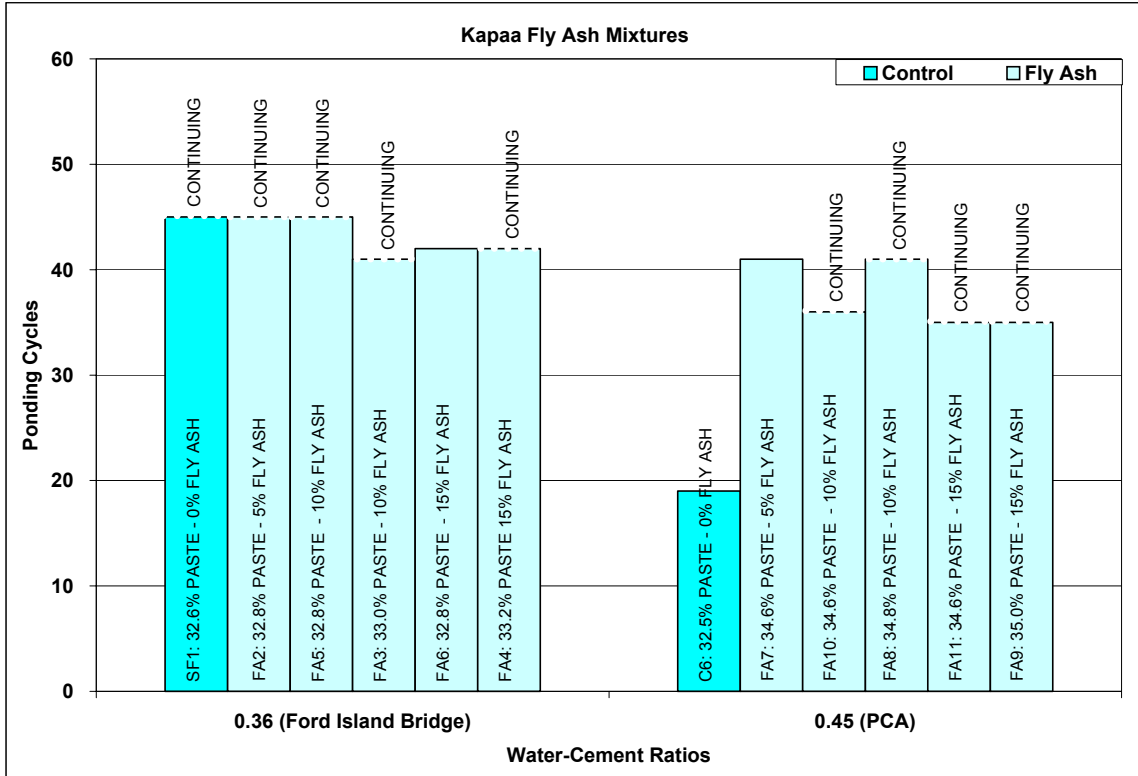


Figure 6-23: Ponding Cycle Results for Kapaa Fly Ash Mixtures

Results of the fly ash mixtures using Halawa aggregates are presented in Figure 6-24. No conclusions can be made regarding the fly ash mixtures with w/c ratios of 0.36 because all are still cycling in the laboratory testing. The results for the fly ash mixtures designed according to PCA with w/c ratios of 0.45 all outperformed their control counterparts regardless of the amount of fly ash.

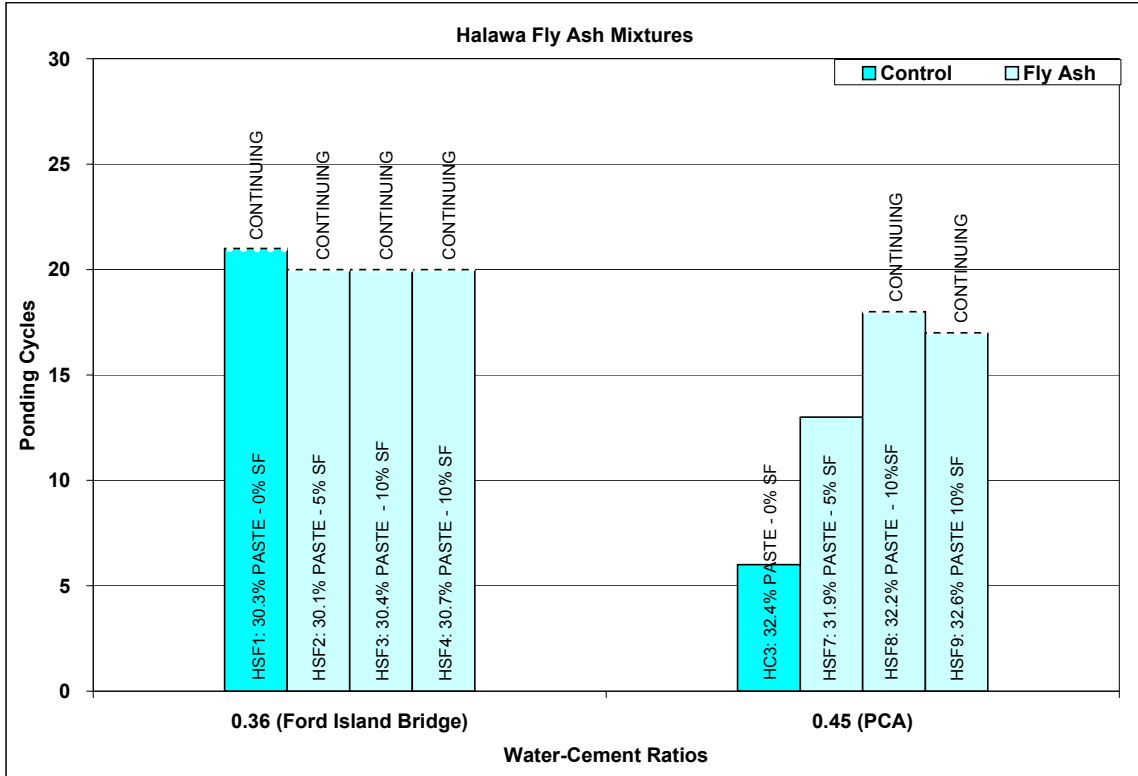


Figure 6-24: Pounding Cycle Results for Halawa Fly Ash Mixtures

## 6.6 Summary

This chapter began with a discussion of the accuracy of each of the electrical tests performed in this study. Also presented were descriptions of the layout and presentation of each of the different electrical tests. Finally using the electrical current results, which were assumed to be accurate, the life cycle results of each of the mixtures were presented.



## CHAPTER 7 SUMMARY AND CONCLUSIONS

### 7.1 Introduction

A study was performed to determine the protective qualities of various corrosion inhibiting admixtures. This chapter summarizes the findings of all of the mechanical, physical and electrical tests performed on these mixtures.

### 7.2 Summary

Compressive test results comparing Kapaa and Halawa control mixtures show that concrete using Halawa aggregates had lower compressive strengths than the same mixtures with Kapaa aggregates. The decrease in strength varied from 8% to 33% with the largest differences for mixtures with the higher water-to-cement ratios. The results also showed that the percentage decrease in compressive strength was similar for mixtures with both low and high paste contents. Compressive test results from the Kapaa and Halawa Rheocrete mixtures showed a similar trend.

The air permeability results were significantly lower than a previous study by Pham and Newtonson (2001). It was concluded that the significantly lower values were due to the added moisture in the concrete in the previous study. The air permeability tests in this study were performed on specimens that were allowed to dry for a significant amount of time before testing. The results of this study were similar to a previous field study by Bola and Newtonson (2000).

Air permeability tests performed on control, DCI, Ferrogard, Rheocrete and silica fume mixtures using Kapaa aggregates all recorded average protective qualities of “fair”. It was also noted that silica fume mixtures provided slightly better air permeability results, however these results still fell in the region indicating a “fair” protective quality. Half of

air permeability results of the latex mixtures using Kapaa aggregates recorded protective qualities lower than “fair”. Latex mixtures did not perform as well on the air permeability results.

Chloride concentration results for the control mixtures using Kapaa aggregates show that mixtures with higher paste contents provided better protection against the ingress of chlorides than their lower paste content counterparts. Also as the water-to-cement ratios were increased, the protection against chlorides reduced.

Chloride concentration results for the DCI mixtures with Kapaa aggregates show the same trend as the control mixtures. The protection against the ingress of chlorides is increased as the paste content increases and the water-to-cement ratio decreases.

Preliminary results of DCI mixtures with water-to-cement ratios of 0.40 show that as the dosage of DCI increases, the protection improves. Also the mixtures with water-to-cement ratios of 0.40 show that the low paste DCI mixtures provide better protection than the control mixture.

Chloride concentrations for the FerroGard, Rheocrete and Latex mixtures show an improvement in chloride protection when compared with their control counterparts.

Results for the silica fume mixtures showed a significant increase in chloride protection when 15% silica fume was added compared to the 5% and 10% counterparts.

The progression of pH values over the number of ponding cycles was plotted for control, DCI, Latex, and silica fume mixtures with Kapaa aggregates. All of the mixtures showed a similar trend with pH values dropping significantly from their initial values.

The final pH values all fall between 12.0 and 12.5, which is below the typical 12.5 value for normal concrete.

The accuracy of the electrical tests performed by the Gecor6 showed mixed results. The corrosion potential proved to be the most accurate of the tests. This test was 81% accurate in measuring corrosion, which was slightly lower than its stated 90% accuracy. However, the corrosion potential test was extremely accurate in predicting the absence of corrosion. Specimens that indicated a low probability of corrosion showed corrosion only 0.4% of the time, significantly lower than the stated 10%.

The corrosion rate tests with the Gecor6 proved to be accurate in predicting corrosion, however it appeared slightly conservative. Finally, no correlation could be determined with concrete resistivity readings in predicting corrosion. This was probably due to the fact that the specimens were saturated during the test, which can significantly affect the results.

Comparing the final ponding cycle results for the Halawa and Kapaa mixtures, early results show a significant improvement in mixtures with water-to-cement ratios of 0.35 when compared to their 0.40 and 0.45 counterparts.

Comparing the ponding cycle results for Kapaa DCI and CNI mixtures, the addition of the calcium nitrate provides a significant improvement over the control mixtures for water-to-cement ratios of 0.40. Also Halawa mixtures using CNI showed the same results.

Preliminary ponding cycle results for the Rheocrete mixtures showed a significant improvement in the Kapaa mixtures when compared to their control counterparts. Rheocrete mixtures using Halawa aggregates however show mixed results and many of these mixtures are still cycling.

Preliminary ponding cycle results for the Kapaa FerroGard mixtures show that the addition of FerroGard provides significantly better results when compared to their control counterparts.

Preliminary ponding cycle results for the Kapaa Latex mixtures show that the addition of latex significantly improves the life of the majority of the mixtures when compared to their control counterpart.

Xypex mixtures with Kapaa aggregates show mixed results when compared to their control counterparts. The majority of the mixtures show results lower than their control counterparts. The Xypex mixtures with water-to-cement ratios of 0.35 performed significantly worse than their control counterparts. It was assumed that this admixture may have not properly consolidated during the mixing.

Preliminary ponding cycle results for the Kapaa and Halawa mixtures with silica fume show these mixtures performing significantly better than their control counterparts. Kapaa and Halawa mixtures with fly ash also show a similar significant improvement in protection against corrosion. This shows that the addition of pozzolans in a concrete mixture can greatly improve the corrosion protection of a concrete mixture.

### **7.3 Conclusions**

1. Concrete using Halawa aggregates had a lower compressive strength than the same mixtures with Kapaa aggregates.
2. The majority of the Kapaa specimens had air permeability results indicating “Fair” performance. However, Latex mixtures did not perform as well on the air permeability results.

3. Mixtures with high paste contents typically had lower chloride concentrations than their low paste counterparts.
4. The pH level at the level of the reinforcing steel dropped from 12.5 to 12.8 to between 12.0 and 12.5 as the number of ponding cycles increased.
5. Correlation of the electrical current and half-cell potential measurements indicated that the half-cell potential readings were accurate in detecting both the absence of corrosion and significant corrosion in the test specimens.
6. Correlation of the electrical current and corrosion rate by linear polarization measurements indicated that the corrosion rate measurements were slightly unconservative in determining significant corrosion in the test specimens.
7. Correlation of the electrical current and concrete resistivity measurements indicated that the concrete resistivity measurements were inconclusive in determining if significant corrosion was occurring in the test specimens.
8. The results of the electrical current tests show that concrete mixtures with w/c ratios of 0.35 or 0.36 performed significantly better than their 0.4 and 0.45 counterparts
9. Preliminary ponding cycles show mixtures using corrosion inhibiting admixtures, except for Xypex mixtures, typically outperformed their control counterparts.
10. The addition of pozzolans (silica fume and fly ash) in a concrete mixture can greatly improve the corrosion protection.



## REFERENCES

- ACI, (2002). *Building Code Requirements for Structural Concrete (318-02) and Commentary (318R-02)*, American Concrete Institute.
- ASTM, (1997). *1997 Annual Book of ASTM Standards*, Easton, Maryland.
- Bola, M. and Newton, C. (2001). "Field Evaluation of Corrosion in Reinforced Concrete Structures in Marine Environment," UHM/CE/00-01.
- Bonded, (2004). "Pro-Crylic" Preliminary Data Sheet, Bonded Materials Co., Honolulu, Hawaii.
- Degussa, (2002). "Rheobuild 1000" Product Information, Master Builders, Inc., [www.masterbuilders.com](http://www.masterbuilders.com).
- Degussa, (2002). "Rheocrete 222+" Product Information, Master Builders, Inc., [www.masterbuilders.com](http://www.masterbuilders.com).
- Degussa, (2002). "Rheocrete CNI" Product Information, Master Builders, Inc., [www.masterbuilders.com](http://www.masterbuilders.com).
- Degussa, (2005). "Rheomac SF100" Product Information, Master Builders, Inc., [www.masterbuilders.com](http://www.masterbuilders.com).
- Gaidis, James M., (2003), "Chemistry of Corrosion Inhibitors," *Cement and Concrete Composites*,
- Grace, (2002). "Daracem 19" Product Information, W.R. Grace & Co.-Conn., [www.graceconstruction.com](http://www.graceconstruction.com).
- Grace, (2002). *Engineering Bulletin 1: Force 10,000, Force 10,000 Microsilica and its uses in Concrete*, W.R. Grace & Co.-Conn., [www.graceconstruction.com](http://www.graceconstruction.com).
- Grace, (2003). "Darex II AEA" Product Information, W.R. Grace & Co.-Conn., [www.graceconstruction.com](http://www.graceconstruction.com).
- Grace, (2003). *Engineering Bulletin 1: DCI, What is Corrosion?*, W.R. Grace & Co.-Conn., [www.graceconstruction.com](http://www.graceconstruction.com).
- Grace, (2003). *Engineering Bulletin 2: DCI, DCI Dosage Rates and ACI Guidelines*, W.R. Grace & Co.-Conn., [www.graceconstruction.com](http://www.graceconstruction.com).
- Grace, (2003). *Engineering Bulletin 3: DCI, The Effects of DCI on the Corrosion Rates of Steel in Concrete*, W.R. Grace & Co.-Conn., [www.graceconstruction.com](http://www.graceconstruction.com).

Grace, (2003). *Engineering Bulletin 5: DCI, How DCI Works*, W.R. Grace & Co.-Conn., [www.graceconstruction.com](http://www.graceconstruction.com).

Kakuda, Donn., (2004). "Examination of Steel Reinforcing Bar Corrosion in Concrete Using Optical and Acoustic Microscopy," University of Hawaii at Manoa.

Kosmatka, Steven H., and Panarese, William C., (1994). "Design and Control of Concrete Mixtures 13<sup>th</sup> Edition," Portland Cement Association.

Phong P. and Newton, C., (2001). "Properties of Concrete Produced With Admixtures Intended to Inhibit Corrosion," UHM/CE/01-01.

Poroscope, (1998). "Poroscope Plus," James Instruments, Inc., Chicago Illinois.

Sika, (2003), "Sika FerroGard 901: Corrosion Inhibiting Admixture" Product Data Sheet, Sika Corp., [www.sikausa.com](http://www.sikausa.com)

Uno, John., (2004). "Corrosion Susceptibility of Concrete Exposed to a Marine Environment," University of Hawaii at Manoa.

## **APPENDIX**



## A.1 List of Appendix Figures

Figure A.1-1: Current Measurements for Kapaa Control Mixture C1.....	145
Figure A.1-2: Corrosion Potential Measurements for Kapaa Control Mixture C1.....	145
Figure A.1-3: Corrosion Rate Measurements for Kapaa Control Mixture C1 .....	146
Figure A.1-4: Corrosion Resistivity Measurements for Kapaa Control Mixture C1.....	146
Figure A.1-5: Current Measurements for Kapaa Control Mixture C2.....	147
Figure A.1-6: Corrosion Potential Measurements for Kapaa Control Mixture C2.....	147
Figure A.1-7: Corrosion Rate Measurements for Kapaa Control Mixture C2 .....	148
Figure A.1-8: Corrosion Resistivity Measurements for Kapaa Control Mixture C2.....	148
Figure A.1-9: Current Measurements for Kapaa Control Mixture C3.....	149
Figure A.1-10: Corrosion Potential Measurements for Kapaa Control Mixture C3.....	149
Figure A.1-11: Corrosion Rate Measurements for Kapaa Control Mixture C3 .....	150
Figure A.1-12: Corrosion Resistivity Measurements for Kapaa Control Mixture C3.....	150
Figure A.1-13: Current Measurements for Kapaa Control Mixture C4.....	151
Figure A.1-14: Corrosion Potential Measurements for Kapaa Control Mixture C4.....	151
Figure A.1-15: Corrosion Rate Measurements for Kapaa Control Mixture C4 .....	152
Figure A.1-16: Corrosion Resistivity Measurements for Kapaa Control Mixture C4.....	152
Figure A.1-17: Current Measurements for Kapaa Control Mixture C5.....	153
Figure A.1-18: Corrosion Potential Measurements for Kapaa Control Mixture C5.....	153
Figure A.1-19: Corrosion Rate Measurements for Kapaa Control Mixture C5 .....	154
Figure A.1-20: Corrosion Resistivity Measurements for Kapaa Control Mixture C5.....	154
Figure A.1-21: Current Measurements for Kapaa Control Mixture C6.....	155
Figure A.1-22: Corrosion Potential Measurements for Kapaa Control Mixture C6.....	155

Figure A.1-23: Corrosion Rate Measurements for Kapaa Control Mixture C6 .....	156
Figure A.1-24: Corrosion Resistivity Measurements for Kapaa Control Mixture C6.....	156
Figure A.1-25: Current Measurements for Halawa Control Mixture HC1.....	157
Figure A.1-26: Current Measurements for Halawa Control Mixture HC2.....	157
Figure A.1-27: Current Measurements for Halawa Control Mixture HC3.....	158
Figure A.1-28: Current Measurements for Halawa Control Mixture HC4.....	158
Figure A.1-29: Current Measurements for Halawa Control Mixture HC5.....	159
Figure A.1-30: Current Measurements for Halawa Control Mixture HC6.....	159
Figure A.1-31: Current Measurements for Kapaa DCI Mixture D1.....	160
Figure A.1-32: Corrosion Potential Measurements for Kapaa DCI Mixture D1.....	160
Figure A.1-33: Corrosion Rate Measurements for Kapaa DCI Mixture D1.....	161
Figure A.1-34: Corrosion Resistivity Measurements for Kapaa DCI Mixture D1.....	161
Figure A.1-35: Current Measurements for Kapaa DCI Mixture D2.....	162
Figure A.1-36: Corrosion Potential Measurements for Kapaa DCI Mixture D2.....	162
Figure A.1-37: Corrosion Rate Measurements for Kapaa DCI Mixture D2.....	163
Figure A.1-38: Corrosion Resistivity Measurements for Kapaa DCI Mixture D2.....	163
Figure A.1-39: Current Measurements for Kapaa DCI Mixture D3.....	164
Figure A.1-40: Corrosion Potential Measurements for Kapaa DCI Mixture D3.....	164
Figure A.1-41: Corrosion Rate Measurements for Kapaa DCI Mixture D3.....	165
Figure A.1-42: Corrosion Resistivity Measurements for Kapaa DCI Mixture D3.....	165
Figure A.1-43: Current Measurements for Kapaa DCI Mixture D4.....	166
Figure A.1-44: Corrosion Potential Measurements for Kapaa DCI Mixture D4.....	166
Figure A.1-45: Corrosion Rate Measurements for Kapaa DCI Mixture D4.....	167

Figure A.1-46: Corrosion Resistivity Measurements for Kapaa DCI Mixture D4.....	167
Figure A.1-47: Current Measurements for Kapaa DCI Mixture D5.....	168
Figure A.1-48: Corrosion Potential Measurements for Kapaa DCI Mixture D5.....	168
Figure A.1-49: Corrosion Rate Measurements for Kapaa DCI Mixture D5.....	169
Figure A.1-50: Corrosion Resistivity Measurements for Kapaa DCI Mixture D5.....	169
Figure A.1-51: Current Measurements for Kapaa DCI Mixture D6.....	170
Figure A.1-52: Corrosion Potential Measurements for Kapaa DCI Mixture D6.....	170
Figure A.1-53: Corrosion Rate Measurements for Kapaa DCI Mixture D6.....	171
Figure A.1-54: Corrosion Resistivity Measurements for Kapaa DCI Mixture D6.....	171
Figure A.1-55: Current Measurements for Kapaa CNI Mixture CNI1.....	172
Figure A.1-56: Corrosion Potential Measurements for Kapaa CNI Mixture CNI1.....	172
Figure A.1-57: Corrosion Rate Measurements for Kapaa CNI Mixture CNI1.....	173
Figure A.1-58: Corrosion Resistivity Measurements for Kapaa CNI Mixture CNI1.....	173
Figure A.1-59: Current Measurements for Kapaa CNI Mixture CNI2.....	174
Figure A.1-60: Corrosion Potential Measurements for Kapaa CNI Mixture CNI2.....	174
Figure A.1-61: Corrosion Rate Measurements for Kapaa CNI Mixture CNI 2.....	175
Figure A.1-62: Corrosion Resistivity Measurements for Kapaa CNI Mixture CNI2.....	175
Figure A.1-63: Current Measurements for Kapaa CNI Mixture CNI3.....	176
Figure A.1-64: Corrosion Potential Measurements for Kapaa CNI Mixture CNI3.....	176
Figure A.1-65: Corrosion Rate Measurements for Kapaa CNI Mixture CNI3.....	177
Figure A.1-66: Corrosion Resistivity Measurements for Kapaa CNI Mixture CNI3.....	177
Figure A.1-67: Current Measurements for Kapaa CNI Mixture CNI4.....	178
Figure A.1-68: Corrosion Potential Measurements for Kapaa CNI Mixture CNI4.....	178

Figure A.1-69: Corrosion Rate Measurements for Kapaa CNI Mixture CNI4.....	179
Figure A.1-70: Corrosion Resistivity Measurements for Kapaa CNI Mixture CNI4.....	179
Figure A.1-71: Current Measurements for Kapaa CNI Mixture CNI5.....	180
Figure A.1-72: Corrosion Rate Measurements for Kapaa CNI Mixture CNI5.....	180
Figure A.1-73: Corrosion Potential Measurements for Kapaa CNI Mixture CNI5.....	181
Figure A.1-74: Corrosion Resistivity Measurements for Kapaa CNI Mixture CNI5.....	181
Figure A.1-75: Current Measurements for Kapaa CNI Mixture CNI6.....	182
Figure A.1-76: Corrosion Rate Measurements for Kapaa CNI Mixture CNI6.....	182
Figure A.1-77: Corrosion Potential Measurements for Kapaa CNI Mixture CNI6.....	183
Figure A.1-78: Corrosion Resistivity Measurements for Kapaa CNI Mixture CNI6.....	183
Figure A.1-79: Current Measurements for Halawa CNI Mixture HCNI1 .....	184
Figure A.1-80: Current Measurements for Halawa CNI Mixture HCNI2.....	184
Figure A.1-81: Current Measurements for Halawa CNI Mixture HCNI3 .....	185
Figure A.1-82: Current Measurements for Halawa CNI Mixture HCNI4.....	185
Figure A.1-83: Current Measurements for Halawa CNI Mixture HCNI5 .....	186
Figure A.1-84: Current Measurements for Halawa CNI Mixture HCNI6.....	186
Figure A.1-85: Current Measurements for Kapaa FerroGard Mixture FER1 .....	187
Figure A.1-86: Corrosion Potential Measurements for Kapaa Ferrogard Mixture FER1 .....	187
Figure A.1-87: Corrosion Rate Measurements for Kapaa Ferrogard Mixture FER1 .....	188
Figure A.1-88: Corrosion Resistivity Measurements for Kapaa Ferrogard Mixture FER1 .....	188
Figure A.1-89: Current Measurements for Kapaa FerroGard Mixture FER2 .....	189

Figure A.1-90: Corrosion Potential Measurements for Kapaa Ferrogard Mixture	
FER2 .....	189
Figure A.1-91: Corrosion Rate Measurements for Kapaa Ferrogard Mixture FER2 .....	190
Figure A.1-92: Corrosion Resistivity Measurements for Kapaa Ferrogard Mixture	
FER2 .....	190
Figure A.1-93: Current Measurements for Kapaa FerroGard Mixture FER3 .....	191
Figure A.1-94: Corrosion Potential Measurements for Kapaa Ferrogard Mixture	
FER3 .....	191
Figure A.1-95: Corrosion Rate Measurements for Kapaa Ferrogard Mixture FER3 .....	192
Figure A.1-96: Corrosion Resistivity Measurements for Kapaa Ferrogard Mixture	
FER3 .....	192
Figure A.1-97: Current Measurements for Kapaa FerroGard Mixture FER4 .....	193
Figure A.1-98: Corrosion Potential Measurements for Kapaa Ferrogard Mixture	
FER4 .....	193
Figure A.1-99: Corrosion Rate Measurements for Kapaa Ferrogard Mixture FER4 .....	194
Figure A.1-100: Corrosion Resistivity Measurements for Kapaa Ferrogard Mixture	
FER4 .....	194
Figure A.1-101: Current Measurements for Kapaa FerroGard Mixture FER5 .....	195
Figure A.1-102: Corrosion Potential Measurements for Kapaa Ferrogard Mixture	
FER5 .....	195
Figure A.1-103: Corrosion Rate Measurements for Kapaa Ferrogard Mixture FER5 ....	196
Figure A.1-104: Corrosion Resistivity Measurements for Kapaa Ferrogard Mixture	
FER5 .....	196

Figure A.1-105: Current Measurements for Kapaa FerroGard Mixture FER6 .....	197
Figure A.1-106: Corrosion Potential Measurements for Kapaa Control Mixture FER6.	197
Figure A.1-107: Corrosion Rate Measurements for Kapaa Ferrogard Mixture FER6 ....	198
Figure A.1-108: Corrosion Resistivity Measurements for Kapaa Ferrogard Mixture FER6 .....	198
Figure A.1-109: Current Measurements for Kapaa Rheocrete Mixture RHE1 .....	199
Figure A.1-110: Corrosion Potential Measurements for Kapaa Rheocrete Mixture RHE1.....	199
Figure A.1-111: Corrosion Rate Measurements for Kapaa Rheocrete Mixture RHE1 ...	200
Figure A.1-112: Corrosion Resistivity Measurements for Kapaa Rheocrete Mixture RHE1.....	200
Figure A.1-113: Current Measurements for Kapaa Rheocrete Mixture RHE2 .....	201
Figure A.1-114: Corrosion Potential Measurements for Kapaa Control Mixture RHE2	201
Figure A.1-115: Corrosion Rate Measurements for Kapaa Rheocrete Mixture RHE2 ...	202
Figure A.1-116: Corrosion Resistivity Measurements for Kapaa Rheocrete Mix RHE2	202
Figure A.1-117: Current Measurements for Kapaa Rheocrete Mixture RHE3 .....	203
Figure A.1-118: Corrosion Potential Measurements for Kapaa Control Mixture RHE3	203
Figure A.1-119: Corrosion Rate Measurements for Kapaa Rheocrete Mixture RHE3 ...	204
Figure A.1-120: Corrosion Resistivity Measurements for Kapaa Rheocrete Mix RHE3	204
Figure A.1-121: Current Measurements for Kapaa Rheocrete Mixture RHE4 .....	205
Figure A.1-122: Corrosion Potential Measurements for Kapaa Control Mixture RHE4	205
Figure A.1-123: Corrosion Rate Measurements for Kapaa Rheocrete Mixture RHE4 ...	206
Figure A.1-124: Corrosion Resistivity Measurements for Kapaa Rheocrete Mix RHE4	206

Figure A.1-125: Current Measurements for Kapaa Rheocrete Mixture RHE5 .....	207
Figure A.1-126: Corrosion Potential Measurements for Kapaa Control Mixture RHE5	207
Figure A.1-127: Corrosion Rate Measurements for Kapaa Rheocrete Mixture RHE5 ...	208
Figure A.1-128: Corrosion Resistivity Measurements for Kapaa Rheocrete Mix RHE5	208
Figure A.1-129: Current Measurements for Kapaa Rheocrete Mixture RHE6 .....	209
Figure A.1-130: Corrosion Potential Measurements for Kapaa Control Mixture RHE6	209
Figure A.1-131: Corrosion Rate Measurements for Kapaa Rheocrete Mixture RHE6 ...	210
Figure A.1-132: Corrosion Resistivity Measurements for Kapaa Rheocrete RHE6 .....	210
Figure A.1-133: Current Measurements for Halawa Rheocrete Mixture HRHE1 .....	211
Figure A.1-134: Current Measurements for Halawa Rheocrete Mixture HRHE2 .....	211
Figure A.1-135: Current Measurements for Halawa Rheocrete Mixture HRHE3 .....	212
Figure A.1-136: Current Measurements for Halawa Rheocrete Mixture HRHE4 .....	212
Figure A.1-137: Current Measurements for Halawa Rheocrete Mixture HRHE5 .....	213
Figure A.1-138: Current Measurements for Halawa Rheocrete Mixture HRHE6 .....	213
Figure A.1-139: Current Measurements for Kapaa Xypex Mixture XYP1 .....	214
Figure A.1-140: Corrosion Potential Measurements for Kapaa Xypex Mixture XYP1 ..	214
Figure A.1-141: Corrosion Rate Measurements for Kapaa Xypex Mixture XYP1 .....	215
Figure A.1-142: Corrosion Resistivity Measurements for Kapaa Xypex Mixture XYP1.....	215
Figure A.1-143: Current Measurements for Kapaa Xypex Mixture XYP2.....	216
Figure A.1-144: Corrosion Potential Measurements for Kapaa Xypex Mixture XYP2..	216
Figure A.1-145: Corrosion Rate Measurements for Kapaa Xypex Mixture XYP2.....	217

Figure A.1-146: Corrosion Resistivity Measurements for Kapaa Xypex Mixture	
XYP2.....	217
Figure A.1-147: Current Measurements for Kapaa Xypex Mixture XYP3.....	218
Figure A.1-148: Corrosion Potential Measurements for Kapaa Xypex Mixture XYP3..	218
Figure A.1-149: Corrosion Rate Measurements for Kapaa Xypex Mixture XYP3.....	219
Figure A.1-150: Corrosion Resistivity Measurements for Kapaa Xypex Mixture	
XYP3.....	219
Figure A.1-151: Current Measurements for Kapaa Xypex Mixture XYP4.....	220
Figure A.1-152: Corrosion Potential Measurements for Kapaa Xypex Mixture XYP4..	220
Figure A.1-153: Corrosion Rate Measurements for Kapaa Xypex Mixture XYP4.....	221
Figure A.1-154: Corrosion Resistivity Measurements for Kapaa Xypex Mixture	
XYP4.....	221
Figure A.1-155: Current Measurements for Kapaa Xypex Mixture XYP5.....	222
Figure A.1-156: Corrosion Potential Measurements for Kapaa Xypex Mixture XYP5..	222
Figure A.1-157: Corrosion Rate Measurements for Kapaa Xypex Mixture XYP5.....	223
Figure A.1-158: Corrosion Resistivity Measurements for Kapaa Xypex Mixture	
XYP5.....	223
Figure A.1-159: Current Measurements for Kapaa Xypex Mixture XYP6.....	224
Figure A.1-160: Corrosion Potential Measurements for Kapaa Xypex Mixture XYP6..	224
Figure A.1-161: Corrosion Rate Measurements for Kapaa Xypex Mixture XYP6.....	225
Figure A.1-162: Corrosion Resistivity Measurements for Kapaa Xypex Mixture	
XYP6.....	225
Figure A.1-163: Current Measurements for Kapaa Latex Mixture L1.....	226

Figure A.1-164: Corrosion Potential Measurements for Kapaa latex Mixture L1 .....	226
Figure A.1-165: Corrosion Rate Measurements for Kapaa latex Mixture L1 .....	227
Figure A.1-166: Corrosion Resistivity Measurements for Kapaa latex Mixture L1 .....	227
Figure A.1-167: Current Measurements for Kapaa Latex Mixture L2 .....	228
Figure A.1-168: Corrosion Potential Measurements for Kapaa latex Mixture L2 .....	228
Figure A.1-169: Corrosion Rate Measurements for Kapaa latex Mixture L2 .....	229
Figure A.1-170: Corrosion Resistivity Measurements for Kapaa latex Mixture L2 .....	229
Figure A.1-171: Current Measurements for Kapaa Latex Mixture L3 .....	230
Figure A.1-172: Corrosion Potential Measurements for Kapaa latex Mixture L3 .....	230
Figure A.1-173: Corrosion Rate Measurements for Kapaa latex Mixture L3 .....	231
Figure A.1-174: Corrosion Resistivity Measurements for Kapaa latex Mixture L3 .....	231
Figure A.1-175: Current Measurements for Kapaa Latex Mixture L4 .....	232
Figure A.1-176: Corrosion Potential Measurements for Kapaa latex Mixture L4 .....	232
Figure A.1-177: Corrosion Rate Measurements for Kapaa latex Mixture L4 .....	233
Figure A.1-178: Corrosion Resistivity Measurements for Kapaa latex Mixture L4 .....	233
Figure A.1-179: Current Measurements for Kapaa Latex Mixture L5 .....	234
Figure A.1-180: Corrosion Potential Measurements for Kapaa latex Mixture LA5 .....	234
Figure A.1-181: Corrosion Rate Measurements for Kapaa latex Mixture L5 .....	235
Figure A.1-182: Corrosion Resistivity Measurements for Kapaa latex Mixture L5 .....	235
Figure A.1-183: Current Measurements for Kapaa Latex Mixture L6 .....	236
Figure A.1-184: Corrosion Potential Measurements for Kapaa latex Mixture LA6 .....	236
Figure A.1-185: Corrosion Rate Measurements for Kapaa latex Mixture L6 .....	237
Figure A.1-186: Corrosion Resistivity Measurements for Kapaa latex Mixture L6 .....	237

Figure A.1-187: Current Measurements for Kapaa Silica Fume Mixture SF1 .....	238
Figure A.1-188: Corrosion Potential Measurements for Kapaa silica fume Mixture SF1 .....	238
Figure A.1-189: Corrosion Rate Measurements for Kapaa silica fume Mixture SF1 .....	239
Figure A.1-190: Corrosion Resistivity Measurements for Kapaa silica fume Mixture SF1 .....	239
Figure A.1-191: Current Measurements for Kapaa Silica Fume Mixture SF2 .....	240
Figure A.1-192: Corrosion Potential Measurements for Kapaa silica fume Mixture SF1 .....	240
Figure A.1-193: Corrosion Rate Measurements for Kapaa silica fume Mixture SF2 .....	241
Figure A.1-194: Corrosion Resistivity Measurements for Kapaa silica fume Mixture SF2 .....	241
Figure A.1-195: Current Measurements for Kapaa Silica Fume Mixture SF3 .....	242
Figure A.1-196: Corrosion Potential Measurements for Kapaa silica fume Mixture SF3 .....	242
Figure A.1-197: Corrosion Rate Measurements for Kapaa silica fume Mixture SF3 .....	243
Figure A.1-198: Corrosion Resistivity Measurements for Kapaa silica fume Mixture SF3 .....	243
Figure A.1-199: Current Measurements for Kapaa Silica Fume Mixture SF4 .....	244
Figure A.1-200: Corrosion Potential Measurements for Kapaa silica fume Mixture SF4 .....	244
Figure A.1-201: Corrosion Rate Measurements for Kapaa silica fume Mixture SF4 .....	245

Figure A.1-202: Corrosion Resistivity Measurements for Kapaa silica fume Mixture	
SF4 .....	245
Figure A.1-203: Current Measurements for Kapaa Silica Fume Mixture SF5 .....	246
Figure A.1-204: Corrosion Potential Measurements for Kapaa silica fume Mixture	
SF5 .....	246
Figure A.1-205: Corrosion Rate Measurements for Kapaa silica fume Mixture SF5 .....	247
Figure A.1-206: Corrosion Resistivity Measurements for Kapaa silica fume Mixture	
SF5 .....	247
Figure A.1-207: Current Measurements for Kapaa Silica Fume Mixture SF6 .....	248
Figure A.1-208: Corrosion Potential Measurements for Kapaa silica fume Mixture	
SF6 .....	248
Figure A.1-209: Corrosion Rate Measurements for Kapaa silica fume Mixture SF6 .....	249
Figure A.1-210: Corrosion Resistivity Measurements for Kapaa silica fume Mixture	
SF6 .....	249
Figure A.1-211: Current Measurements for Kapaa Silica Fume Mixture SF7 .....	250
Figure A.1-212: Corrosion Potential Measurements for Kapaa silica fume Mixture	
SF7 .....	250
Figure A.1-213: Corrosion Rate Measurements for Kapaa silica fume Mixture SF7 .....	251
Figure A.1-214: Corrosion Resistivity Measurements for Kapaa silica fume Mixture	
SF7 .....	251
Figure A.1-215: Current Measurements for Kapaa Silica Fume Mixture SF8 .....	252
Figure A.1-216: Corrosion Potential Measurements for Kapaa silica fume Mixture	
SF8 .....	252

Figure A.1-217: Corrosion Rate Measurements for Kapaa silica fume Mixture SF8 .....	253
Figure A.1-218: Corrosion Resistivity Measurements for Kapaa silica fume Mixture SF8 .....	253
Figure A.1-219: Current Measurements for Kapaa Silica Fume Mixture SF9.....	254
Figure A.1-220: Corrosion Potential Measurements for Kapaa silica fume Mixture SF9 .....	254
Figure A.1-221: Corrosion Rate Measurements for Kapaa silica fume Mixture SF9 .....	255
Figure A.1-222: Corrosion Resistivity Measurements for Kapaa silica fume Mixture SF9 .....	255
Figure A.1-223: Current Measurements for Kapaa Silica Fume Mixture SF10.....	256
Figure A.1-224: Corrosion Potential Measurements for Kapaa silica fume Mixture SF10 .....	256
Figure A.1-225: Corrosion Rate Measurements for Kapaa silica fume Mixture SF10 ...	257
Figure A.1-226: Corrosion Resistivity Measurements for Kapaa silica fume Mix SF10	257
Figure A.1-227: Current Measurements for Kapaa Silica Fume Mixture SF11 .....	258
Figure A.1-228: Corrosion Potential Measurements for Kapaa silica fume Mixture SF11 .....	258
Figure A.1-229: Corrosion Rate Measurements for Kapaa silica fume Mixture SF11 ...	259
Figure A.1-230: Corrosion Resistivity Measurements for Kapaa SF Mixture SF11.....	259
Figure A.1-231: Current Measurements for Halawa Silica Fume Mixture HSF1 .....	260
Figure A.1-232: Current Measurements for Halawa Silica Fume Mixture HSF2 .....	260
Figure A.1-233: Current Measurements for Halawa Silica Fume Mixture HSF3 .....	261
Figure A.1-234: Current Measurements for Halawa Silica Fume Mixture HSF4.....	261

Figure A.1-235: Current Measurements for Halawa Silica Fume Mixture HSF5 .....	262
Figure A.1-236: Current Measurements for Halawa Silica Fume Mixture HSF6 .....	262
Figure A.1-237: Current Measurements for Halawa Rheomac Mixture HSF-RH2 .....	263
Figure A.1-238: Current Measurements for Halawa Rheomac Mixture HSF-RH3 .....	263
Figure A.1-239: Current Measurements for Halawa Rheomac Mixture HSF-RH4 .....	264
Figure A.1-240: Current Measurements for Halawa Rheomac Mixture HSF-RH5 .....	264
Figure A.1-241: Current Measurements for Halawa Rheomac Mixture HSF-RH6 .....	265
Figure A.1-242: Current Measurements for Halawa Rheomac Mixture HSF-RH7 .....	265
Figure A.1-243: Current Measurements for Kapaa Fly Ash Mixture FA2.....	266
Figure A.1-244: Corrosion Potential for Kapaa Fly Ash Mixture FA2.....	266
Figure A.1-245: Corrosion Rate for Kapaa Fly Ash Mixture FA2.....	267
Figure A.1-246: Corrosion Resistivity for Kapaa Fly Ash Mixture FA2.....	267
Figure A.1-247: Current Measurements for Kapaa Fly Ash Mixture FA3.....	268
Figure A.1-248: Corrosion Potential for Kapaa Fly Ash Mixture FA3.....	268
Figure A.1-249: Corrosion Rate for Kapaa Fly Ash Mixture FA3.....	269
Figure A.1-250: Corrosion Resistivity for Kapaa Fly Ash Mixture FA3.....	269
Figure A.1-251: Current Measurements for Kapaa Fly Ash Mixture FA4.....	270
Figure A.1-252: Corrosion Potential for Kapaa Fly Ash Mixture FA4.....	270
Figure A.1-253: Corrosion Rate for Kapaa Fly Ash Mixture FA4.....	271
Figure A.1-254: Corrosion Resistivity for Kapaa Fly Ash Mixture FA4.....	271
Figure A.1-255: Current Measurements for Kapaa Fly Ash Mixture FA5.....	272
Figure A.1-256: Corrosion Potential for Kapaa Fly Ash Mixture FA5.....	272
Figure A.1-257: Corrosion Rate for Kapaa Fly Ash Mixture FA5.....	273

Figure A.1-258: Corrosion Resistivity for Kapaa Fly Ash Mixture FA5 .....	273
Figure A.1-259: Current Measurements for Kapaa Fly Ash Mixture FA6.....	274
Figure A.1-260: Corrosion Potential for Kapaa Fly Ash Mixture FA6.....	274
Figure A.1-261: Corrosion Rate for Kapaa Fly Ash Mixture FA6.....	275
Figure A.1-262: Corrosion Resistivity for Kapaa Fly Ash Mixture FA6.....	275
Figure A.1-263: Current Measurements for Kapaa Fly Ash Mixture FA7.....	276
Figure A.1-264: Corrosion Potential for Kapaa Fly Ash Mixture FA7 .....	276
Figure A.1-265: Corrosion Rate for Kapaa Fly Ash Mixture FA7.....	277
Figure A.1-266: Corrosion Resistivity for Kapaa Fly Ash Mixture FA7.....	277
Figure A.1-267: Current Measurements for Kapaa Fly Ash Mixture FA8.....	278
Figure A.1-268: Corrosion Potential for Kapaa Fly Ash Mixture FA8.....	278
Figure A.1-269: Corrosion Rate for Kapaa Fly Ash Mixture FA8.....	279
Figure A.1-270: Corrosion Resistivity for Kapaa Fly Ash Mixture FA8.....	279
Figure A.1-271: Current Measurements for Kapaa Fly Ash Mixture FA9.....	280
Figure A.1-272: Corrosion Potential for Kapaa Fly Ash Mixture FA9 .....	280
Figure A.1-273: Corrosion Rate for Kapaa Fly Ash Mixture FA9.....	281
Figure A.1-274: Corrosion Resistivity for Kapaa Fly Ash Mixture FA9.....	281
Figure A.1-275: Current Measurements for Kapaa Fly Ash Mixture FA10.....	282
Figure A.1-276: Corrosion Potential for Kapaa Fly Ash Mixture FA10.....	282
Figure A.1-277: Corrosion Rate for Kapaa Fly Ash Mixture FA10.....	283
Figure A.1-278: Corrosion Resistivity for Kapaa Fly Ash Mixture FA10.....	283
Figure A.1-279: Current Measurements for Kapaa Fly Ash Mixture FA11.....	284
Figure A.1-280: Corrosion Potential for Kapaa Fly Ash Mixture FA11 .....	284

Figure A.1-281: Corrosion Rate for Kapaa Fly Ash Mixture FA11.....	285
Figure A.1-282: Corrosion Resistivity for Kapaa Fly Ash Mixture FA11 .....	285
Figure A.1-283: Current Measurements for Halawa Fly Ash Mixture HFA2.....	286
Figure A.1-284: Current Measurements for Halawa Fly Ash Mixture HFA3.....	286
Figure A.1-285: Current Measurements for Halawa Fly Ash Mixture HFA4.....	287
Figure A.1-286: Current Measurements for Halawa Fly Ash Mixture HFA5.....	287
Figure A.1-287: Current Measurements for Halawa Fly Ash Mixture HFA7.....	288
Figure A.1-288: Current Measurements for Halawa Fly Ash Mixture HFA8.....	288
Figure A.1-289: Current Measurements for Halawa Fly Ash Mixture HFA9.....	289



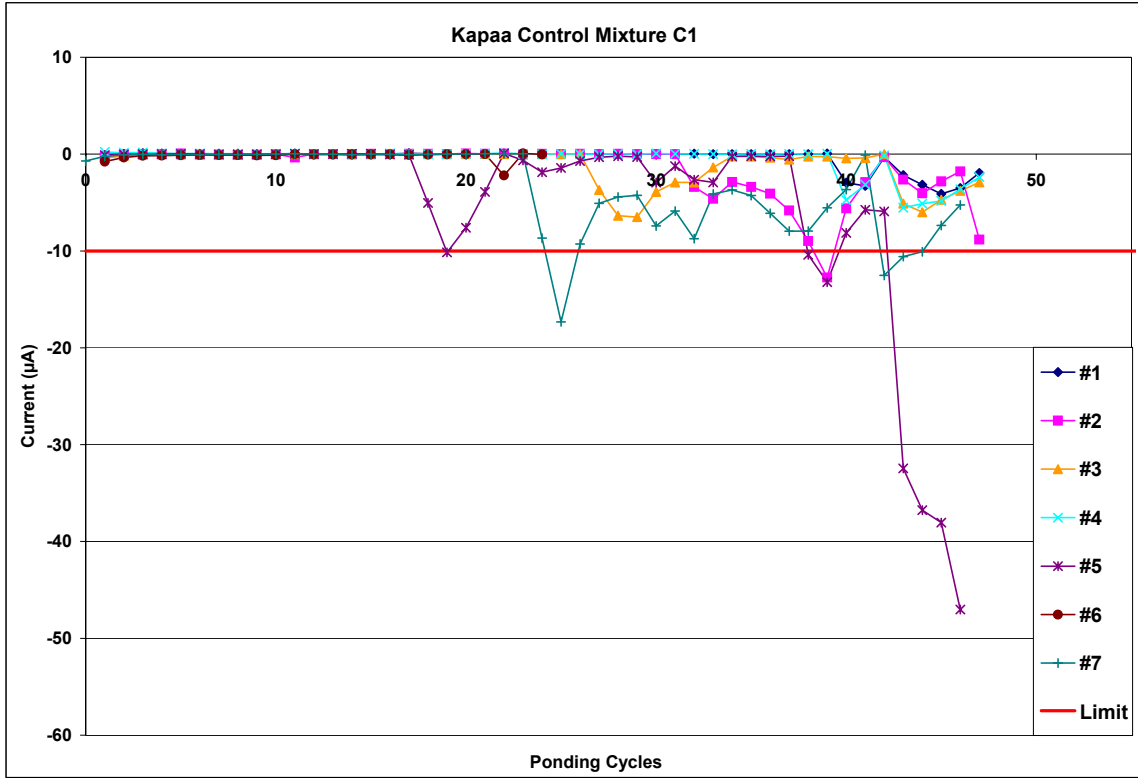


Figure A.1-1: Current Measurements for Kapaa Control Mixture C1

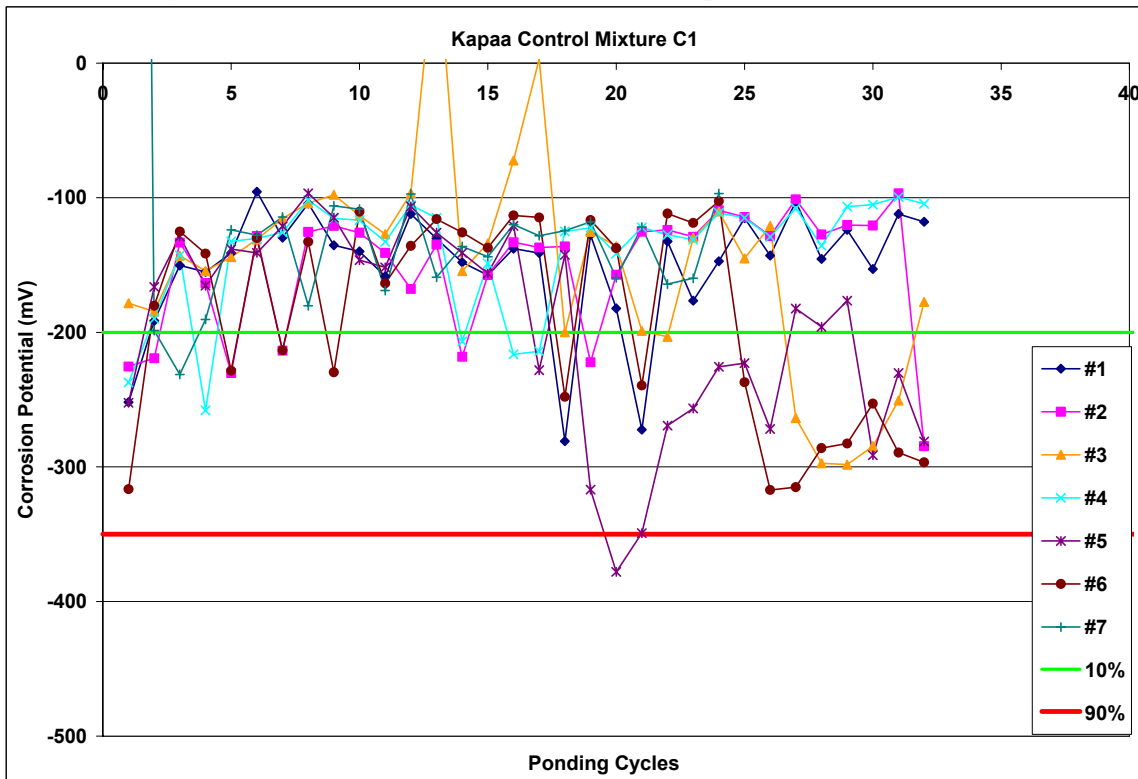


Figure A.1-2: Corrosion Potential Measurements for Kapaa Control Mixture C1

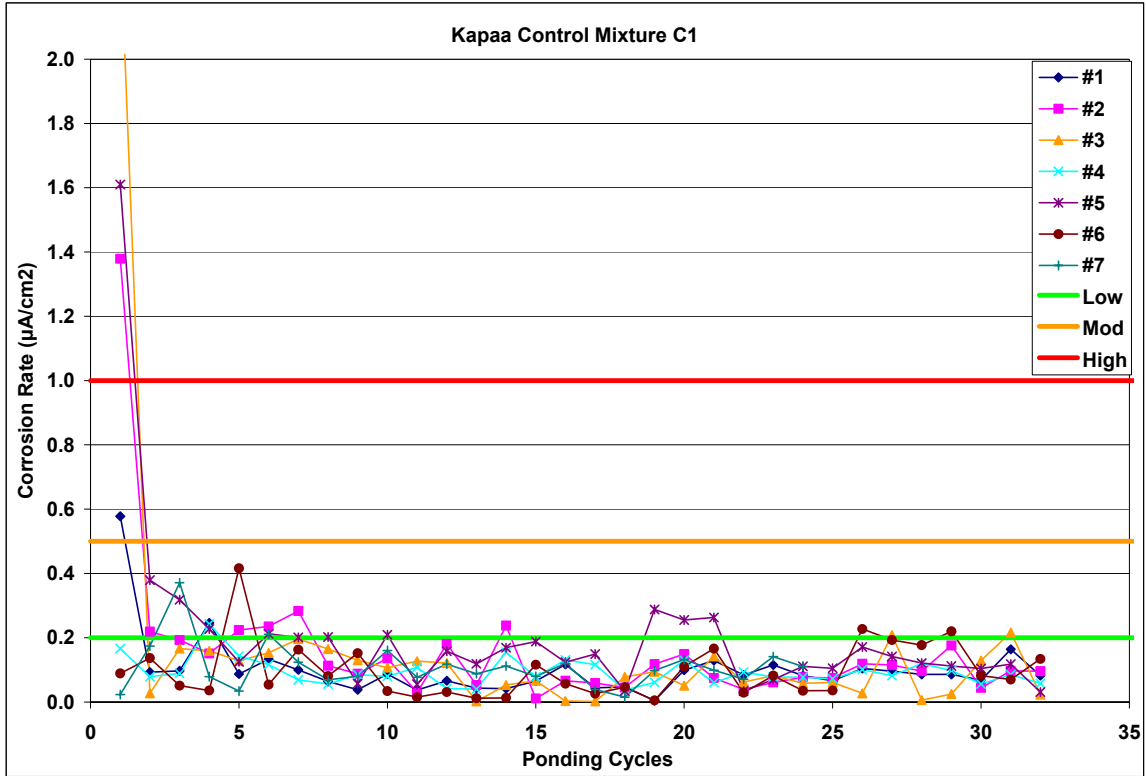


Figure A.1-3: Corrosion Rate Measurements for Kapaa Control Mixture C1

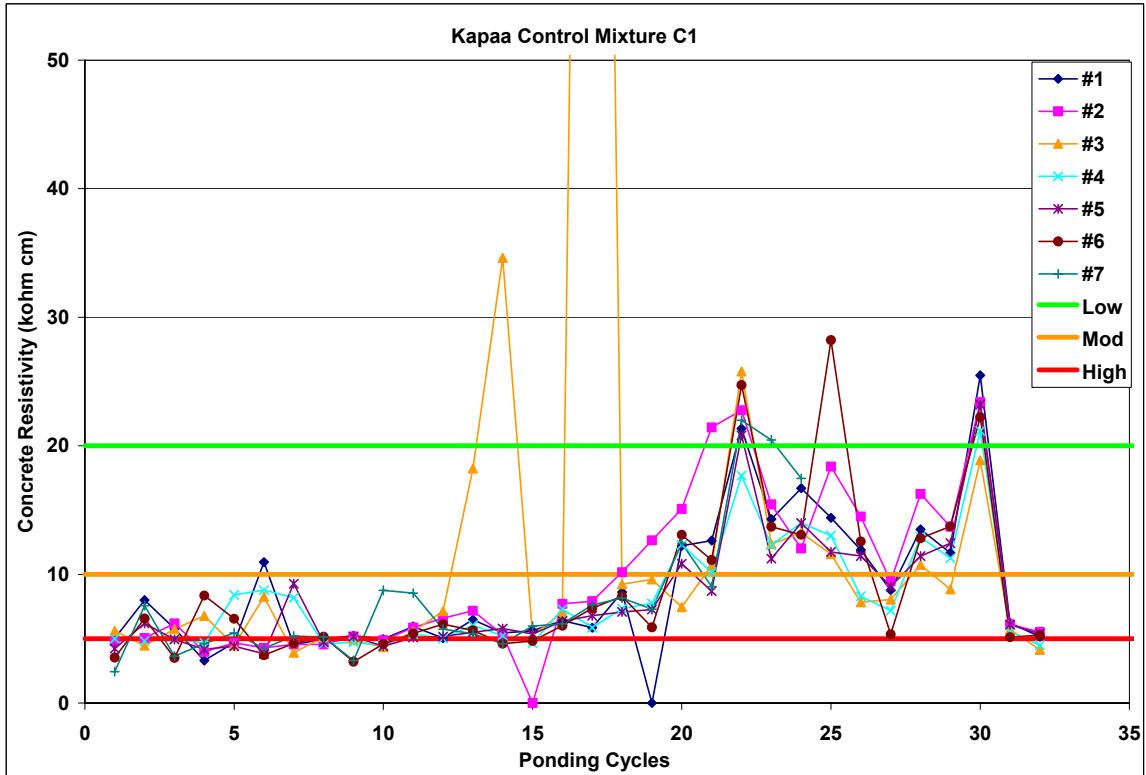


Figure A.1-4: Corrosion Resistivity Measurements for Kapaa Control Mixture C1

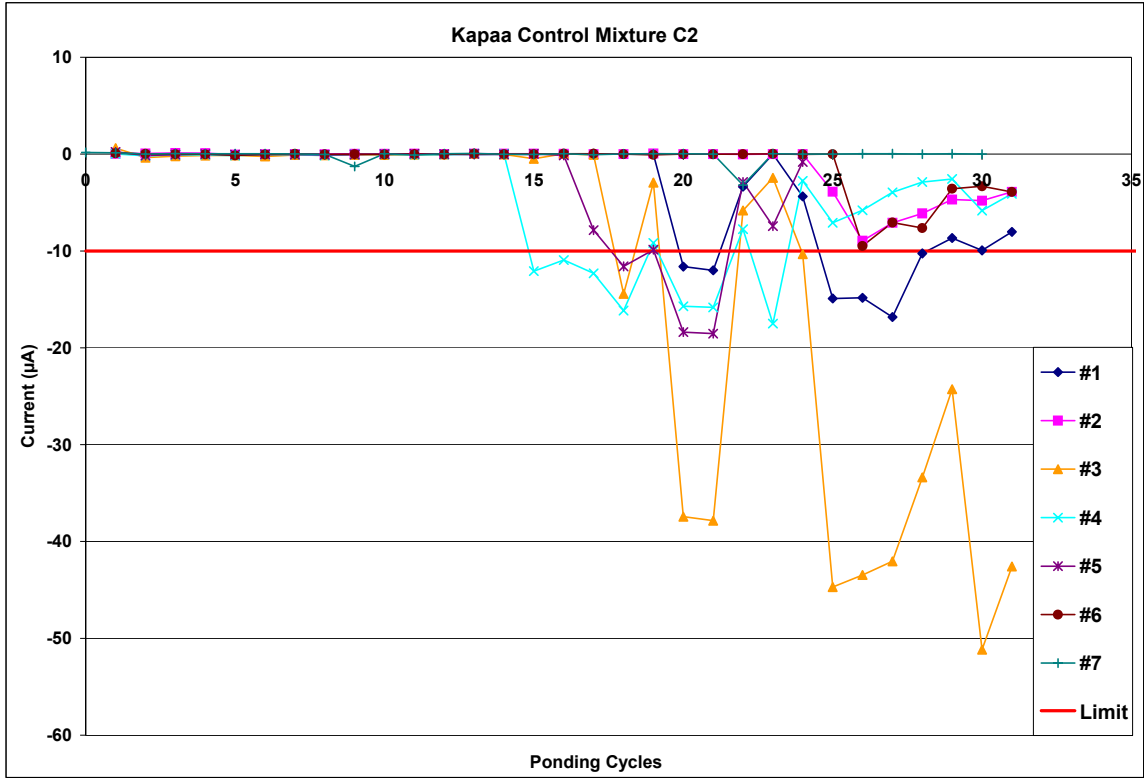


Figure A.1-5: Current Measurements for Kapaa Control Mixture C2

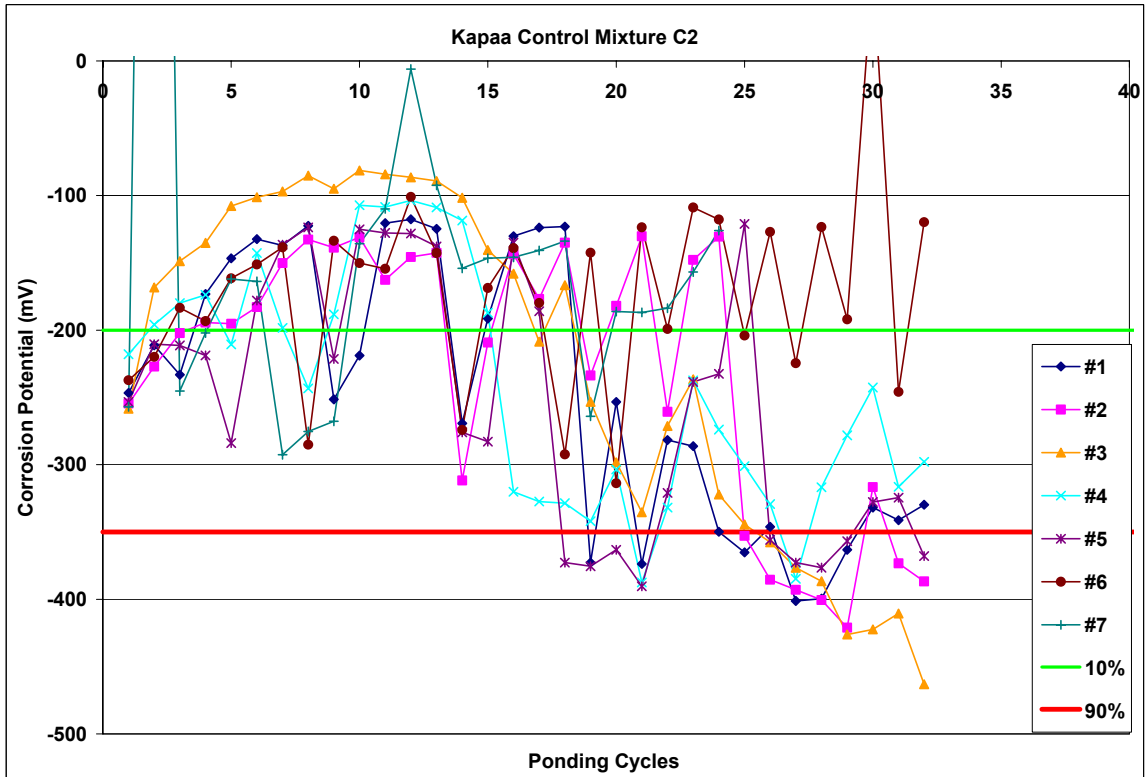


Figure A.1-6: Corrosion Potential Measurements for Kapaa Control Mixture C2

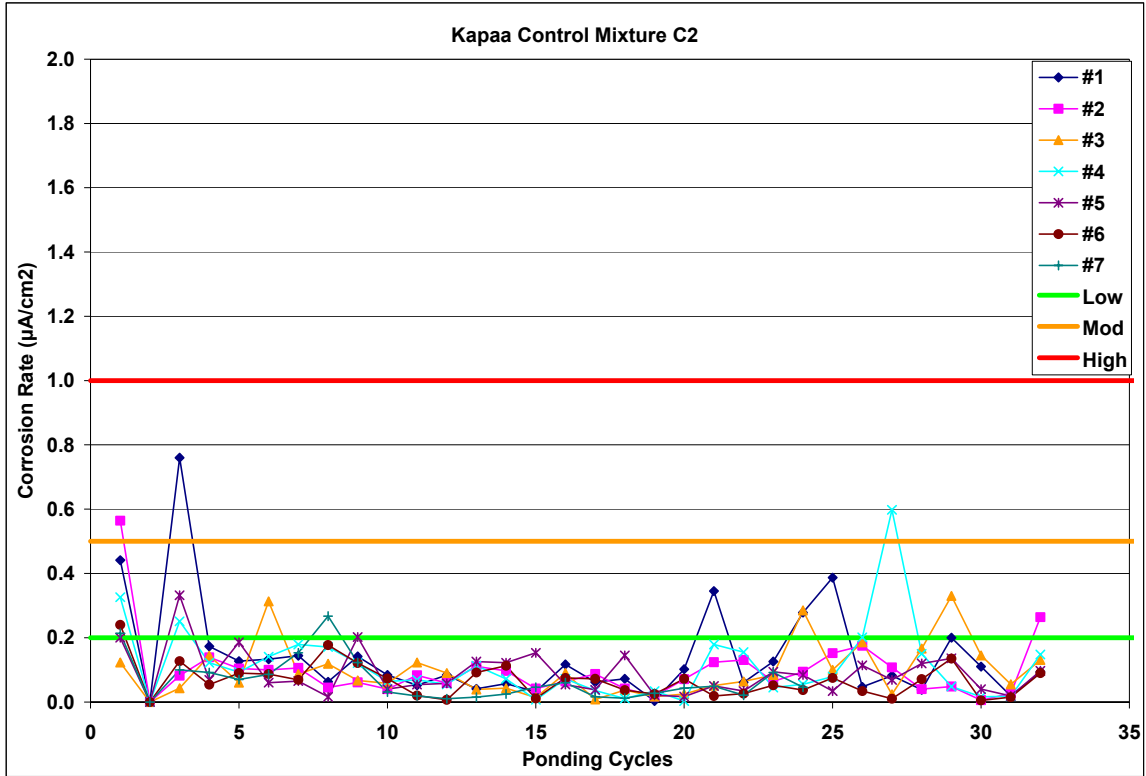


Figure A.1-7: Corrosion Rate Measurements for Kapaa Control Mixture C2

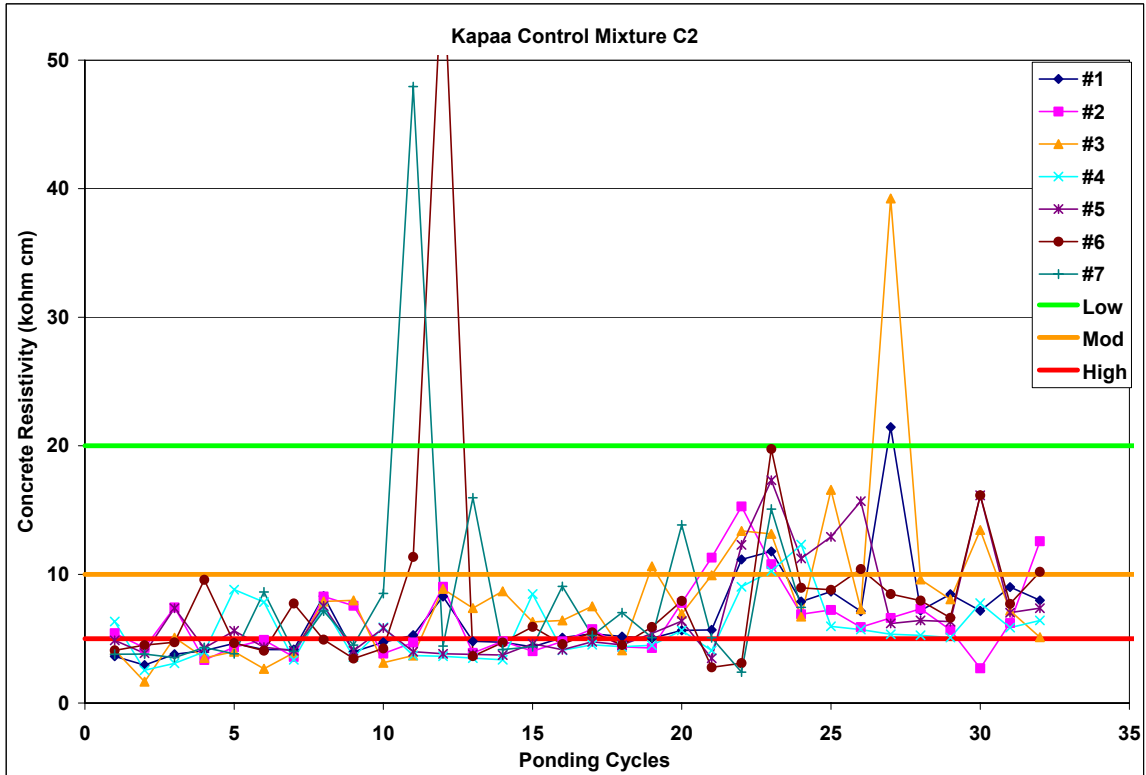


Figure A.1-8: Corrosion Resistivity Measurements for Kapaa Control Mixture C2

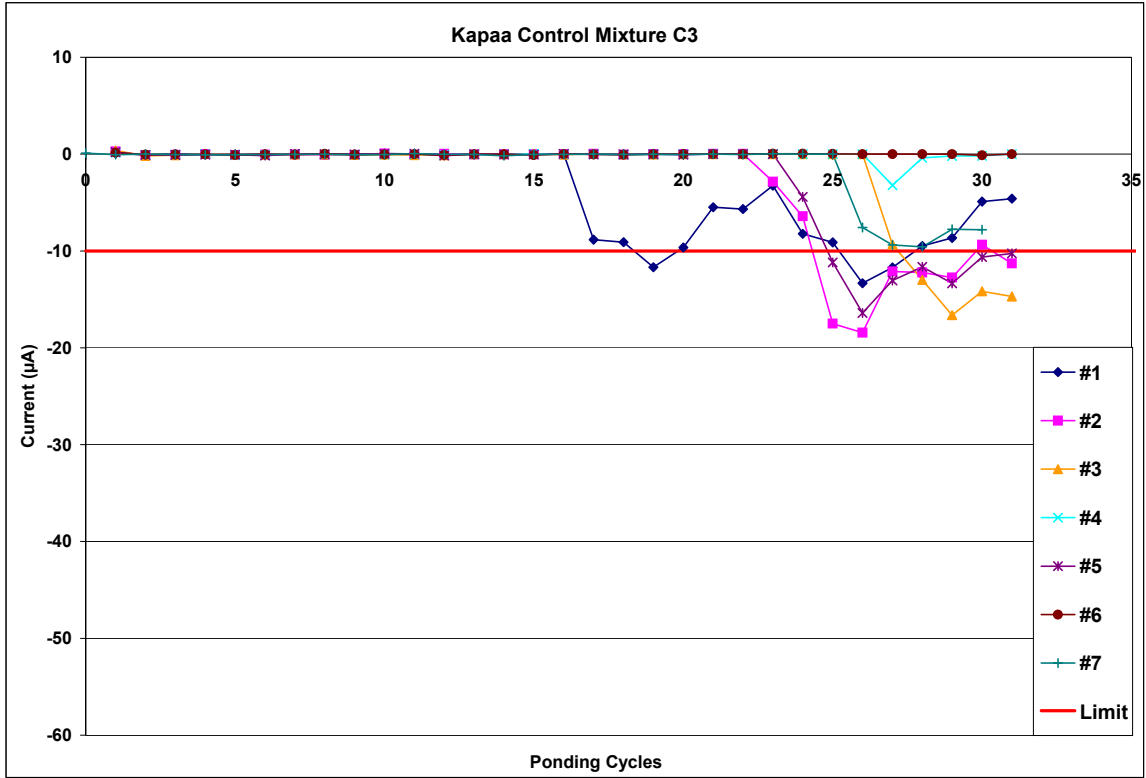


Figure A.1-9: Current Measurements for Kapaa Control Mixture C3

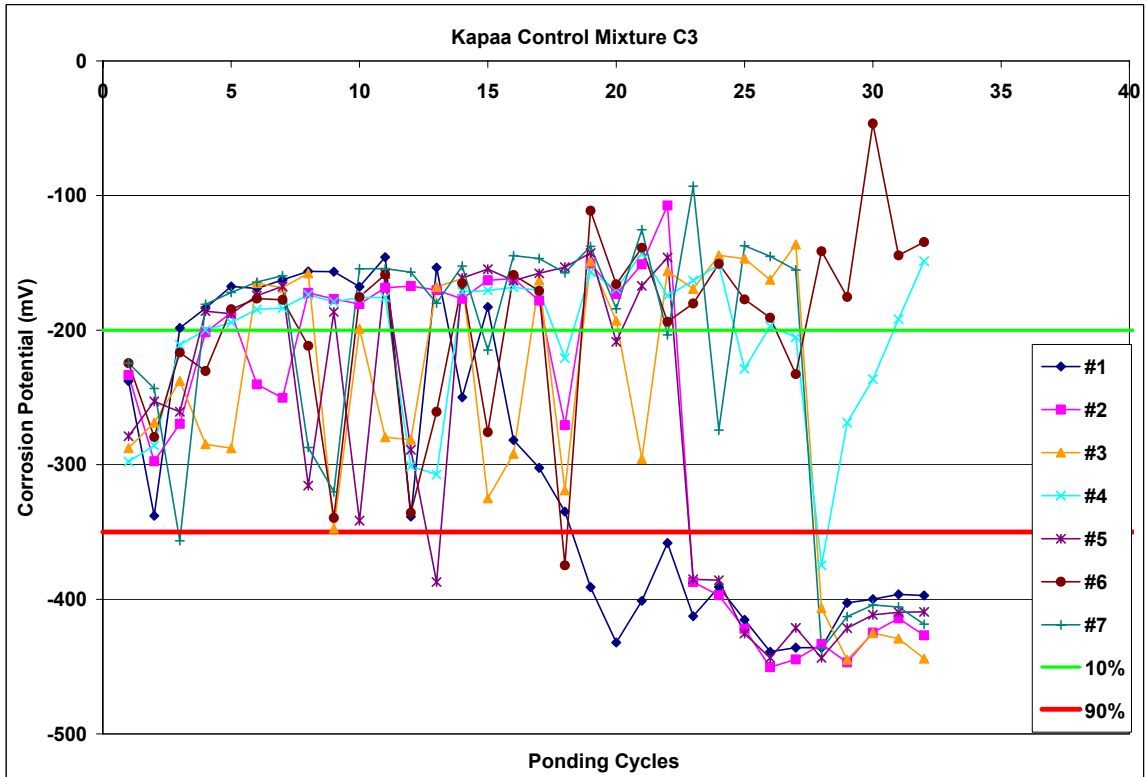


Figure A.1-10: Corrosion Potential Measurements for Kapaa Control Mixture C3

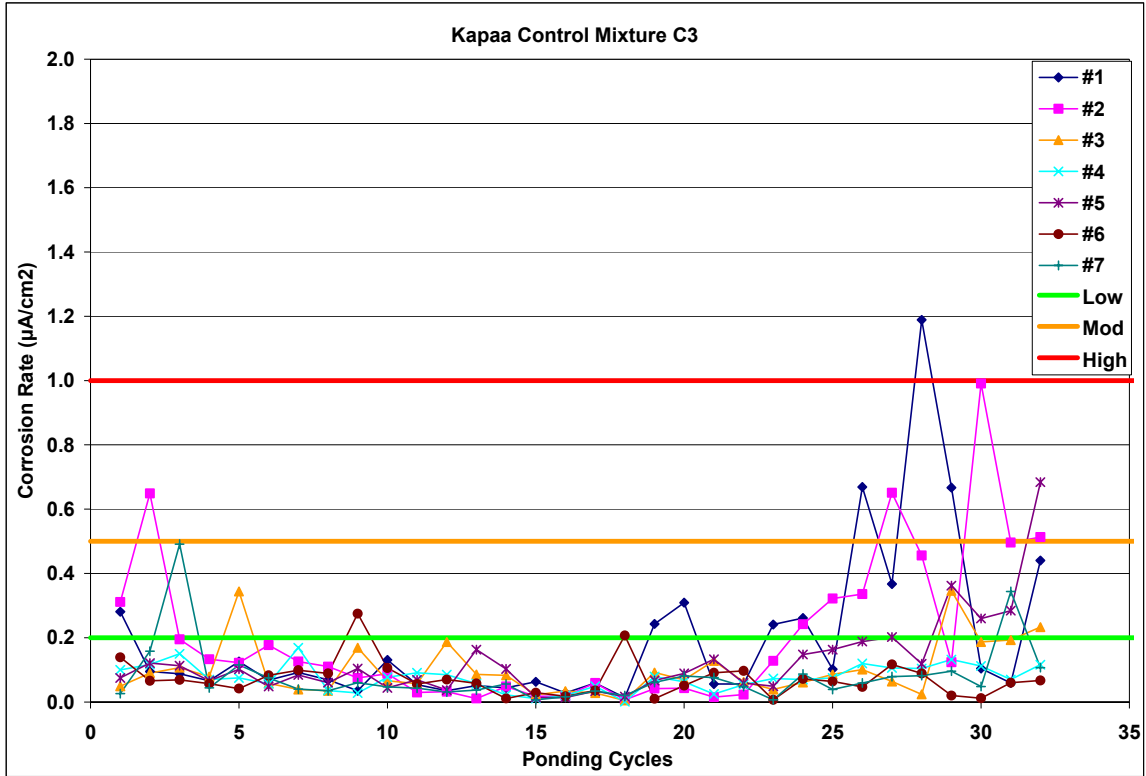


Figure A.1-11: Corrosion Rate Measurements for Kapaa Control Mixture C3

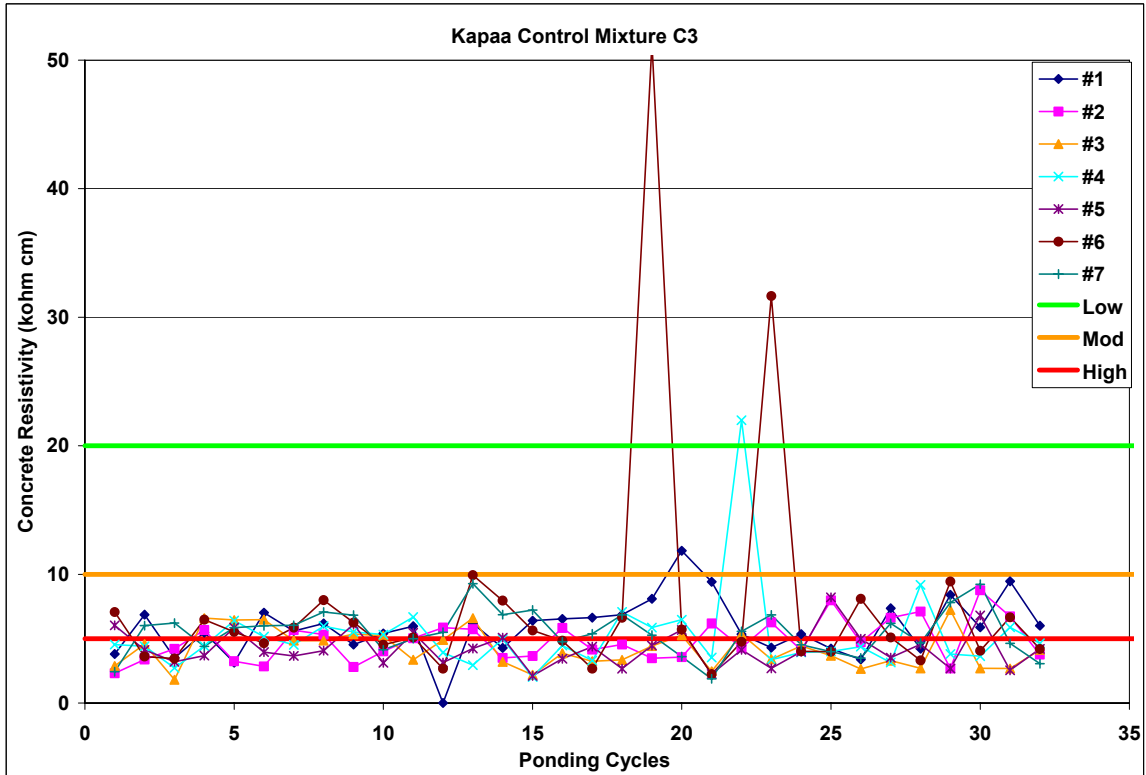


Figure A.1-12: Corrosion Resistivity Measurements for Kapaa Control Mixture C3

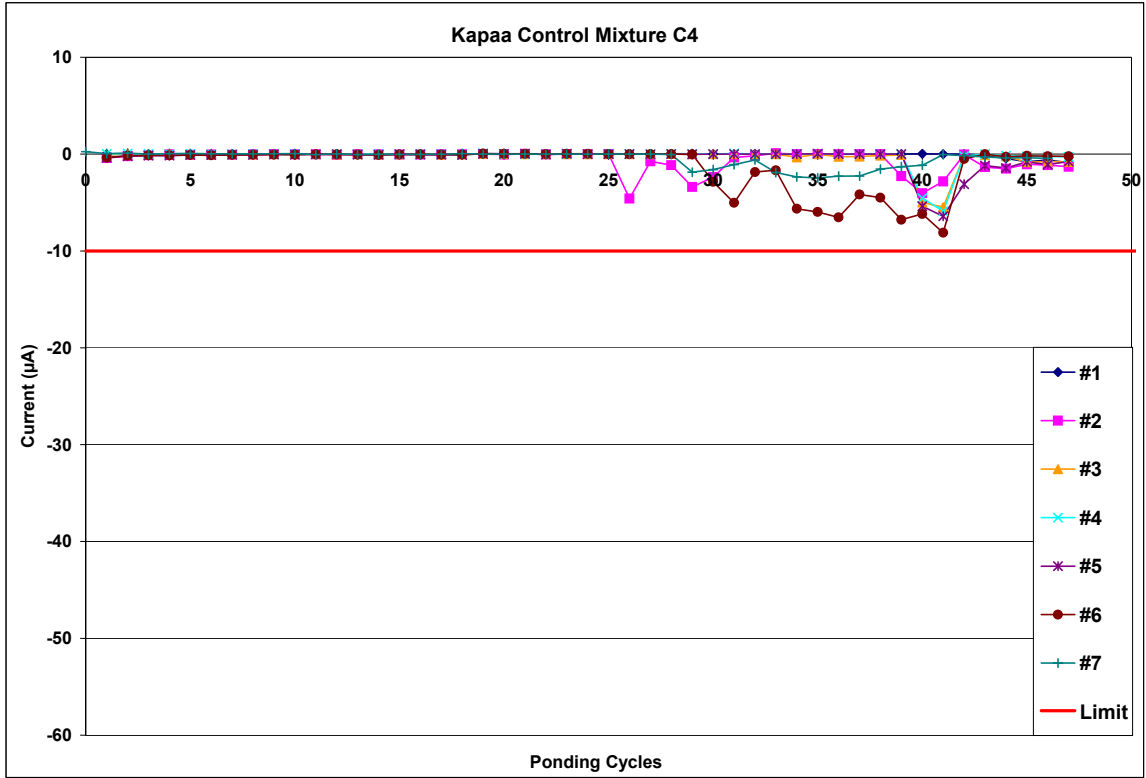


Figure A.1-13: Current Measurements for Kapaa Control Mixture C4

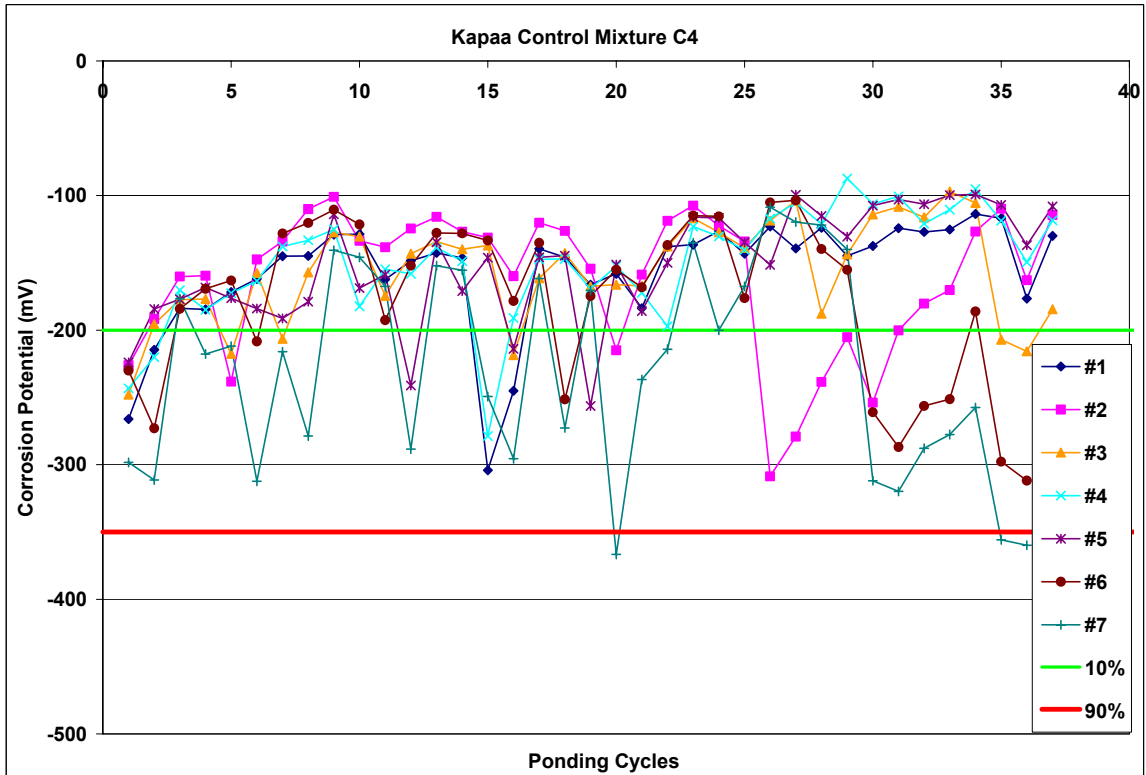


Figure A.1-14: Corrosion Potential Measurements for Kapaa Control Mixture C4

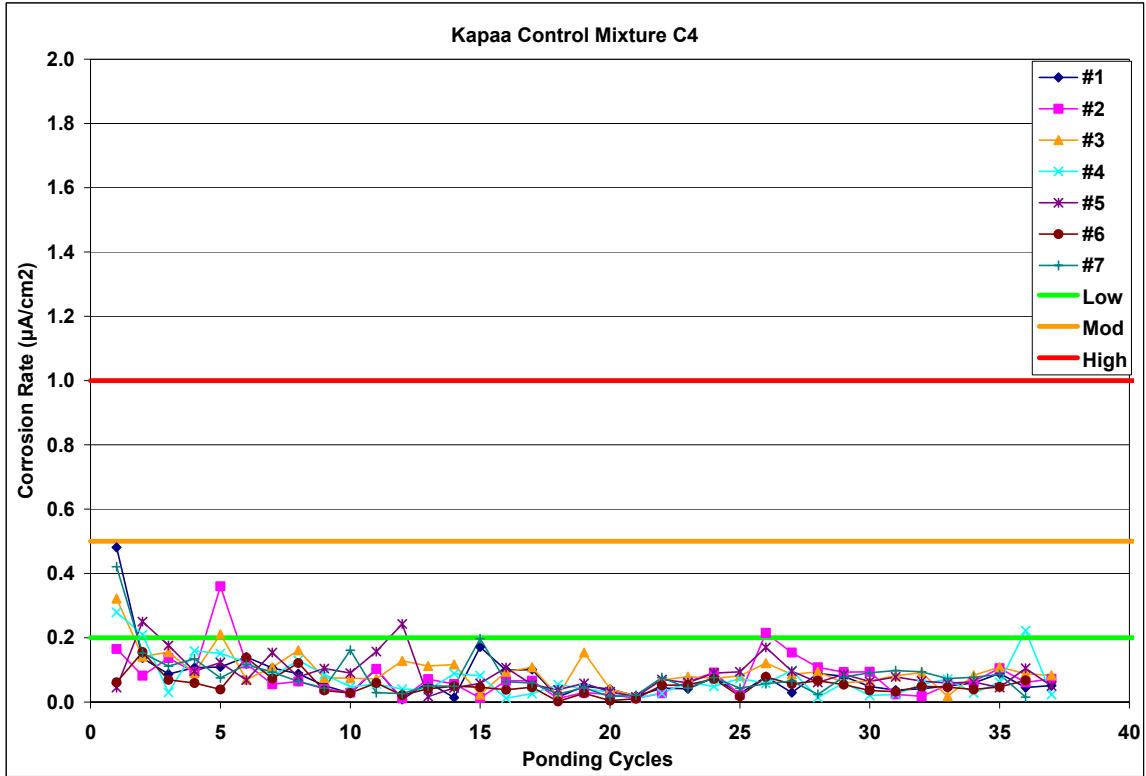


Figure A.1-15: Corrosion Rate Measurements for Kapaa Control Mixture C4

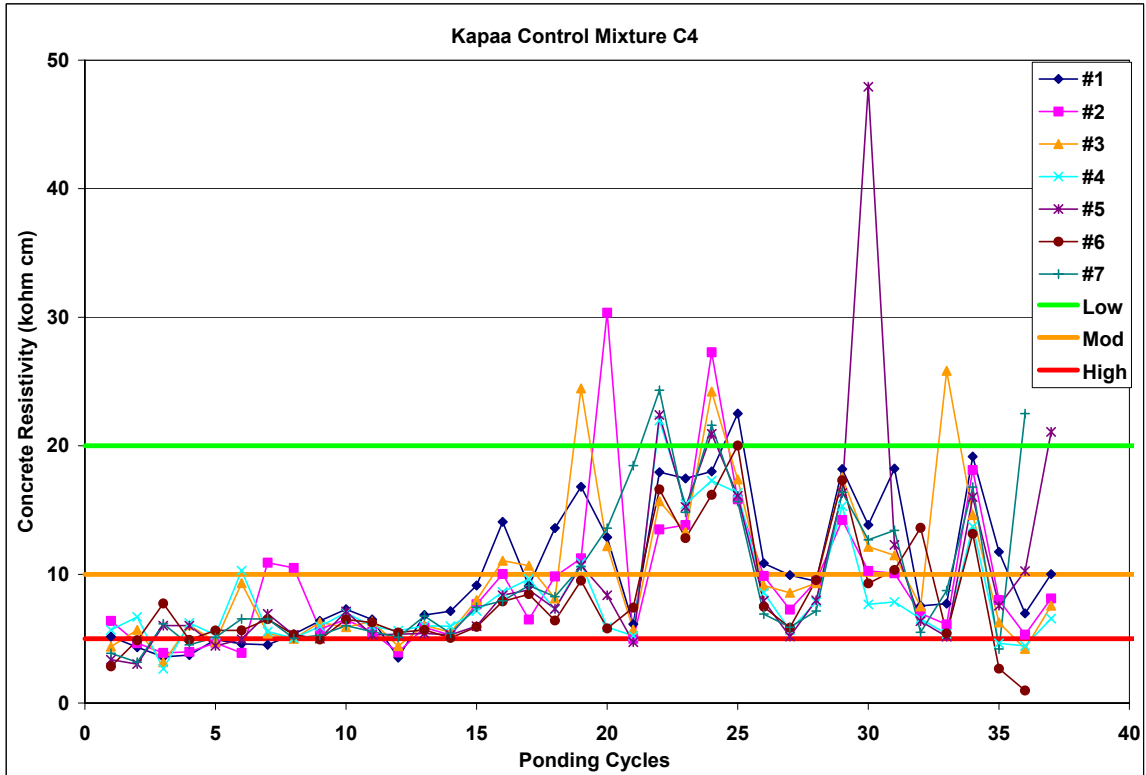


Figure A.1-16: Corrosion Resistivity Measurements for Kapaa Control Mixture C4

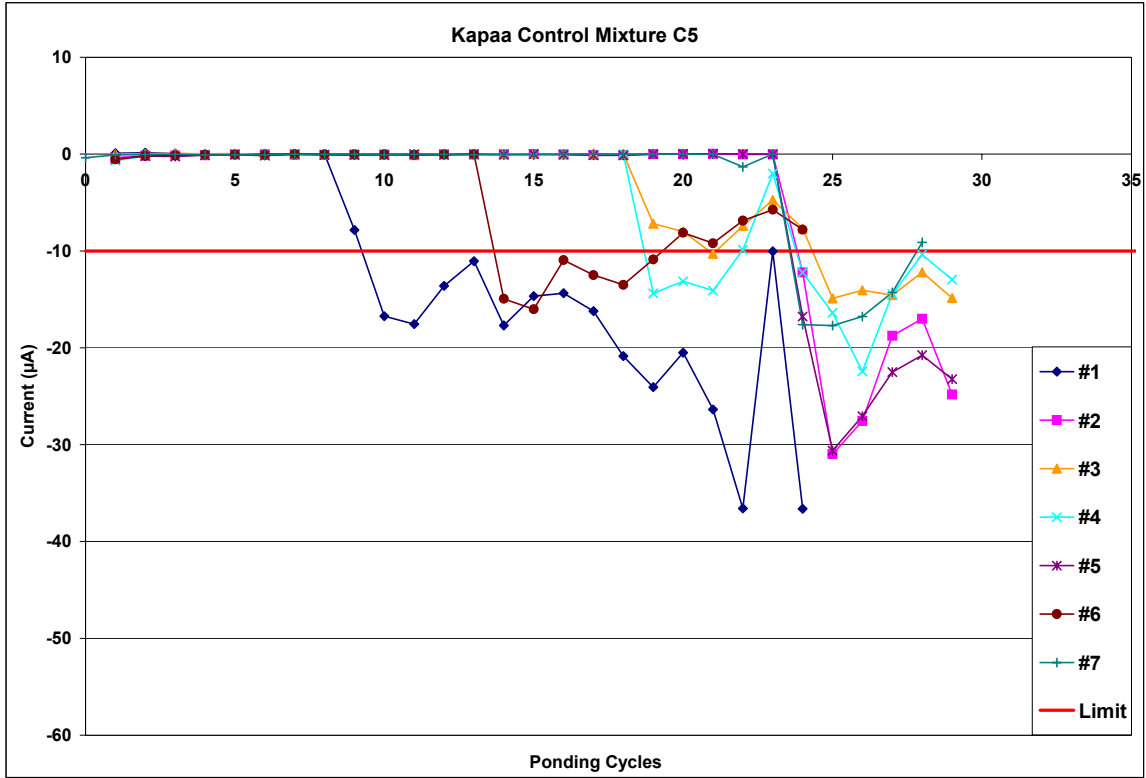


Figure A.1-17: Current Measurements for Kapaa Control Mixture C5

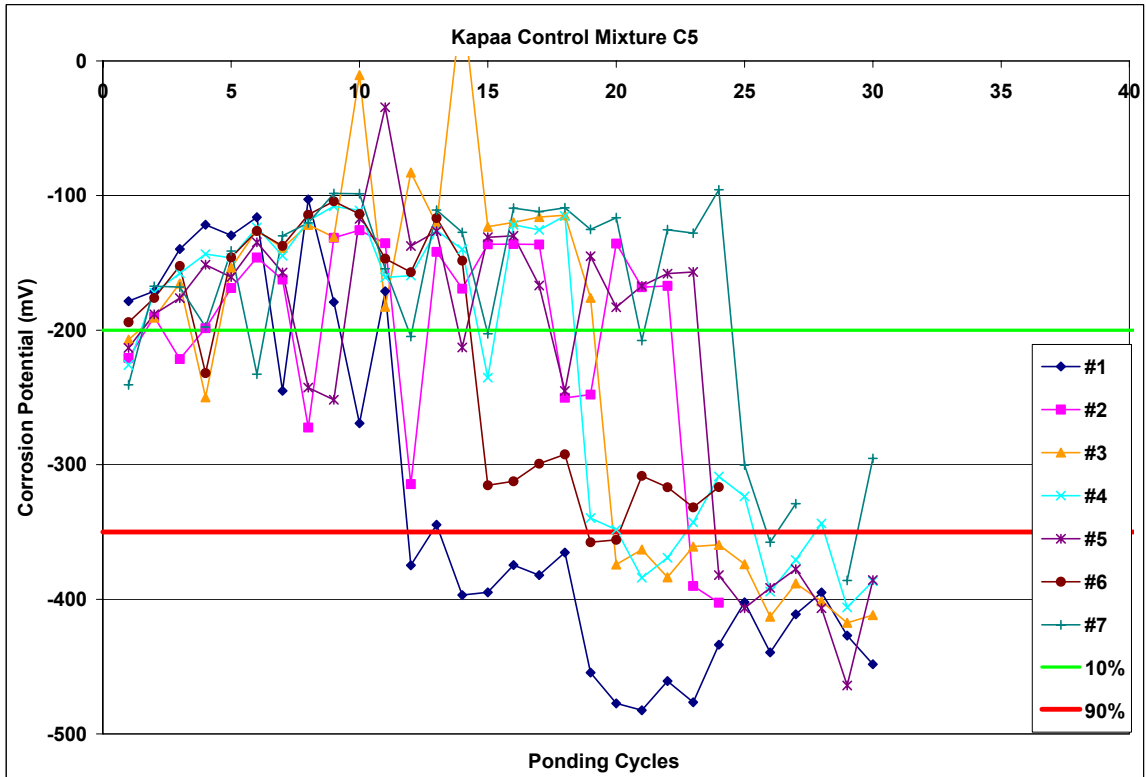


Figure A.1-18: Corrosion Potential Measurements for Kapaa Control Mixture C5

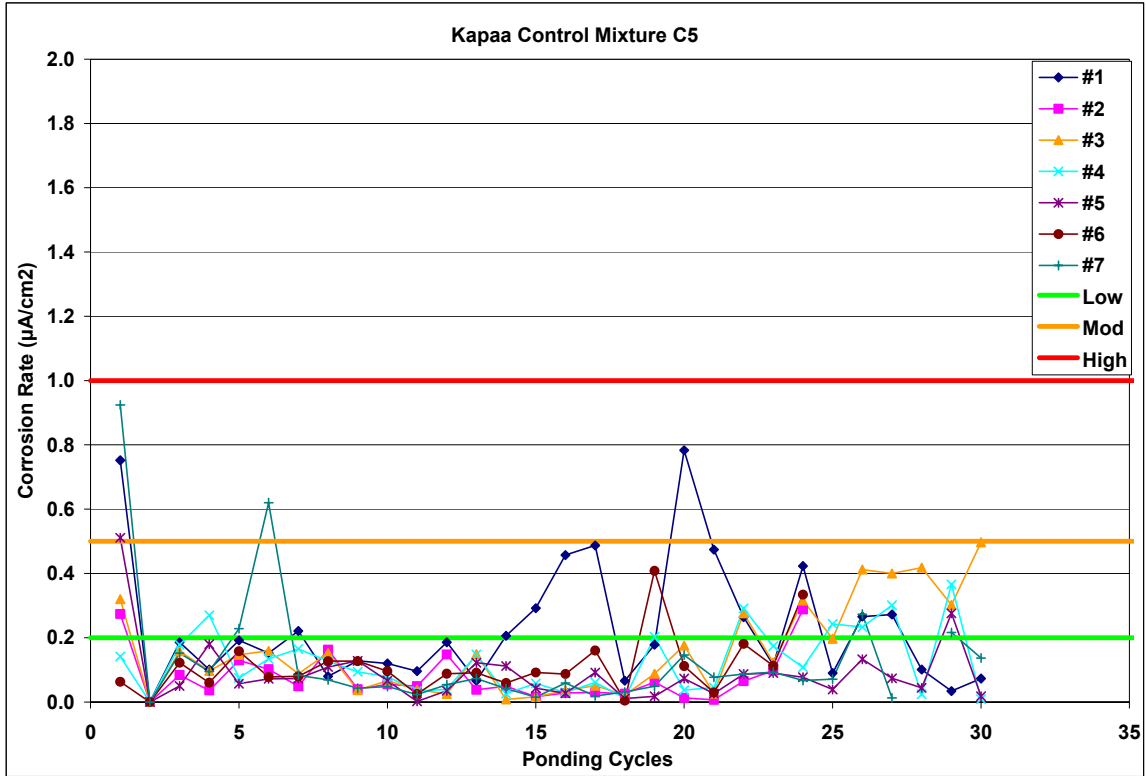


Figure A.1-19: Corrosion Rate Measurements for Kapaa Control Mixture C5

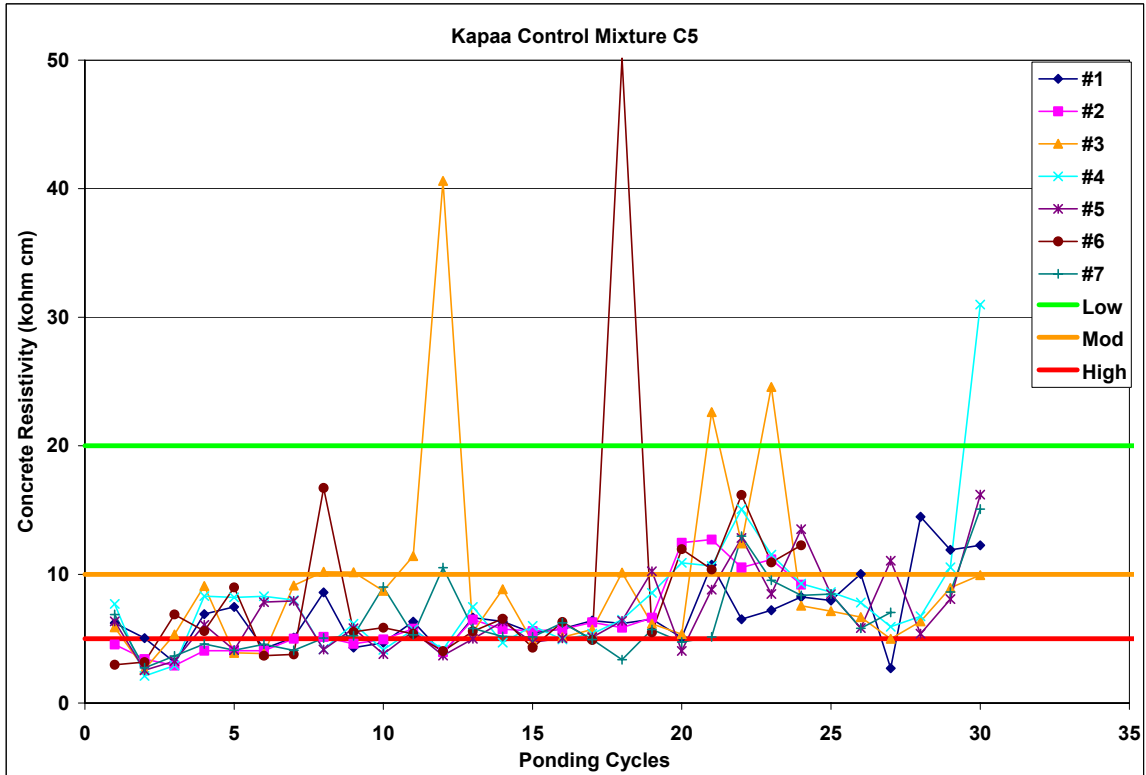


Figure A.1-20: Corrosion Resistivity Measurements for Kapaa Control Mixture C5

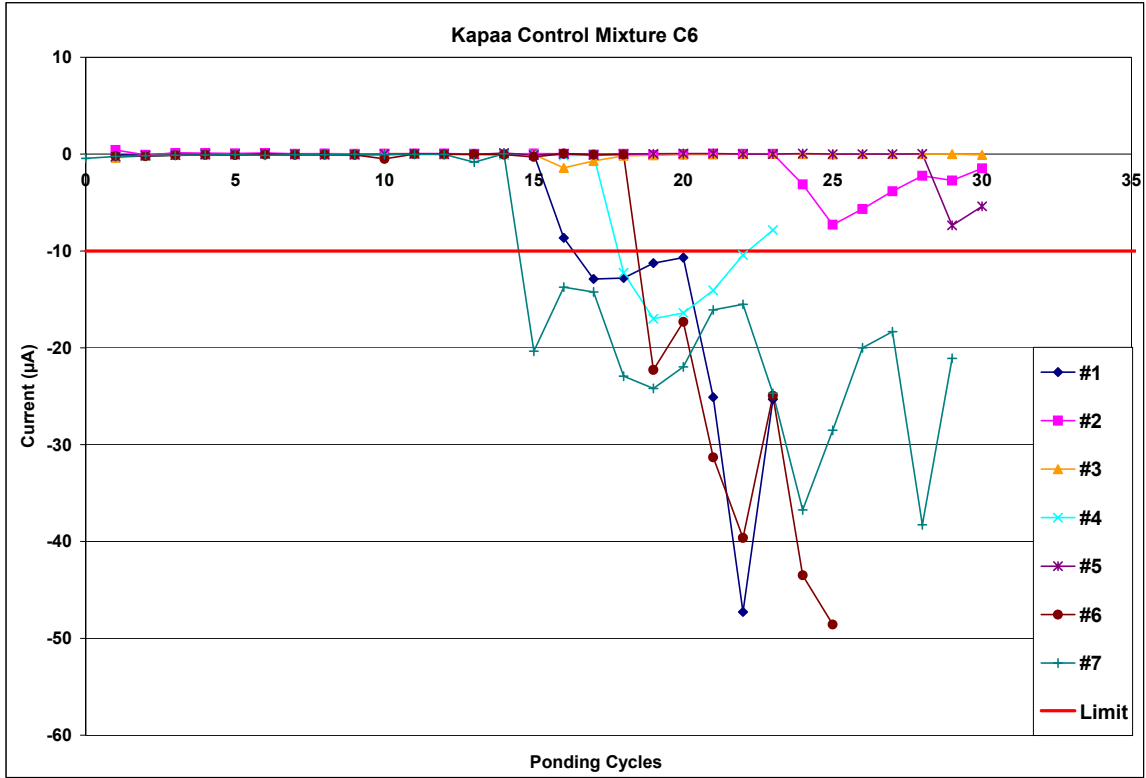


Figure A.1-21: Current Measurements for Kapaa Control Mixture C6

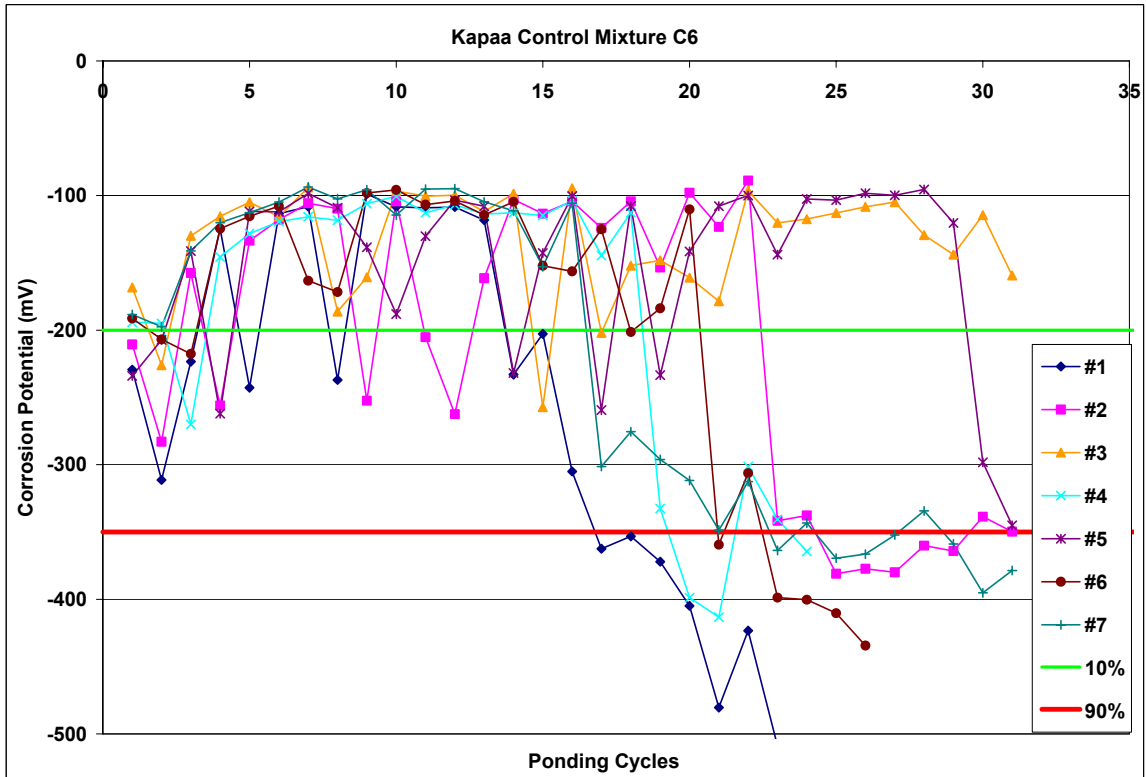


Figure A.1-22: Corrosion Potential Measurements for Kapaa Control Mixture C6

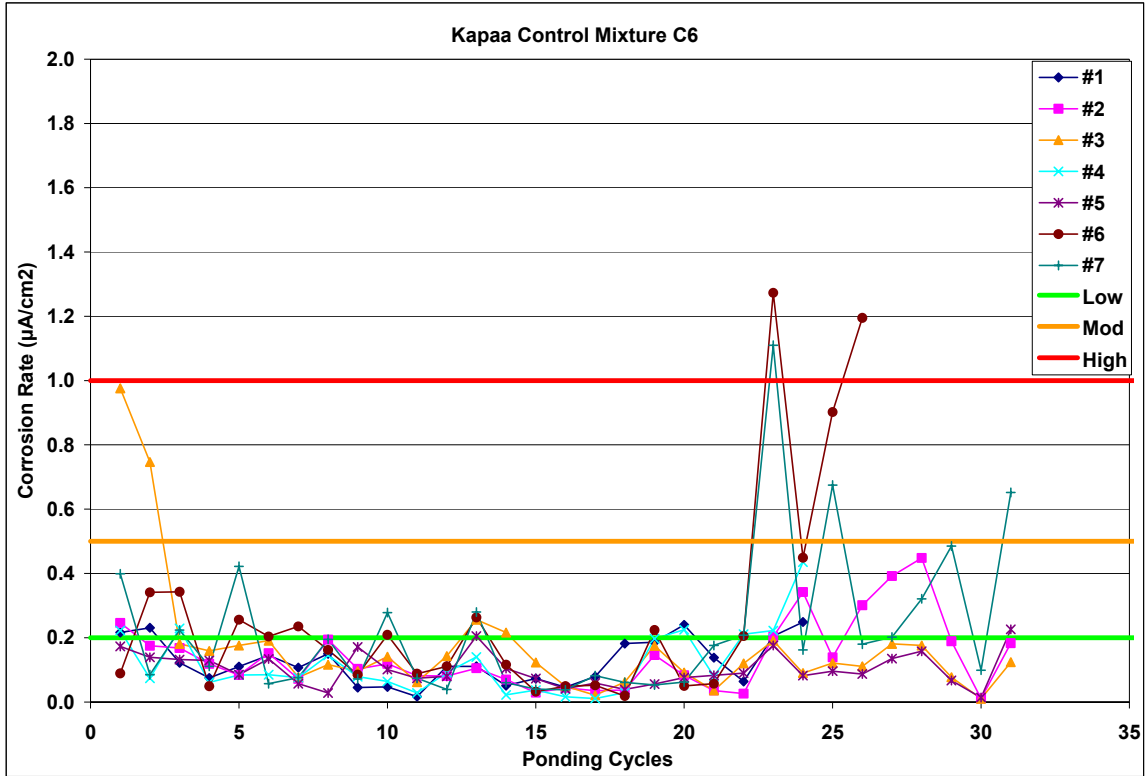


Figure A.1-23: Corrosion Rate Measurements for Kapaa Control Mixture C6

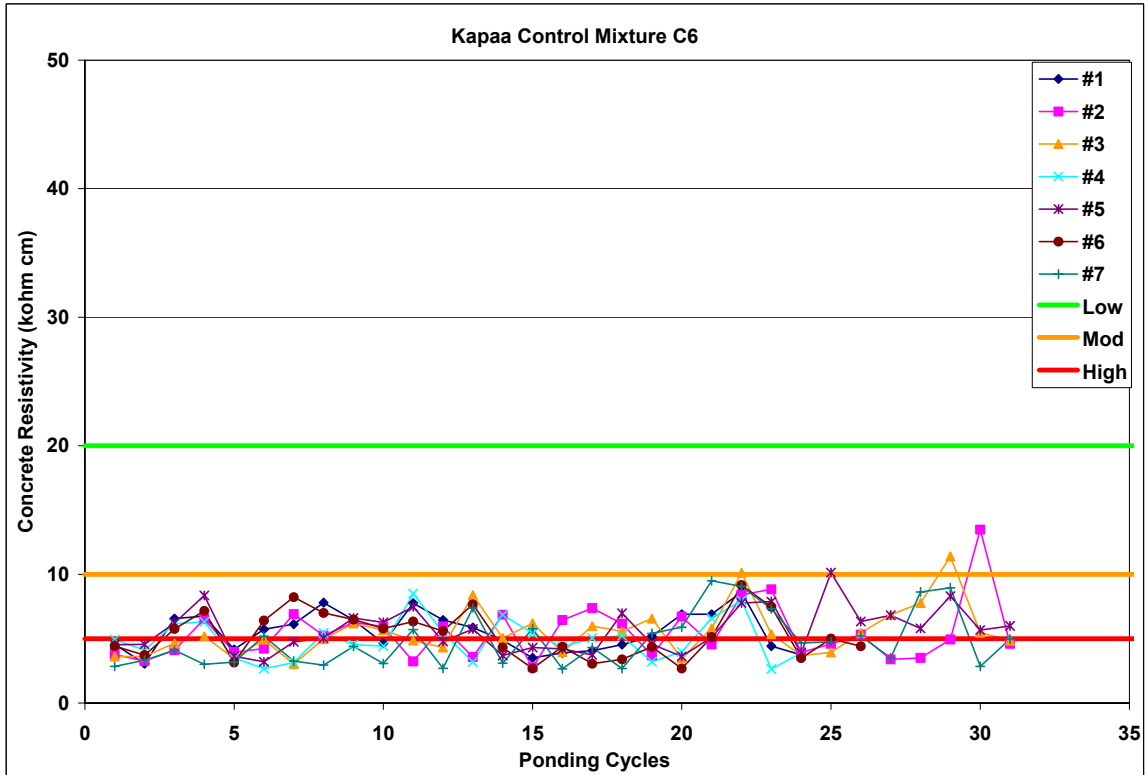


Figure A.1-24: Corrosion Resistivity Measurements for Kapaa Control Mixture C6

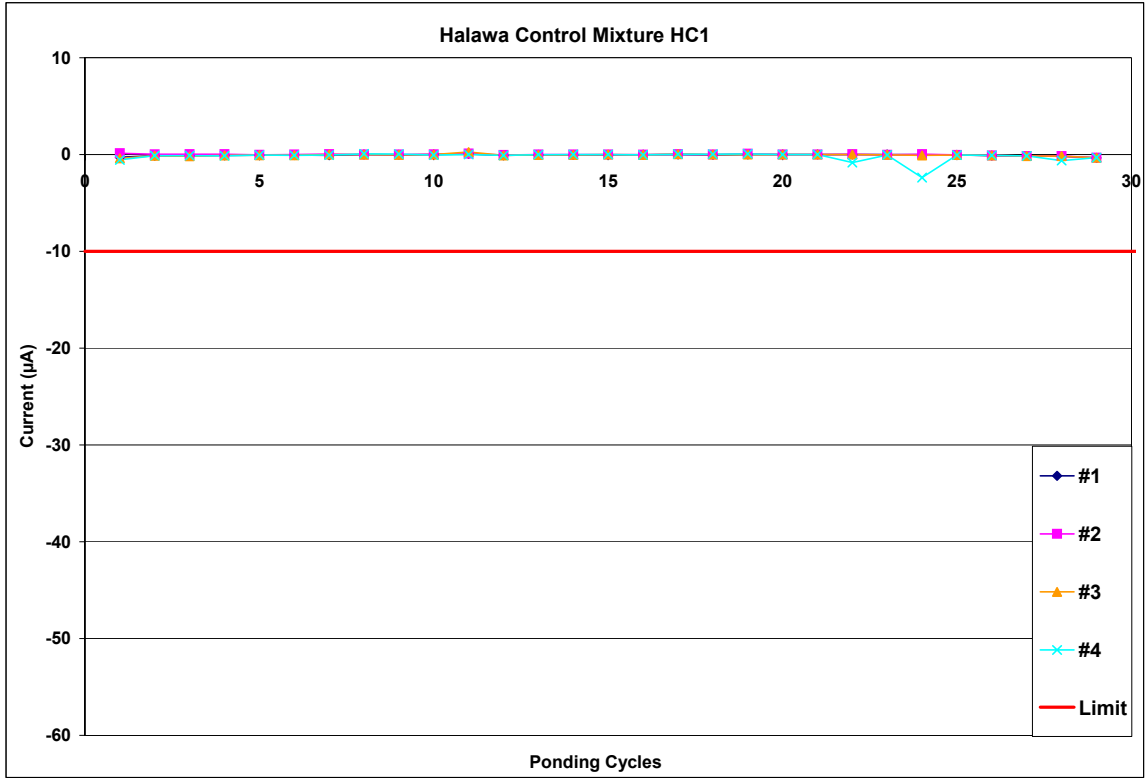


Figure A.1-25: Current Measurements for Halawa Control Mixture HC1

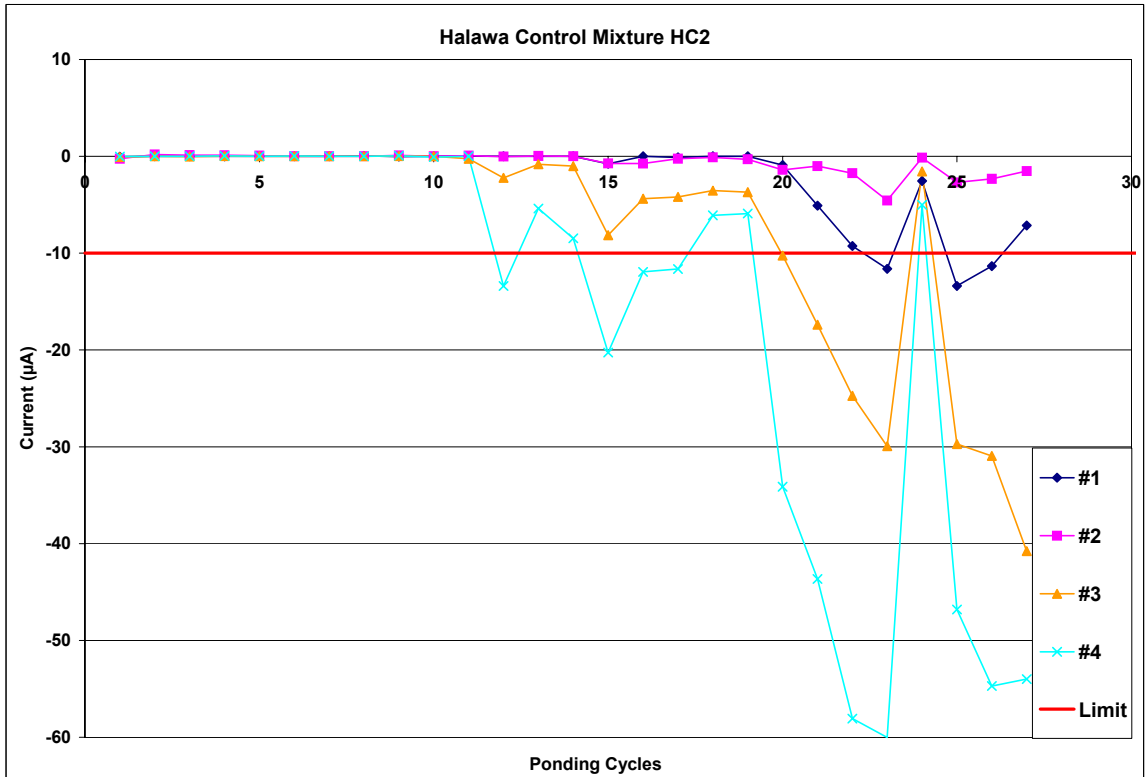


Figure A.1-26: Current Measurements for Halawa Control Mixture HC2

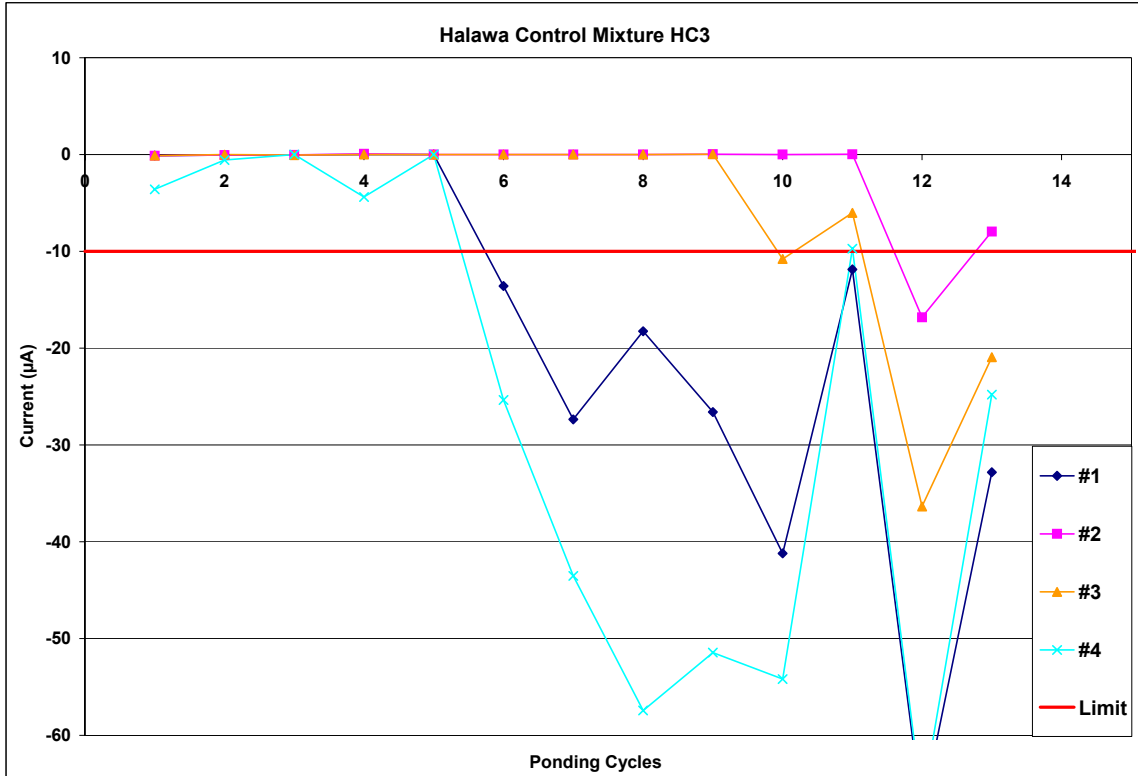


Figure A.1-27: Current Measurements for Halawa Control Mixture HC3

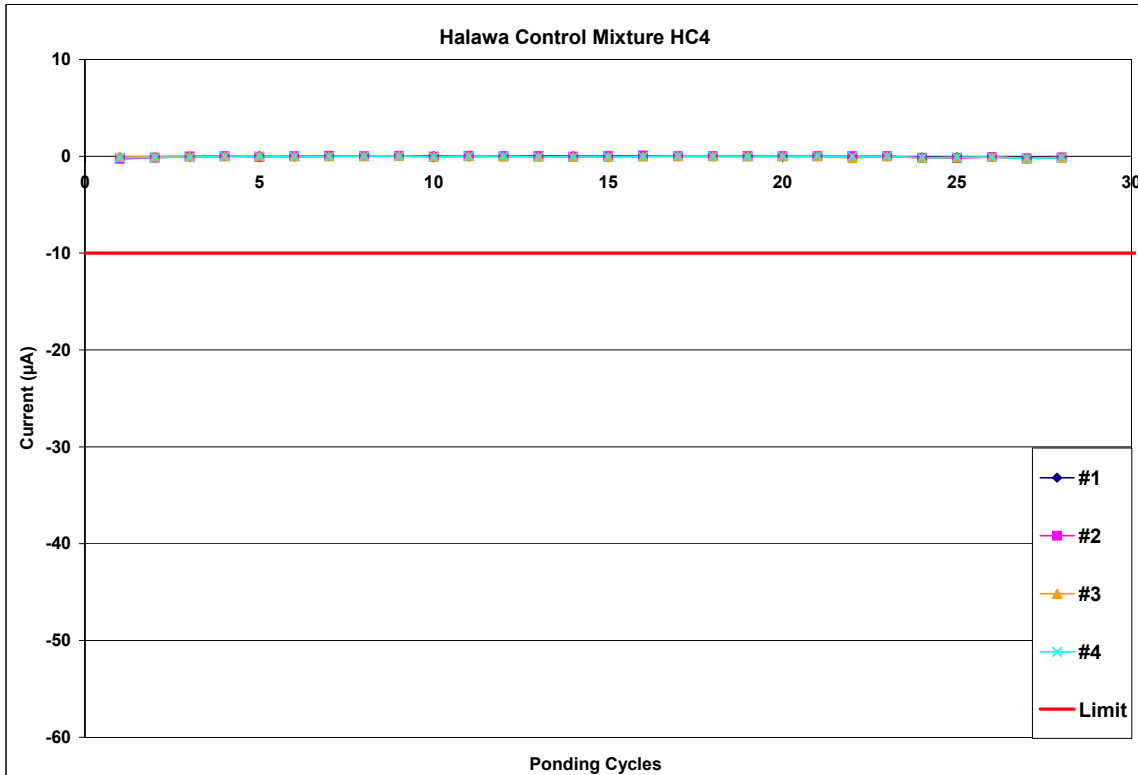


Figure A.1-28: Current Measurements for Halawa Control Mixture HC4

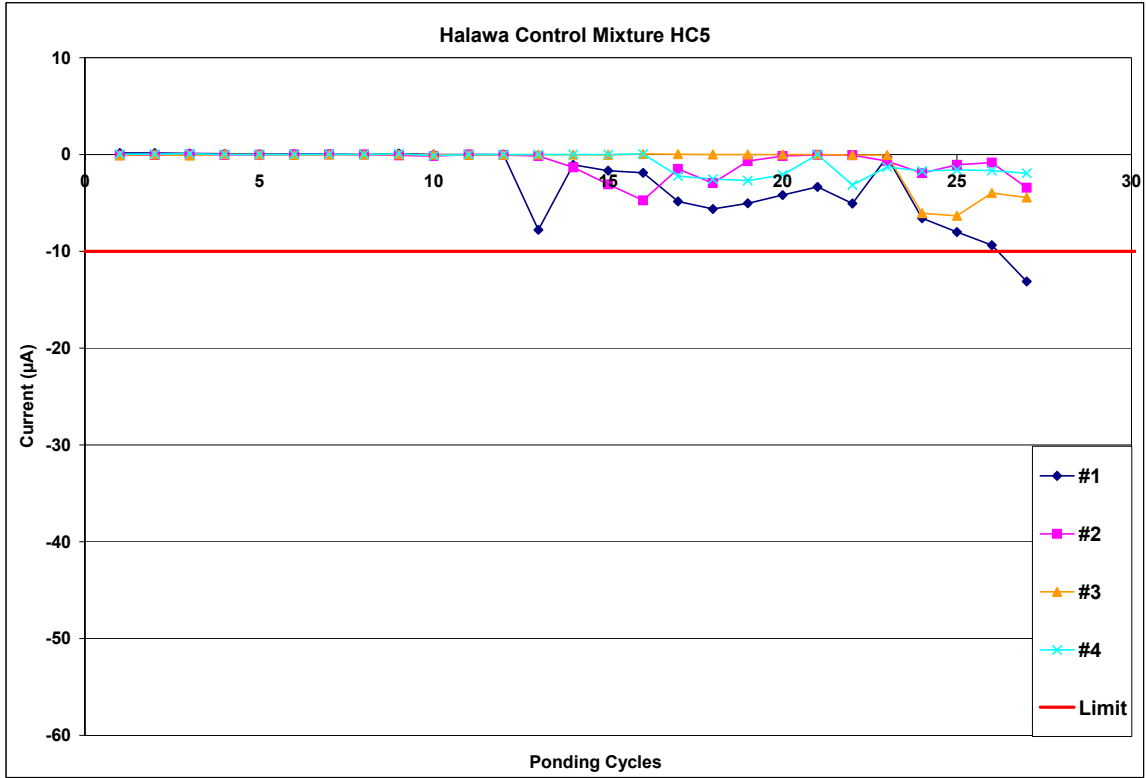


Figure A.1-29: Current Measurements for Halawa Control Mixture HC5

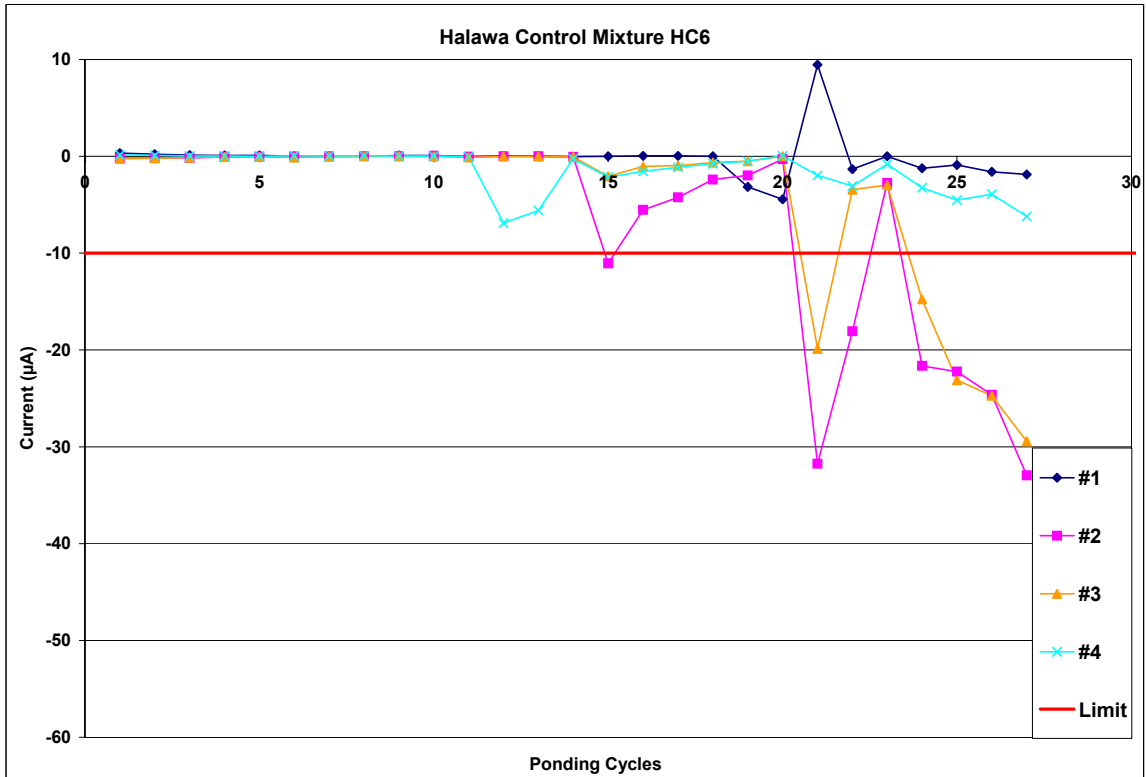


Figure A.1-30: Current Measurements for Halawa Control Mixture HC6

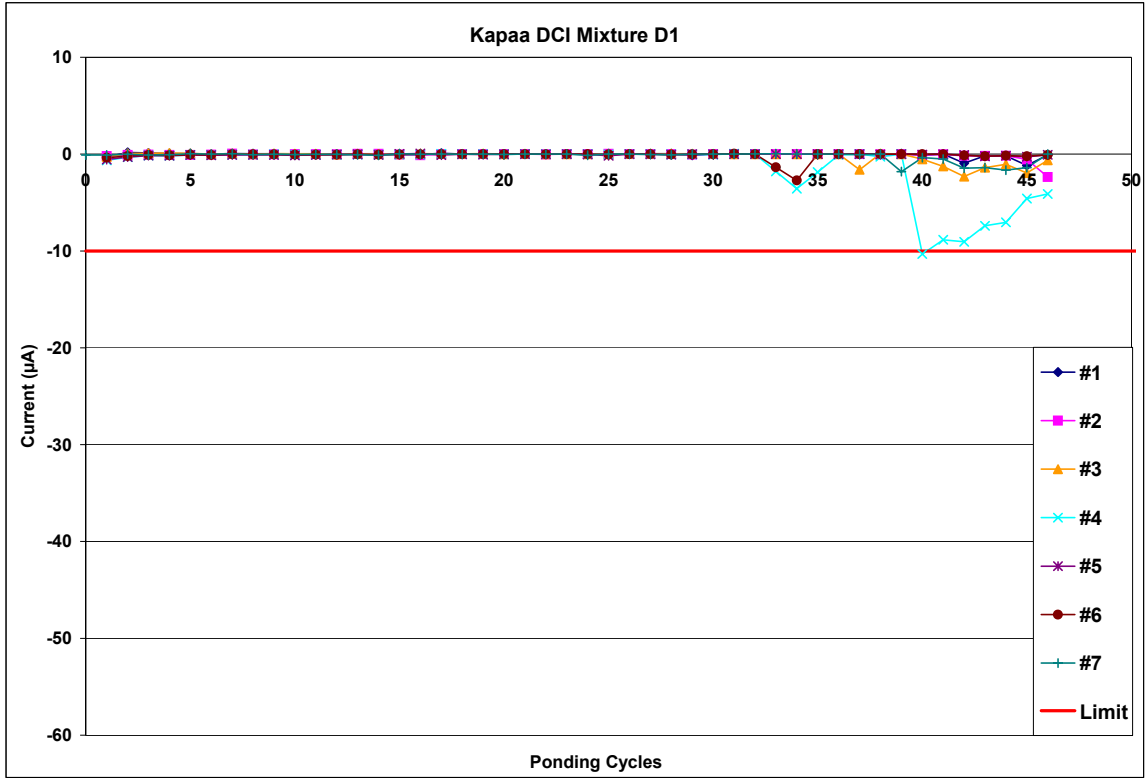


Figure A.1-31: Current Measurements for Kapaa DCI Mixture D1

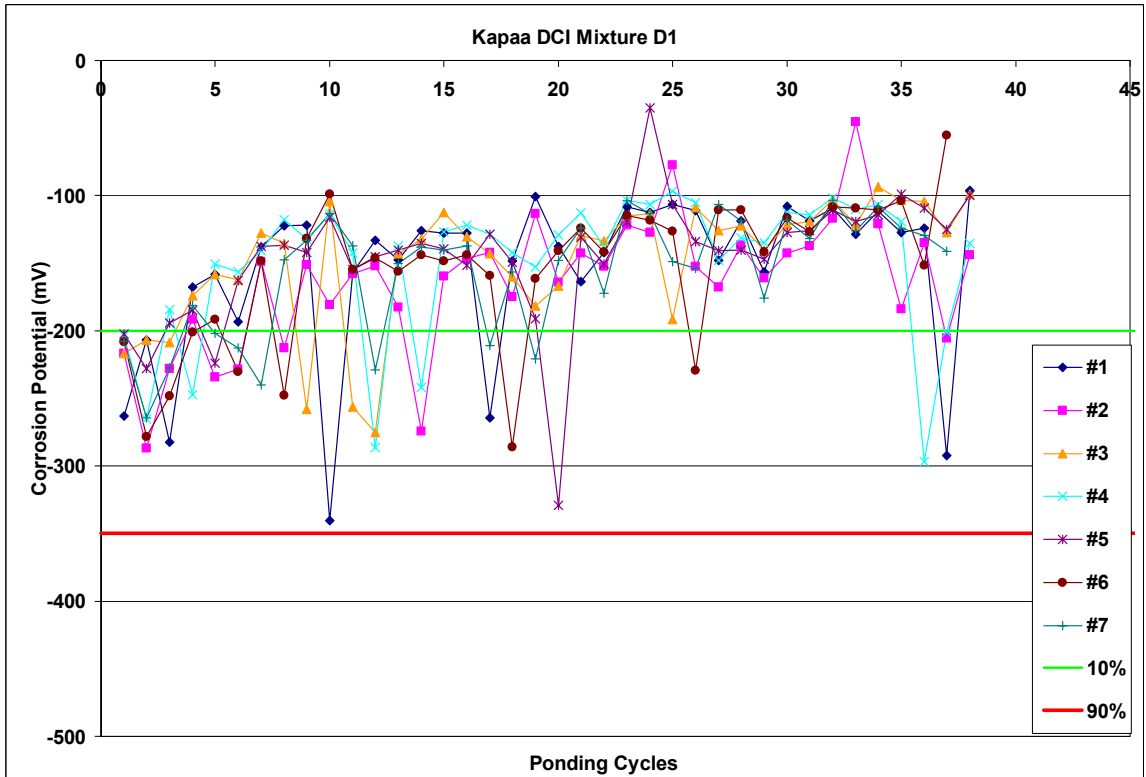


Figure A.1-32: Corrosion Potential Measurements for Kapaa DCI Mixture D1.

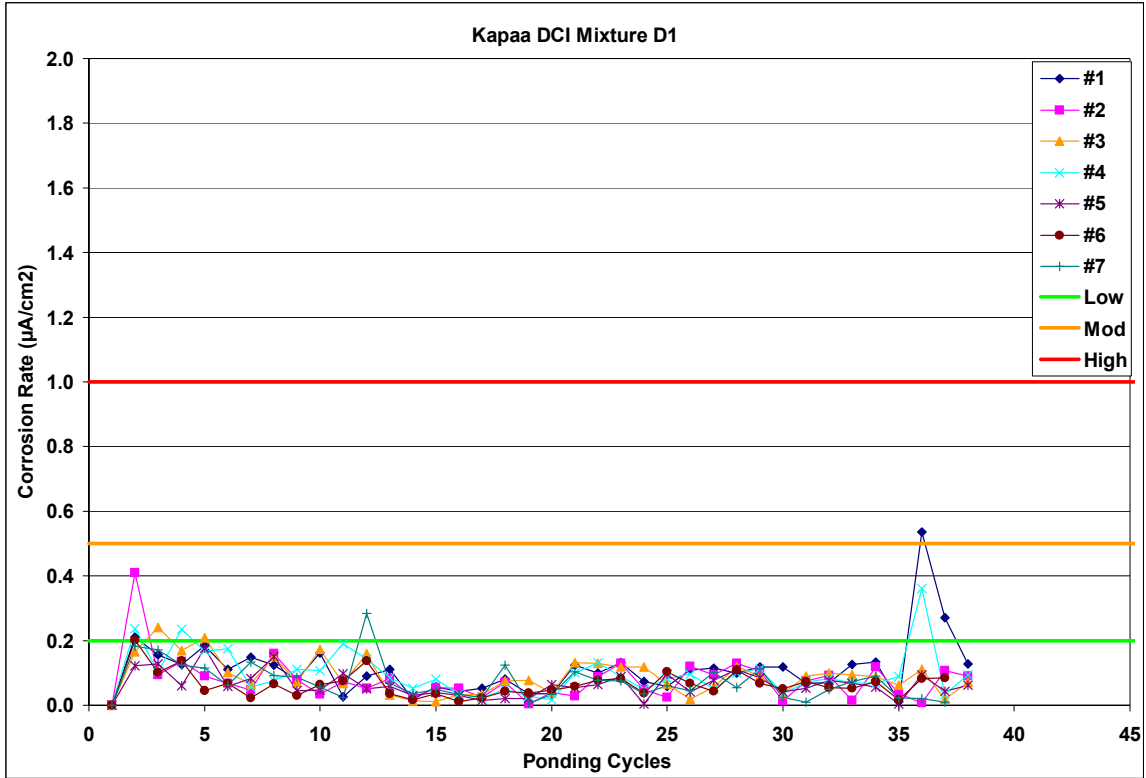


Figure A.1-33: Corrosion Rate Measurements for Kapaa DCI Mixture D1

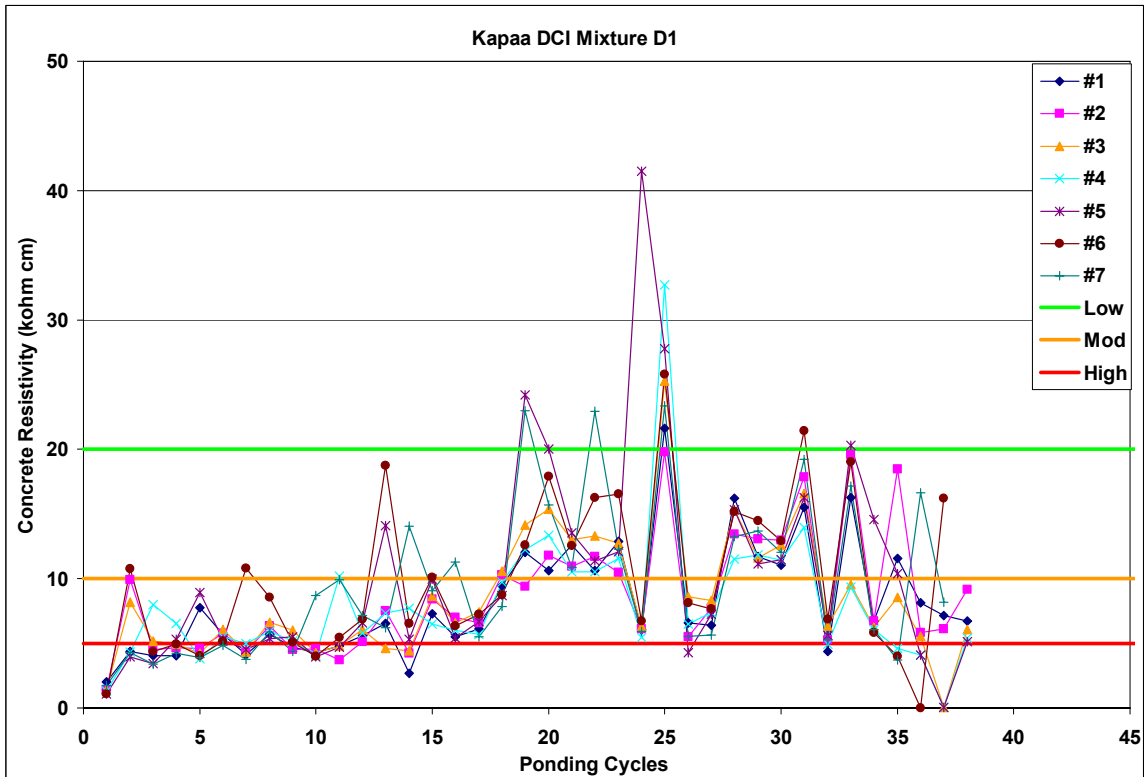


Figure A.1-34: Corrosion Resistivity Measurements for Kapaa DCI Mixture D1

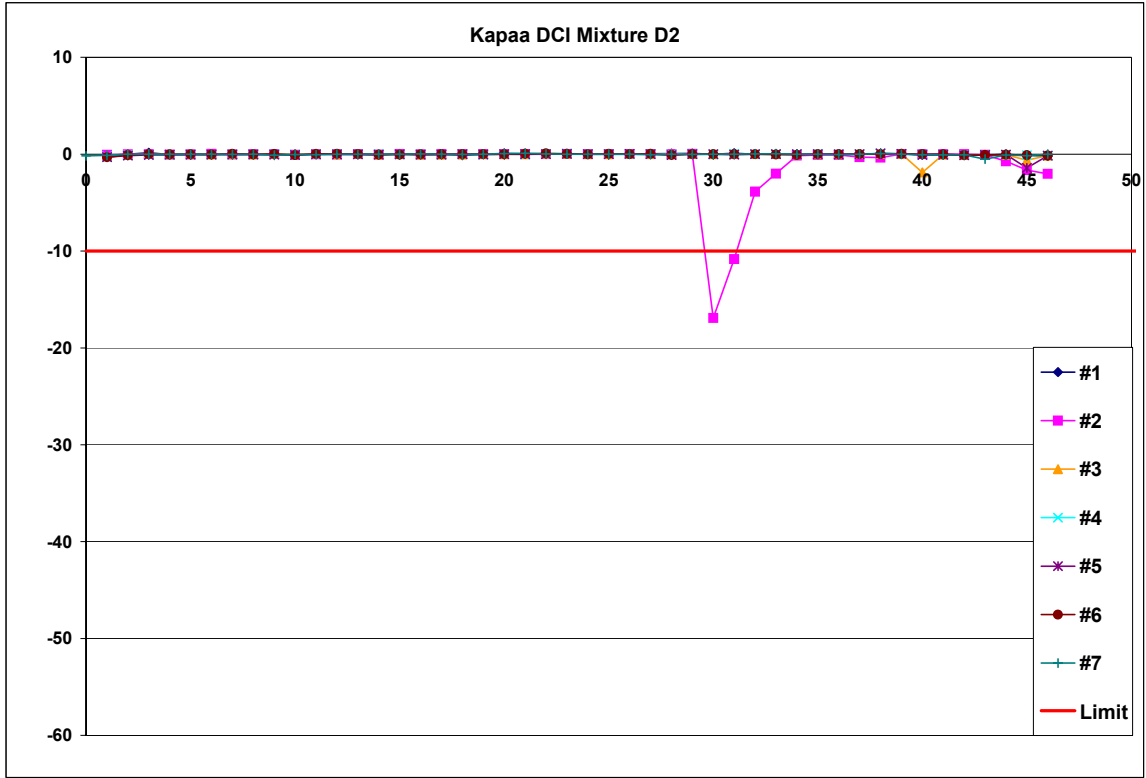


Figure A.1-35: Current Measurements for Kapaa DCI Mixture D2

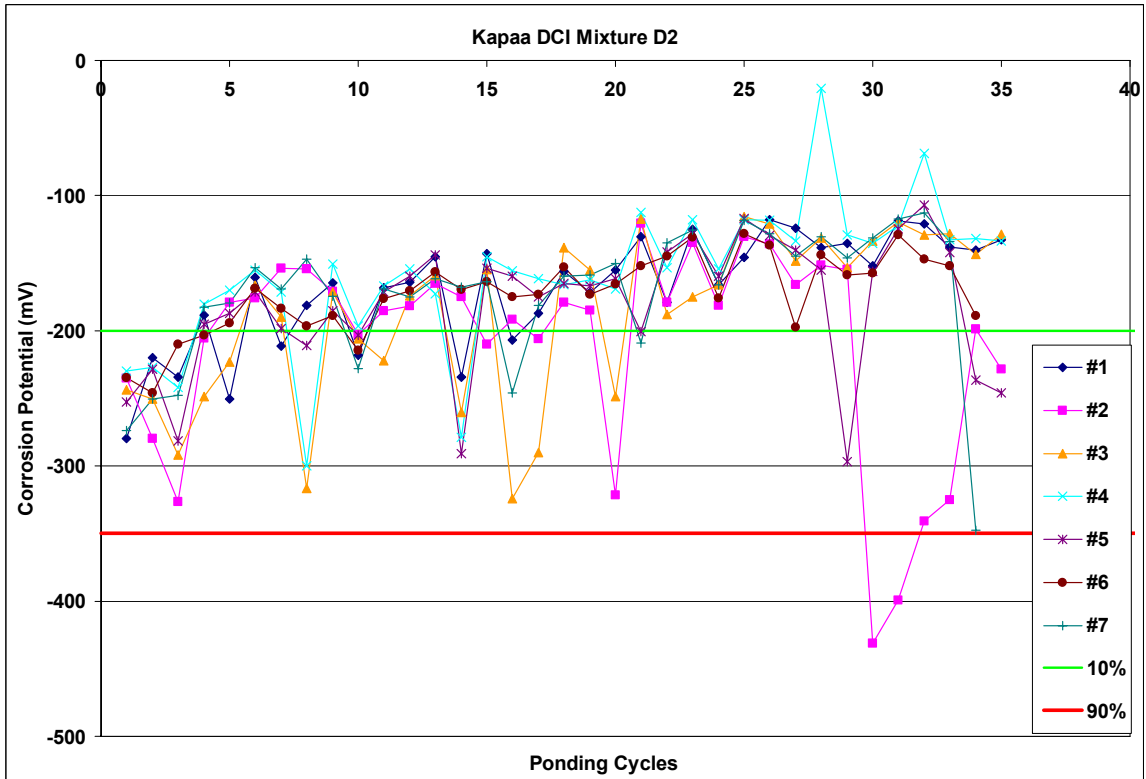


Figure A.1-36: Corrosion Potential Measurements for Kapaa DCI Mixture D2

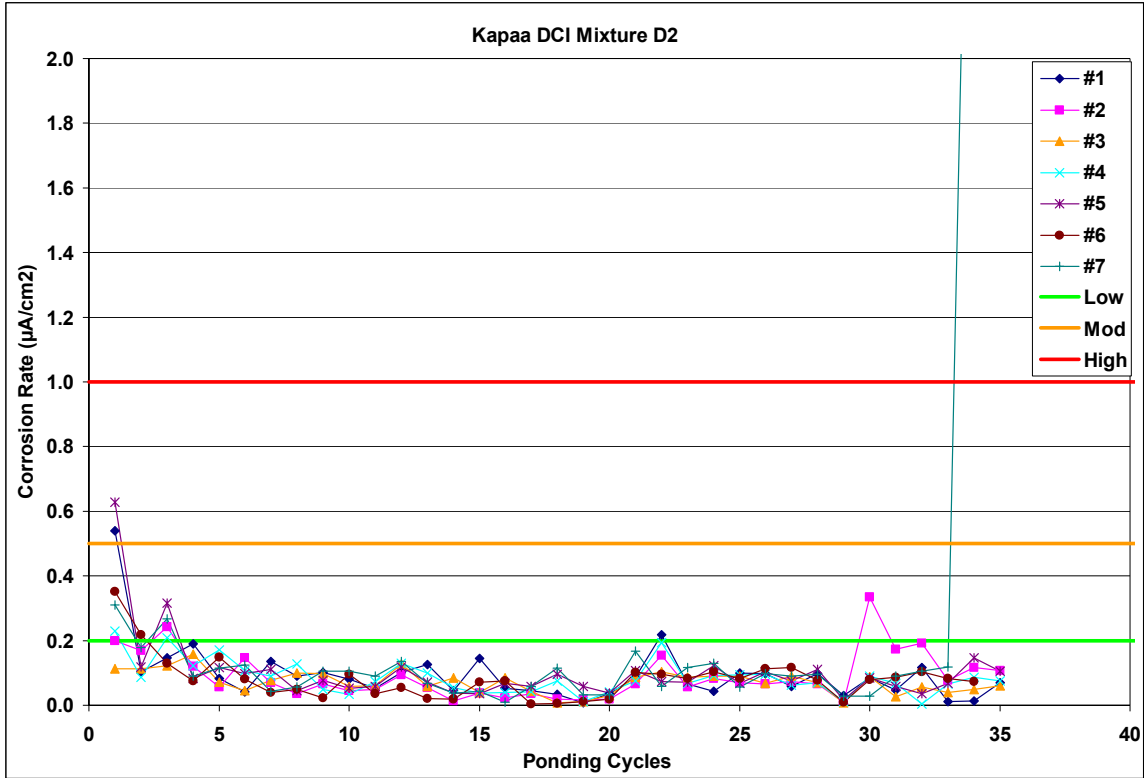


Figure A.1-37: Corrosion Rate Measurements for Kapaa DCI Mixture D2

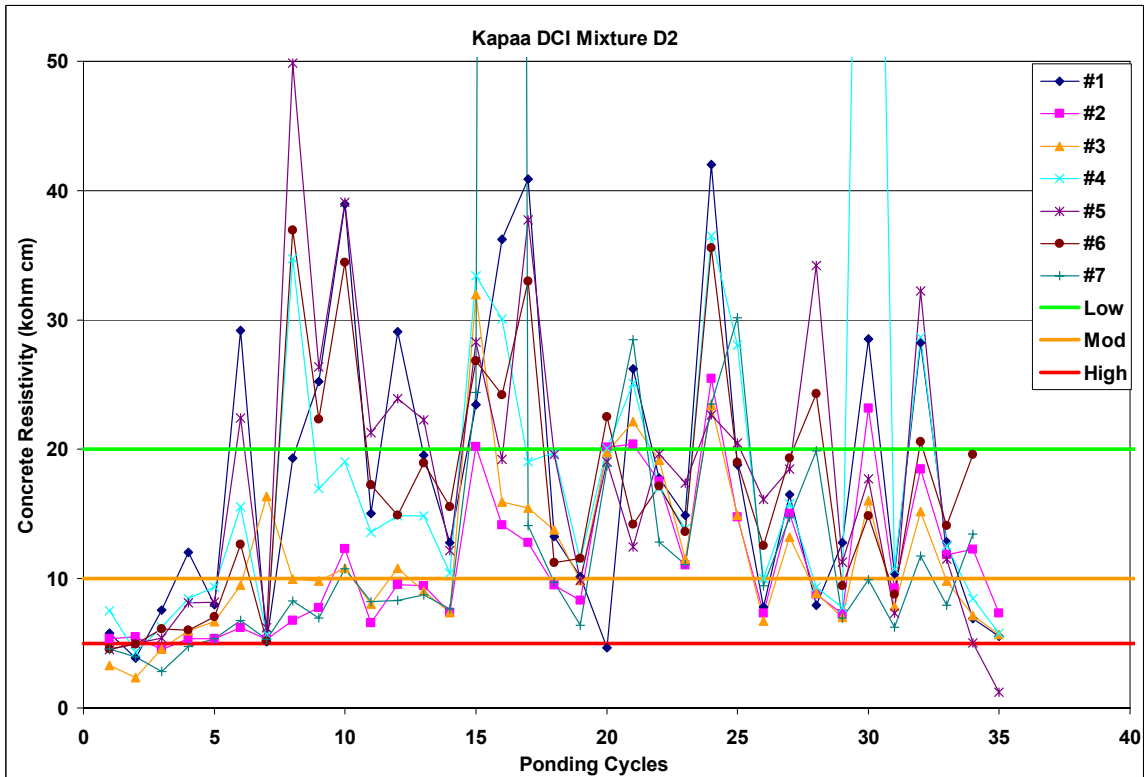


Figure A.1-38: Corrosion Resistivity Measurements for Kapaa DCI Mixture D2

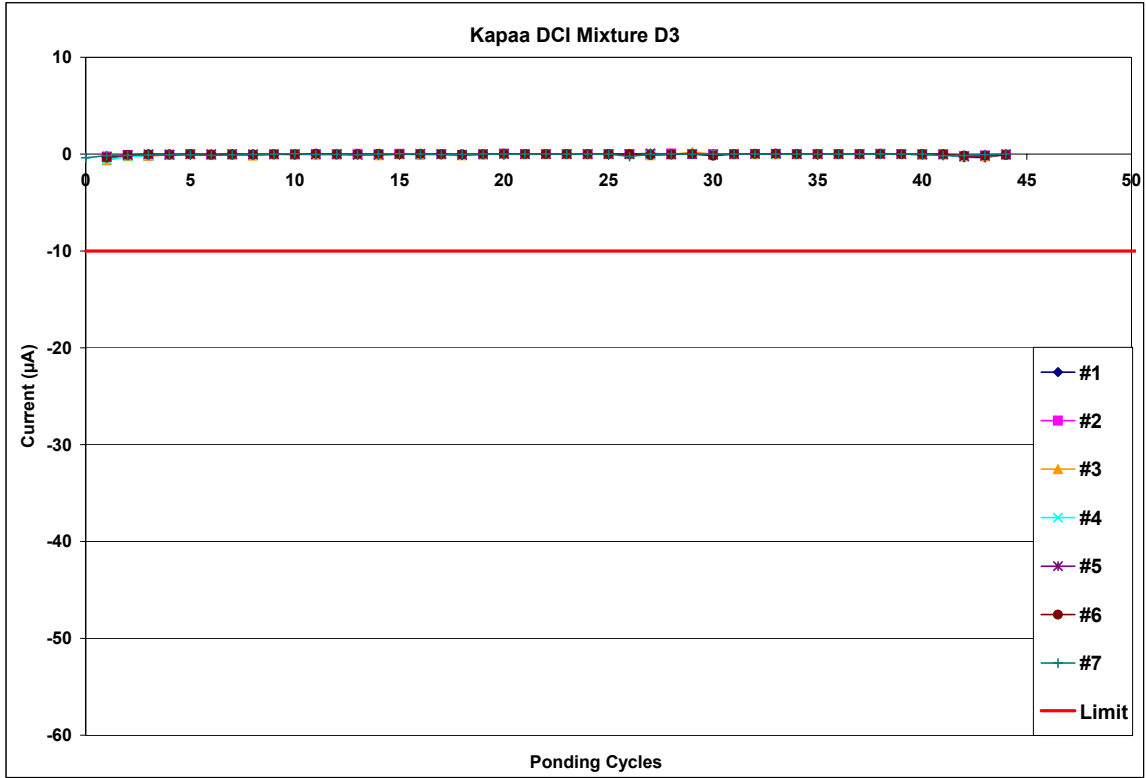


Figure A.1-39: Current Measurements for Kapaa DCI Mixture D3

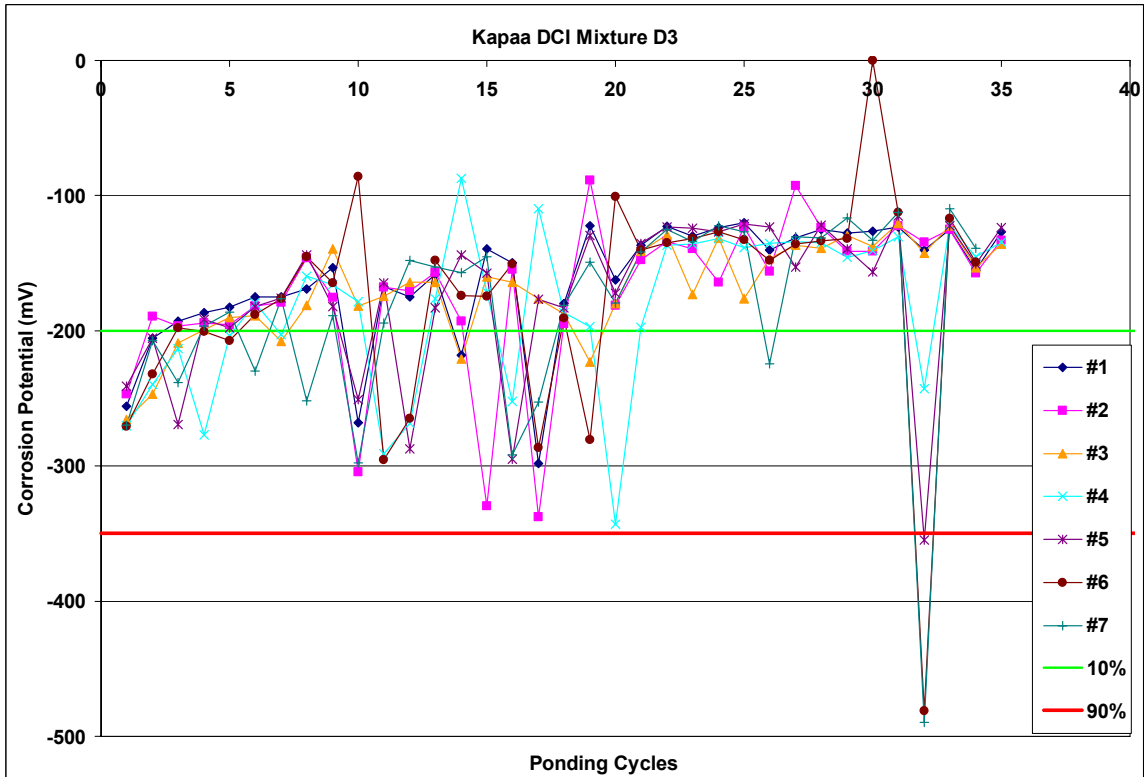


Figure A.1-40: Corrosion Potential Measurements for Kapaa DCI Mixture D3

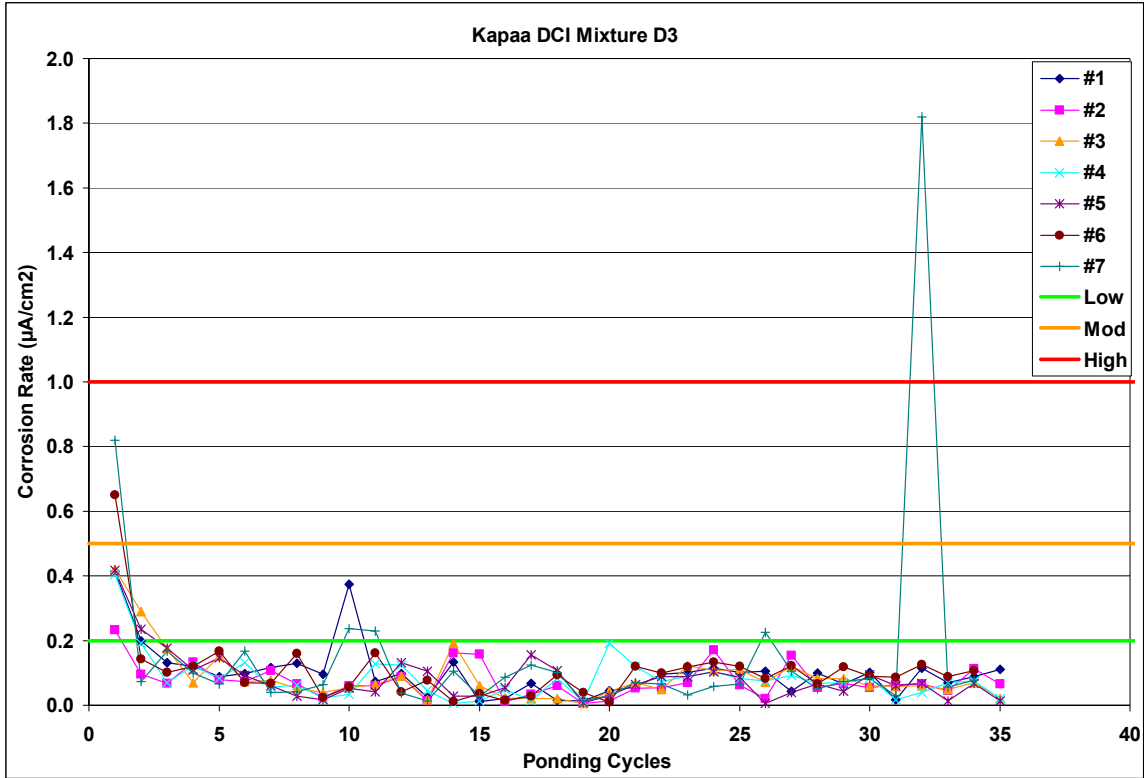


Figure A.1-41: Corrosion Rate Measurements for Kapaa DCI Mixture D3

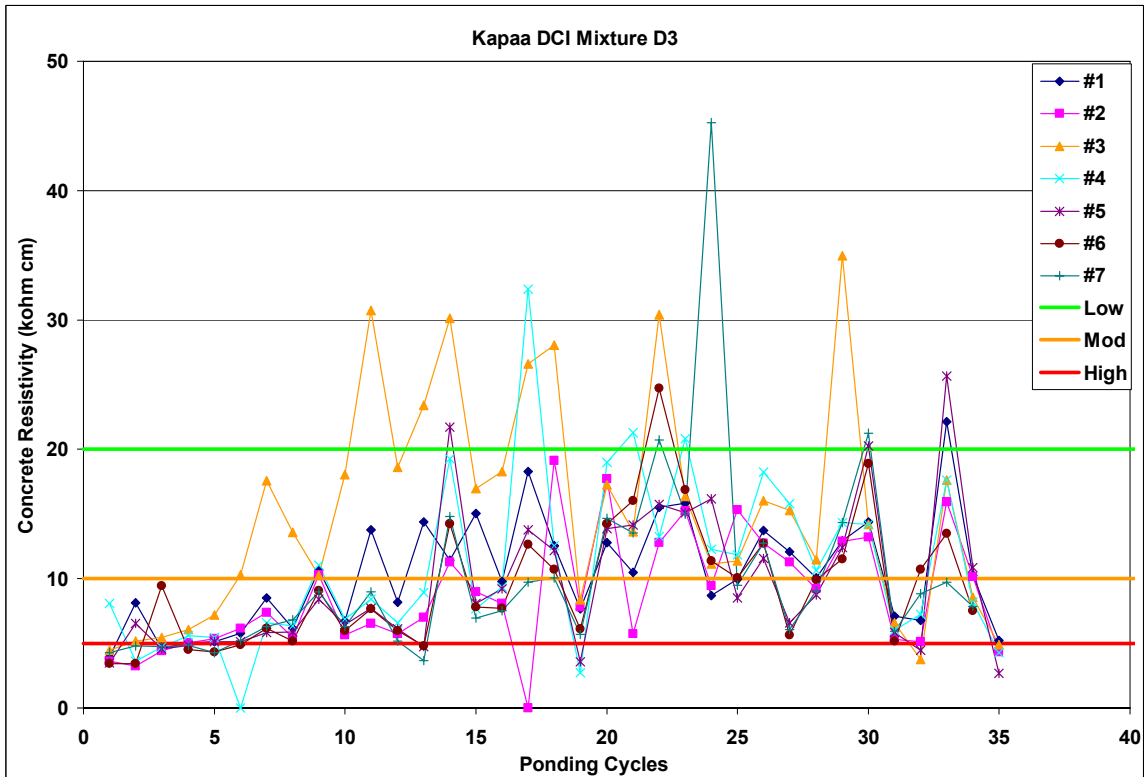


Figure A.1-42: Corrosion Resistivity Measurements for Kapaa DCI Mixture D3

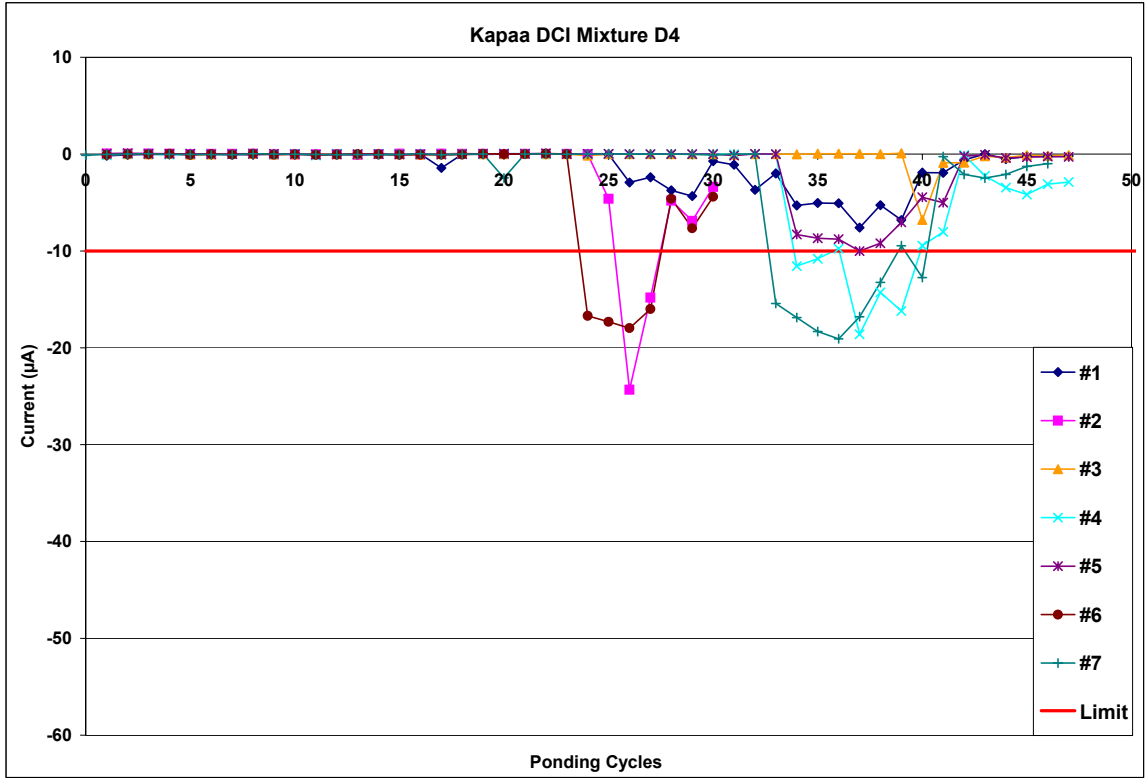


Figure A.1-43: Current Measurements for Kapaa DCI Mixture D4

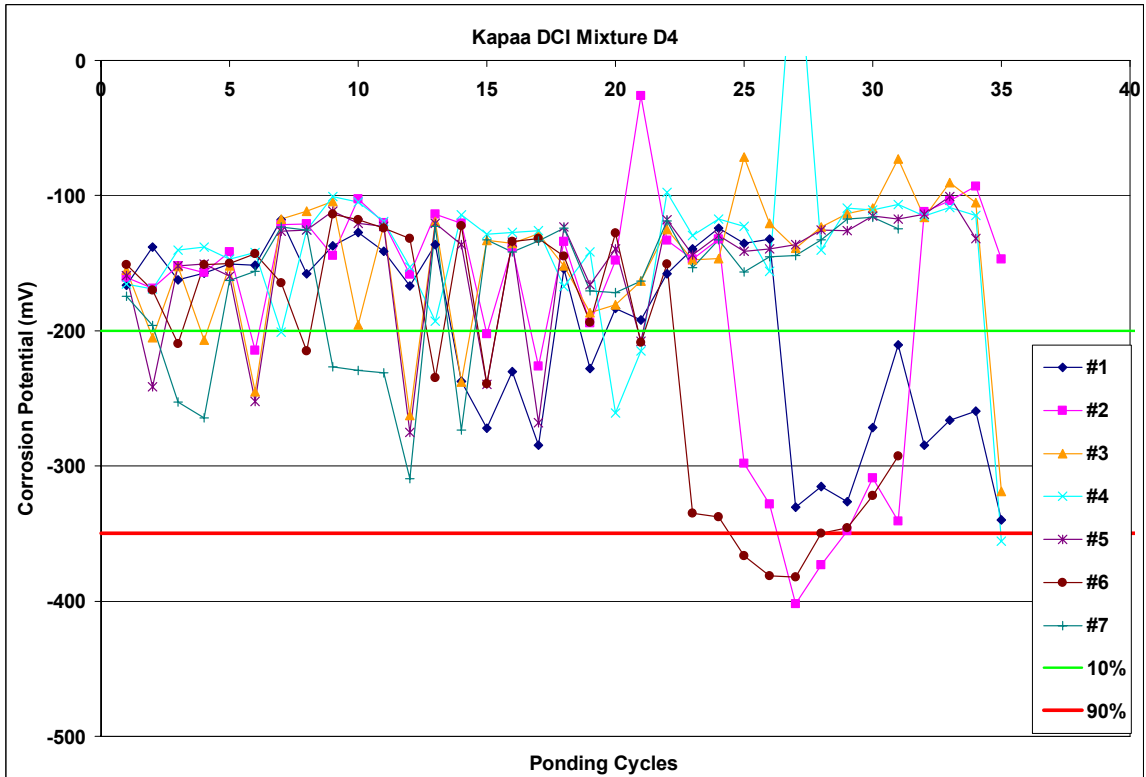


Figure A.1-44: Corrosion Potential Measurements for Kapaa DCI Mixture D4

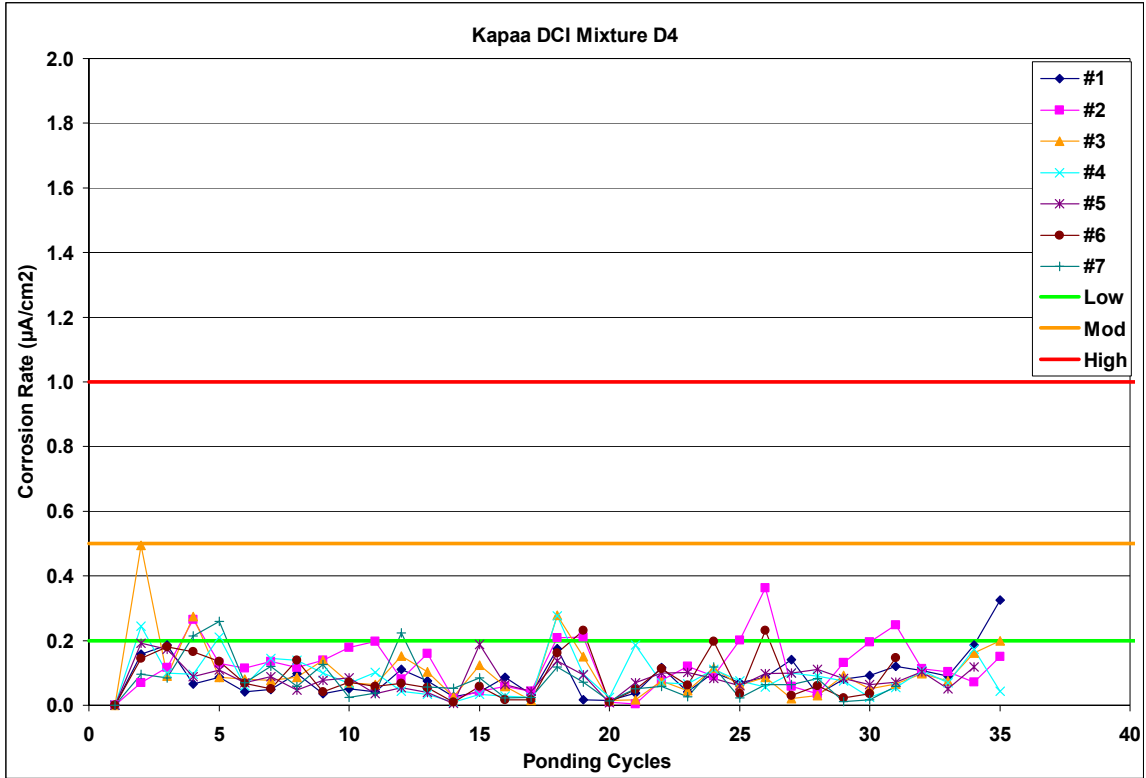


Figure A.1-45: Corrosion Rate Measurements for Kapaa DCI Mixture D4

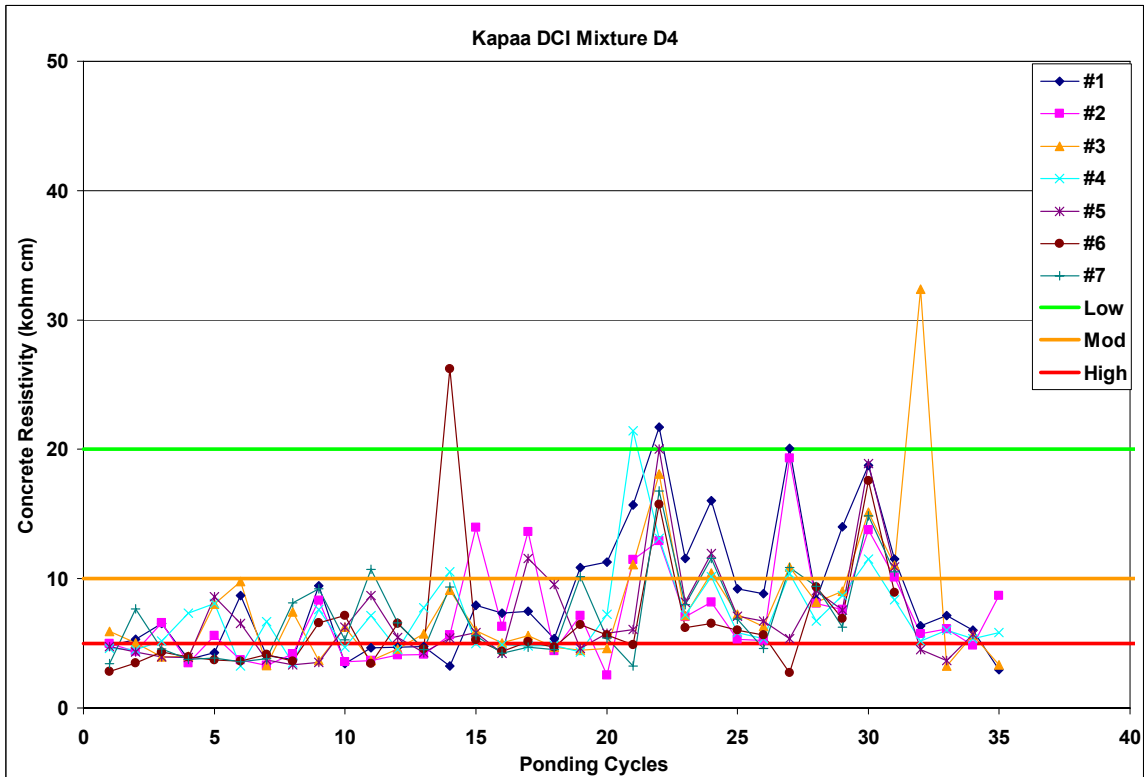


Figure A.1-46: Corrosion Resistivity Measurements for Kapaa DCI Mixture D4

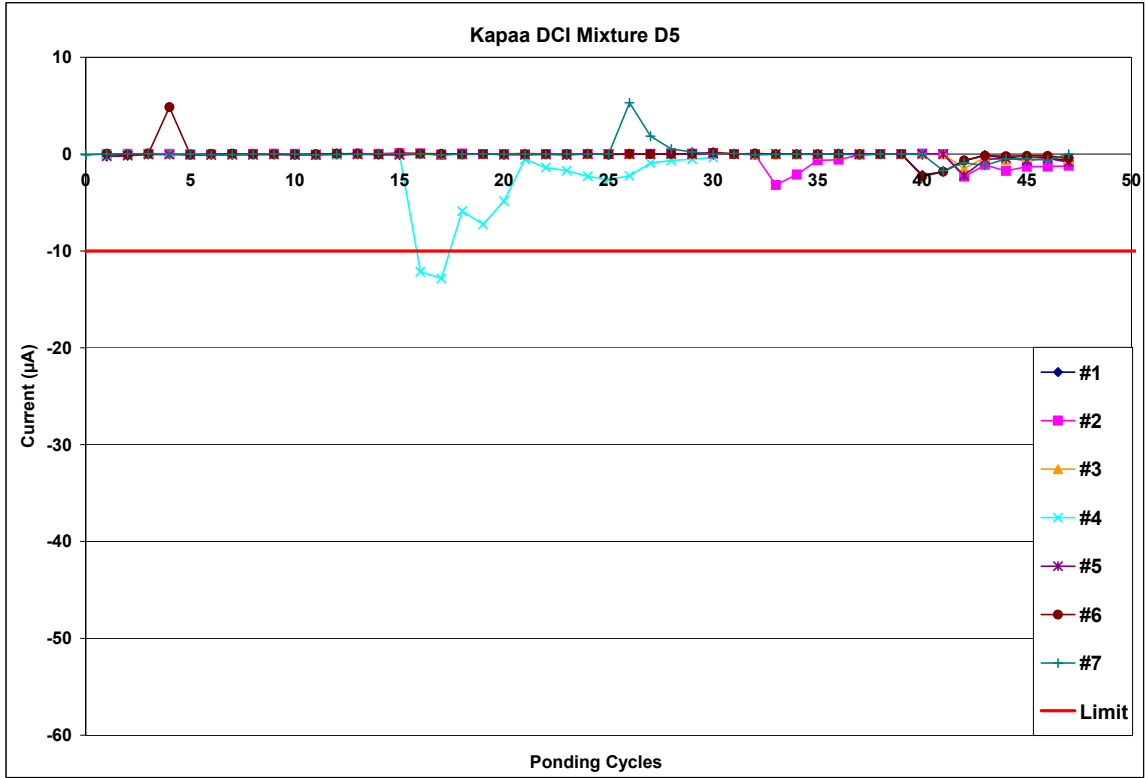


Figure A.1-47: Current Measurements for Kapaa DCI Mixture D5

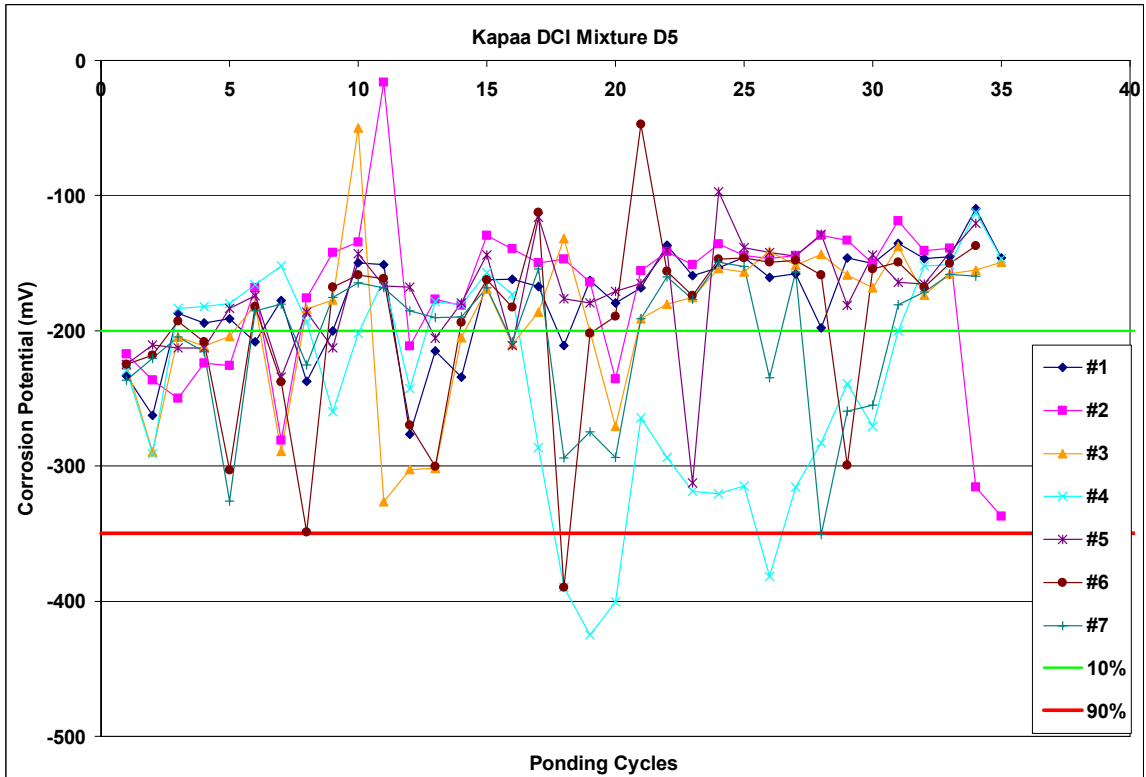


Figure A.1-48: Corrosion Potential Measurements for Kapaa DCI Mixture D5

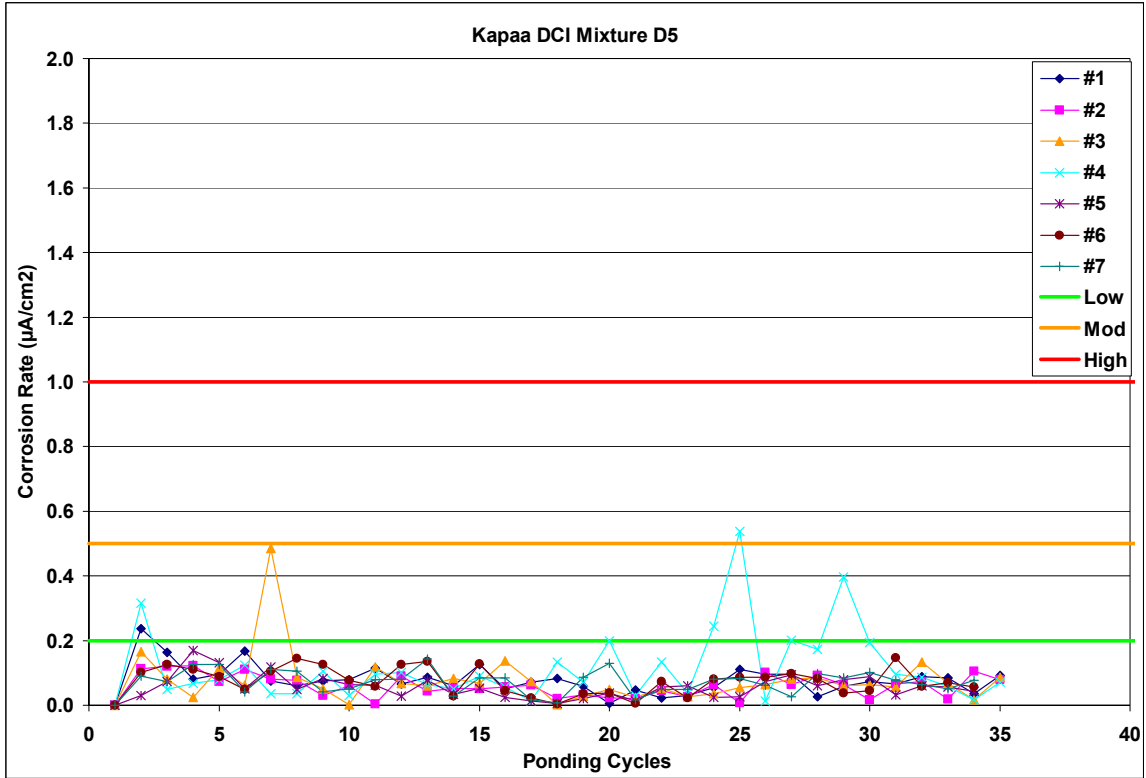


Figure A.1-49: Corrosion Rate Measurements for Kapaa DCI Mixture D5

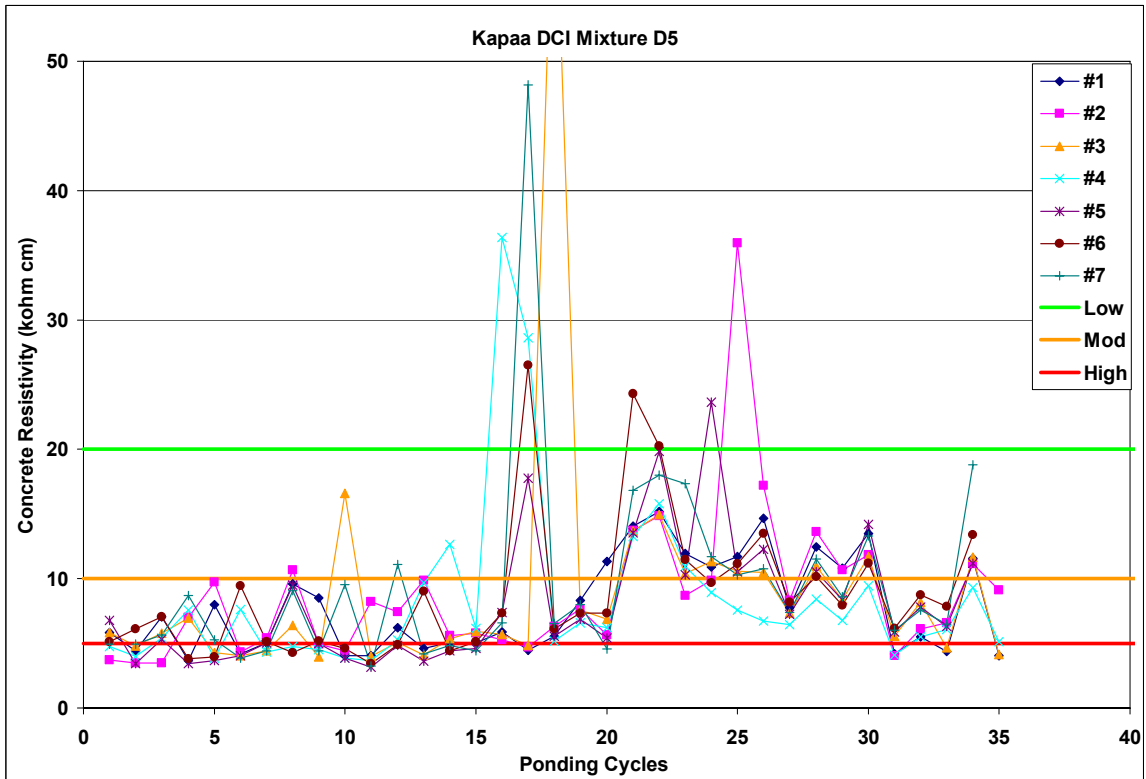


Figure A.1-50: Corrosion Resistivity Measurements for Kapaa DCI Mixture D5

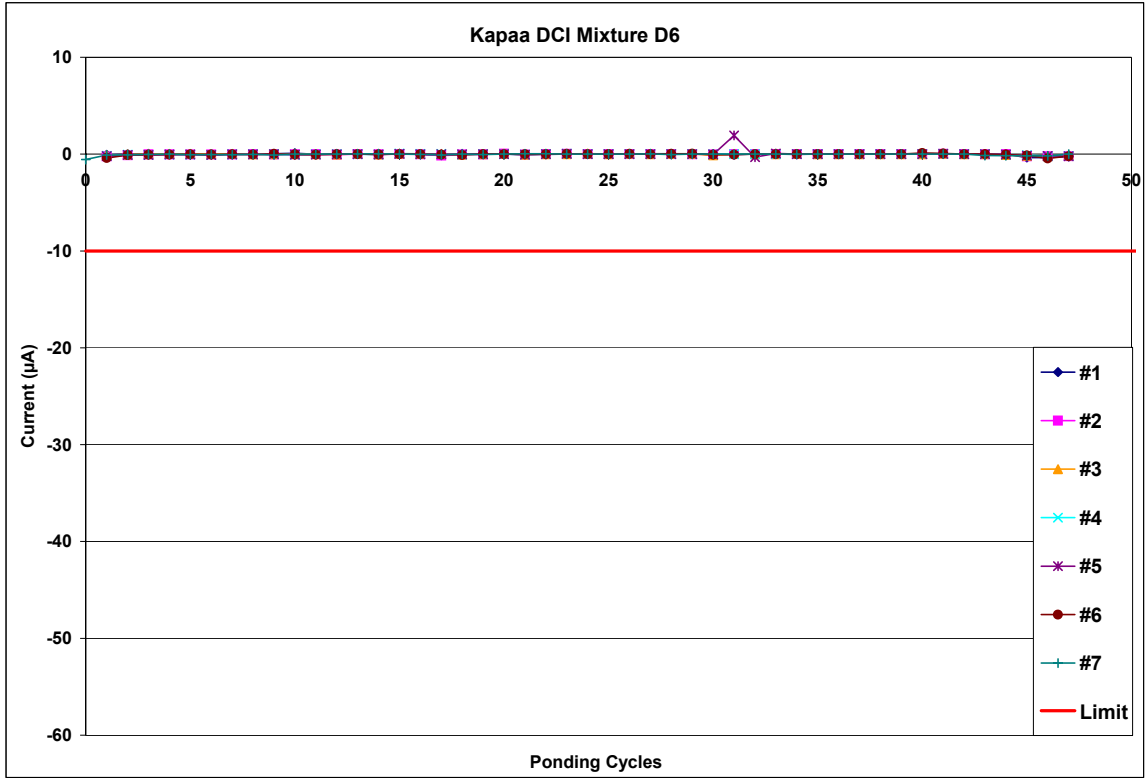


Figure A.1-51: Current Measurements for Kapaa DCI Mixture D6

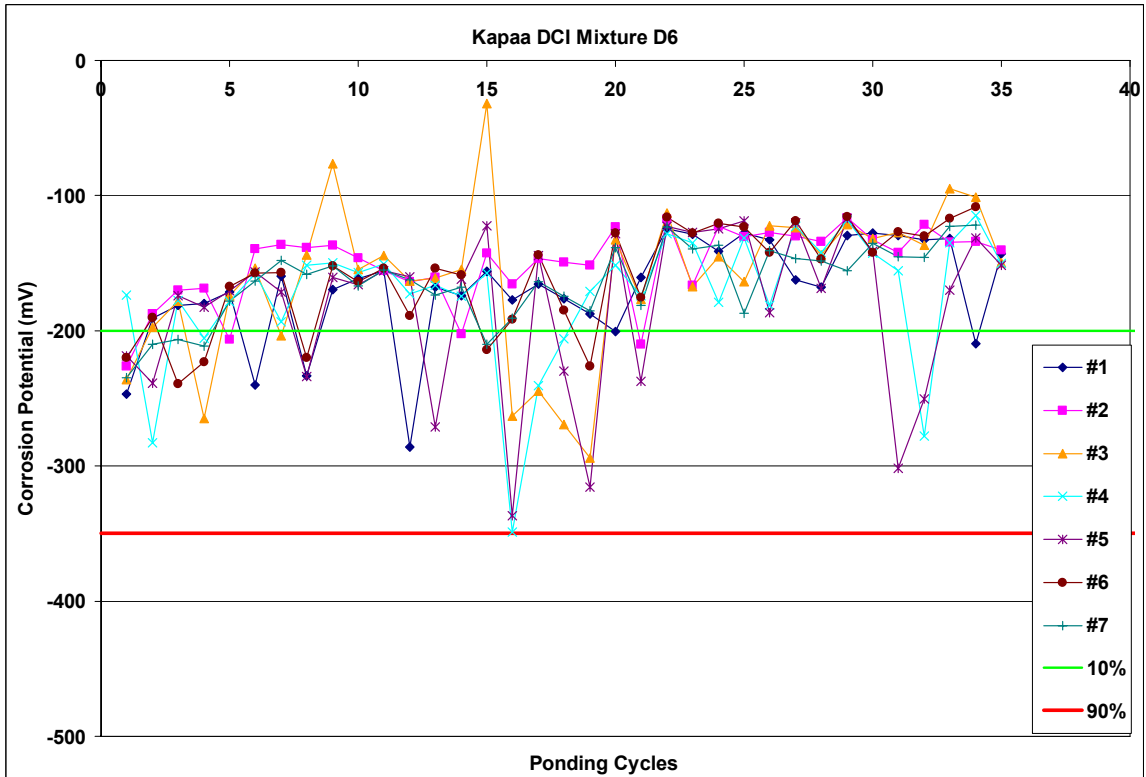


Figure A.1-52: Corrosion Potential Measurements for Kapaa DCI Mixture D6

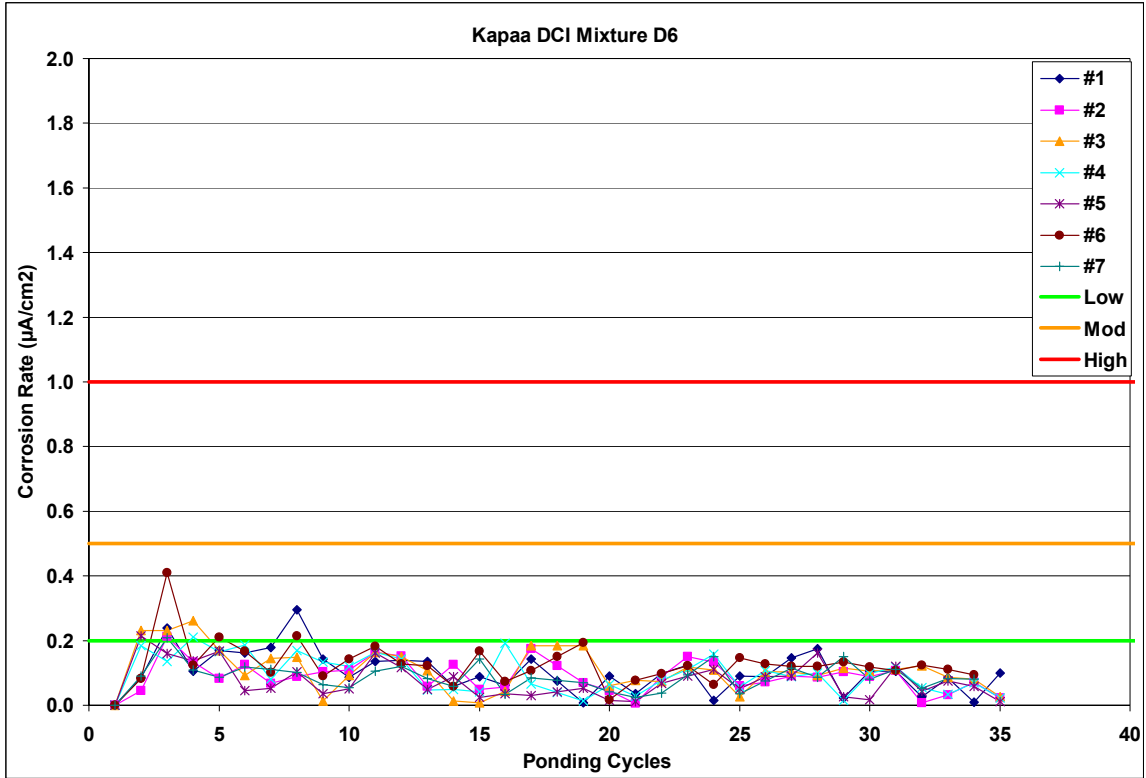


Figure A.1-53: Corrosion Rate Measurements for Kapaa DCI Mixture D6

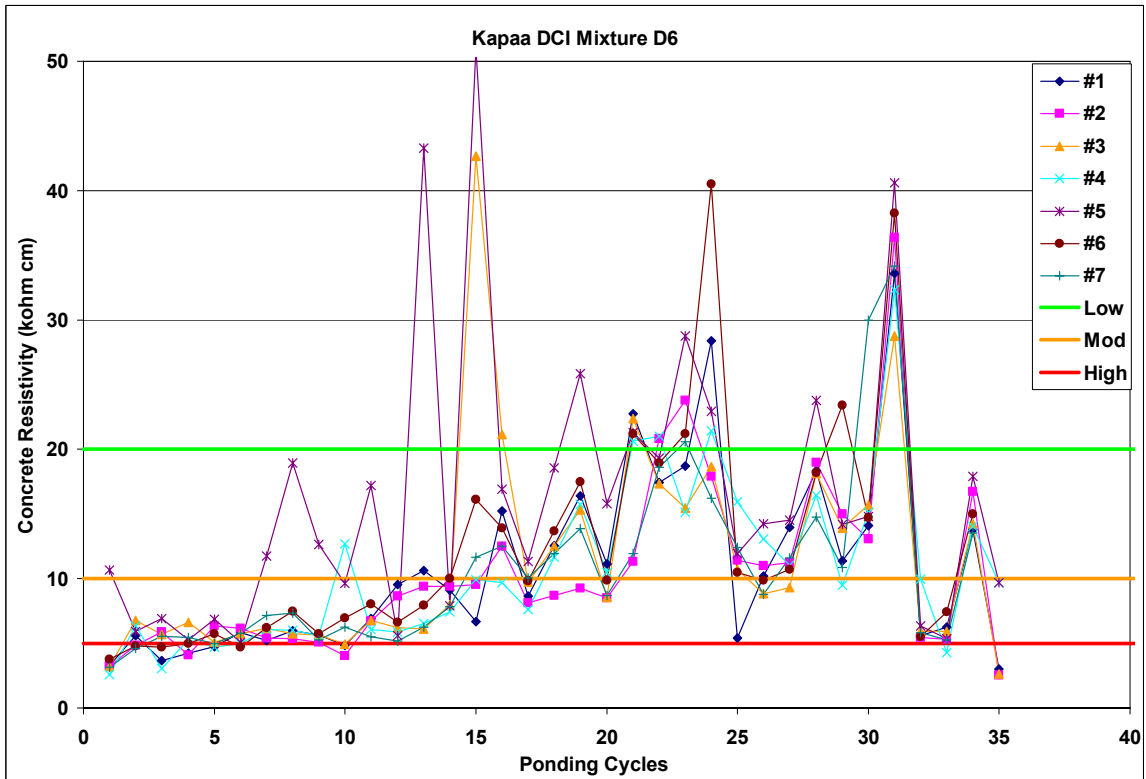


Figure A.1-54: Corrosion Resistivity Measurements for Kapaa DCI Mixture D6

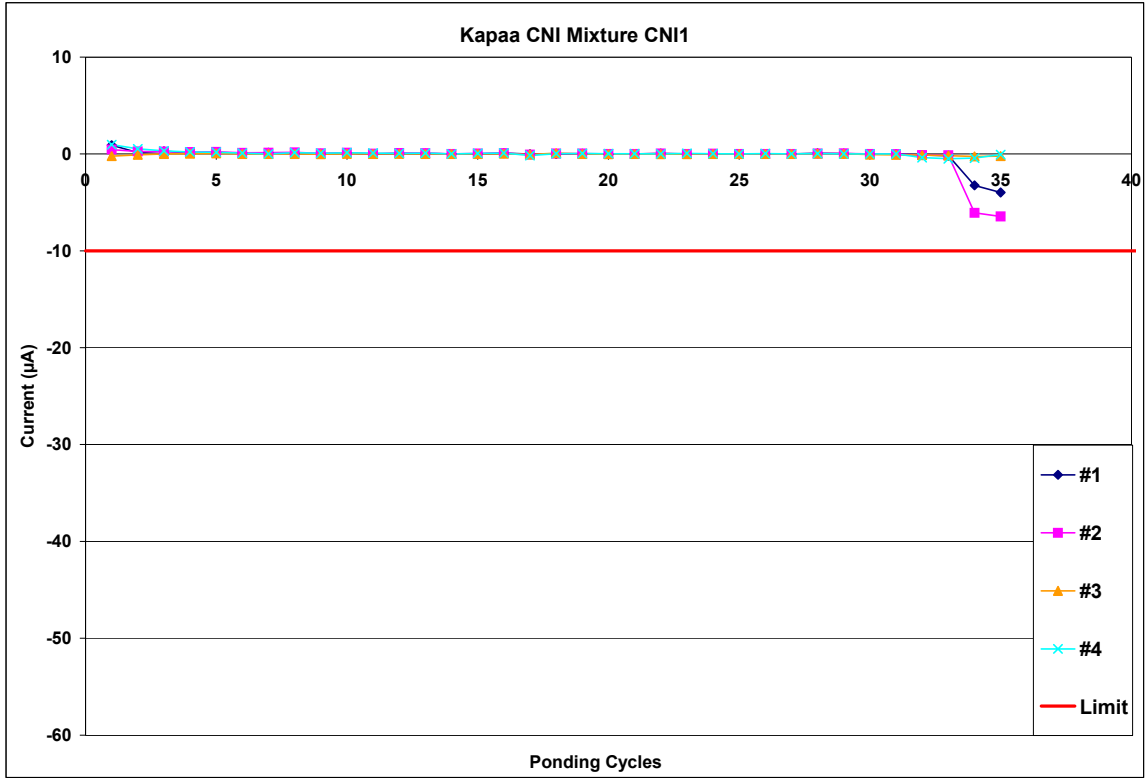


Figure A.1-55: Current Measurements for Kapaa CNI Mixture CNI1

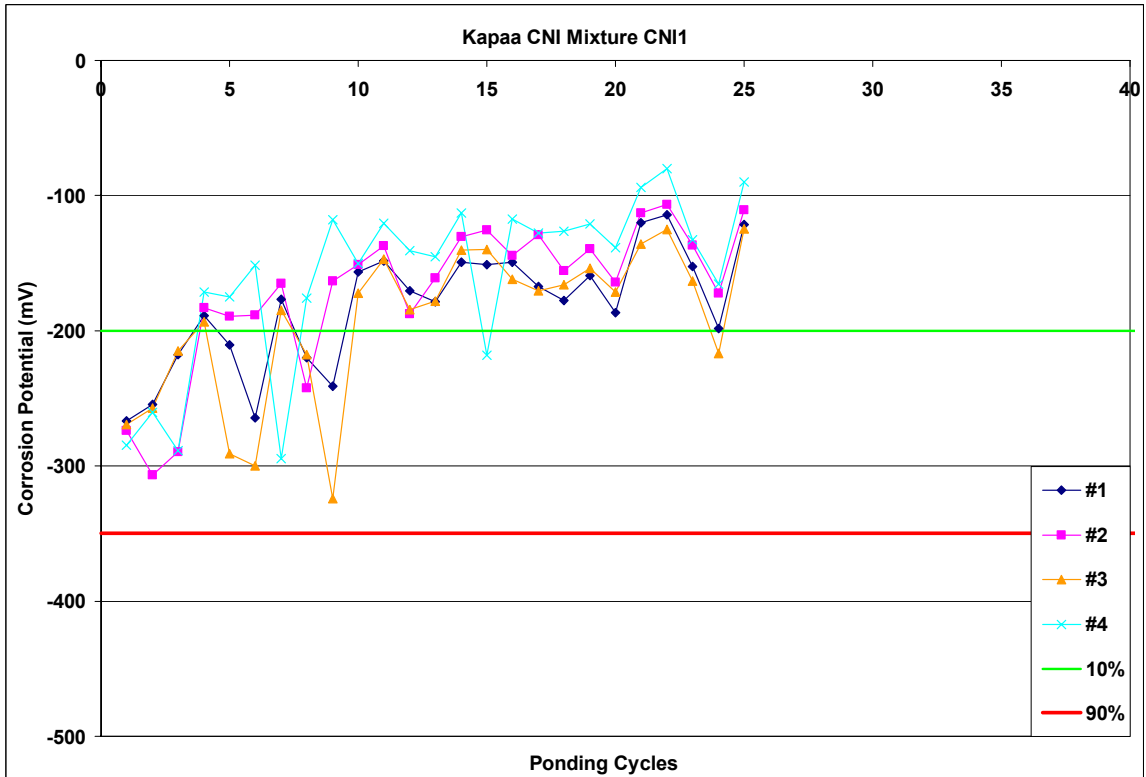


Figure A.1-56: Corrosion Potential Measurements for Kapaa CNI Mixture CNI1

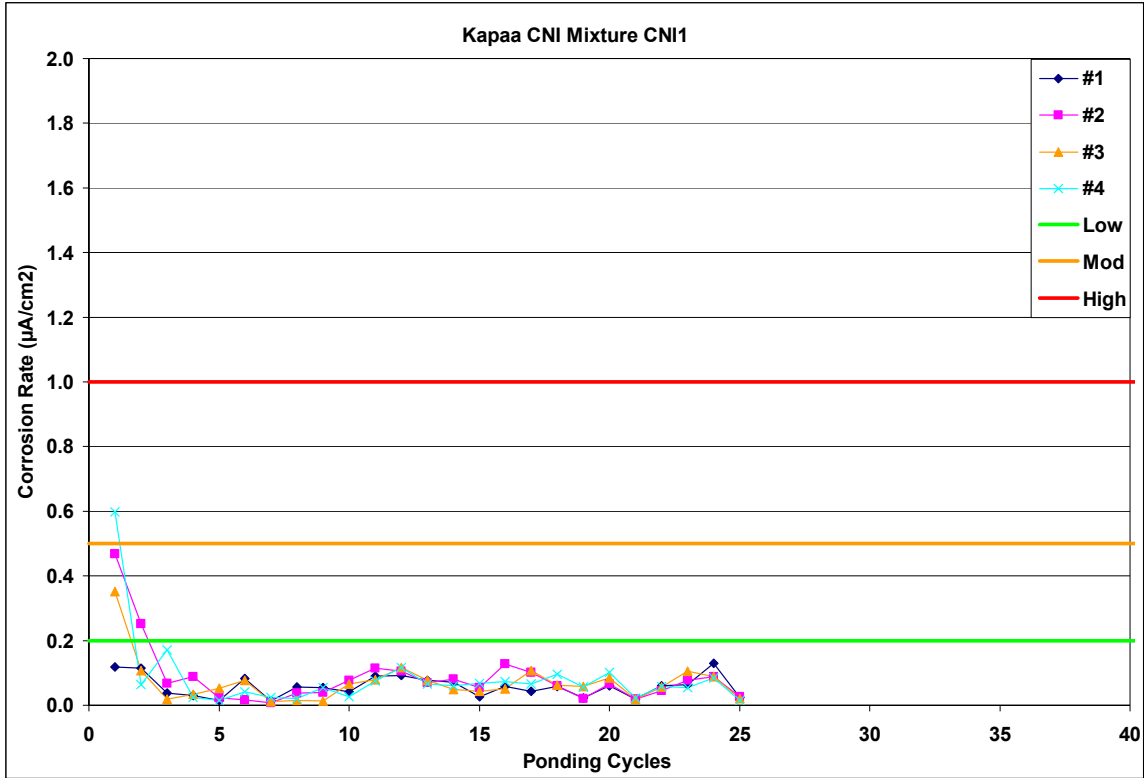


Figure A.1-57: Corrosion Rate Measurements for Kapaa CNI Mixture CNI1

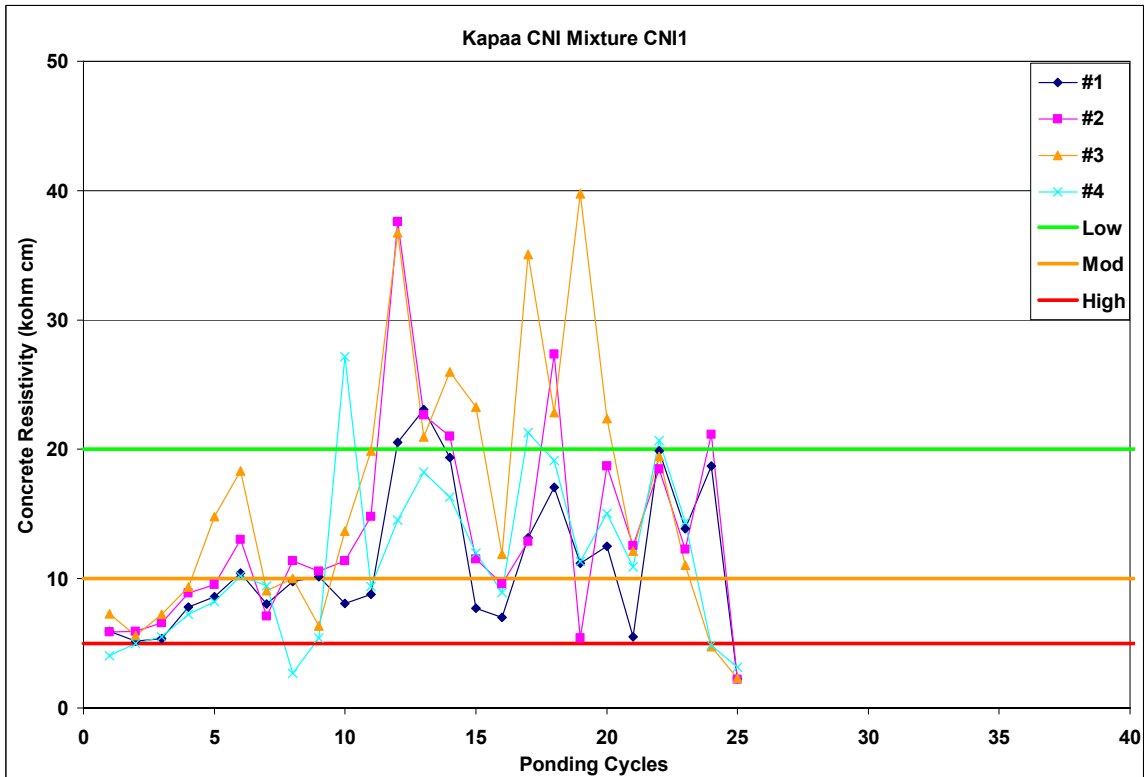


Figure A.1-58: Corrosion Resistivity Measurements for Kapaa CNI Mixture CNI1

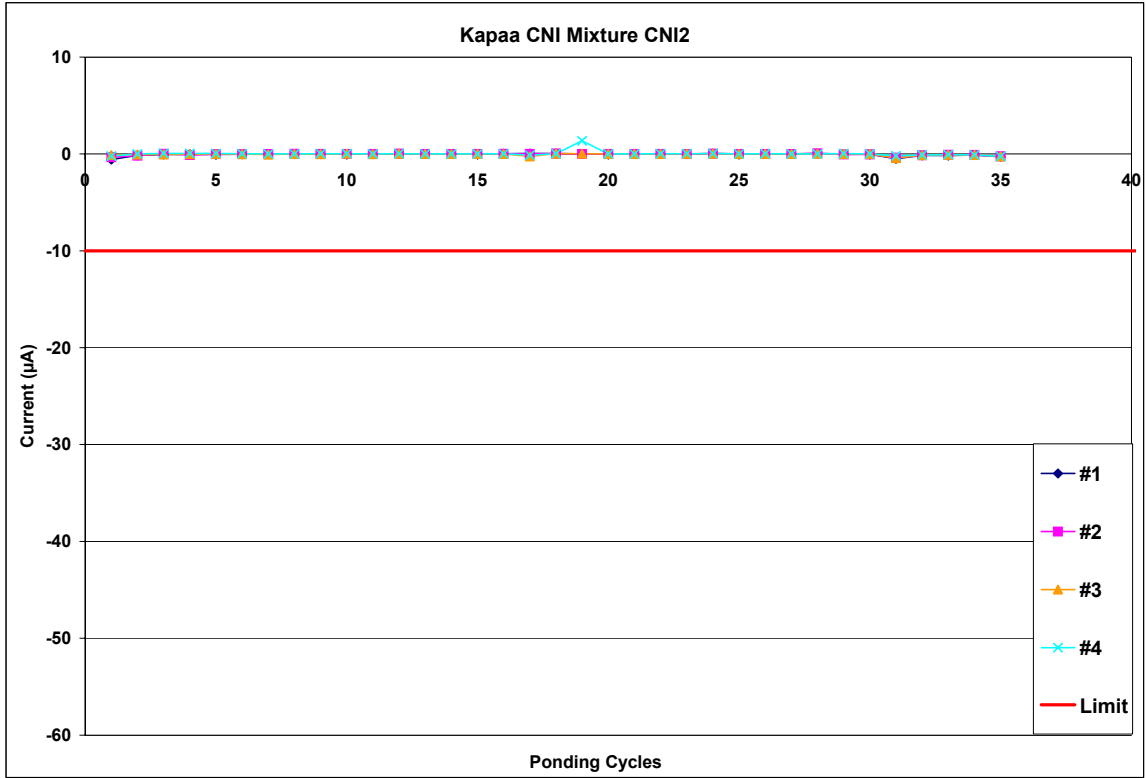


Figure A.1-59: Current Measurements for Kapaa CNI Mixture CNI2

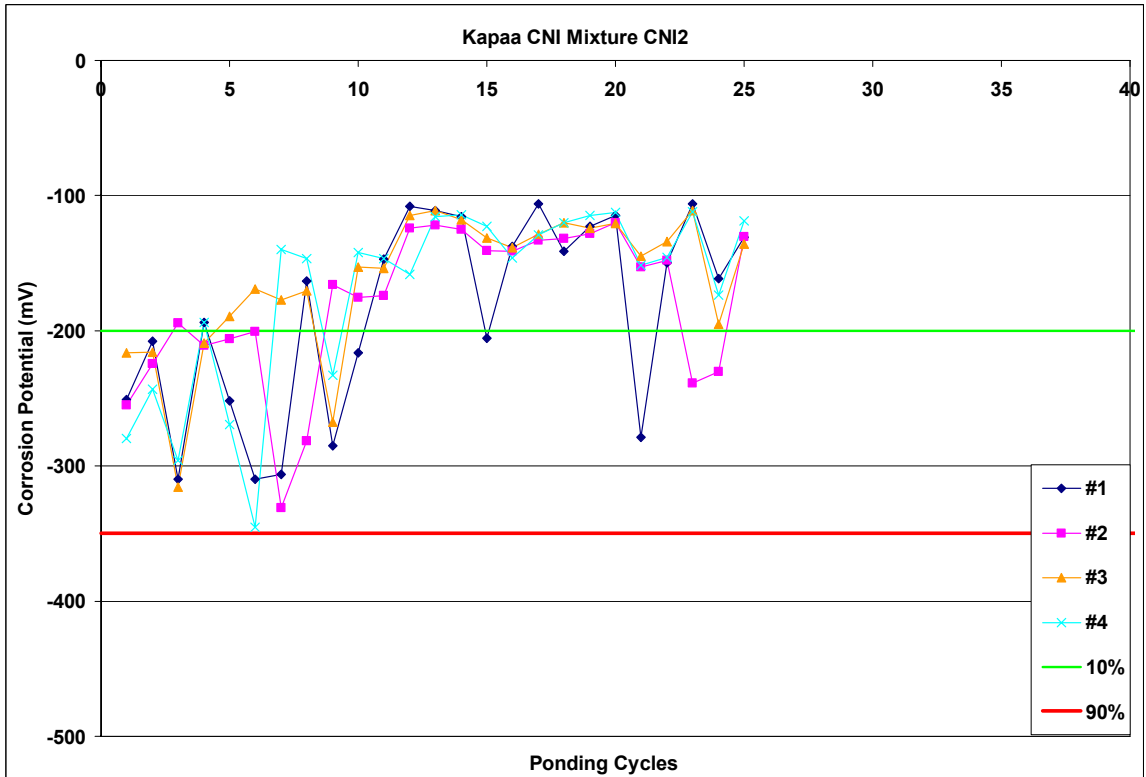


Figure A.1-60: Corrosion Potential Measurements for Kapaa CNI Mixture CNI2

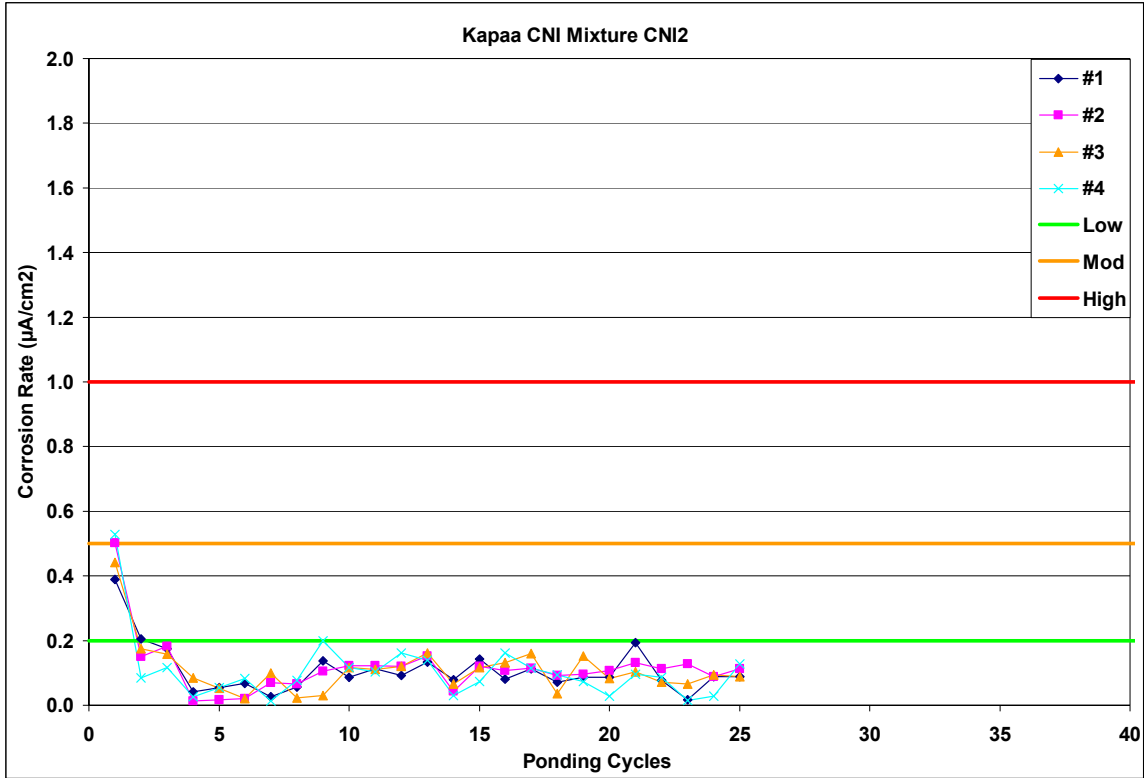


Figure A.1-61: Corrosion Rate Measurements for Kapaa CNI Mixture CNI 2

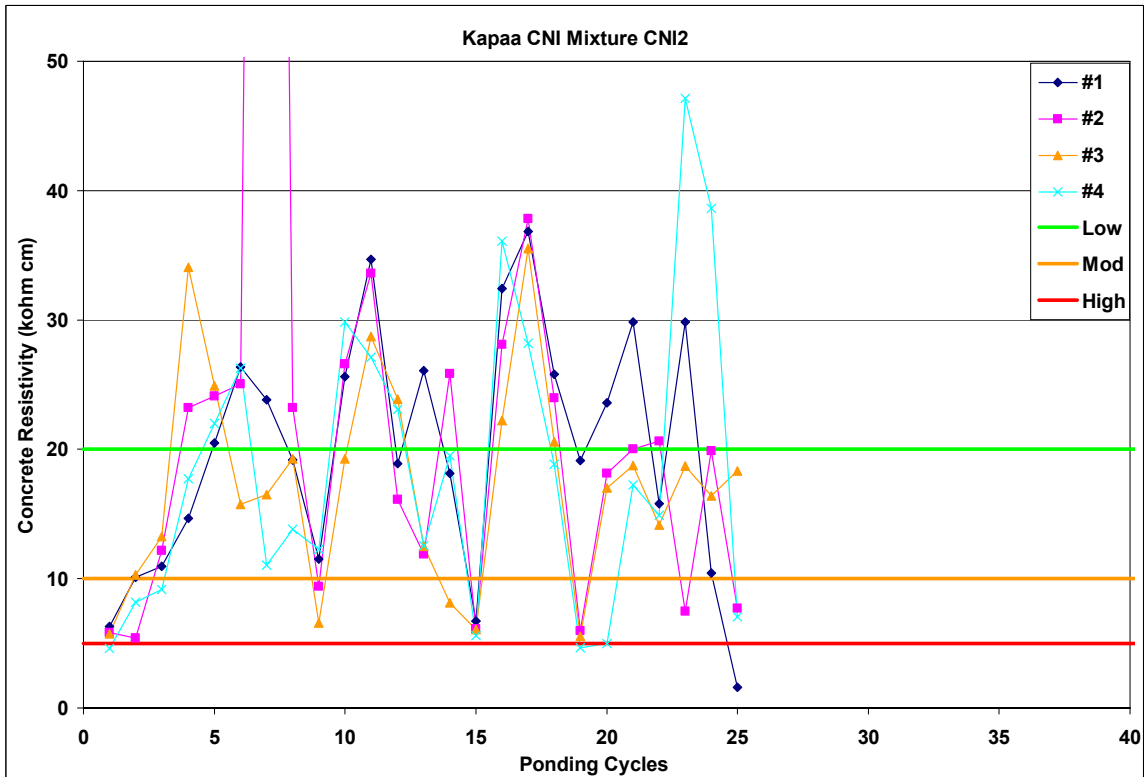


Figure A.1-62: Corrosion Resistivity Measurements for Kapaa CNI Mixture CNI2

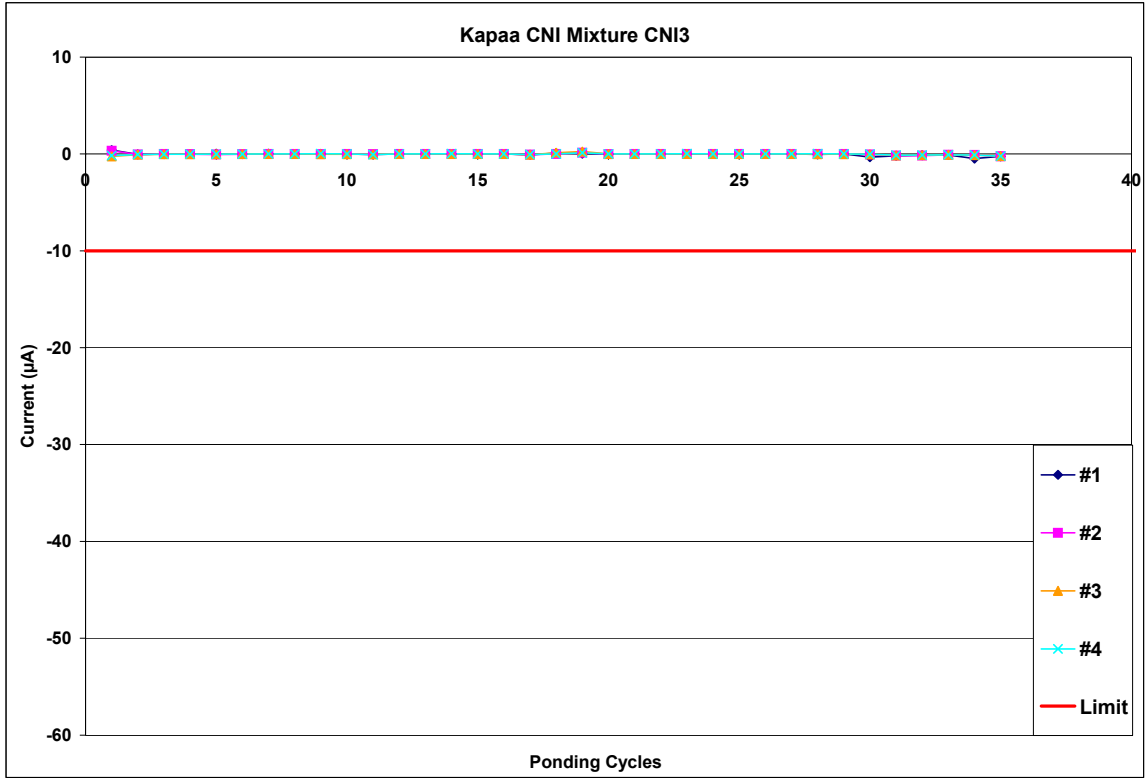


Figure A.1-63: Current Measurements for Kapaa CNI Mixture CNI3

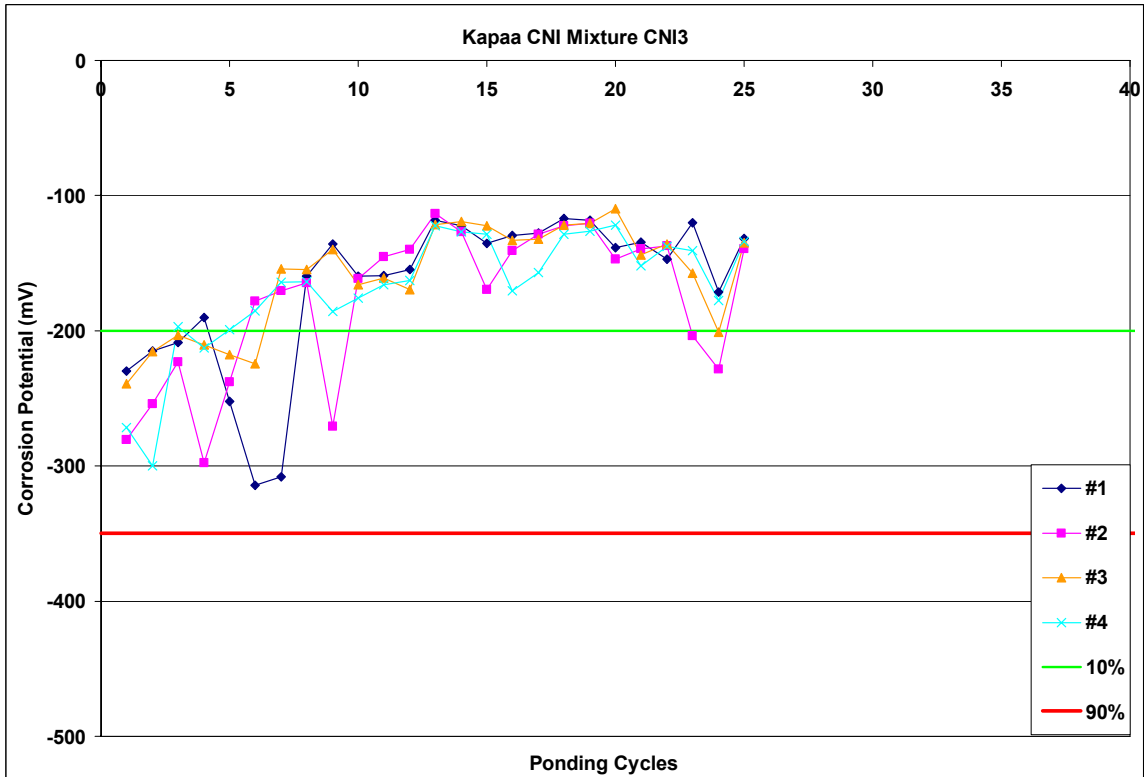


Figure A.1-64: Corrosion Potential Measurements for Kapaa CNI Mixture CNI3

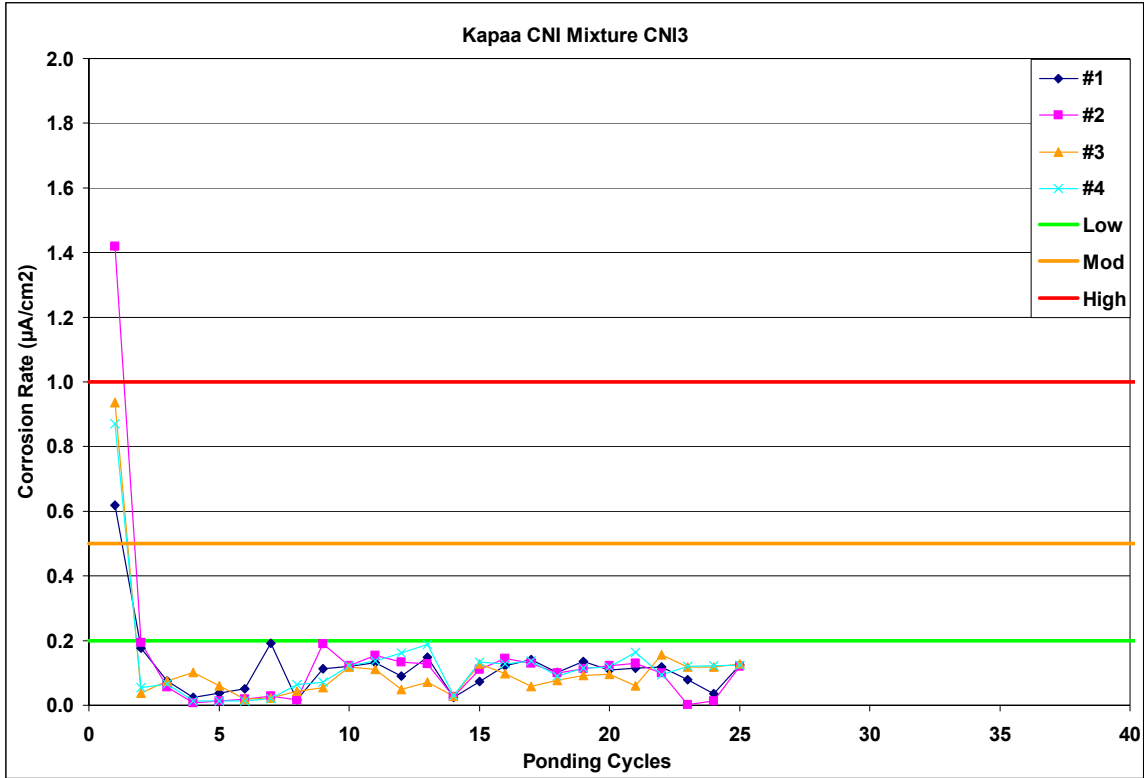


Figure A.1-65: Corrosion Rate Measurements for Kapaa CNI Mixture CNI3

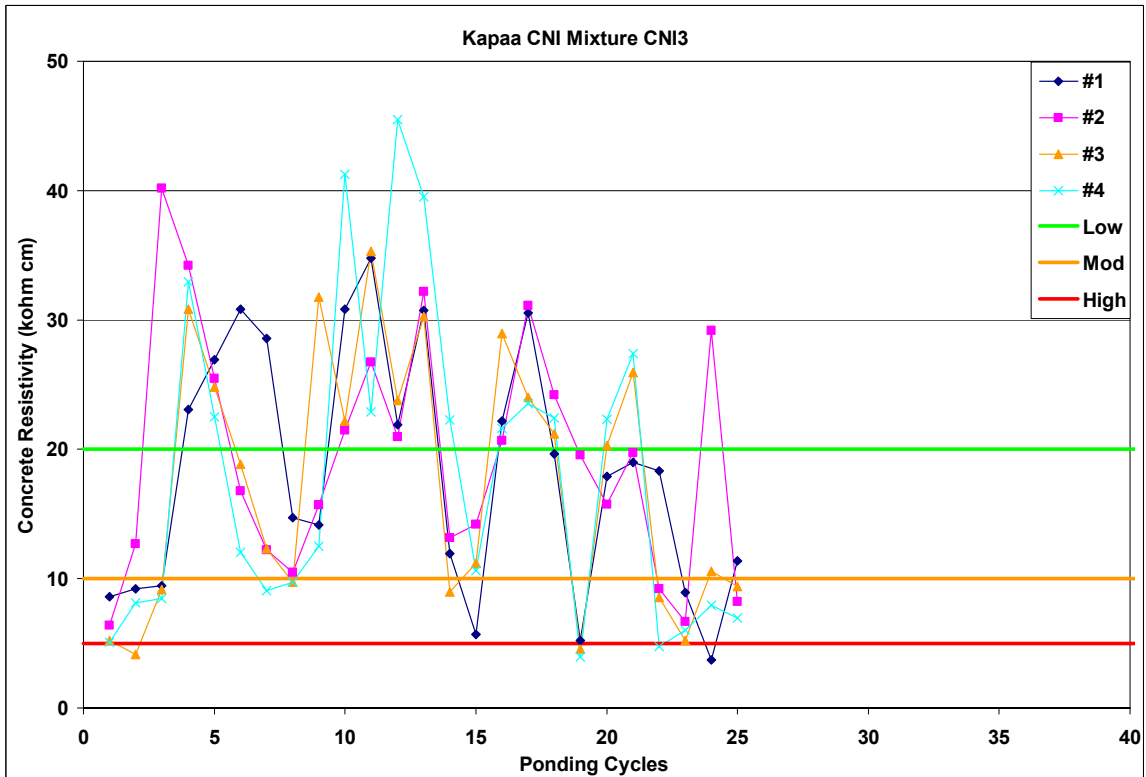


Figure A.1-66: Corrosion Resistivity Measurements for Kapaa CNI Mixture CNI3

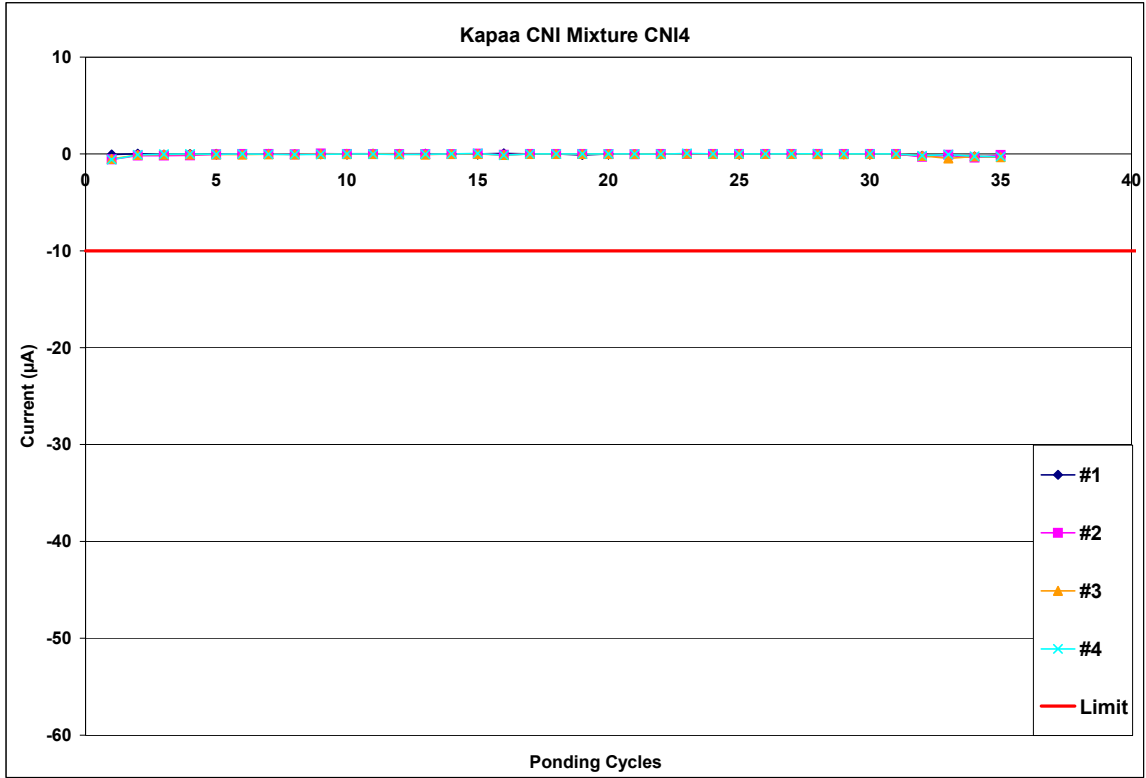


Figure A.1-67: Current Measurements for Kapaa CNI Mixture CNI4

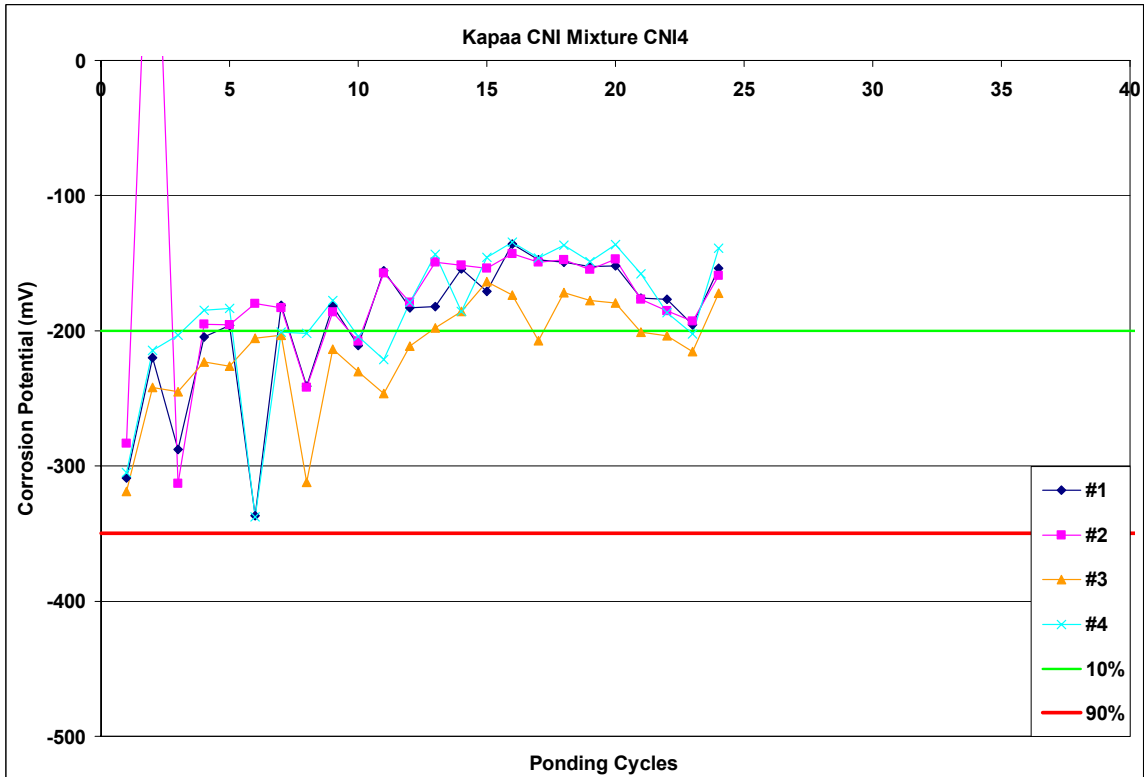


Figure A.1-68: Corrosion Potential Measurements for Kapaa CNI Mixture CNI4

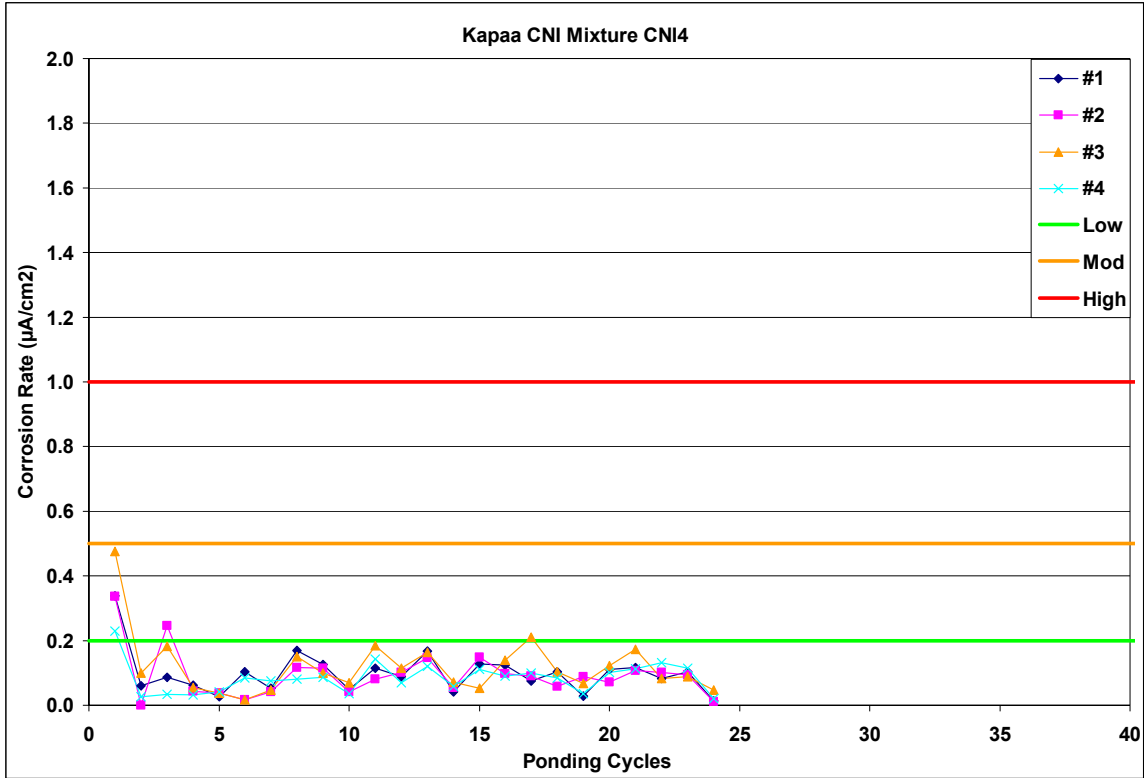


Figure A.1-69: Corrosion Rate Measurements for Kapaa CNI Mixture CNI4

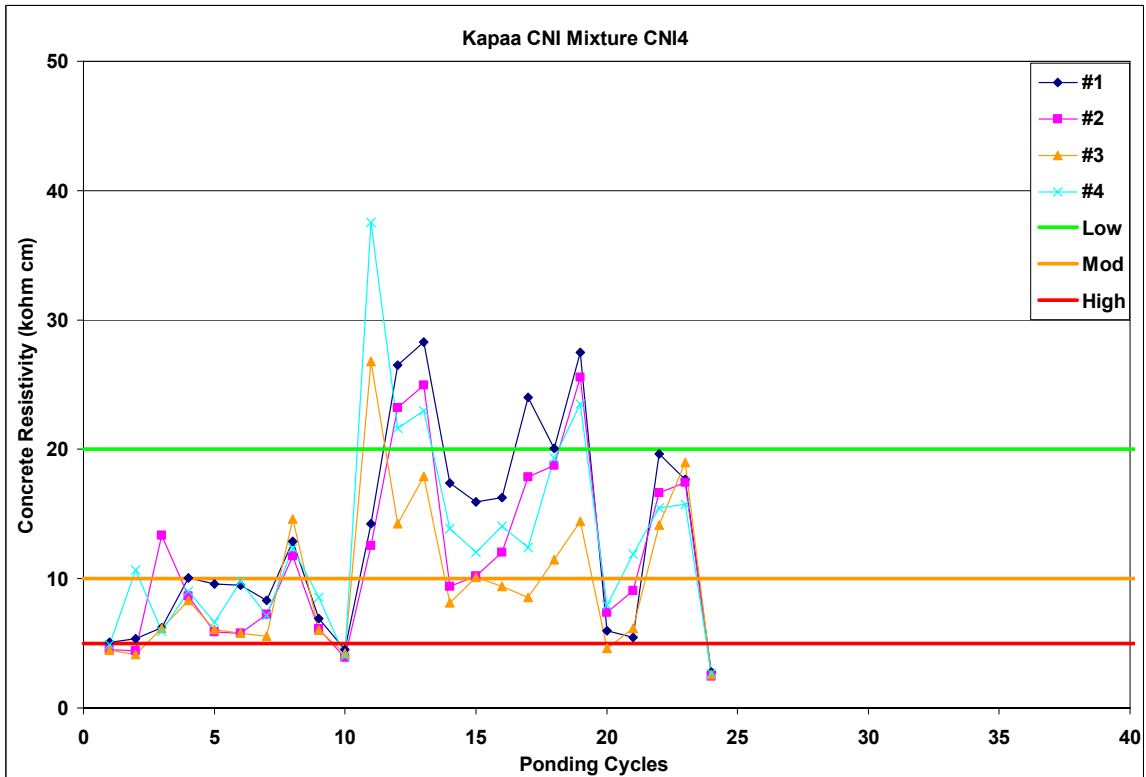


Figure A.1-70: Corrosion Resistivity Measurements for Kapaa CNI Mixture CNI4

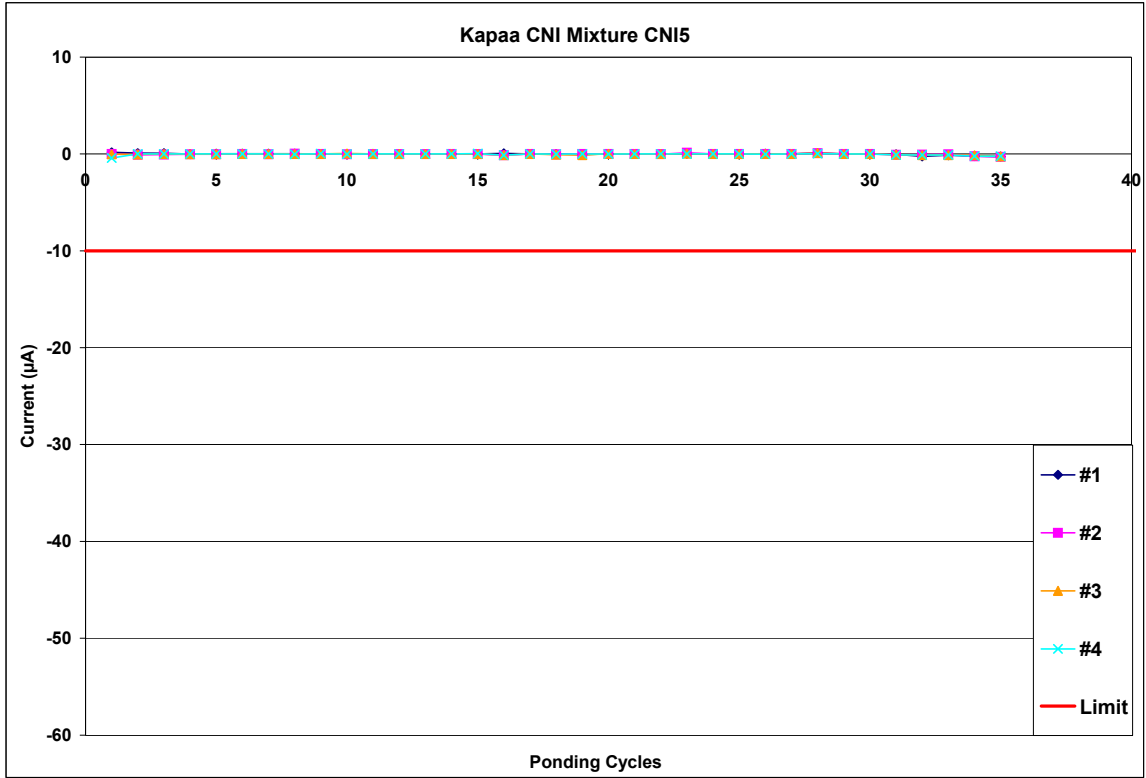


Figure A.1-71: Current Measurements for Kapaa CNI Mixture CNI5

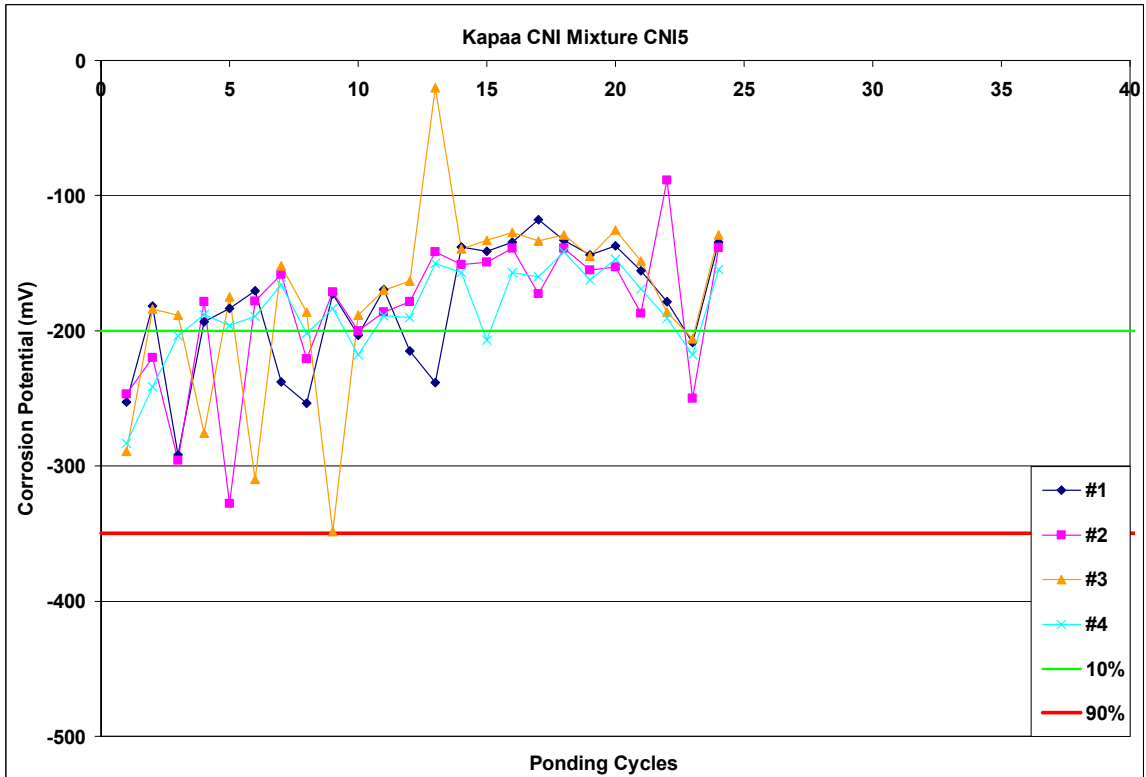


Figure A.1-72: Corrosion Rate Measurements for Kapaa CNI Mixture CNI5

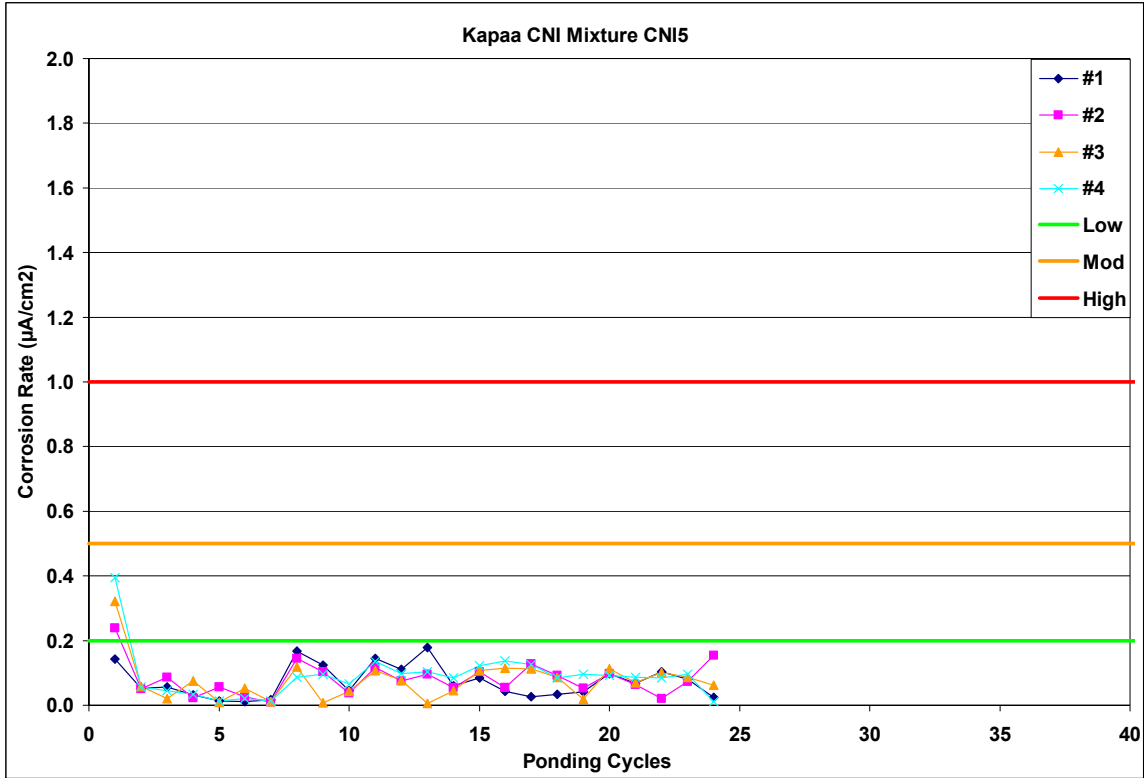


Figure A.1-73: Corrosion Potential Measurements for Kapaa CNI Mixture CNI5

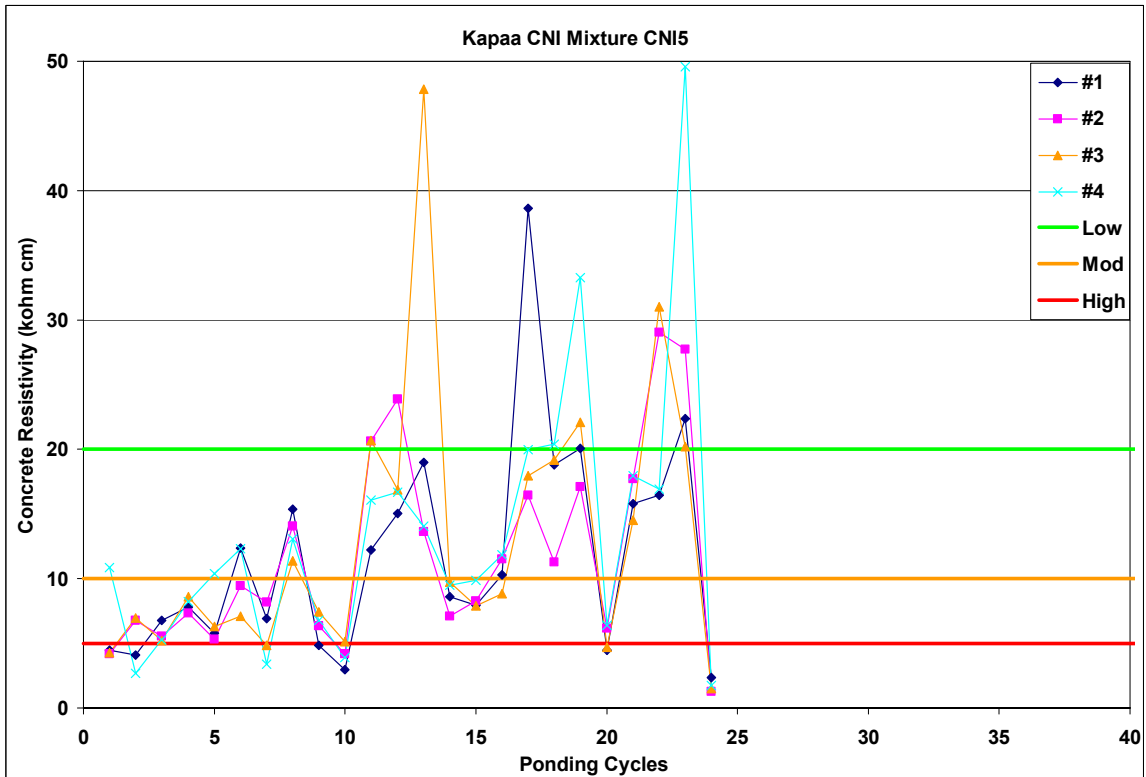


Figure A.1-74: Corrosion Resistivity Measurements for Kapaa CNI Mixture CNI5

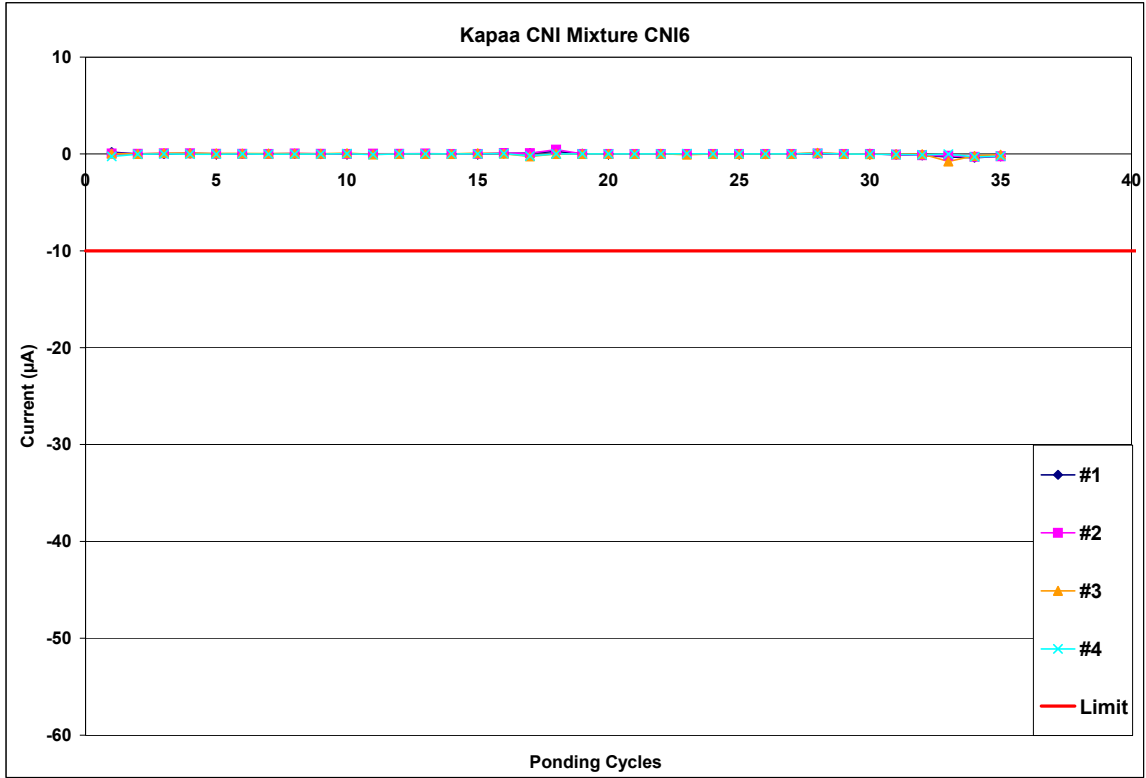


Figure A.1-75: Current Measurements for Kapaa CNI Mixture CNI6

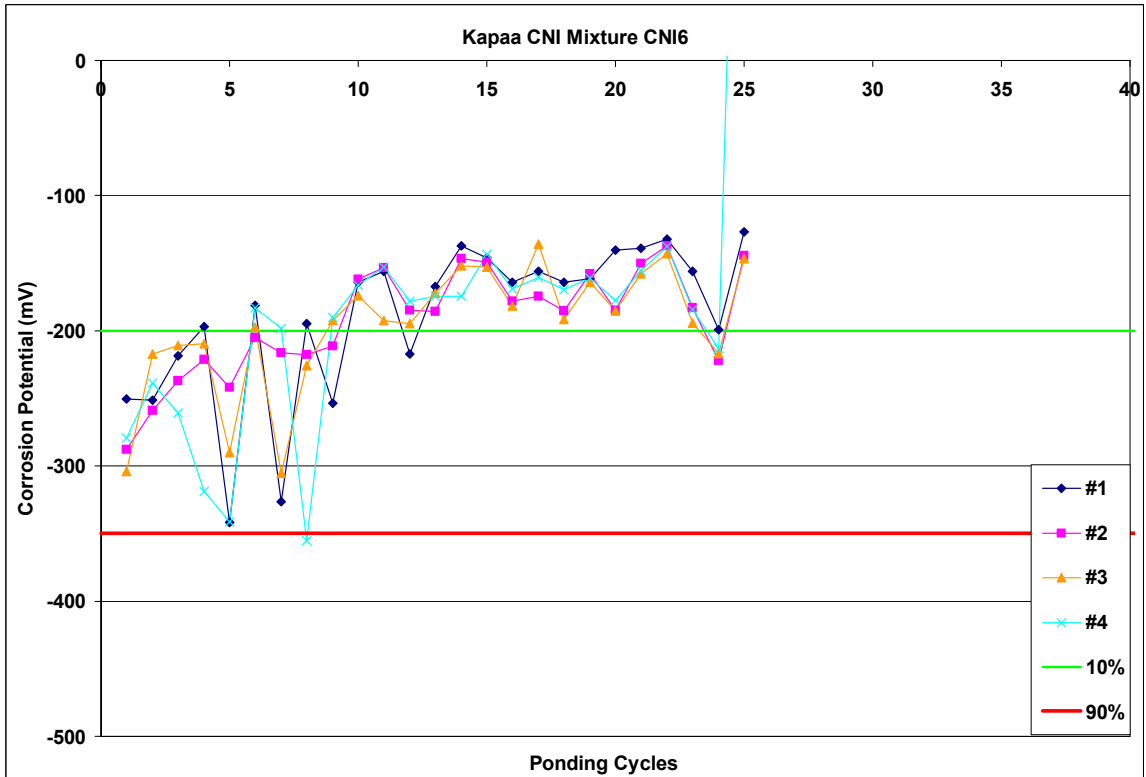


Figure A.1-76: Corrosion Rate Measurements for Kapaa CNI Mixture CNI6

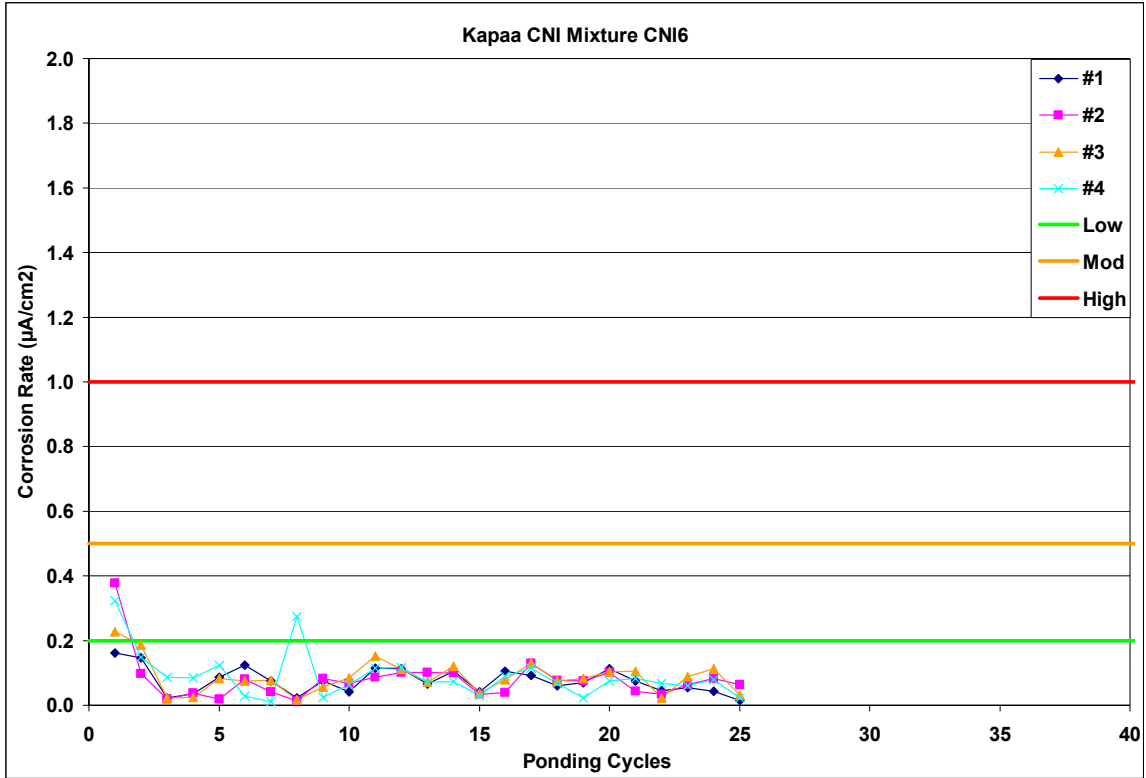


Figure A.1-77: Corrosion Potential Measurements for Kapaa CNI Mixture CNI6

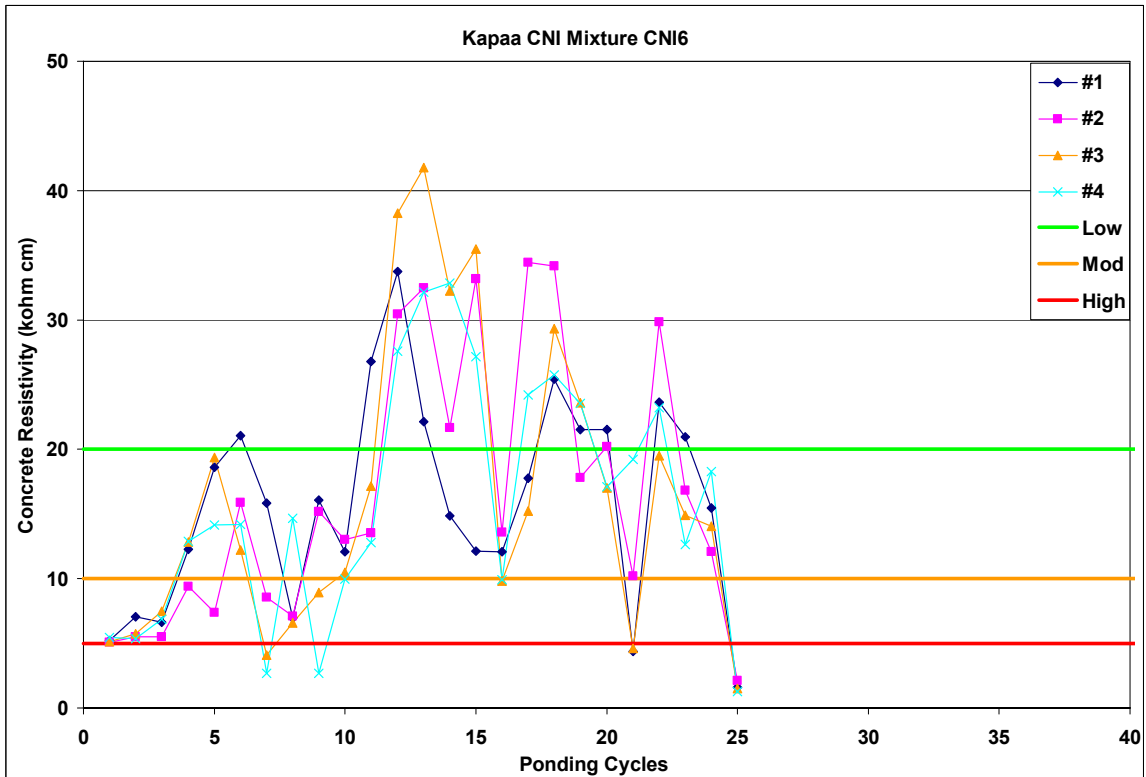


Figure A.1-78: Corrosion Resistivity Measurements for Kapaa CNI Mixture CNI6

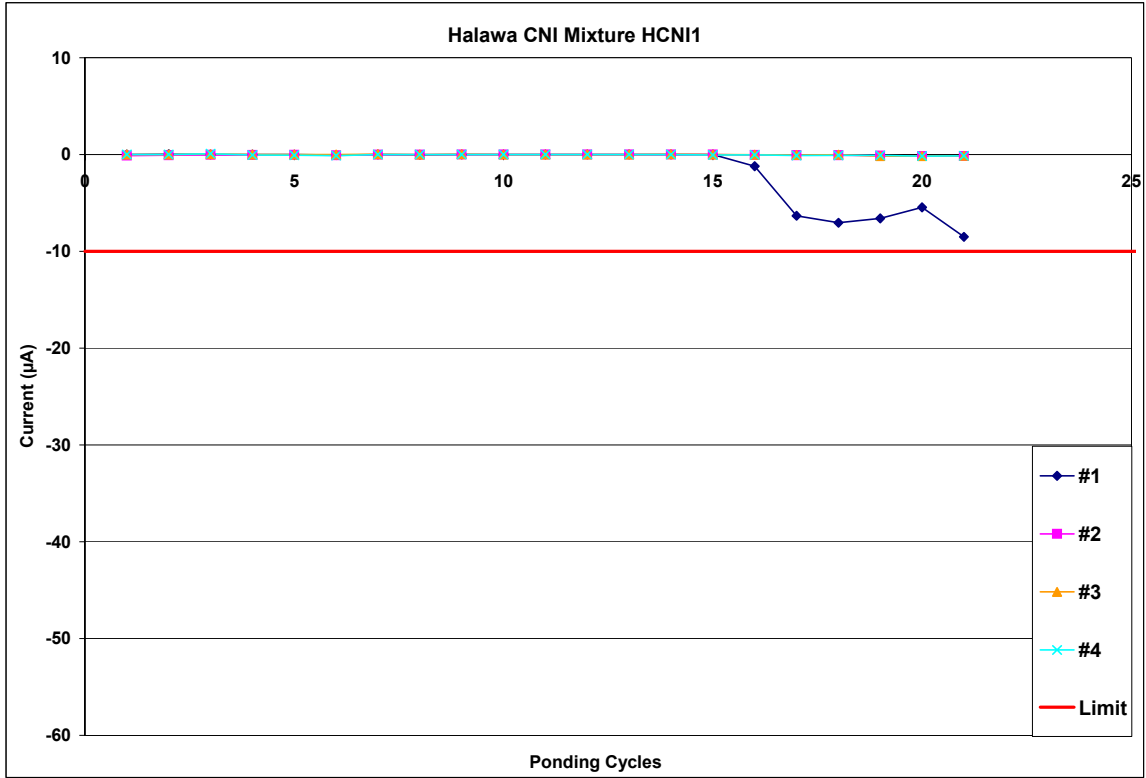


Figure A.1-79: Current Measurements for Halawa CNI Mixture HCNI1

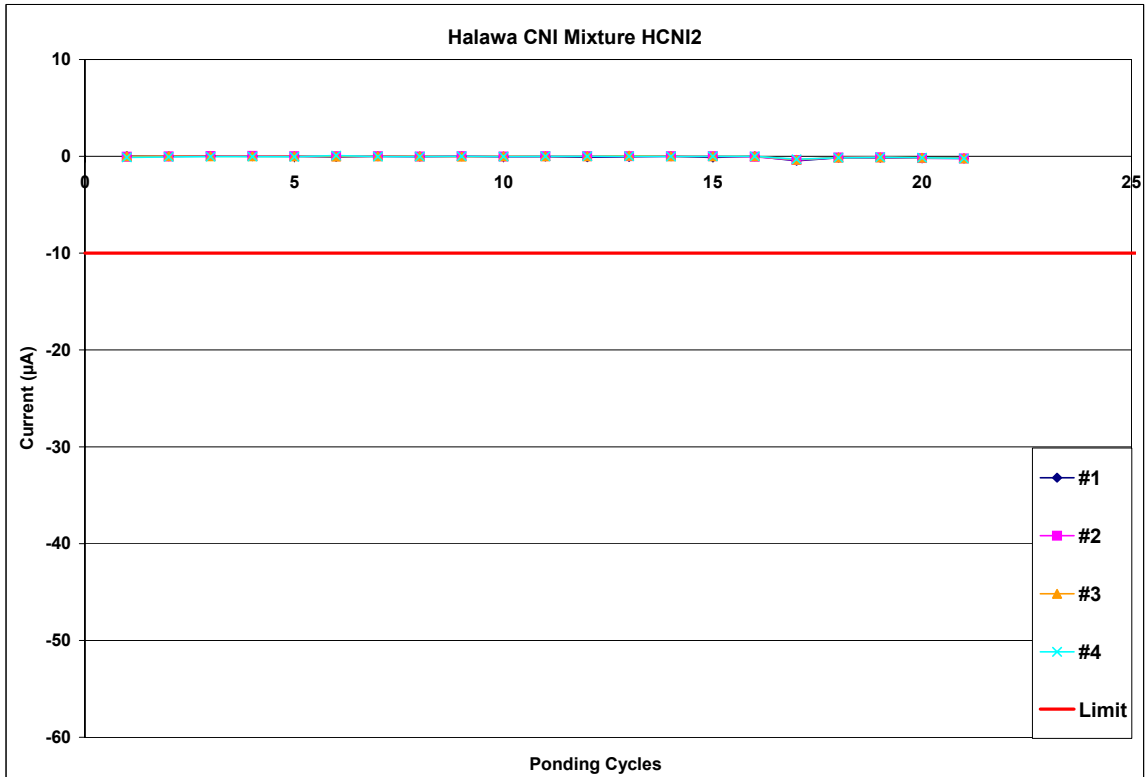


Figure A.1-80: Current Measurements for Halawa CNI Mixture HCNI2

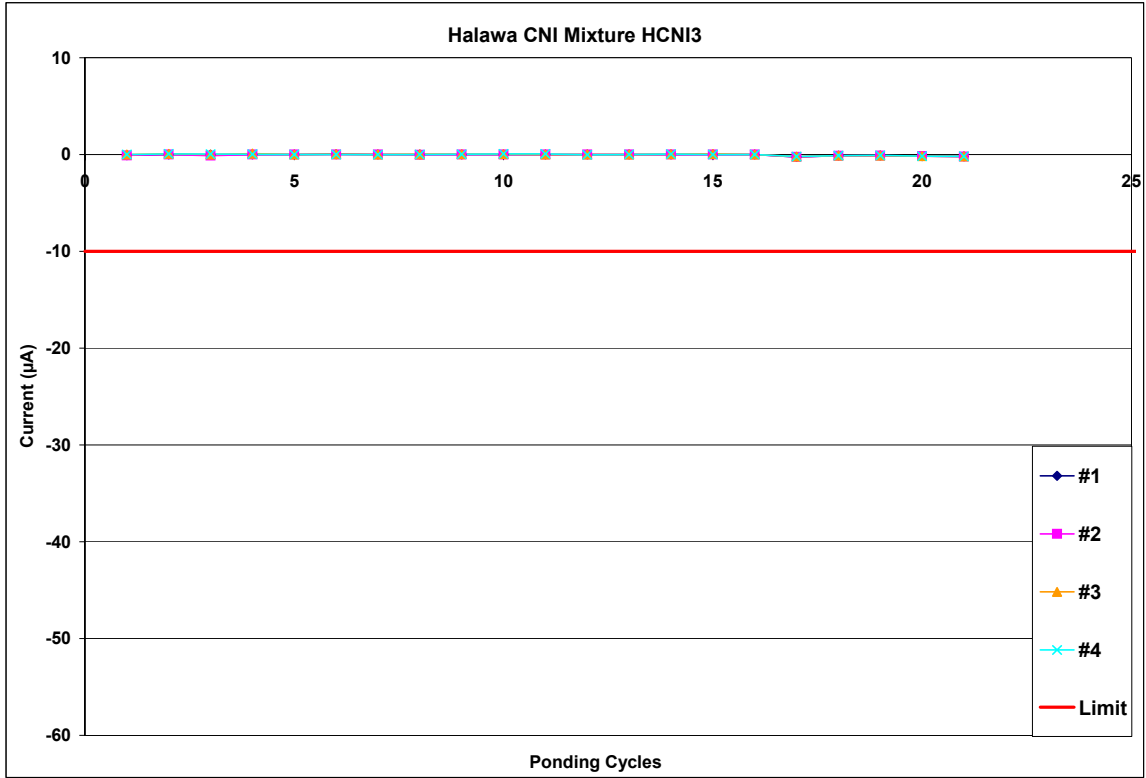


Figure A.1-81: Current Measurements for Halawa CNI Mixture HCNI3

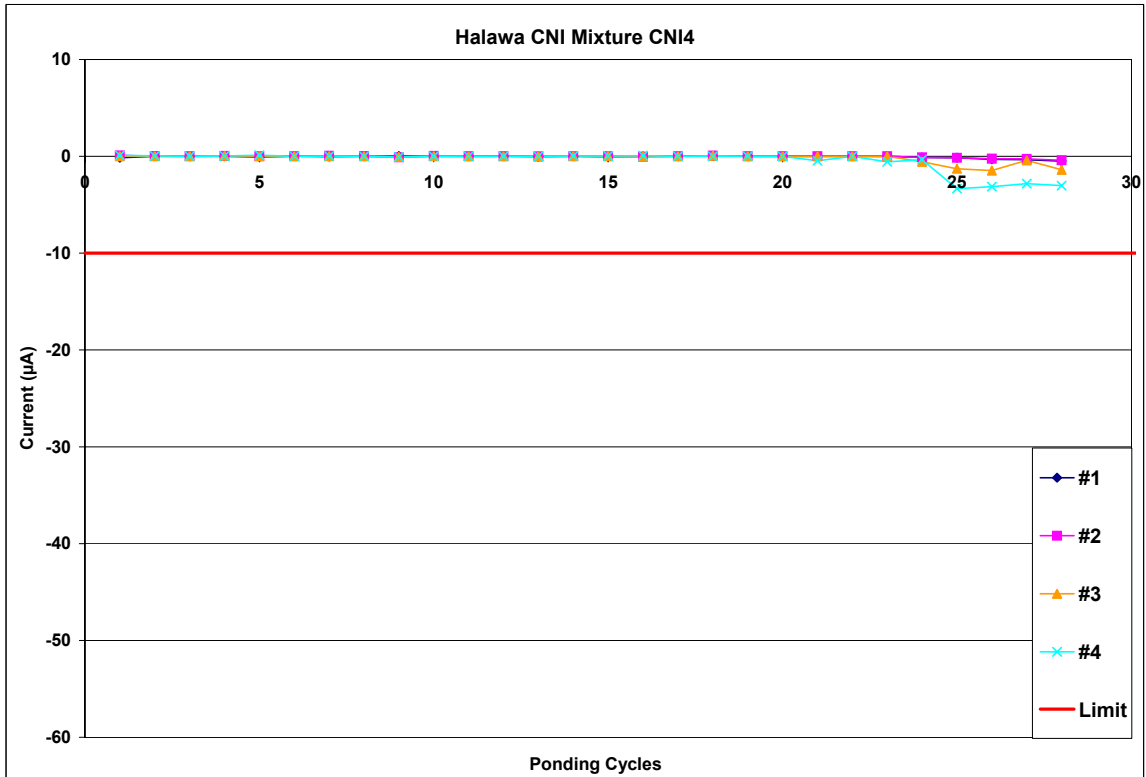


Figure A.1-82: Current Measurements for Halawa CNI Mixture HCNI4

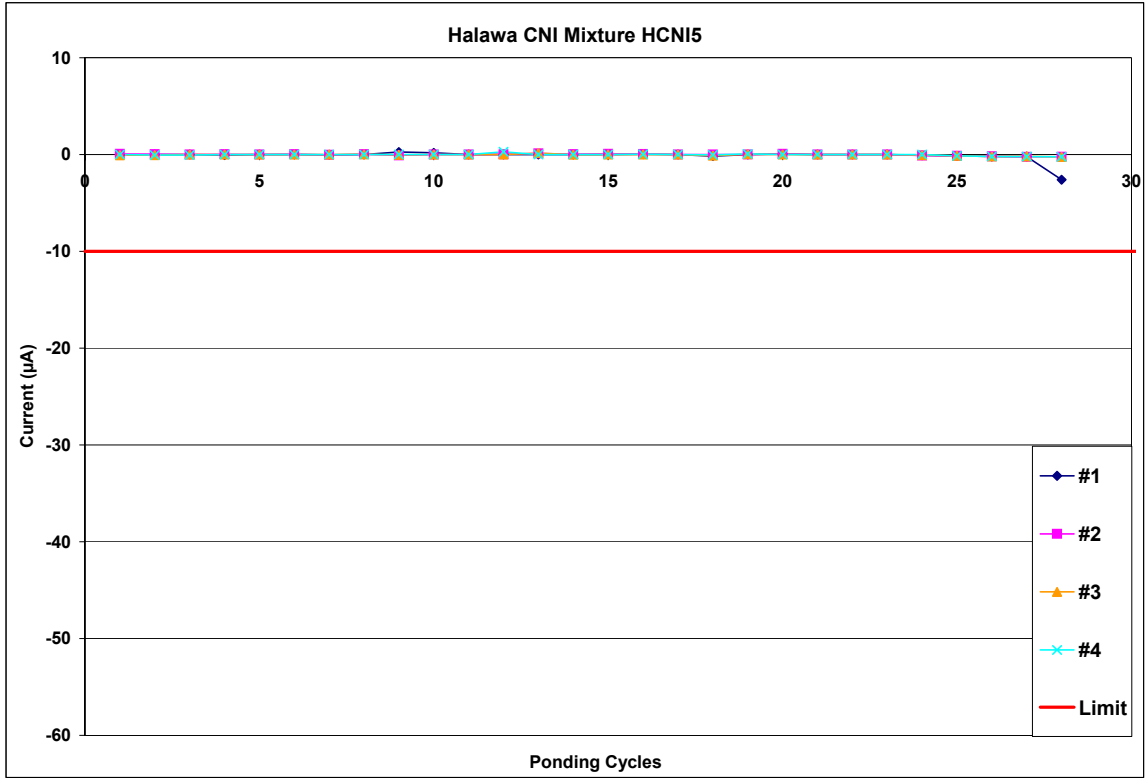


Figure A.1-83: Current Measurements for Halawa CNI Mixture HCNI5

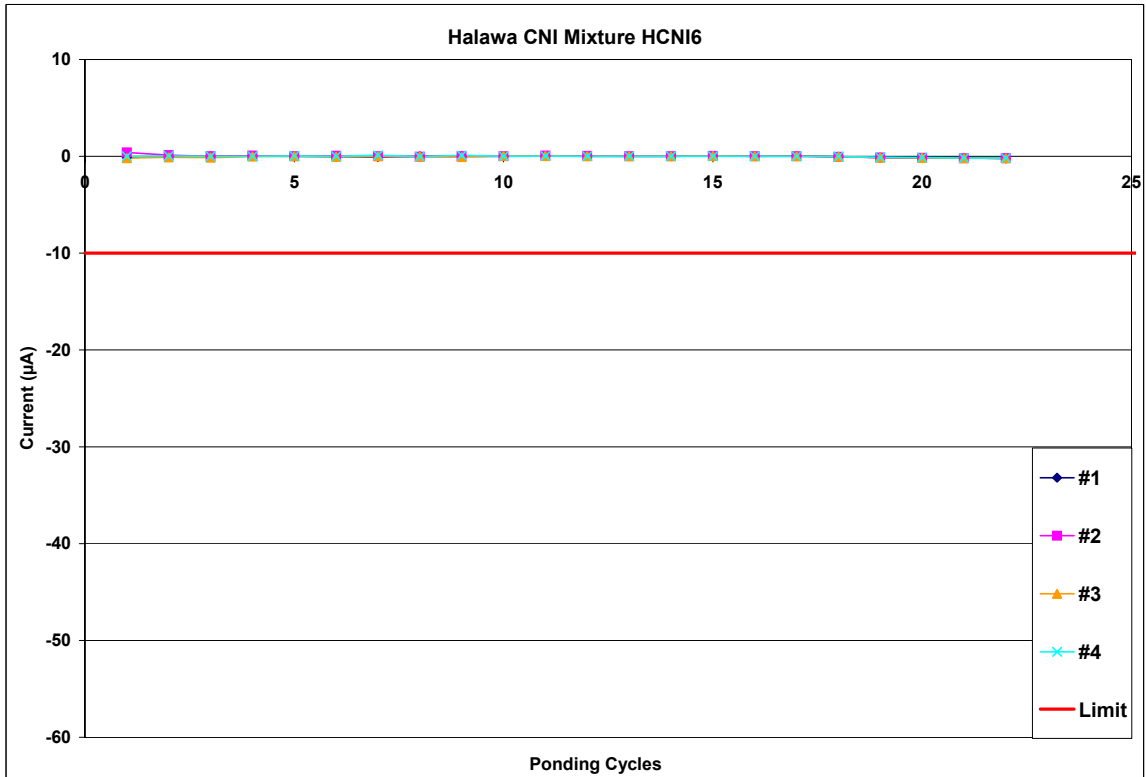


Figure A.1-84: Current Measurements for Halawa CNI Mixture HCNI6

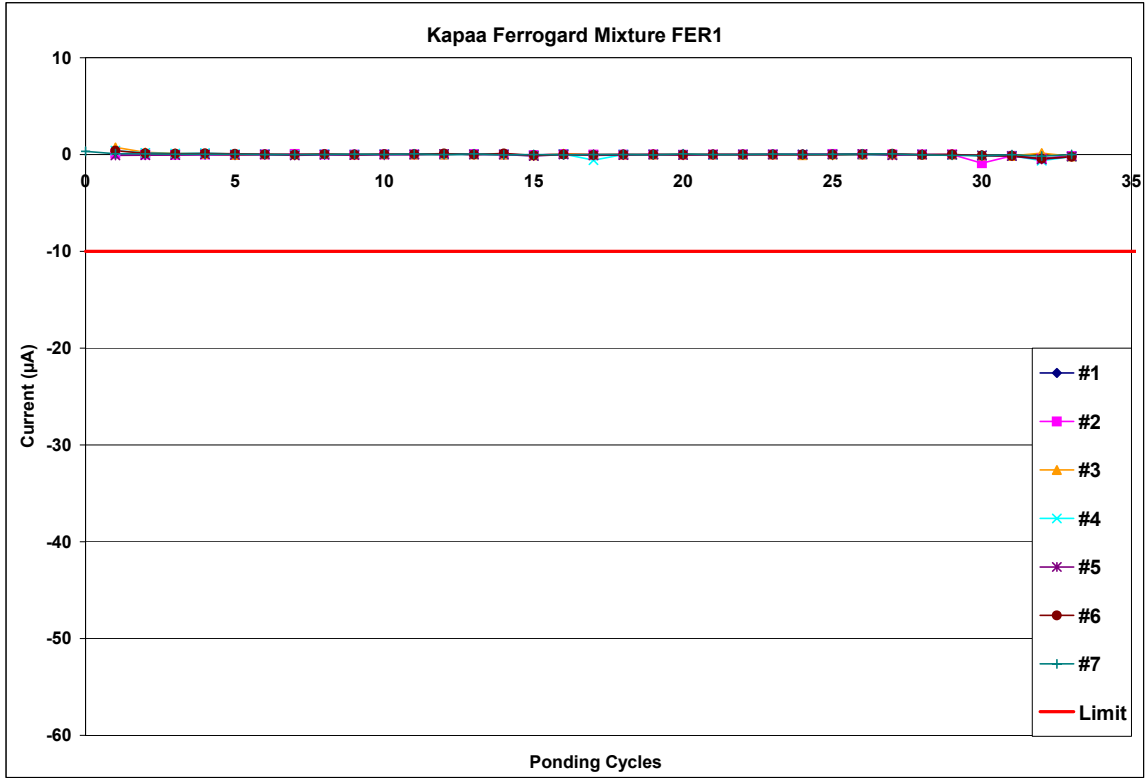


Figure A.1-85: Current Measurements for Kapaa FerroGard Mixture FER1

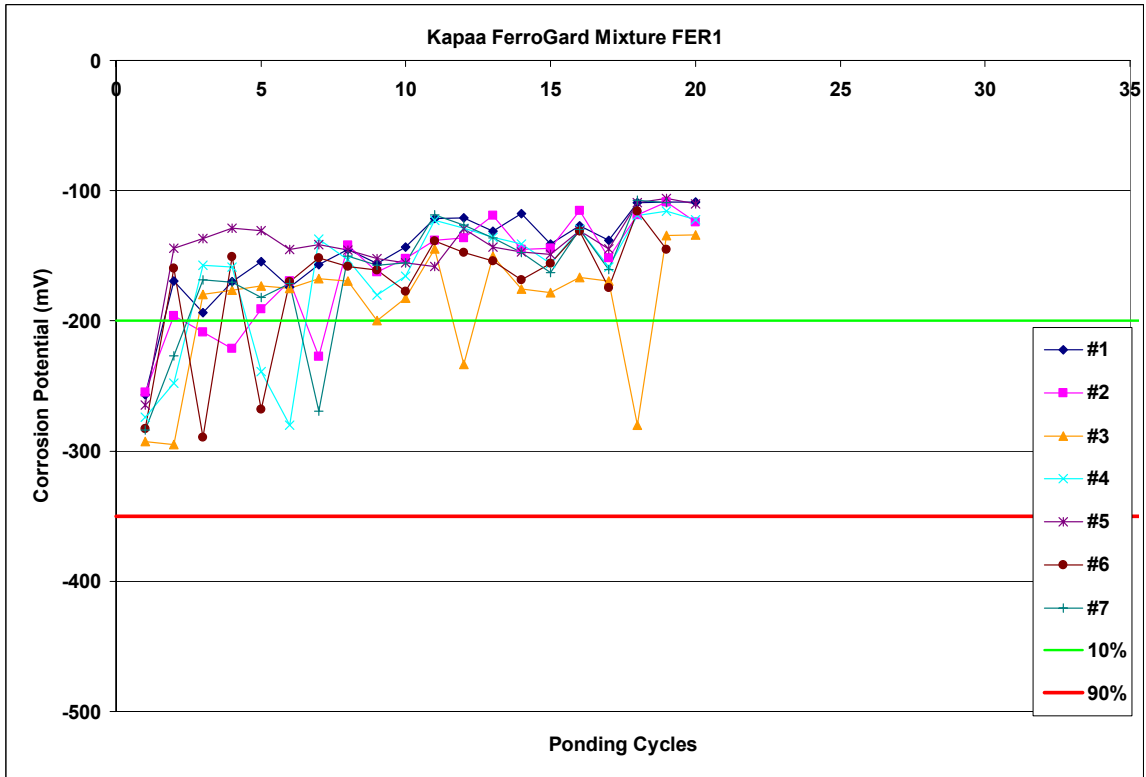


Figure A.1-86: Corrosion Potential Measurements for Kapaa FerroGard Mixture FER1

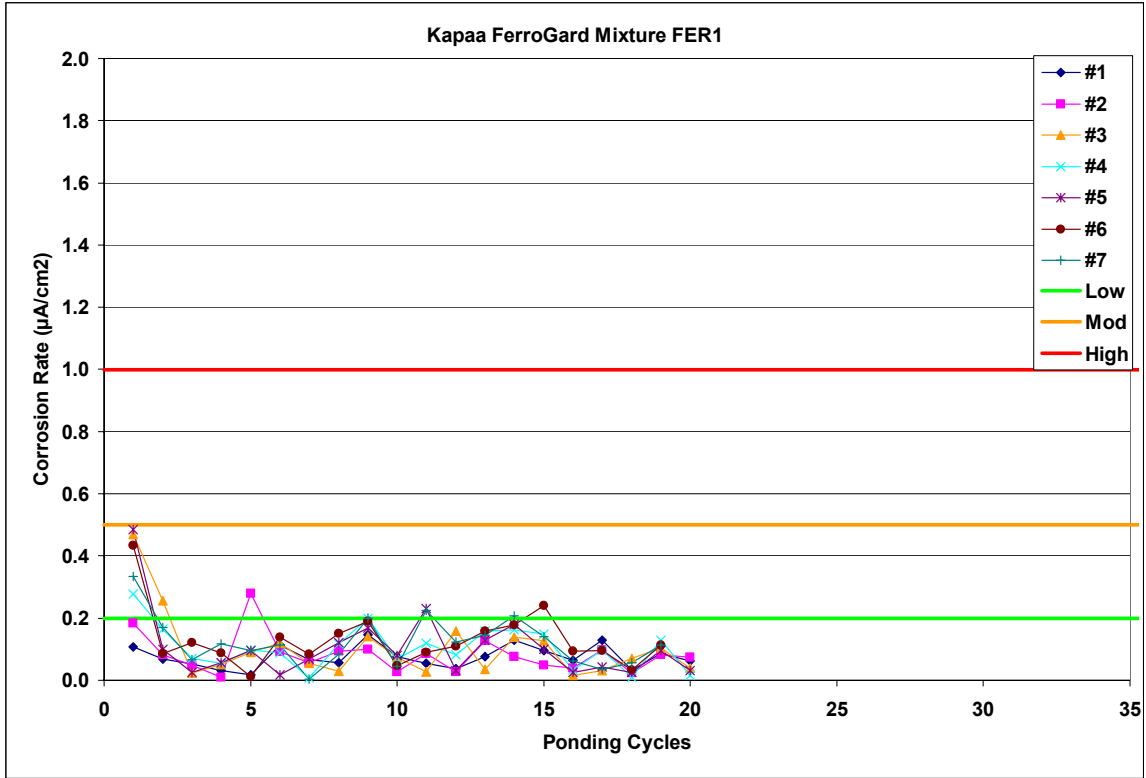


Figure A.1-87: Corrosion Rate Measurements for Kapaa FerroGard Mixture FER1

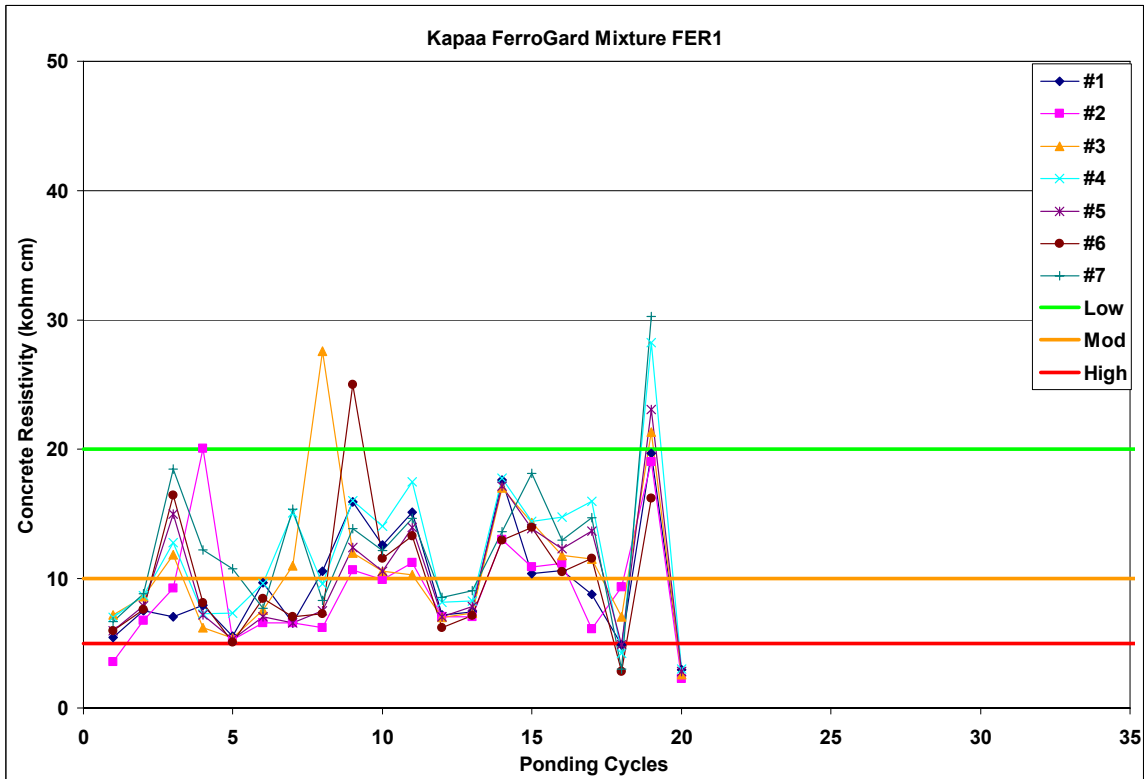


Figure A.1-88: Corrosion Resistivity Measurements for Kapaa FerroGard Mixture FER1

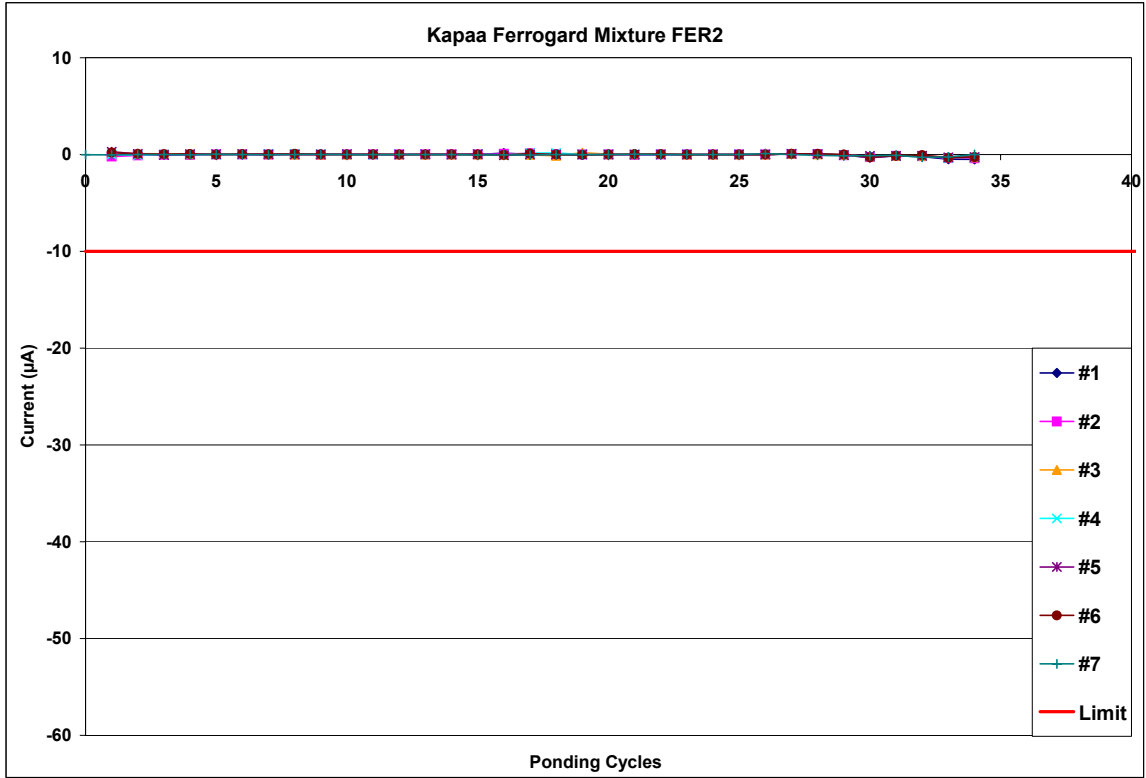


Figure A.1-89: Current Measurements for Kapaa FerroGard Mixture FER2

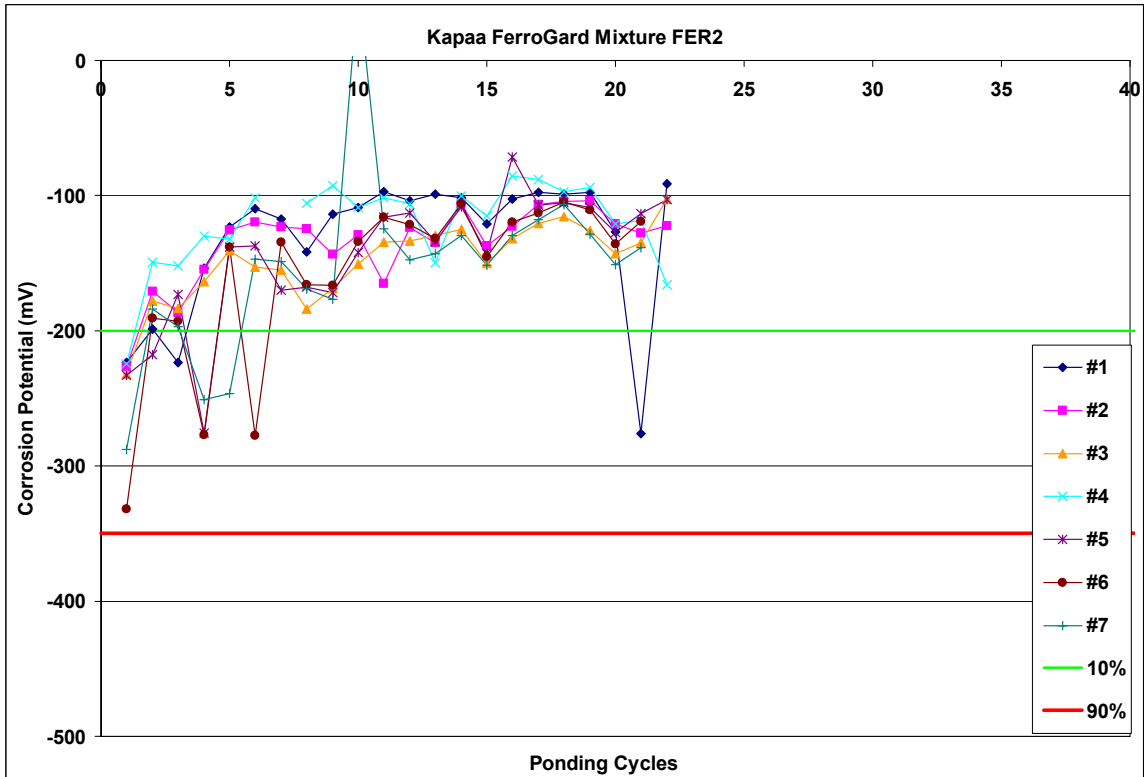


Figure A.1-90: Corrosion Potential Measurements for Kapaa FerroGard Mixture FER2

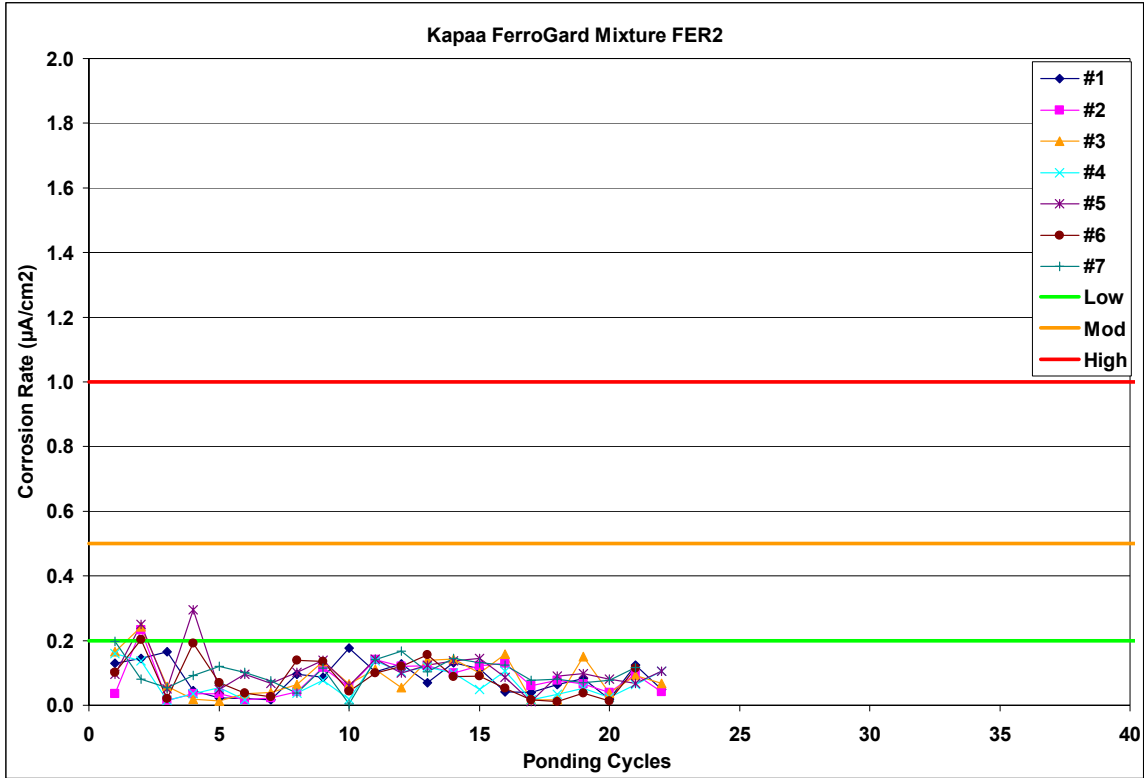


Figure A.1-91: Corrosion Rate Measurements for Kapaa FerroGard Mixture FER2

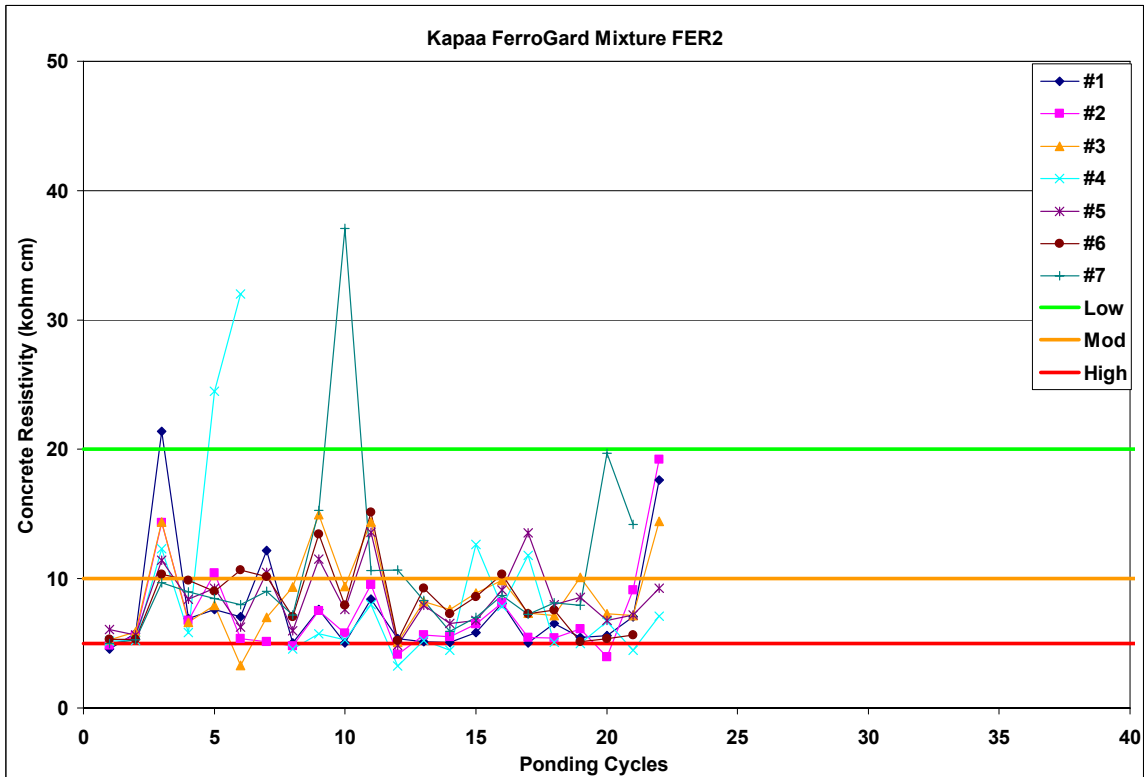


Figure A.1-92: Corrosion Resistivity Measurements for Kapaa FerroGard Mixture FER2

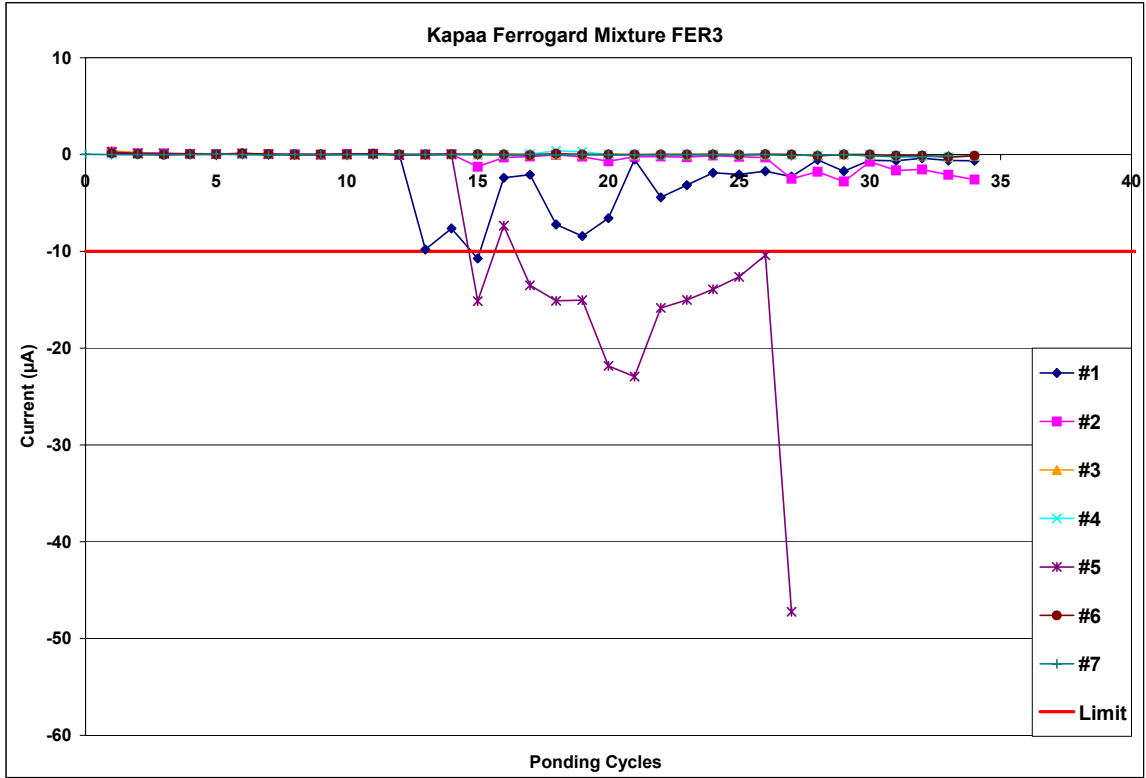


Figure A.1-93: Current Measurements for Kapaa FerroGard Mixture FER3

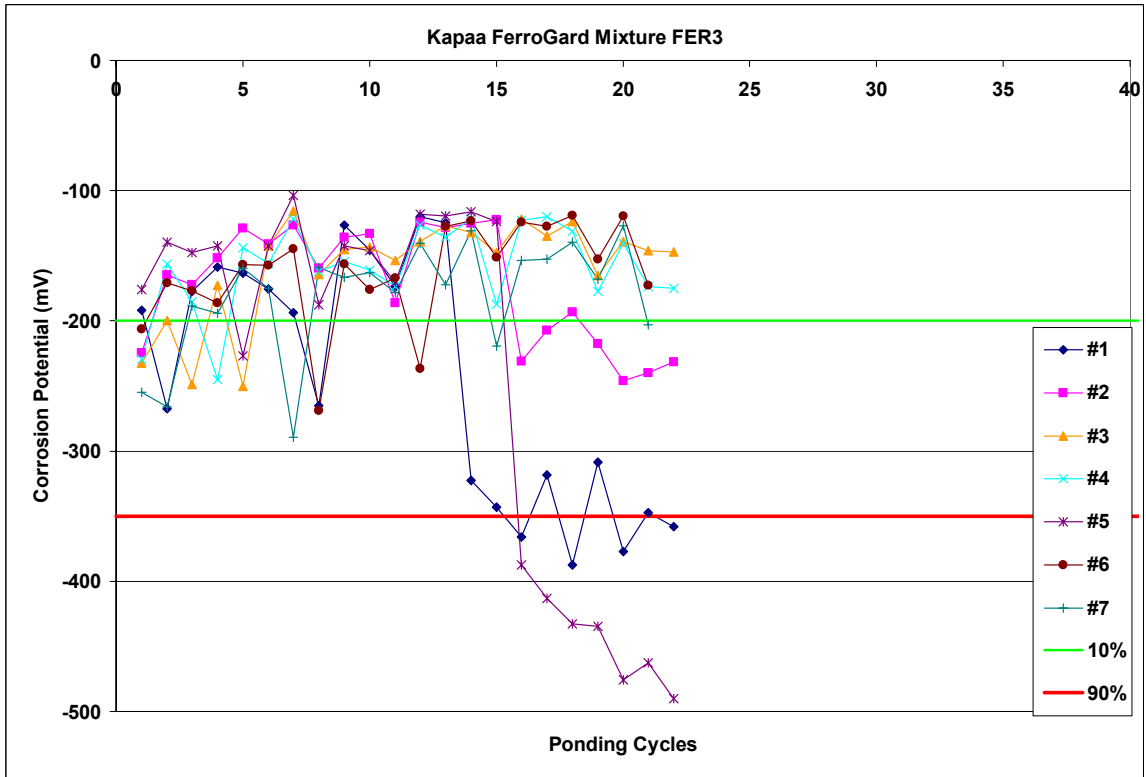


Figure A.1-94: Corrosion Potential Measurements for Kapaa FerroGard Mixture FER3

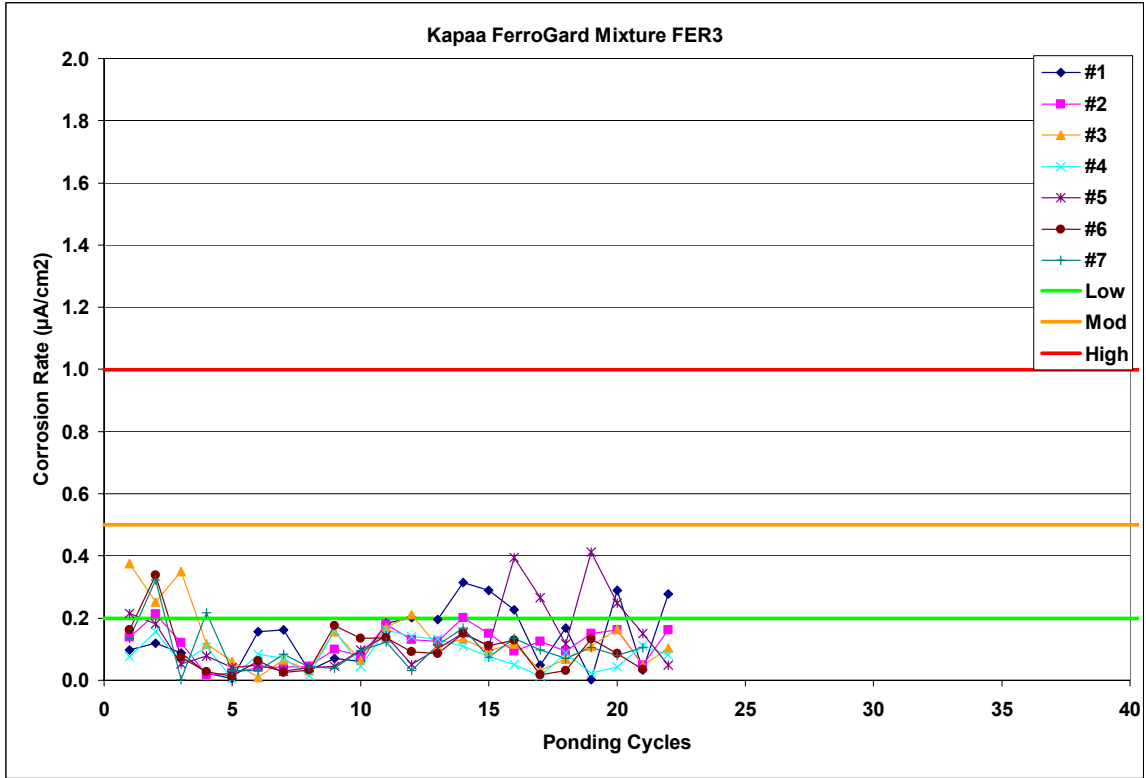


Figure A.1-95: Corrosion Rate Measurements for Kapaa FerroGard Mixture FER3

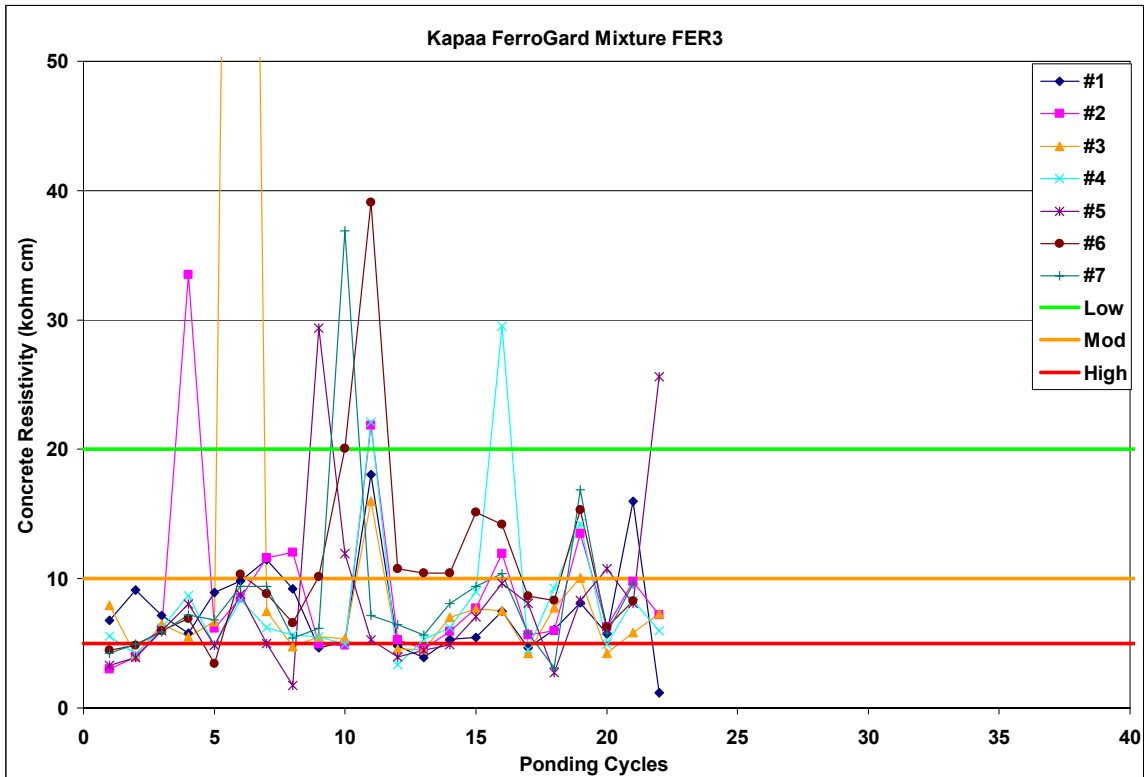


Figure A.1-96: Corrosion Resistivity Measurements for Kapaa FerroGard Mixture FER3

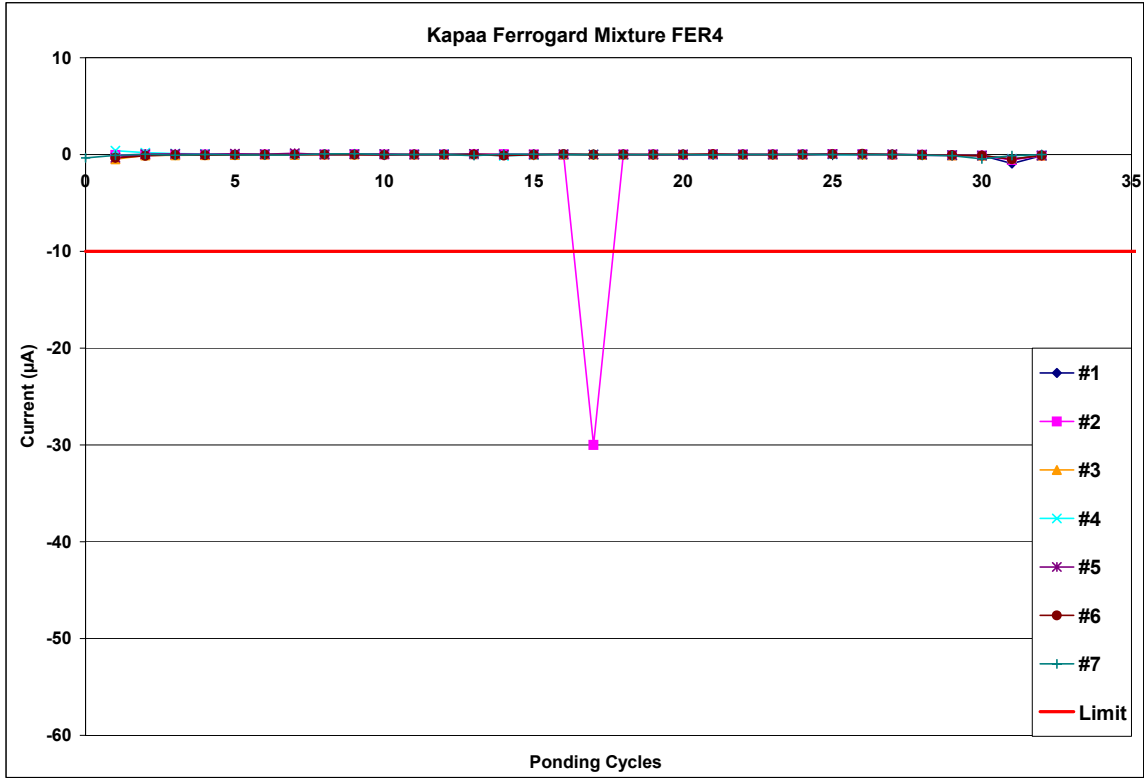


Figure A.1-97: Current Measurements for Kapaa FerroGard Mixture FER4

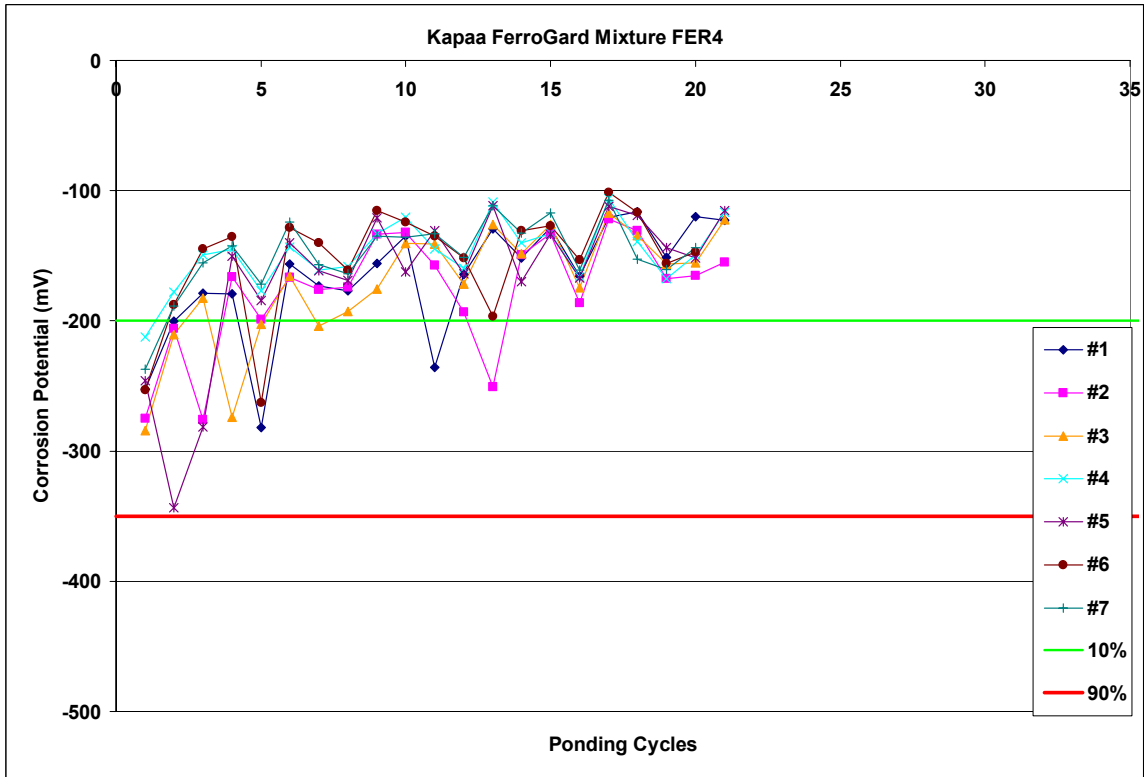


Figure A.1-98: Corrosion Potential Measurements for Kapaa FerroGard Mixture FER4

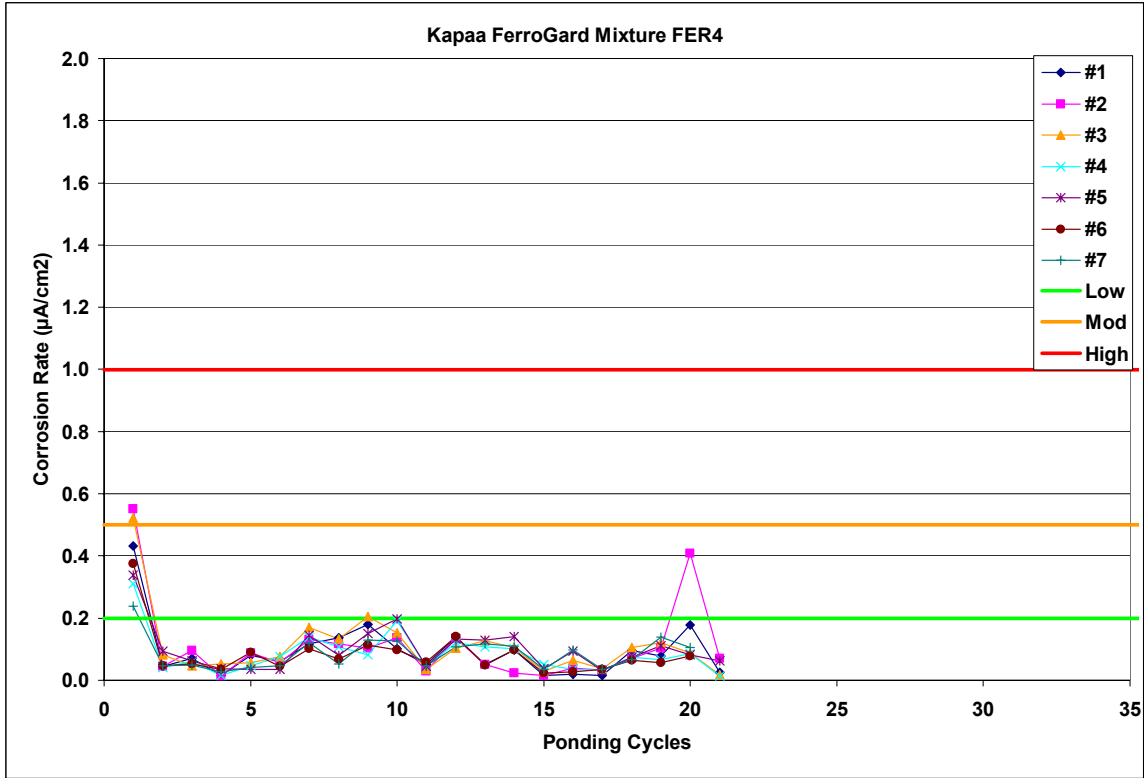


Figure A.1-99: Corrosion Rate Measurements for Kapaa FerroGard Mixture FER4

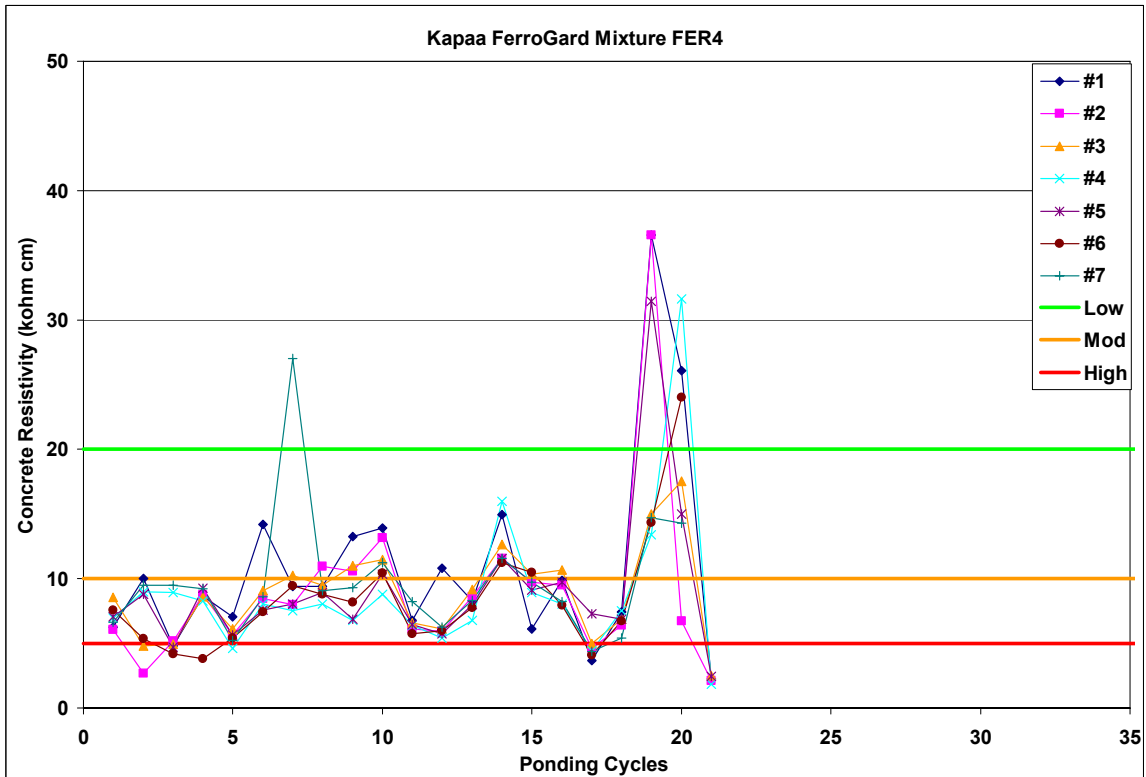


Figure A.1-100: Corrosion Resistivity Measurements for Kapaa FerroGard Mixture FER4

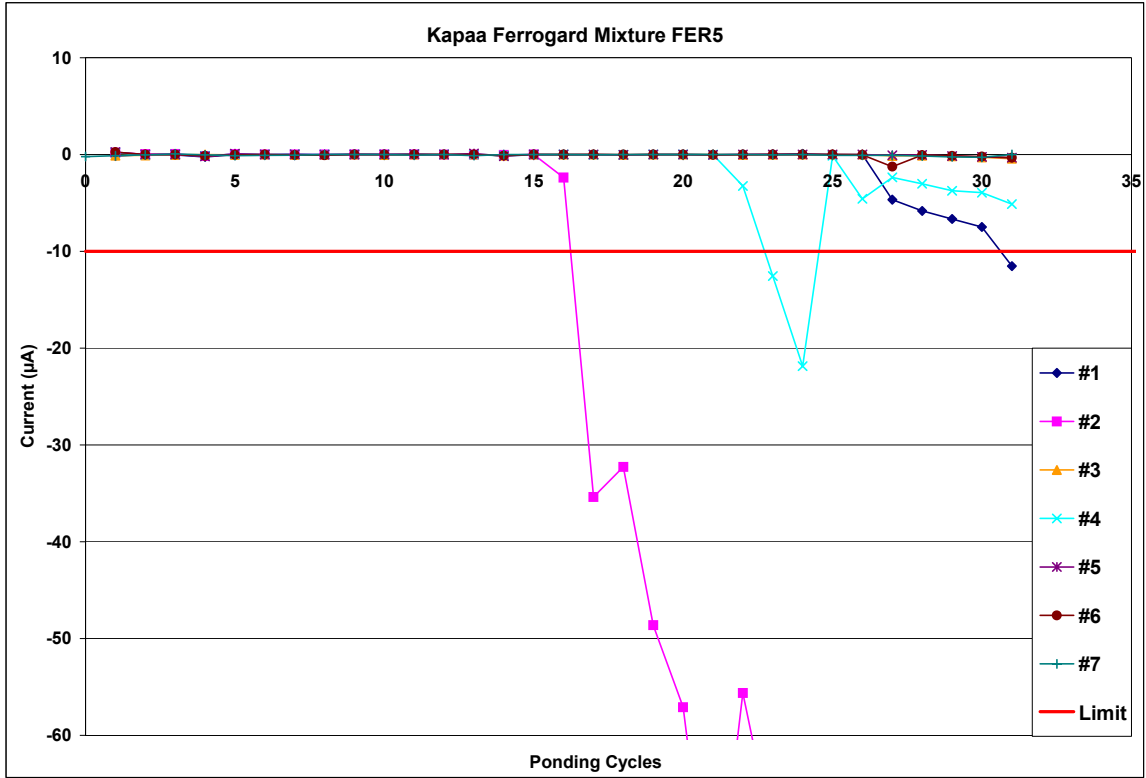


Figure A.1-101: Current Measurements for Kapaa FerroGard Mixture FER5

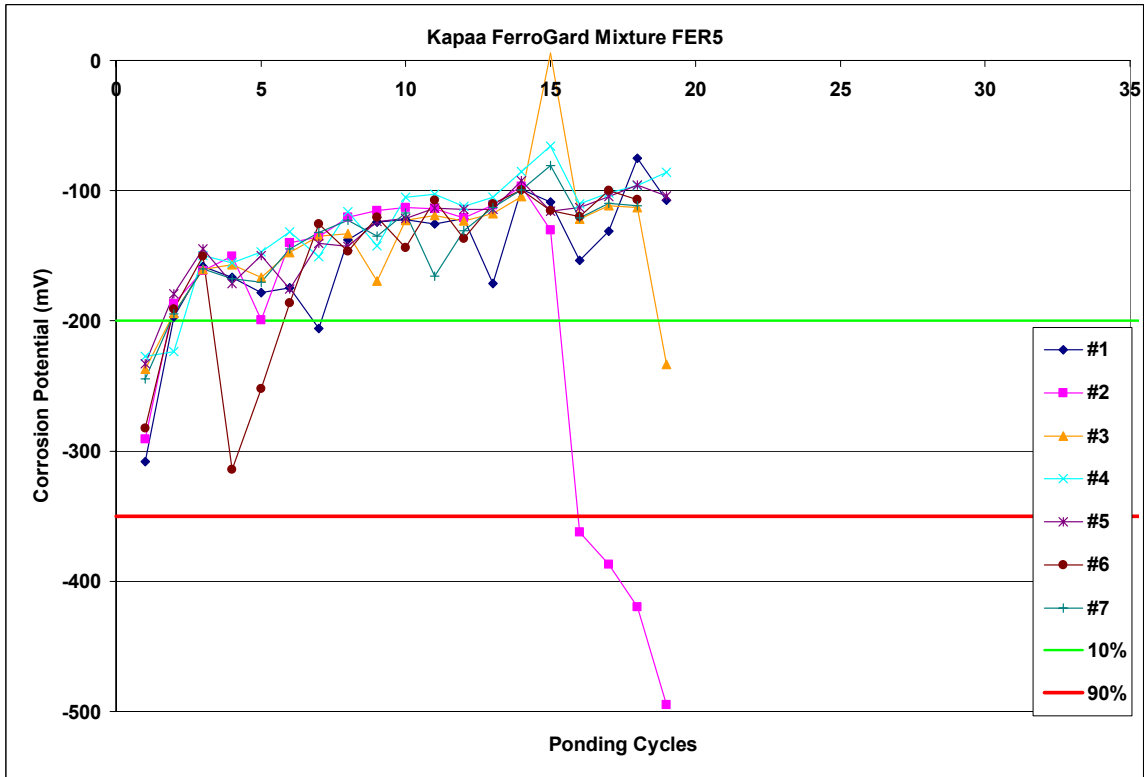


Figure A.1-102: Corrosion Potential Measurements for Kapaa FerroGard Mixture FER5

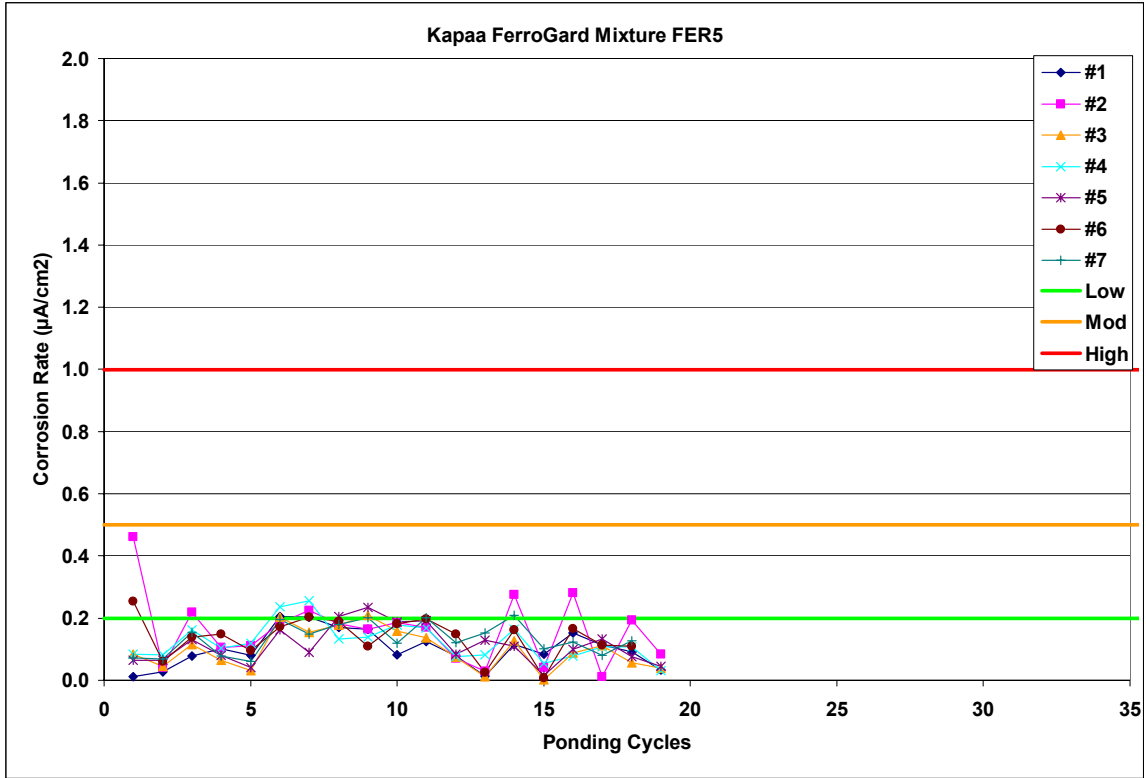


Figure A.1-103: Corrosion Rate Measurements for Kapaa FerroGard Mixture FER5

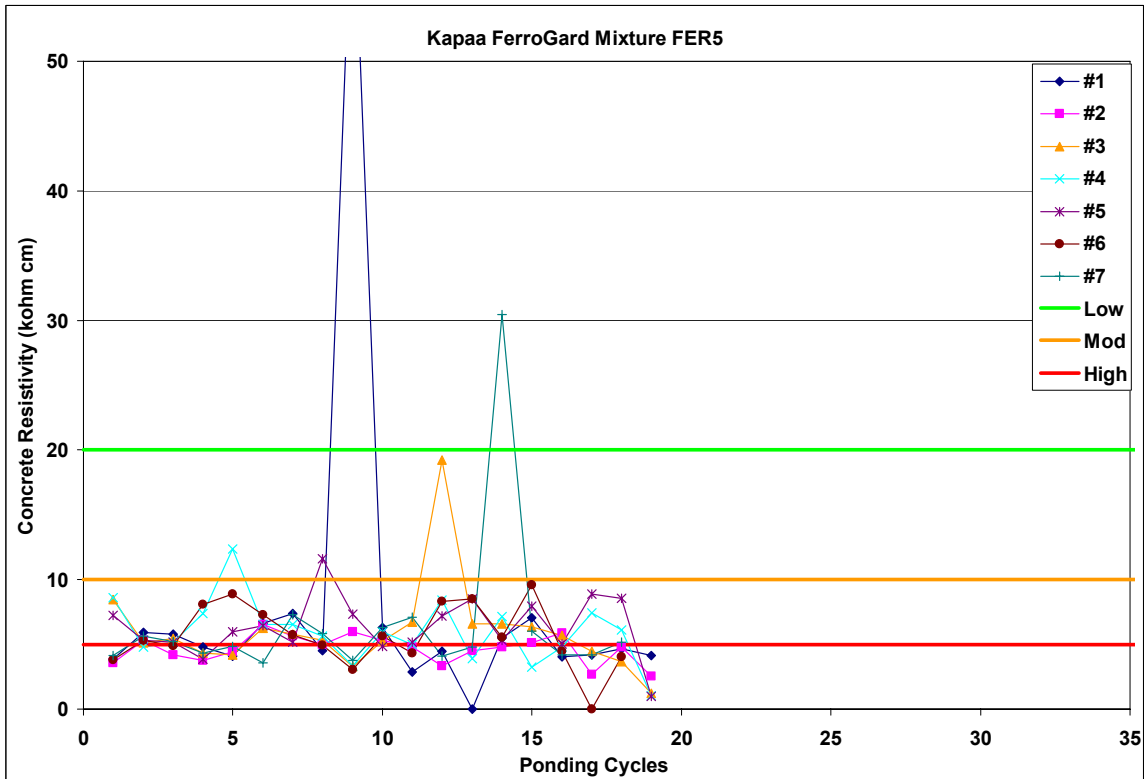


Figure A.1-104: Corrosion Resistivity Measurements for Kapaa FerroGard Mixture FER5

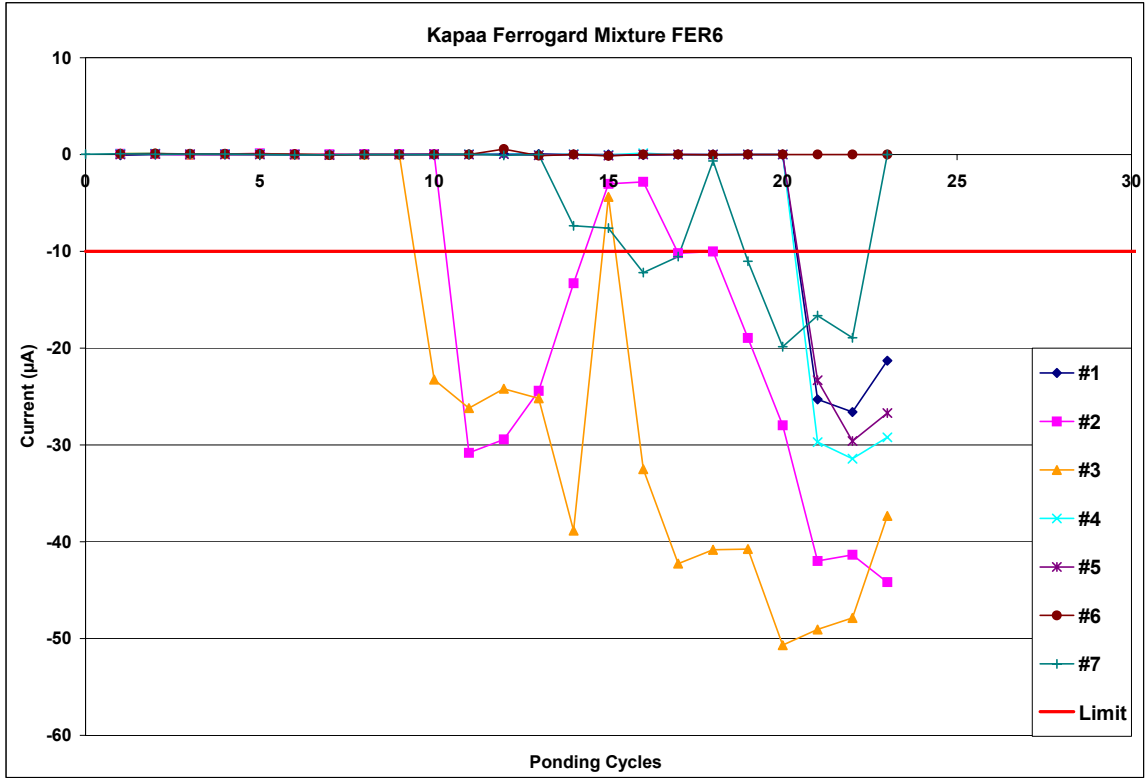


Figure A.1-105: Current Measurements for Kapaa FerroGard Mixture FER6

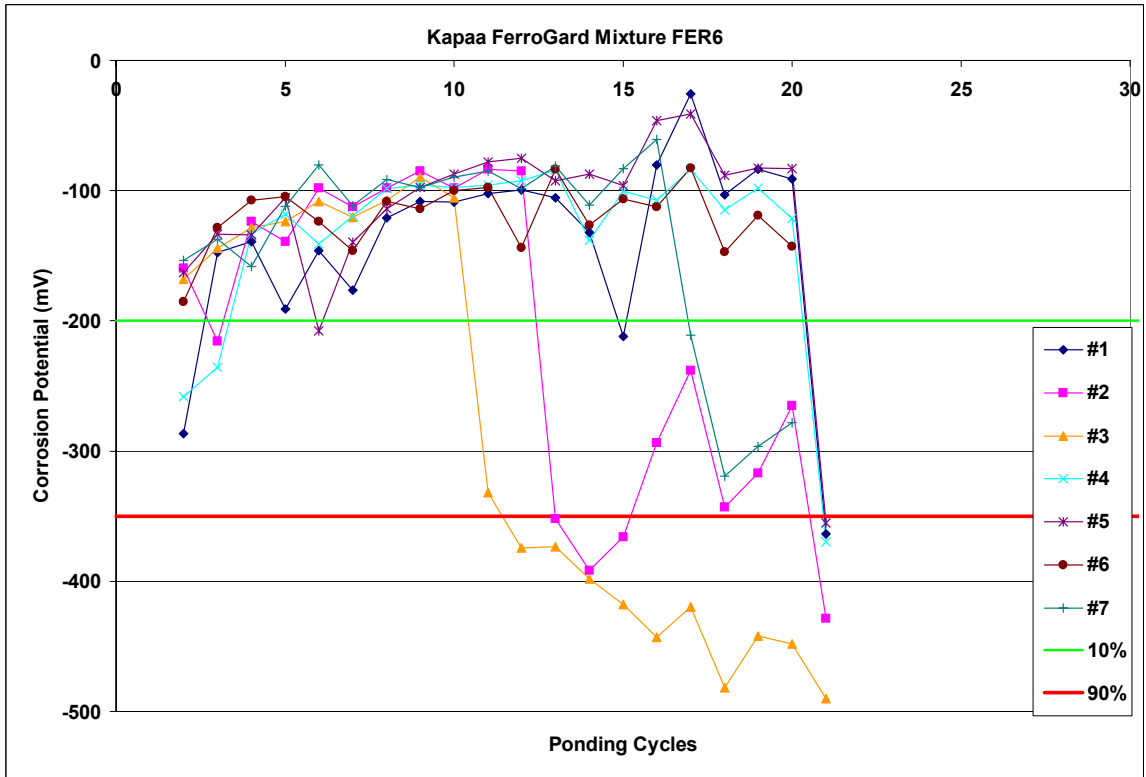


Figure A.1-106: Corrosion Potential Measurements for Kapaa Control Mixture FER6

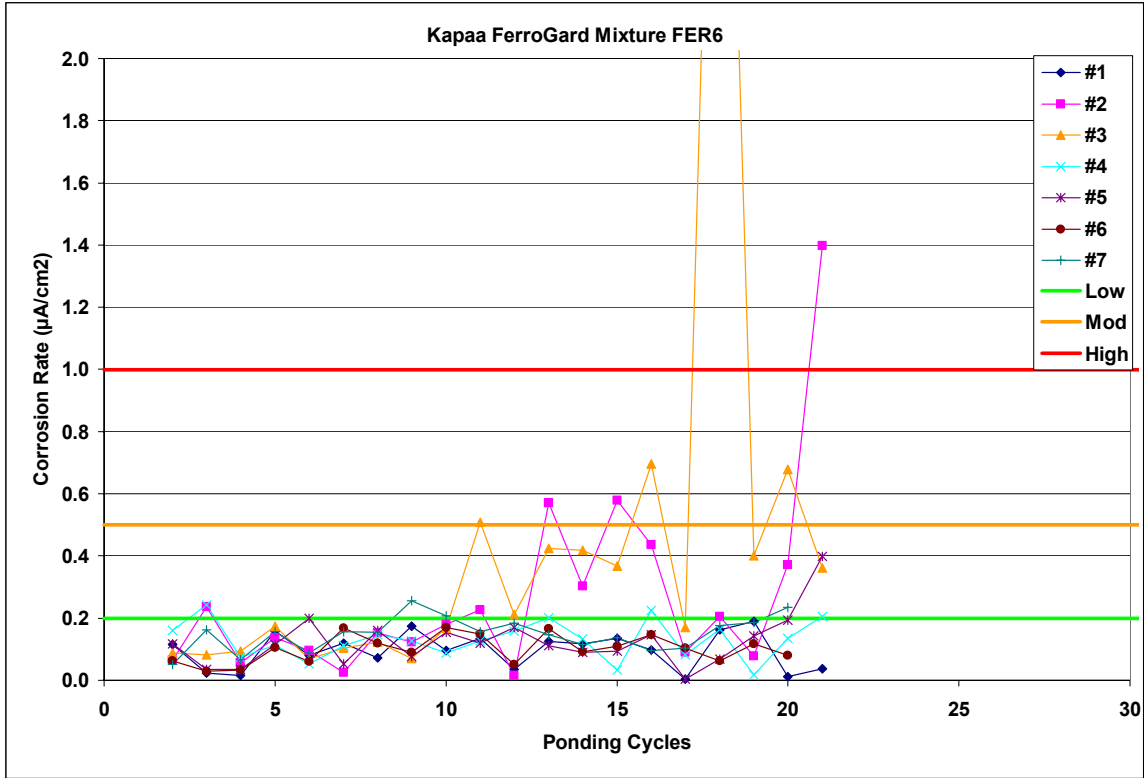


Figure A.1-107: Corrosion Rate Measurements for Kapaa FerroGard Mixture FER6

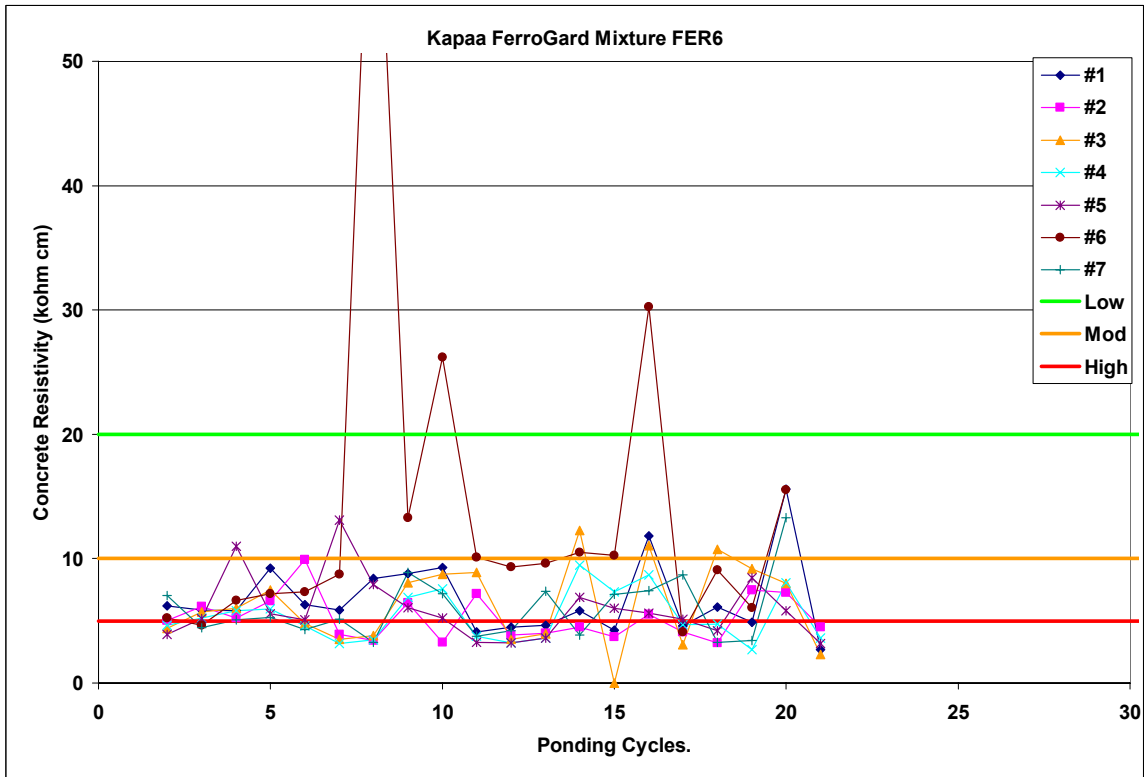


Figure A.1-108: Corrosion Resistivity Measurements for Kapaa FerroGard Mixture FER6

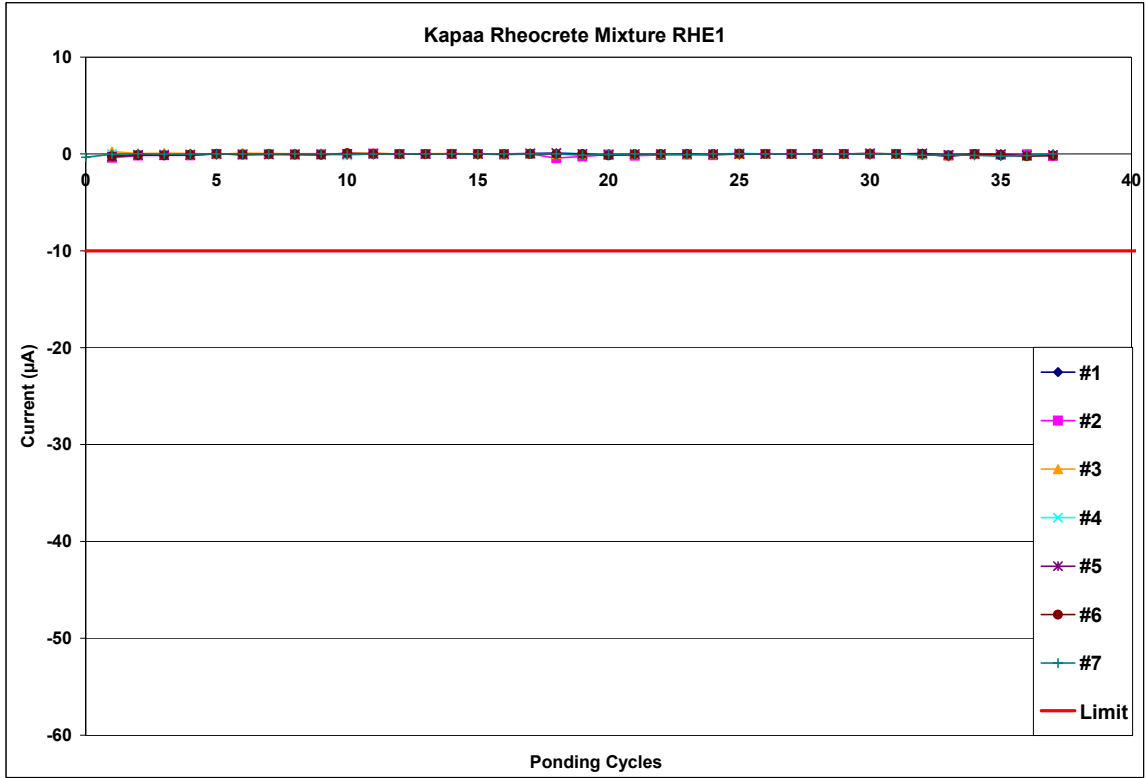


Figure A.1-109: Current Measurements for Kapaa Rheocrete Mixture RHE1

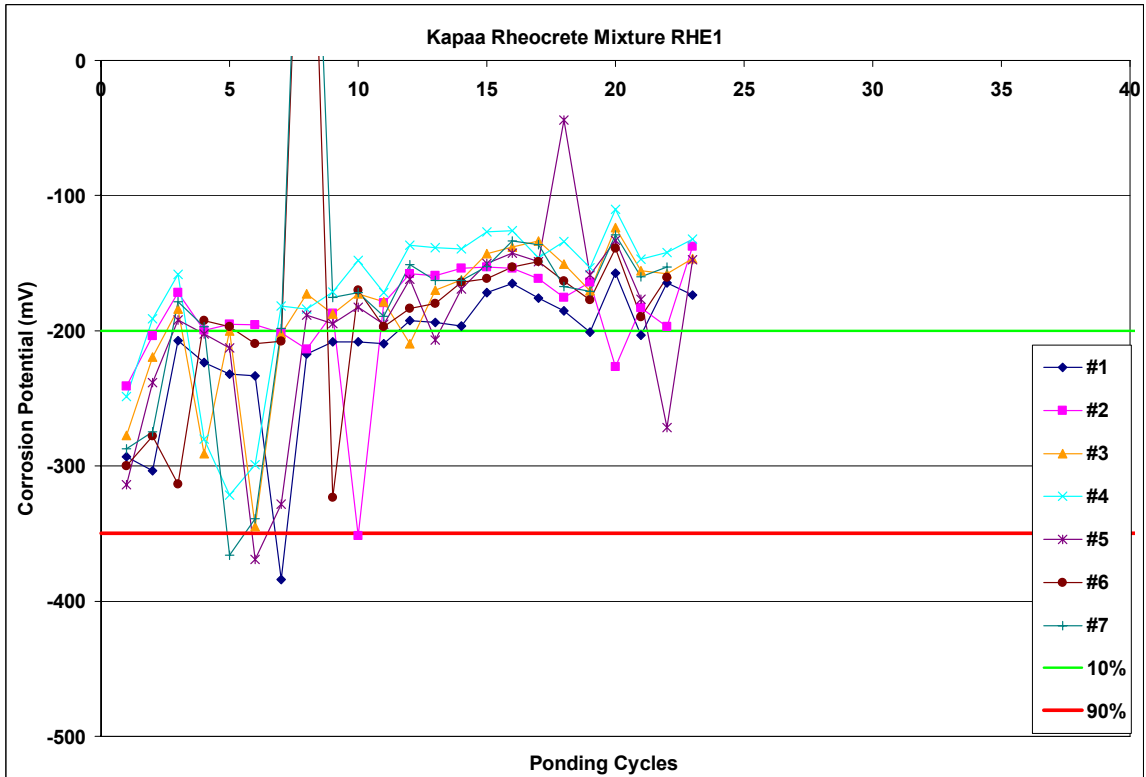


Figure A.1-110: Corrosion Potential Measurements for Kapaa Rheocrete Mixture RHE1

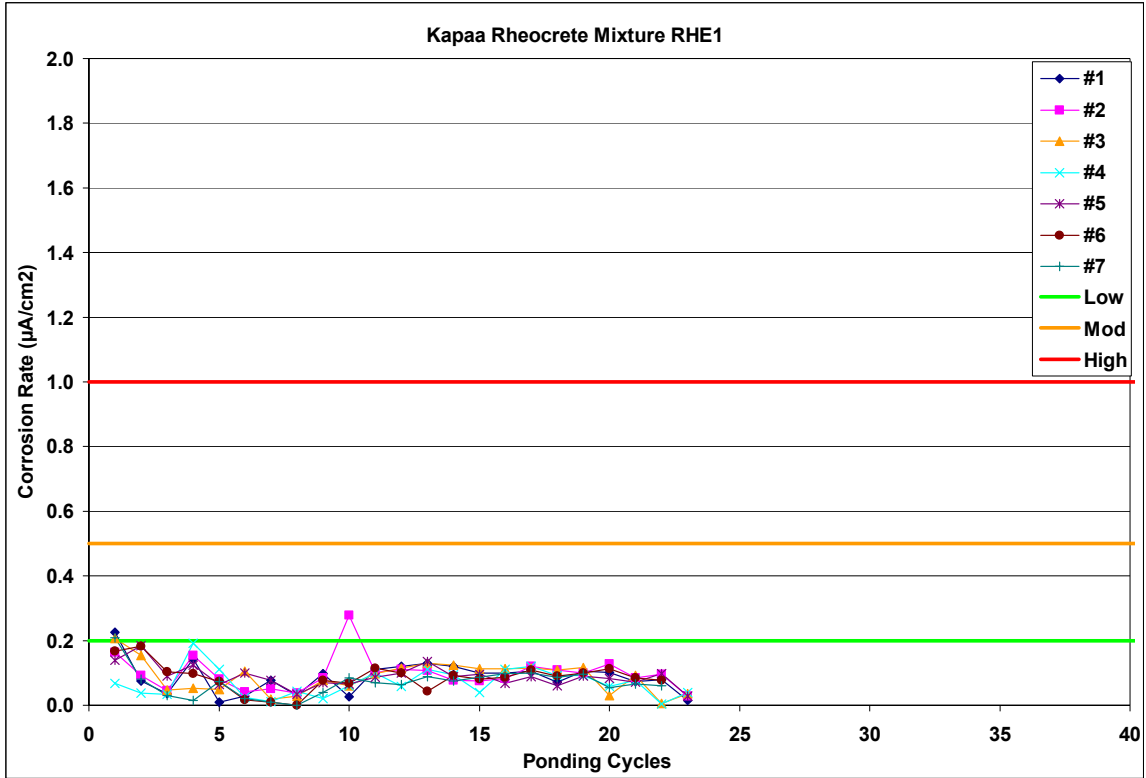


Figure A.1-111: Corrosion Rate Measurements for Kapaa Rheocrete Mixture RHE1

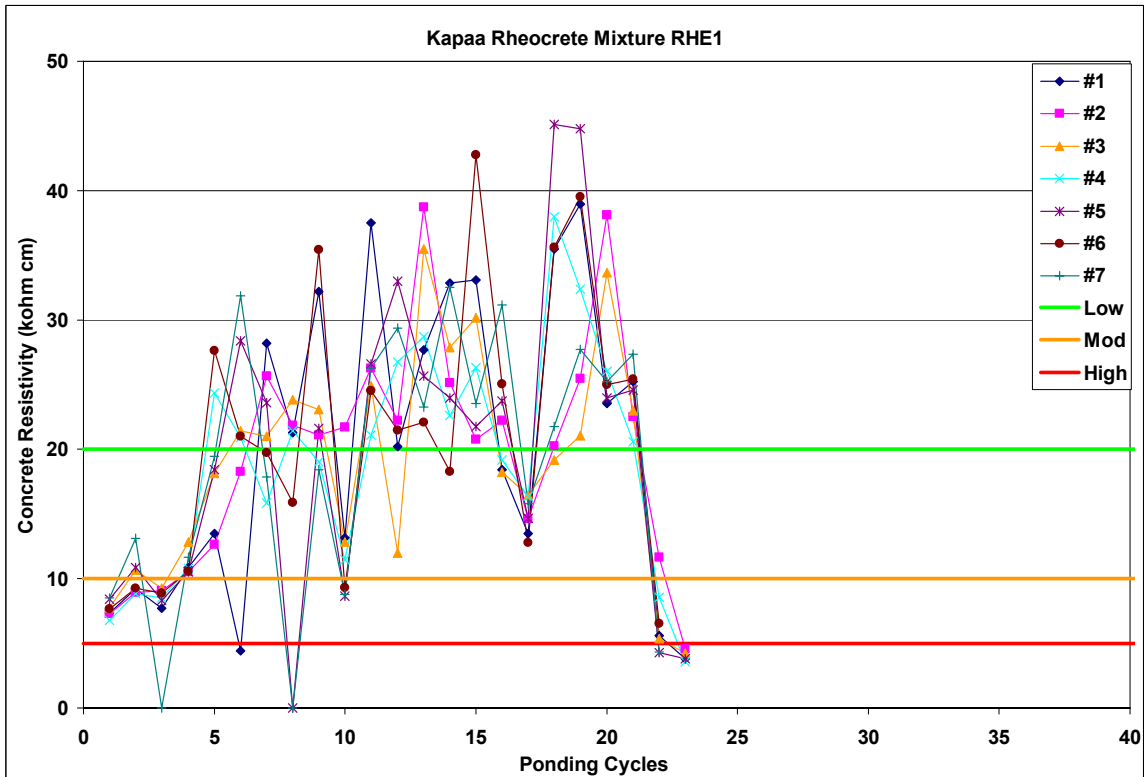


Figure A.1-112: Corrosion Resistivity Measurements for Kapaa Rheocrete Mixture RHE1

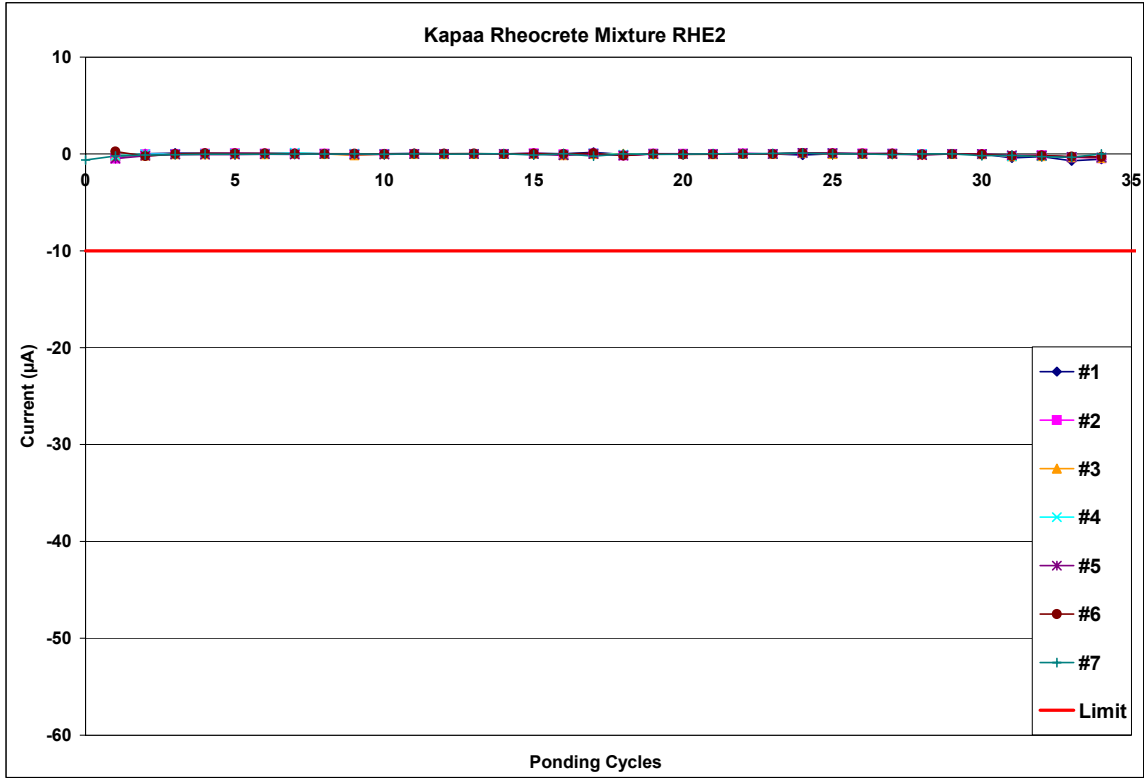


Figure A.1-113: Current Measurements for Kapaa Rheocrete Mixture RHE2

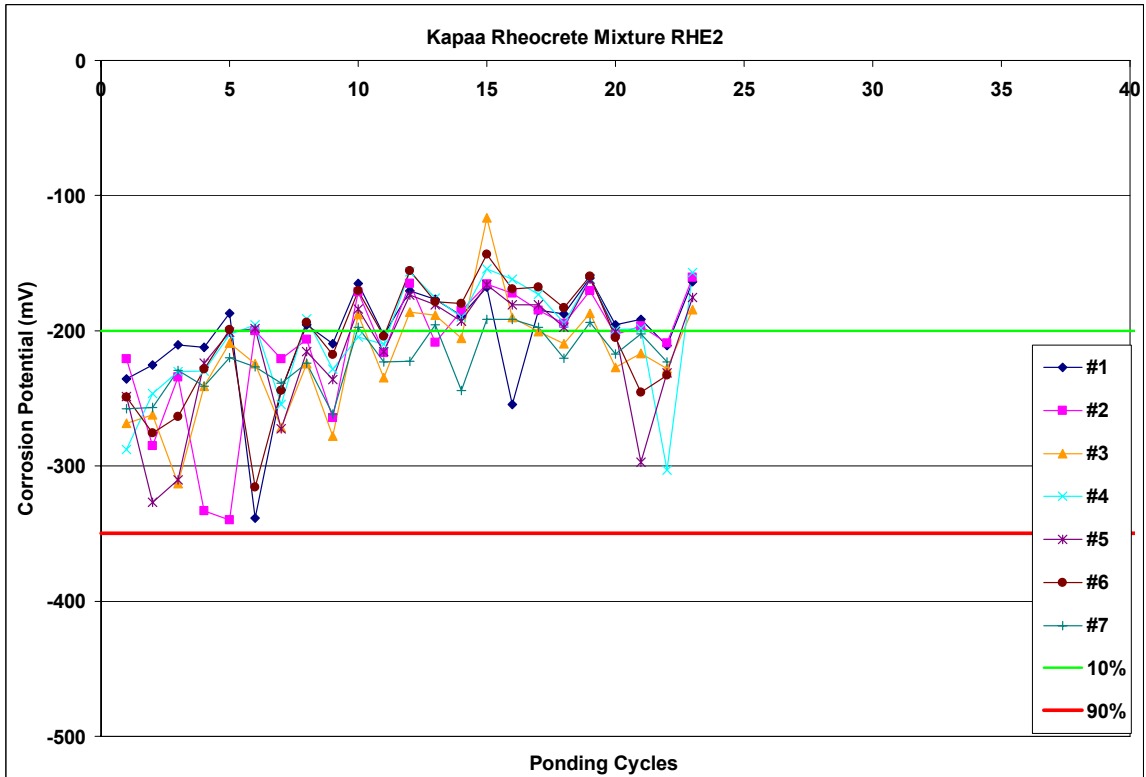


Figure A.1-114: Corrosion Potential Measurements for Kapaa Control Mixture RHE2

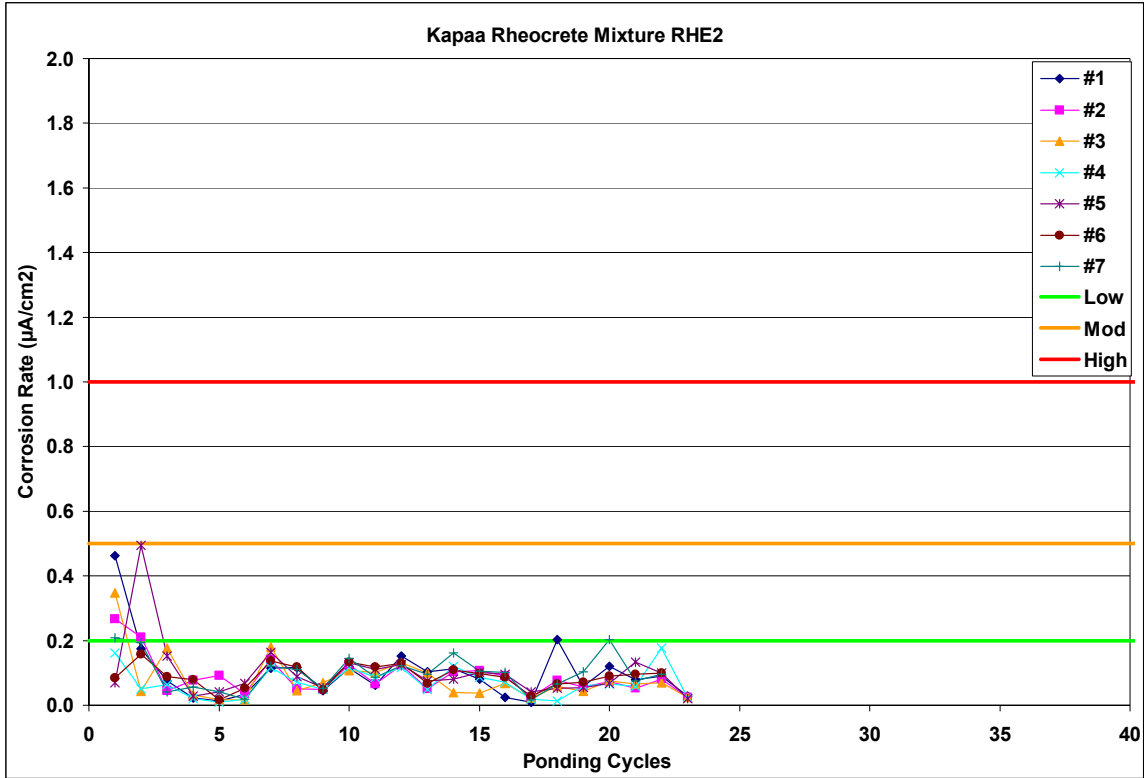


Figure A.1-115: Corrosion Rate Measurements for Kapaa Rheocrete Mixture RHE2

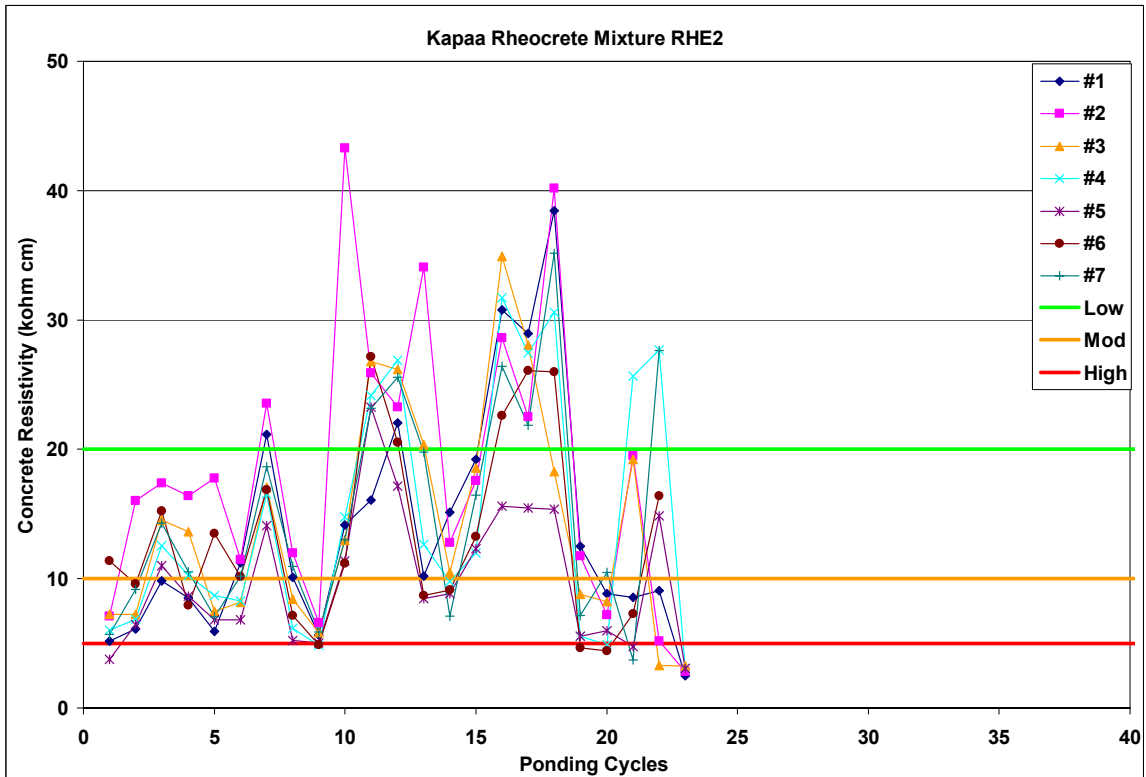


Figure A.1-116: Corrosion Resistivity Measurements for Kapaa Rheocrete Mix RHE2

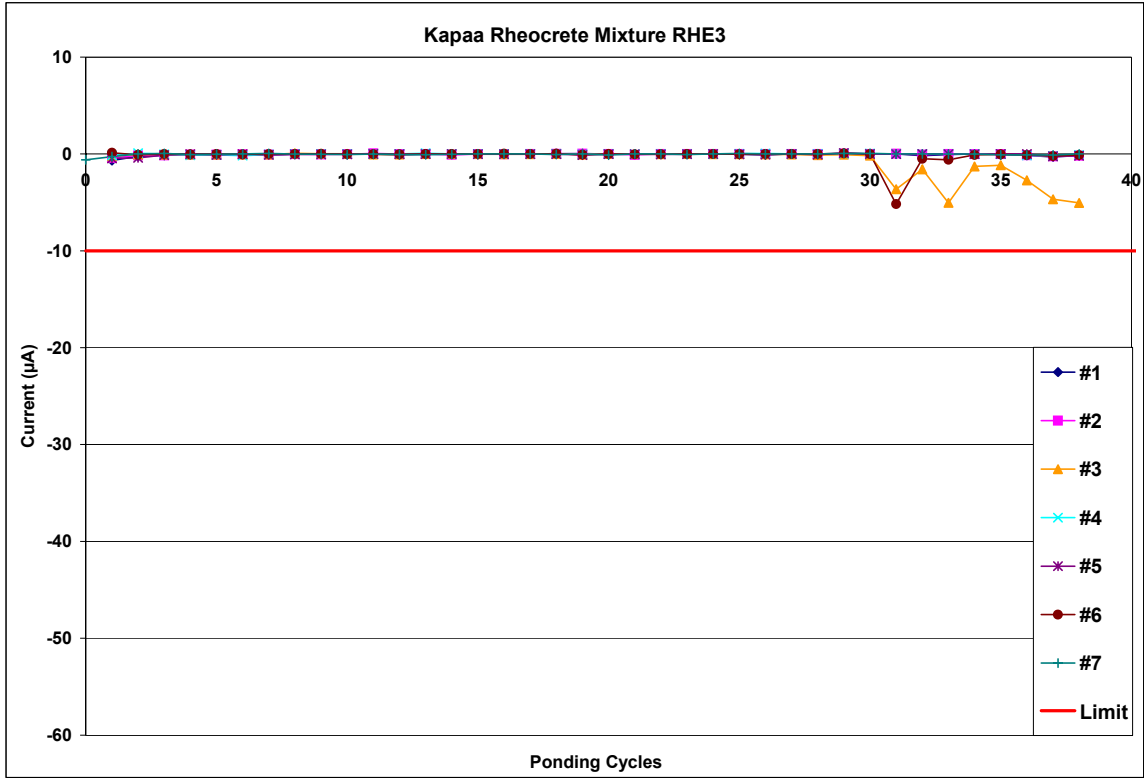


Figure A.1-117: Current Measurements for Kapaa Rheocrete Mixture RHE3

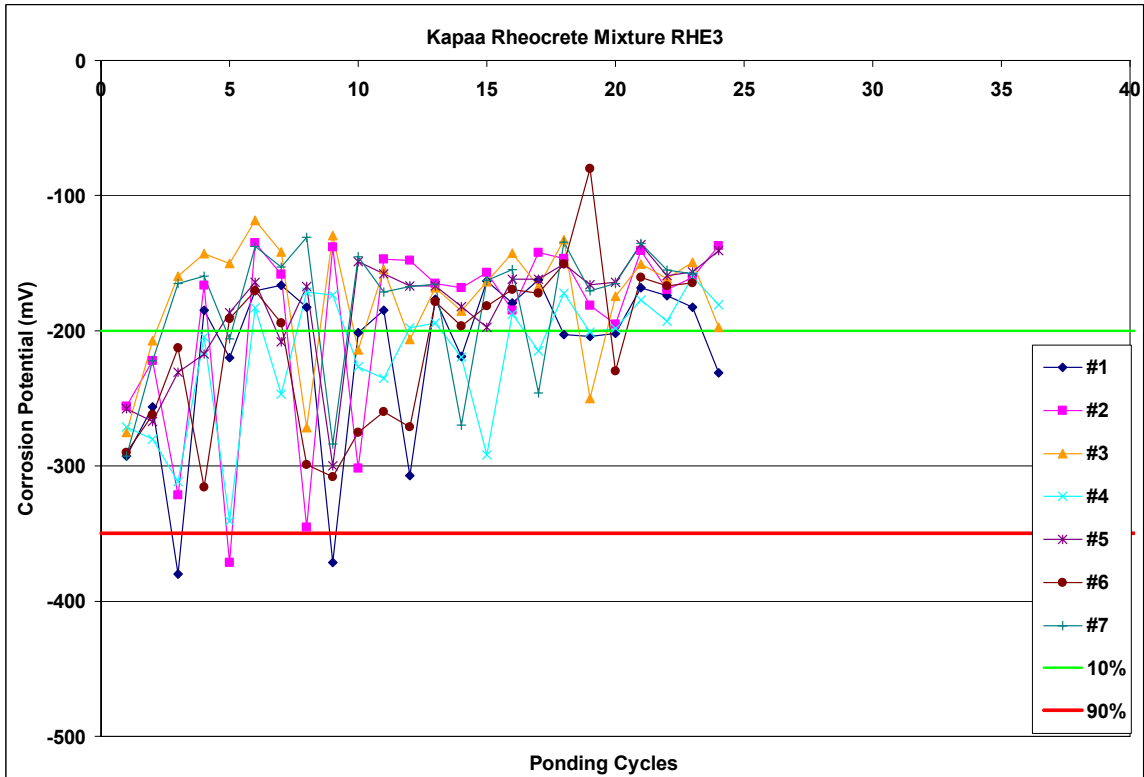


Figure A.1-118: Corrosion Potential Measurements for Kapaa Control Mixture RHE3

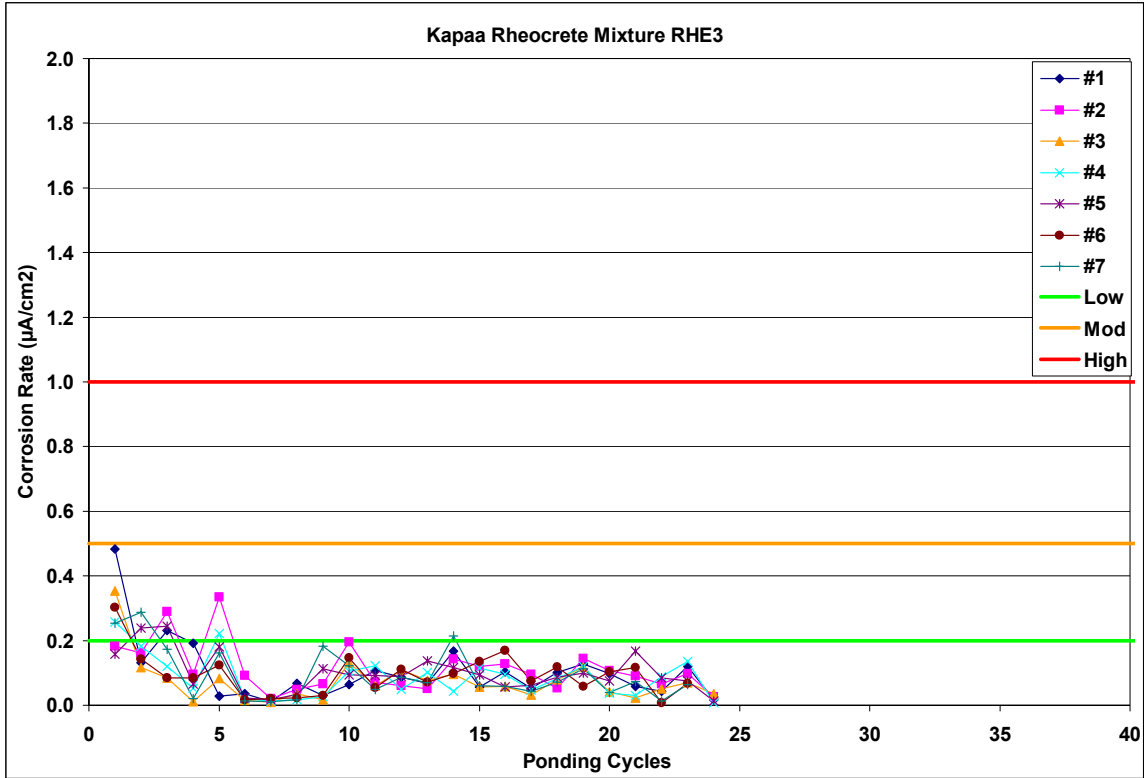


Figure A.1-119: Corrosion Rate Measurements for Kapaa Rheocrete Mixture RHE3

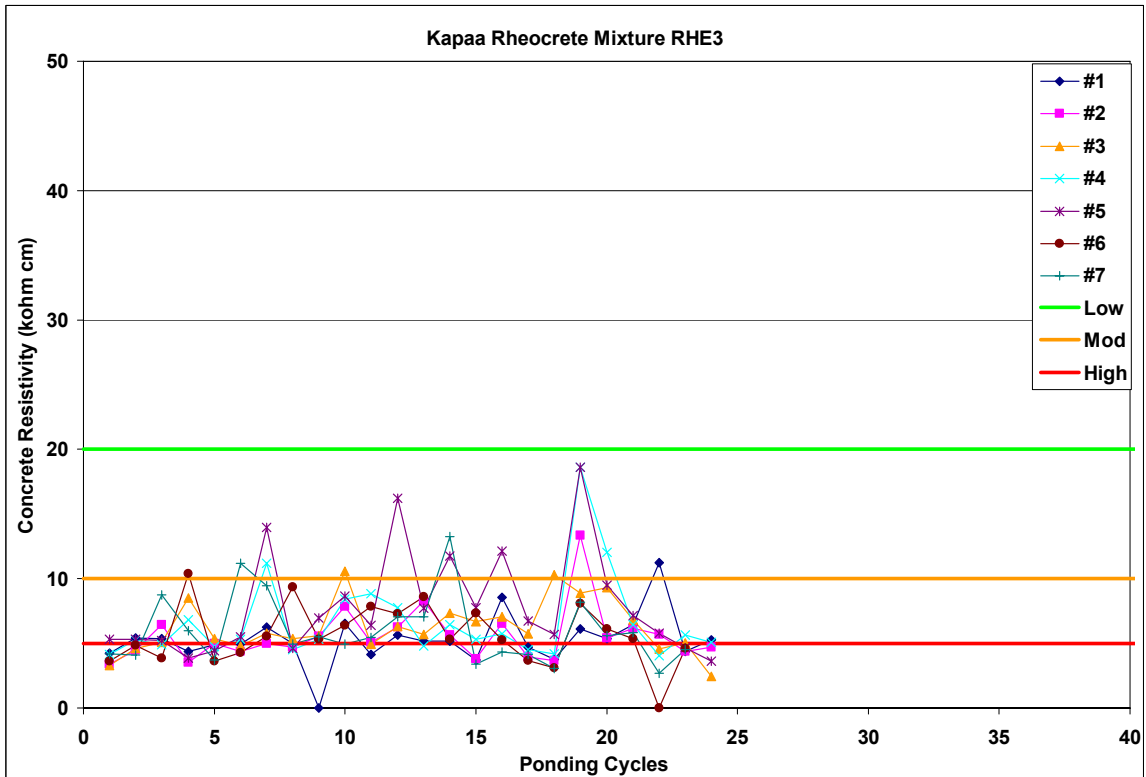


Figure A.1-120: Corrosion Resistivity Measurements for Kapaa Rheocrete Mix RHE3

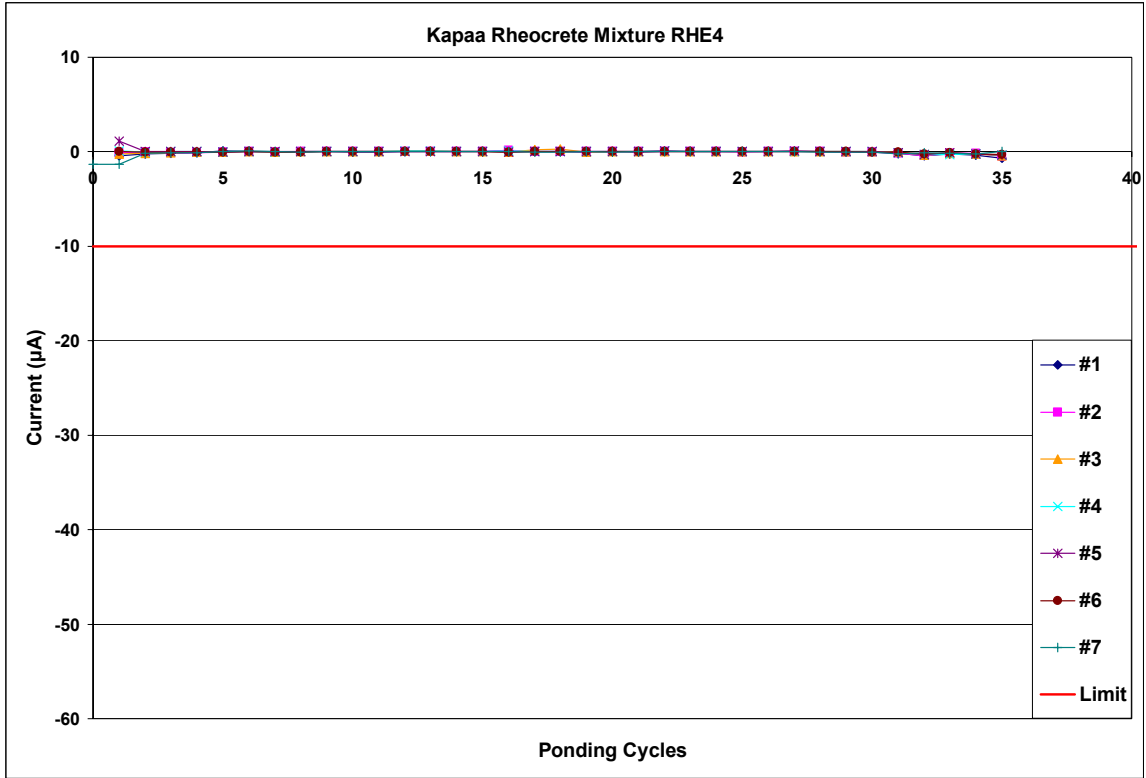


Figure A.1-121: Current Measurements for Kapaa Rheocrete Mixture RHE4

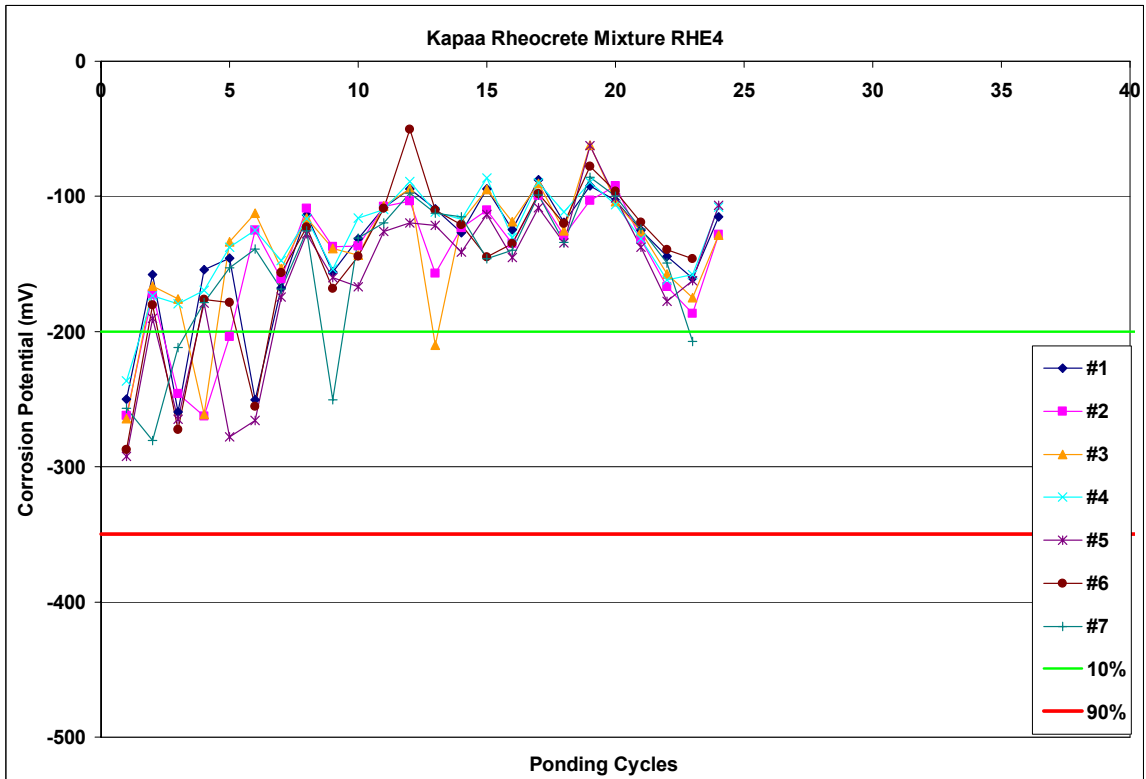


Figure A.1-122: Corrosion Potential Measurements for Kapaa Control Mixture RHE4

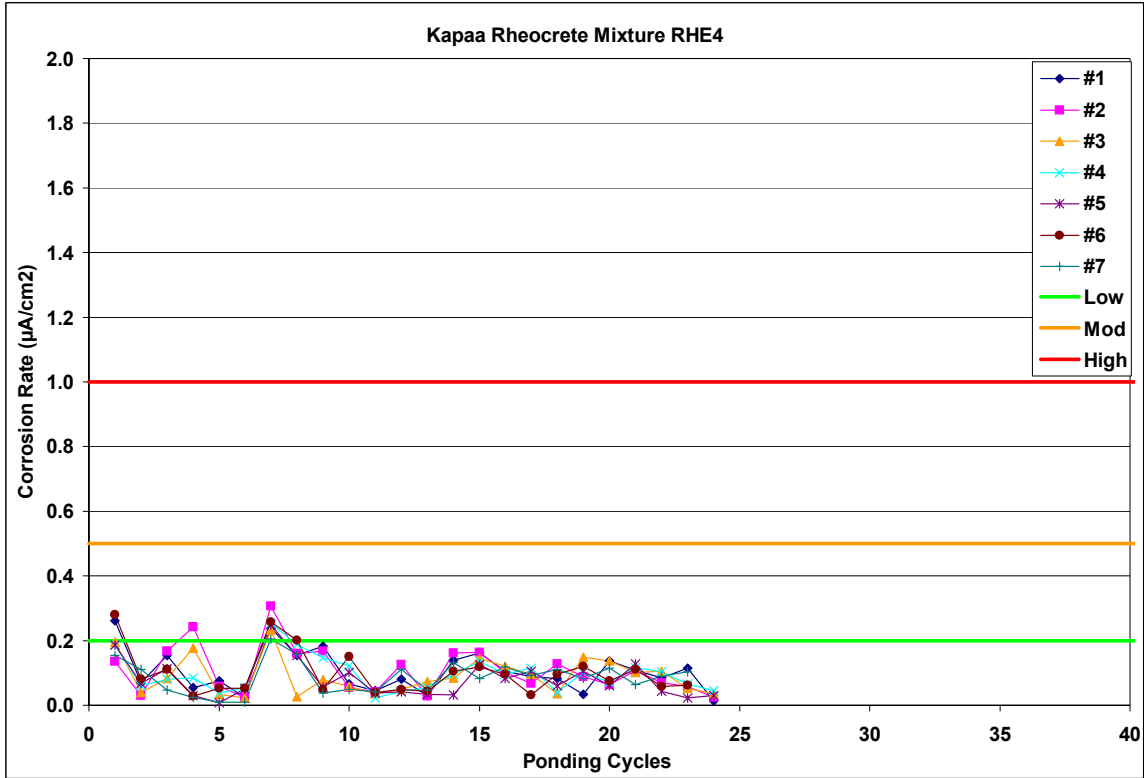


Figure A.1-123: Corrosion Rate Measurements for Kapaa Rheocrete Mixture RHE4

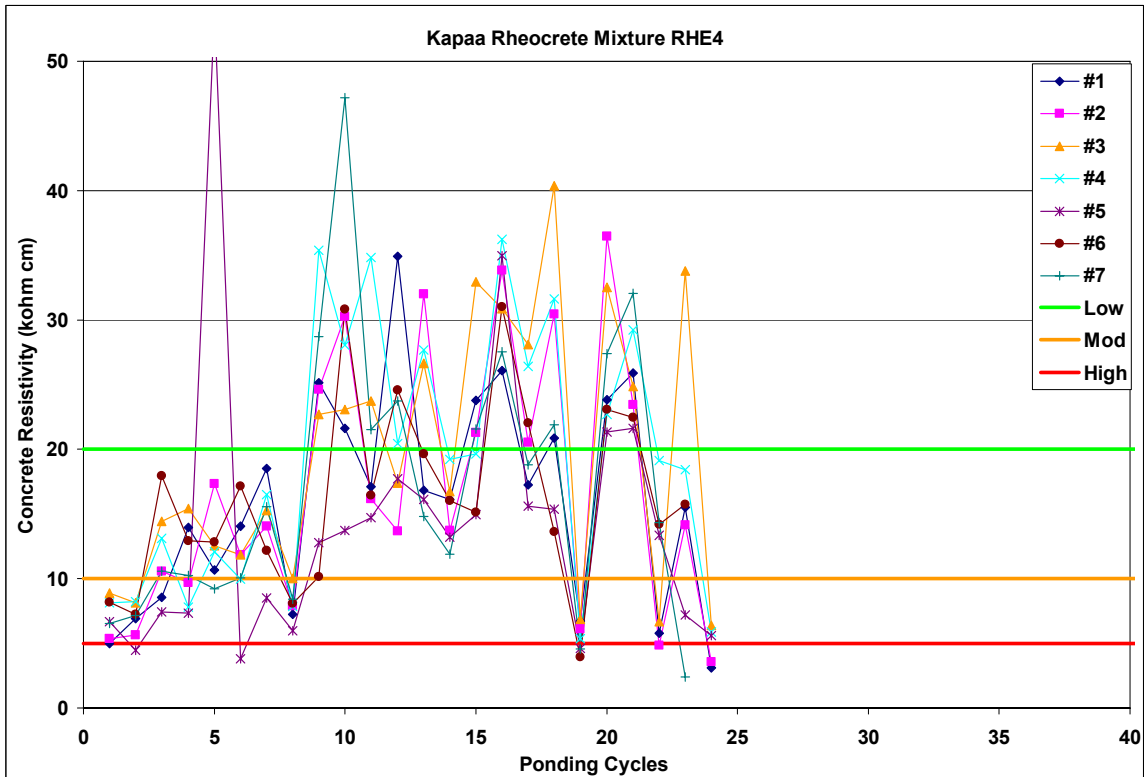


Figure A.1-124: Corrosion Resistivity Measurements for Kapaa Rheocrete Mix RHE4

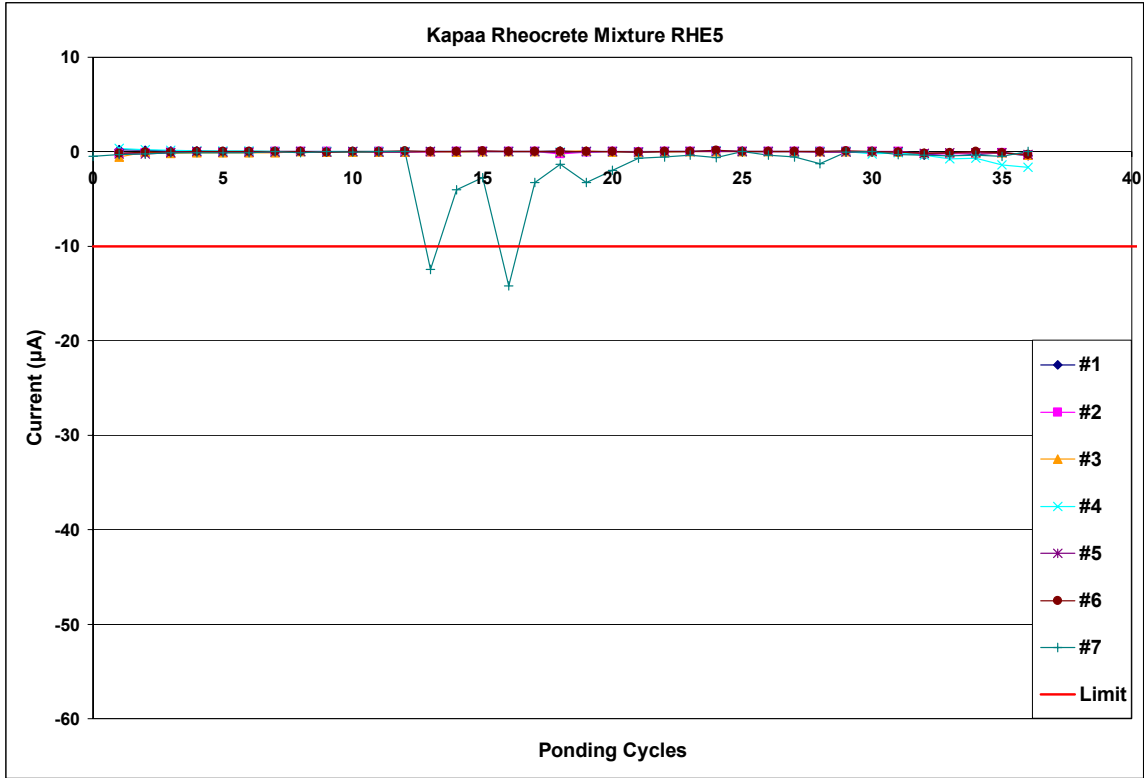


Figure A.1-125: Current Measurements for Kapaa Rheocrete Mixture RHE5

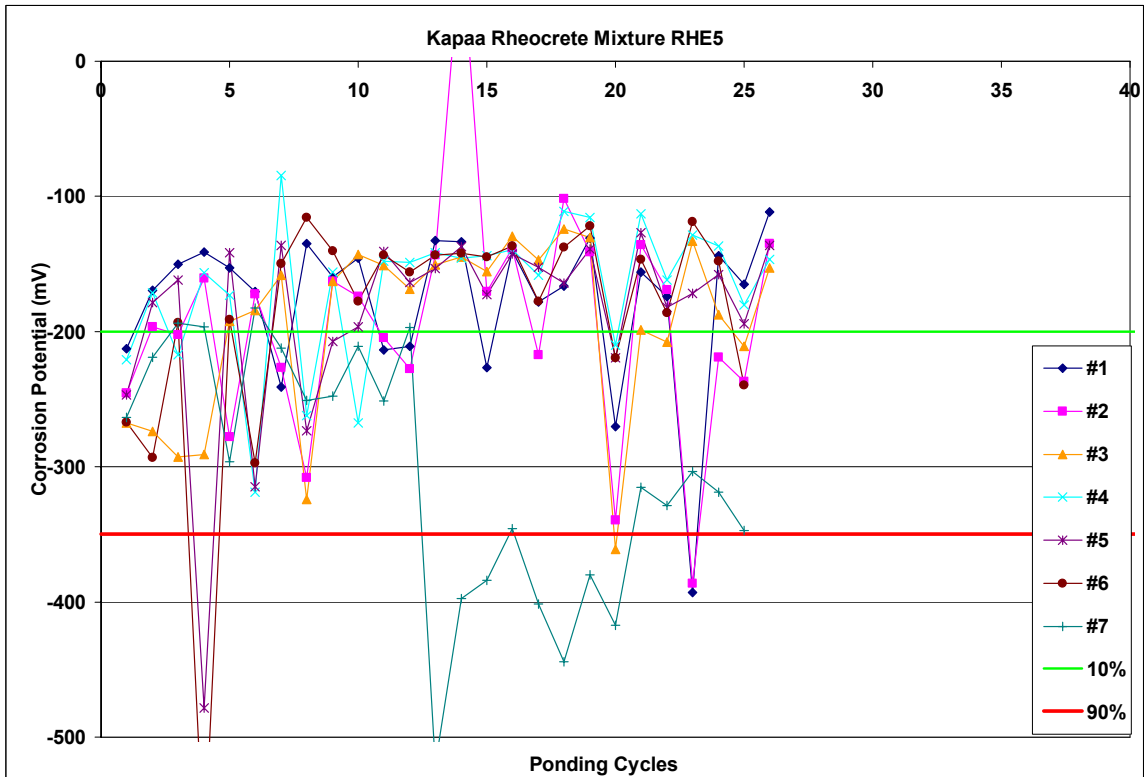


Figure A.1-126: Corrosion Potential Measurements for Kapaa Control Mixture RHE5

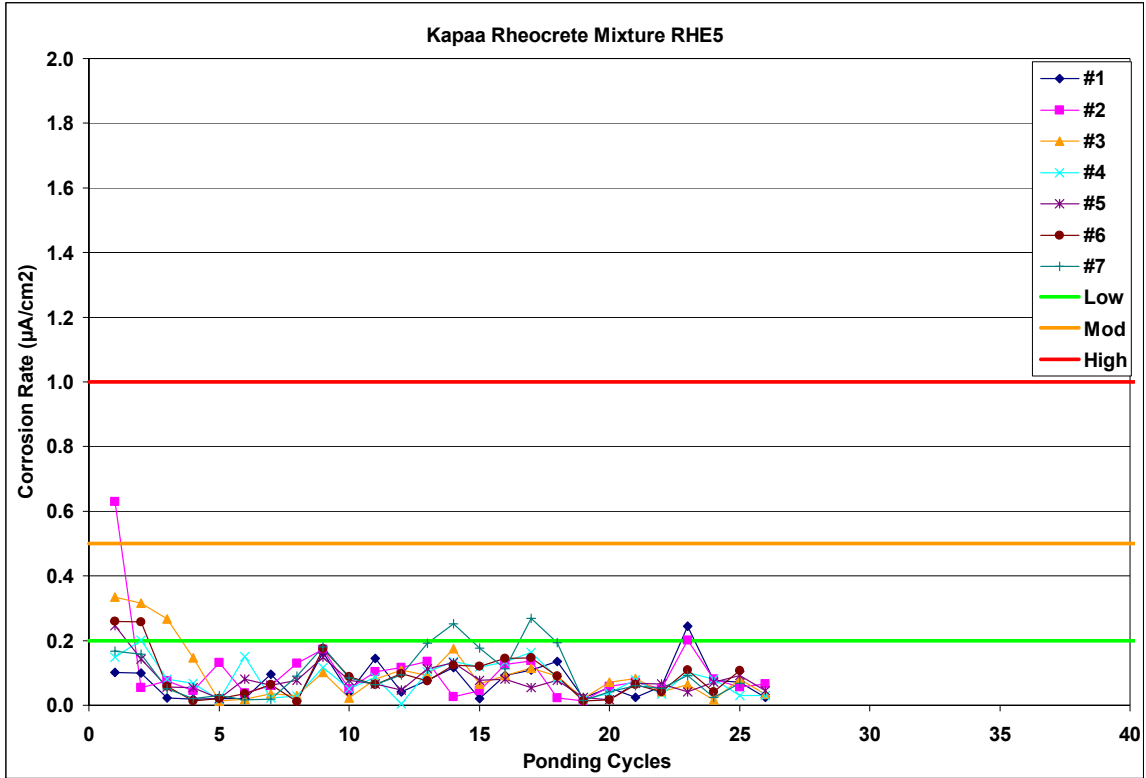


Figure A.1-127: Corrosion Rate Measurements for Kapaa Rheocrete Mixture RHE5

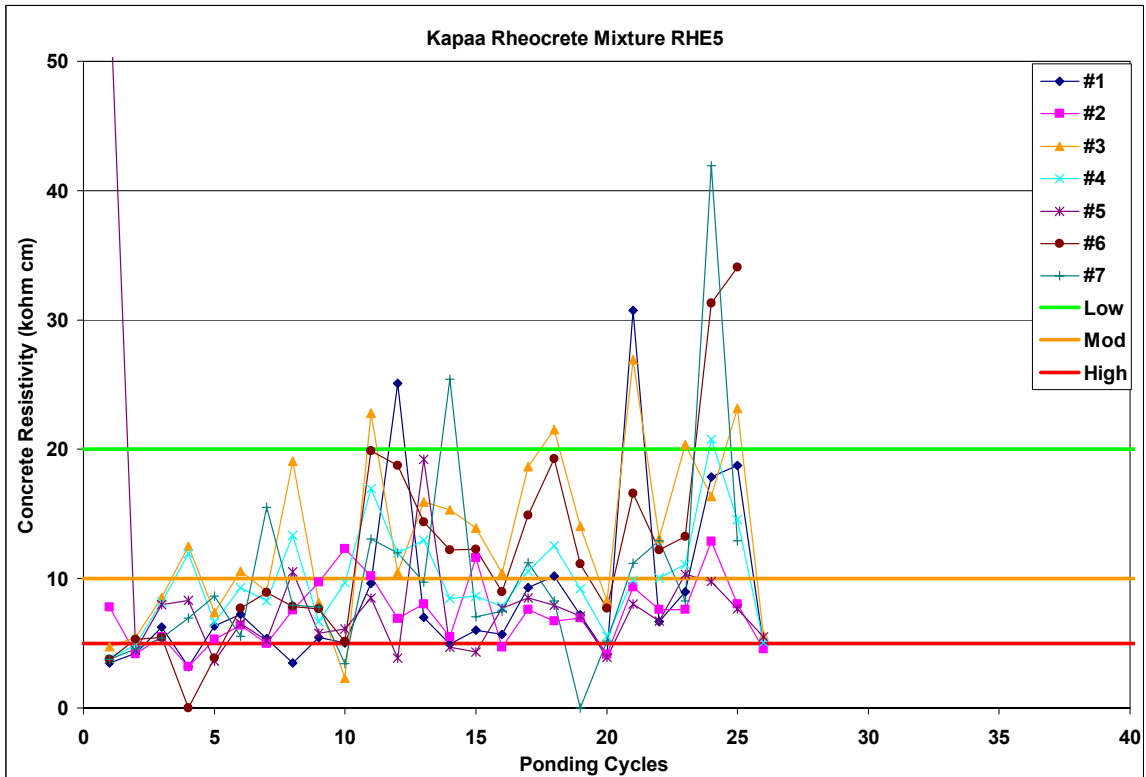


Figure A.1-128: Corrosion Resistivity Measurements for Kapaa Rheocrete Mix RHE5

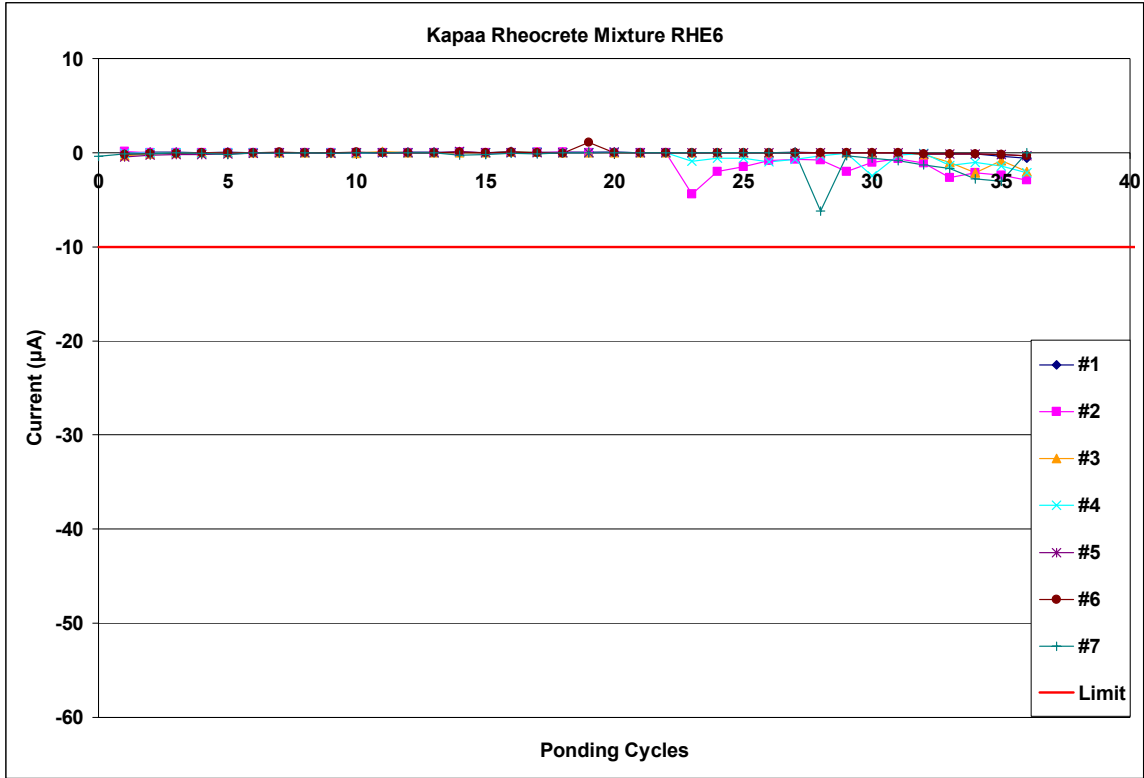


Figure A.1-129: Current Measurements for Kapaa Rheocrete Mixture RHE6

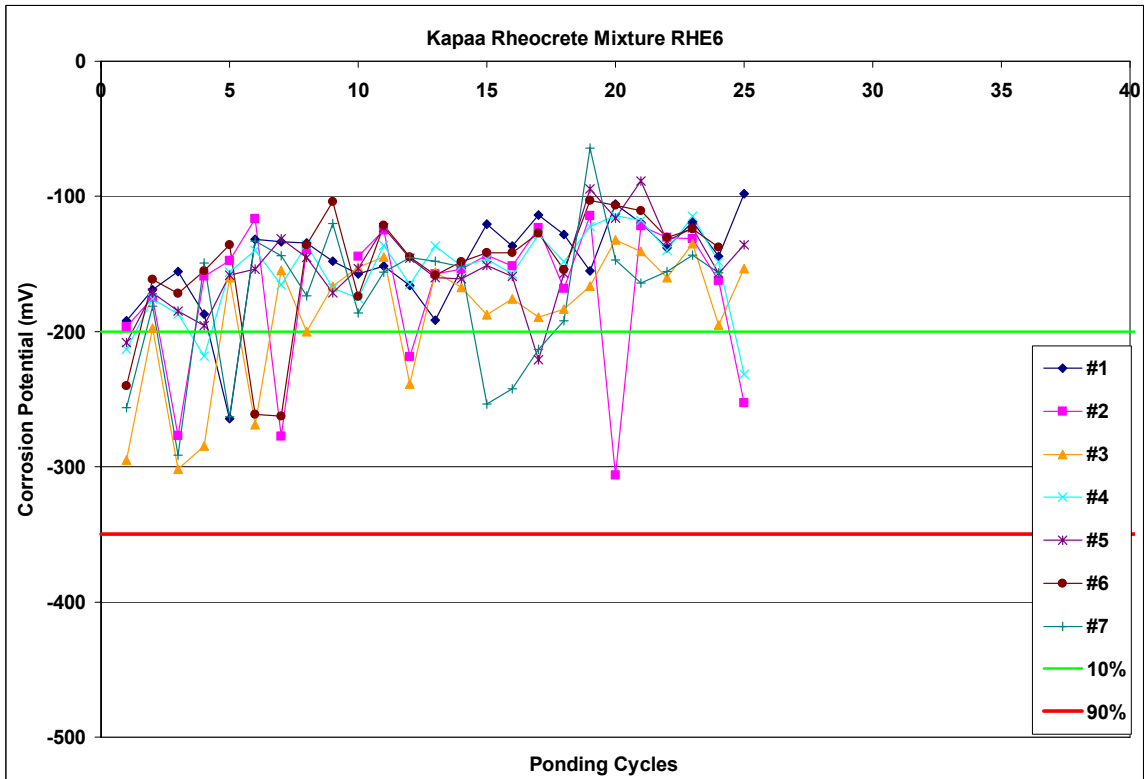


Figure A.1-130: Corrosion Potential Measurements for Kapaa Control Mixture RHE6

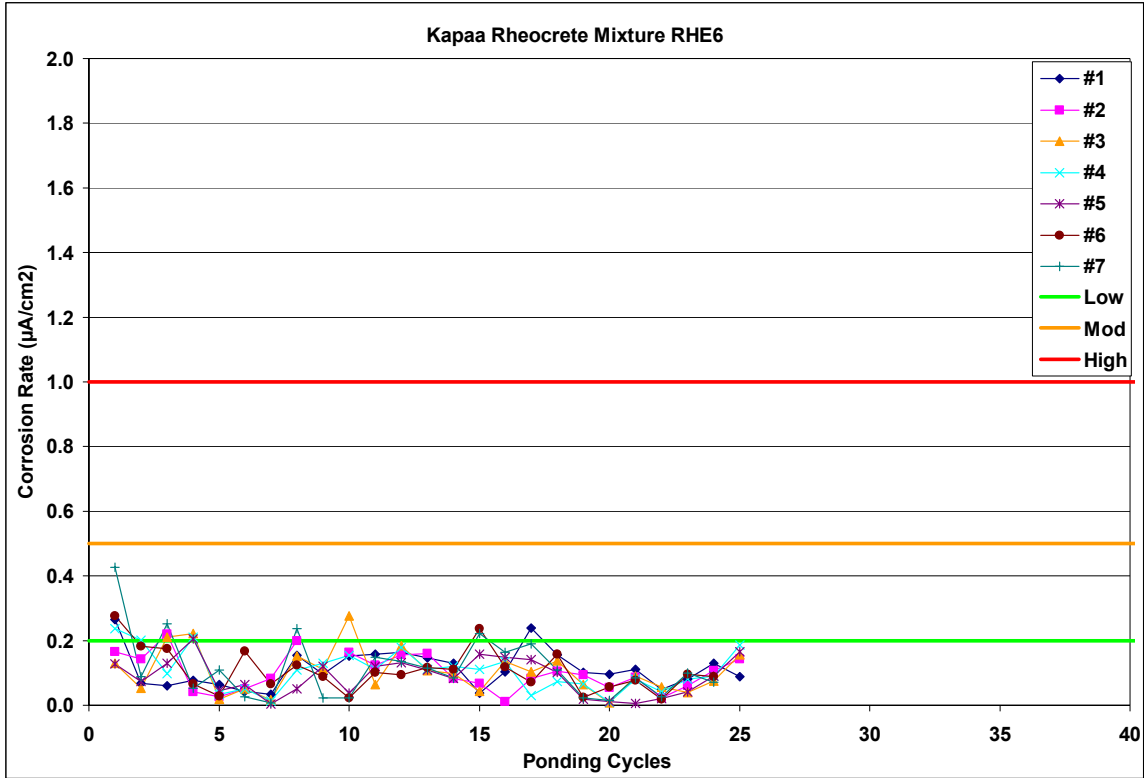


Figure A.1-131: Corrosion Rate Measurements for Kapaa Rheocrete Mixture RHE6

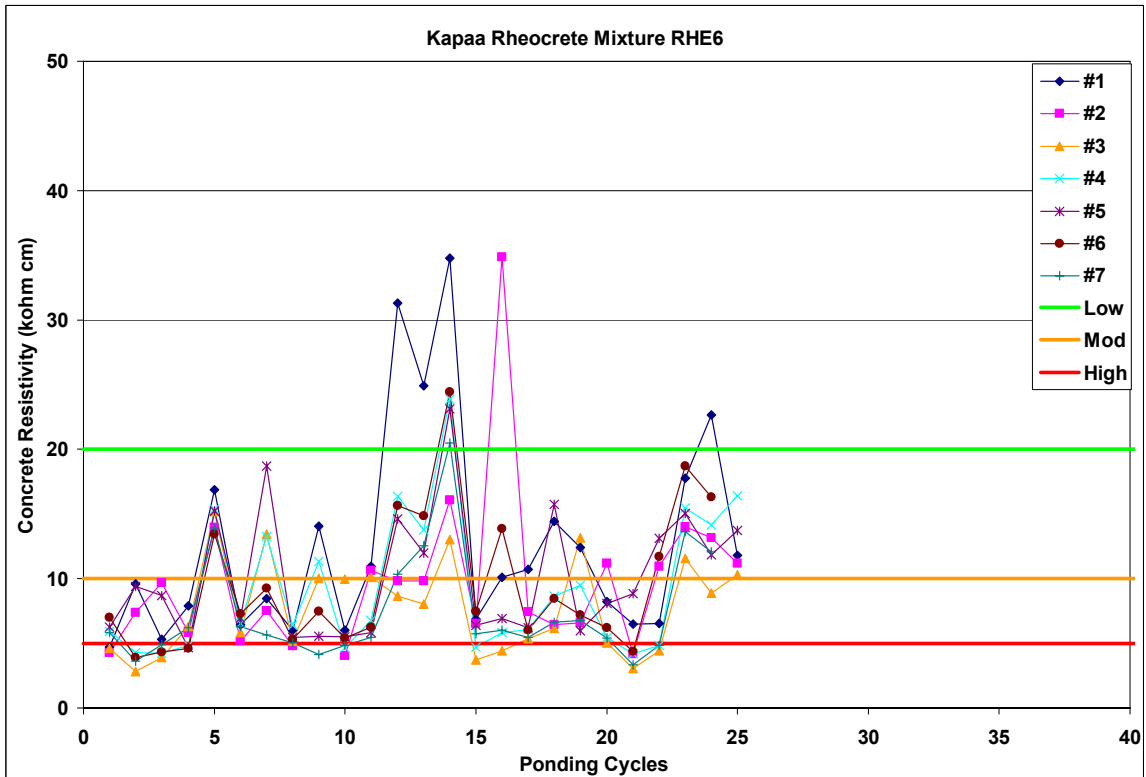


Figure A.1-132: Corrosion Resistivity Measurements for Kapaa Rheocrete RHE6

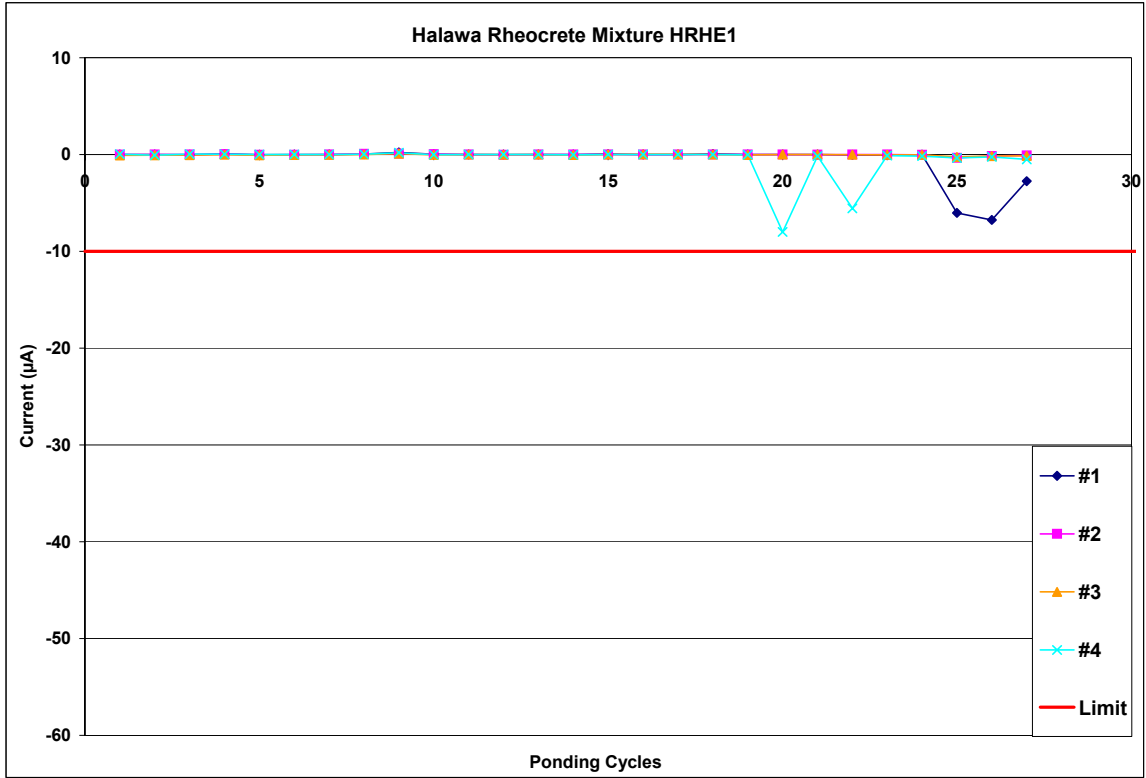


Figure A.1-133: Current Measurements for Halawa Rheocrete Mixture HRHE1

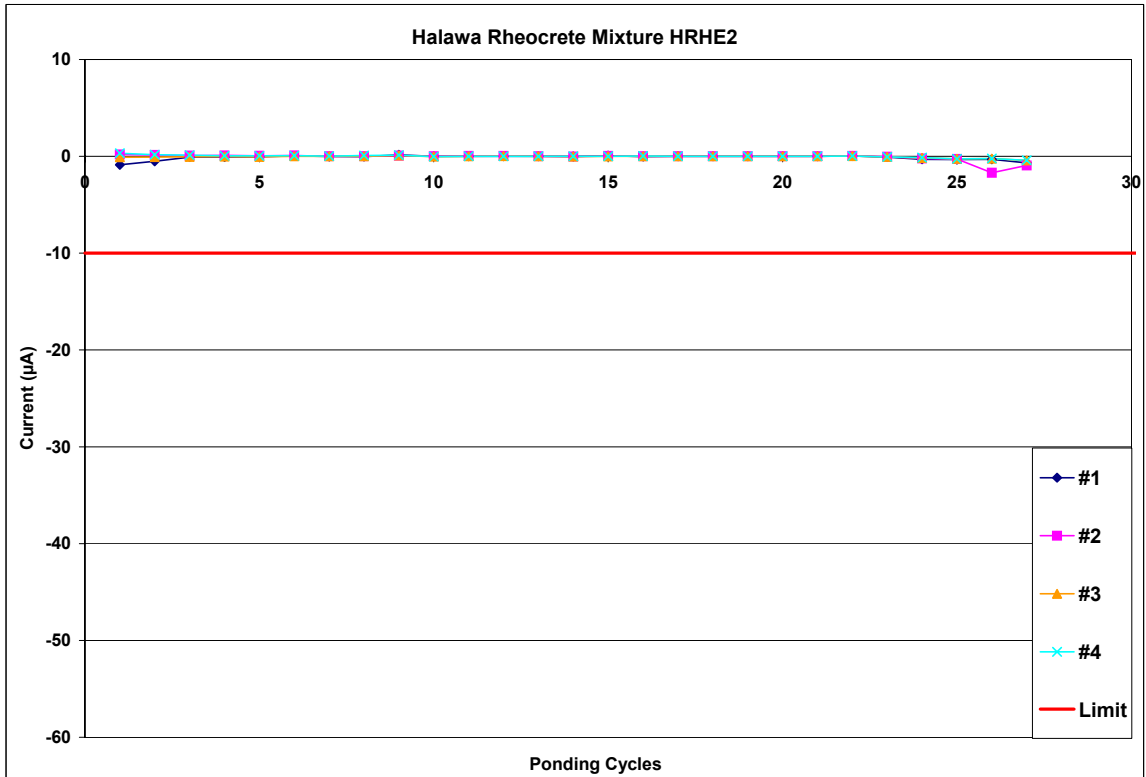


Figure A.1-134: Current Measurements for Halawa Rheocrete Mixture HRHE2

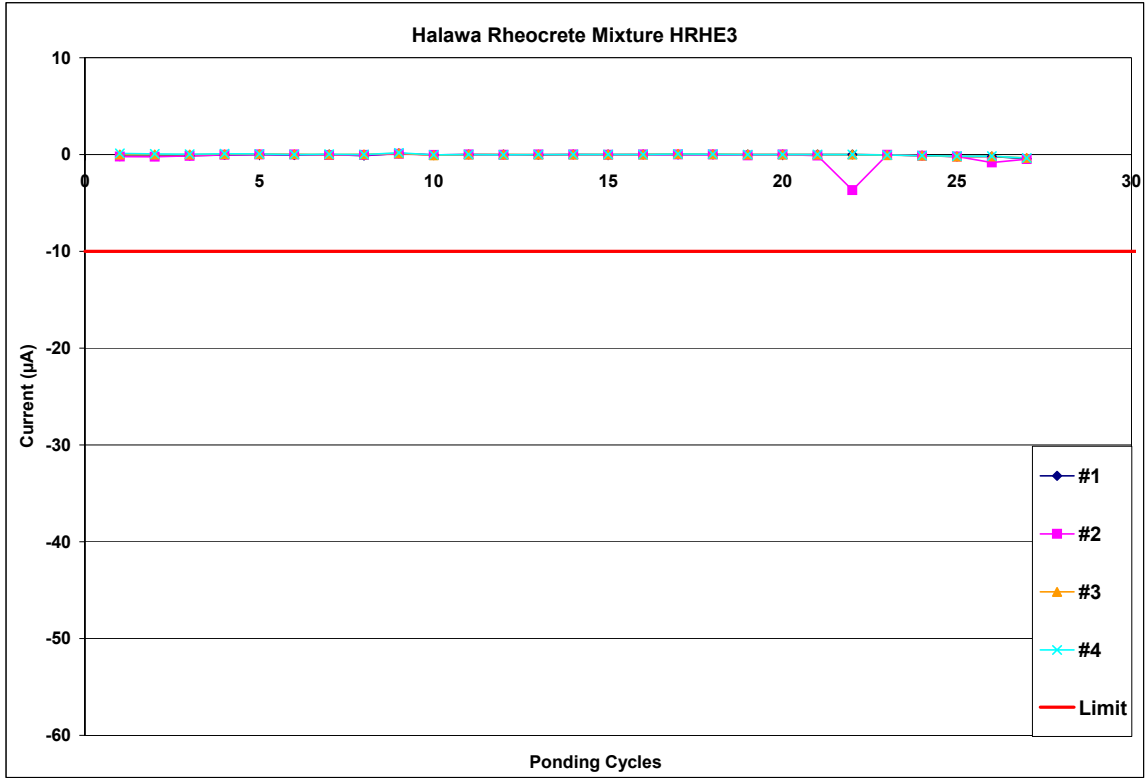


Figure A.1-135: Current Measurements for Halawa Rheocrete Mixture HRHE3

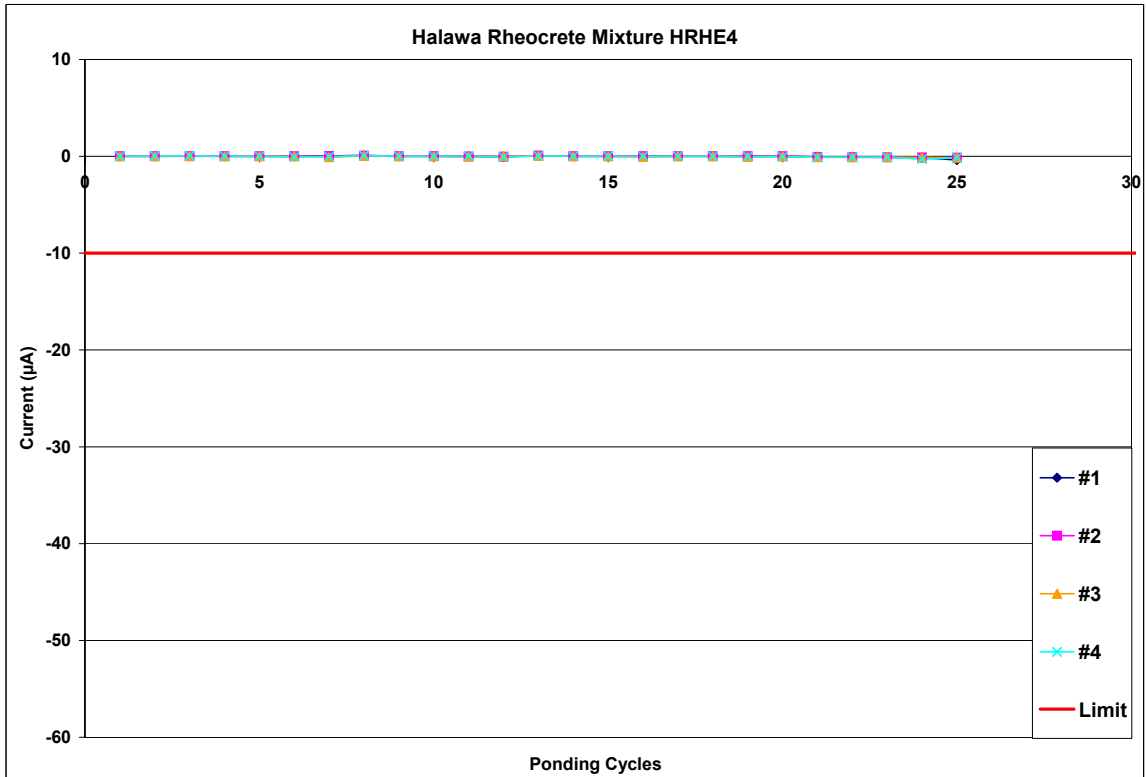


Figure A.1-136: Current Measurements for Halawa Rheocrete Mixture HRHE4

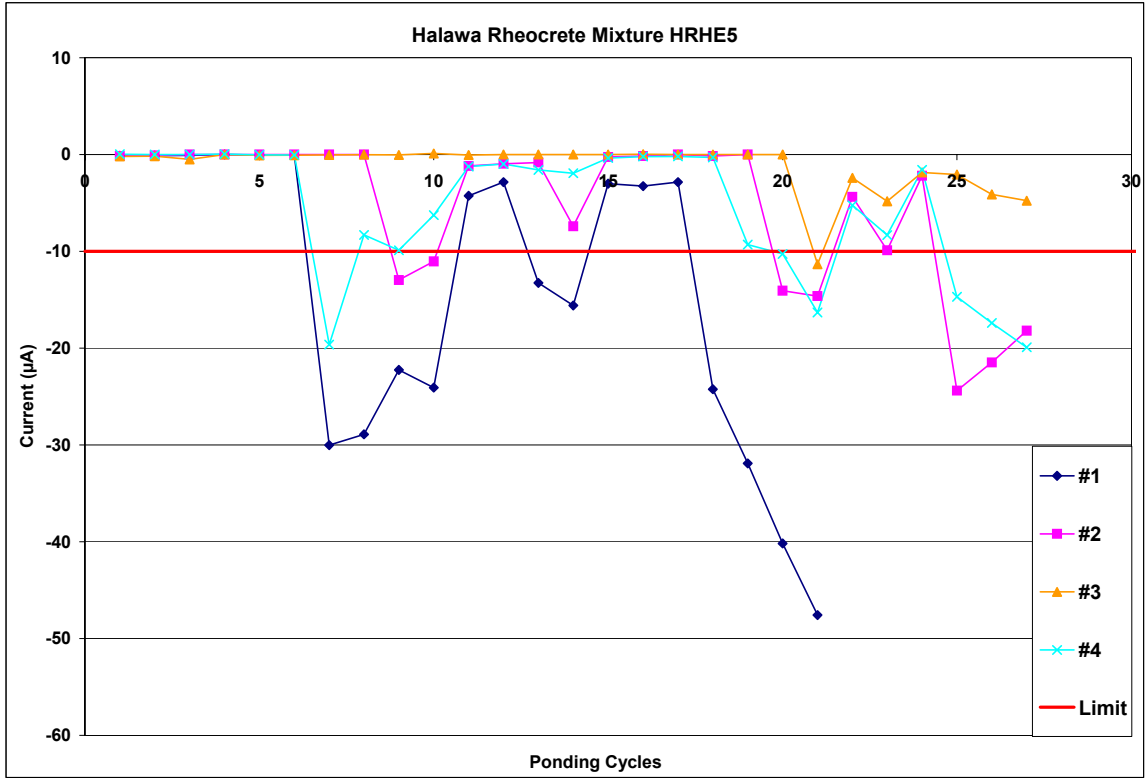


Figure A.1-137: Current Measurements for Halawa Rheocrete Mixture HRHE5

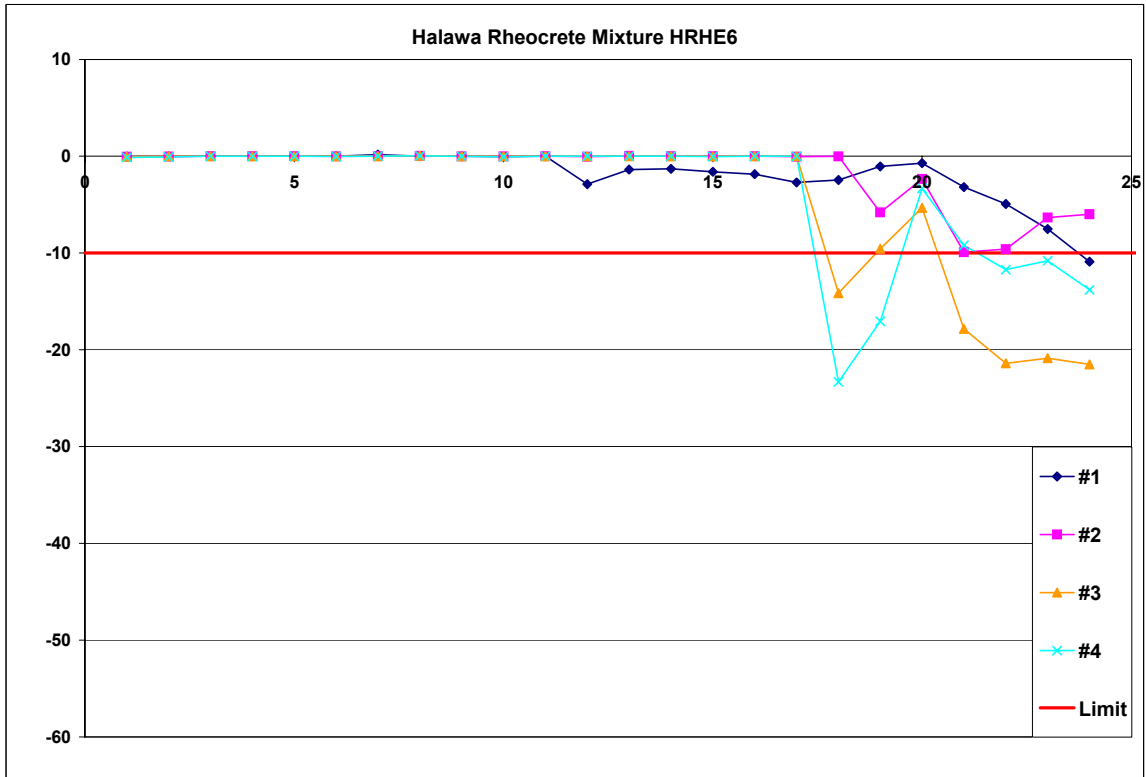


Figure A.1-138: Current Measurements for Halawa Rheocrete Mixture HRHE6

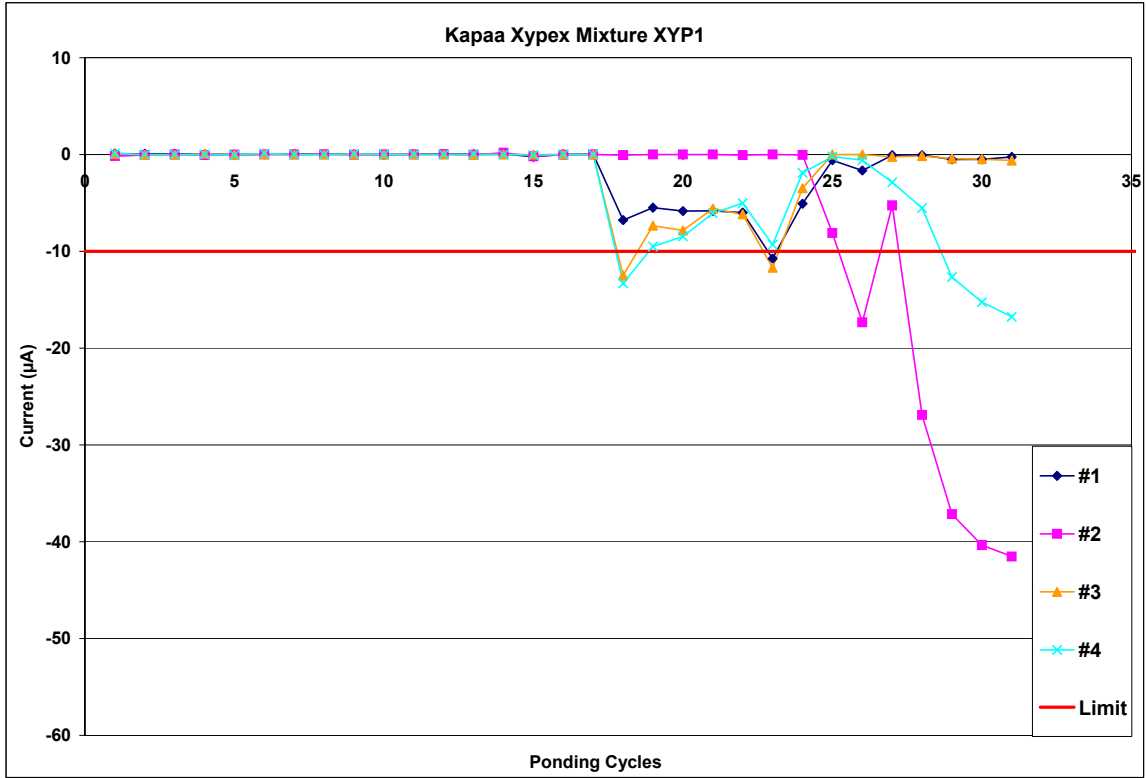


Figure A.1-139: Current Measurements for Kapaa Xypex Mixture XYP1

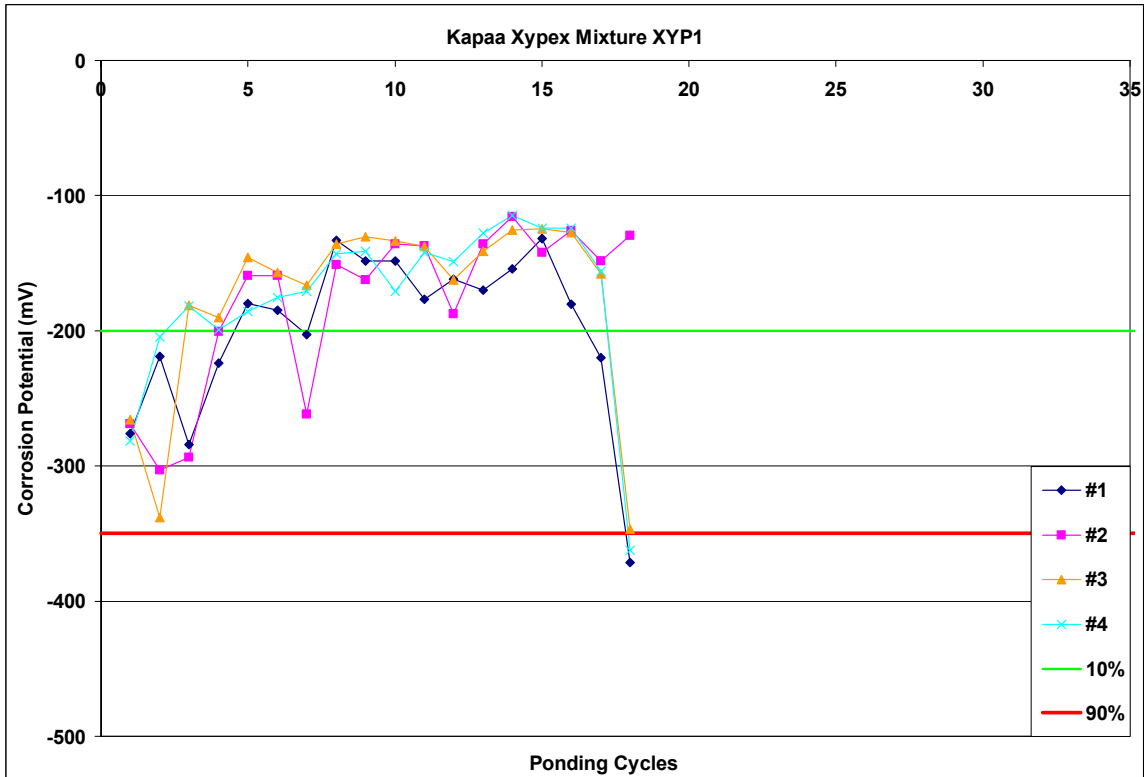


Figure A.1-140: Corrosion Potential Measurements for Kapaa Xypex Mixture XYP1

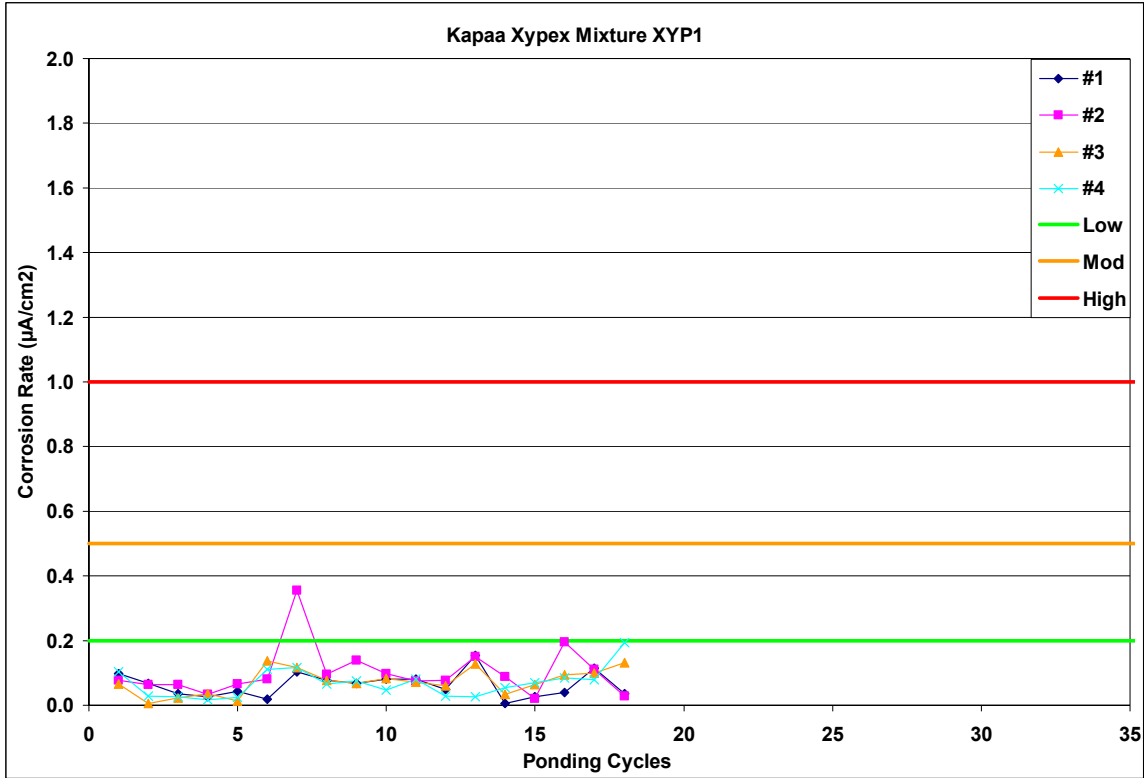


Figure A.1-141: Corrosion Rate Measurements for Kapaa Xypex Mixture XYP1

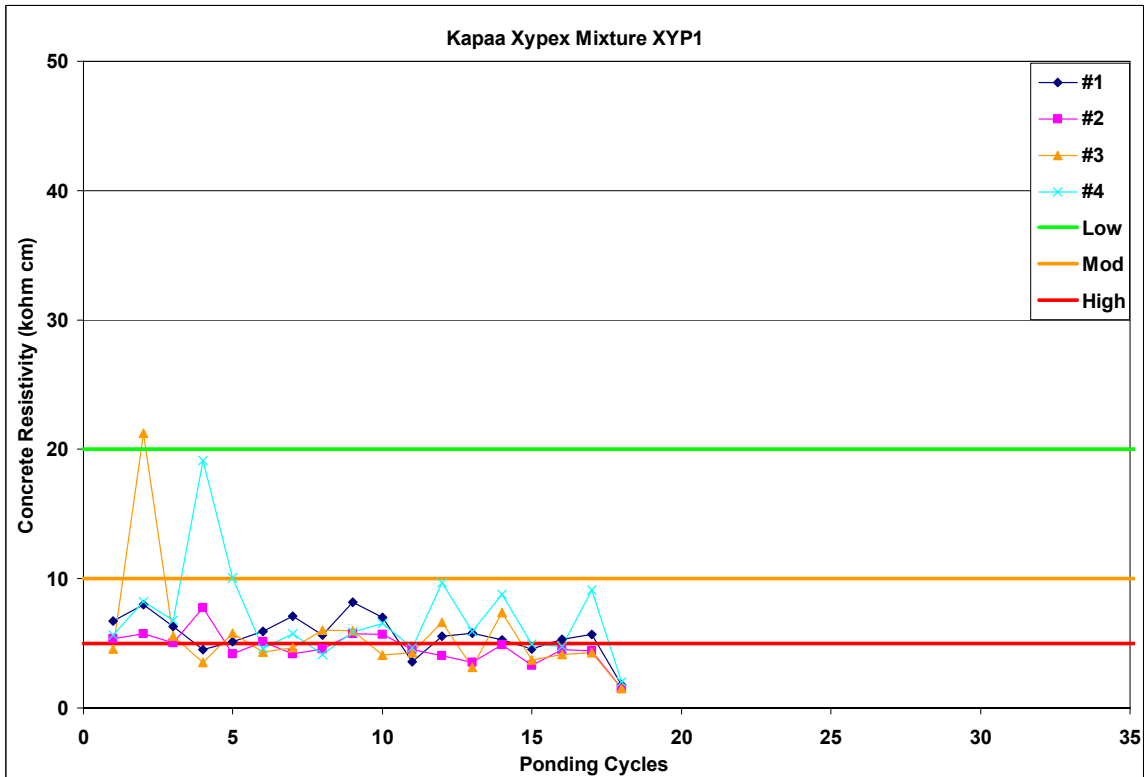


Figure A.1-142: Corrosion Resistivity Measurements for Kapaa Xypex Mixture XYP1

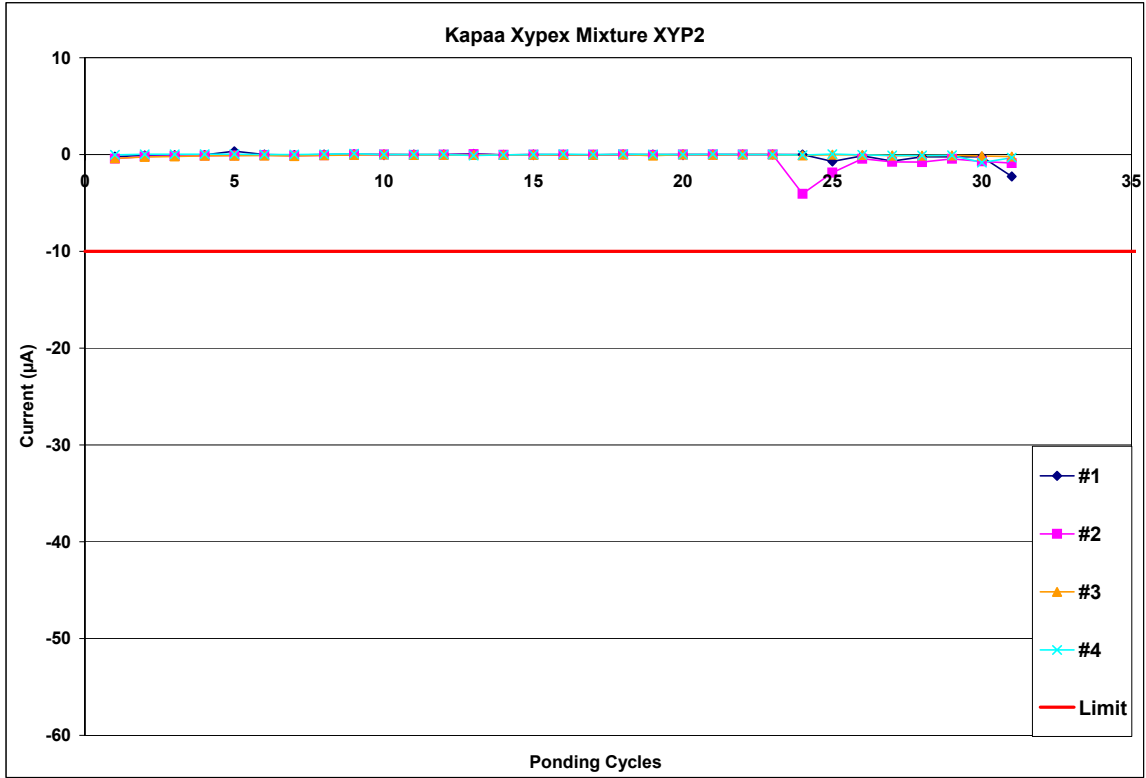


Figure A.1-143: Current Measurements for Kapaa Xypex Mixture XYP2

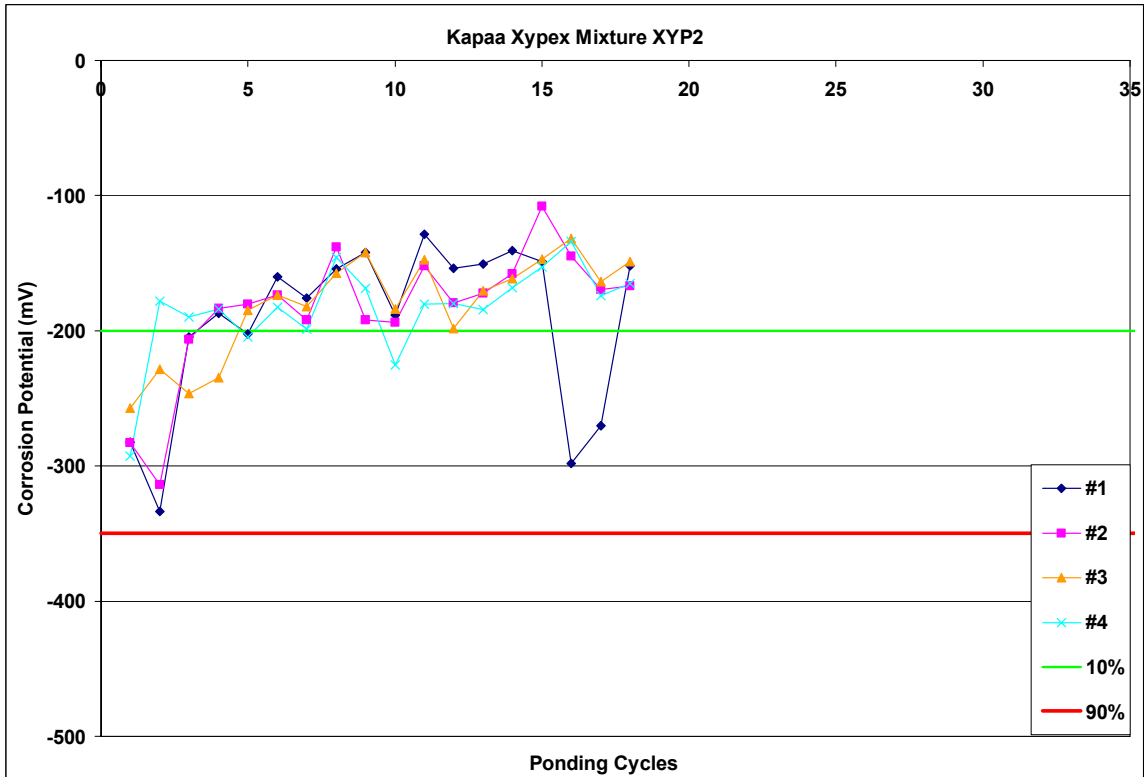


Figure A.1-144: Corrosion Potential Measurements for Kapaa Xypex Mixture XYP2

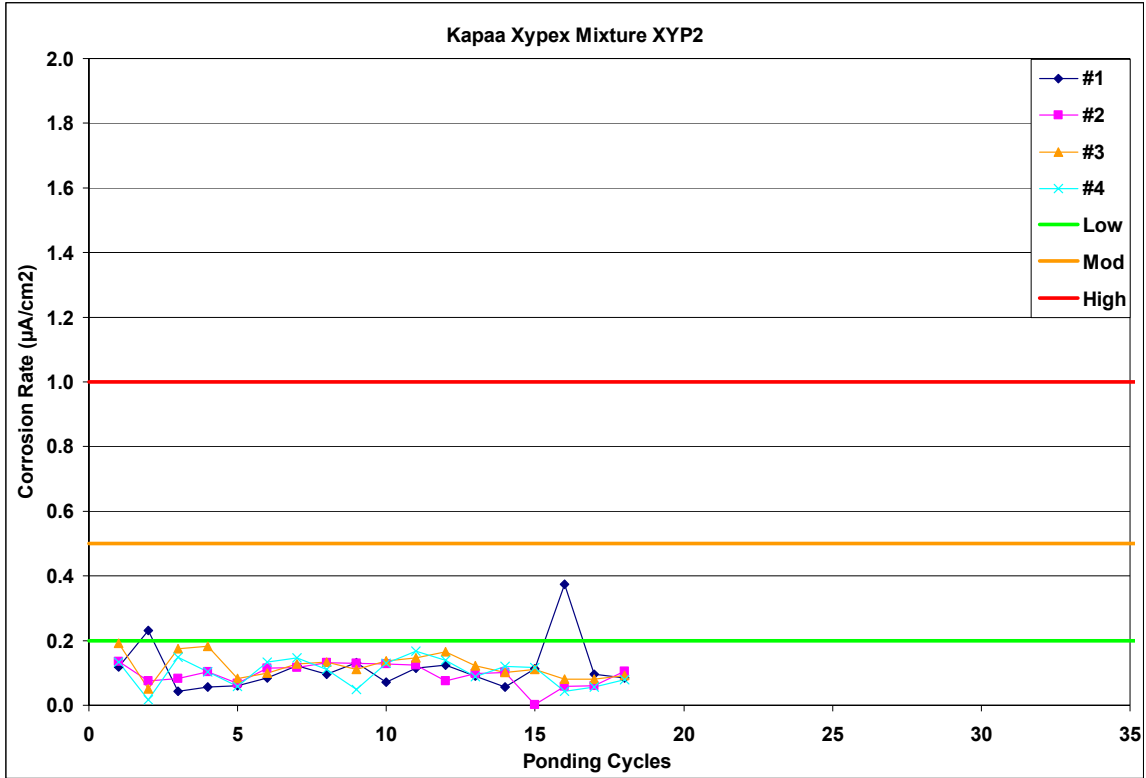


Figure A.1-145: Corrosion Rate Measurements for Kapaa Xypex Mixture XYP2

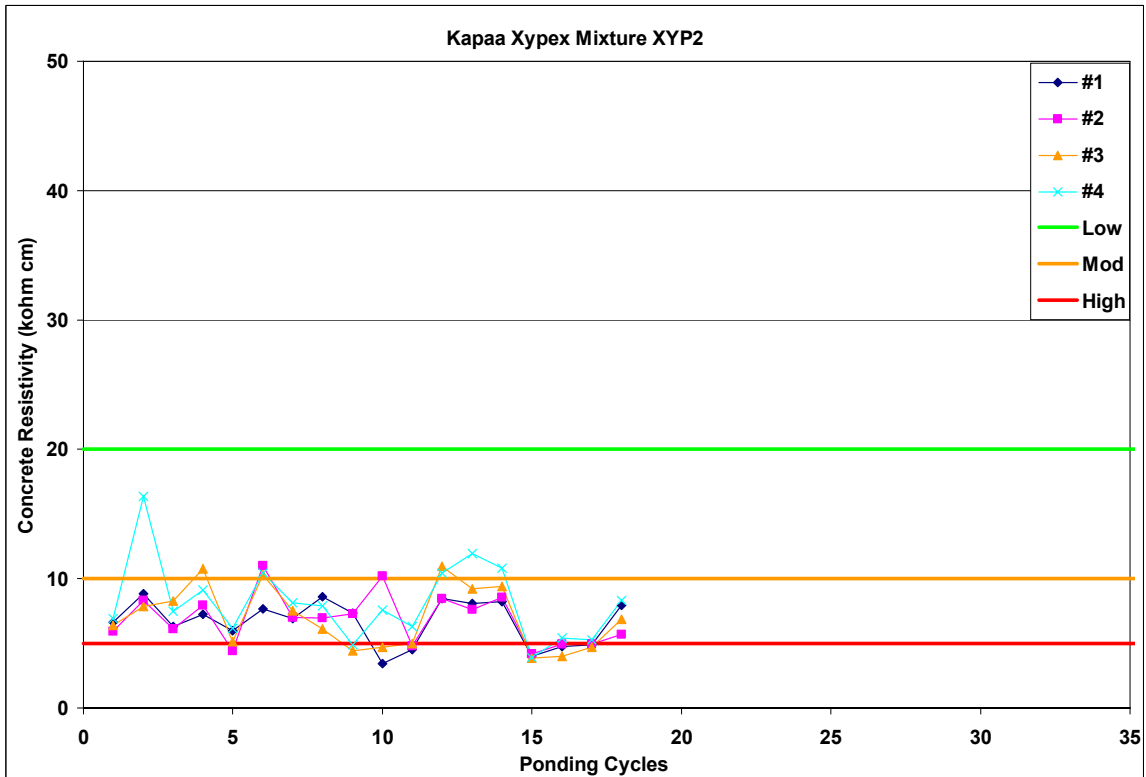


Figure A.1-146: Corrosion Resistivity Measurements for Kapaa Xypex Mixture XYP2

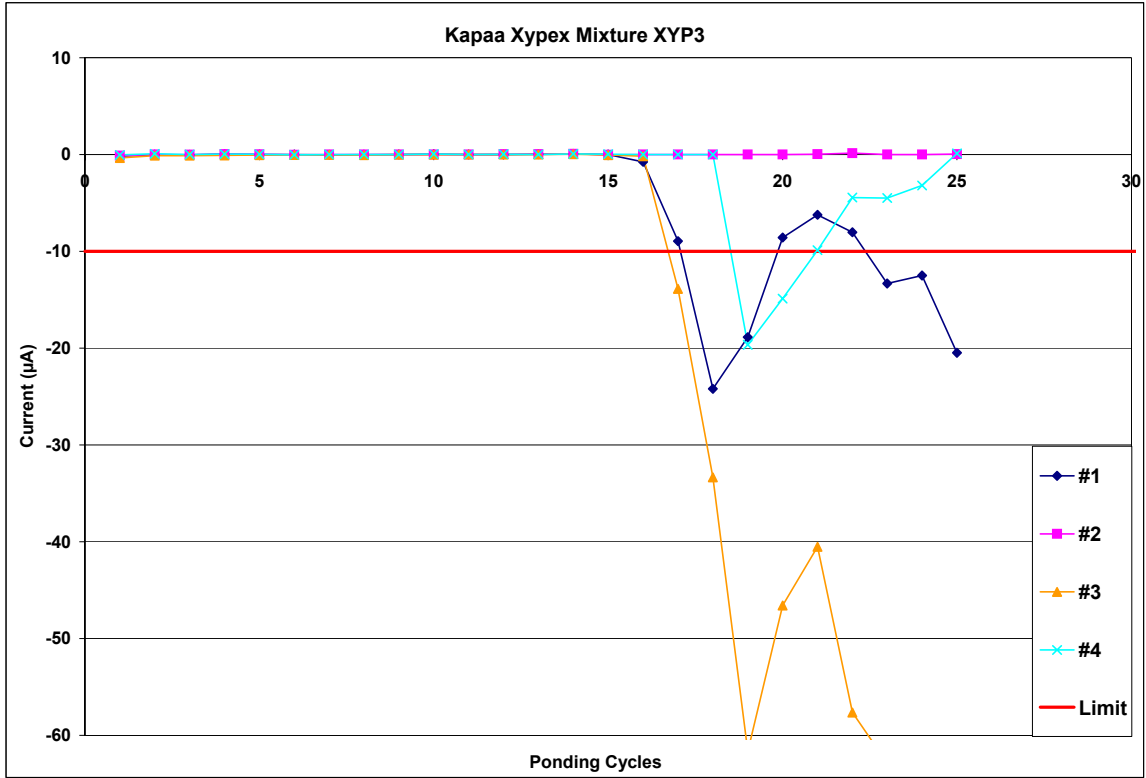


Figure A.1-147: Current Measurements for Kapaa Xypex Mixture XYP3

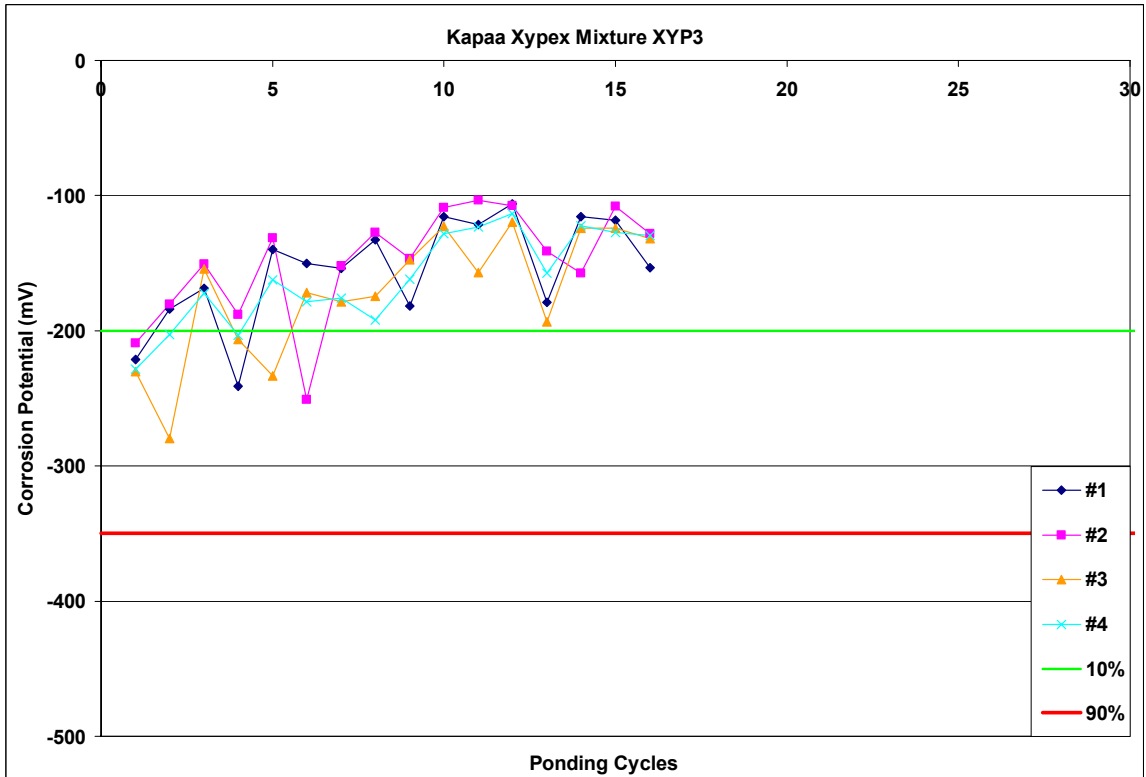


Figure A.1-148: Corrosion Potential Measurements for Kapaa Xypex Mixture XYP3

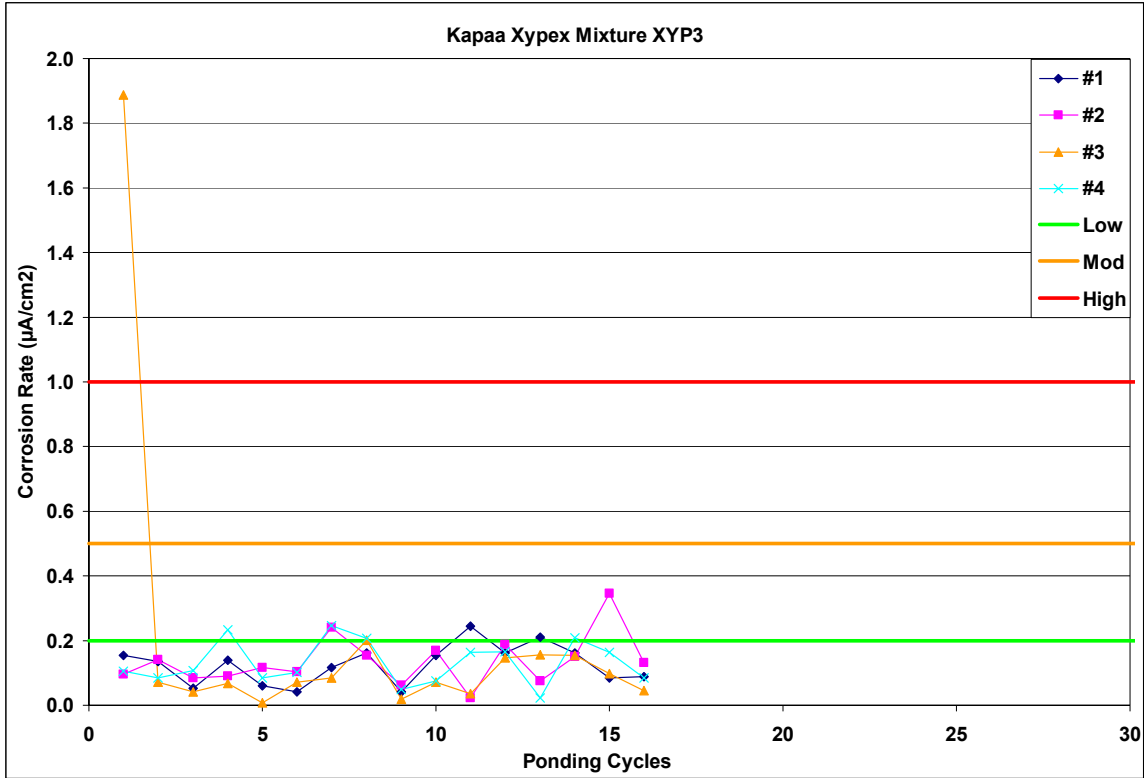


Figure A.1-149: Corrosion Rate Measurements for Kapaa Xypex Mixture YYP3

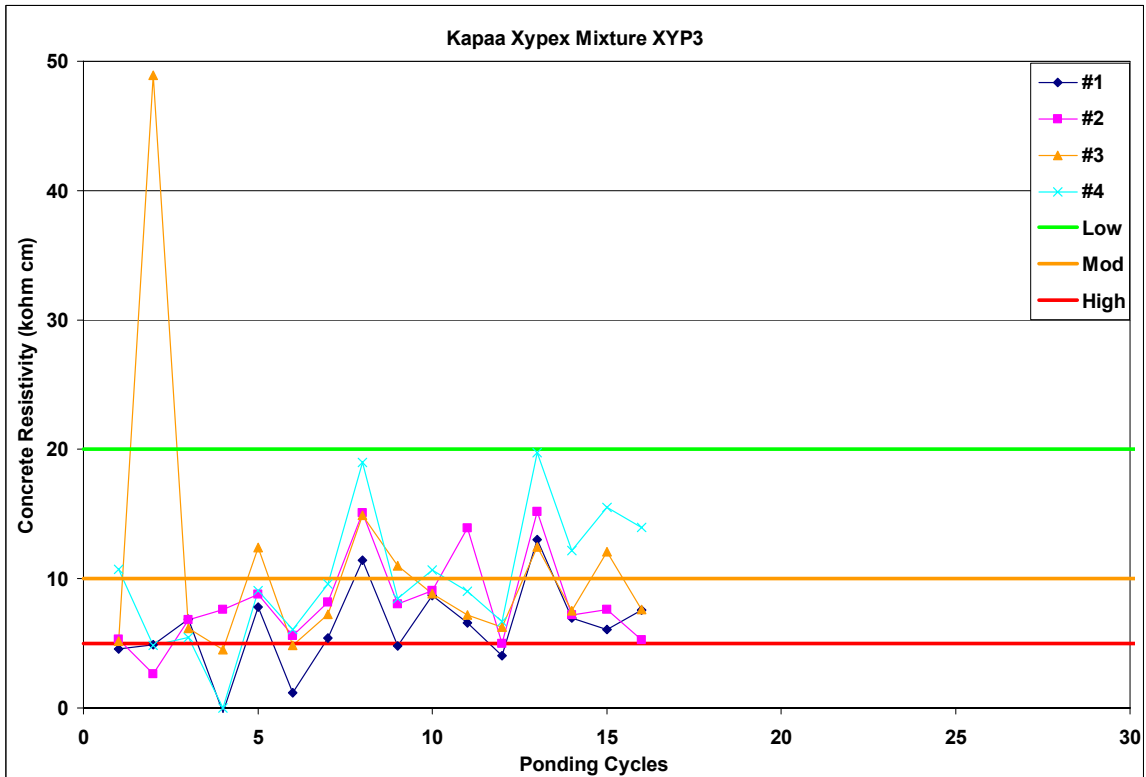


Figure A.1-150: Corrosion Resistivity Measurements for Kapaa Xypex Mixture YYP3

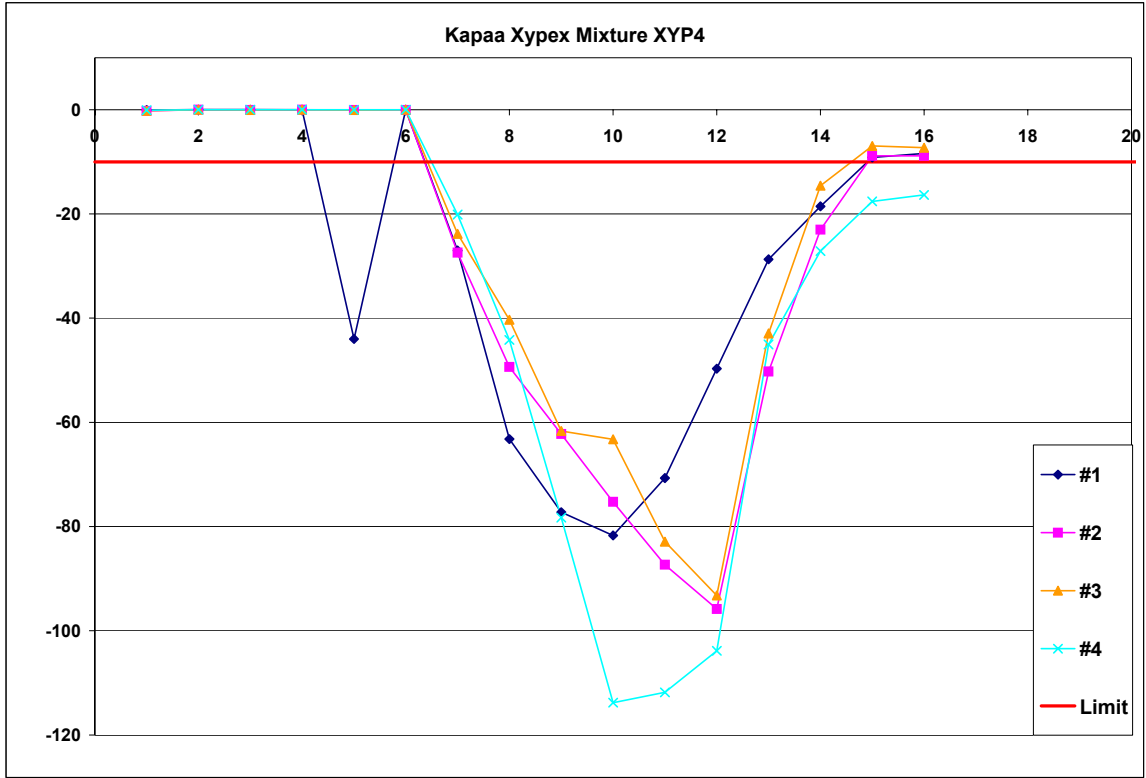


Figure A.1-151: Current Measurements for Kapaa Xypex Mixture XYP4

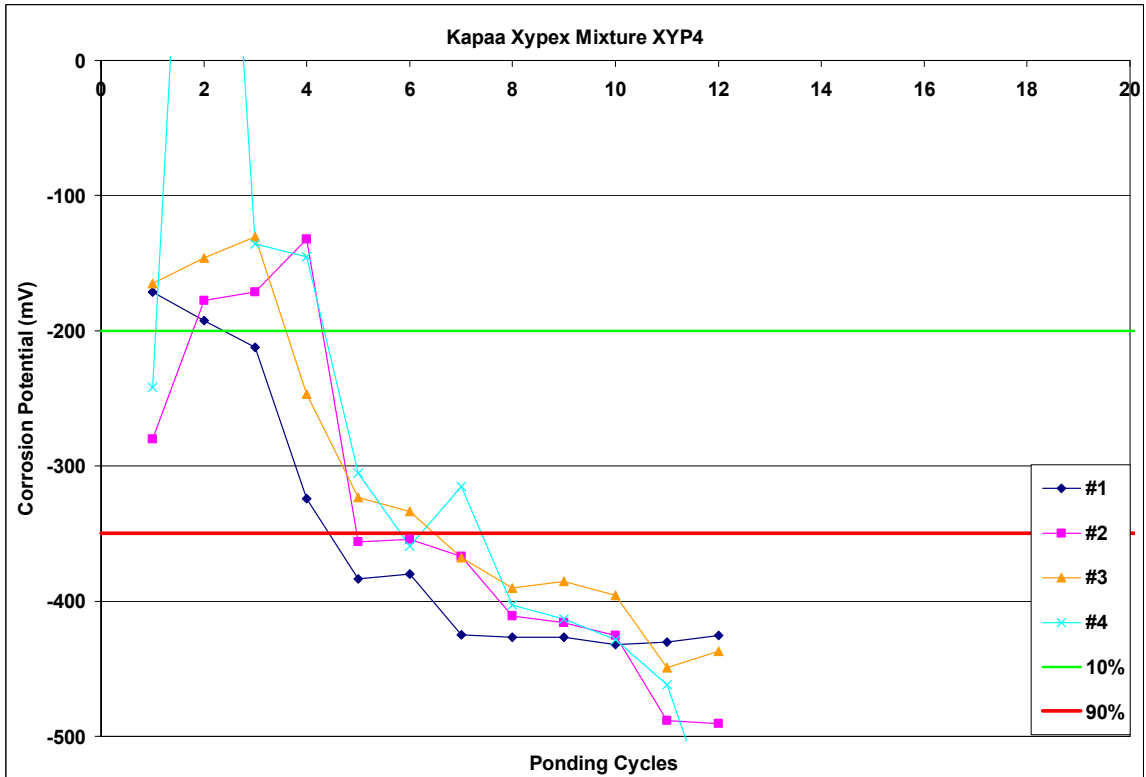


Figure A.1-152: Corrosion Potential Measurements for Kapaa Xypex Mixture XYP4

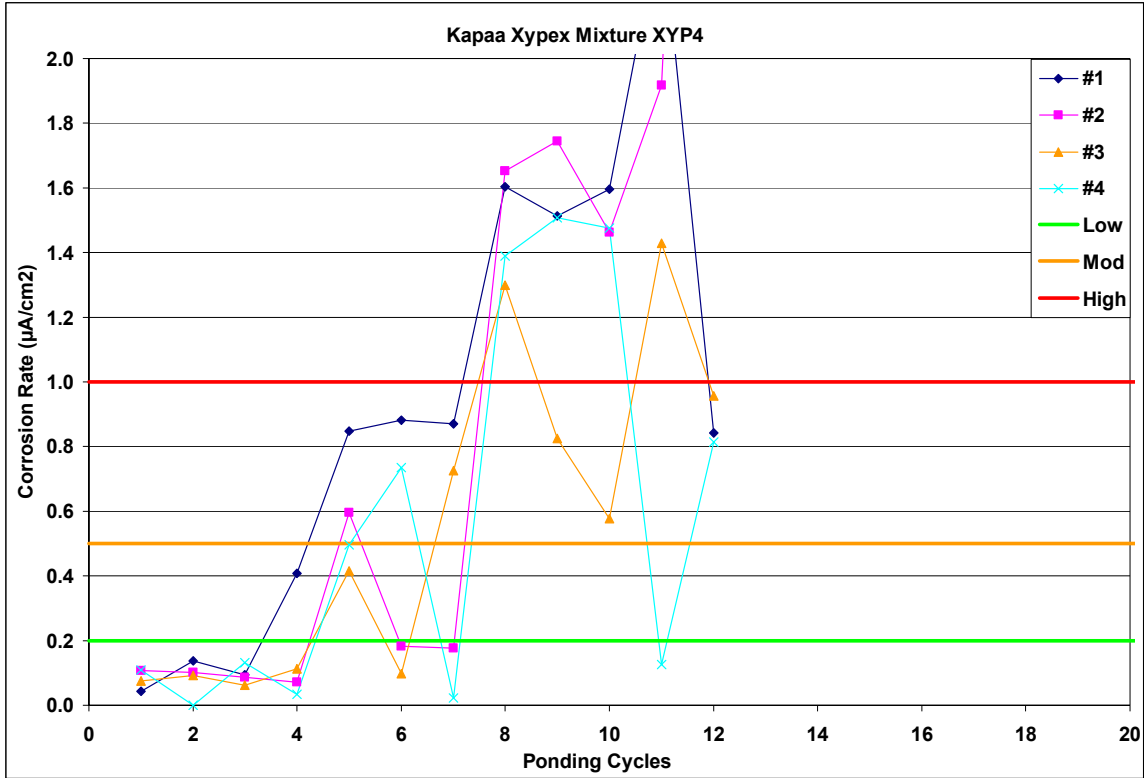


Figure A.1-153: Corrosion Rate Measurements for Kapaa Xypex Mixture XYP4

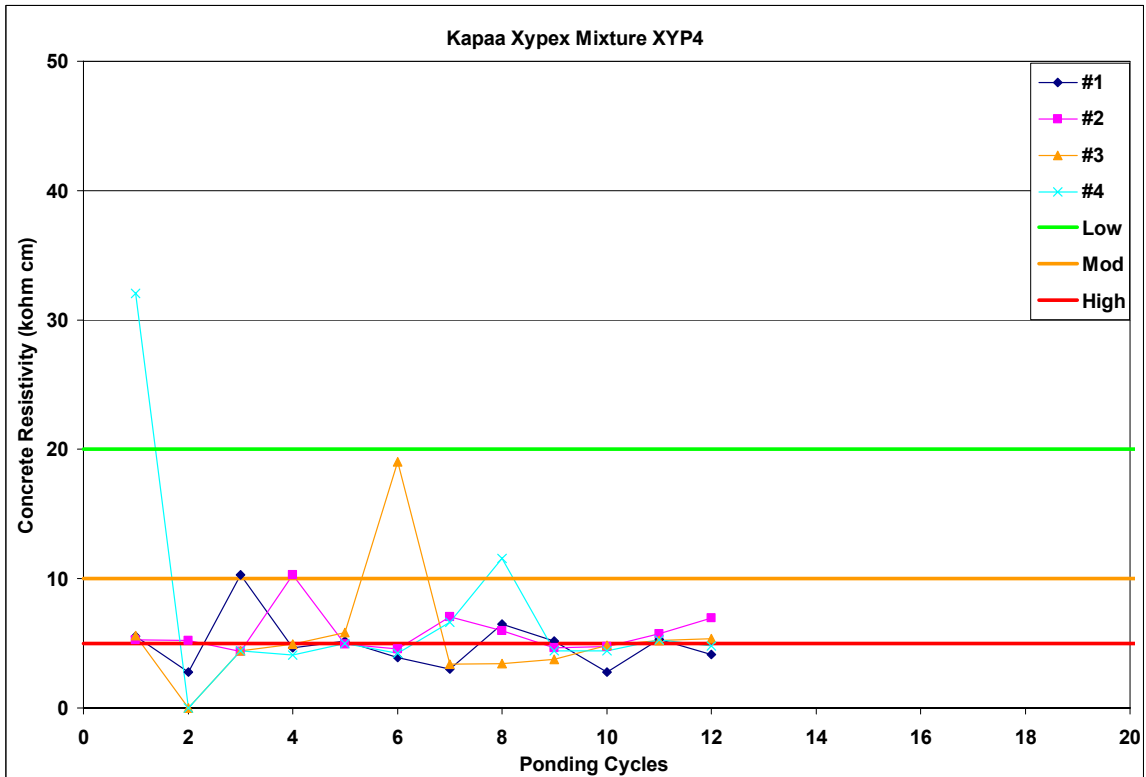


Figure A.1-154: Corrosion Resistivity Measurements for Kapaa Xypex Mixture XYP4

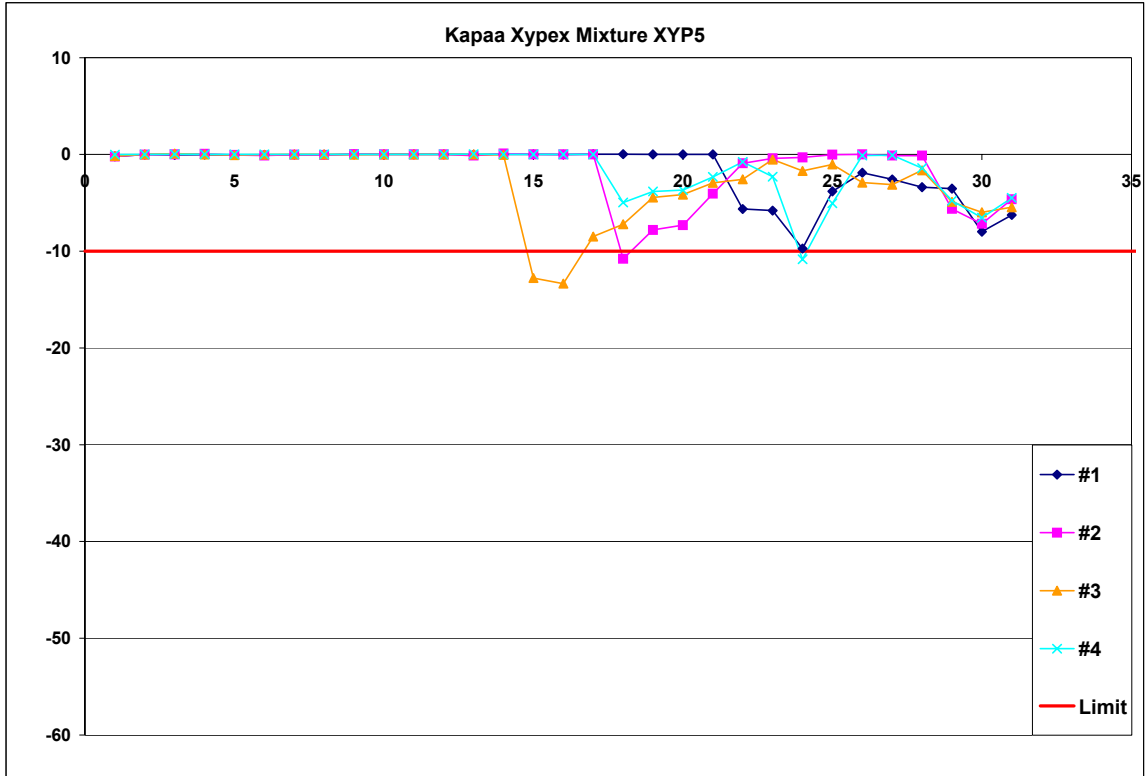


Figure A.1-155: Current Measurements for Kapaa Xypex Mixture XYP5

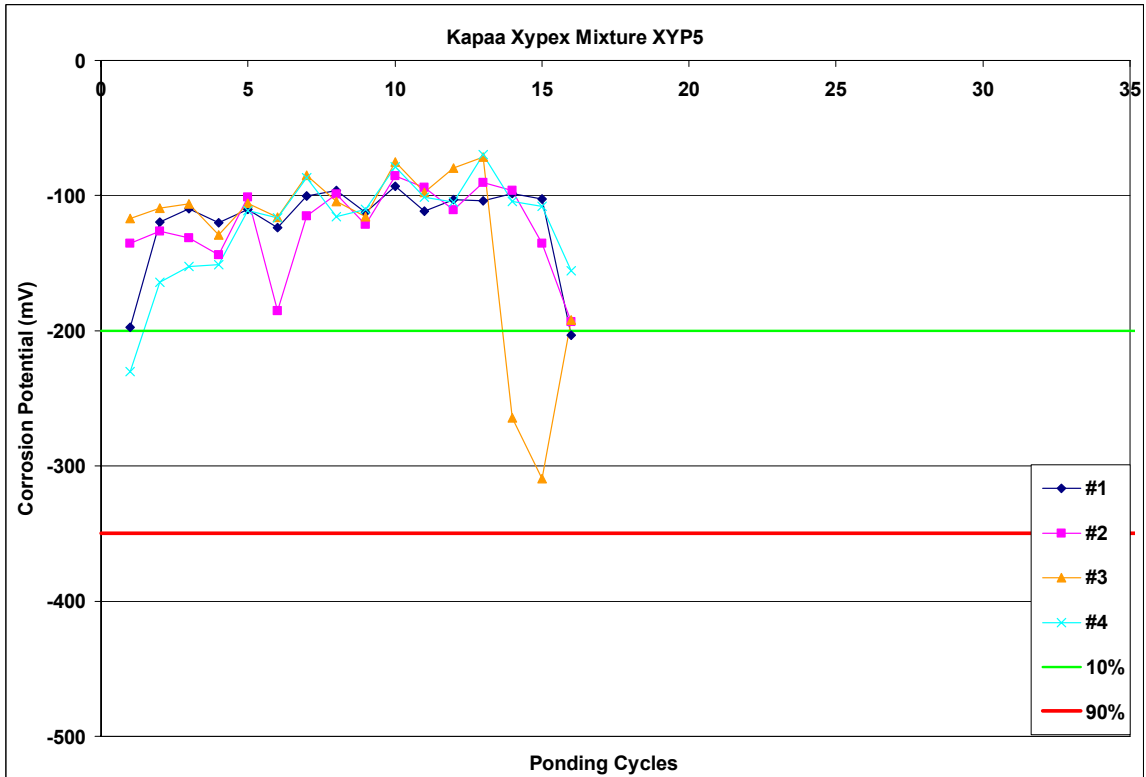


Figure A.1-156: Corrosion Potential Measurements for Kapaa Xypex Mixture XYP5

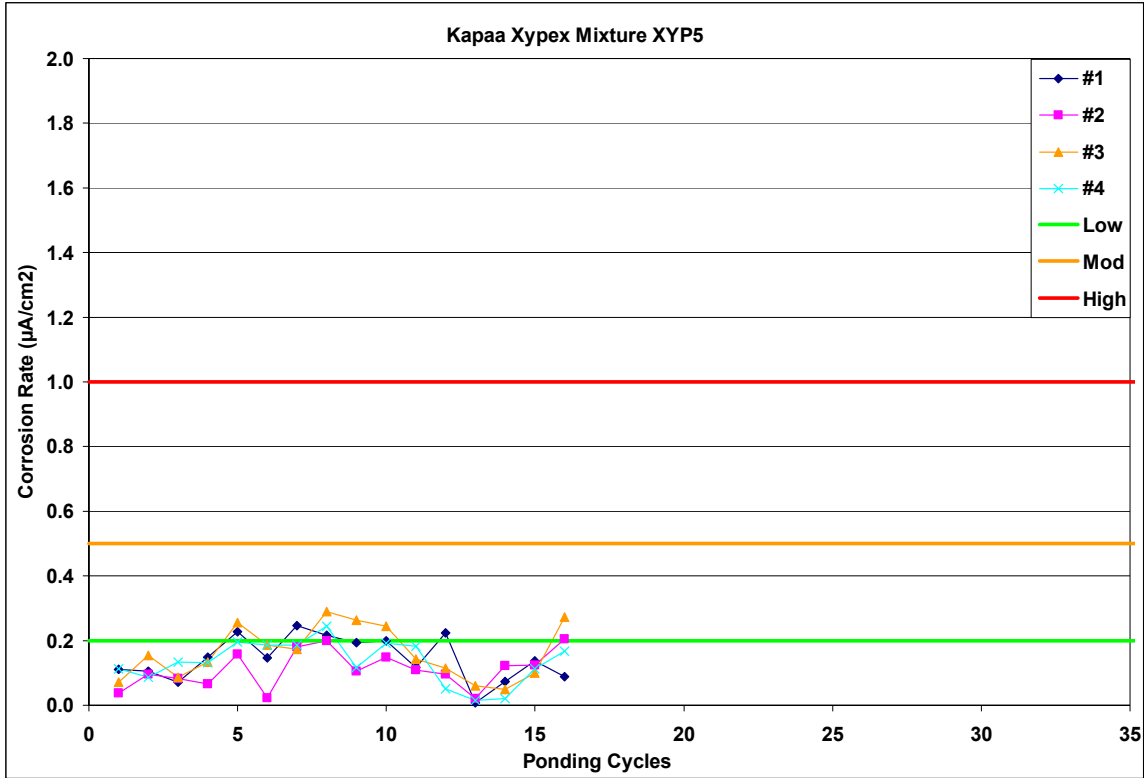


Figure A.1-157: Corrosion Rate Measurements for Kapaa Xypex Mixture XYP5

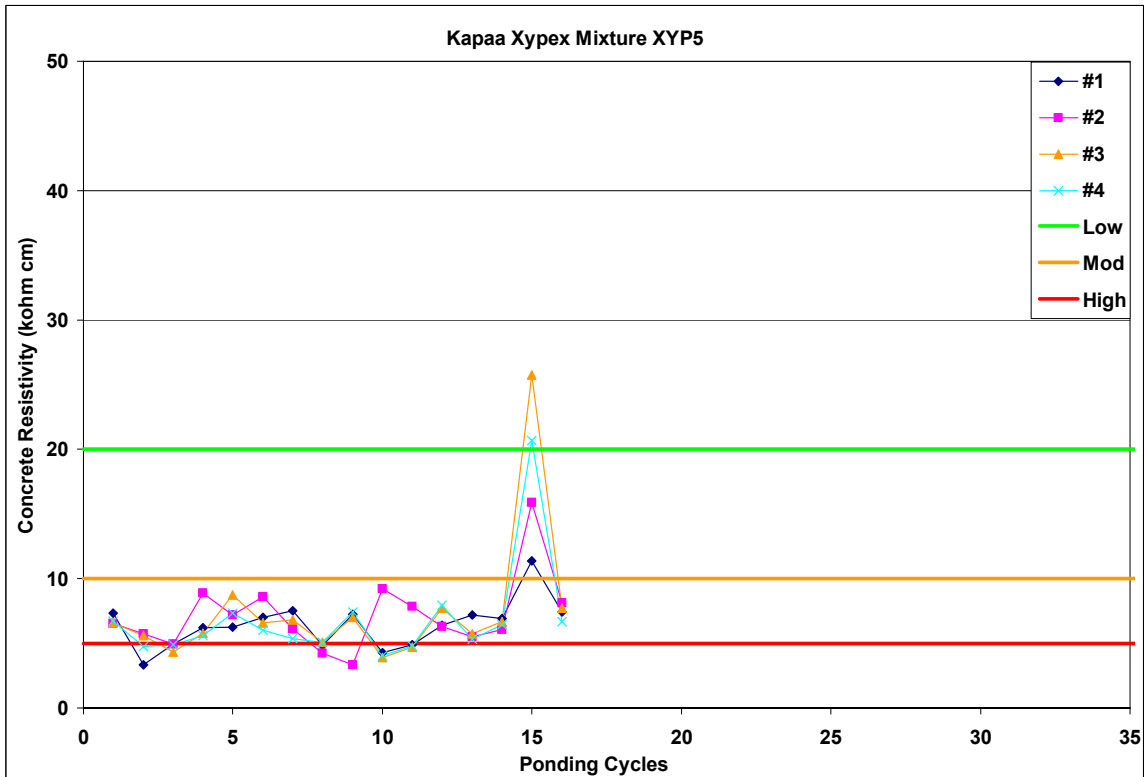


Figure A.1-158: Corrosion Resistivity Measurements for Kapaa Xypex Mixture XYP5

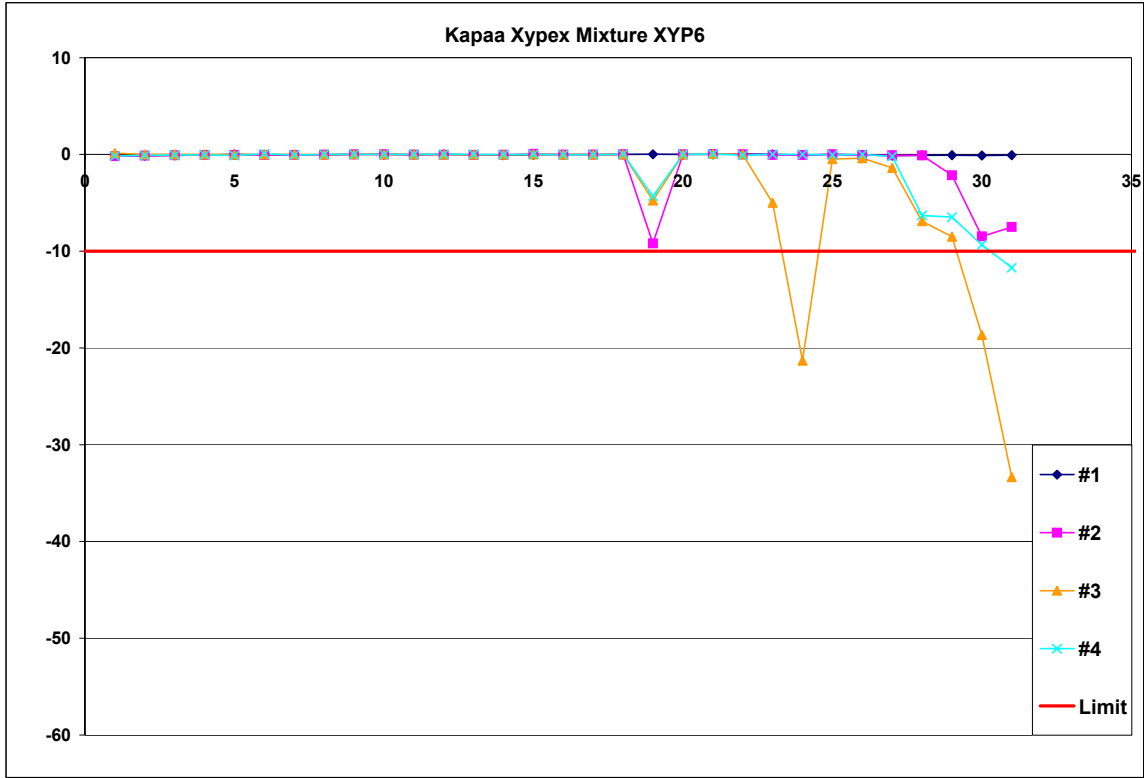


Figure A.1-159: Current Measurements for Kapaa Xypex Mixture XYP6

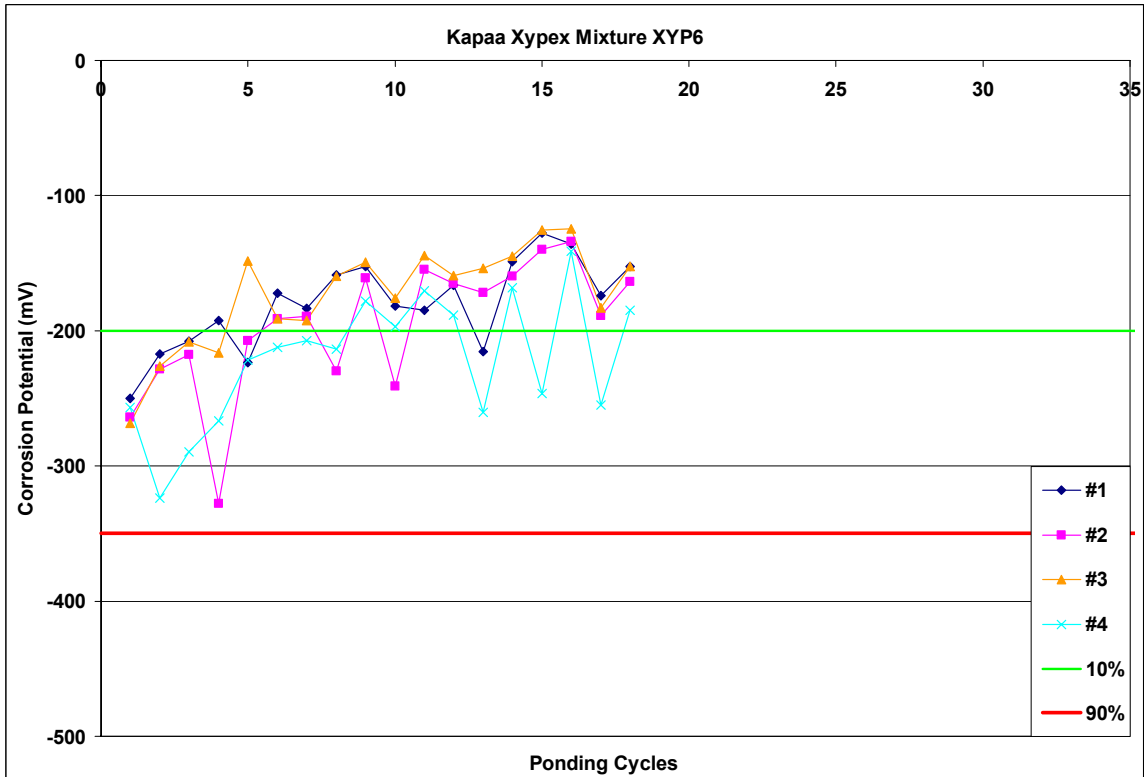


Figure A.1-160: Corrosion Potential Measurements for Kapaa Xypex Mixture XYP6

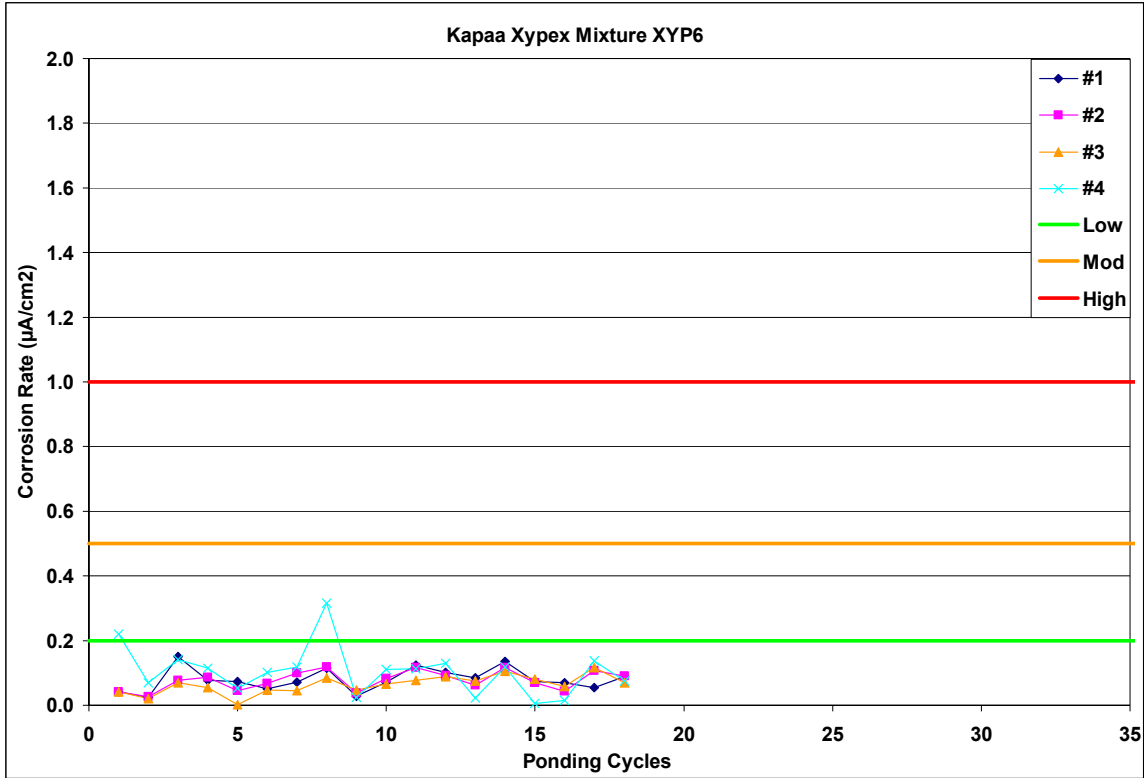


Figure A.1-161: Corrosion Rate Measurements for Kapaa Xypex Mixture XYP6

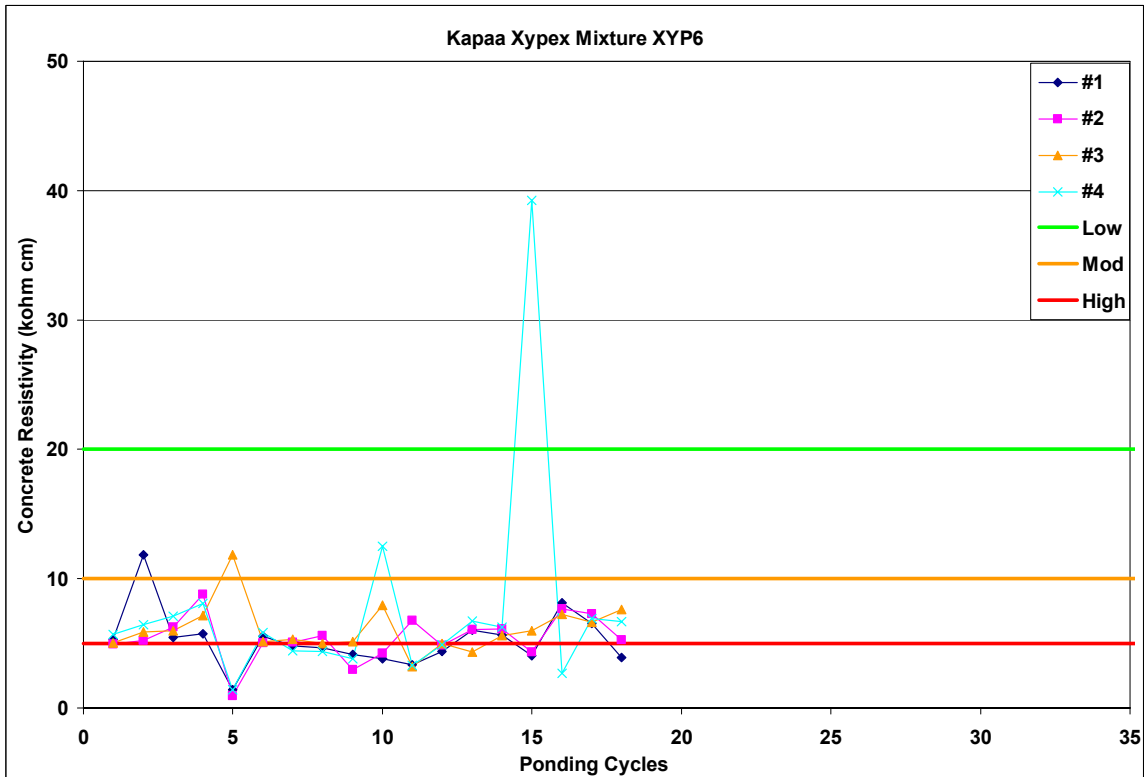


Figure A.1-162: Corrosion Resistivity Measurements for Kapaa Xypex Mixture XYP6

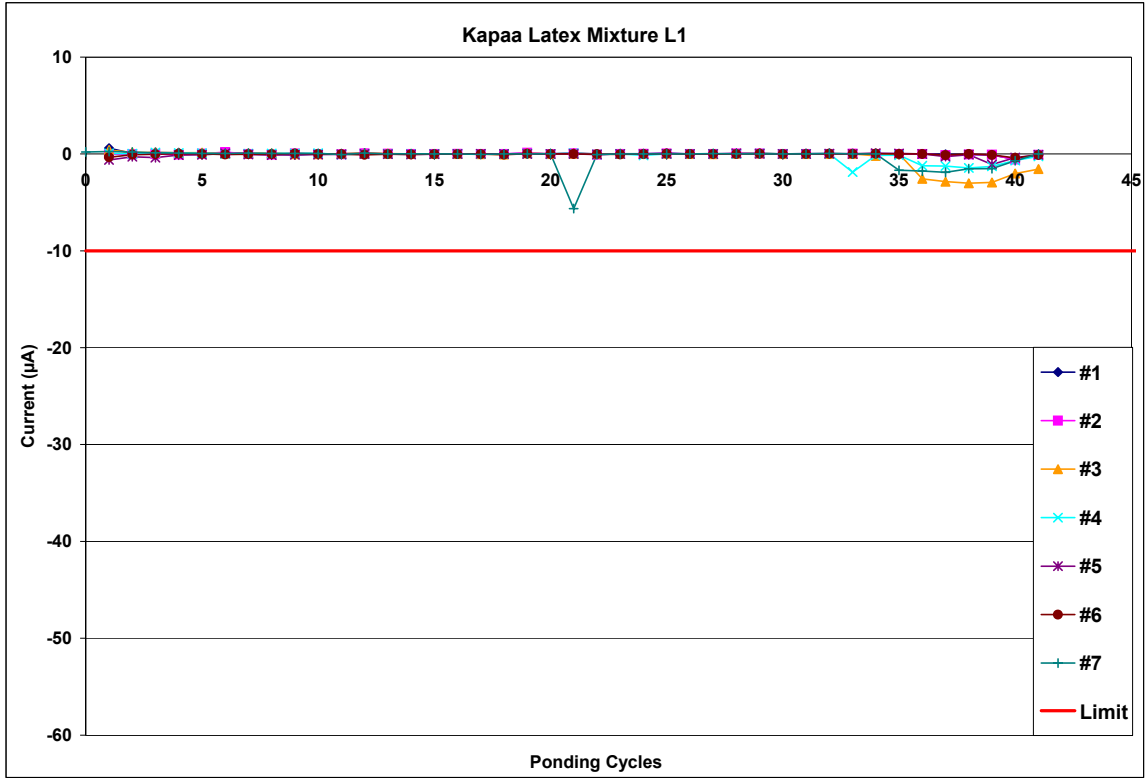


Figure A.1-163: Current Measurements for Kapaa Latex Mixture L1

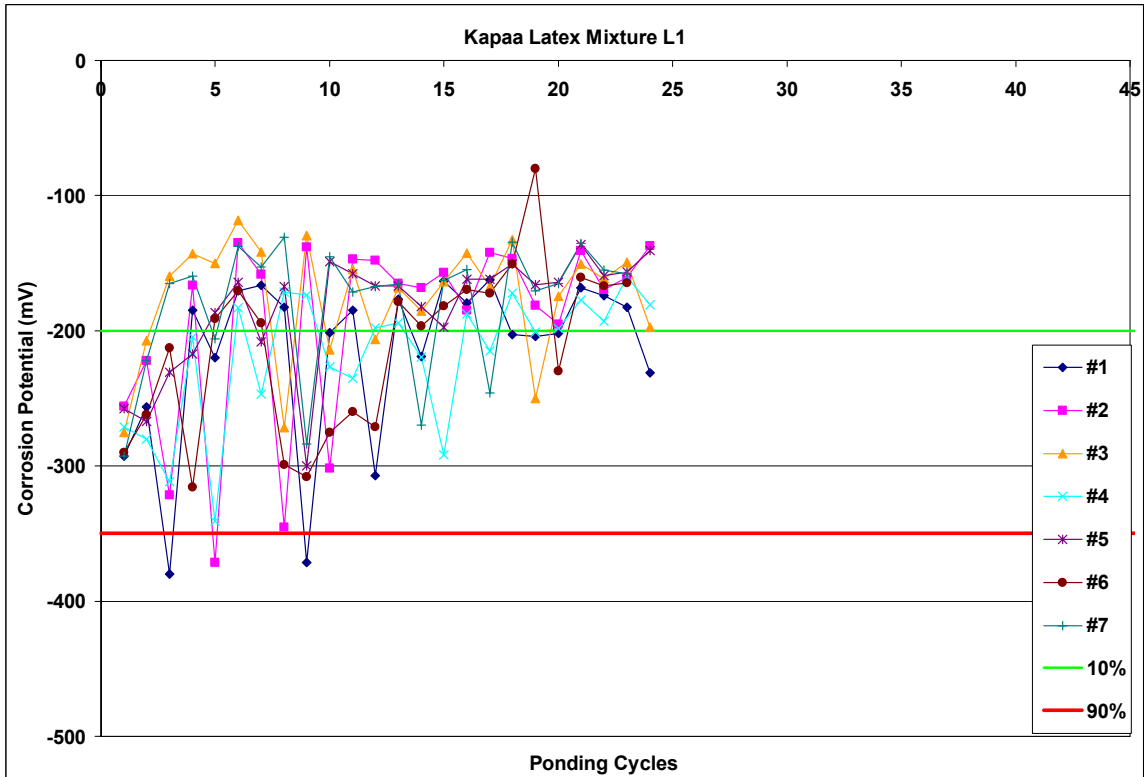


Figure A.1-164: Corrosion Potential Measurements for Kapaa latex Mixture L1

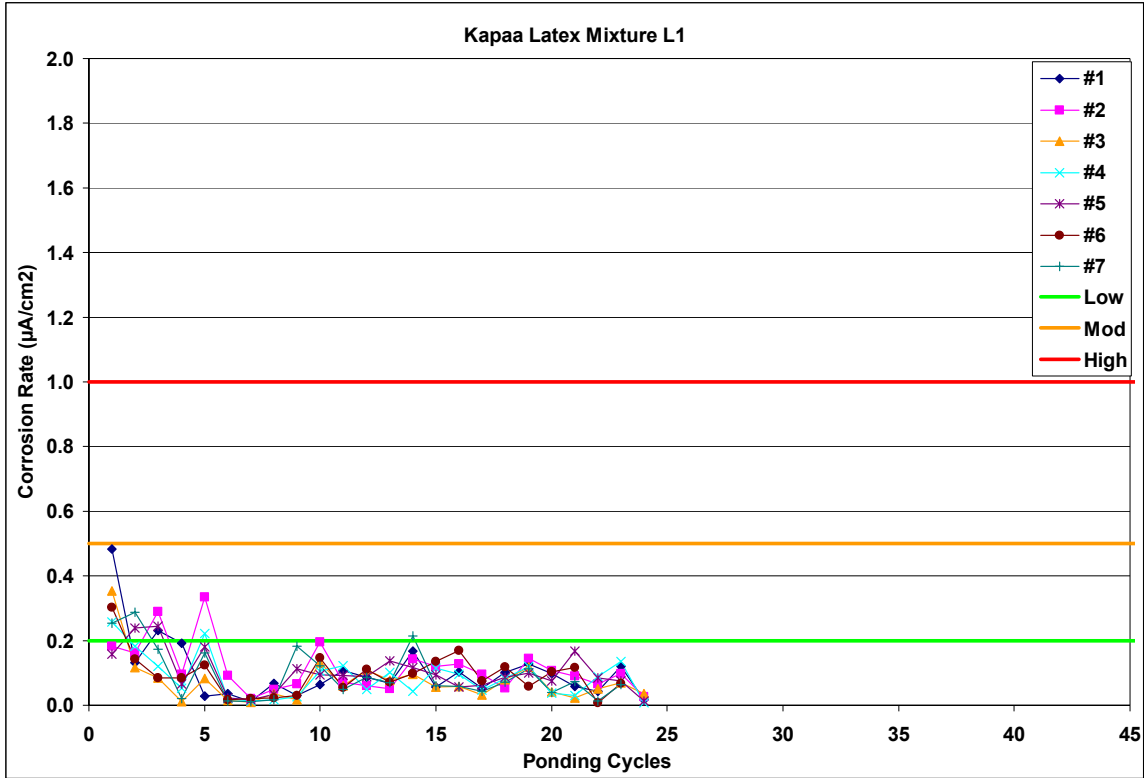


Figure A.1-165: Corrosion Rate Measurements for Kapaa latex Mixture L1

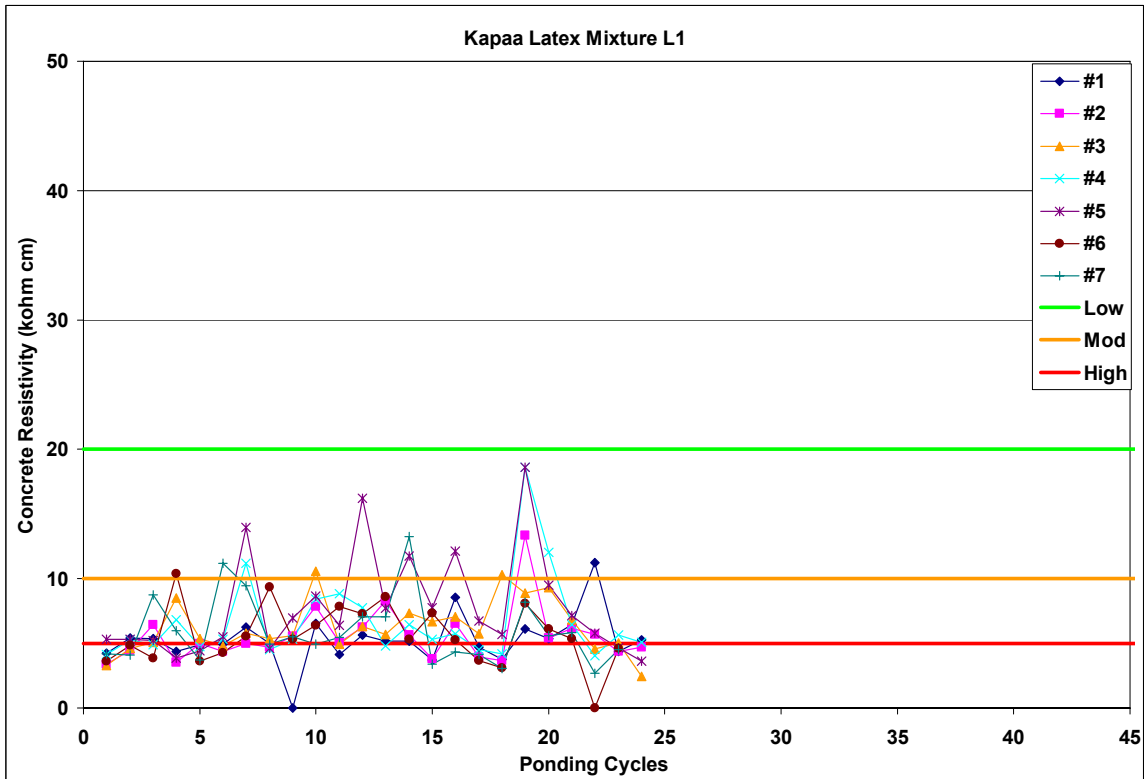


Figure A.1-166: Corrosion Resistivity Measurements for Kapaa latex Mixture L1

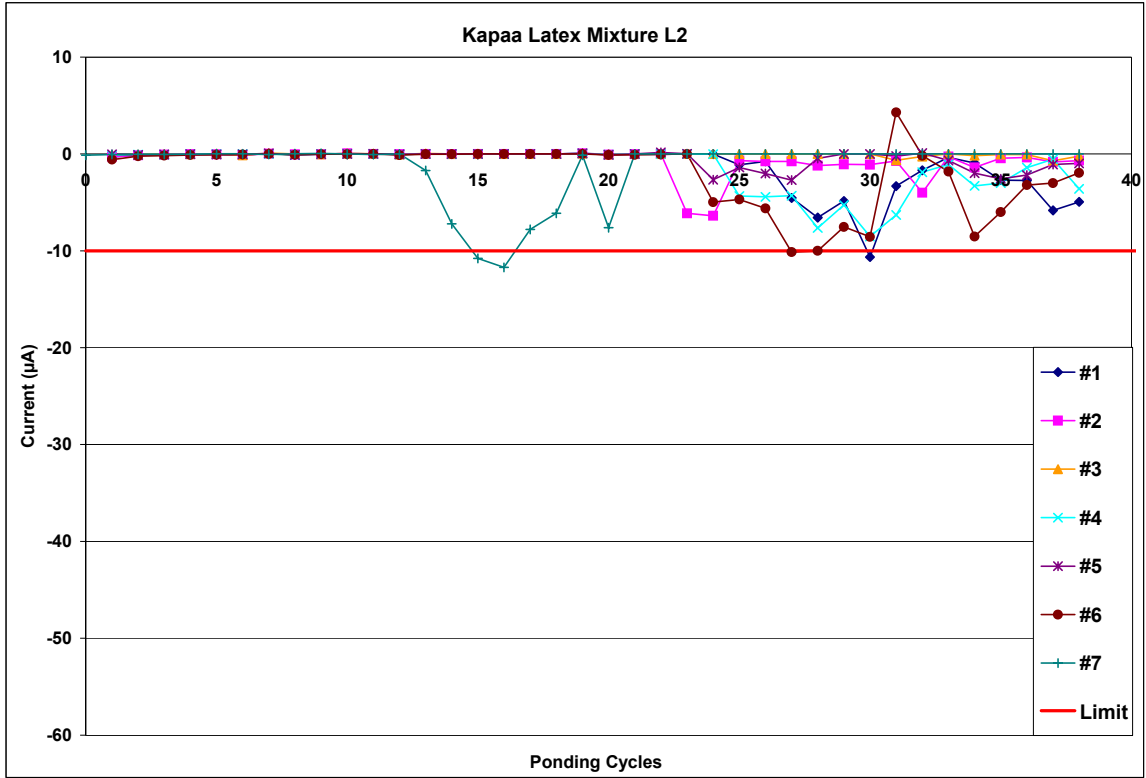


Figure A.1-167: Current Measurements for Kapaa Latex Mixture L2

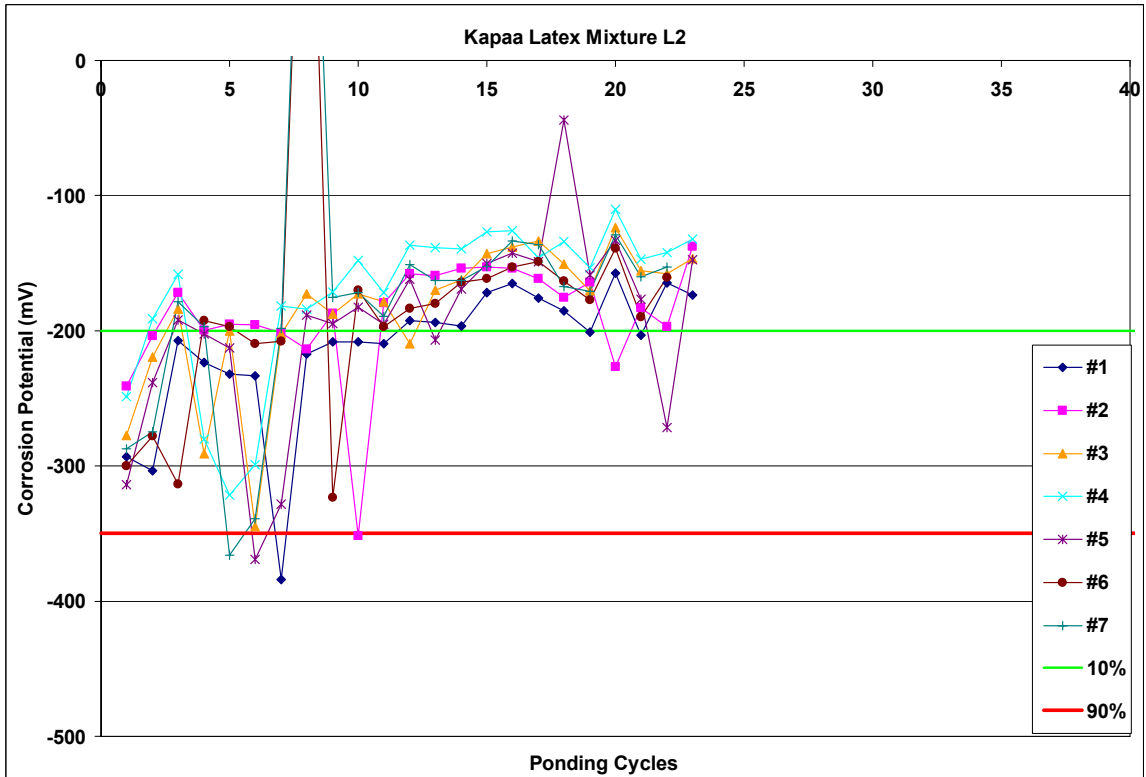


Figure A.1-168: Corrosion Potential Measurements for Kapaa latex Mixture L2

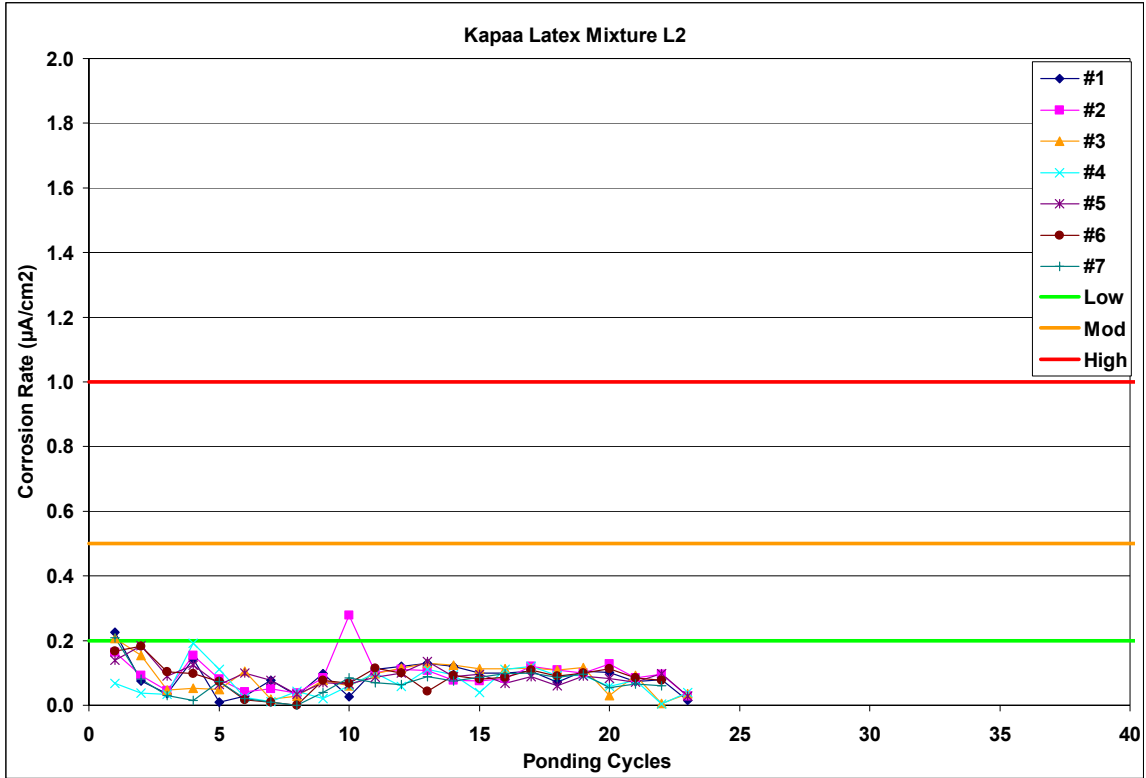


Figure A.1-169: Corrosion Rate Measurements for Kapaa latex Mixture L2

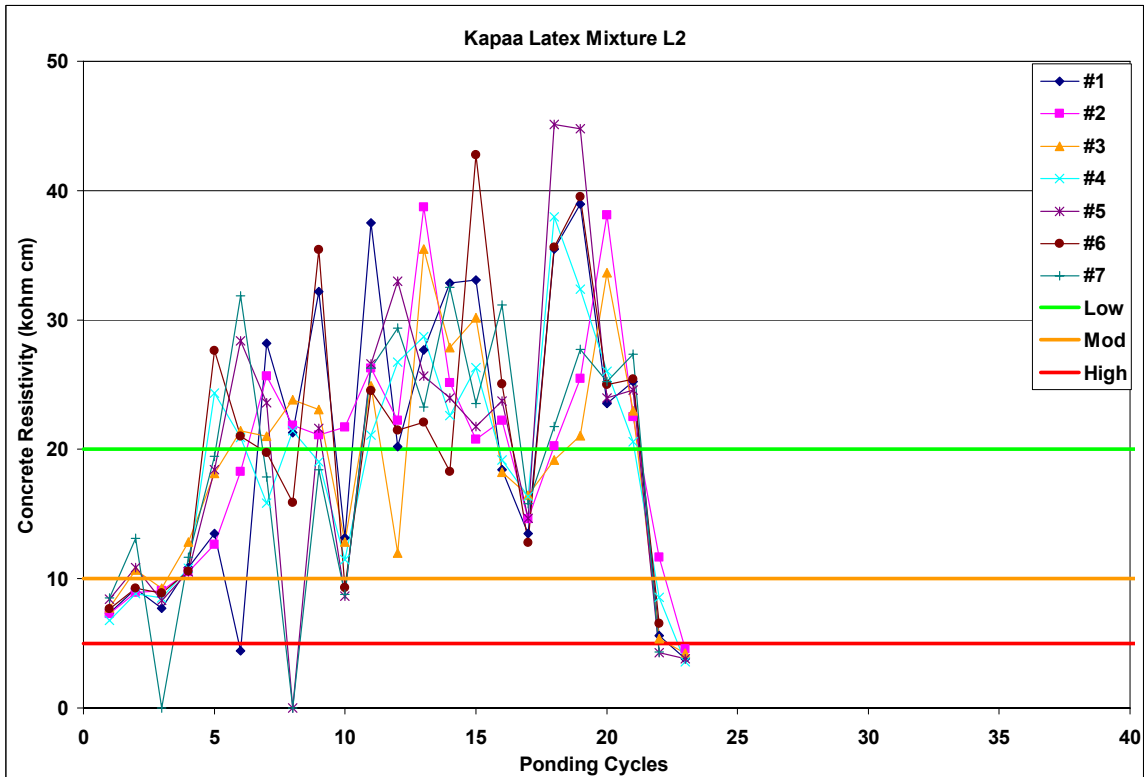


Figure A.1-170: Corrosion Resistivity Measurements for Kapaa latex Mixture L2

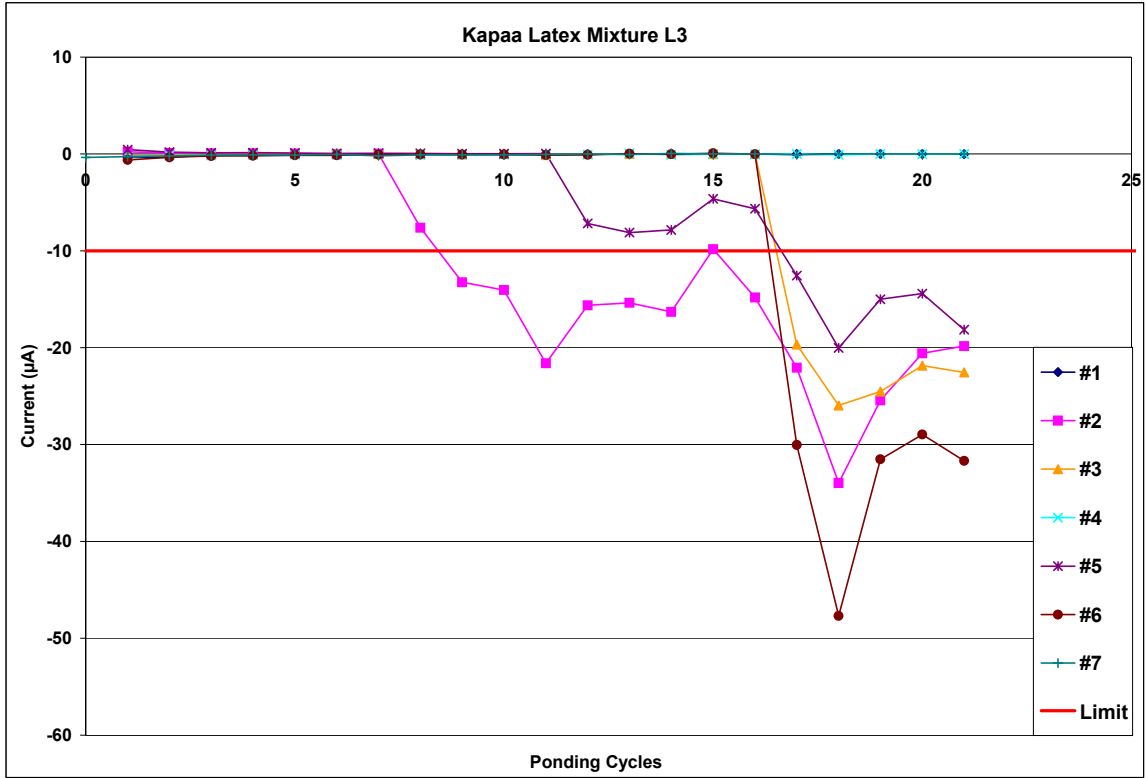


Figure A.1-171: Current Measurements for Kapaa Latex Mixture L3

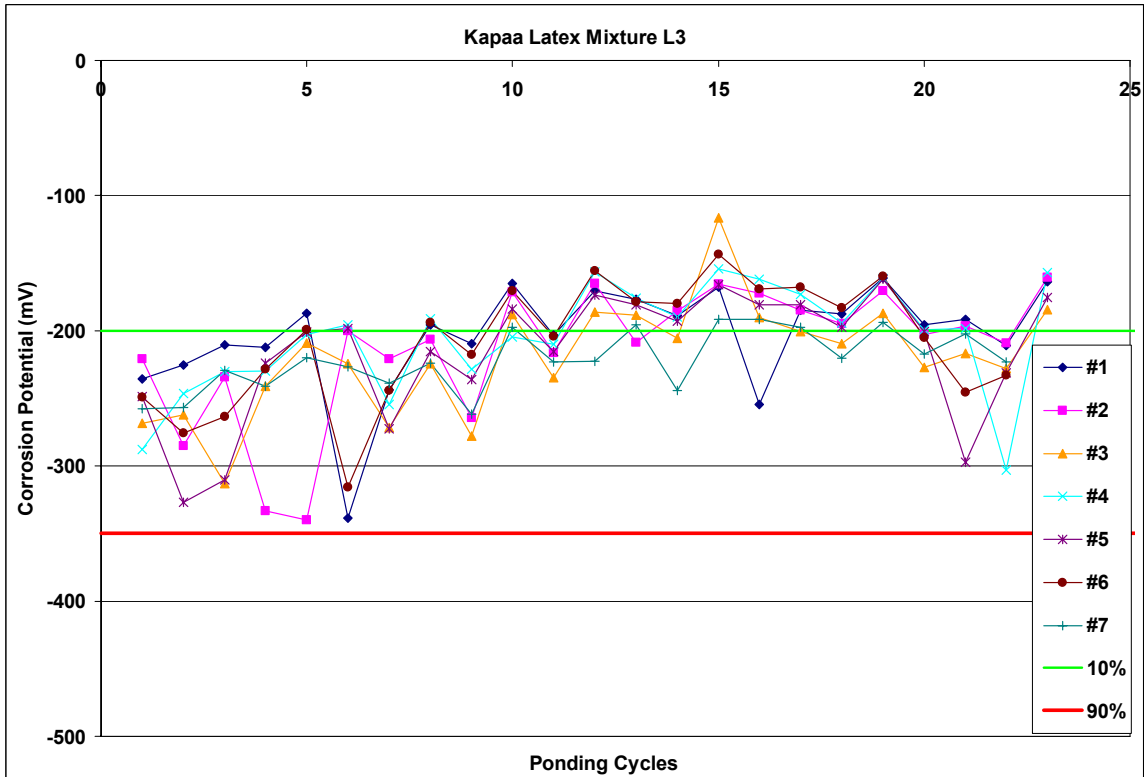


Figure A.1-172: Corrosion Potential Measurements for Kapaa latex Mixture L3

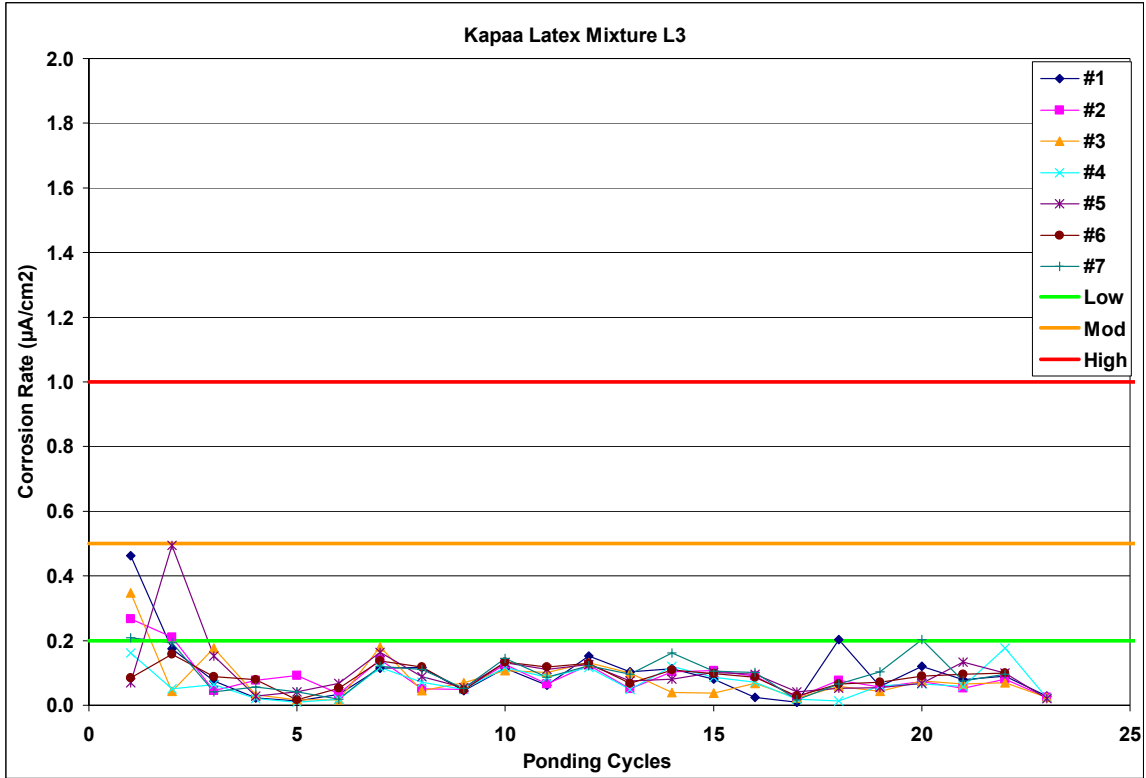


Figure A.1-173: Corrosion Rate Measurements for Kapaa latex Mixture L3

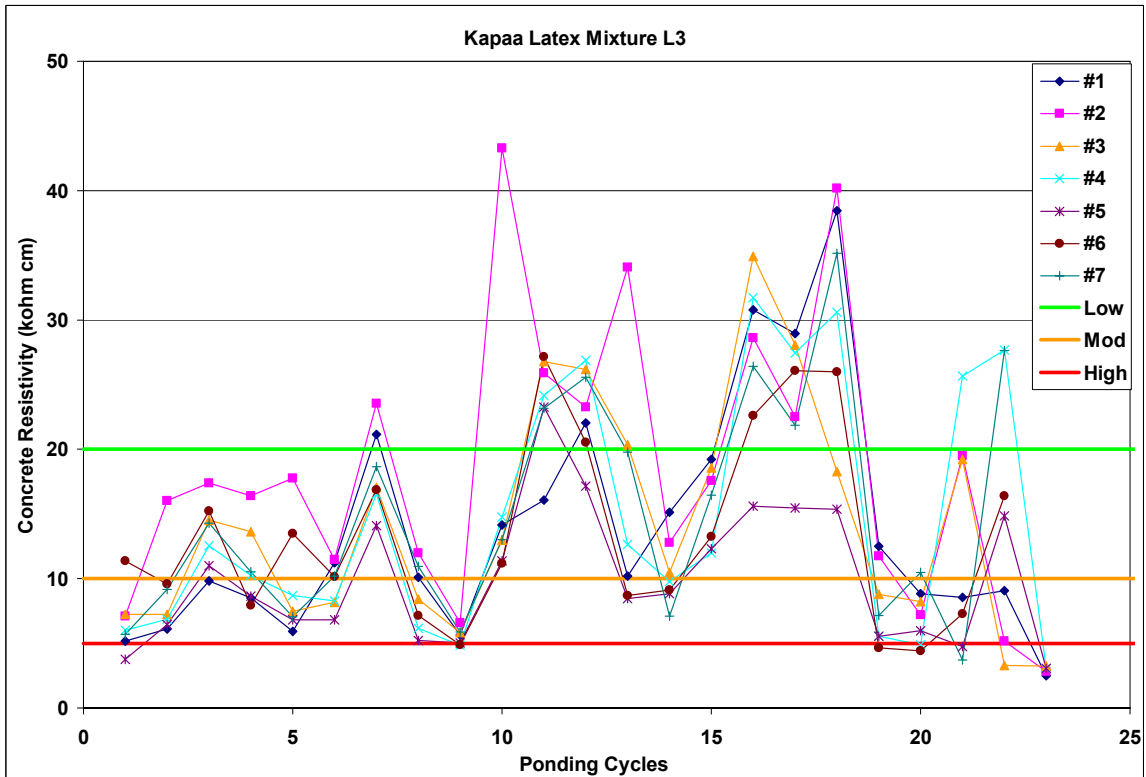


Figure A.1-174: Corrosion Resistivity Measurements for Kapaa latex Mixture L3

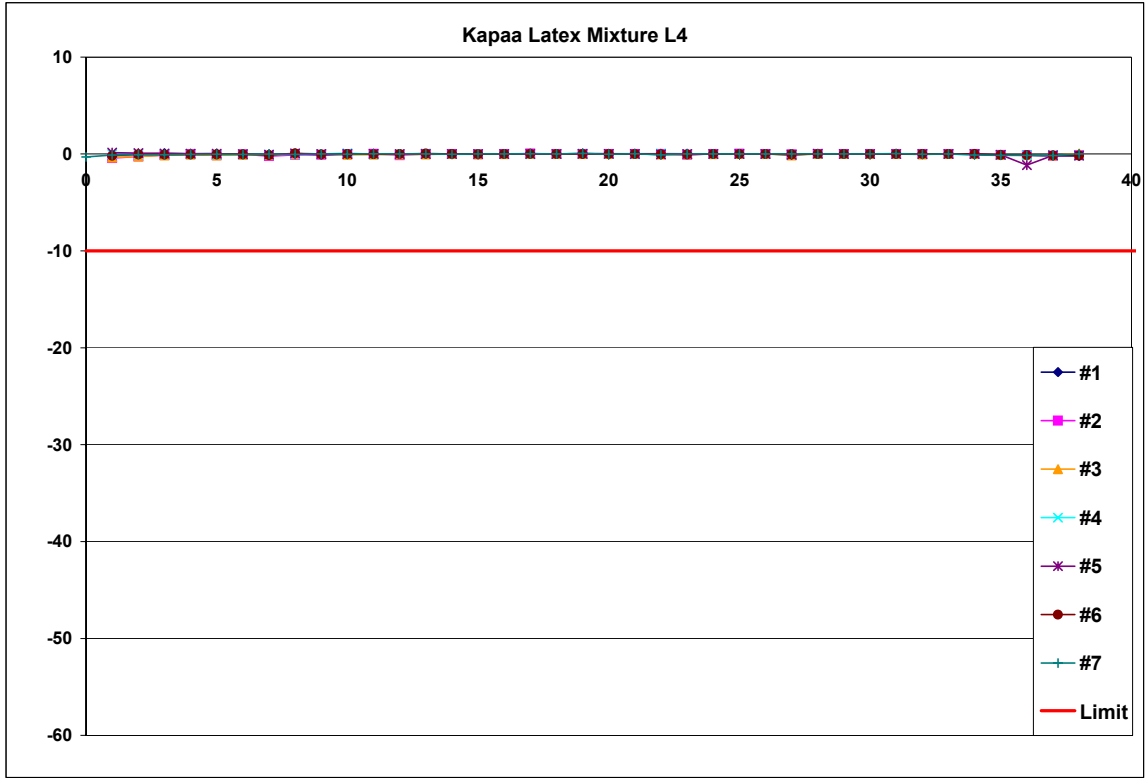


Figure A.1-175: Current Measurements for Kapaa Latex Mixture L4

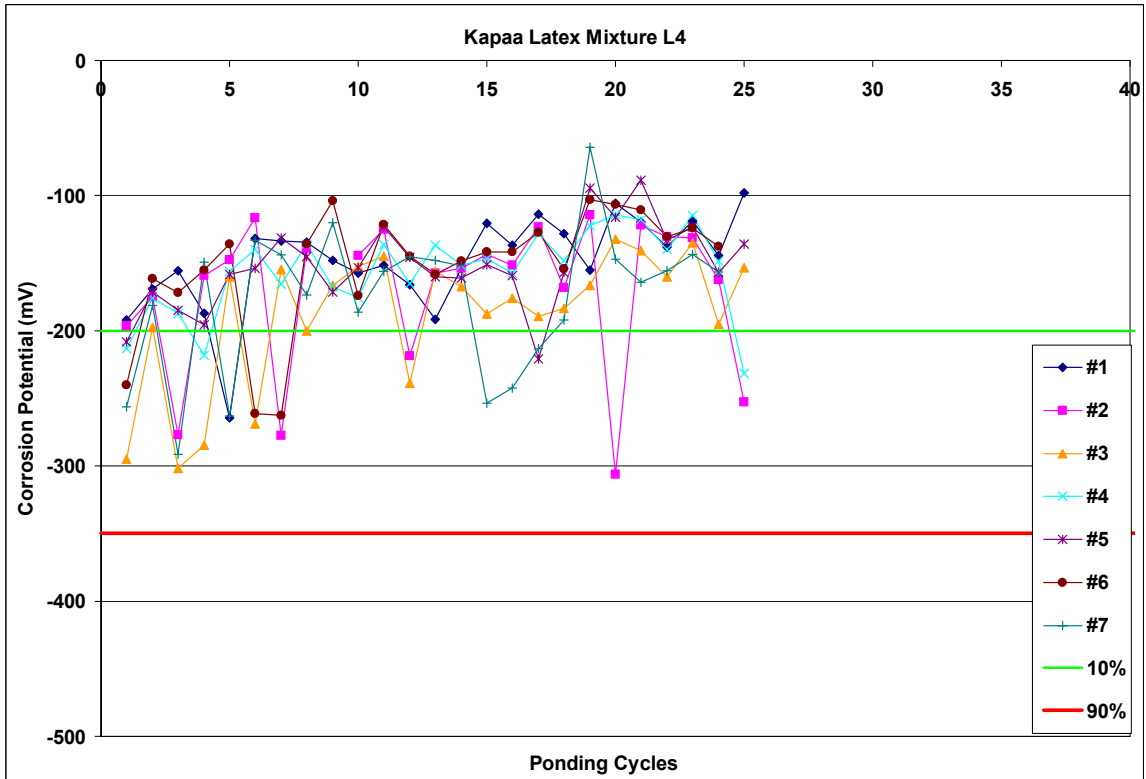


Figure A.1-176: Corrosion Potential Measurements for Kapaa latex Mixture L4

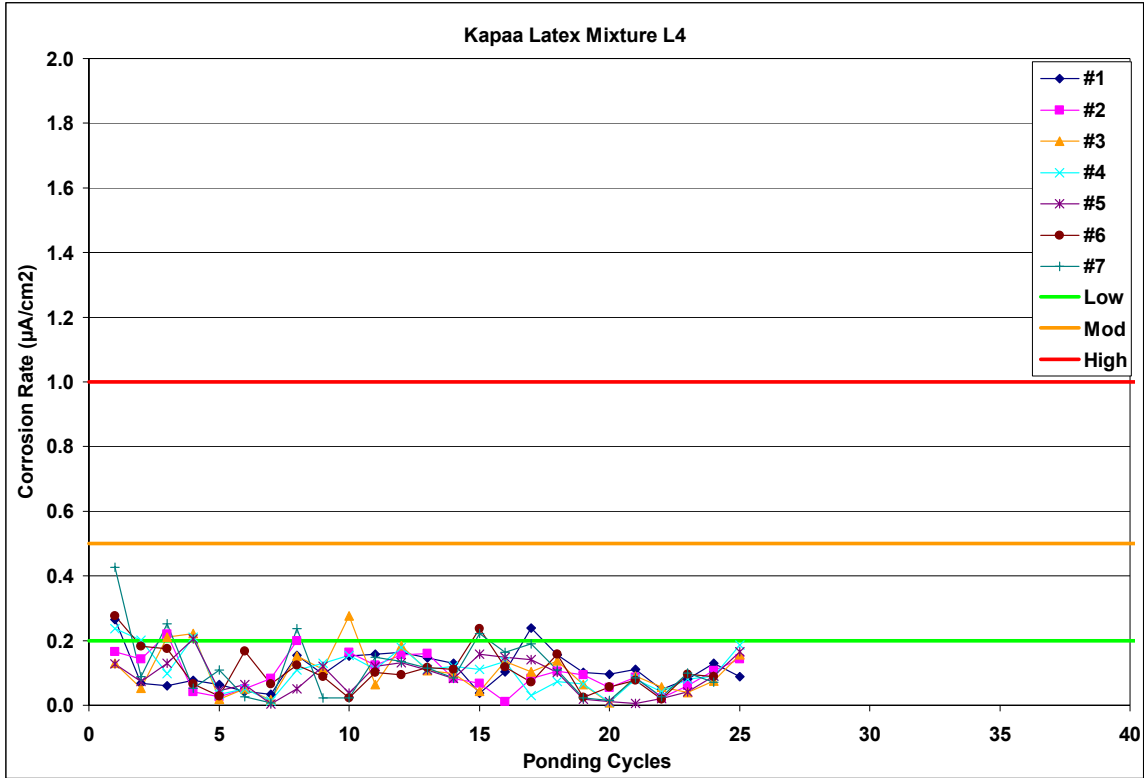


Figure A.1-177: Corrosion Rate Measurements for Kapaa latex Mixture L4

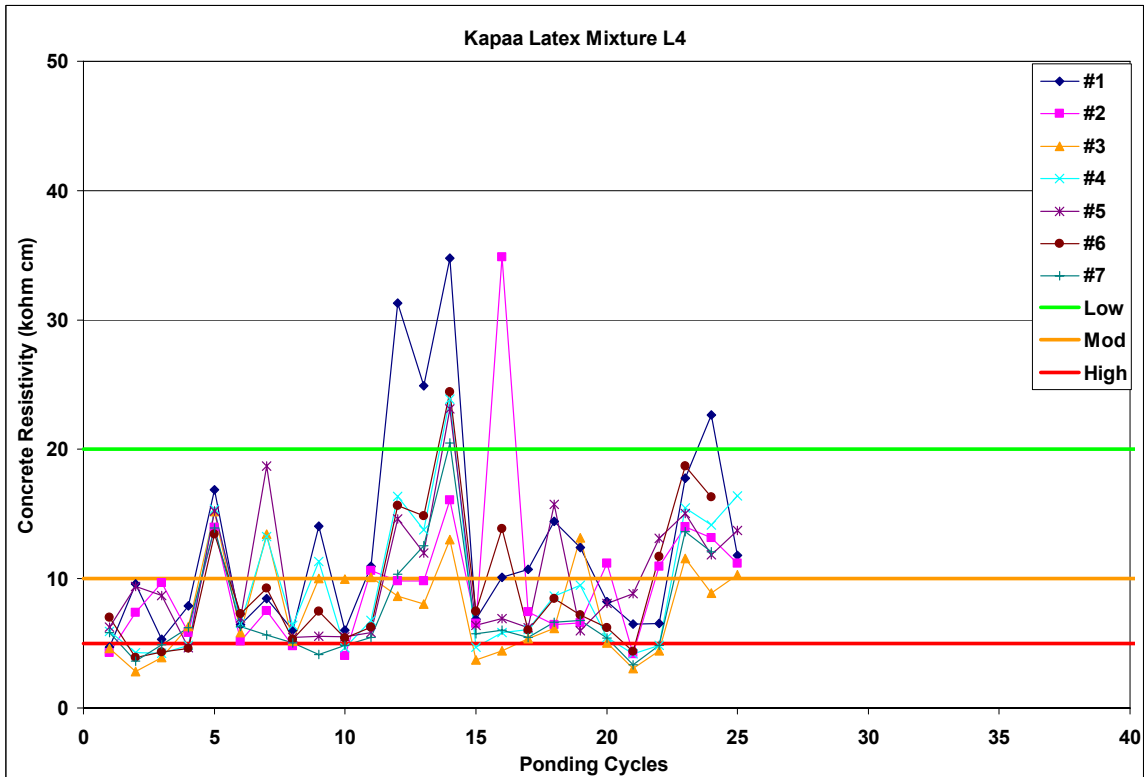


Figure A.1-178: Corrosion Resistivity Measurements for Kapaa latex Mixture L4

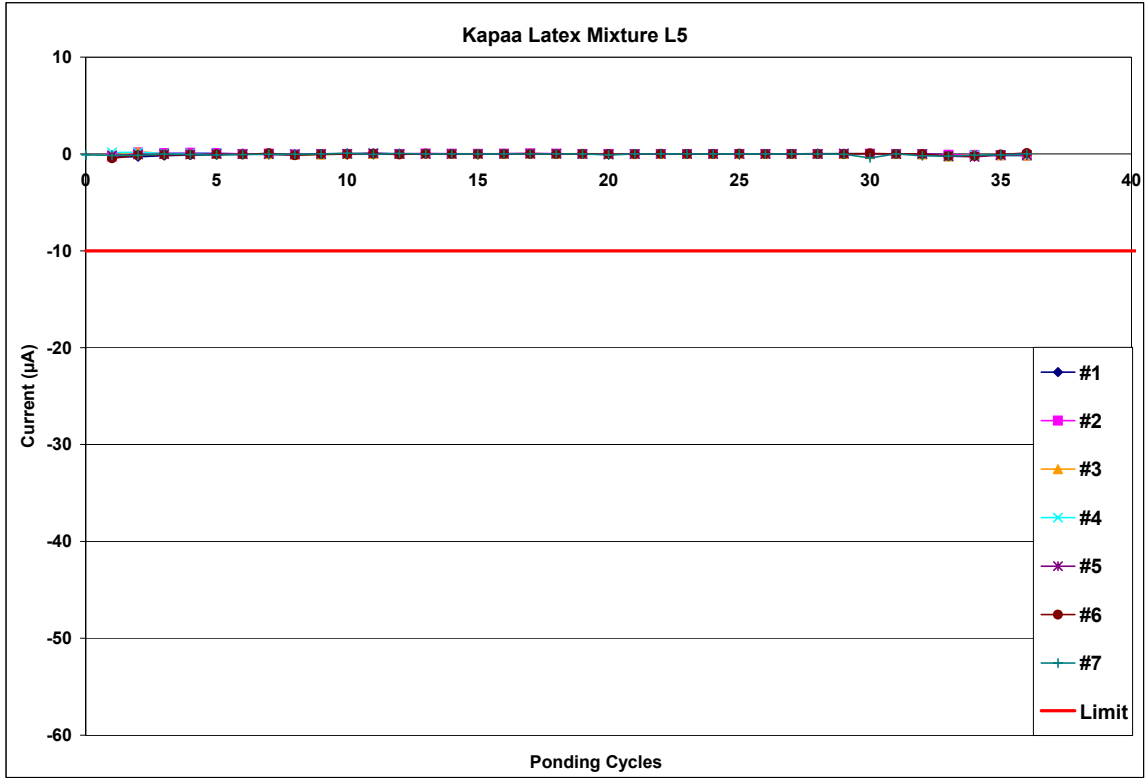


Figure A.1-179: Current Measurements for Kapaa Latex Mixture L5

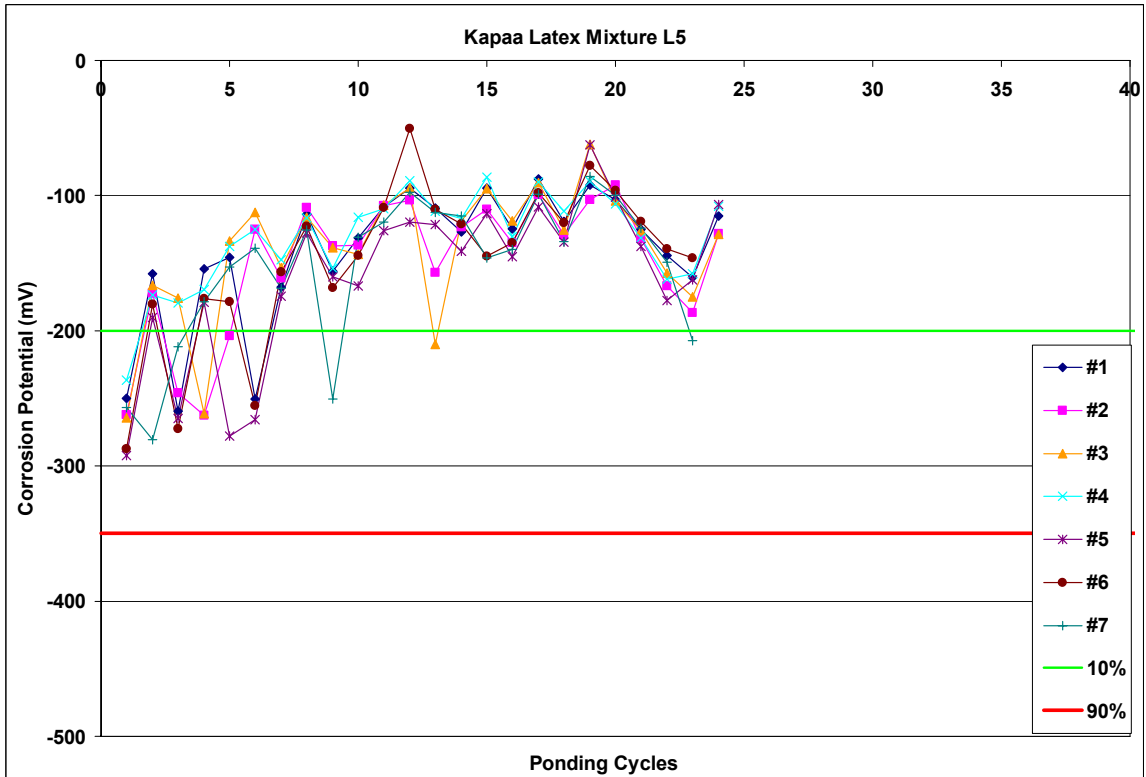


Figure A.1-180: Corrosion Potential Measurements for Kapaa latex Mixture LA5

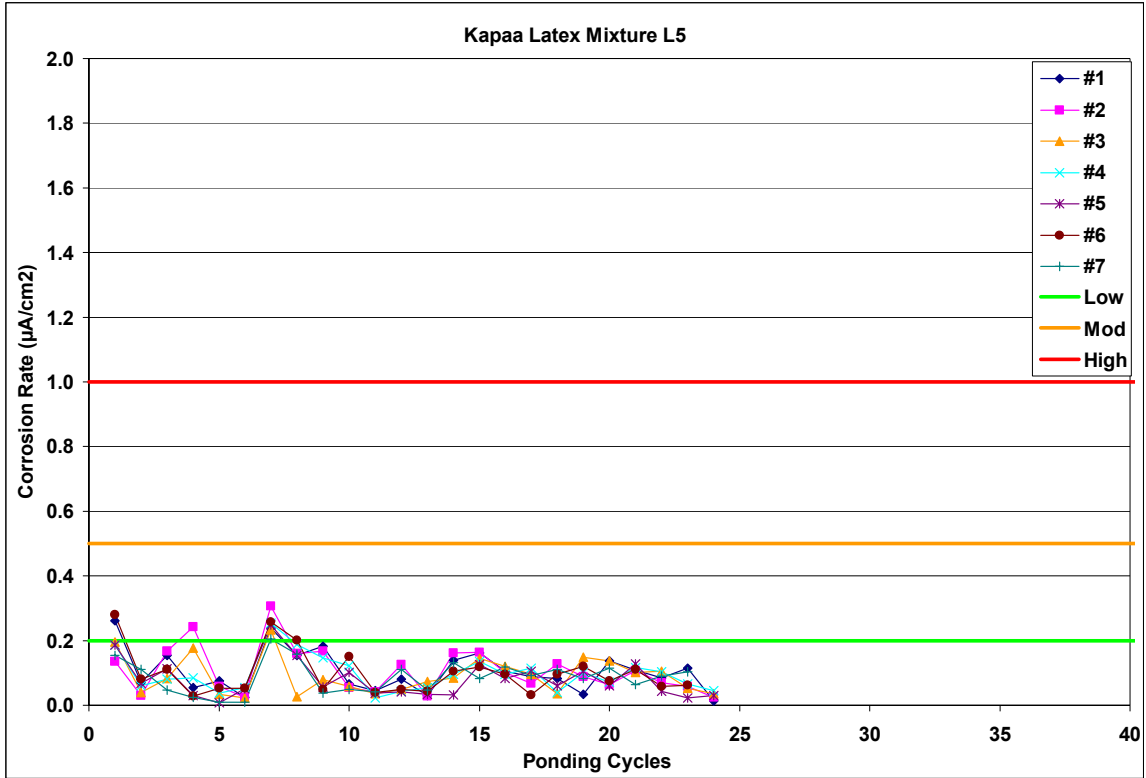


Figure A.1-181: Corrosion Rate Measurements for Kapaa latex Mixture L5

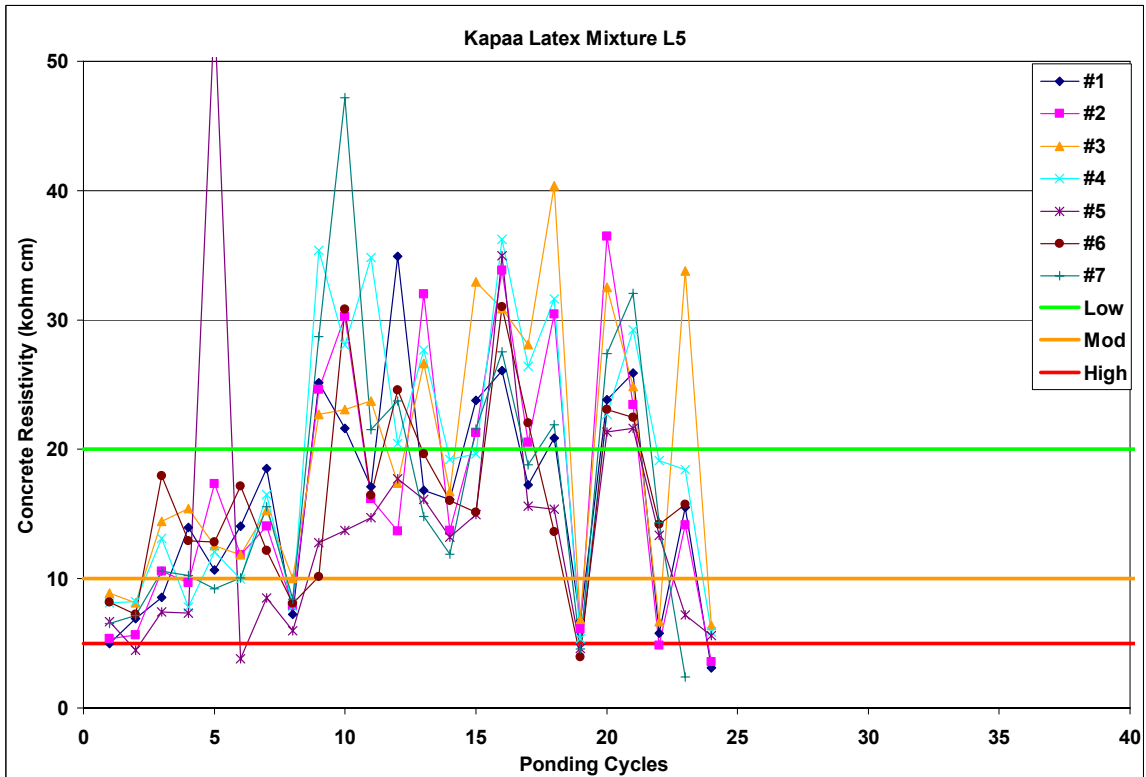


Figure A.1-182: Corrosion Resistivity Measurements for Kapaa latex Mixture L5

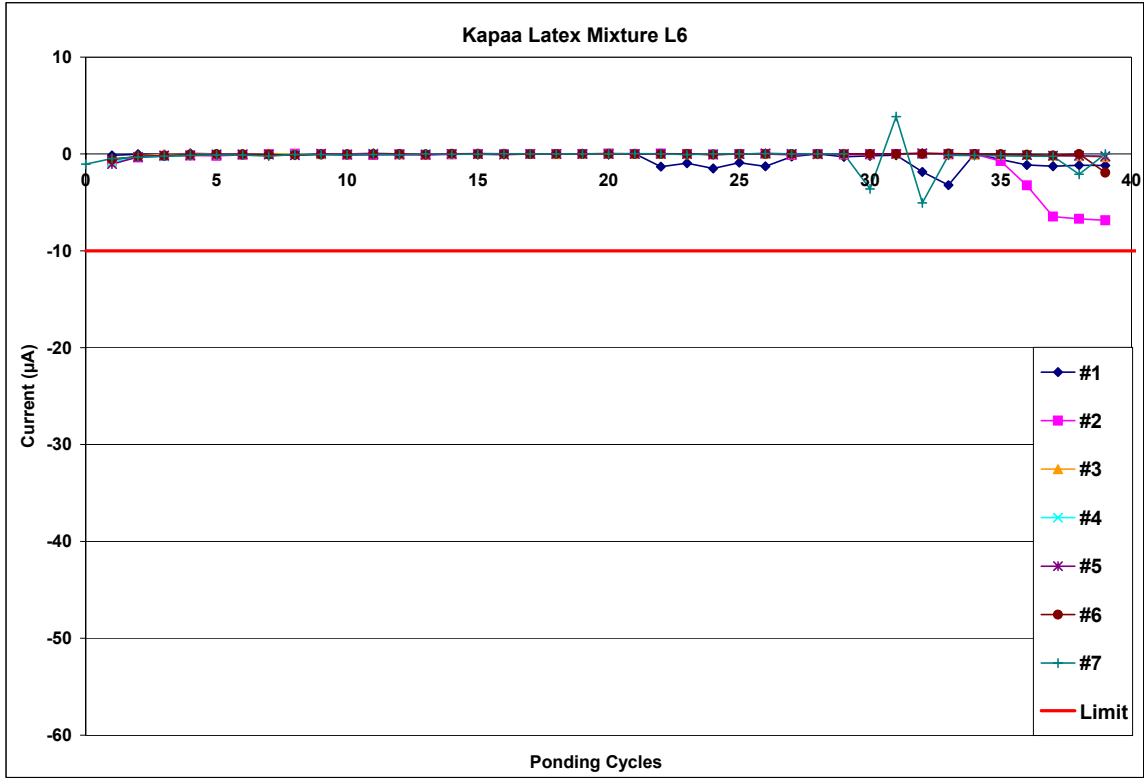


Figure A.1-183: Current Measurements for Kapaa Latex Mixture L6

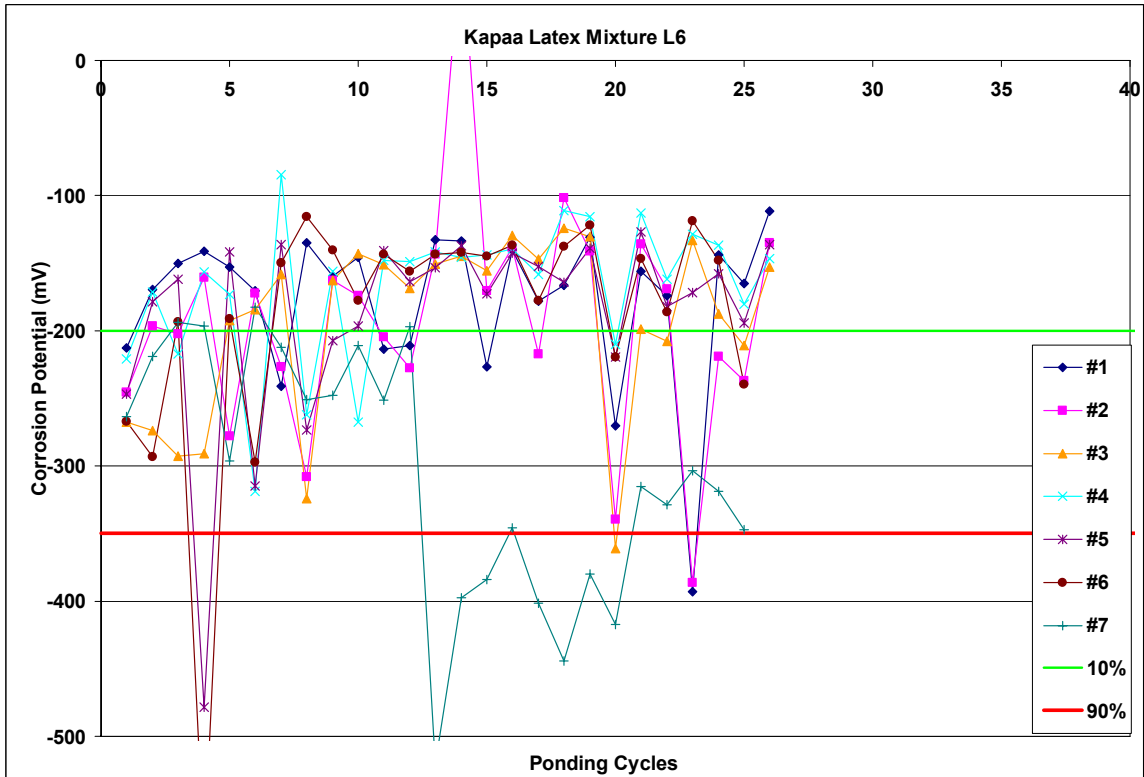


Figure A.1-184: Corrosion Potential Measurements for Kapaa latex Mixture LA6

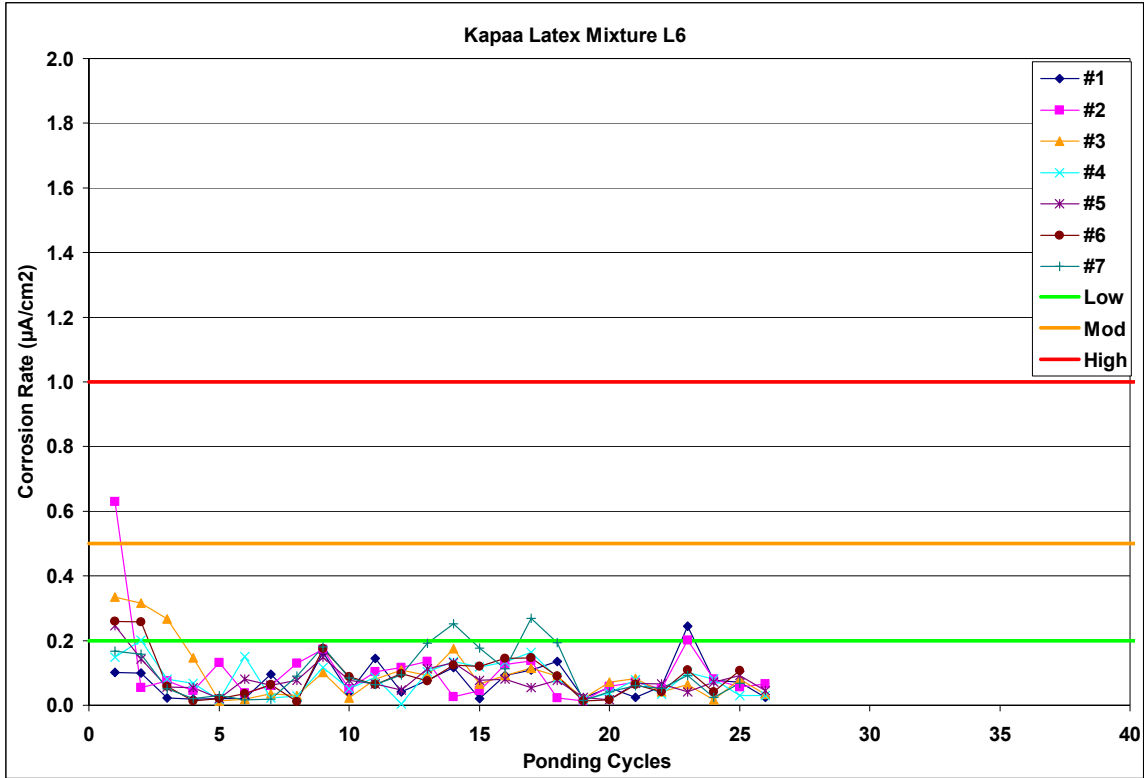


Figure A.1-185: Corrosion Rate Measurements for Kapaa latex Mixture L6

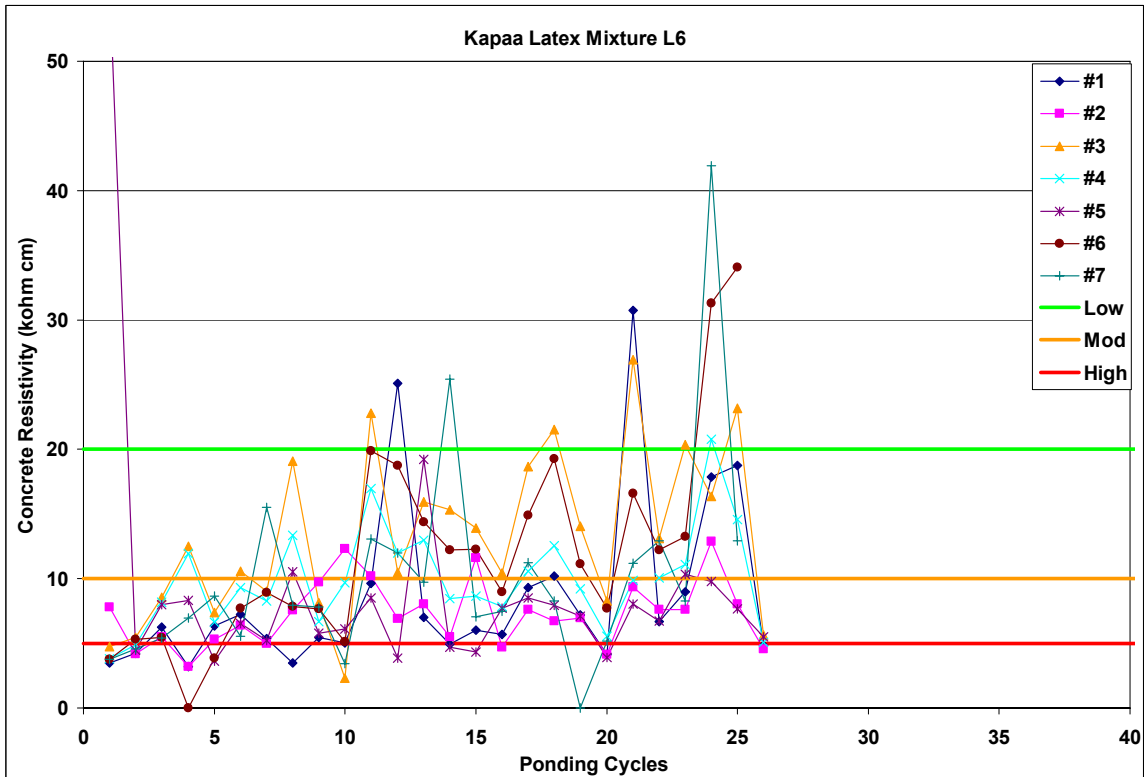


Figure A.1-186: Corrosion Resistivity Measurements for Kapaa latex Mixture L6

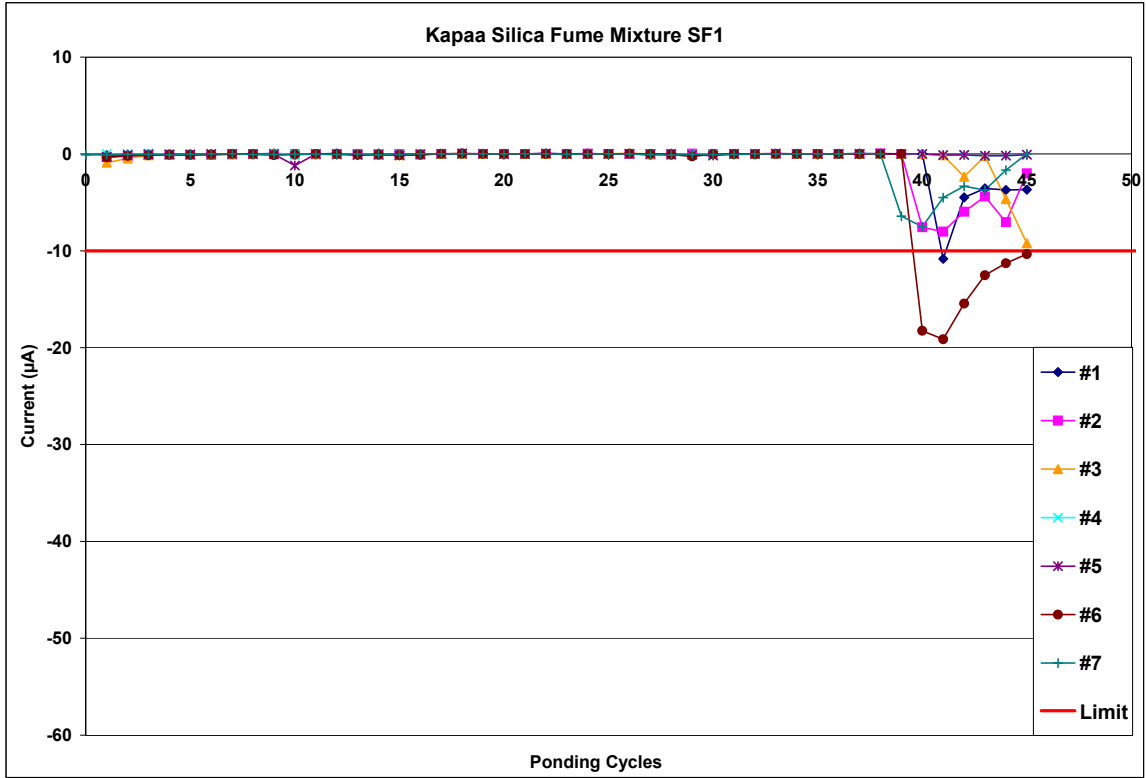


Figure A.1-187: Current Measurements for Kapaa Silica Fume Mixture SF1

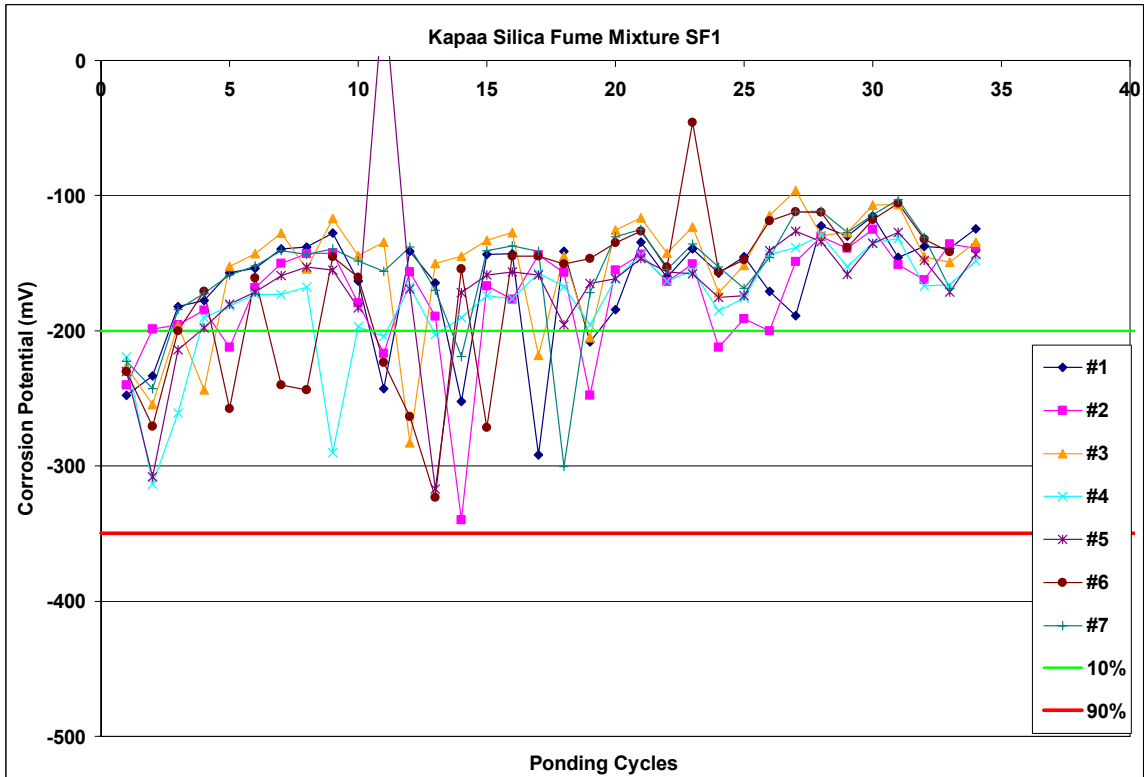


Figure A.1-188: Corrosion Potential Measurements for Kapaa silica fume Mixture SF1

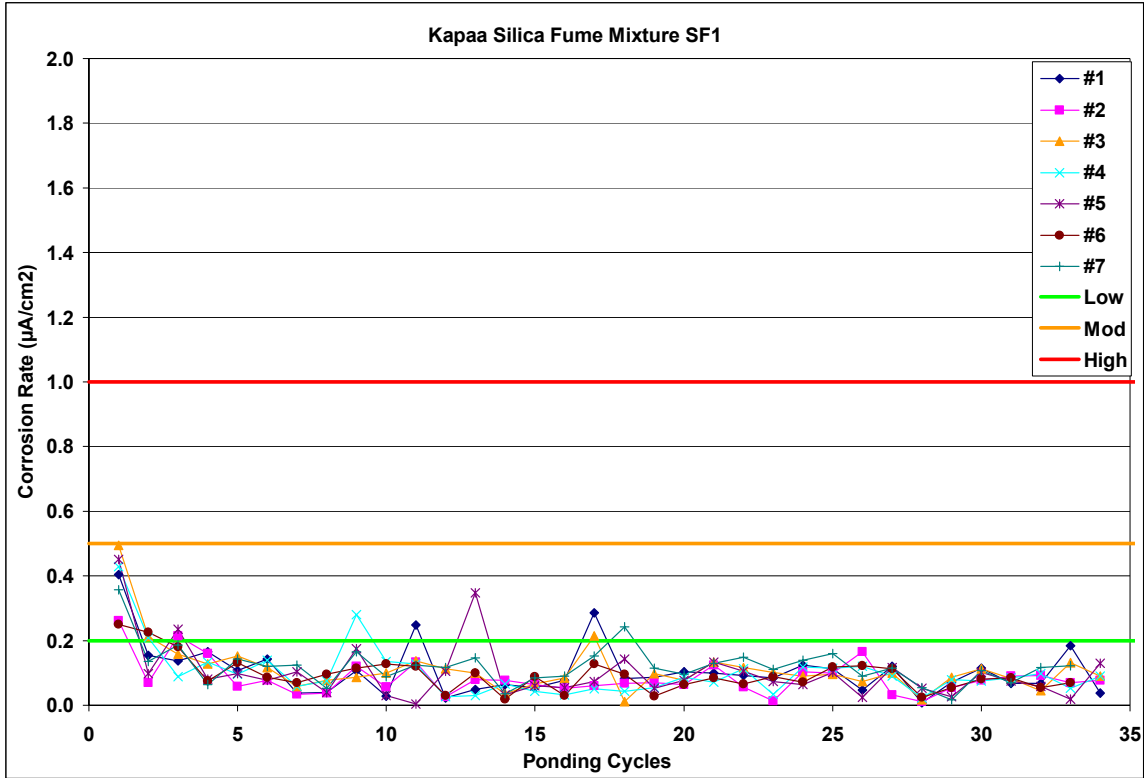


Figure A.1-189: Corrosion Rate Measurements for Kapaa silica fume Mixture SF1

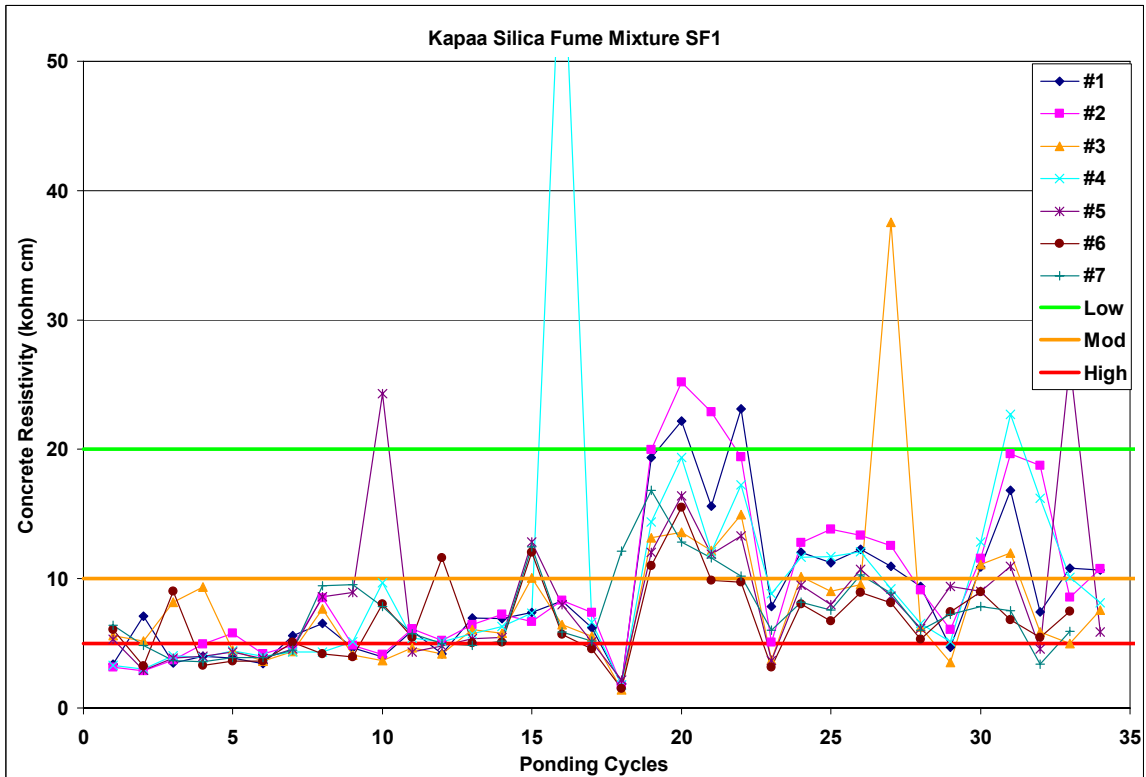


Figure A.1-190: Corrosion Resistivity Measurements for Kapaa silica fume Mixture SF1

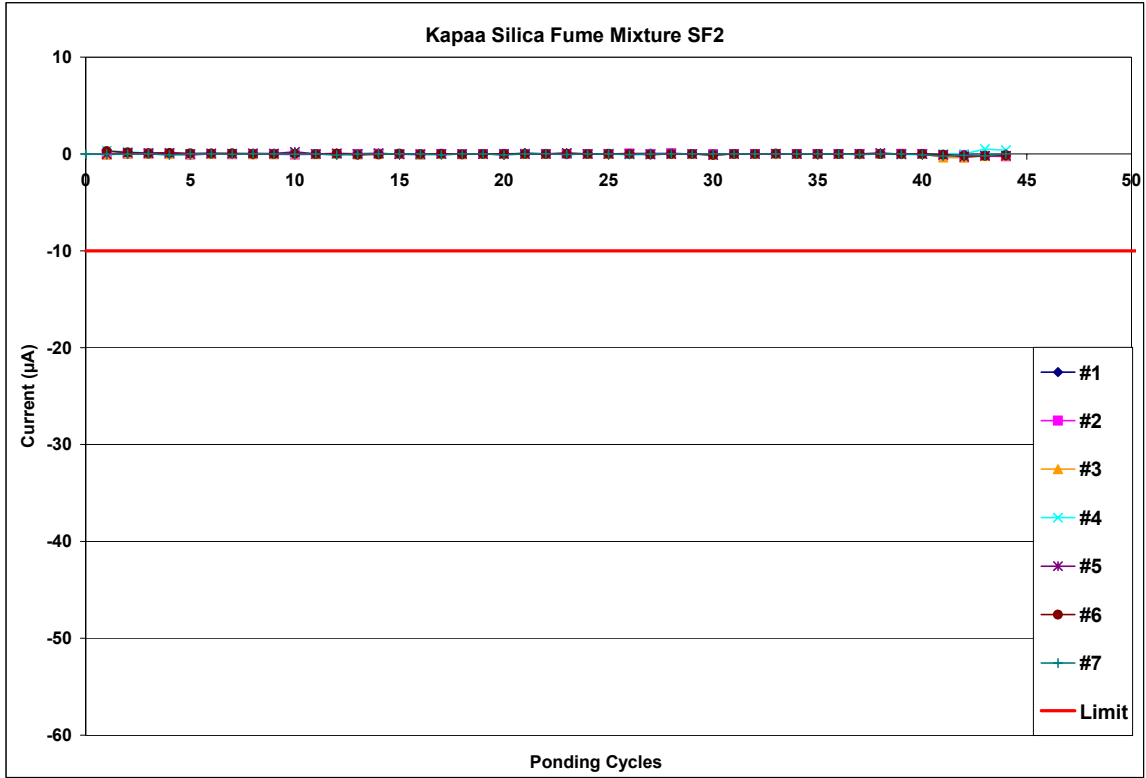


Figure A.1-191: Current Measurements for Kapaa Silica Fume Mixture SF2

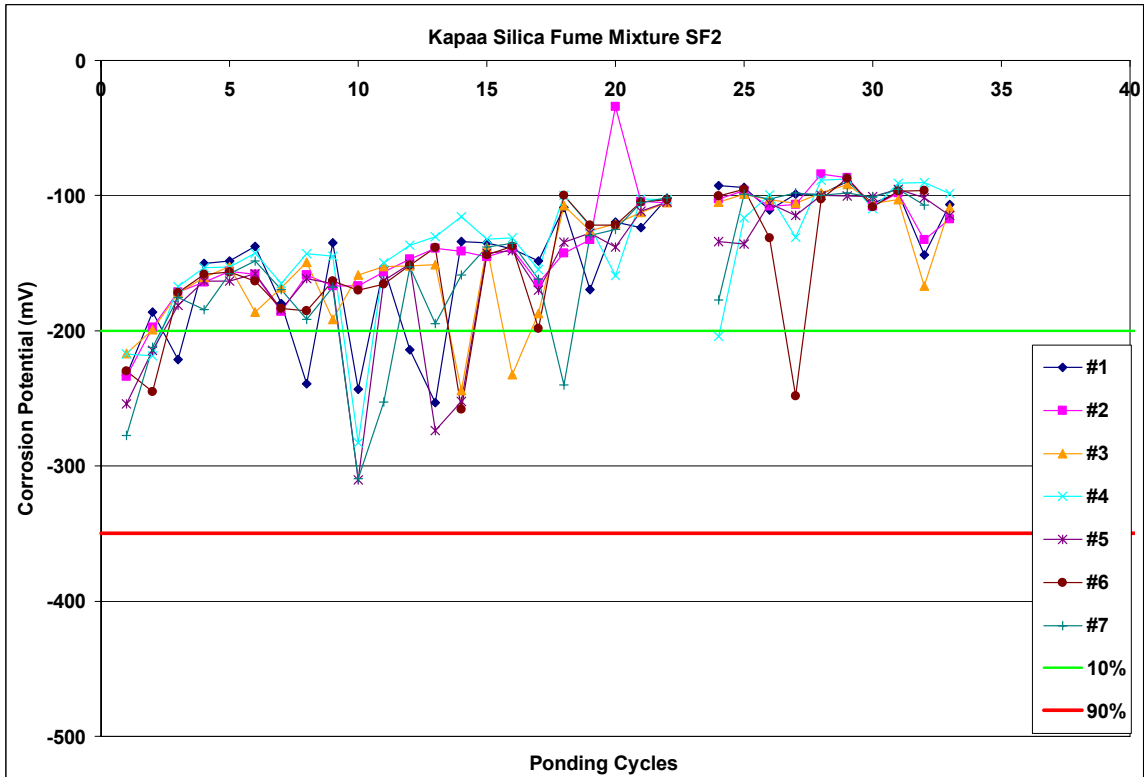


Figure A.1-192: Corrosion Potential Measurements for Kapaa silica fume Mixture SF1

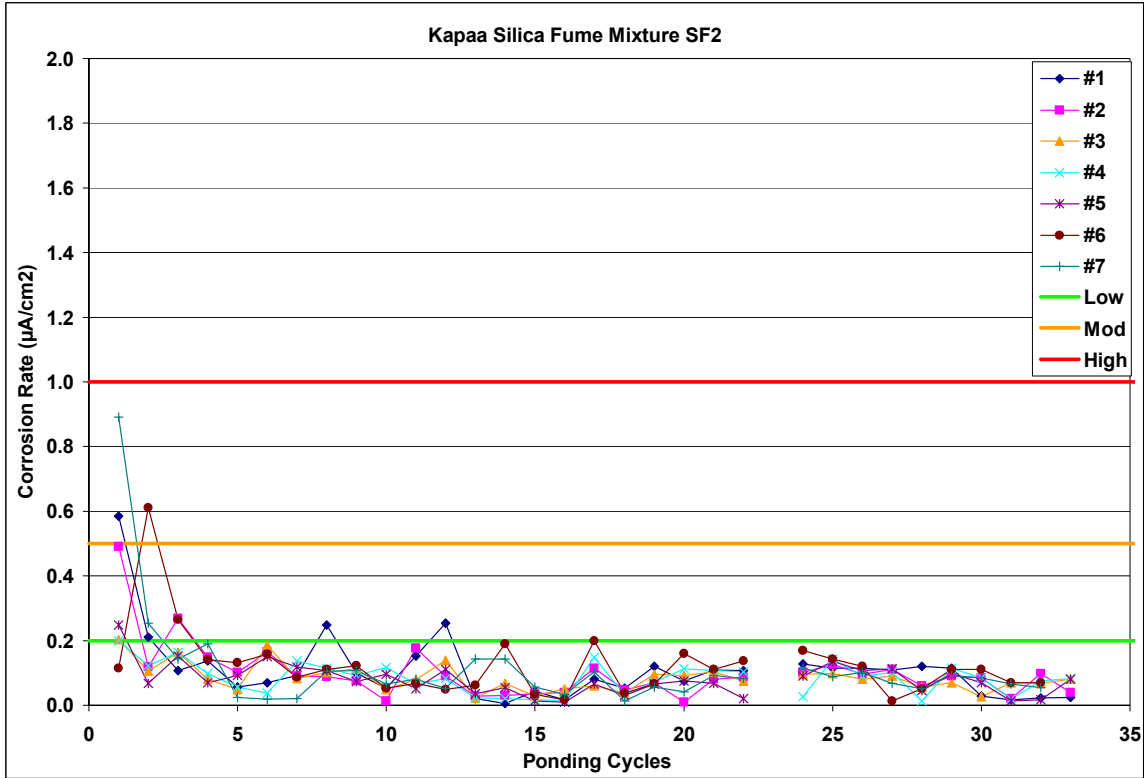


Figure A.1-193: Corrosion Rate Measurements for Kapaa silica fume Mixture SF2

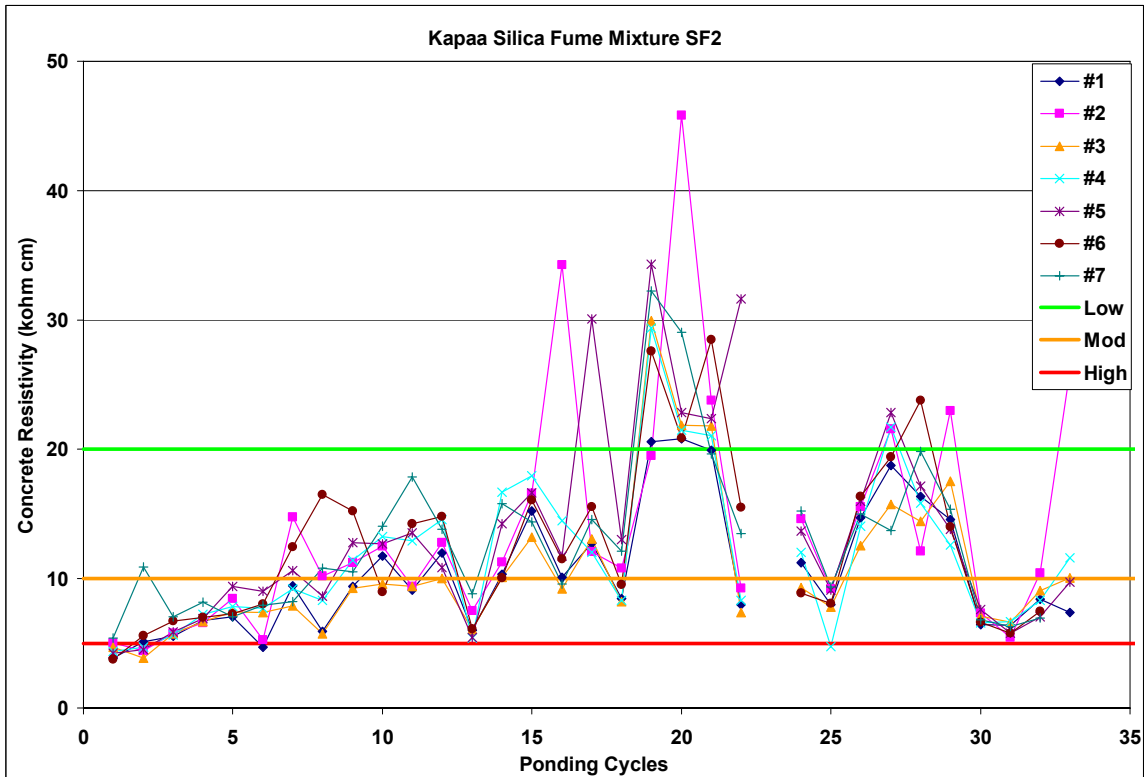


Figure A.1-194: Corrosion Resistivity Measurements for Kapaa silica fume Mixture SF2

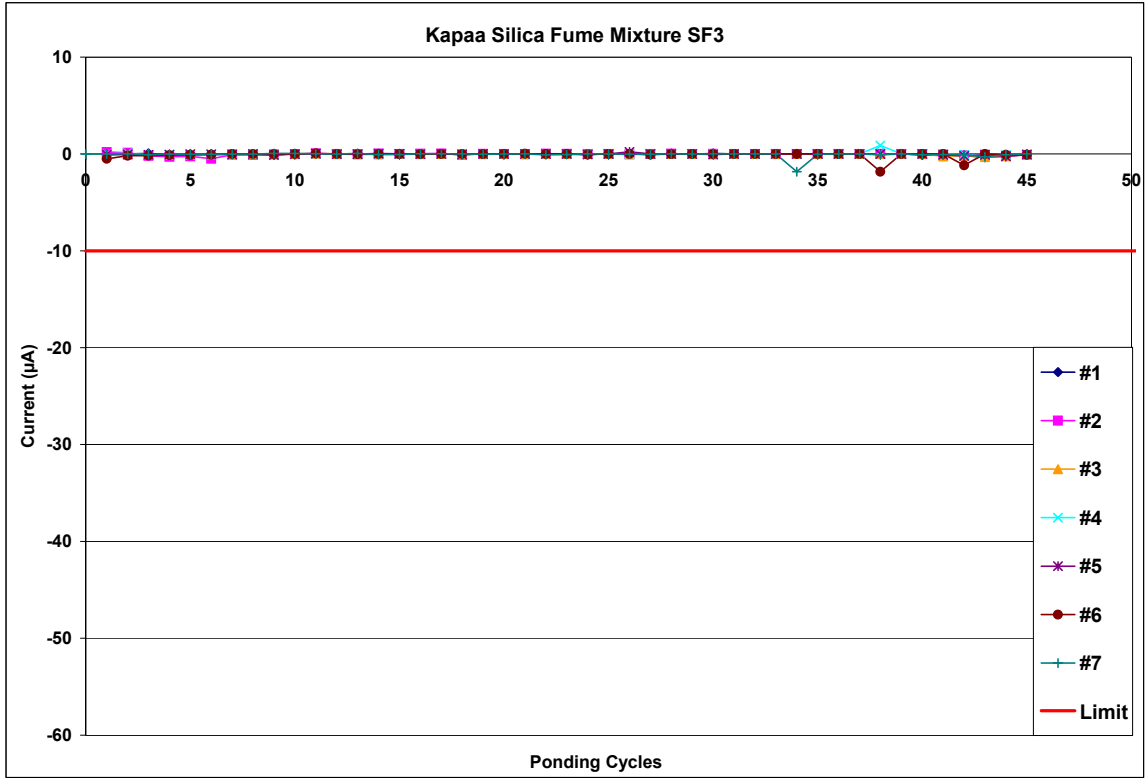


Figure A.1-195: Current Measurements for Kapaa Silica Fume Mixture SF3

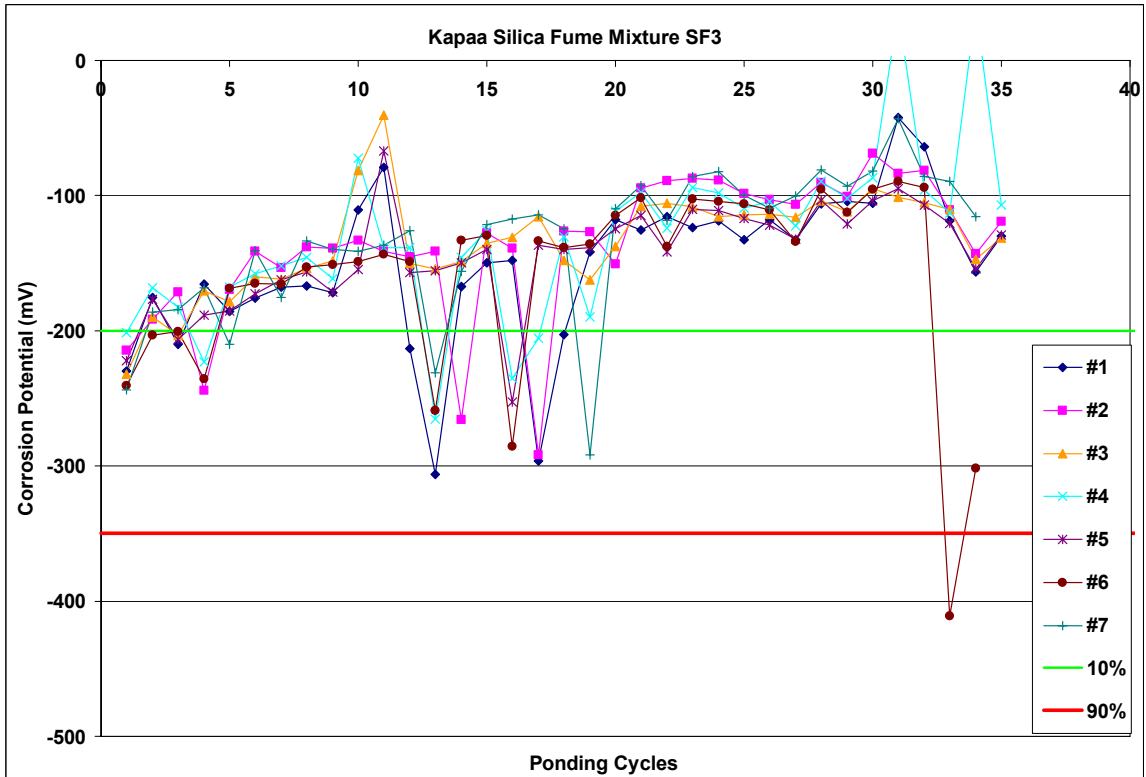


Figure A.1-196: Corrosion Potential Measurements for Kapaa silica fume Mixture SF3

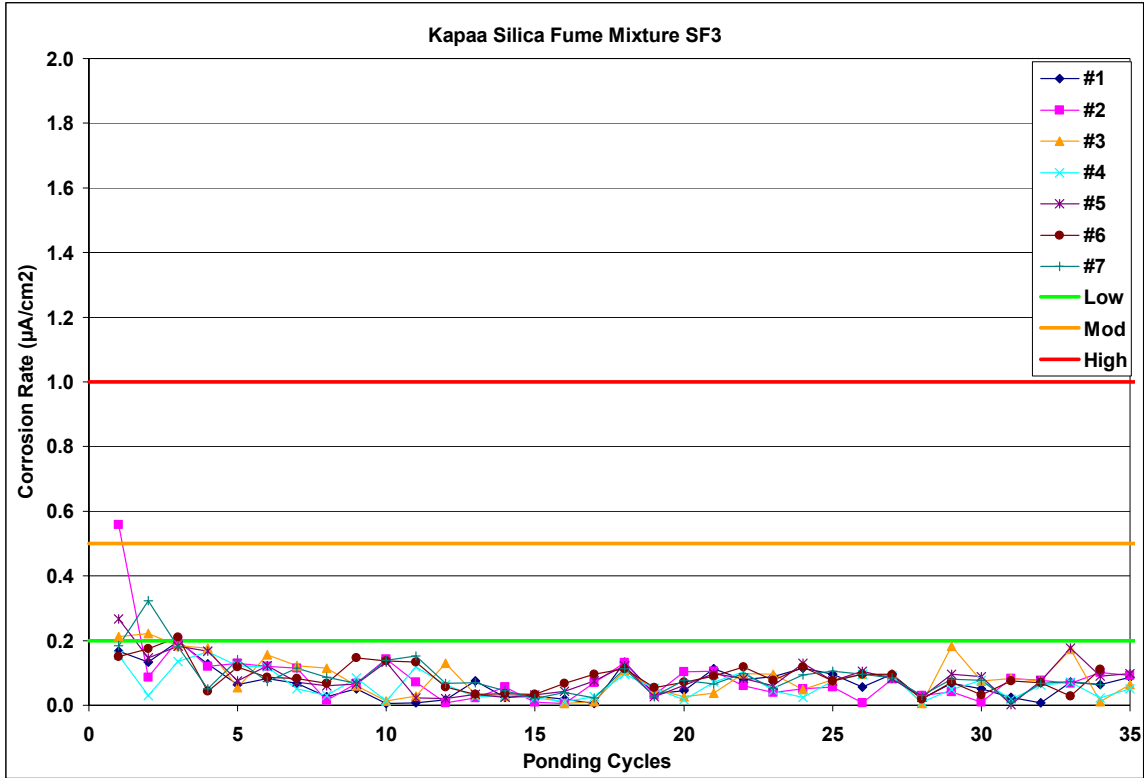


Figure A.1-197: Corrosion Rate Measurements for Kapaa silica fume Mixture SF3

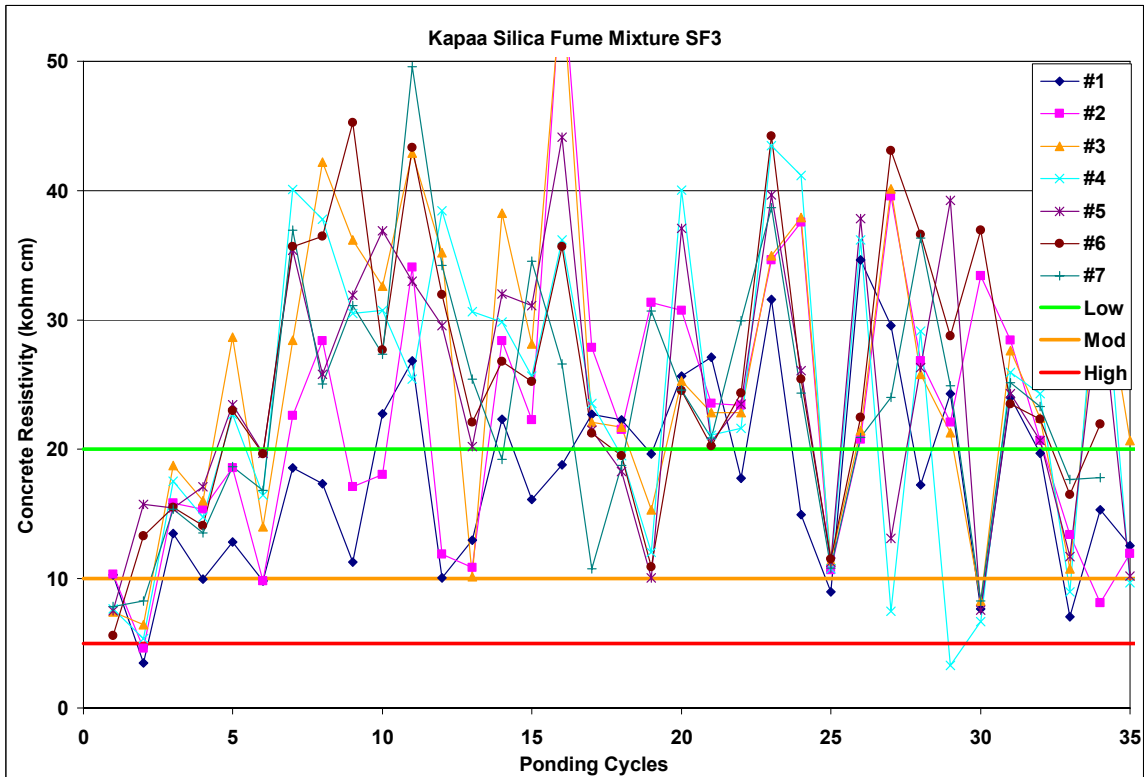


Figure A.1-198: Corrosion Resistivity Measurements for Kapaa silica fume Mixture SF3

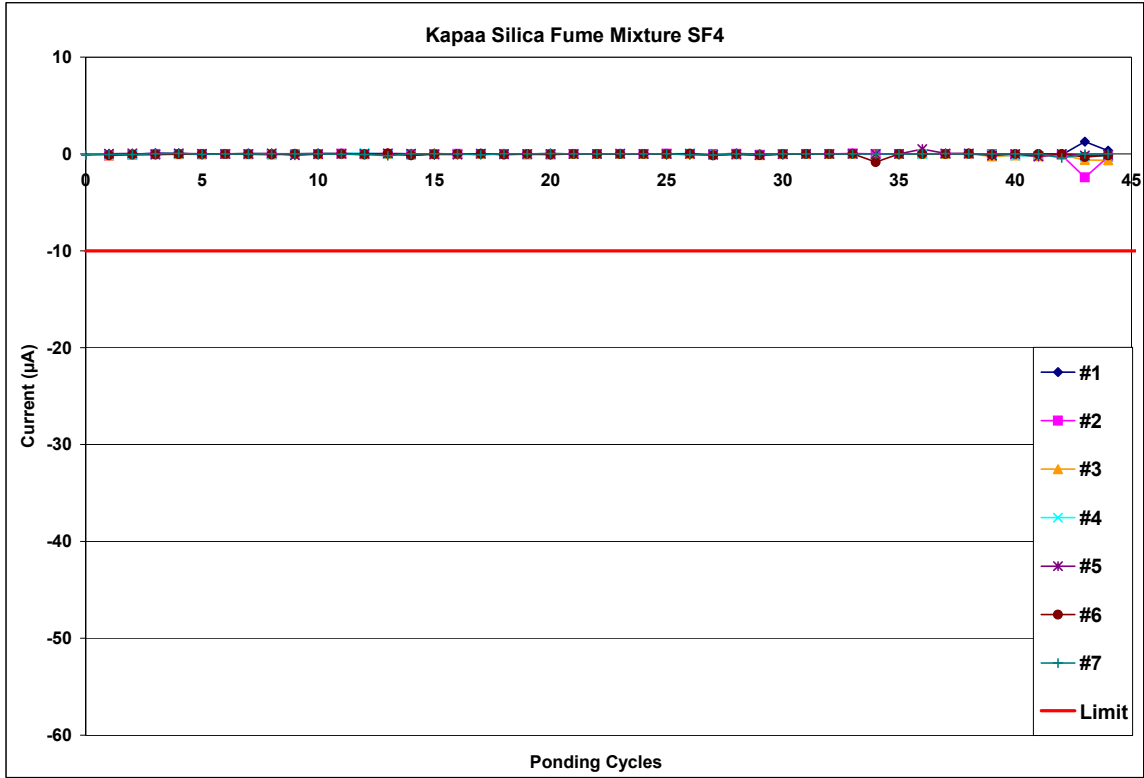


Figure A.1-199: Current Measurements for Kapaa Silica Fume Mixture SF4

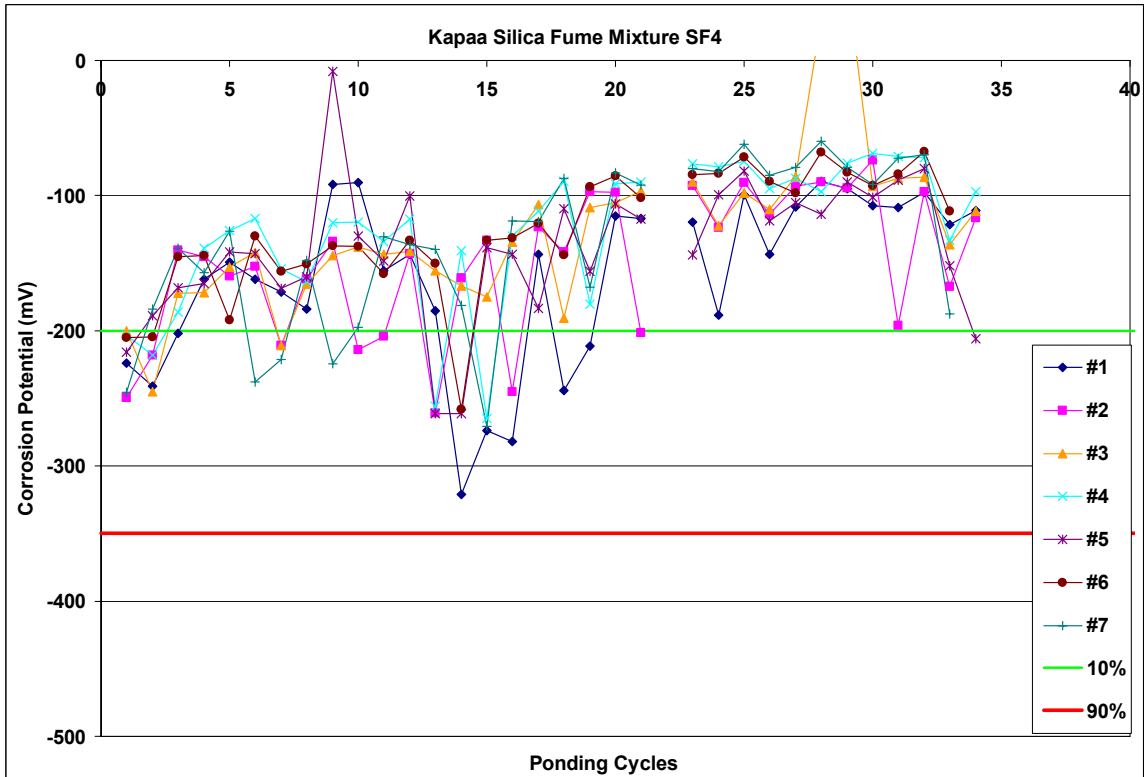


Figure A.1-200: Corrosion Potential Measurements for Kapaa silica fume Mixture SF4

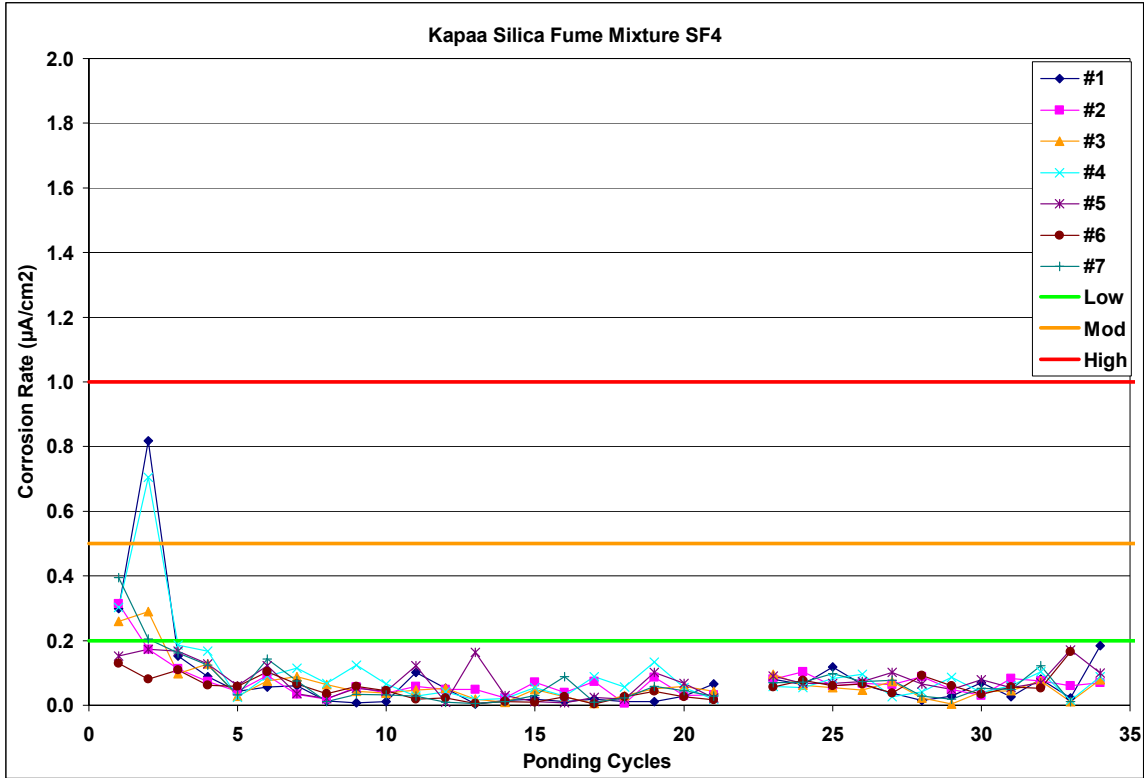


Figure A.1-201: Corrosion Rate Measurements for Kapaa silica fume Mixture SF4

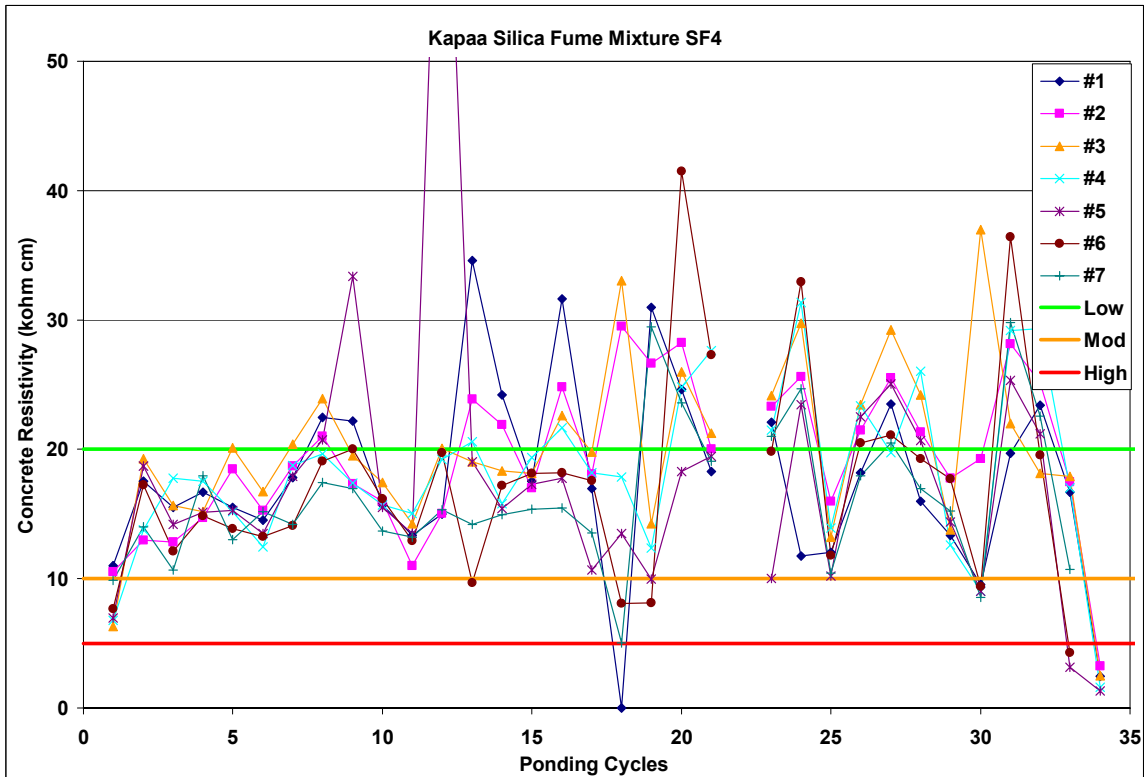


Figure A.1-202: Corrosion Resistivity Measurements for Kapaa silica fume Mixture SF4

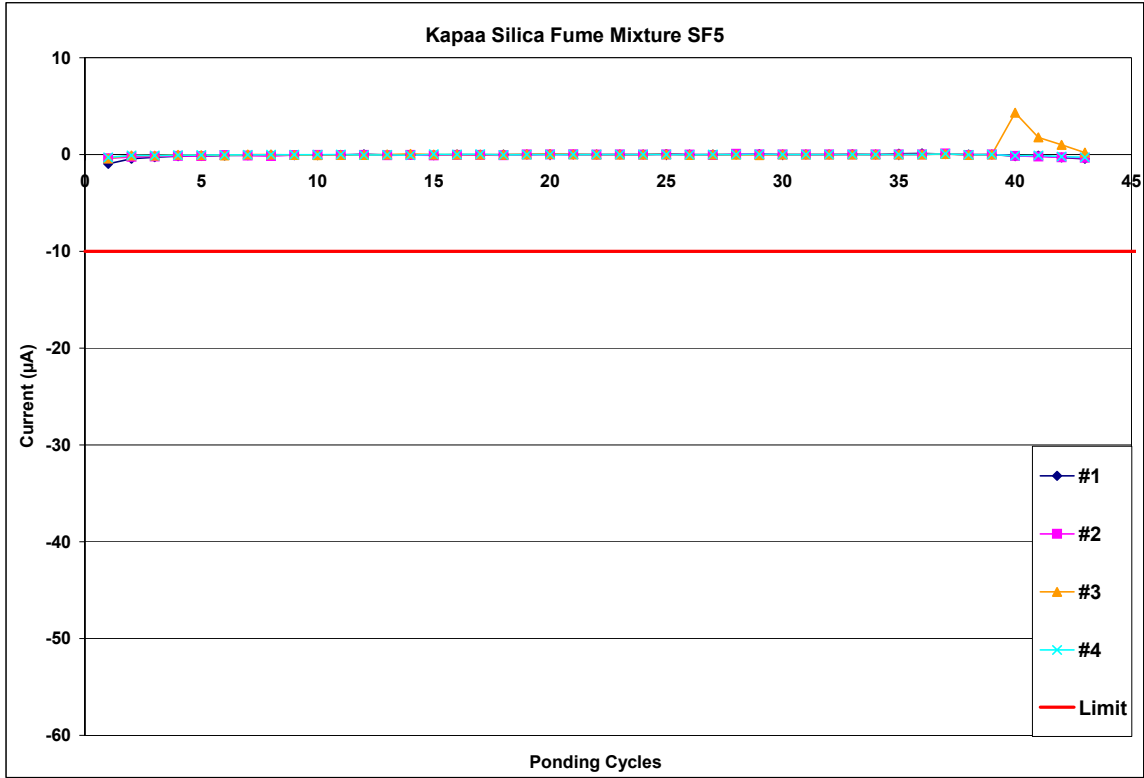


Figure A.1-203: Current Measurements for Kapaa Silica Fume Mixture SF5

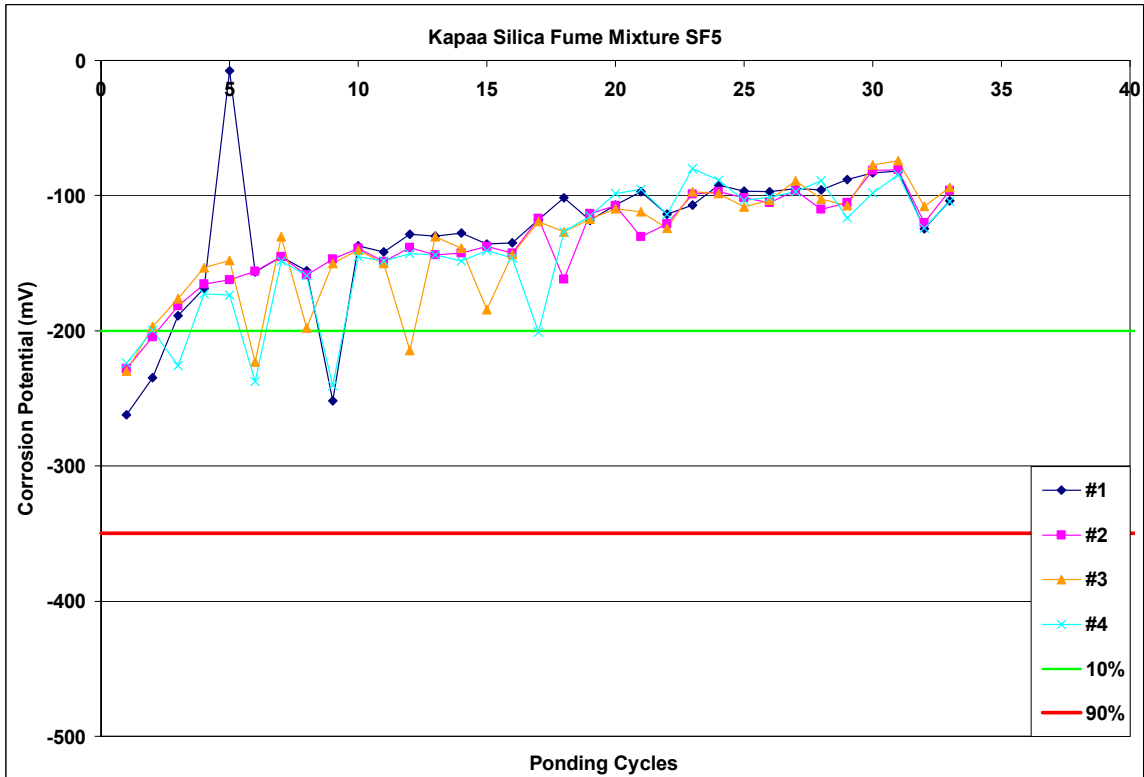


Figure A.1-204: Corrosion Potential Measurements for Kapaa silica fume Mixture SF5

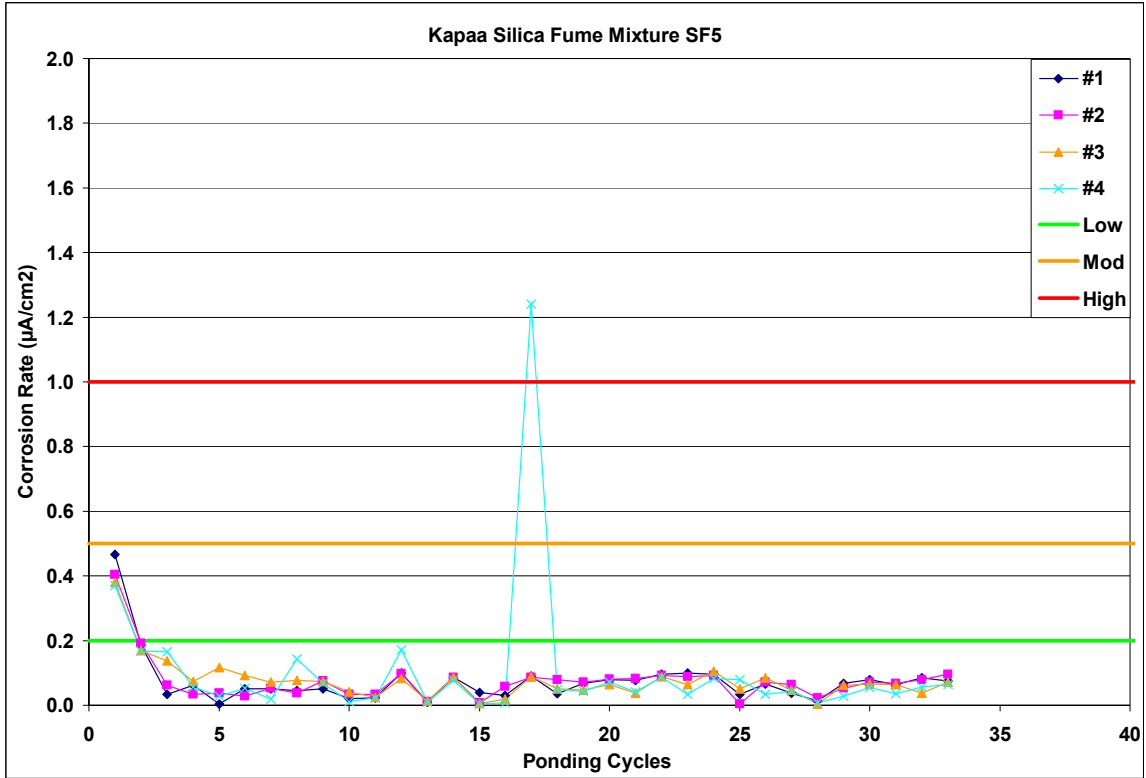


Figure A.1-205: Corrosion Rate Measurements for Kapaa silica fume Mixture SF5

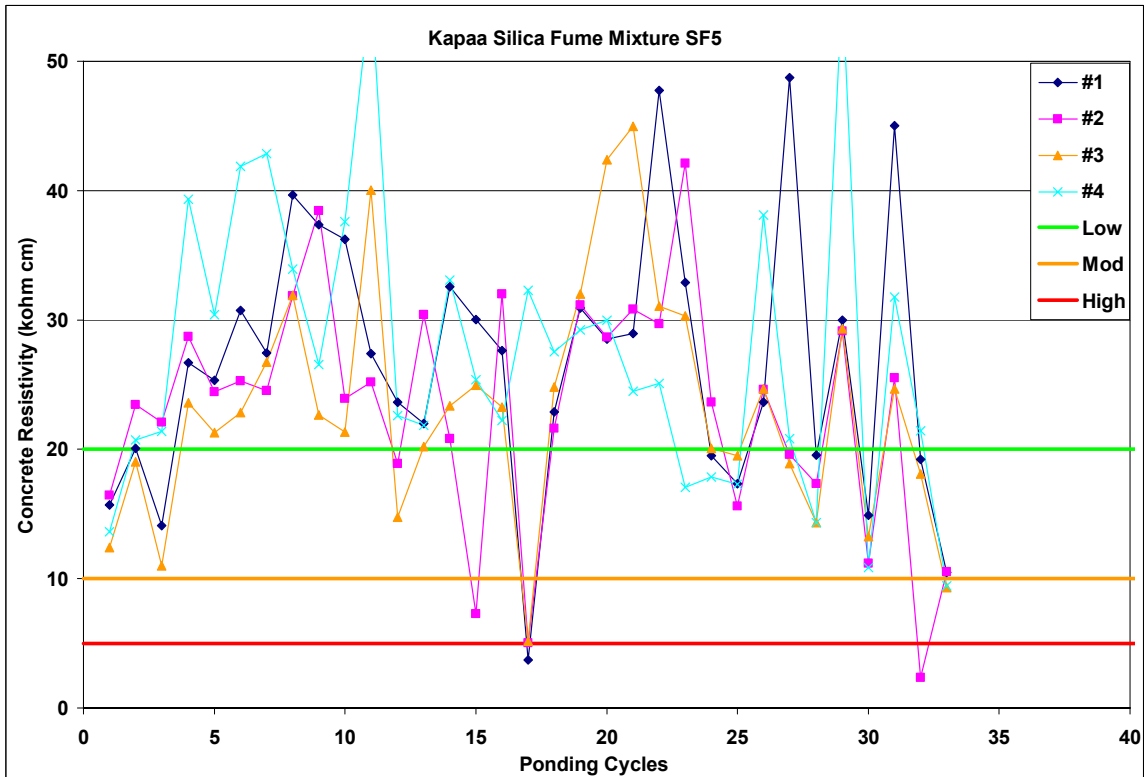


Figure A.1-206: Corrosion Resistivity Measurements for Kapaa silica fume Mixture SF5

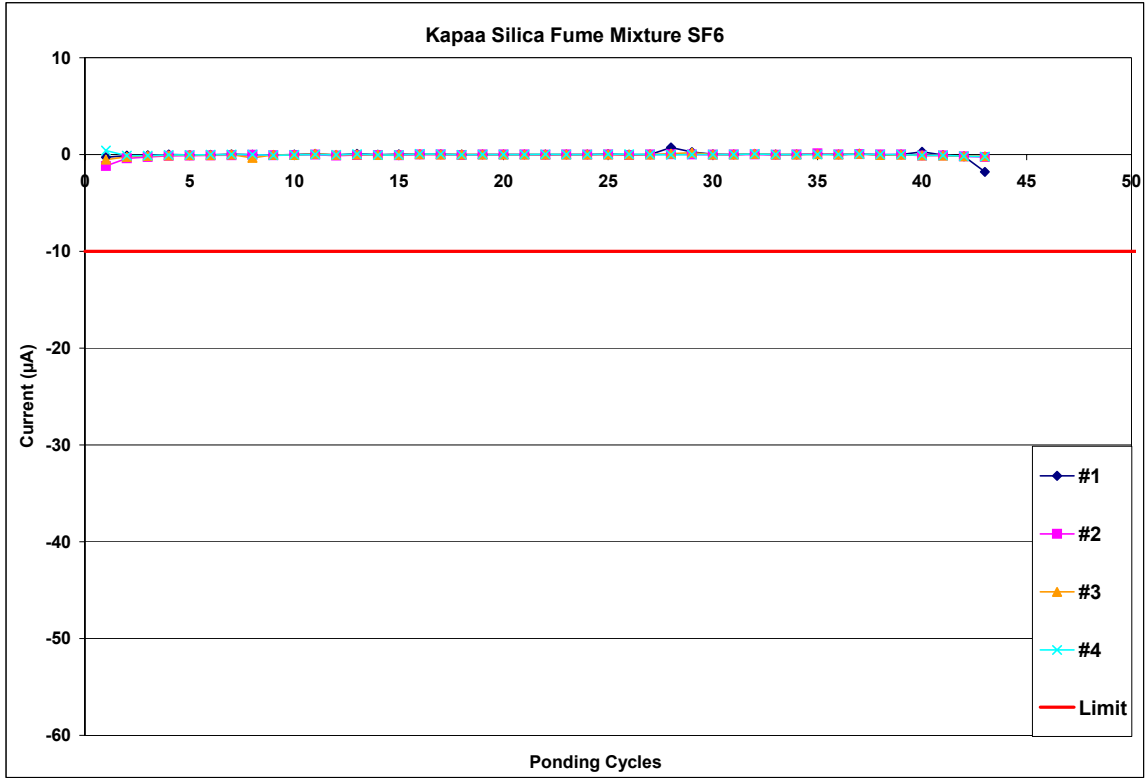


Figure A.1-207: Current Measurements for Kapaa Silica Fume Mixture SF6

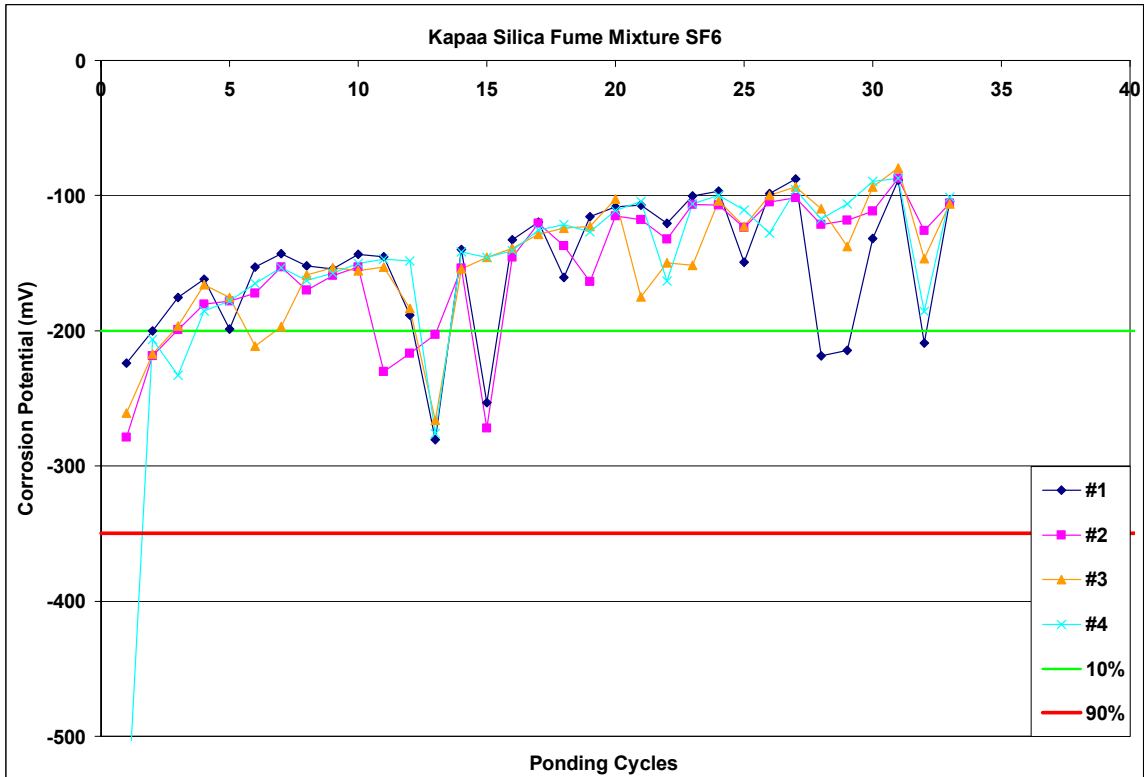


Figure A.1-208: Corrosion Potential Measurements for Kapaa silica fume Mixture SF6

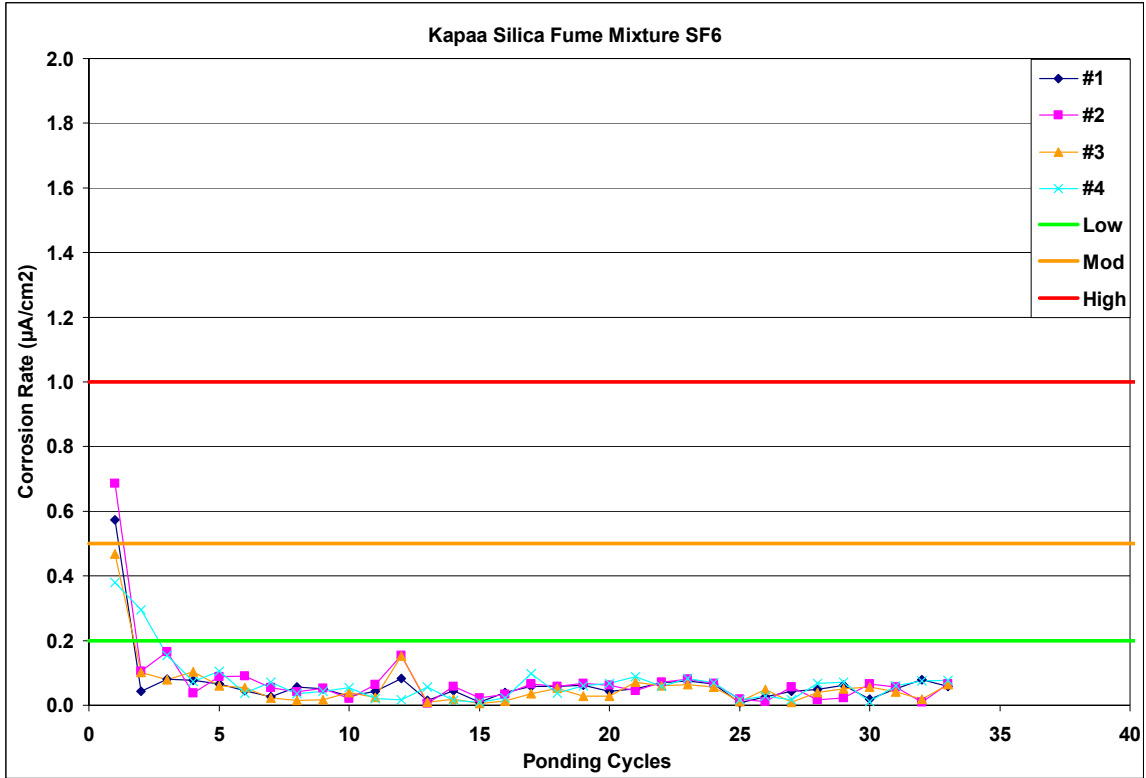


Figure A.1-209: Corrosion Rate Measurements for Kapaa silica fume Mixture SF6

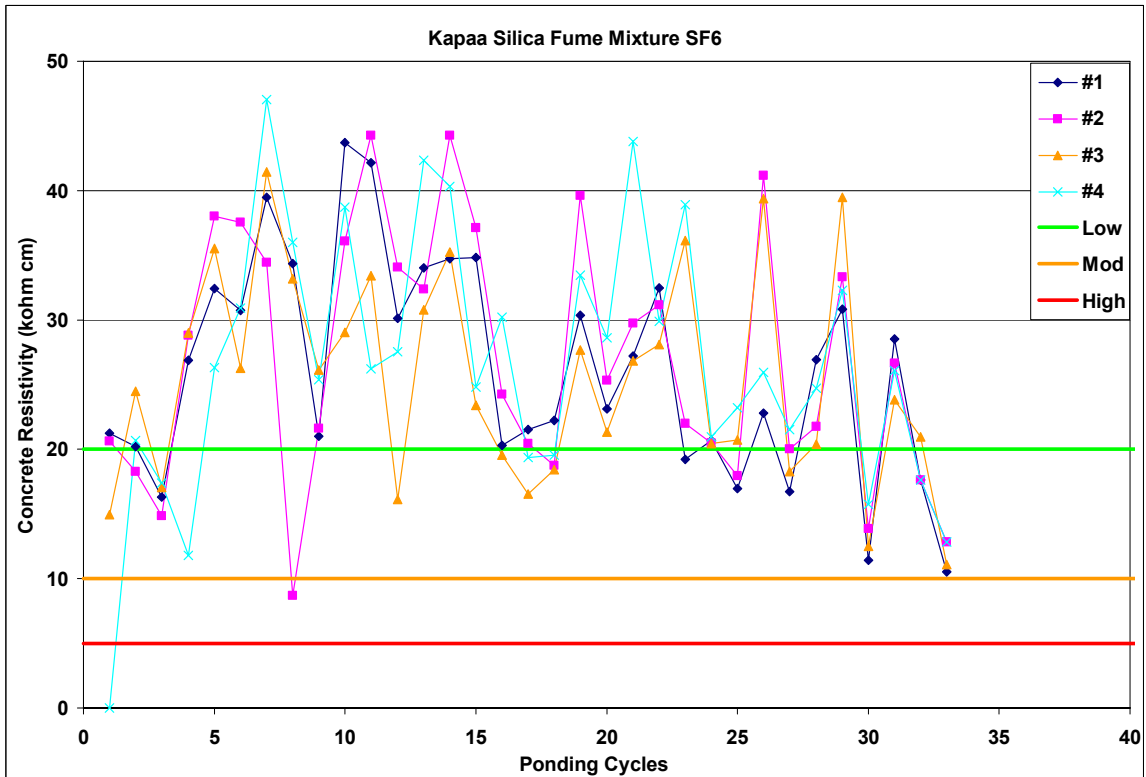


Figure A.1-210: Corrosion Resistivity Measurements for Kapaa silica fume Mixture SF6

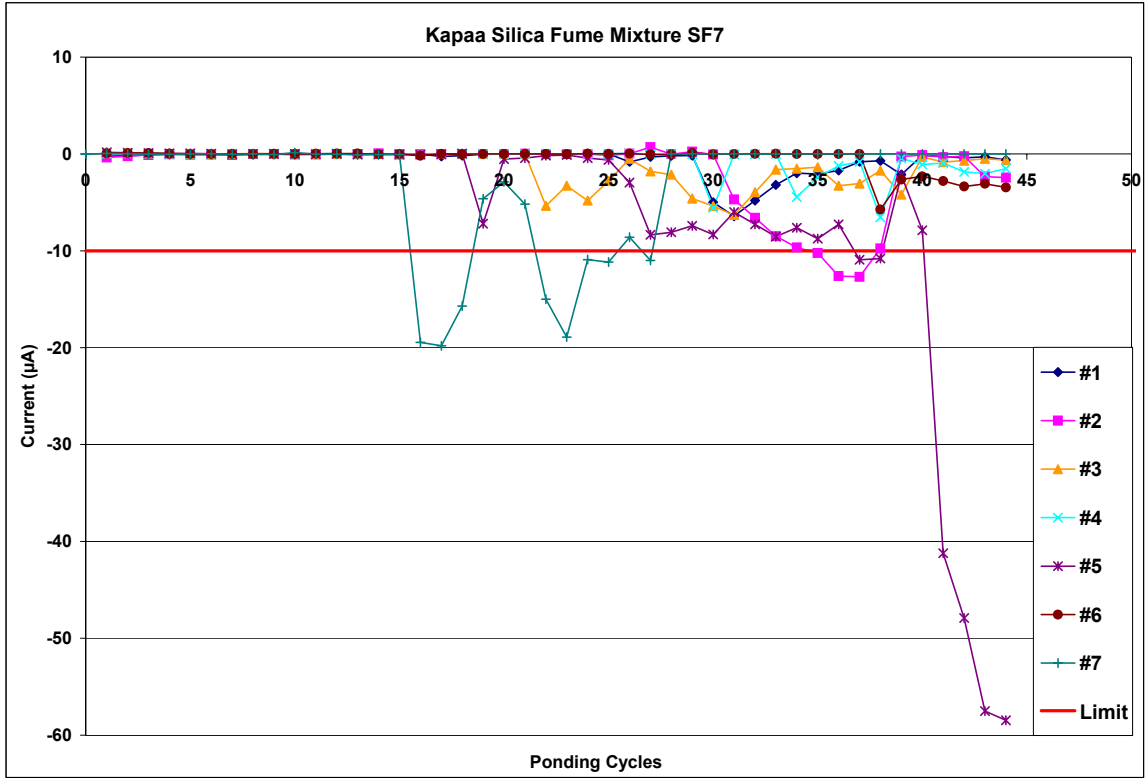


Figure A.1-211: Current Measurements for Kapaa Silica Fume Mixture SF7

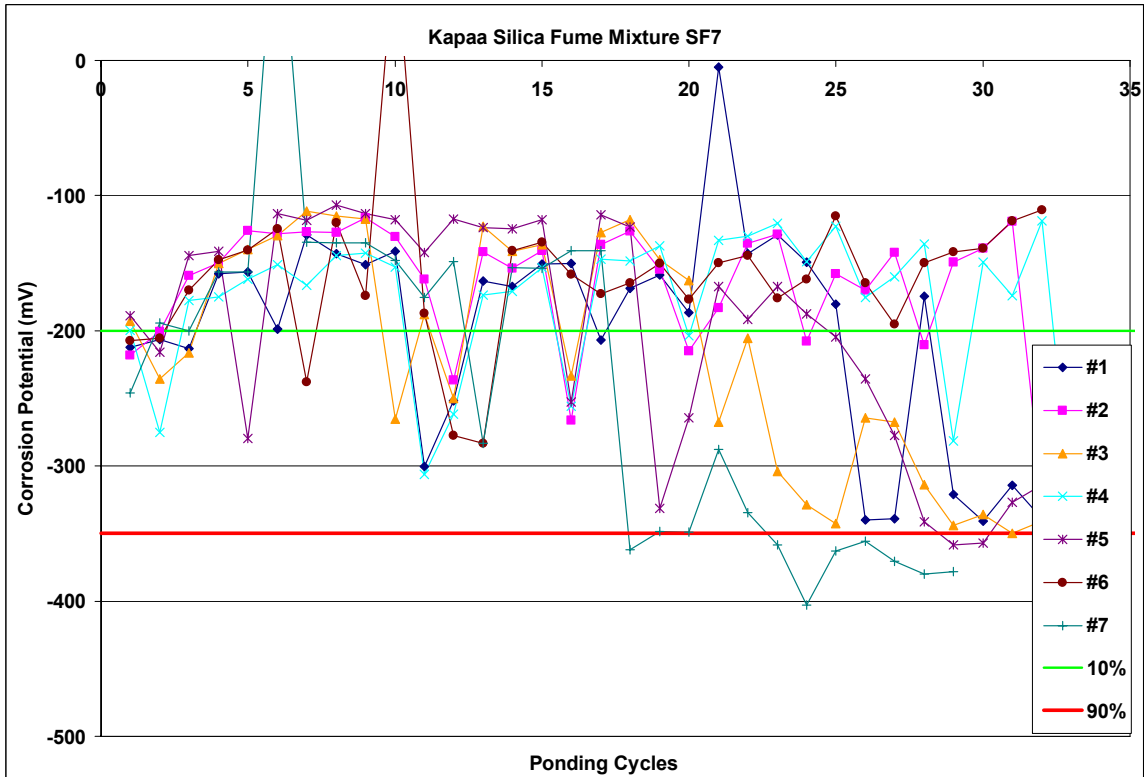


Figure A.1-212: Corrosion Potential Measurements for Kapaa silica fume Mixture SF7

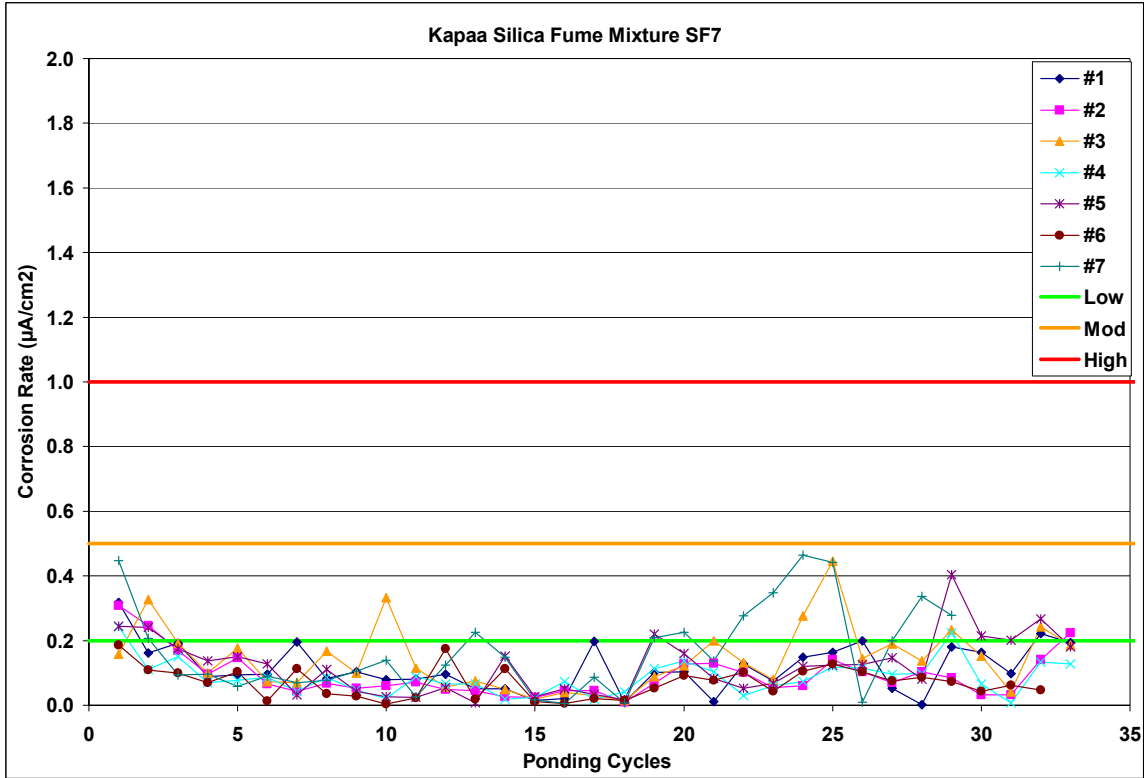


Figure A.1-213: Corrosion Rate Measurements for Kapaa silica fume Mixture SF7

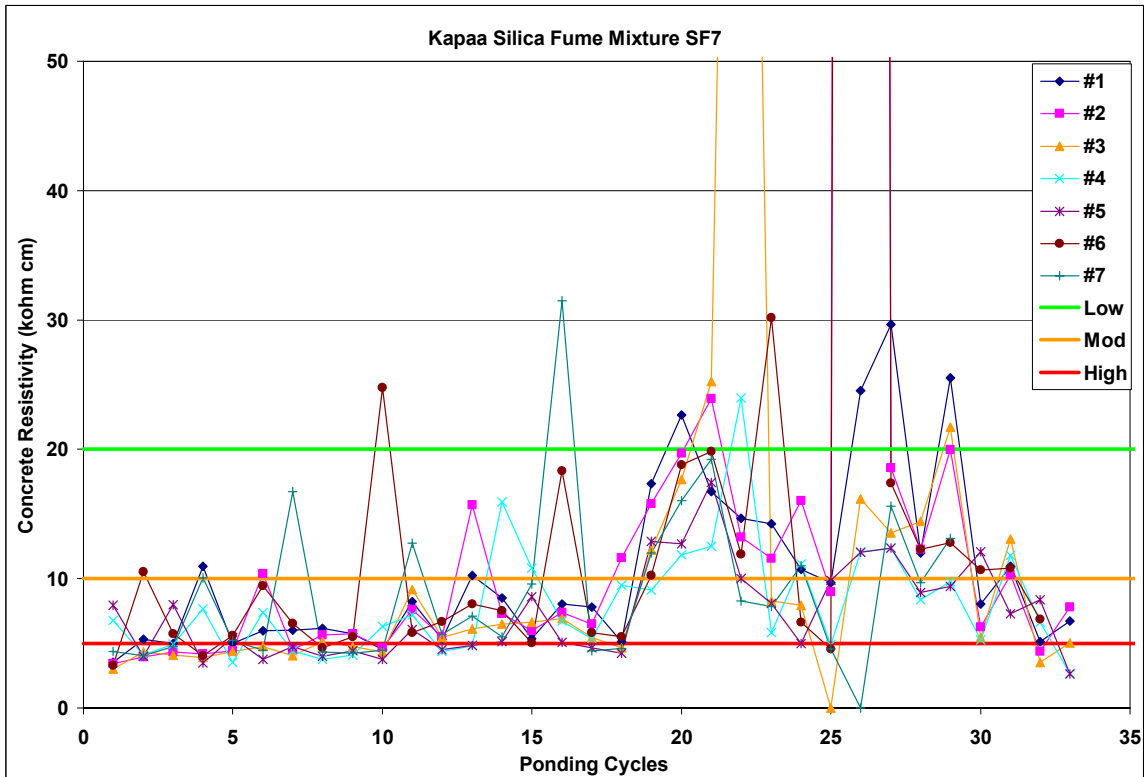


Figure A.1-214: Corrosion Resistivity Measurements for Kapaa silica fume Mixture SF7

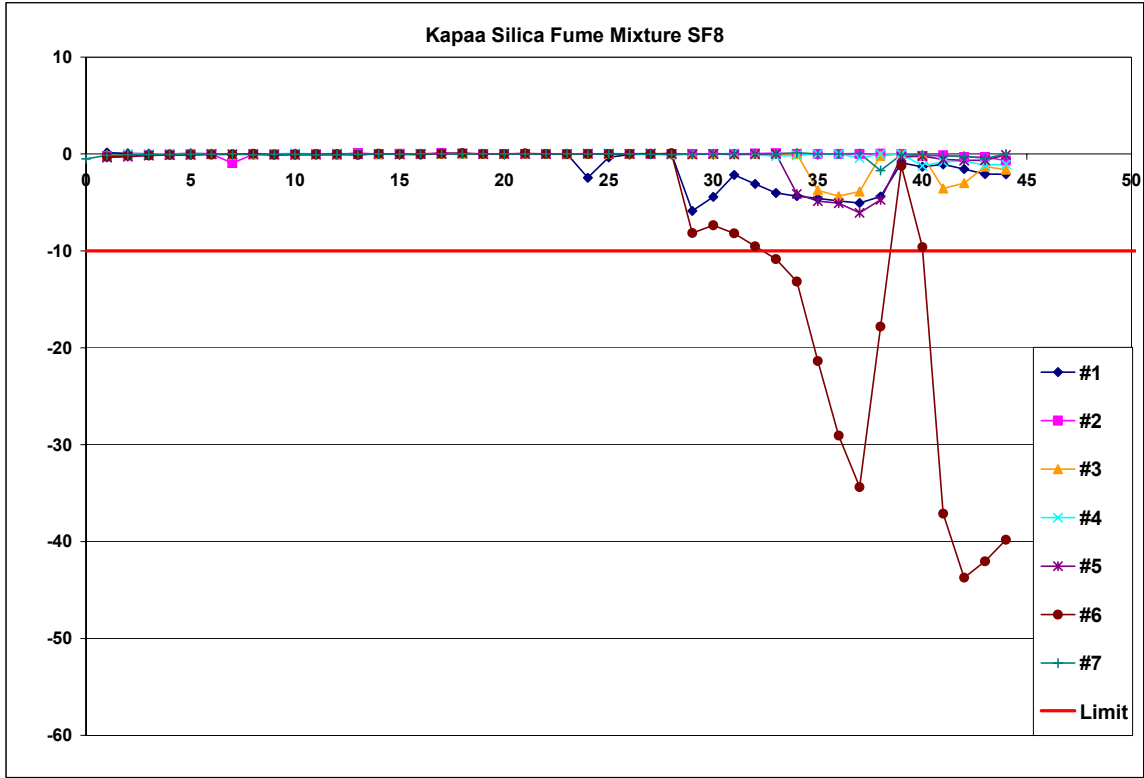


Figure A.1-215: Current Measurements for Kapaa Silica Fume Mixture SF8

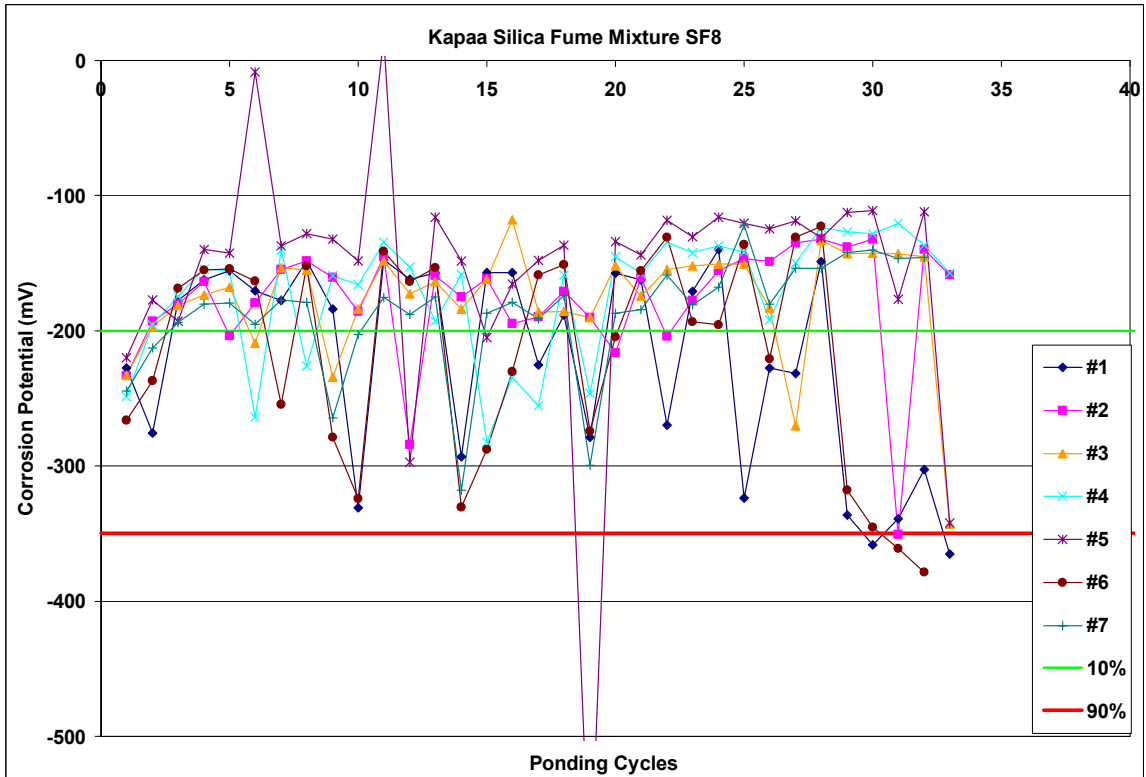


Figure A.1-216: Corrosion Potential Measurements for Kapaa silica fume Mixture SF8

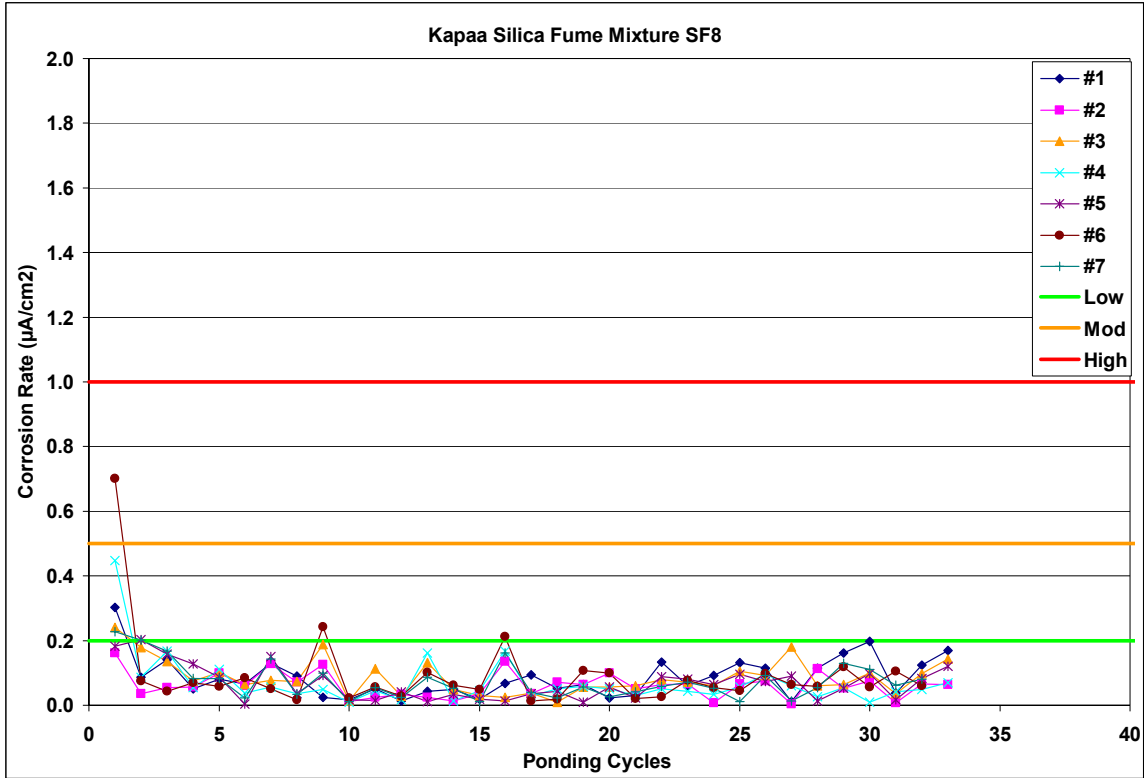


Figure A.1-217: Corrosion Rate Measurements for Kapaa silica fume Mixture SF8

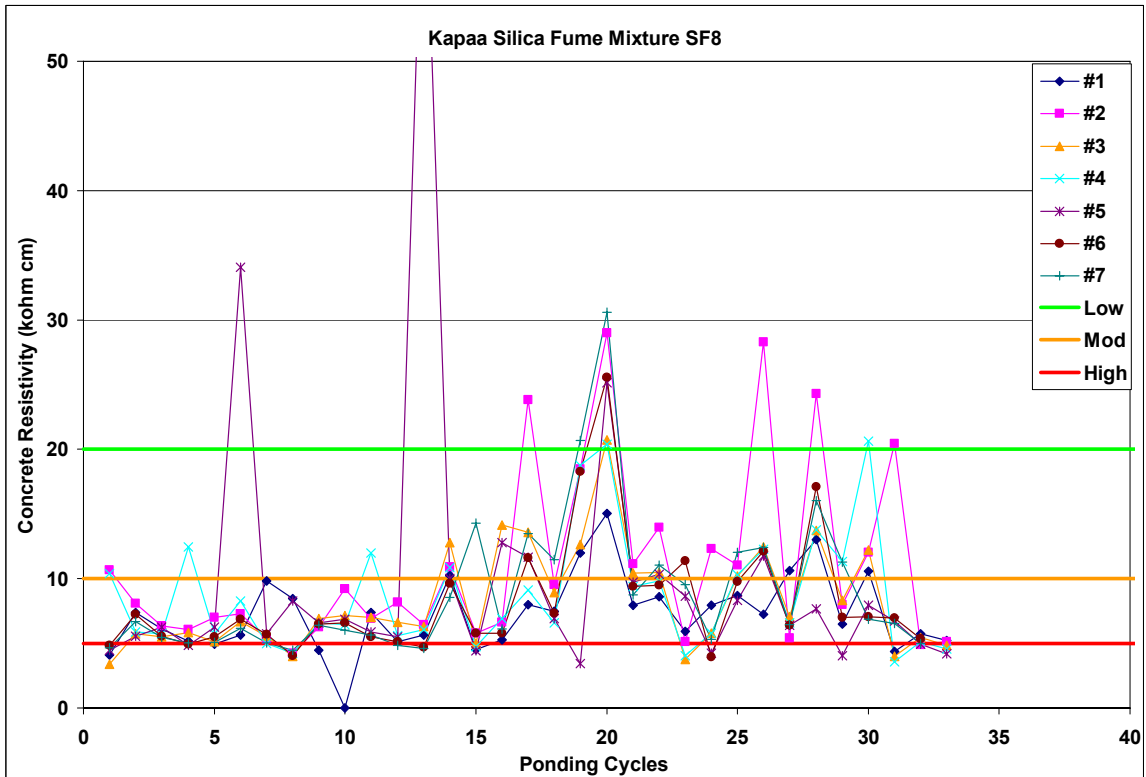


Figure A.1-218: Corrosion Resistivity Measurements for Kapaa silica fume Mixture SF8

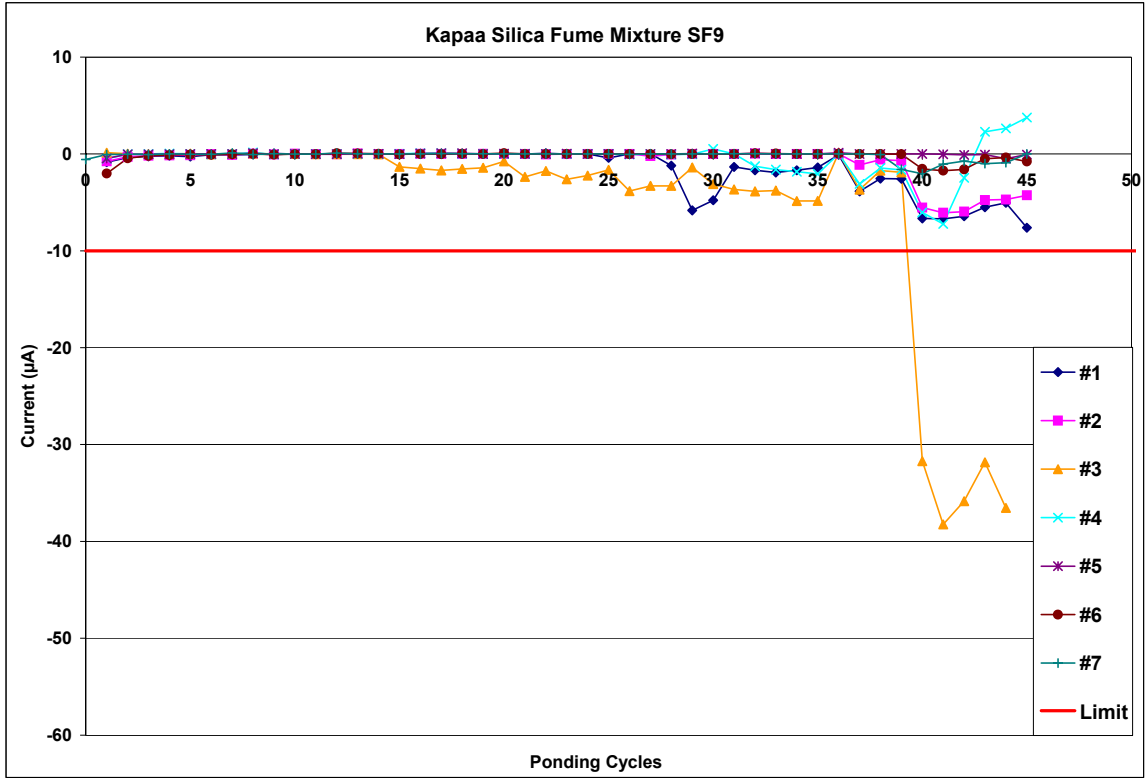


Figure A.1-219: Current Measurements for Kapaa Silica Fume Mixture SF9

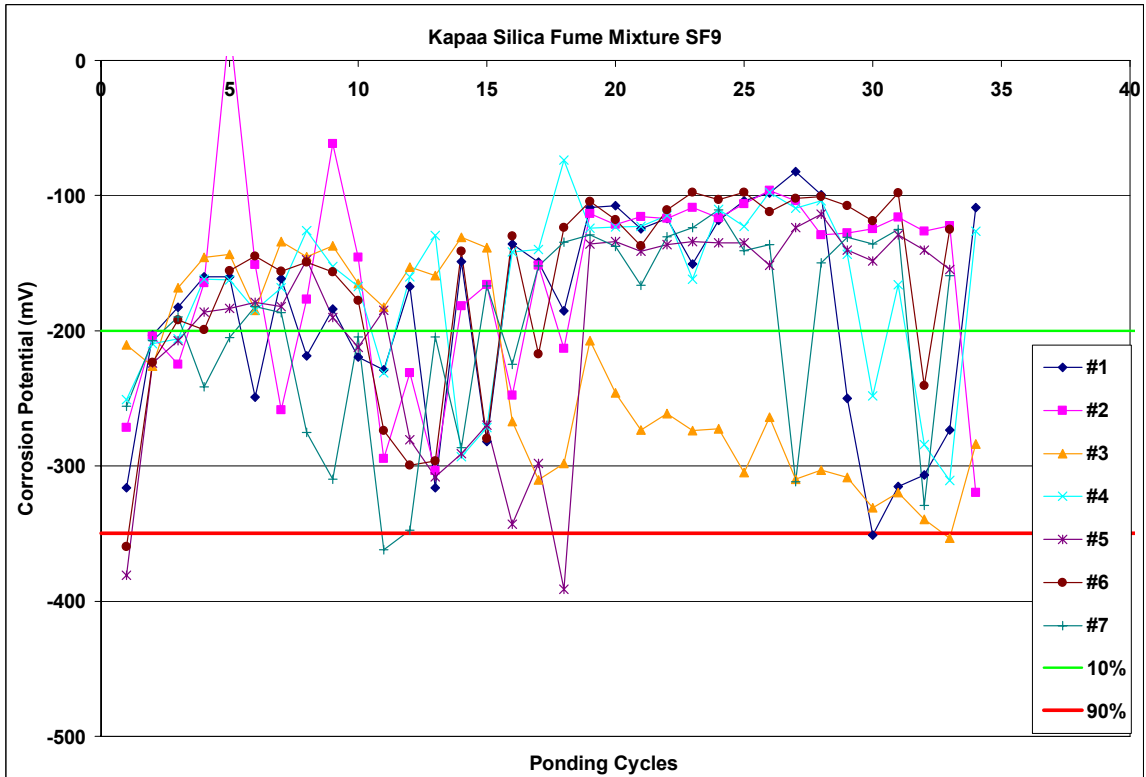


Figure A.1-220: Corrosion Potential Measurements for Kapaa silica fume Mixture SF9

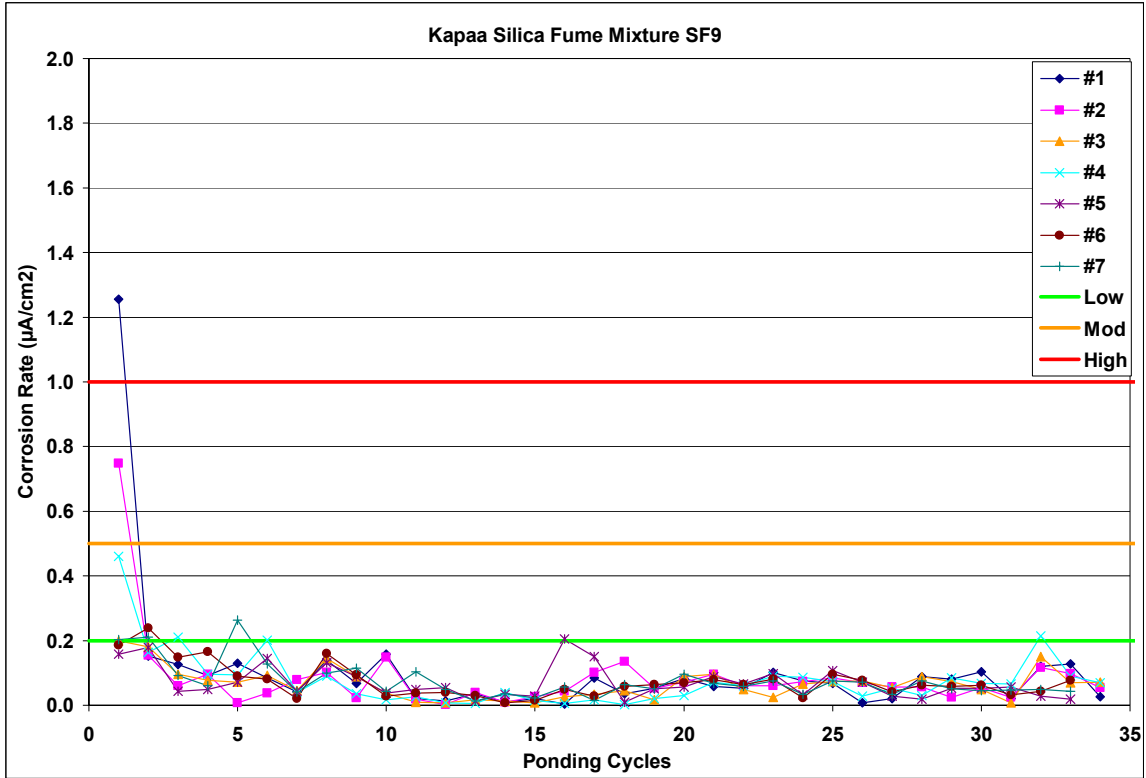


Figure A.1-221: Corrosion Rate Measurements for Kapaa silica fume Mixture SF9

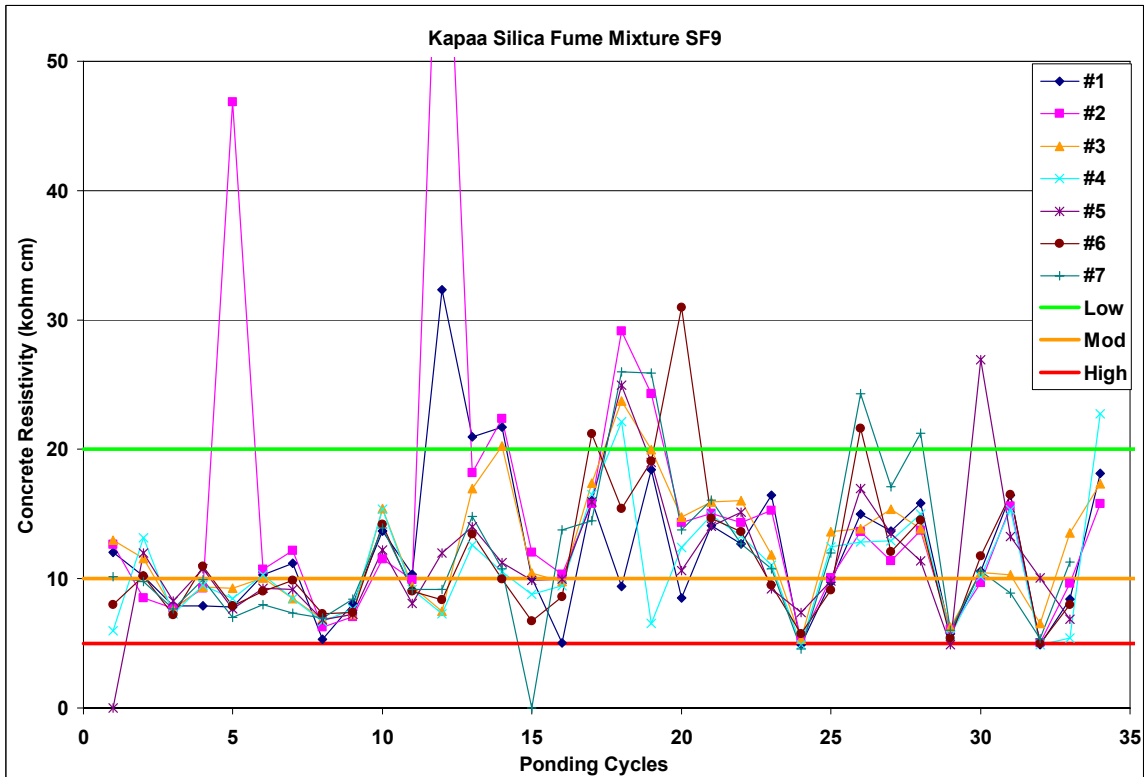


Figure A.1-222: Corrosion Resistivity Measurements for Kapaa silica fume Mixture SF9

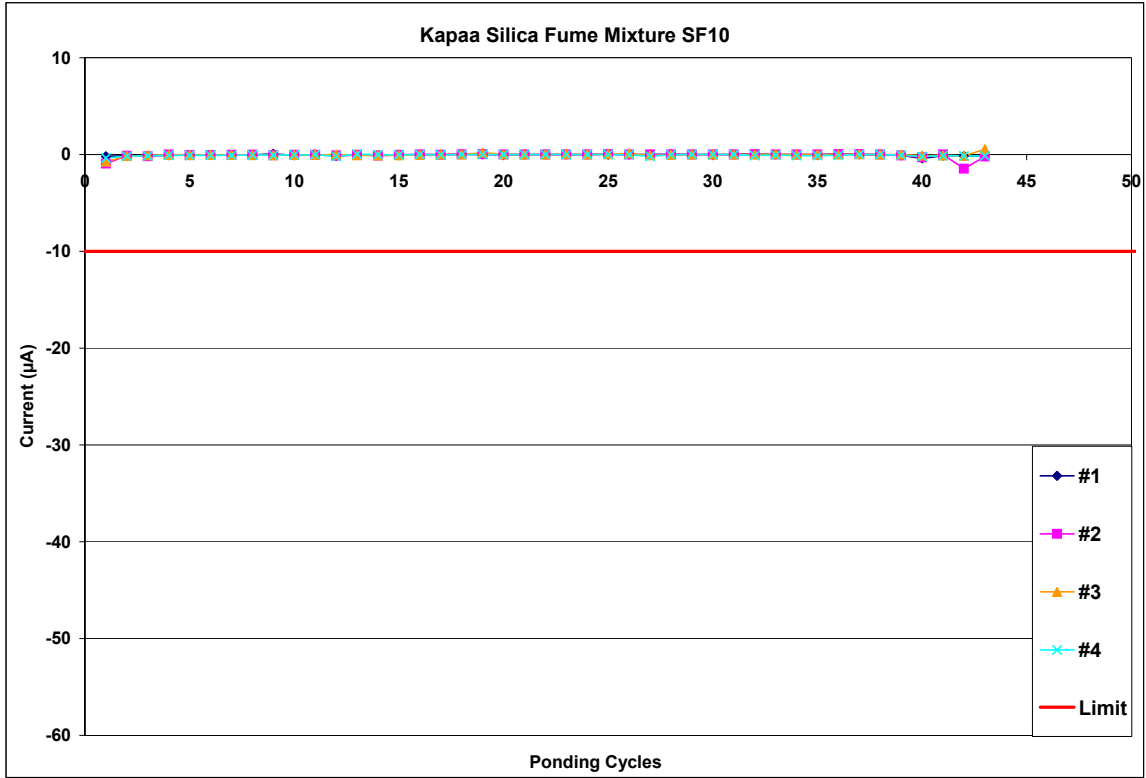


Figure A.1-223: Current Measurements for Kapaa Silica Fume Mixture SF10

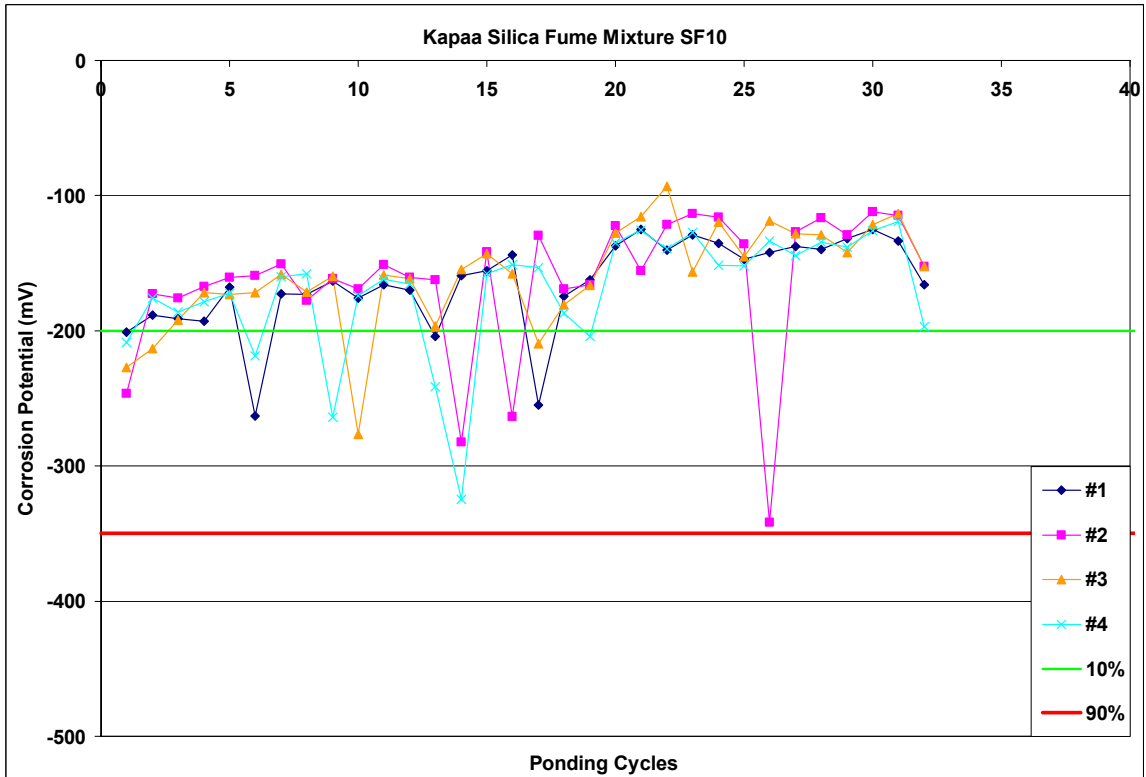


Figure A.1-224: Corrosion Potential Measurements for Kapaa silica fume Mixture SF10

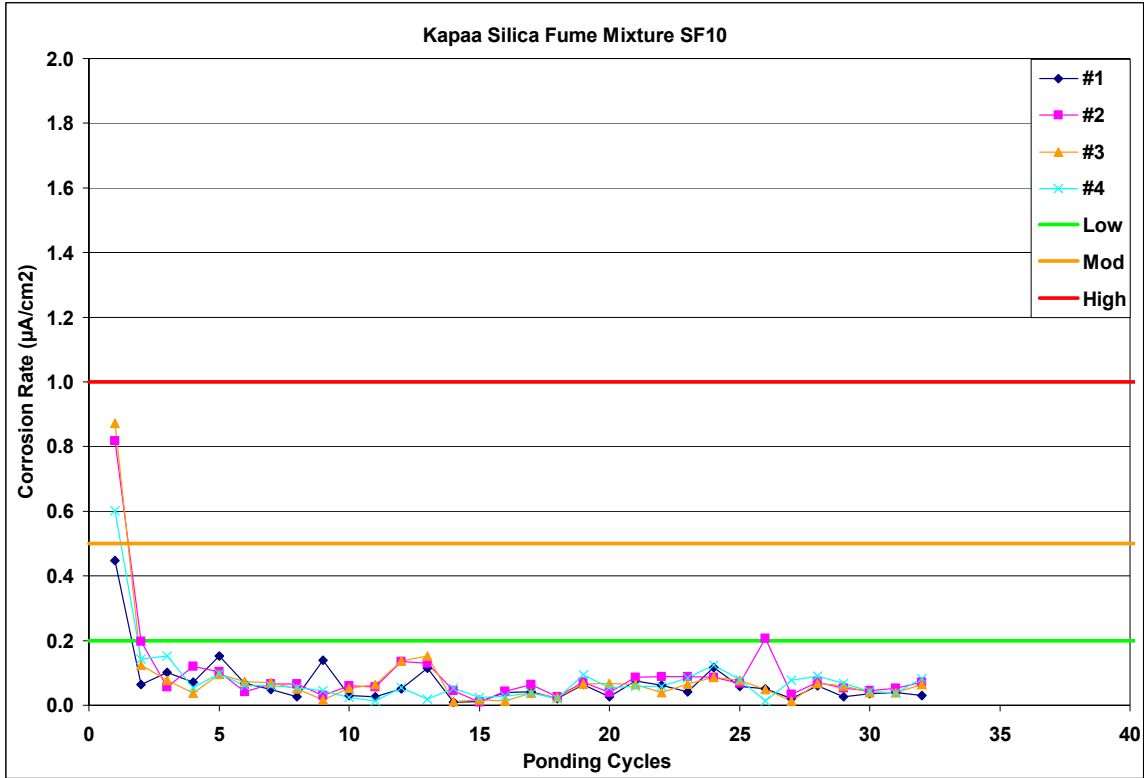


Figure A.1-225: Corrosion Rate Measurements for Kapaa silica fume Mixture SF10

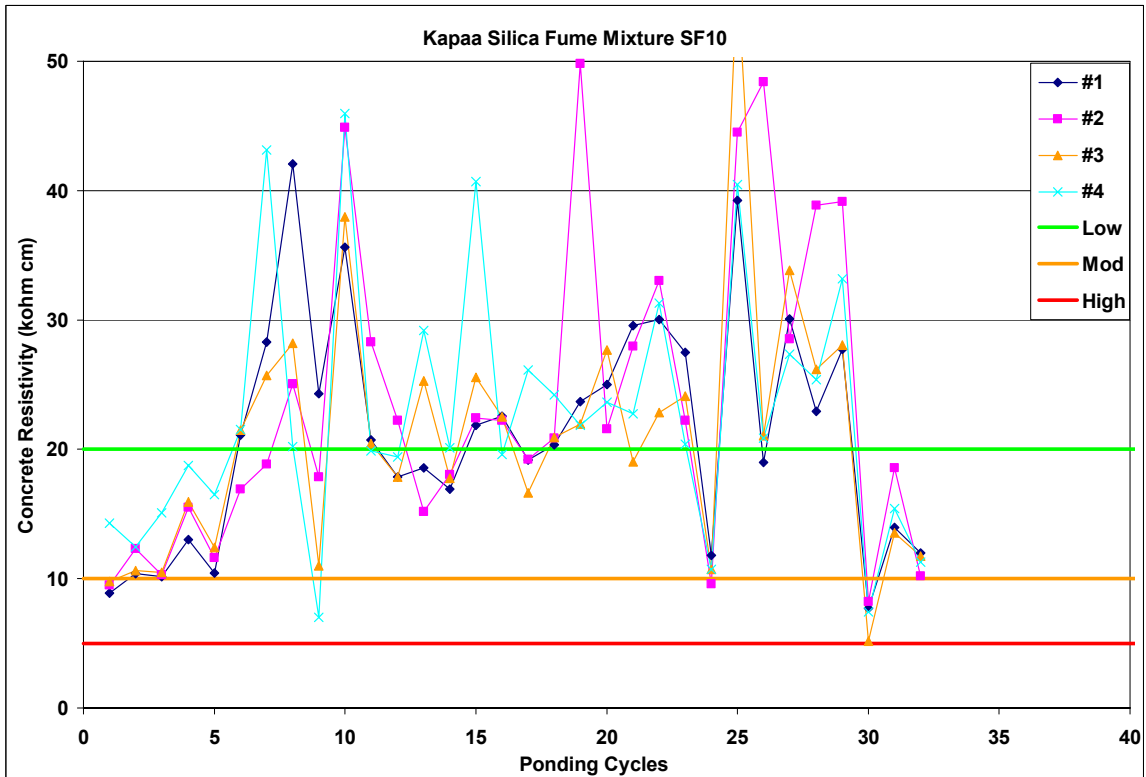


Figure A.1-226: Corrosion Resistivity Measurements for Kapaa silica fume Mix SF10

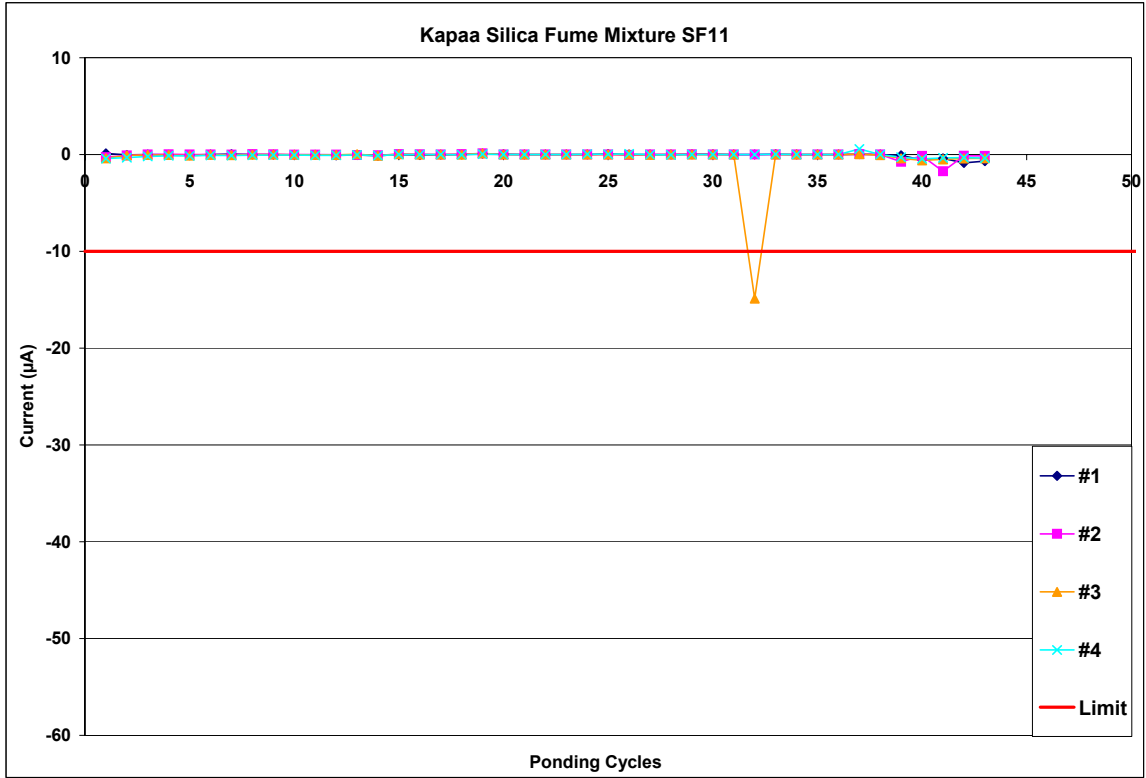


Figure A.1-227: Current Measurements for Kapaa Silica Fume Mixture SF11

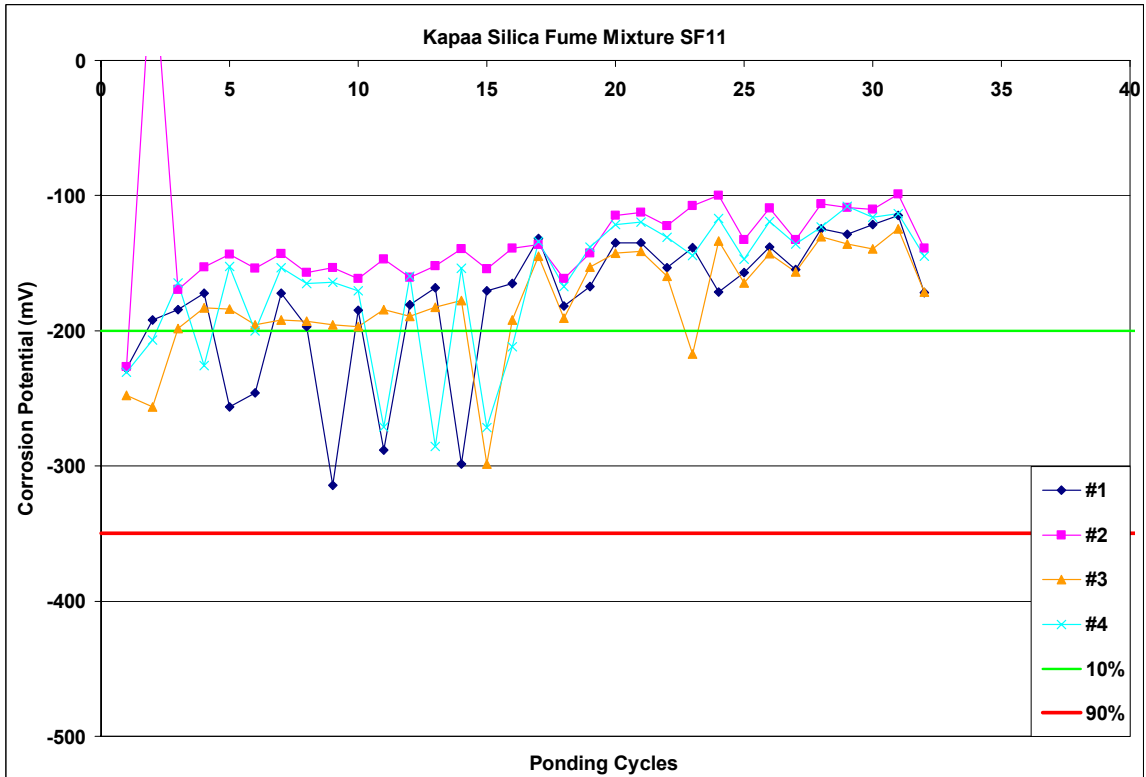


Figure A.1-228: Corrosion Potential Measurements for Kapaa silica fume Mixture SF11

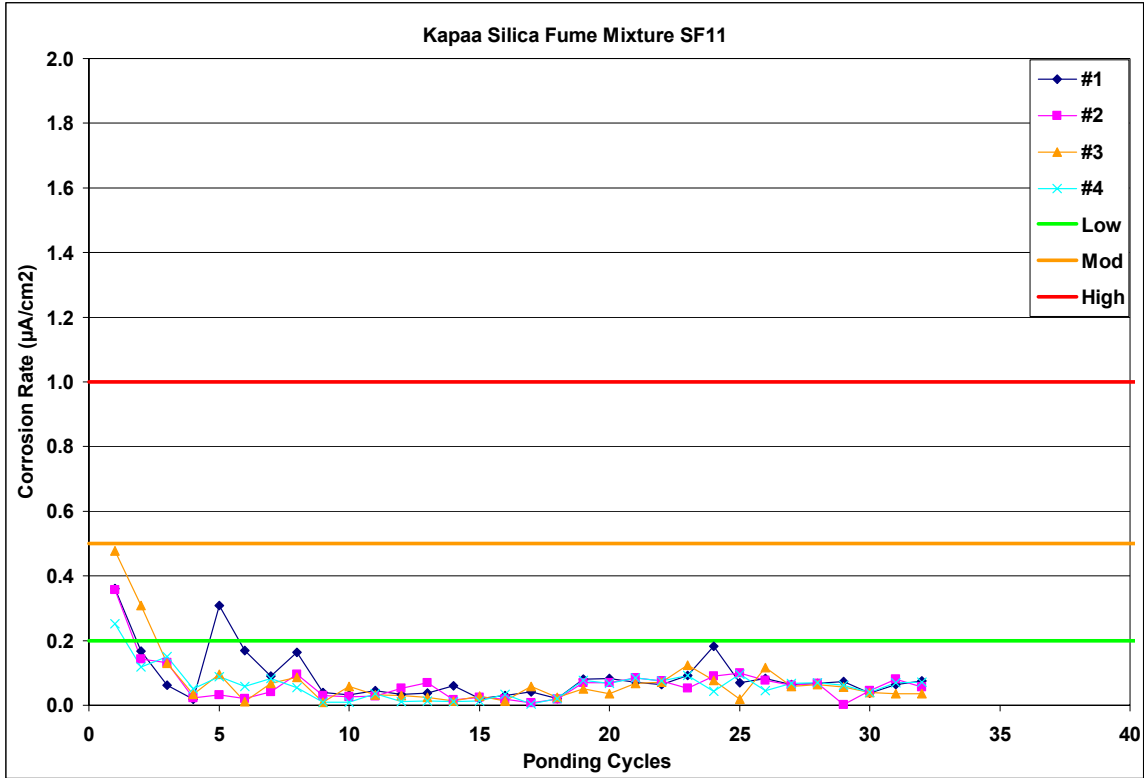


Figure A.1-229: Corrosion Rate Measurements for Kapaa silica fume Mixture SF11

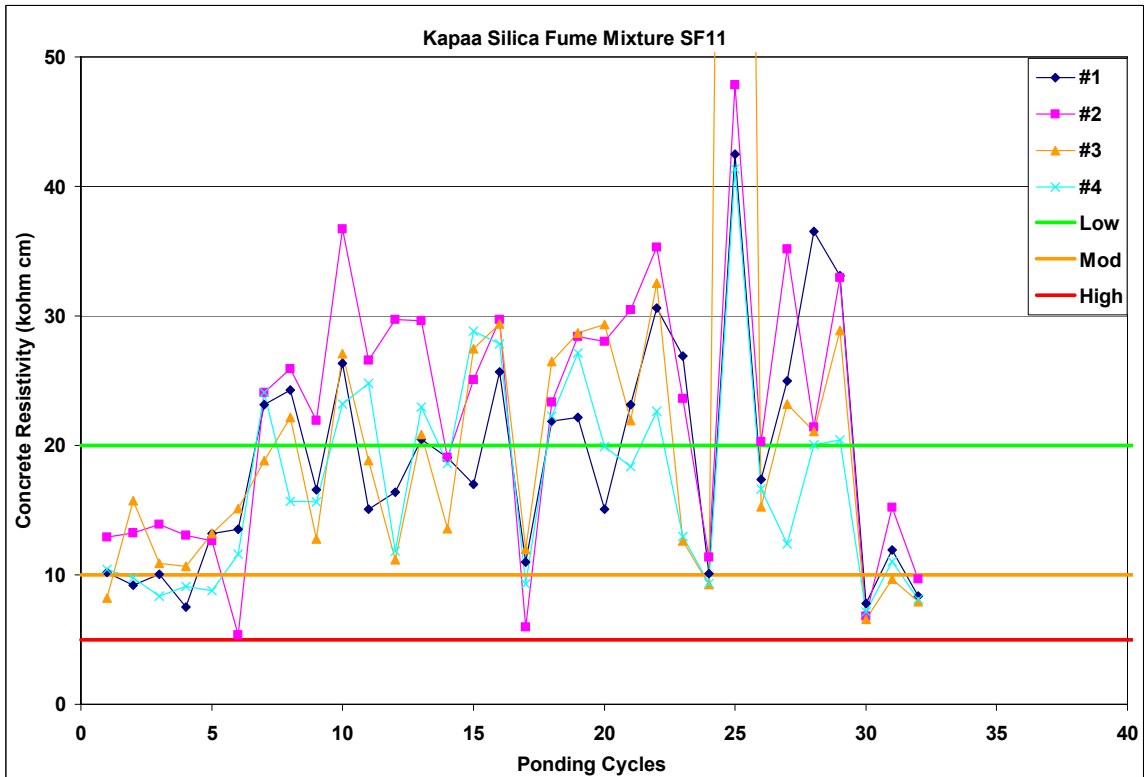


Figure A.1-230: Corrosion Resistivity Measurements for Kapaa SF Mixture SF11

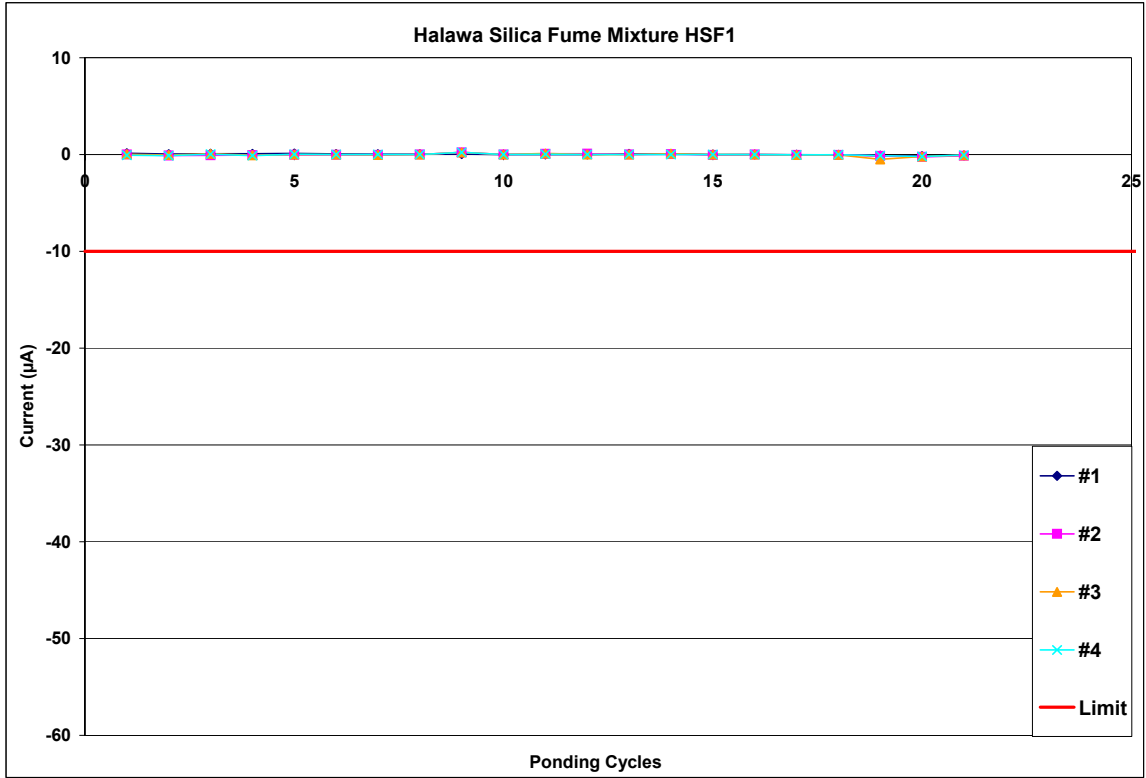


Figure A.1-231: Current Measurements for Halawa Silica Fume Mixture HSF1

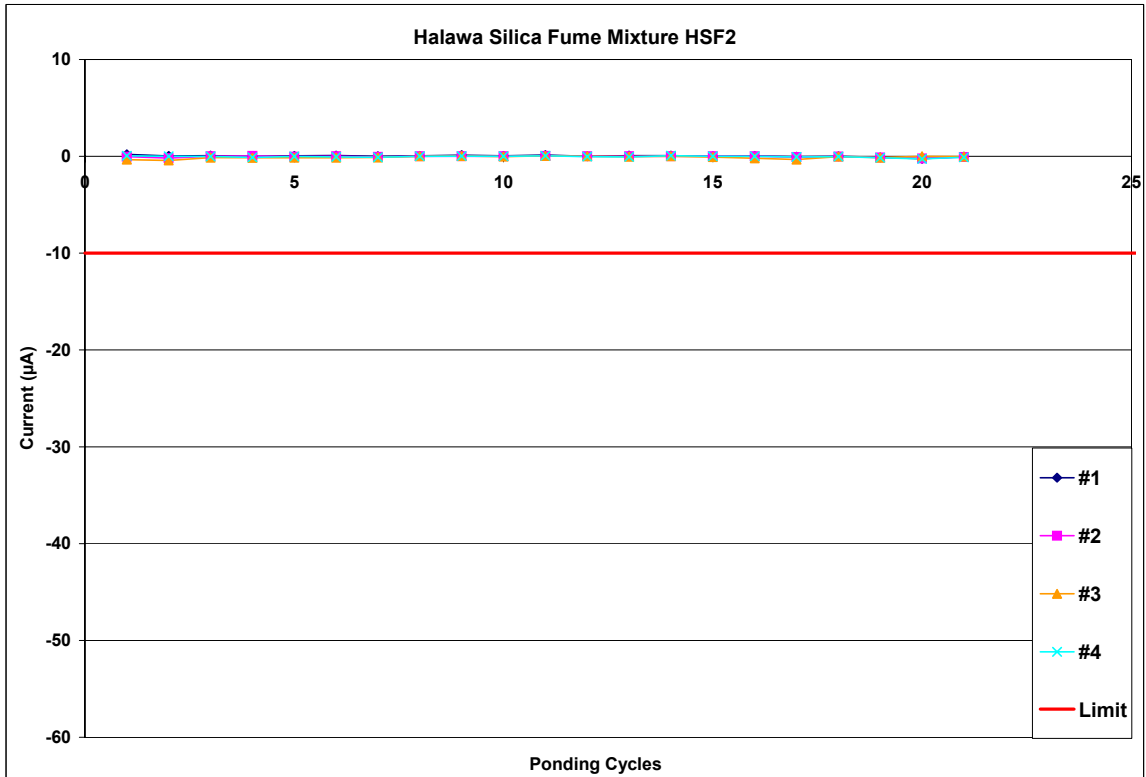


Figure A.1-232: Current Measurements for Halawa Silica Fume Mixture HSF2

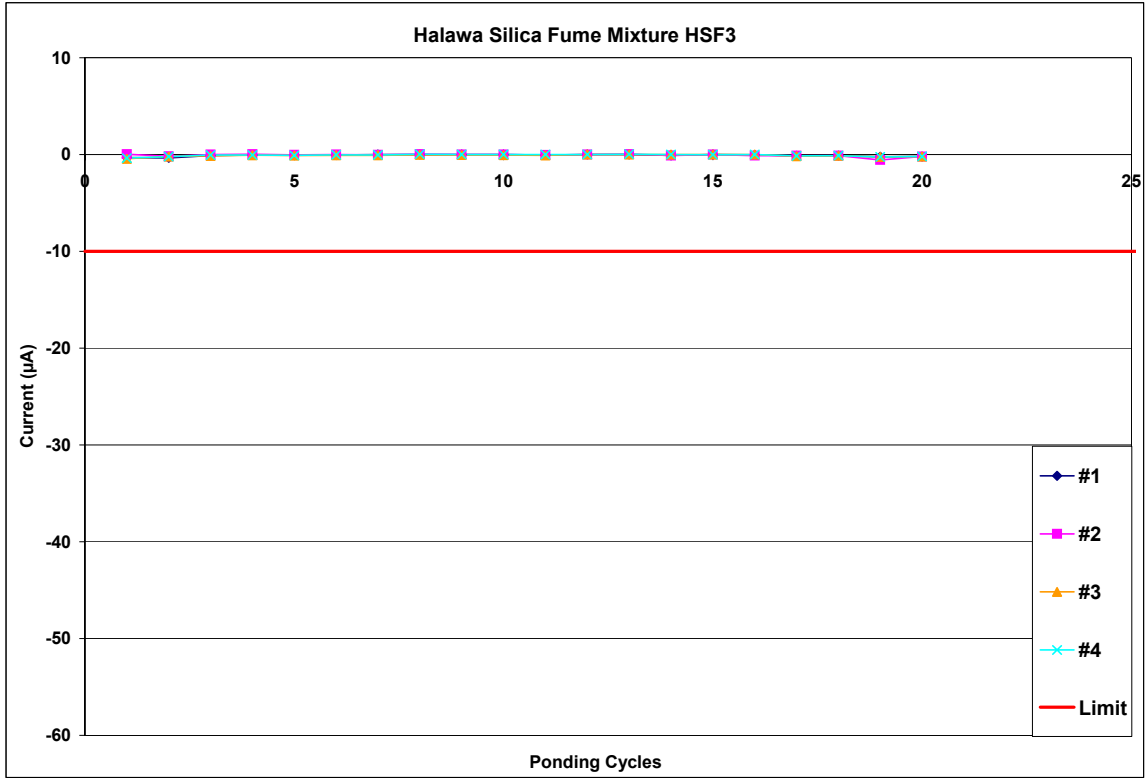


Figure A.1-233: Current Measurements for Halawa Silica Fume Mixture HSF3

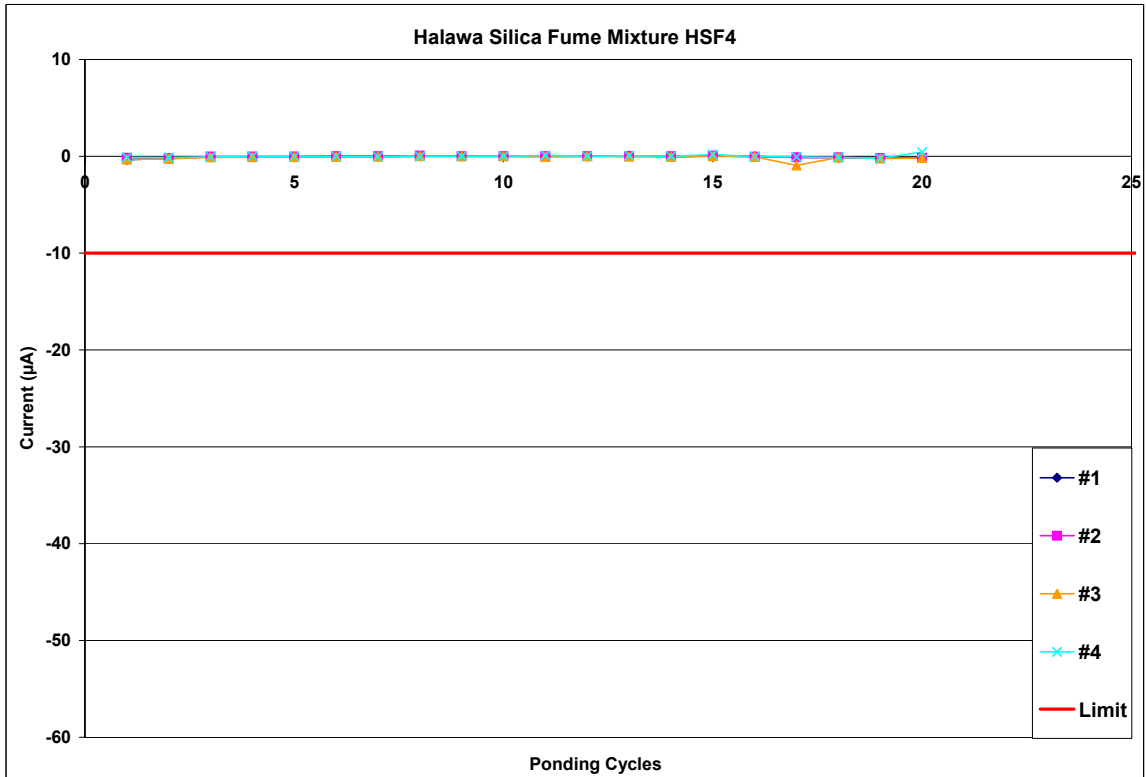


Figure A.1-234: Current Measurements for Halawa Silica Fume Mixture HSF4

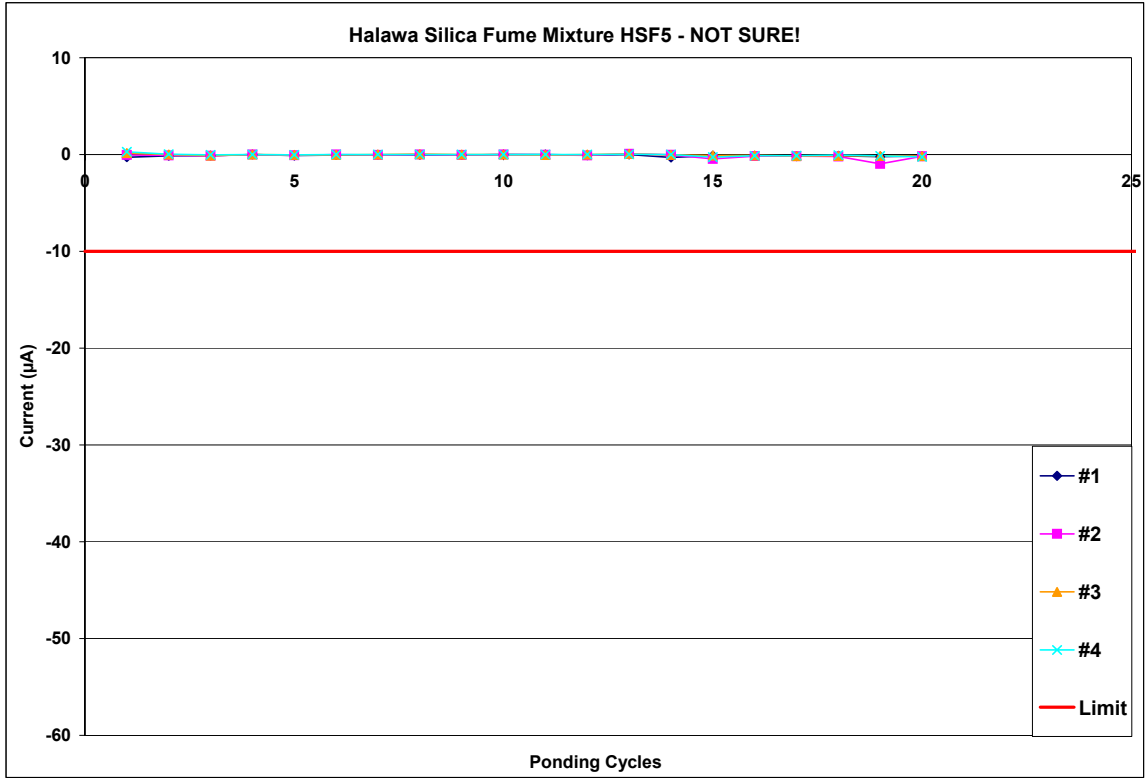


Figure A.1-235: Current Measurements for Halawa Silica Fume Mixture HSF5

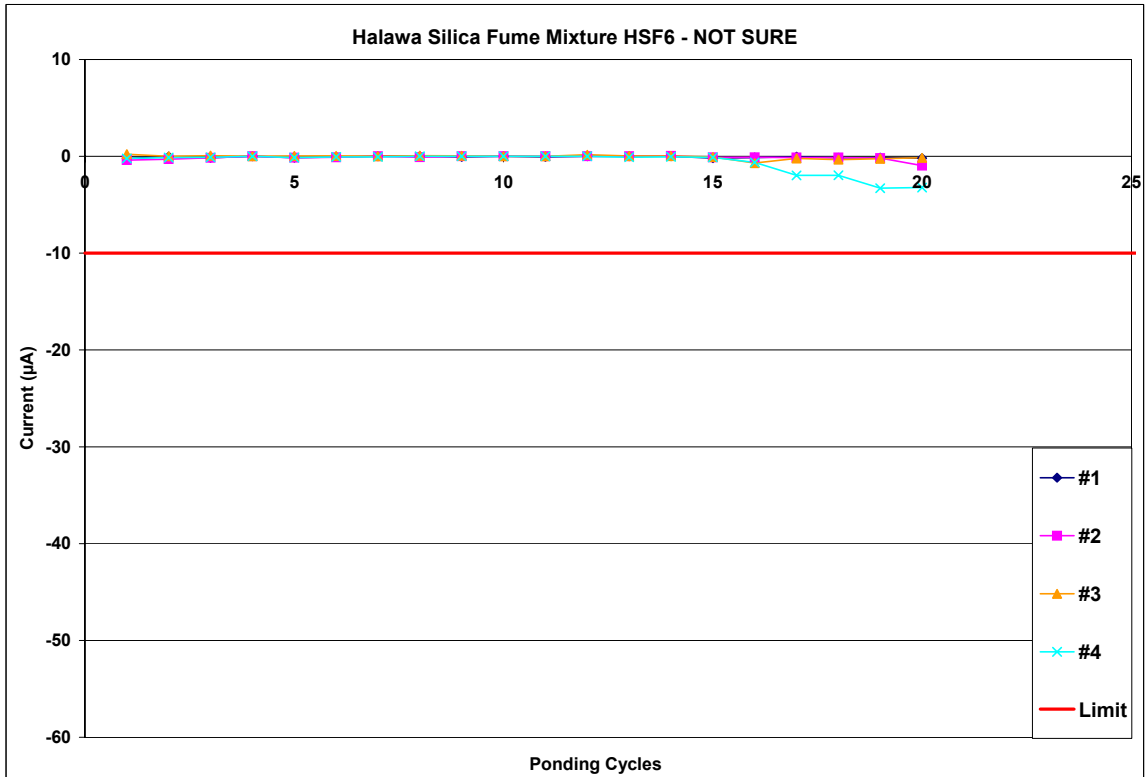


Figure A.1-236: Current Measurements for Halawa Silica Fume Mixture HSF6

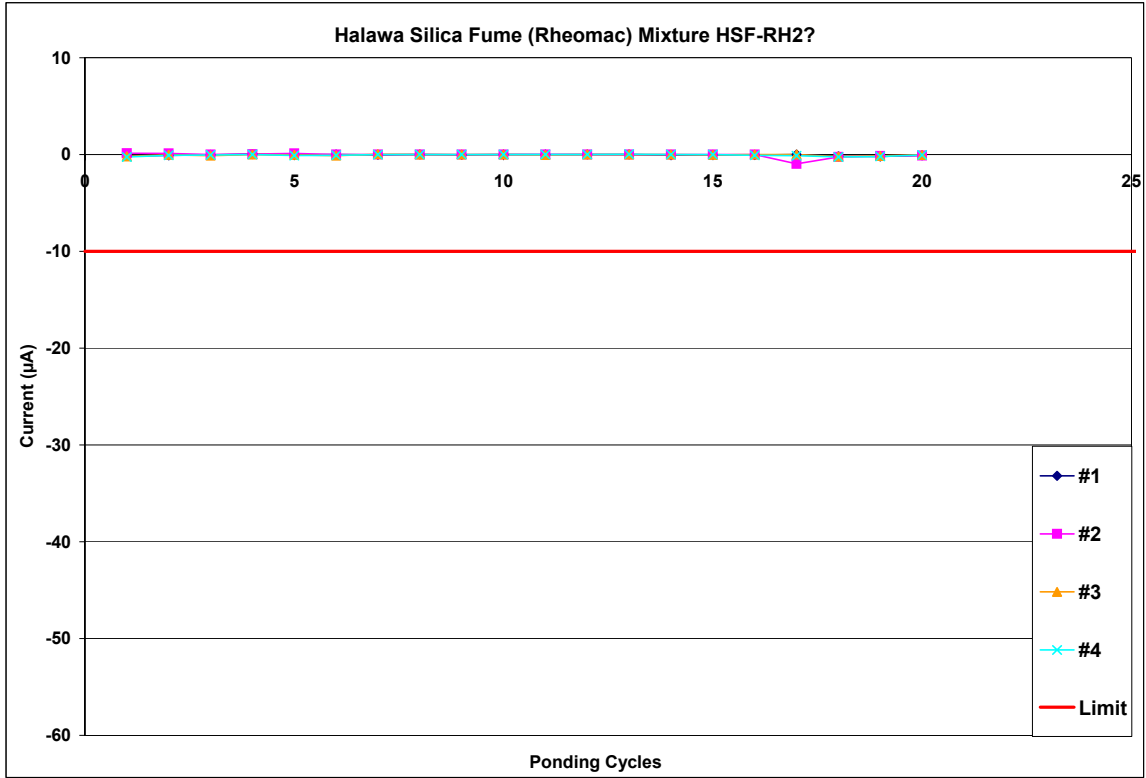


Figure A.1-237: Current Measurements for Halawa Rheomac Mixture HSF-RH2

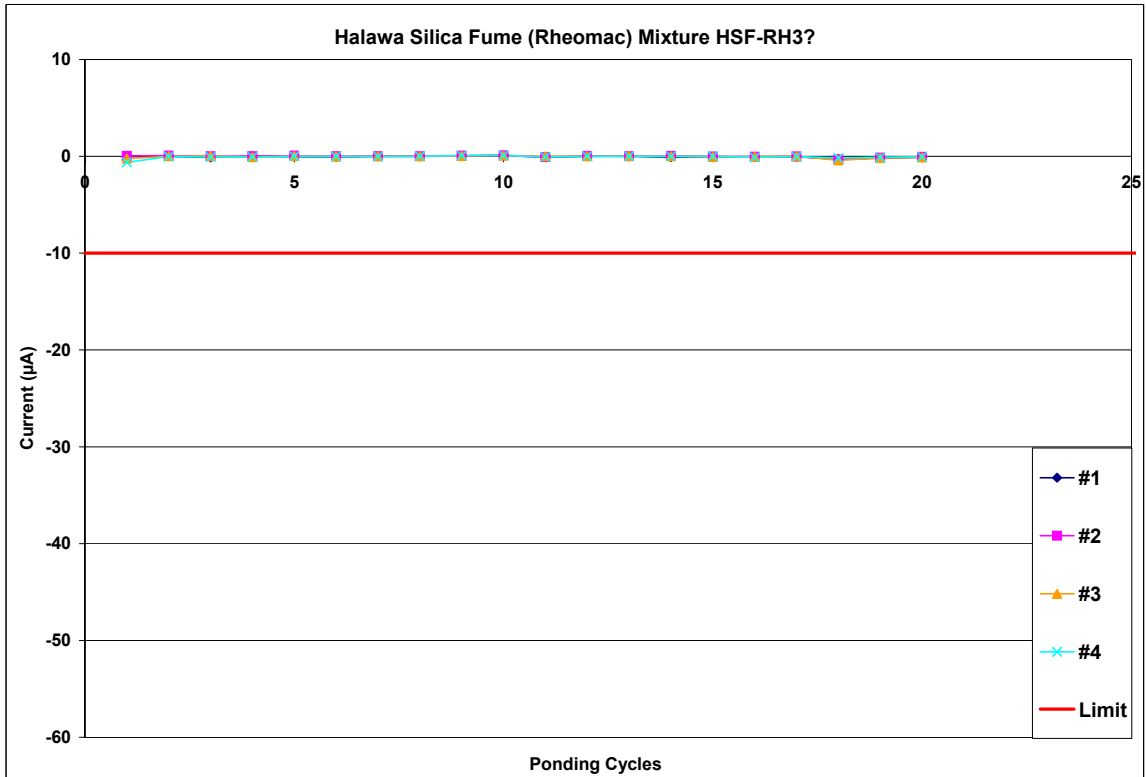


Figure A.1-238: Current Measurements for Halawa Rheomac Mixture HSF-RH3

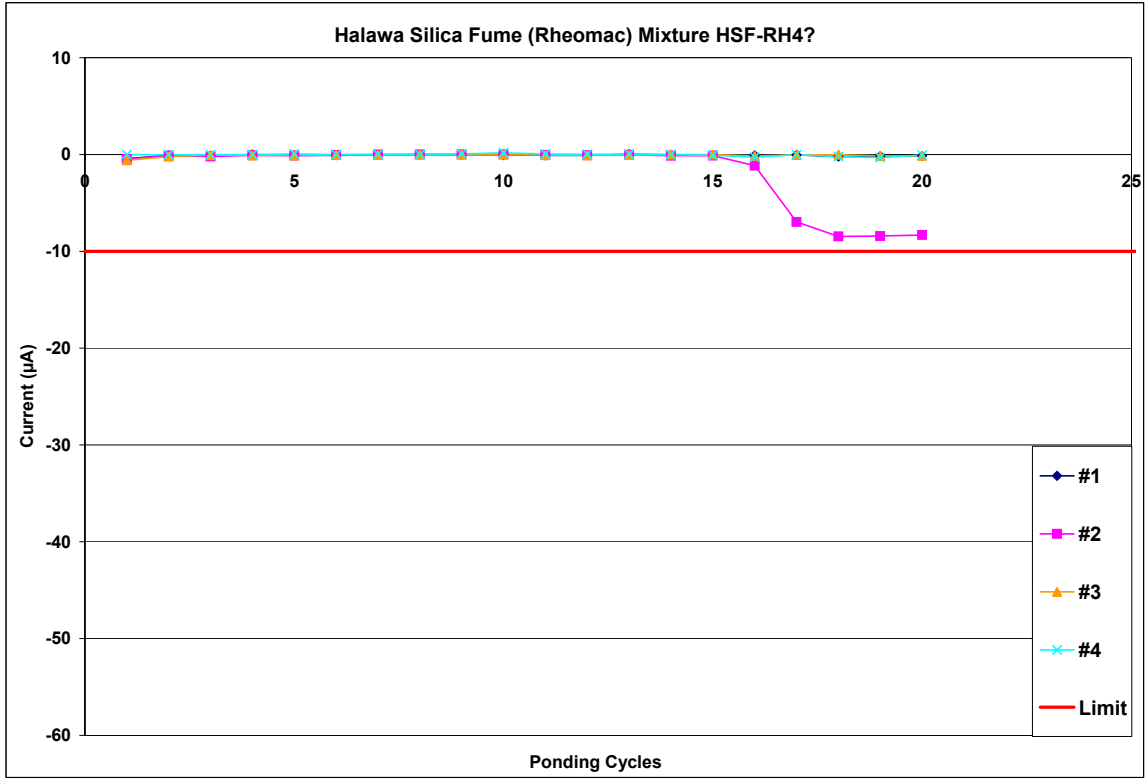


Figure A.1-239: Current Measurements for Halawa Rheomac Mixture HSF-RH4

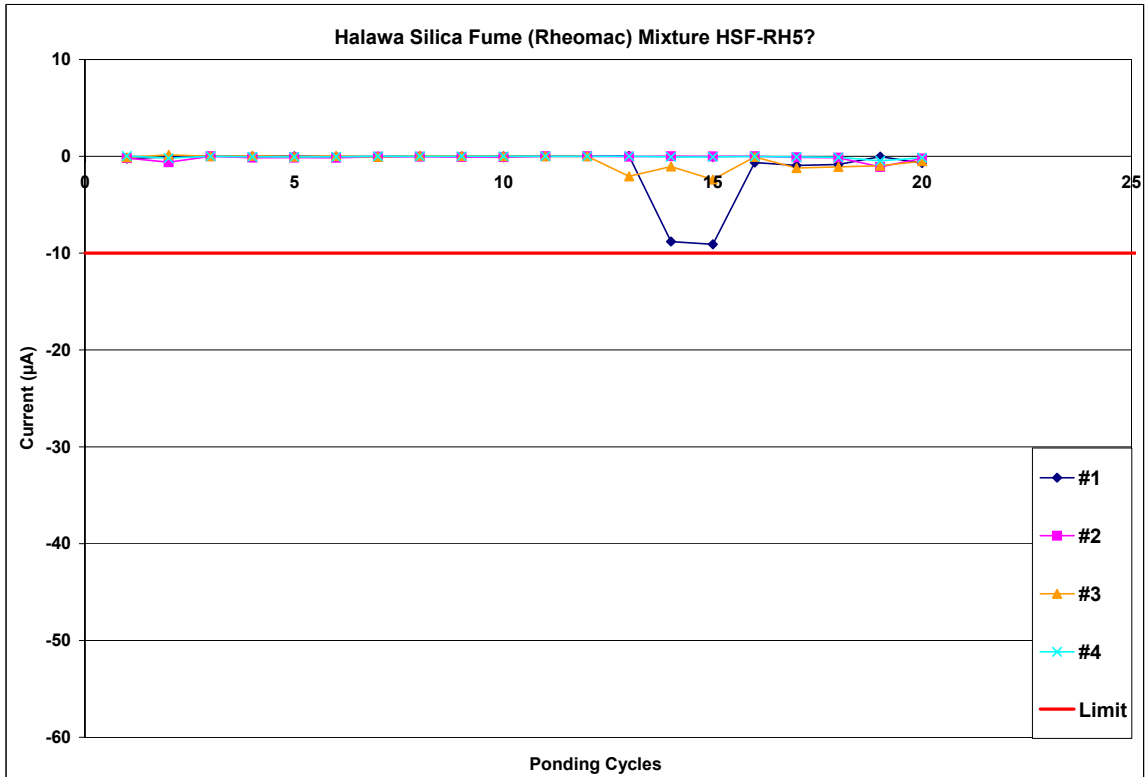


Figure A.1-240: Current Measurements for Halawa Rheomac Mixture HSF-RH5

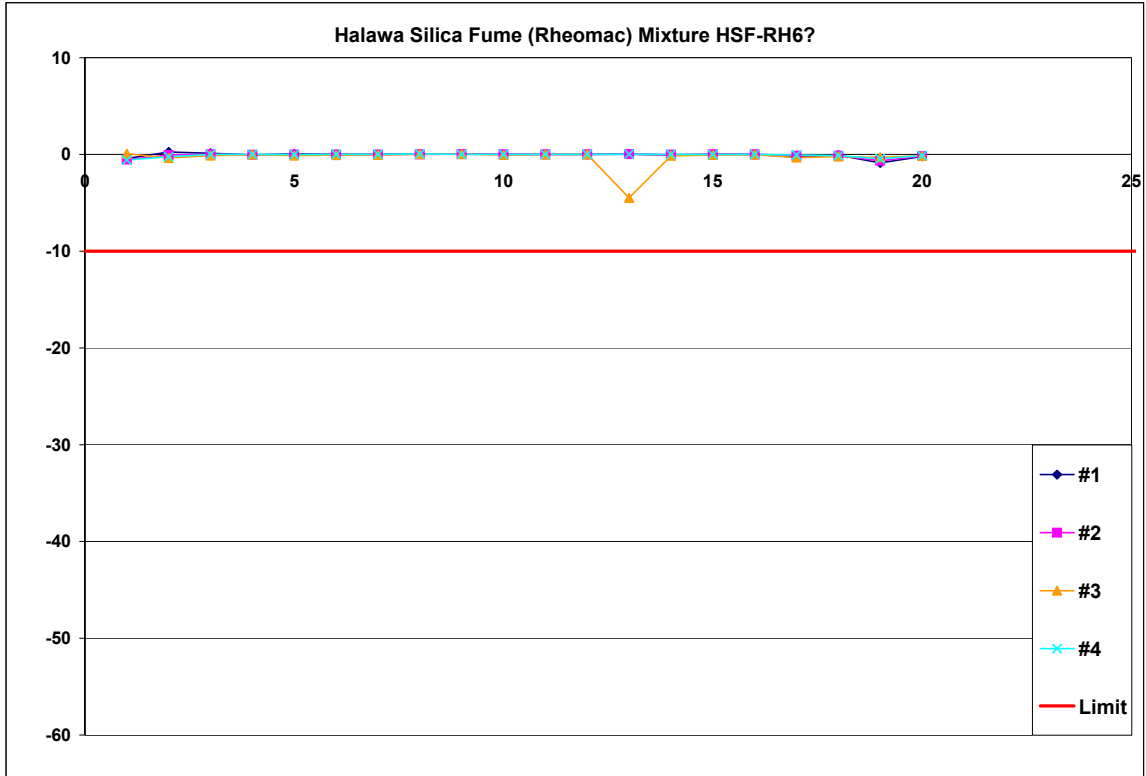


Figure A.1-241: Current Measurements for Halawa Rheomac Mixture HSF-RH6

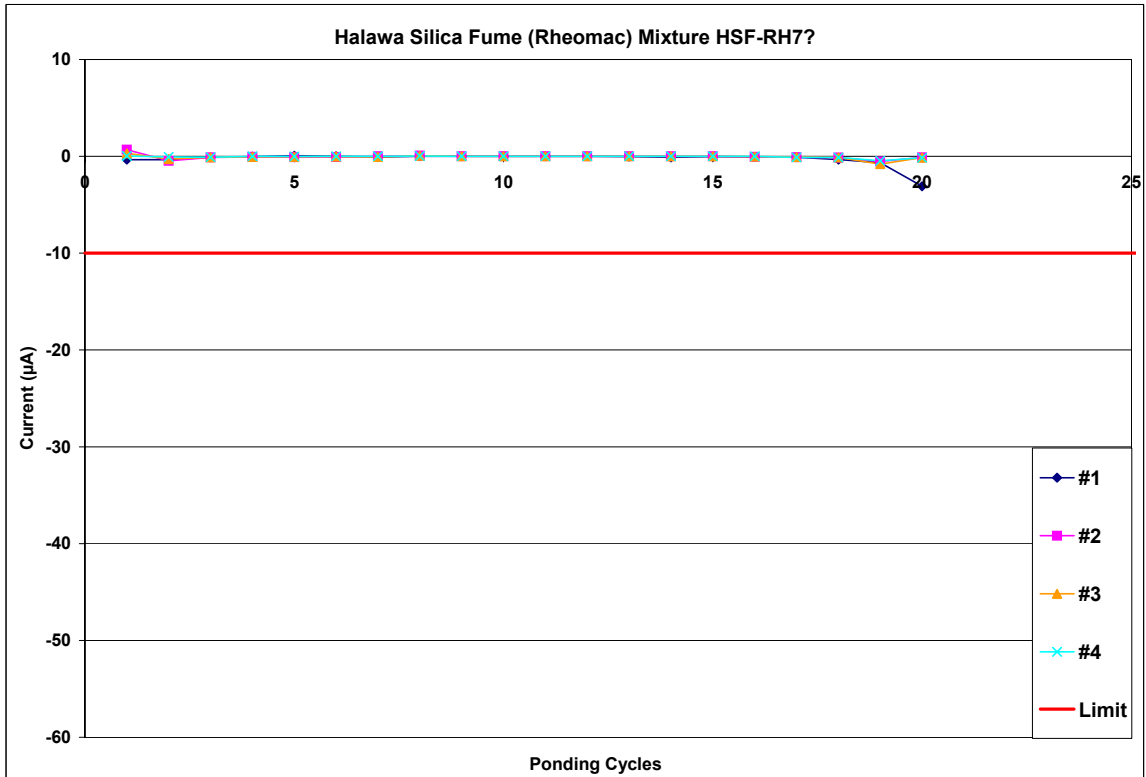


Figure A.1-242: Current Measurements for Halawa Rheomac Mixture HSF-RH7

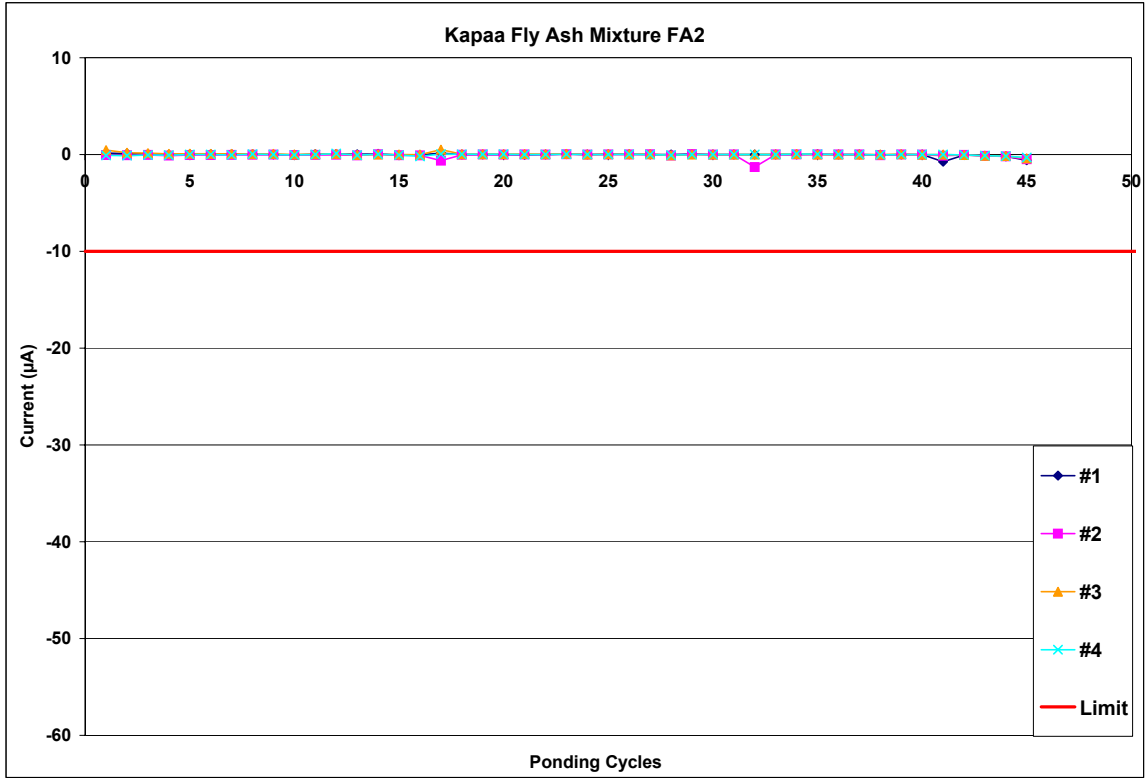


Figure A.1-243: Current Measurements for Kapaa Fly Ash Mixture FA2

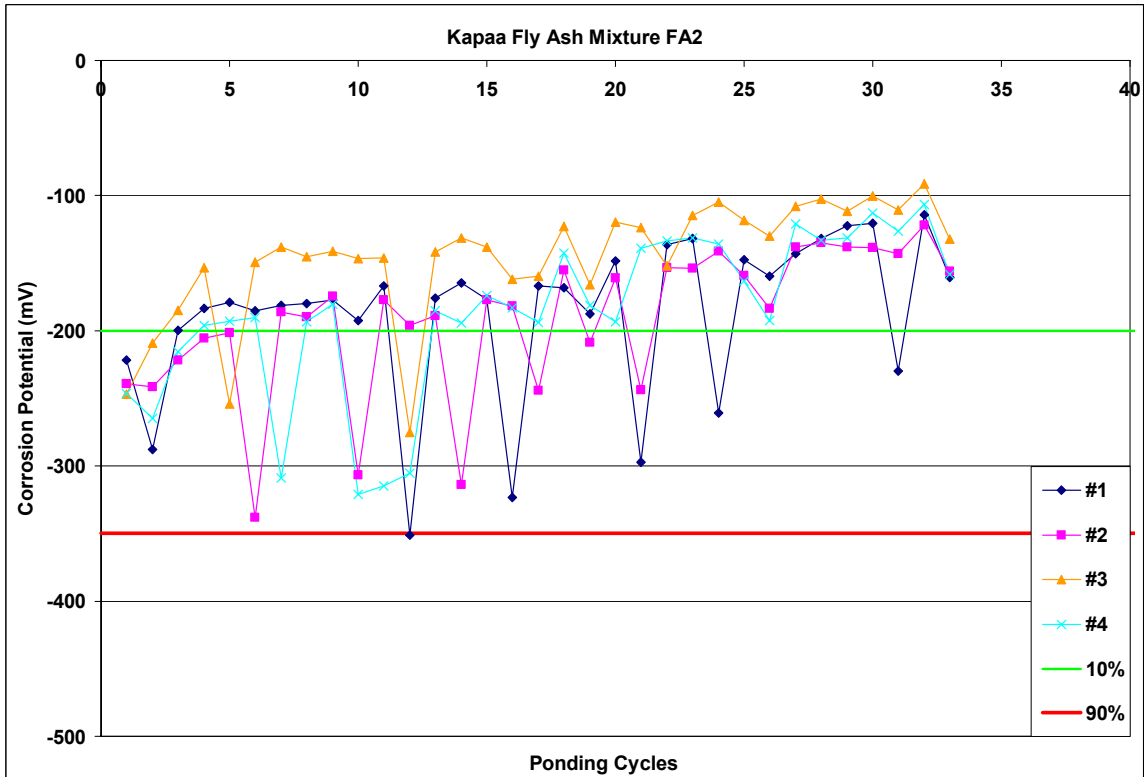


Figure A.1-244: Corrosion Potential for Kapaa Fly Ash Mixture FA2

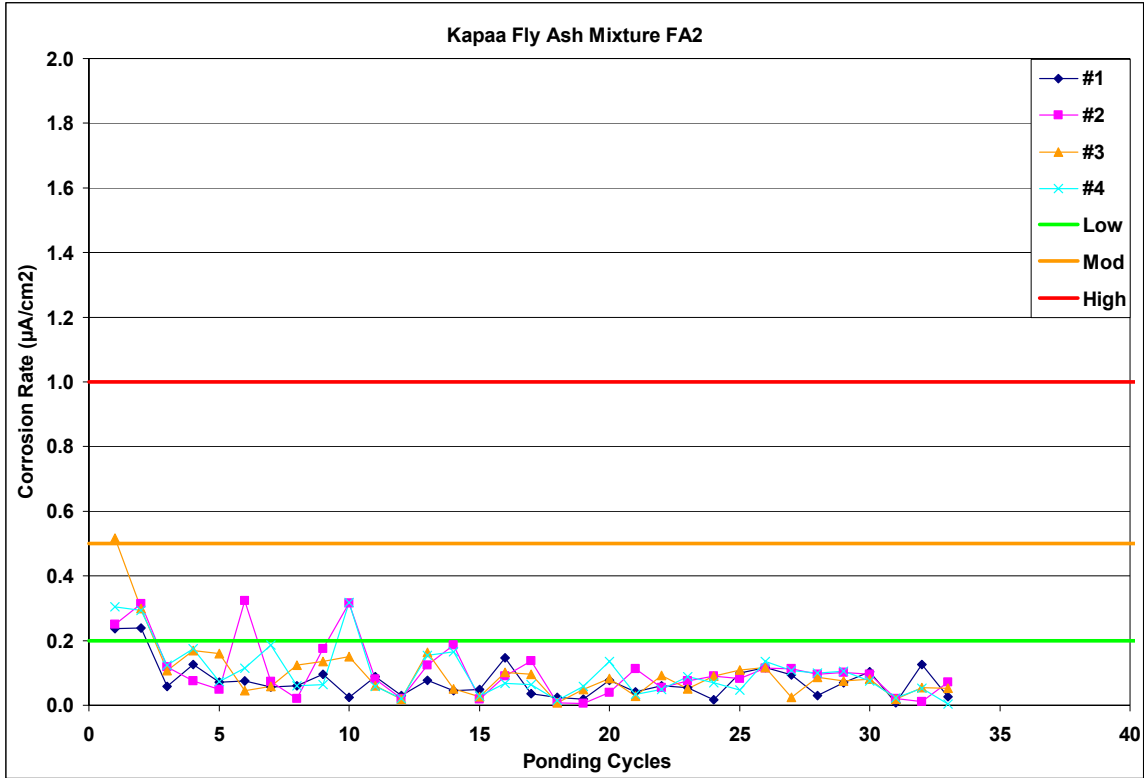


Figure A.1-245: Corrosion Rate for Kapaa Fly Ash Mixture FA2

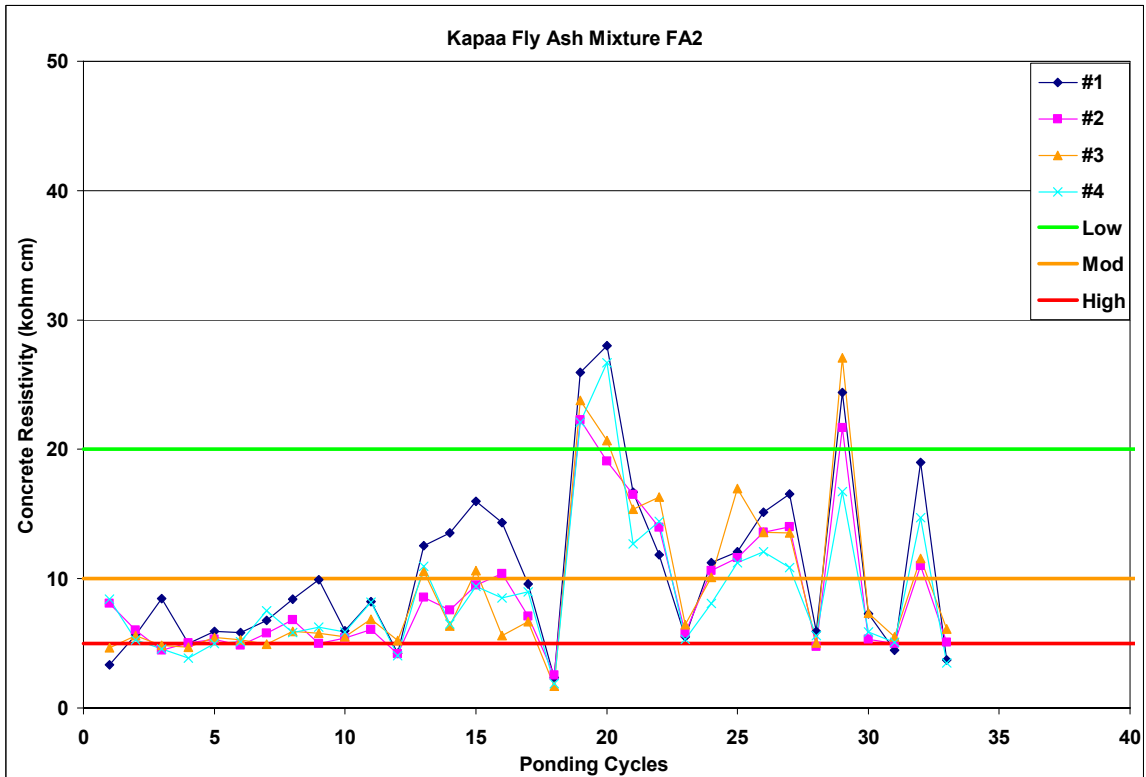


Figure A.1-246: Corrosion Resistivity for Kapaa Fly Ash Mixture FA2

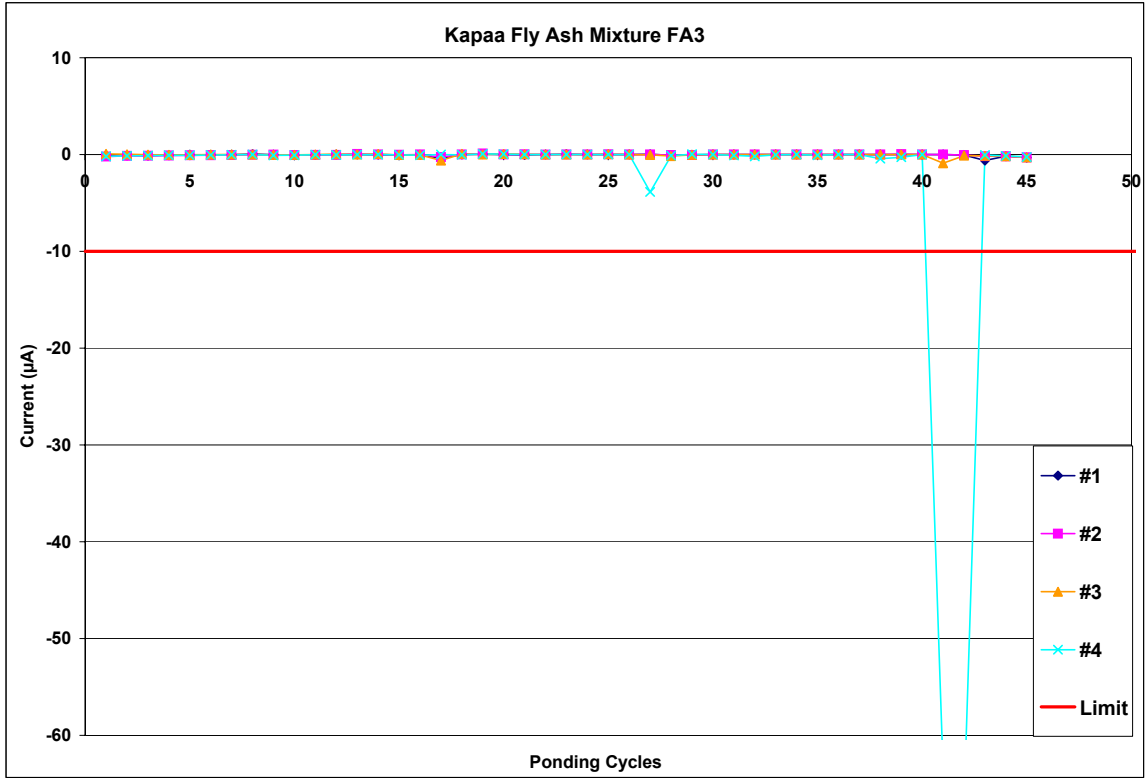


Figure A.1-247: Current Measurements for Kapaa Fly Ash Mixture FA3

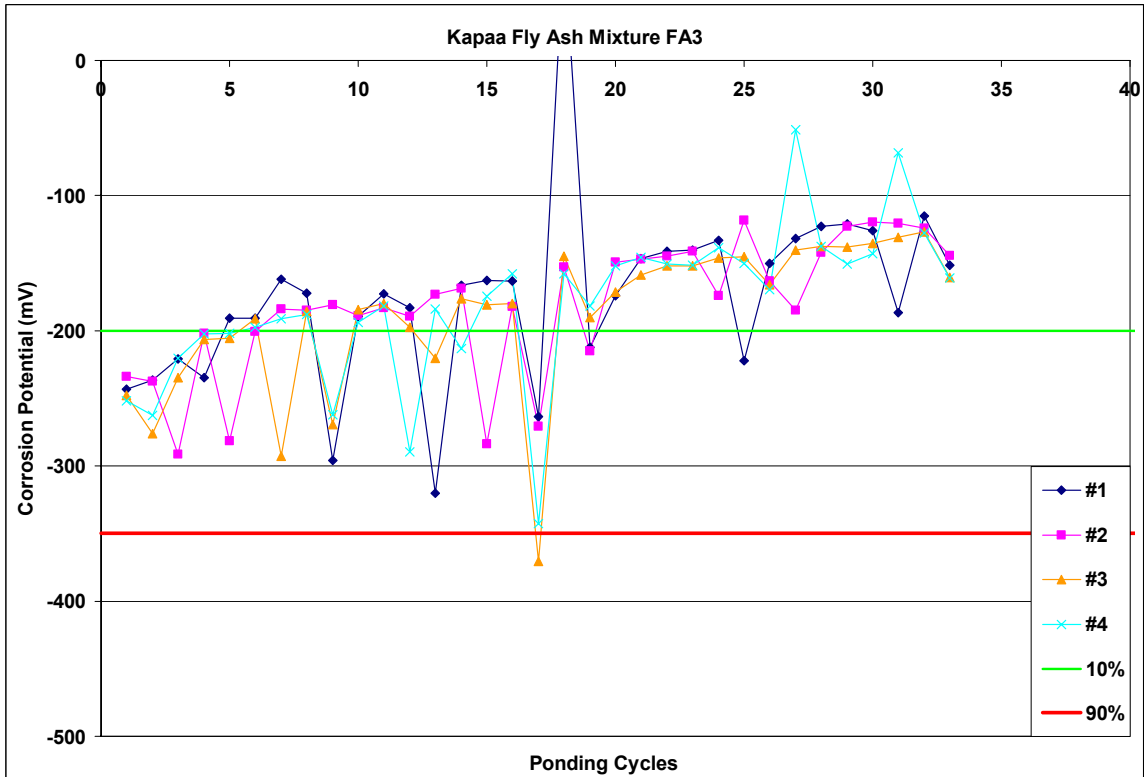


Figure A.1-248: Corrosion Potential for Kapaa Fly Ash Mixture FA3

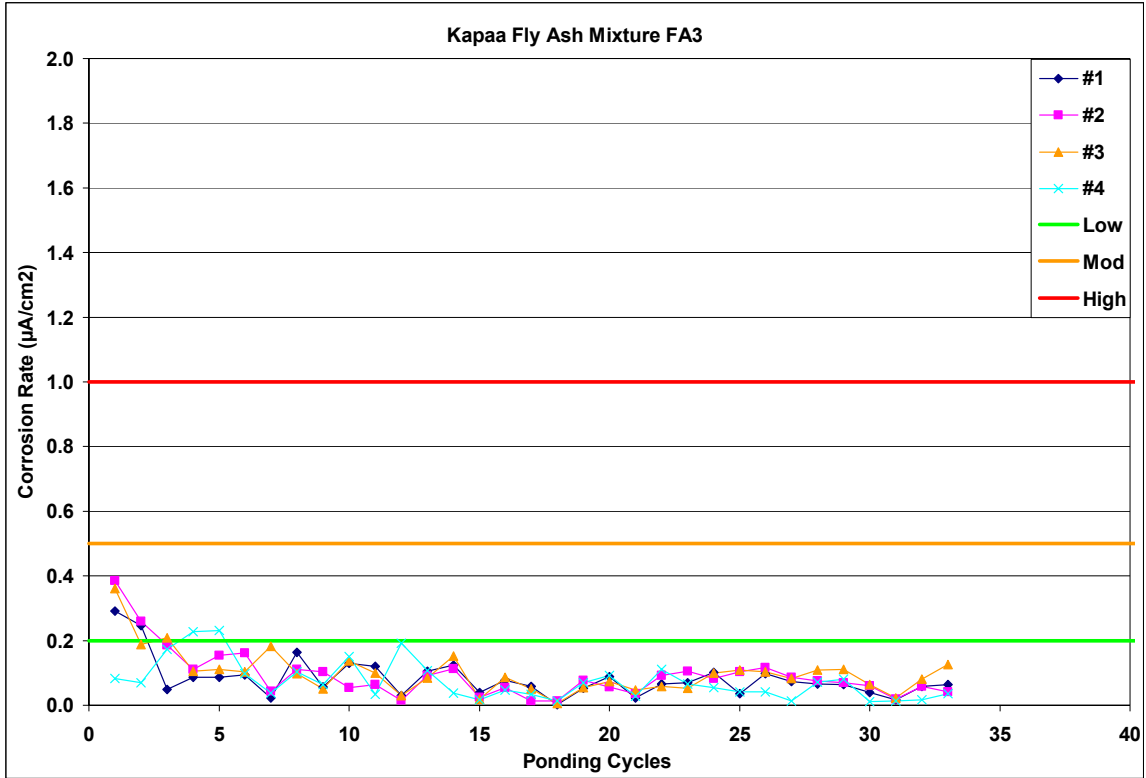


Figure A.1-249: Corrosion Rate for Kapaa Fly Ash Mixture FA3

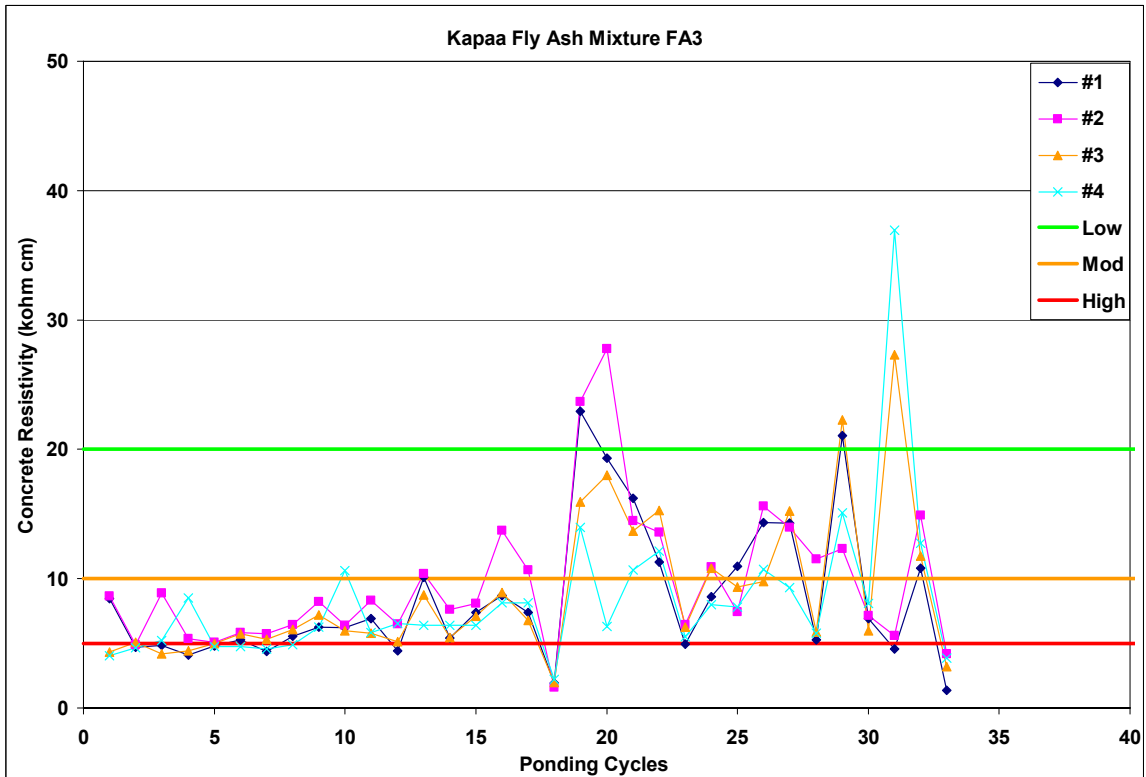


Figure A.1-250: Corrosion Resistivity for Kapaa Fly Ash Mixture FA3

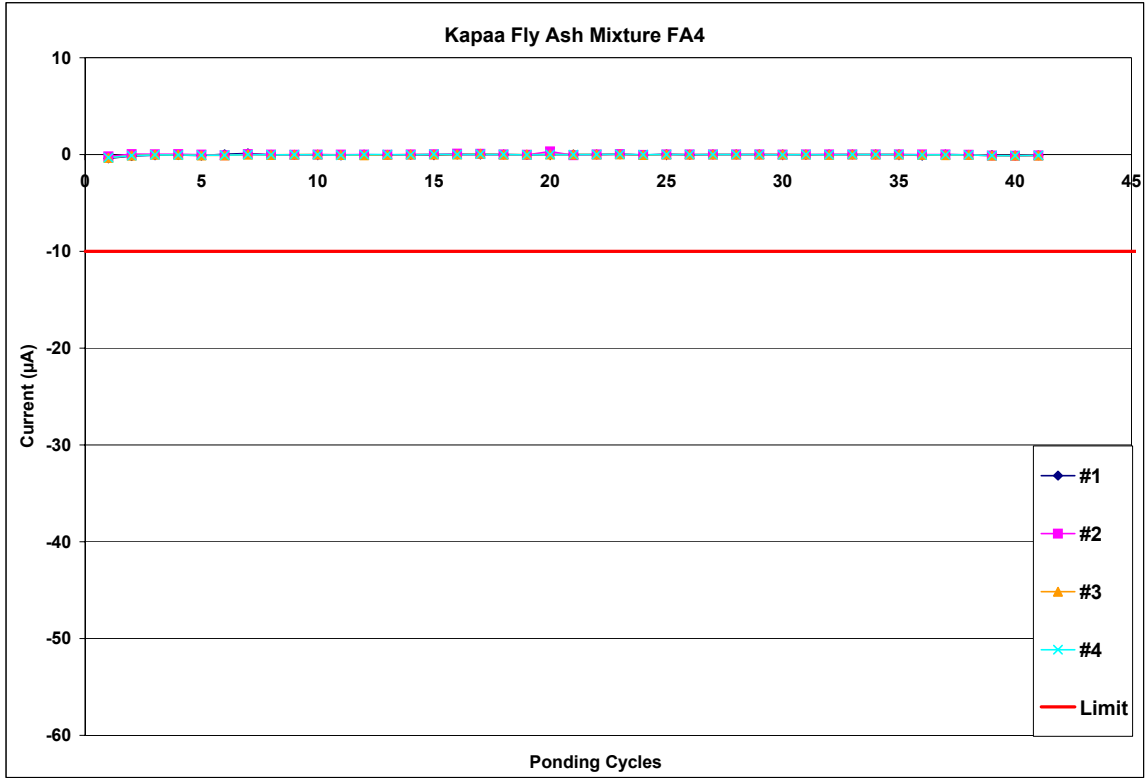


Figure A.1-251: Current Measurements for Kapaa Fly Ash Mixture FA4



Figure A.1-252: Corrosion Potential for Kapaa Fly Ash Mixture FA4

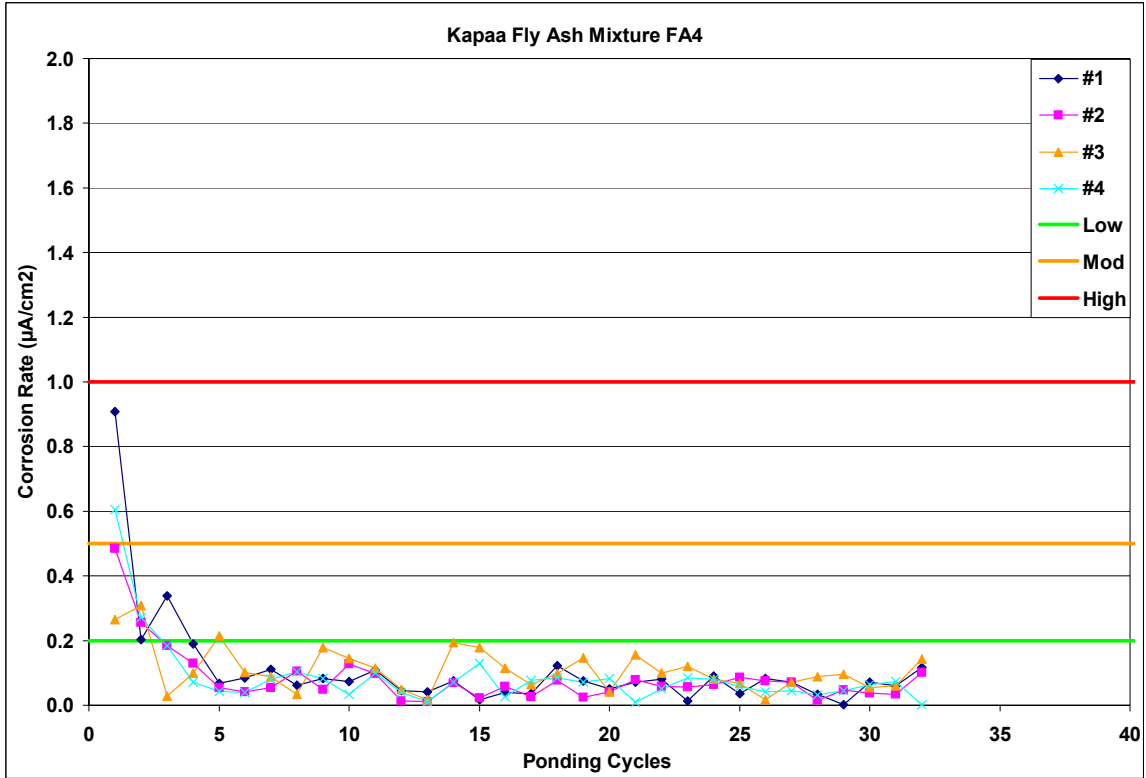


Figure A.1-253: Corrosion Rate for Kapaa Fly Ash Mixture FA4

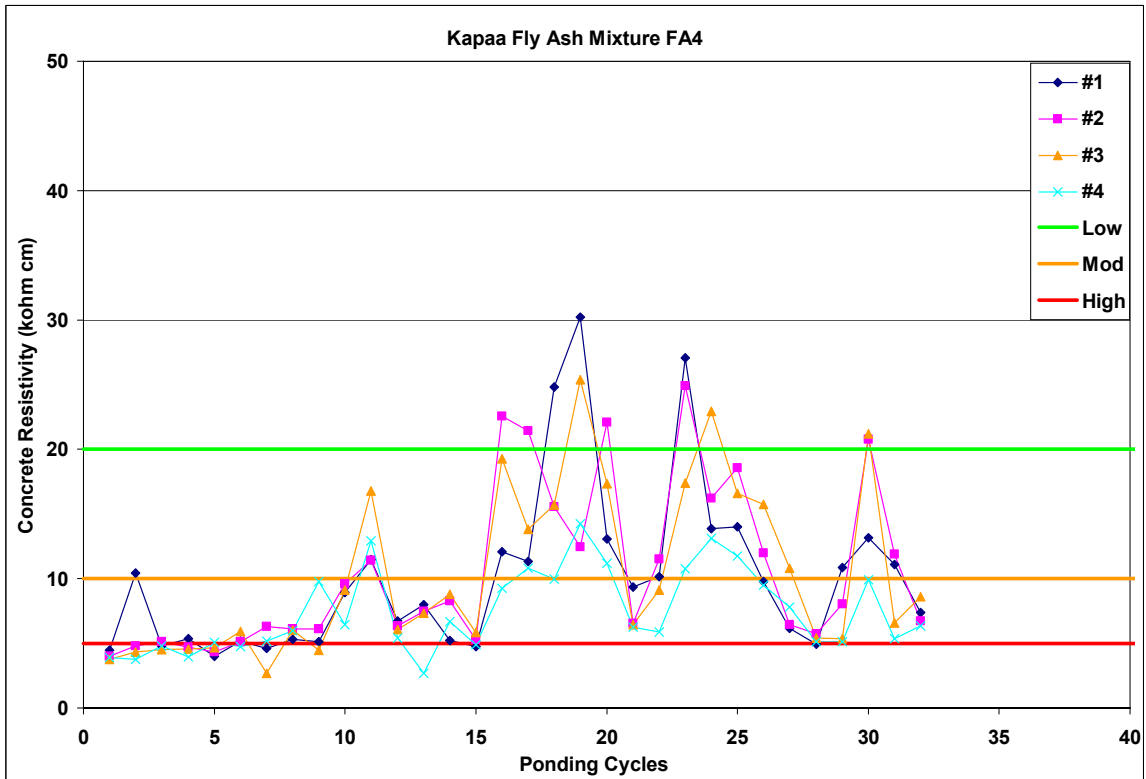


Figure A.1-254: Corrosion Resistivity for Kapaa Fly Ash Mixture FA4

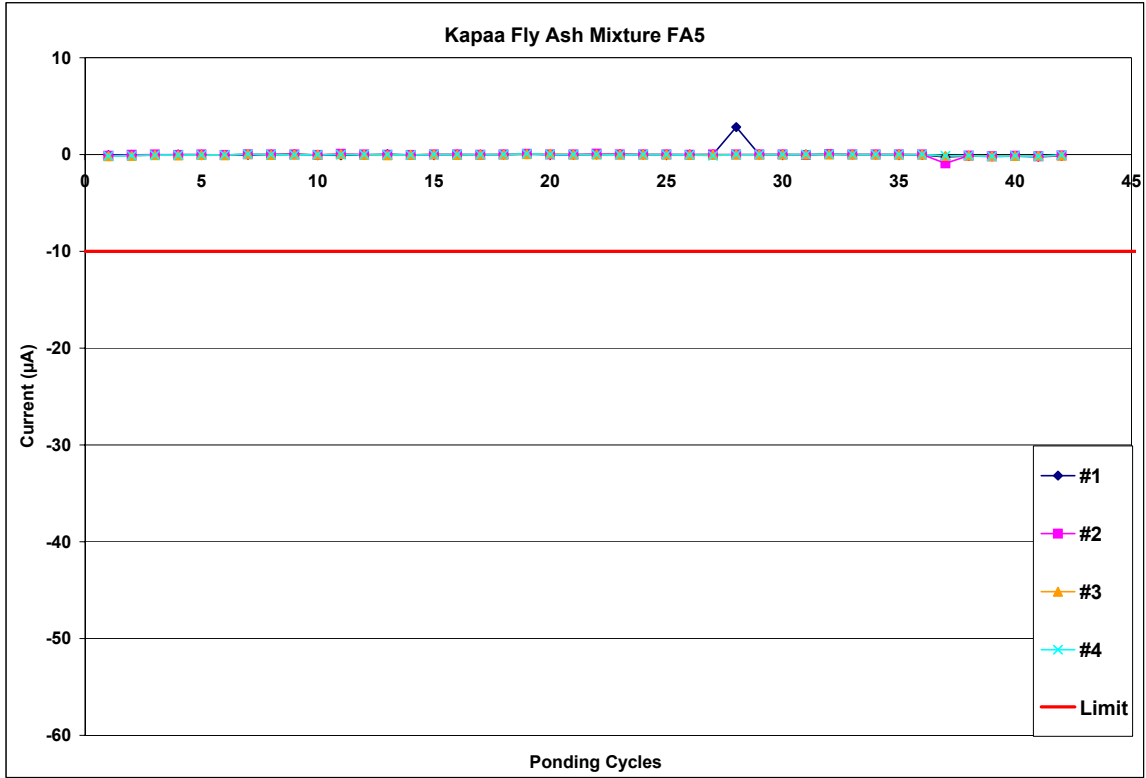


Figure A.1-255: Current Measurements for Kapaa Fly Ash Mixture FA5

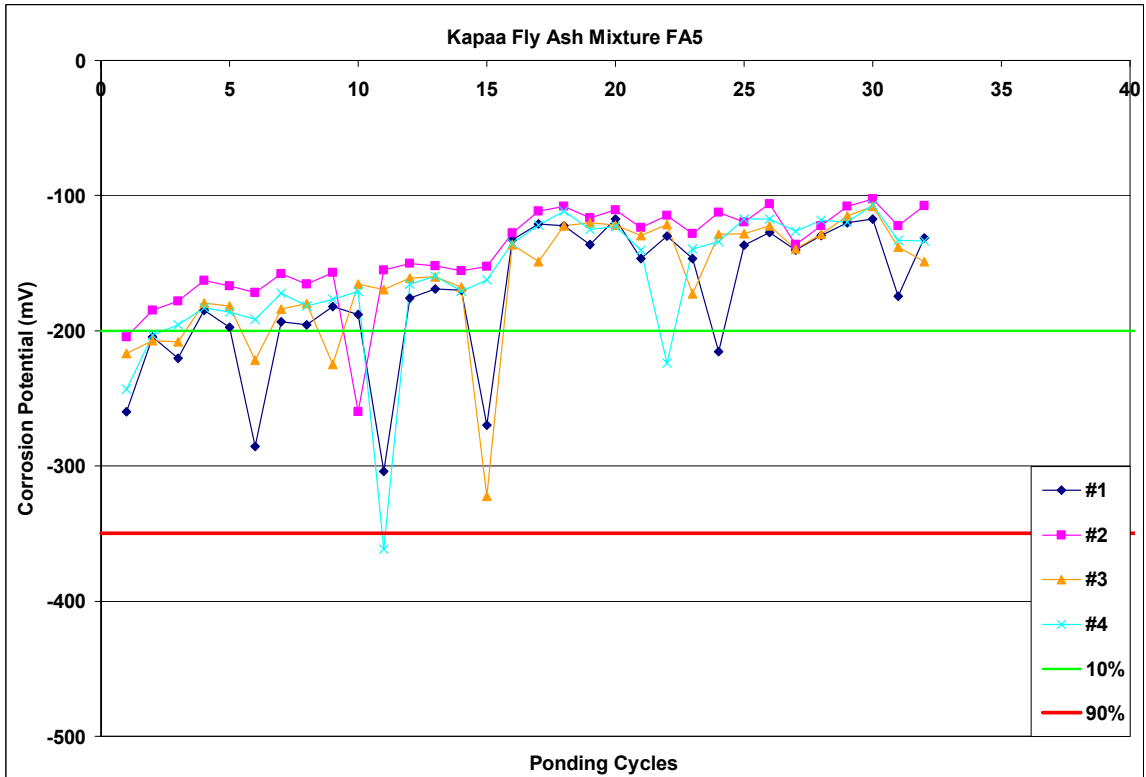


Figure A.1-256: Corrosion Potential for Kapaa Fly Ash Mixture FA5

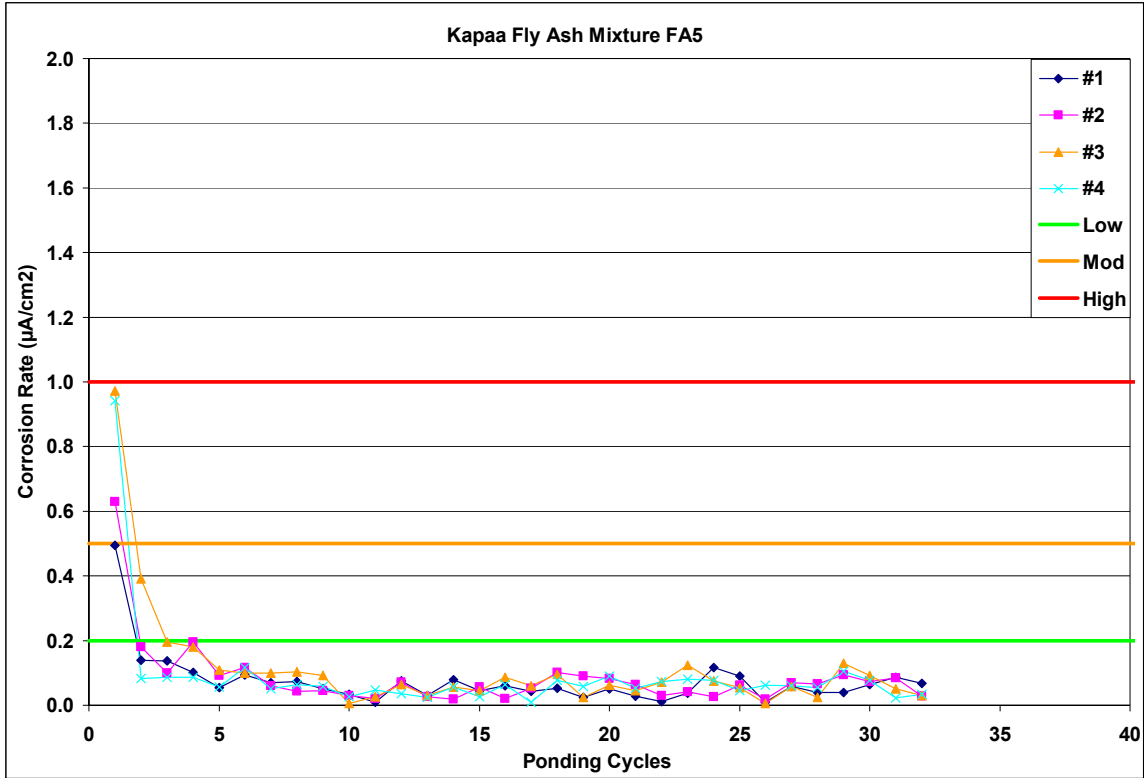


Figure A.1-257: Corrosion Rate for Kapaa Fly Ash Mixture FA5

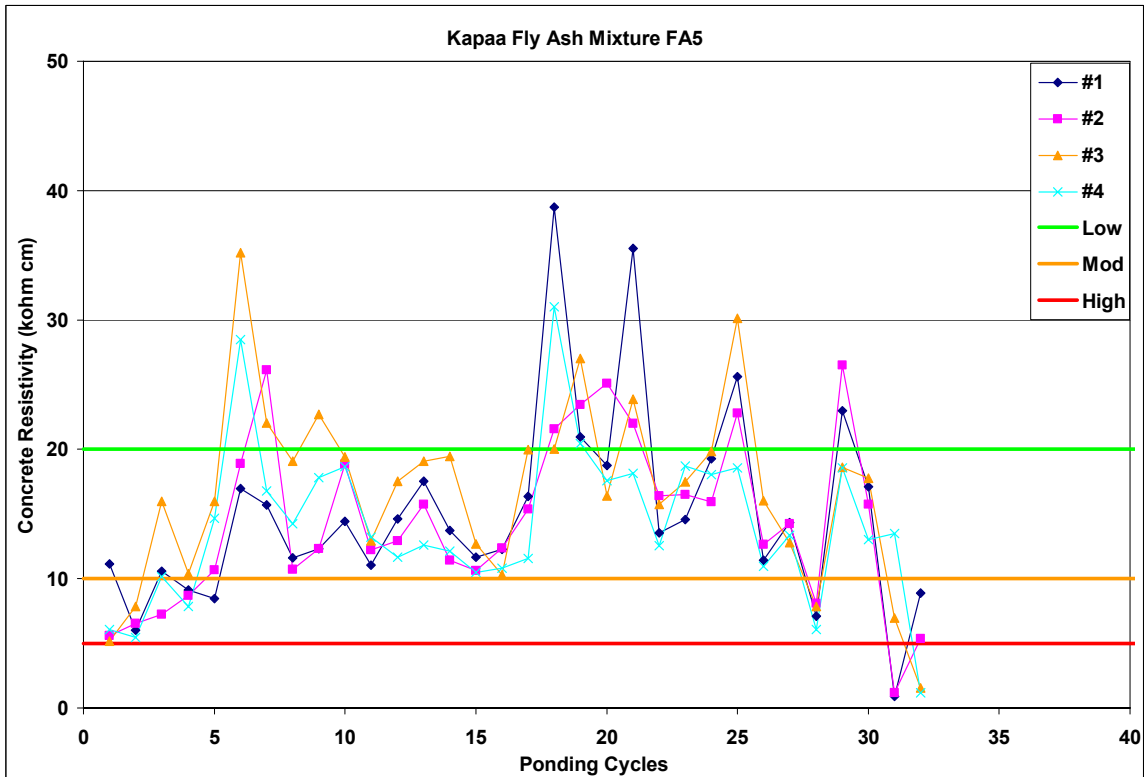


Figure A.1-258: Corrosion Resistivity for Kapaa Fly Ash Mixture FA5

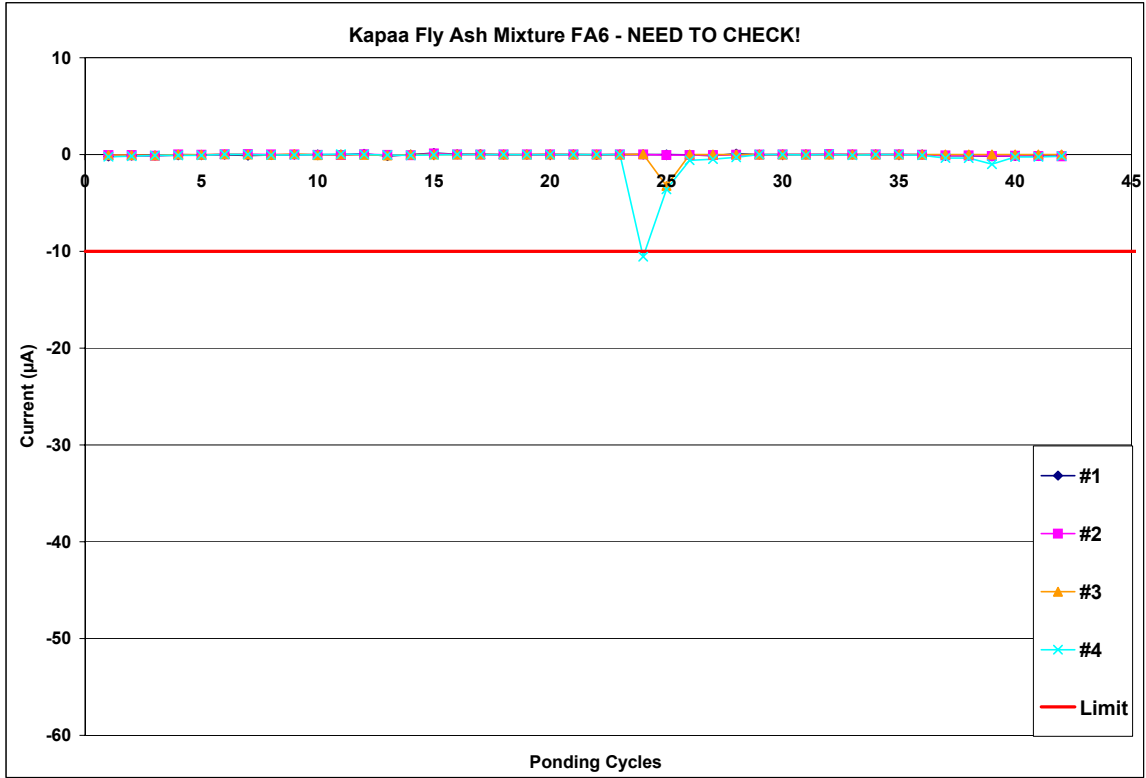


Figure A.1-259: Current Measurements for Kapaa Fly Ash Mixture FA6

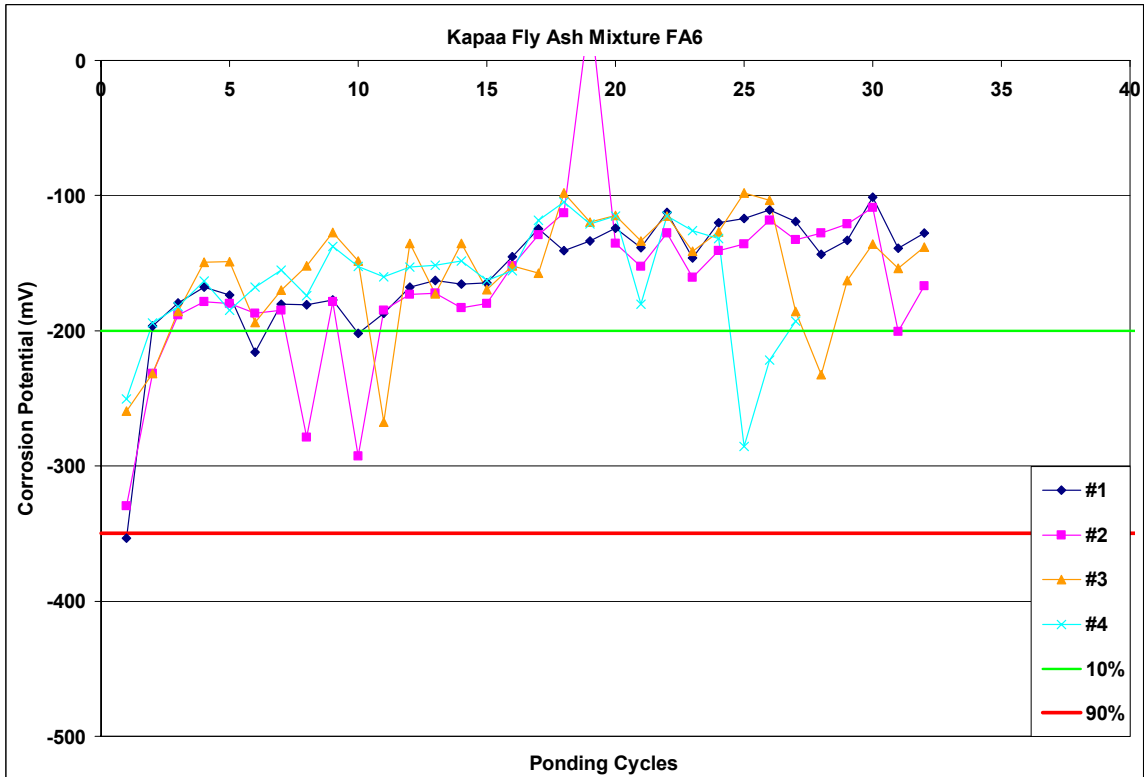


Figure A.1-260: Corrosion Potential for Kapaa Fly Ash Mixture FA6

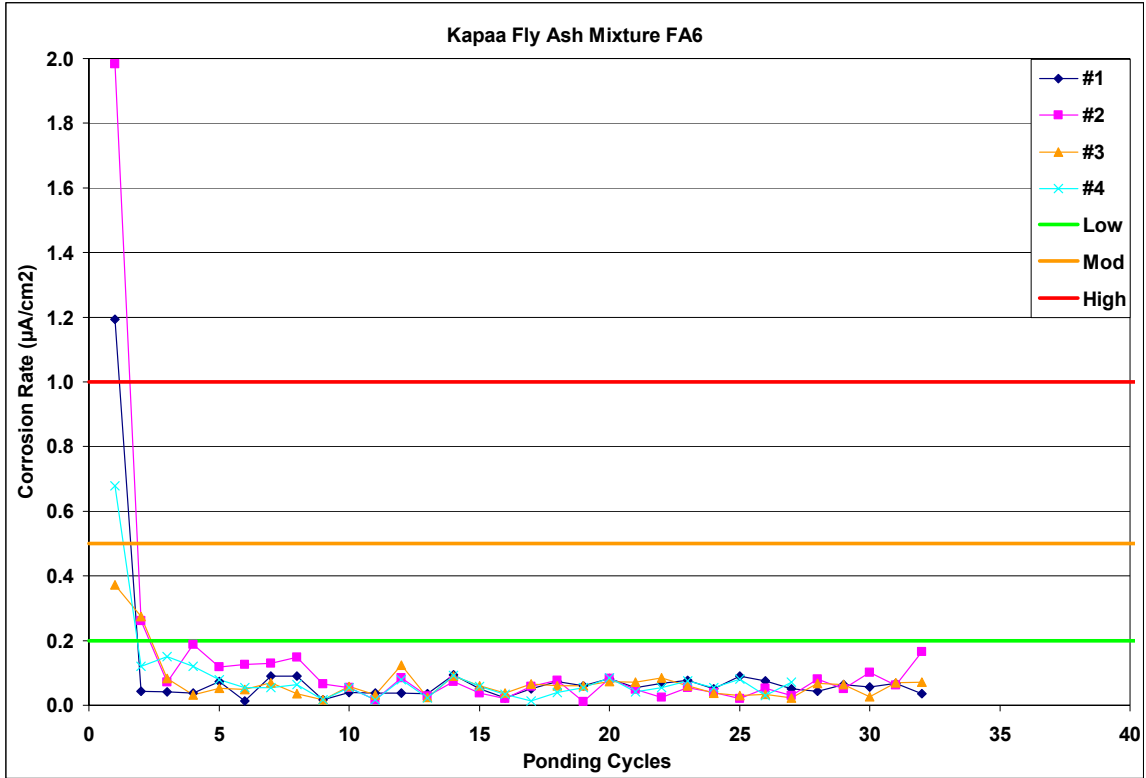


Figure A.1-261: Corrosion Rate for Kapaa Fly Ash Mixture FA6

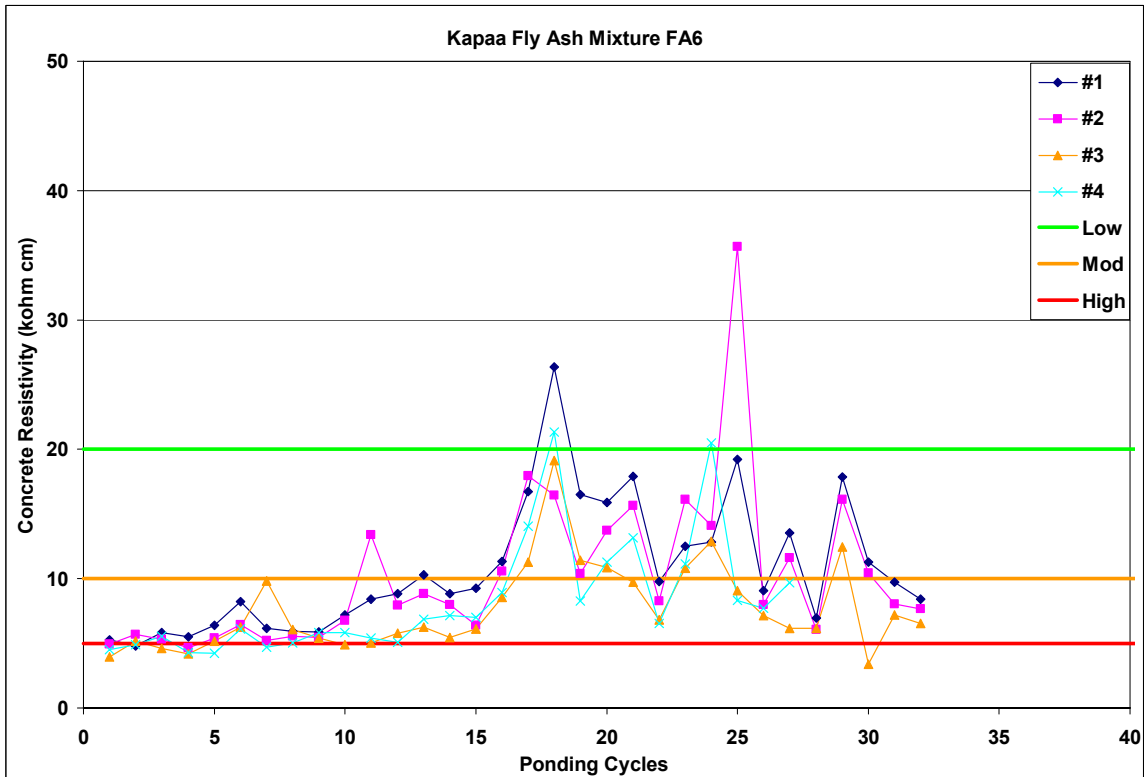


Figure A.1-262: Corrosion Resistivity for Kapaa Fly Ash Mixture FA6

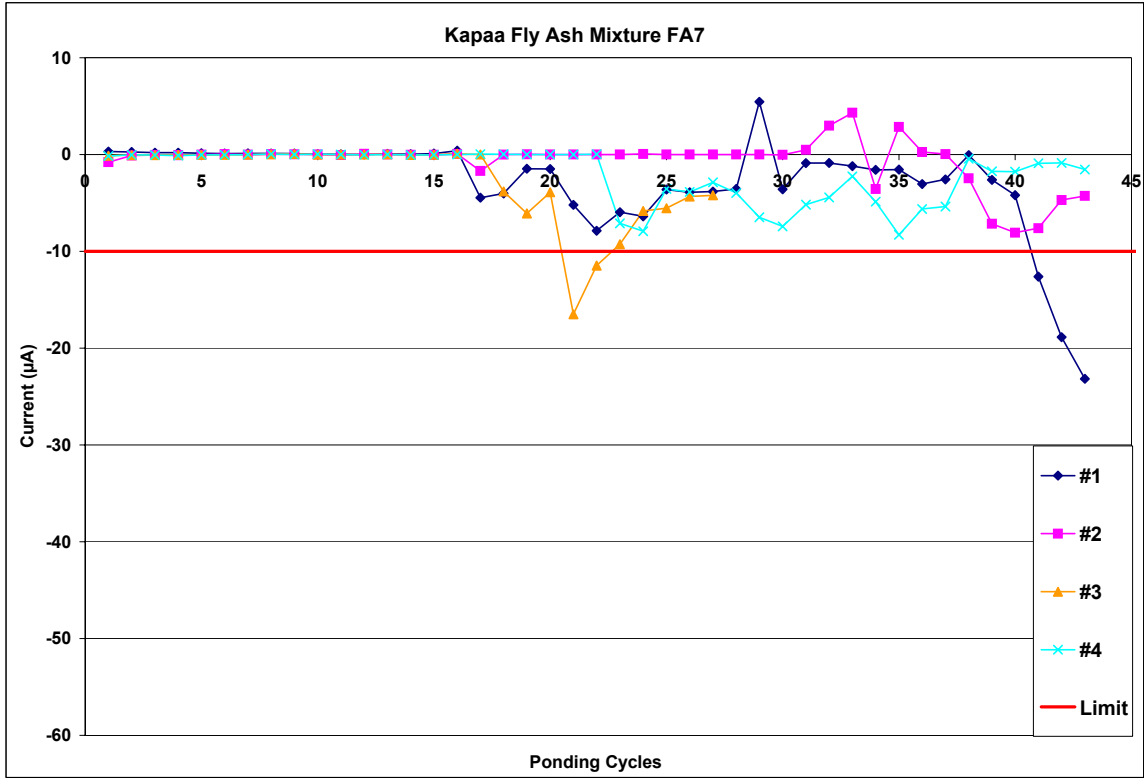


Figure A.1-263: Current Measurements for Kapaa Fly Ash Mixture FA7

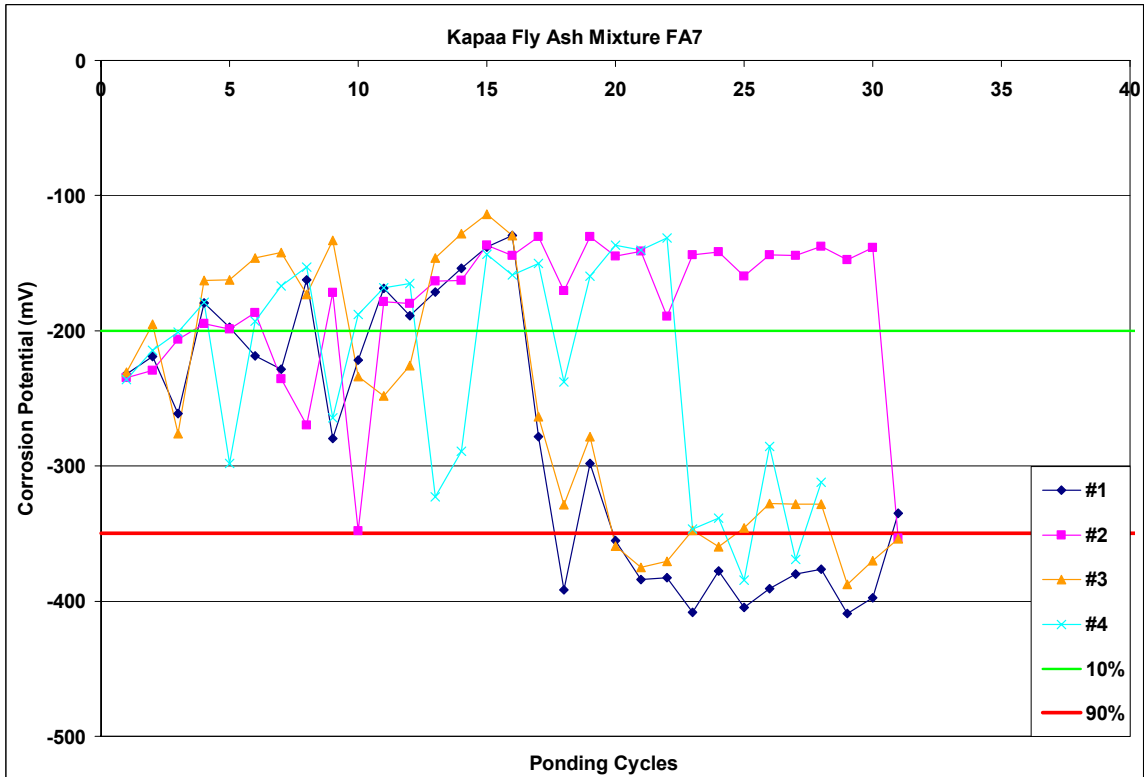


Figure A.1-264: Corrosion Potential for Kapaa Fly Ash Mixture FA7

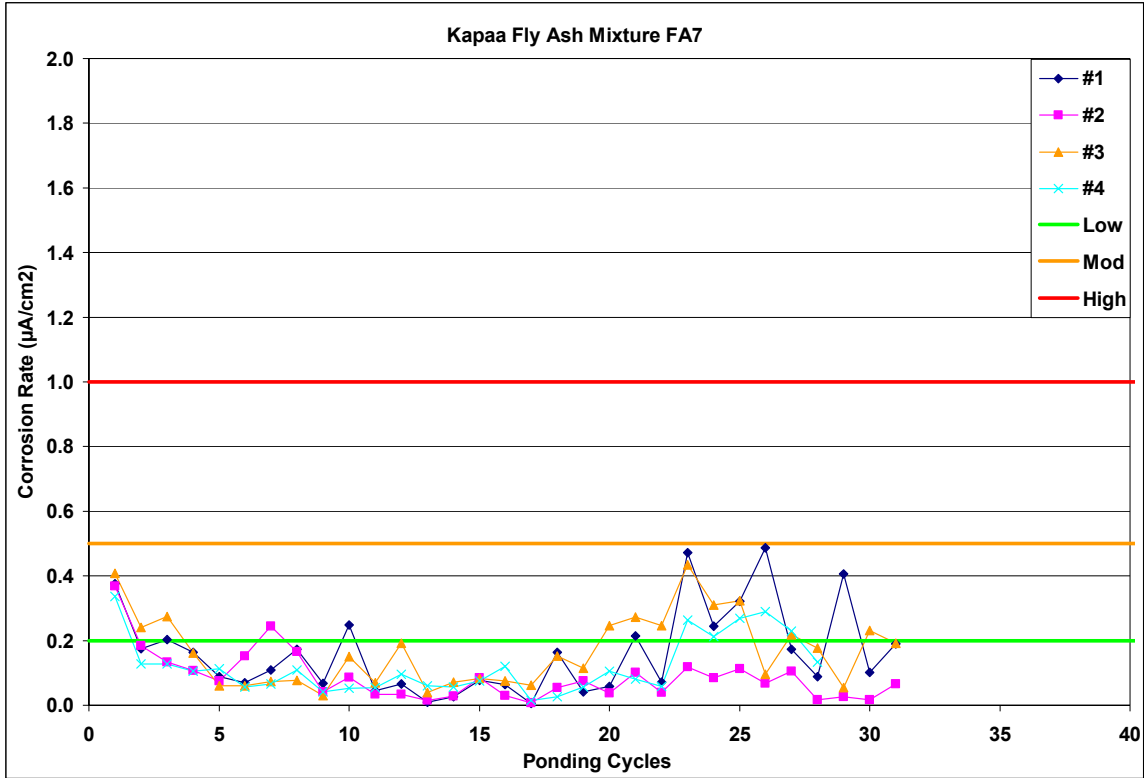


Figure A.1-265: Corrosion Rate for Kapaa Fly Ash Mixture FA7

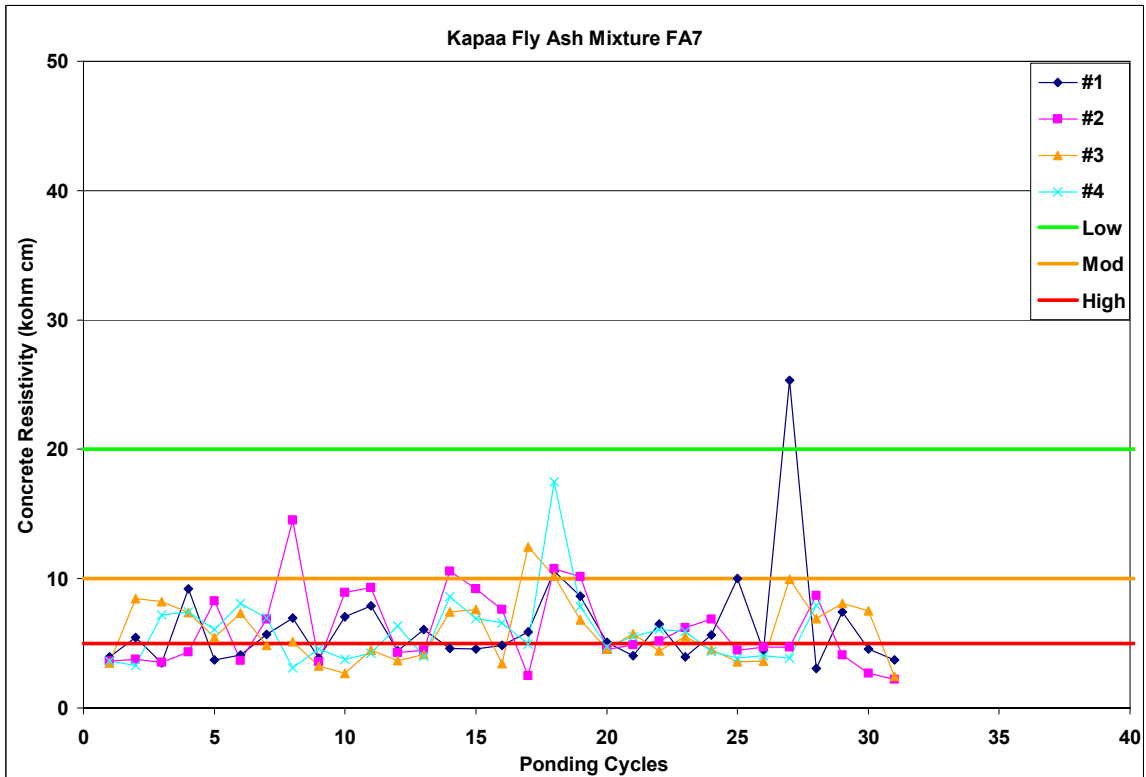


Figure A.1-266: Corrosion Resistivity for Kapaa Fly Ash Mixture FA7

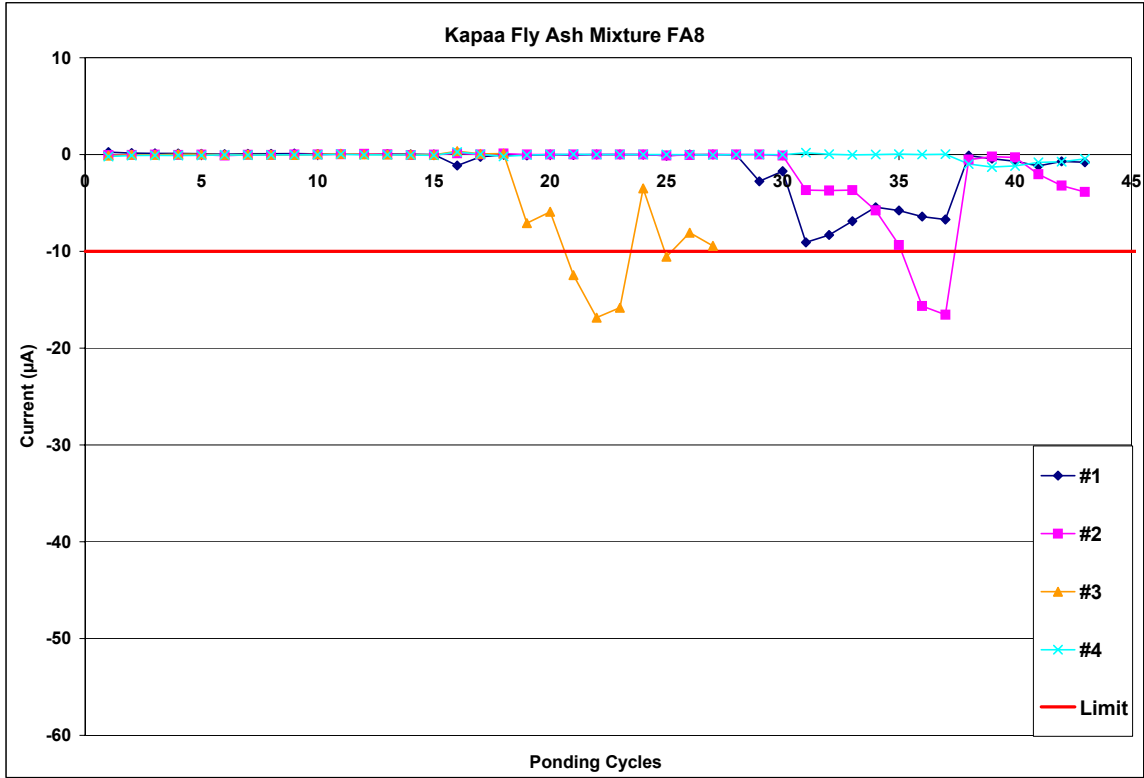


Figure A.1-267: Current Measurements for Kapaa Fly Ash Mixture FA8

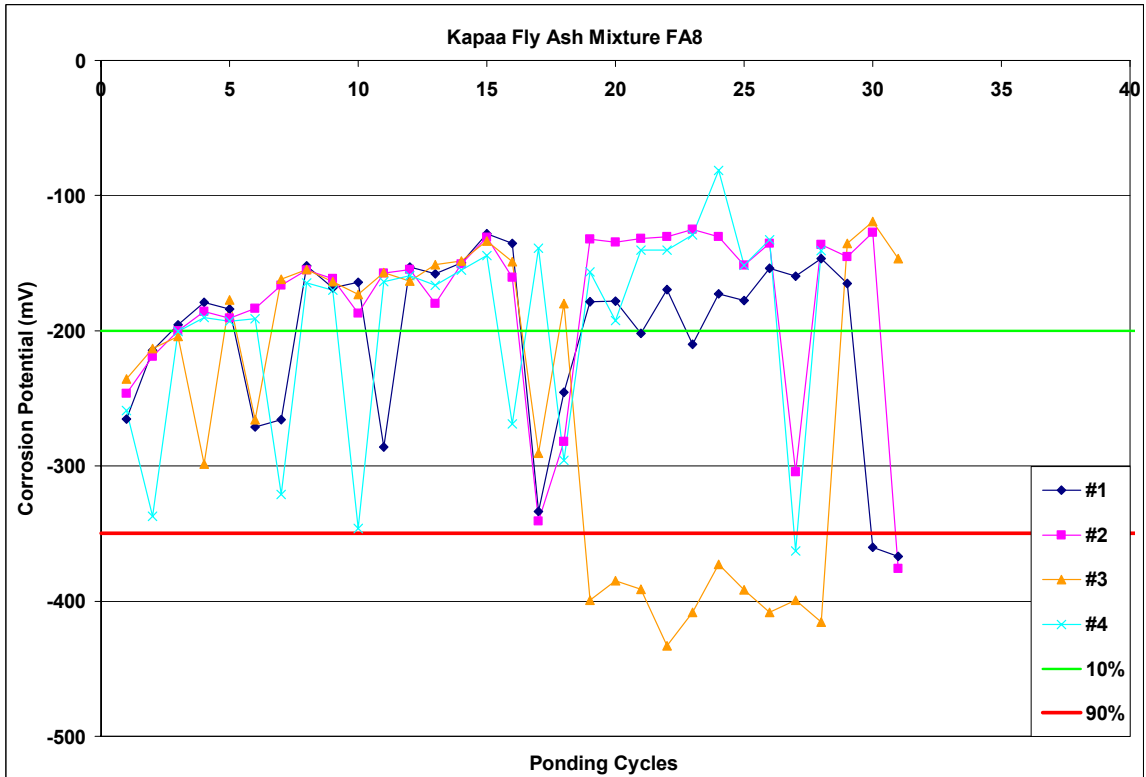


Figure A.1-268: Corrosion Potential for Kapaa Fly Ash Mixture FA8

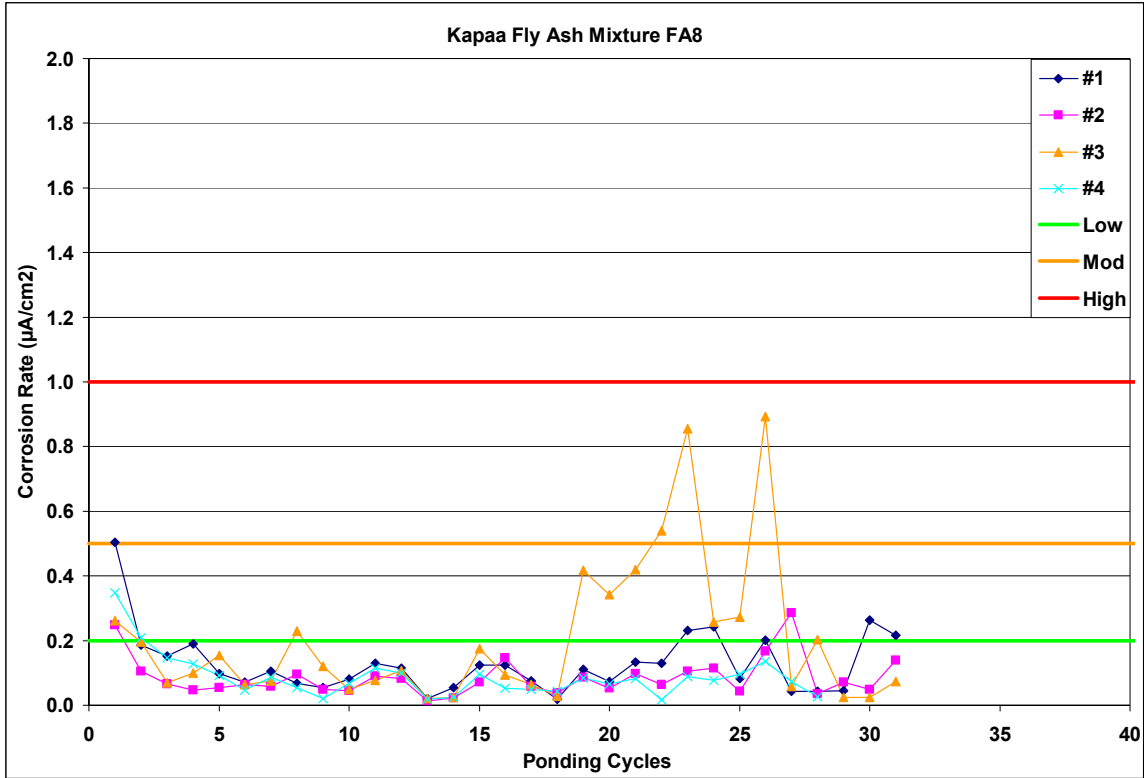


Figure A.1-269: Corrosion Rate for Kapaa Fly Ash Mixture FA8

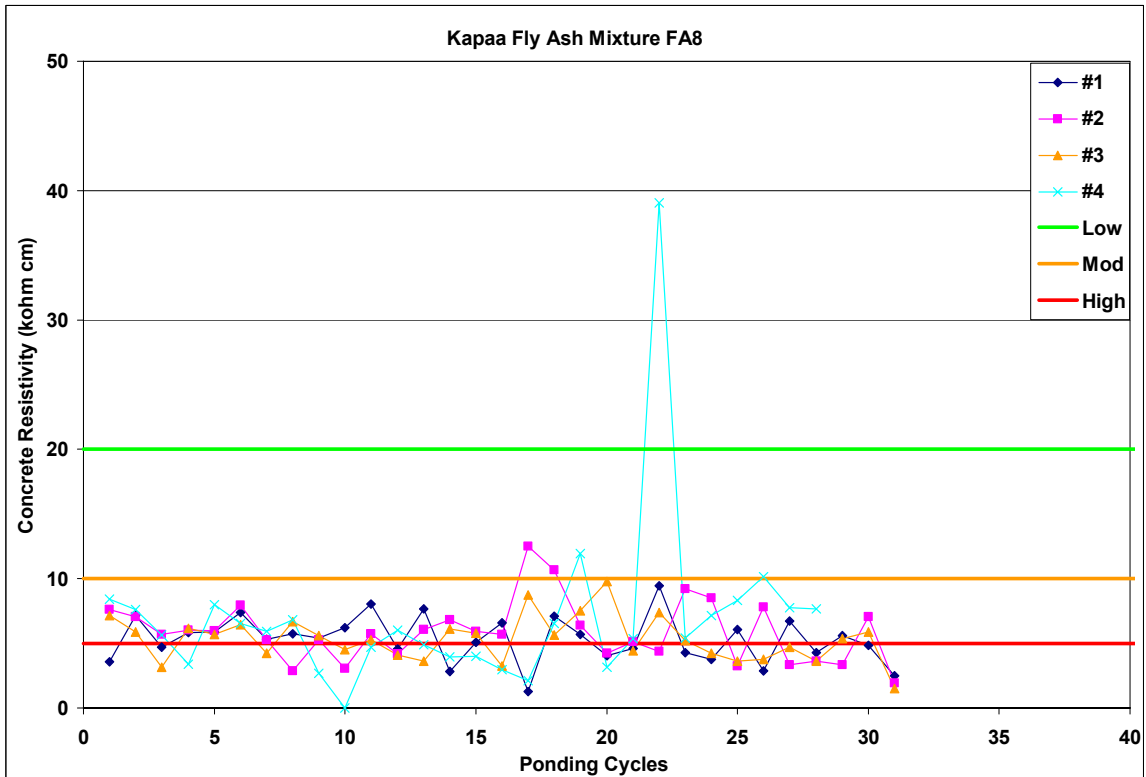


Figure A.1-270: Corrosion Resistivity for Kapaa Fly Ash Mixture FA8

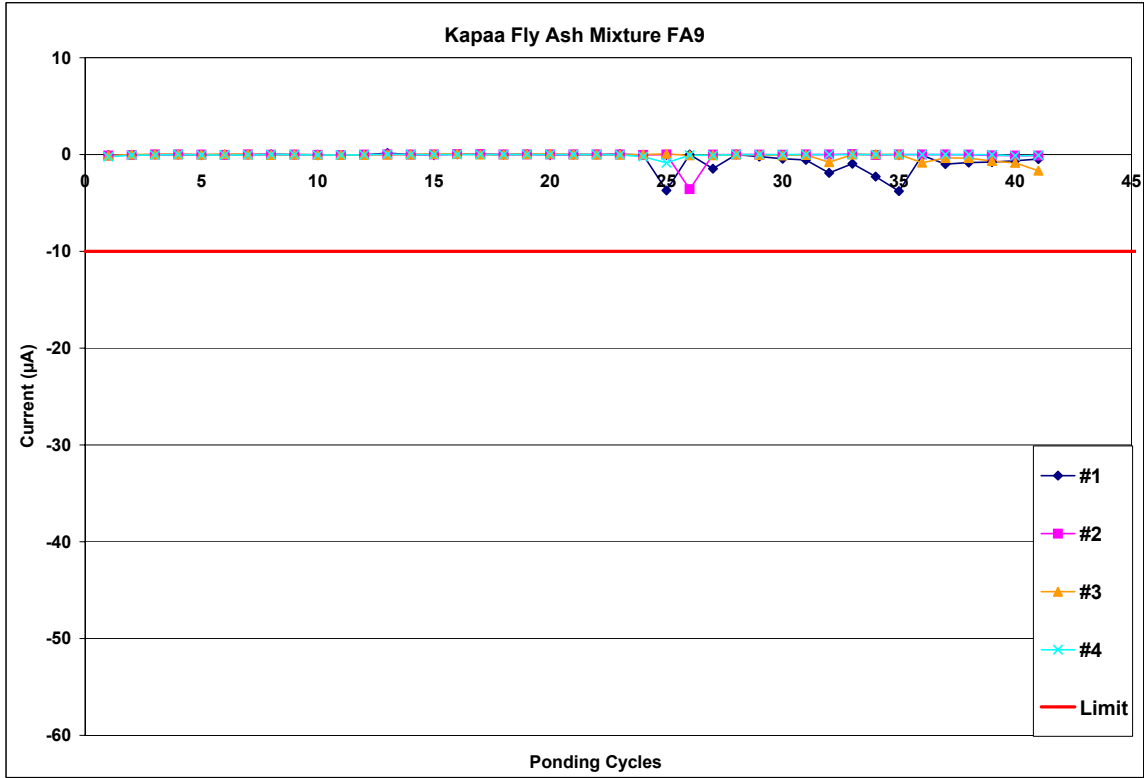


Figure A.1-271: Current Measurements for Kapaa Fly Ash Mixture FA9

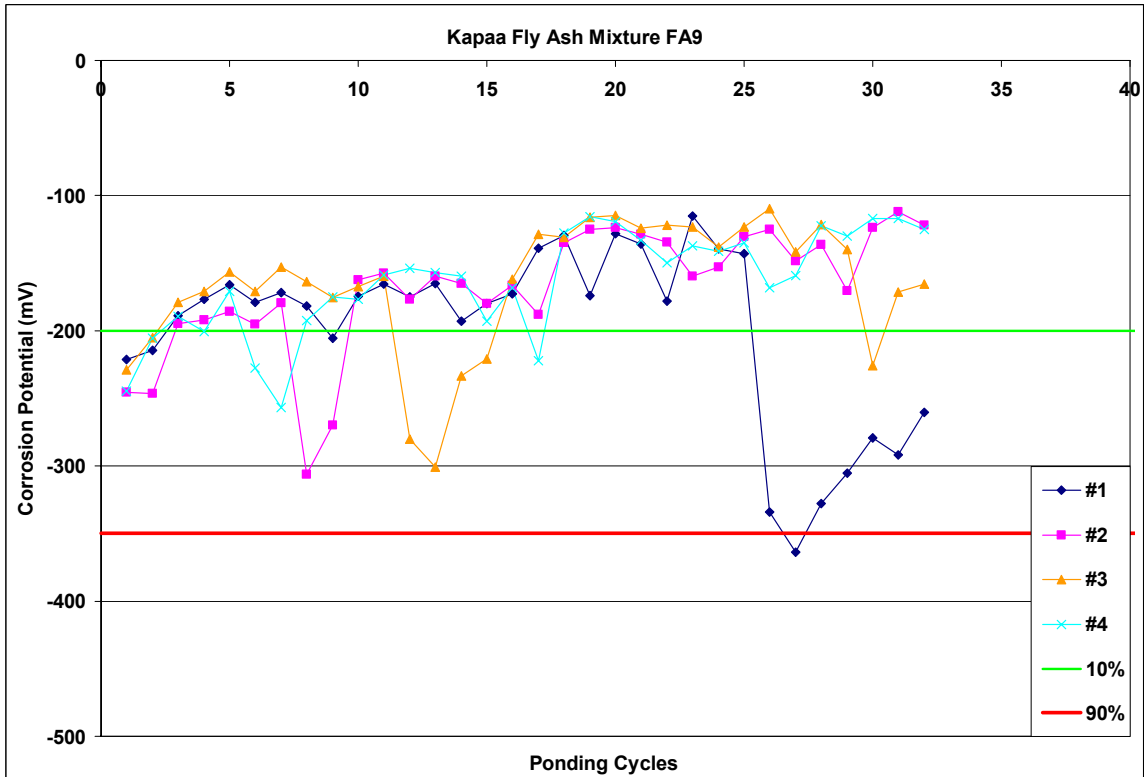


Figure A.1-272: Corrosion Potential for Kapaa Fly Ash Mixture FA9

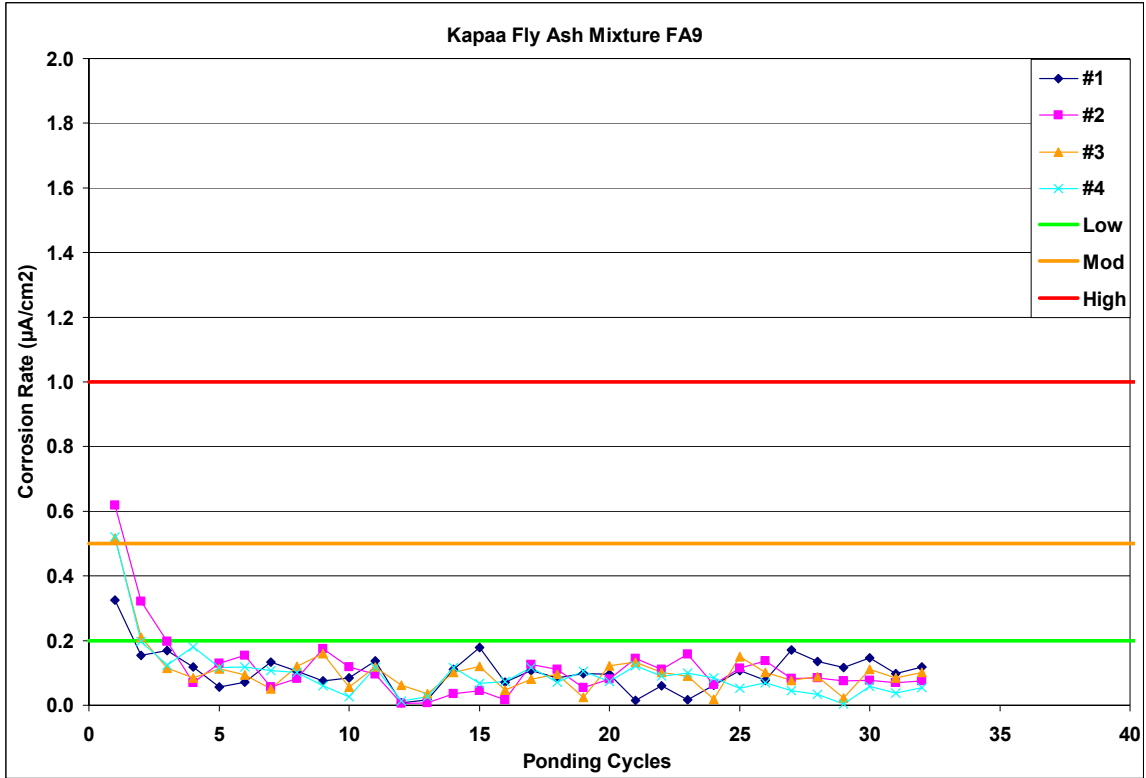


Figure A.1-273: Corrosion Rate for Kapaa Fly Ash Mixture FA9

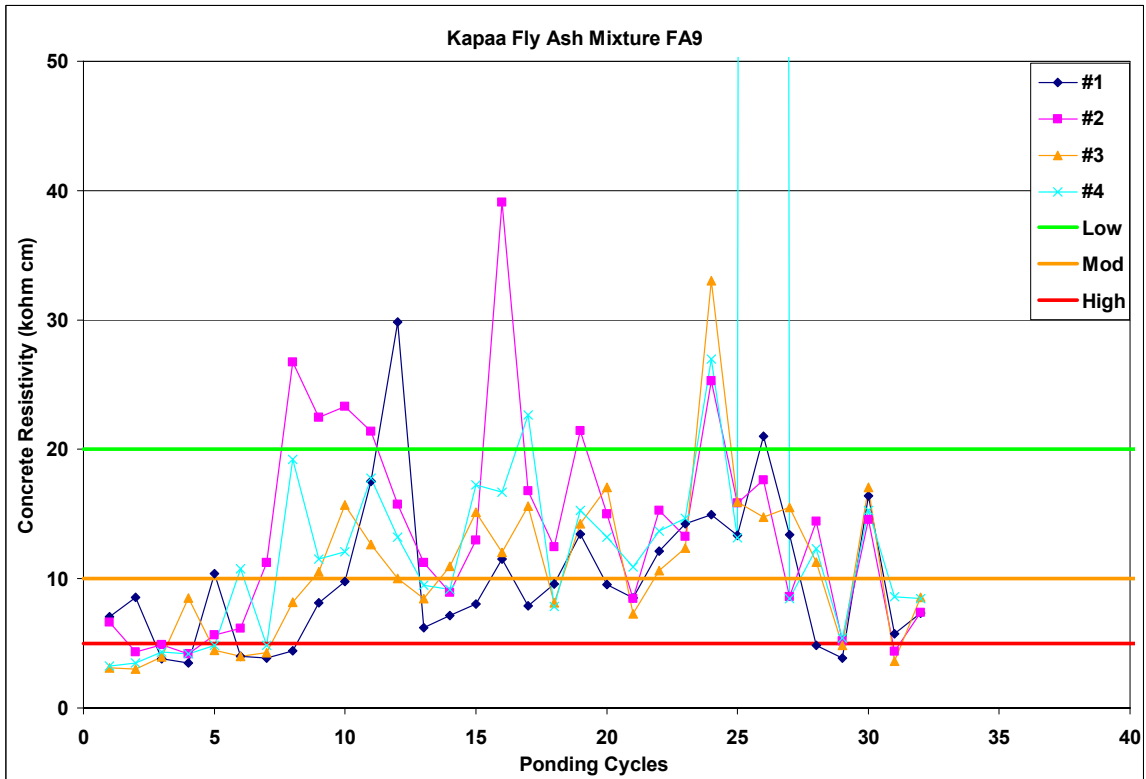


Figure A.1-274: Corrosion Resistivity for Kapaa Fly Ash Mixture FA9

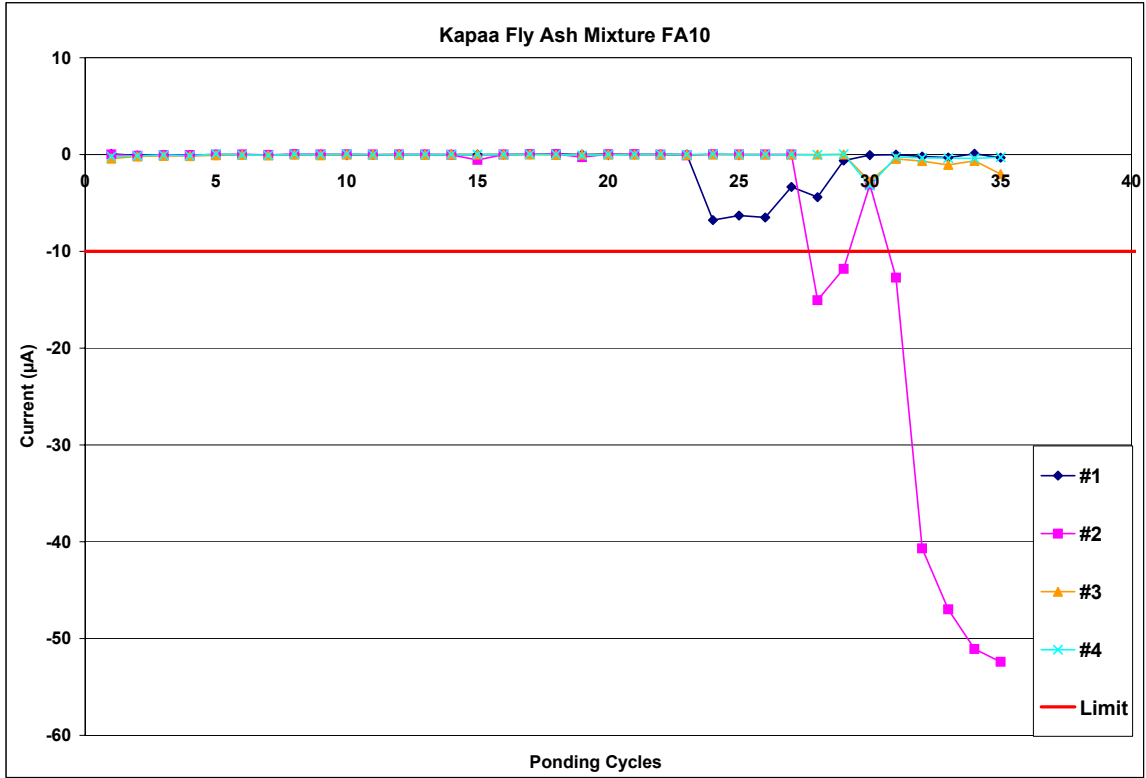


Figure A.1-275: Current Measurements for Kapaa Fly Ash Mixture FA10

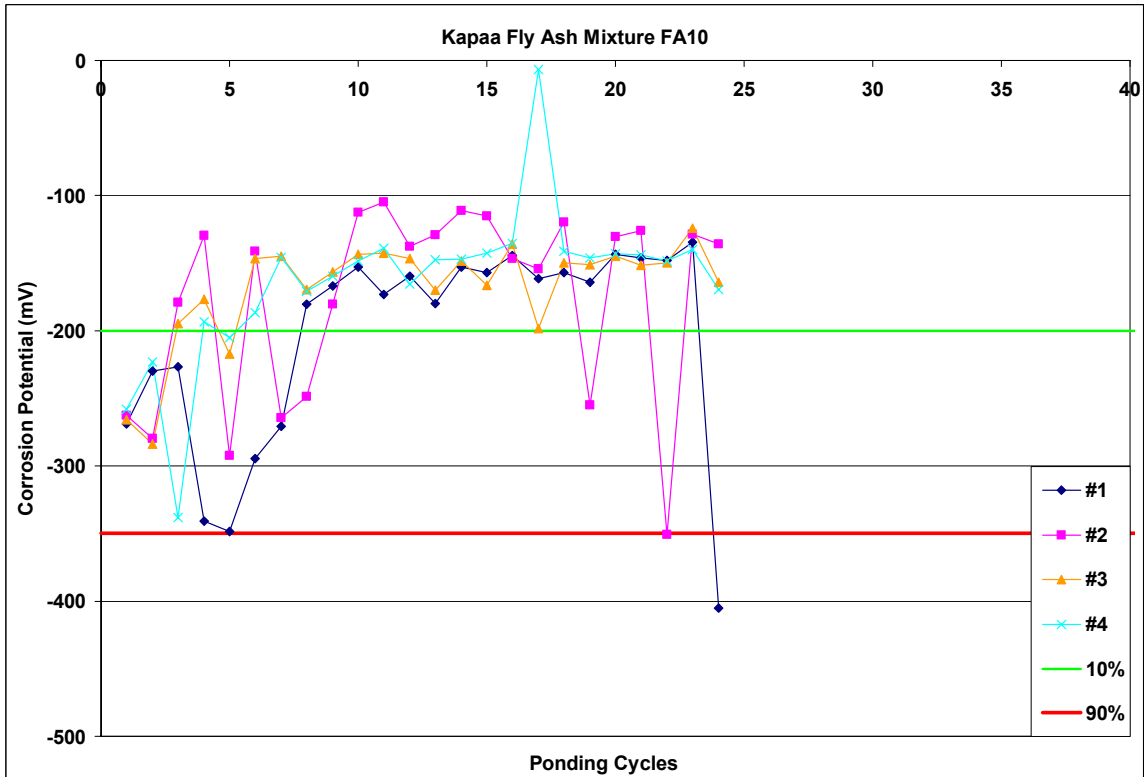


Figure A.1-276: Corrosion Potential for Kapaa Fly Ash Mixture FA10

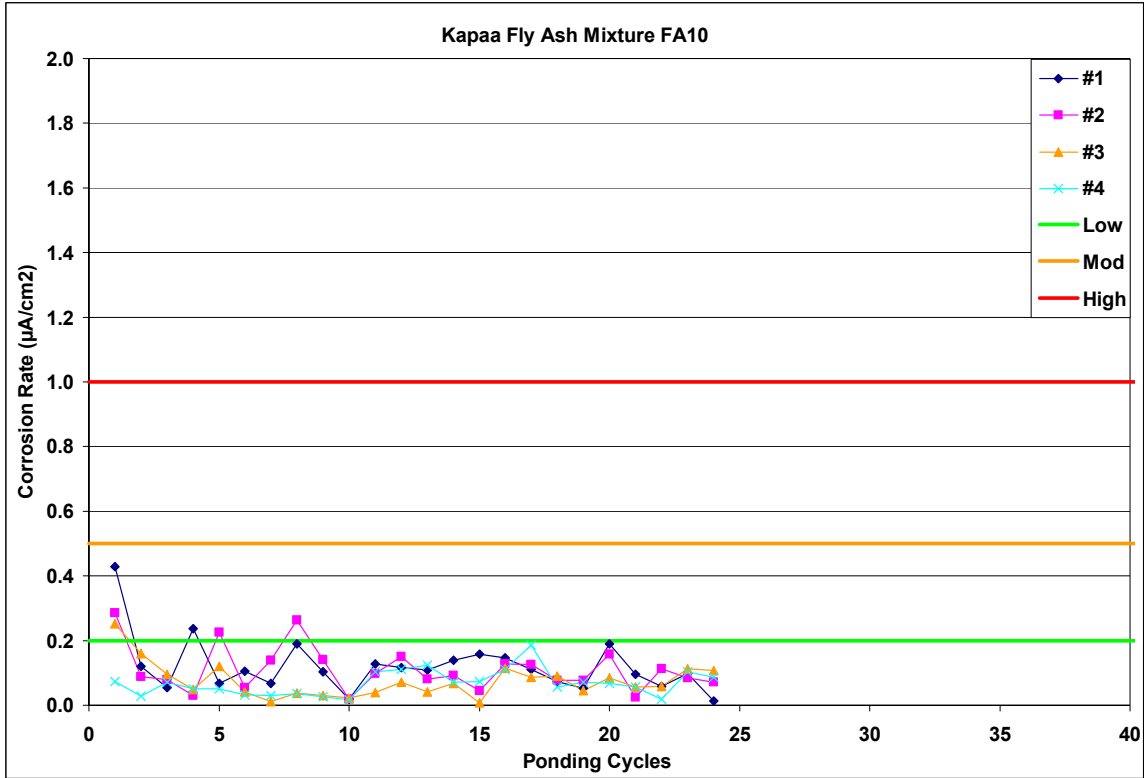


Figure A.1-277: Corrosion Rate for Kapaa Fly Ash Mixture FA10

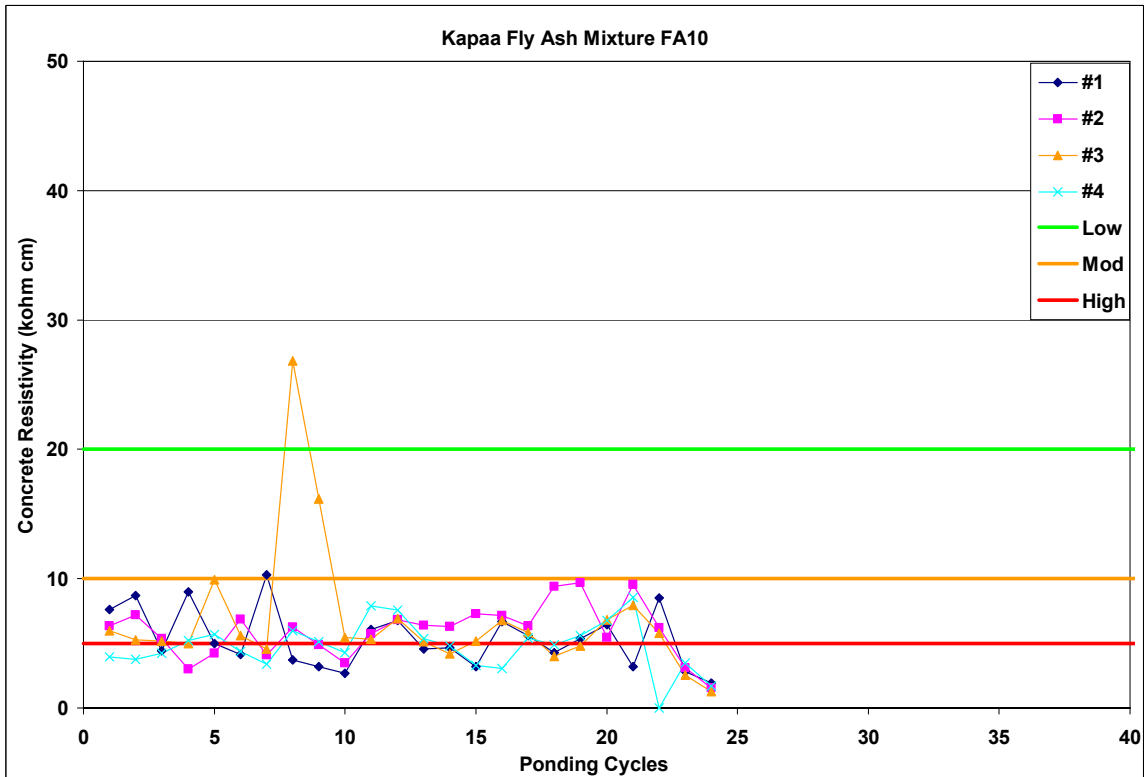


Figure A.1-278: Corrosion Resistivity for Kapaa Fly Ash Mixture FA10

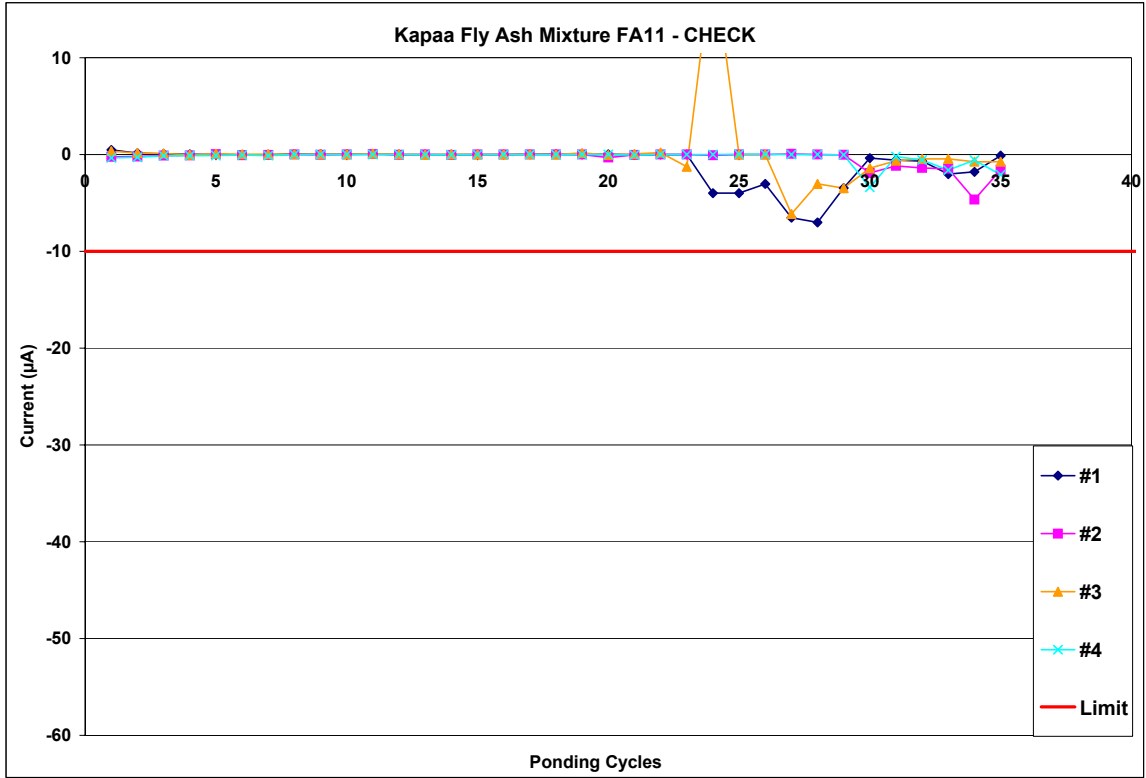


Figure A.1-279: Current Measurements for Kapaa Fly Ash Mixture FA11

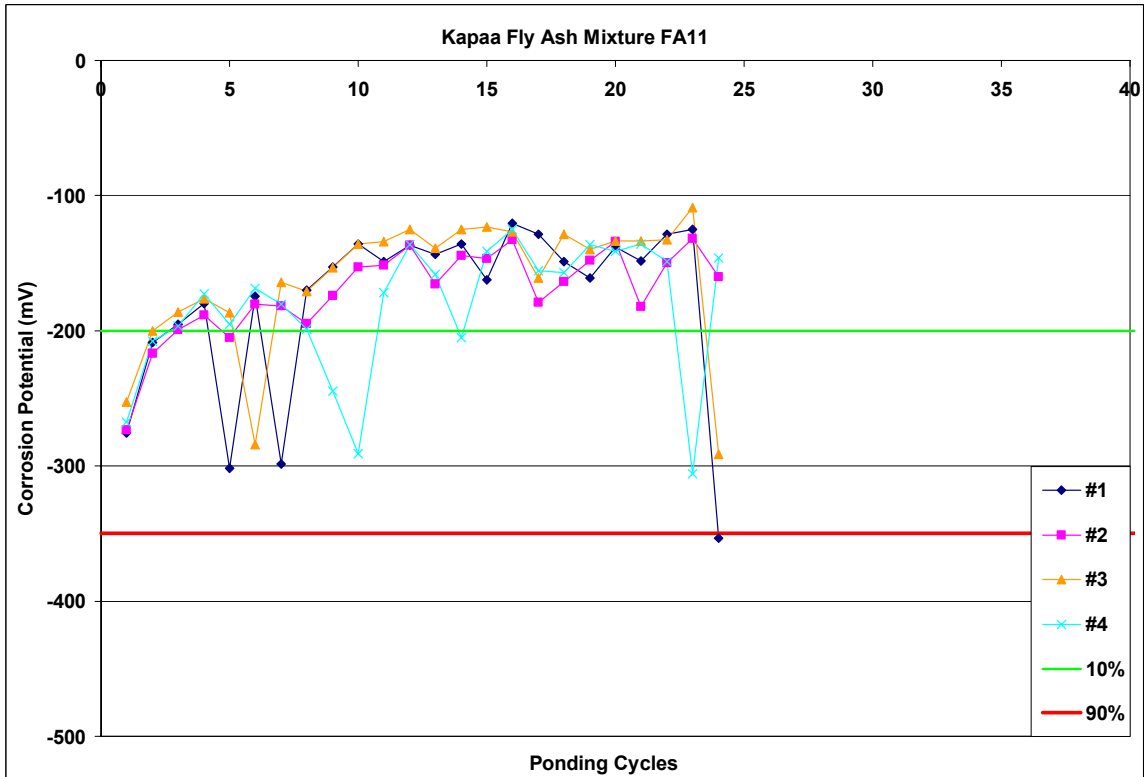


Figure A.1-280: Corrosion Potential for Kapaa Fly Ash Mixture FA11

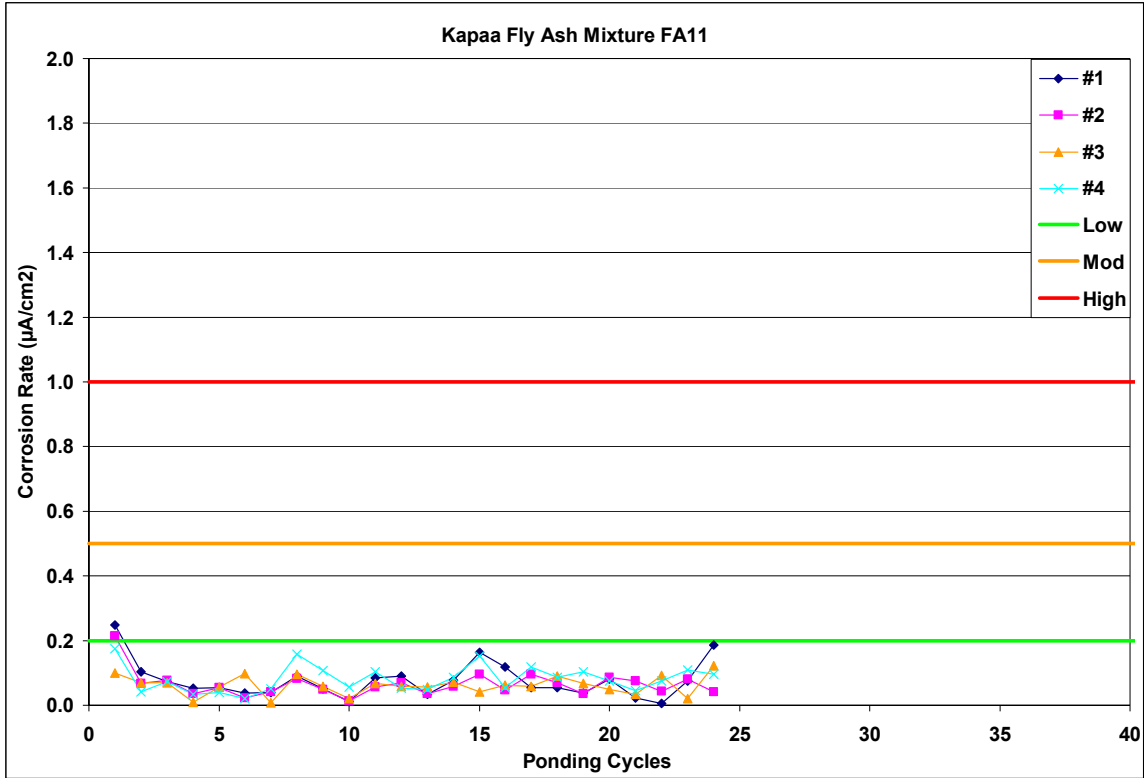


Figure A.1-281: Corrosion Rate for Kapaa Fly Ash Mixture FA11

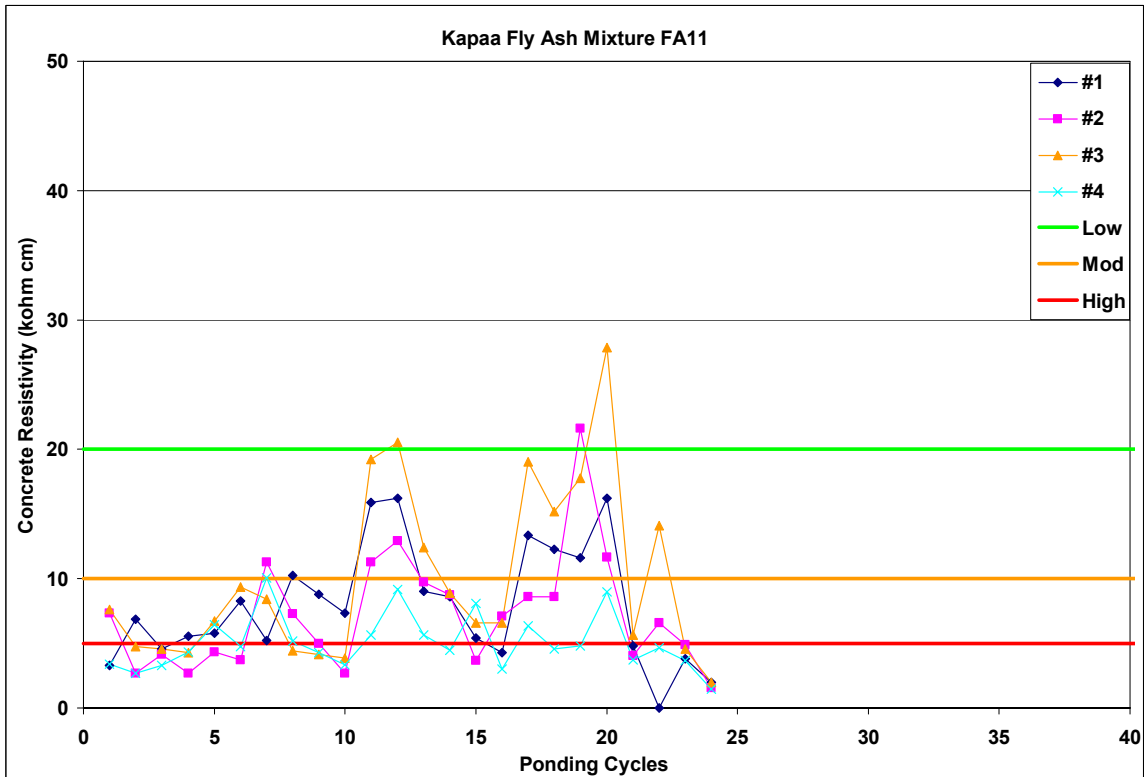


Figure A.1-282: Corrosion Resistivity for Kapaa Fly Ash Mixture FA11

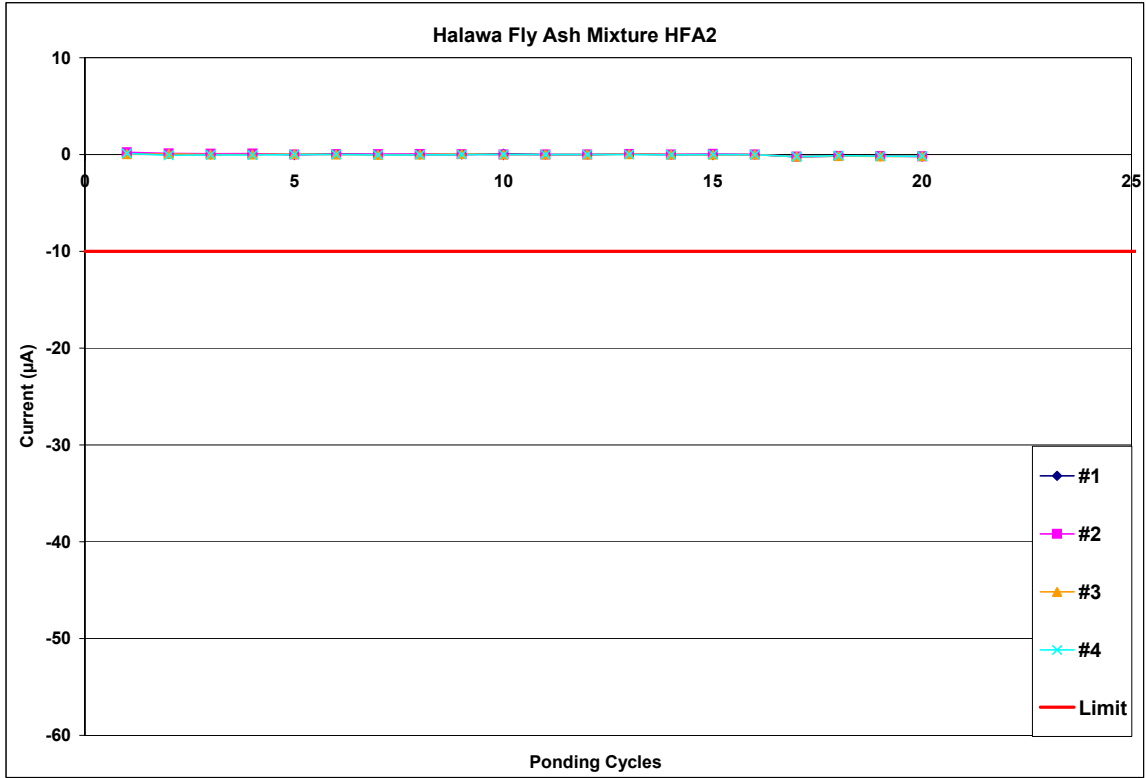


Figure A.1-283: Current Measurements for Halawa Fly Ash Mixture HFA2

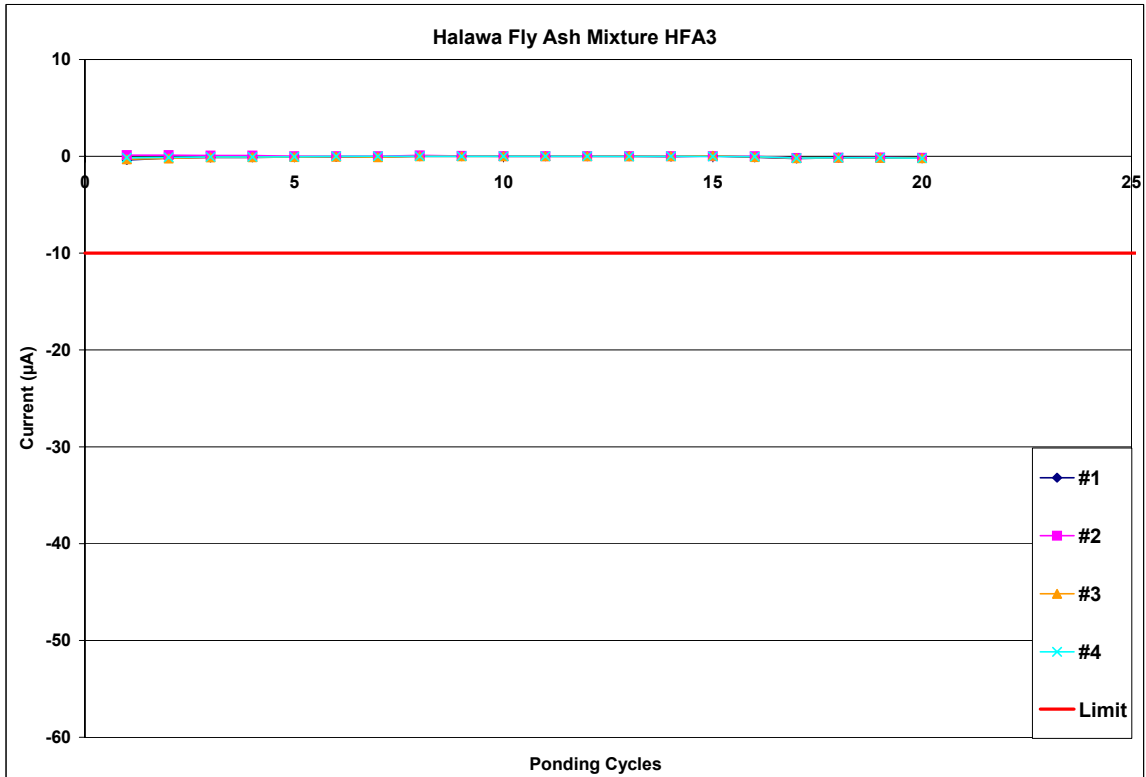


Figure A.1-284: Current Measurements for Halawa Fly Ash Mixture HFA3

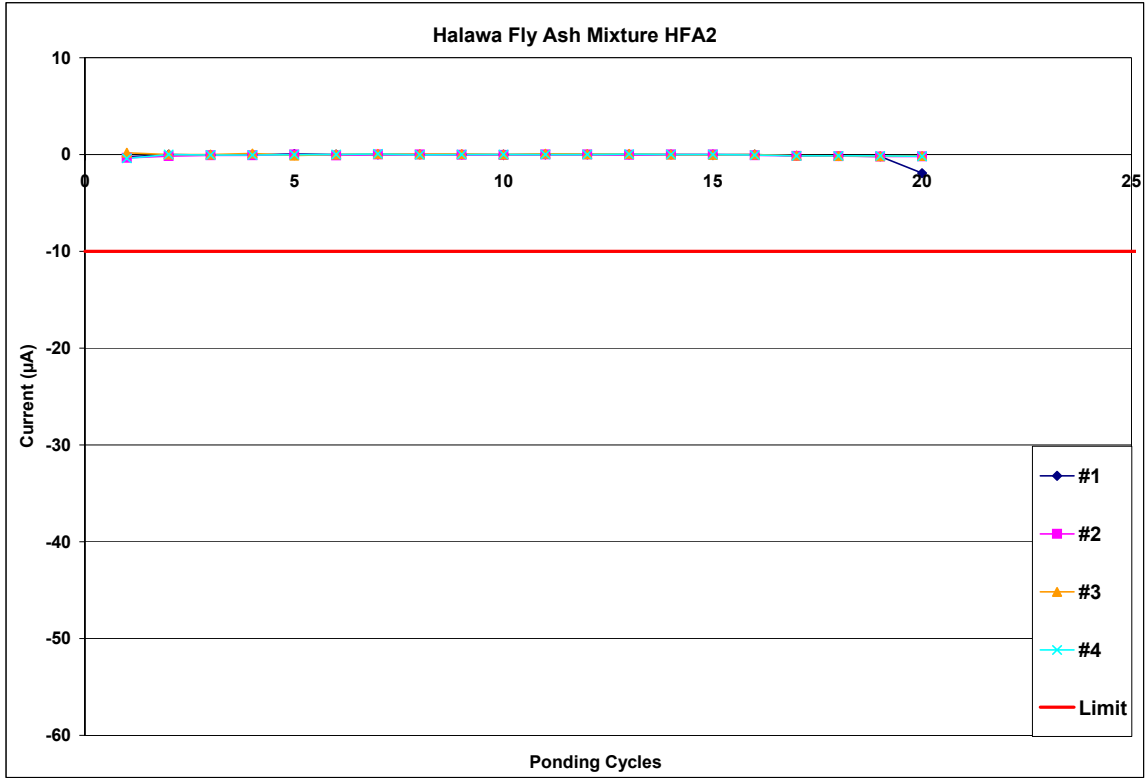


Figure A.1-285: Current Measurements for Halawa Fly Ash Mixture HFA4

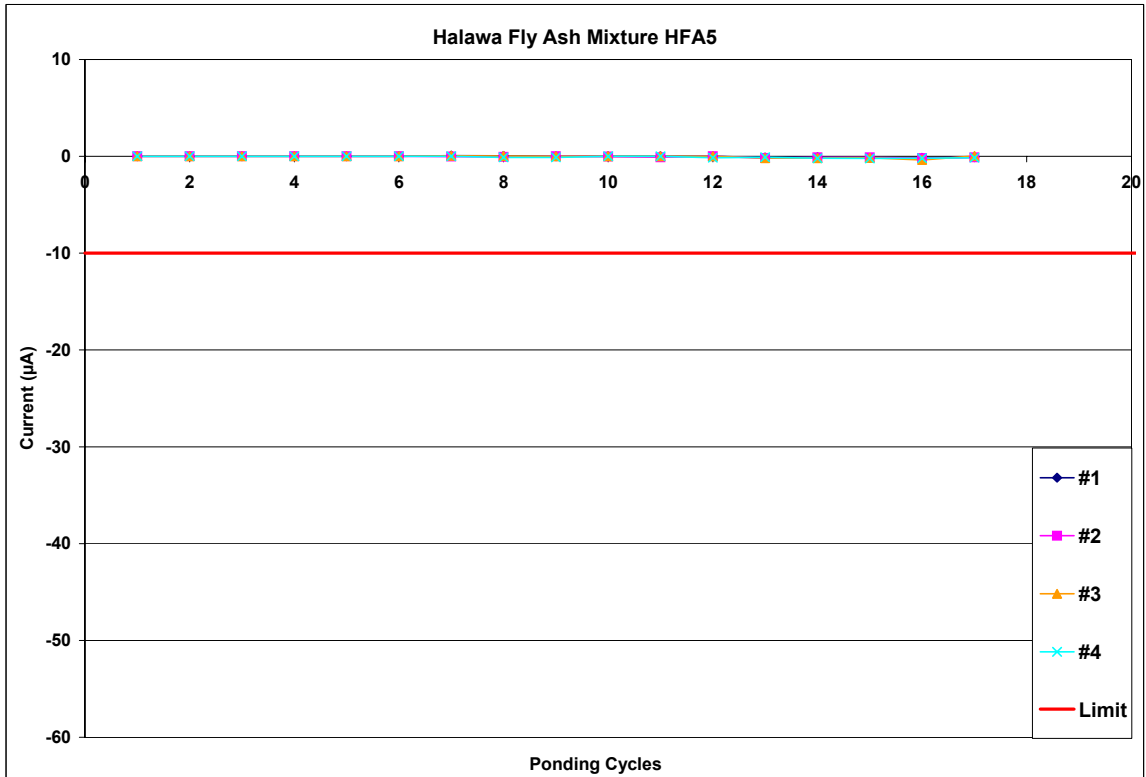


Figure A.1-286: Current Measurements for Halawa Fly Ash Mixture HFA5

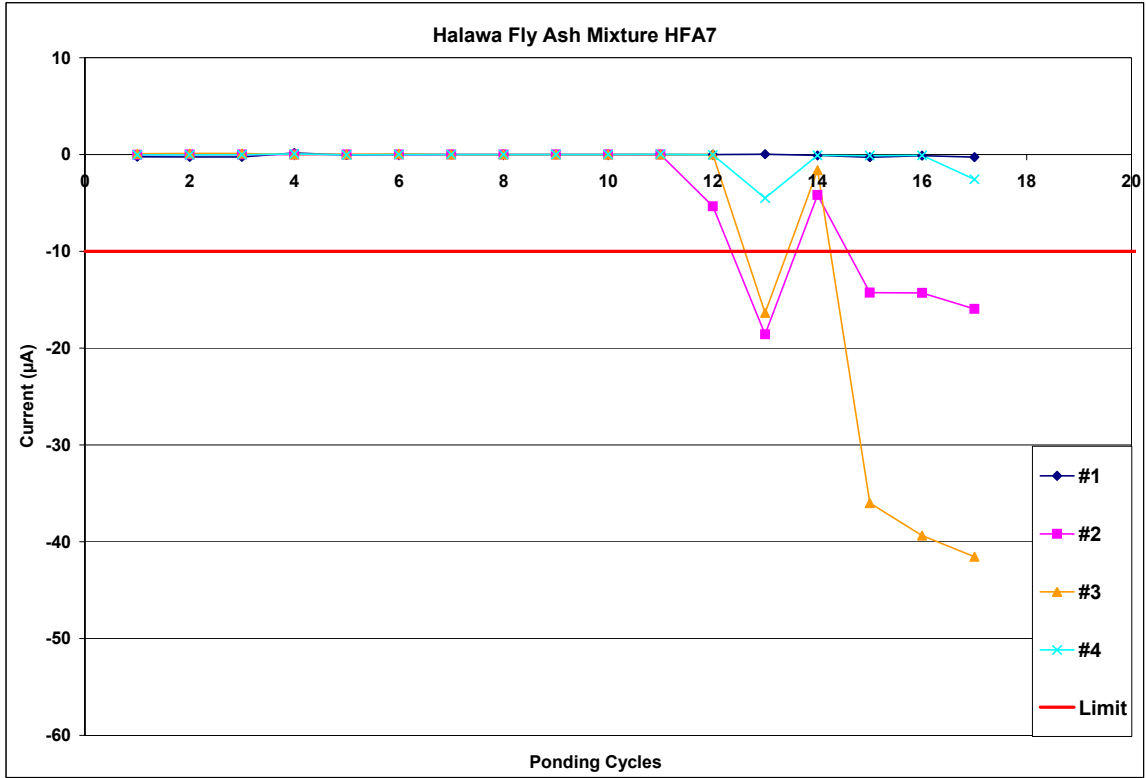


Figure A.1-287: Current Measurements for Halawa Fly Ash Mixture HFA7

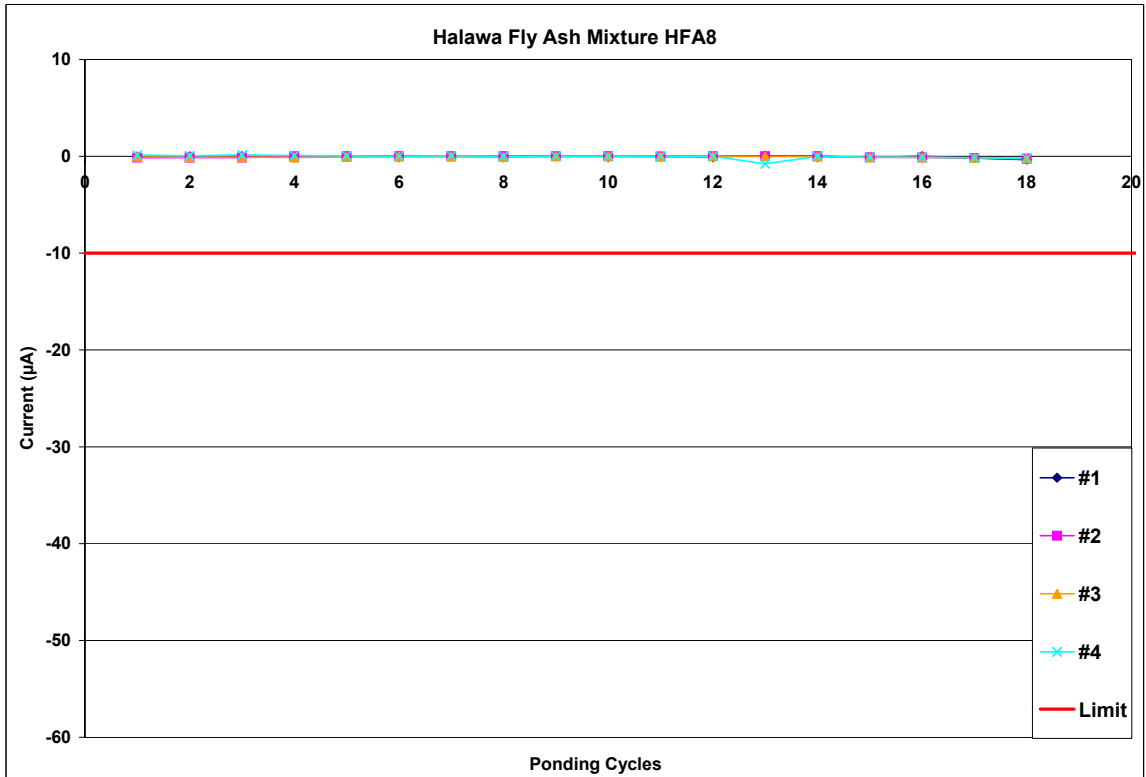


Figure A.1-288: Current Measurements for Halawa Fly Ash Mixture HFA8

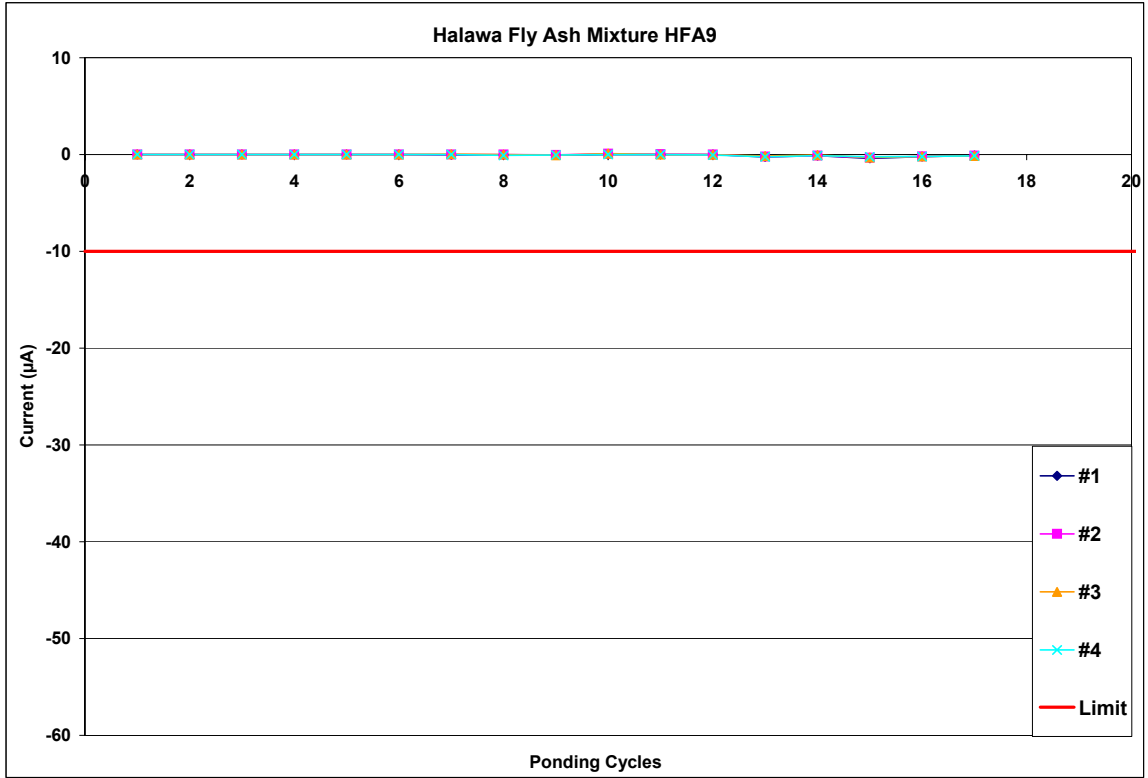


Figure A.1-289: Current Measurements for Halawa Fly Ash Mixture HFA9